USGS
science for a changing world

Geologic Studies in Alaska by the U.S. Geological Survey, 1996

Professional Paper 1595

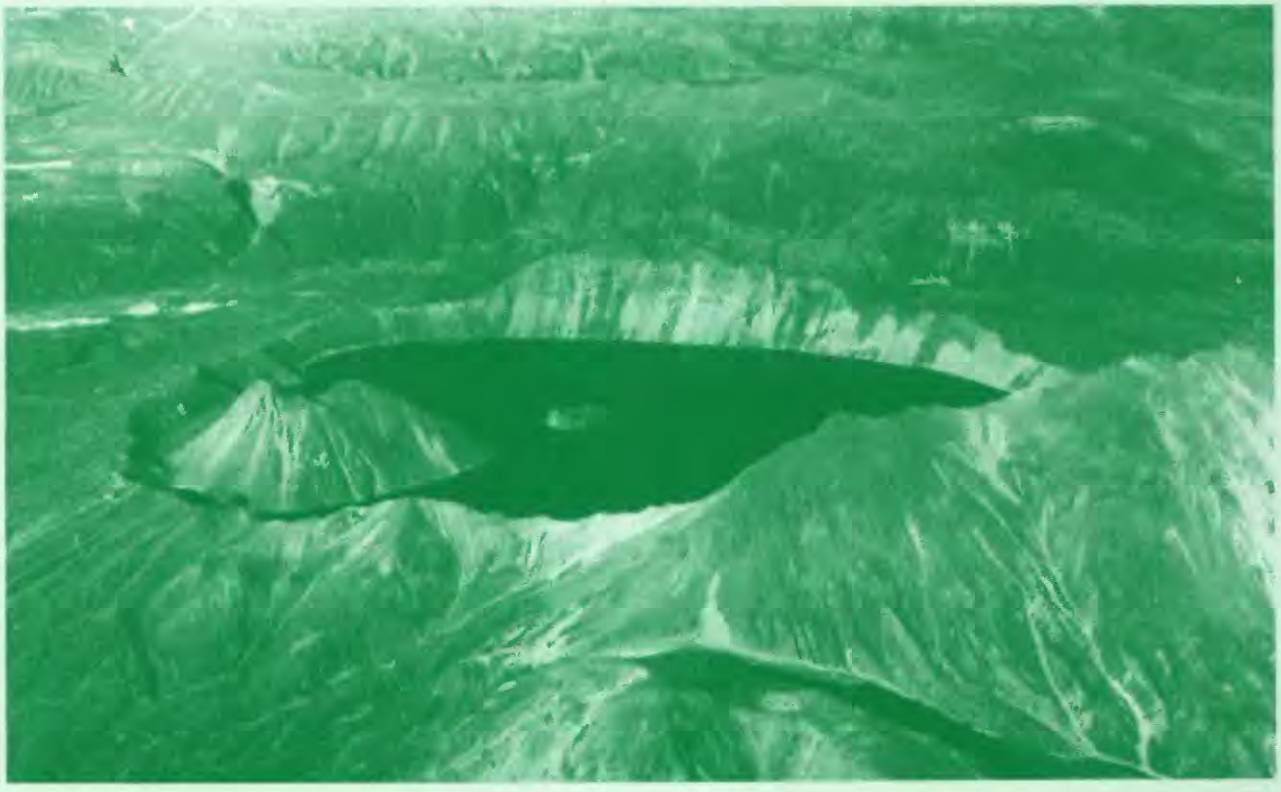

U.S. Department of the Interior
U.S. Geological Survey

Availability of Publications of the U.S. Geological Survey

Order U.S. Geological Survey (USGS) publications from the offices listed below. Detailed ordering instructions, along with prices of the last offerings, are given in the current-year issues of the catalog "New Publications of the U.S. Geological Survey."

Books, Maps, and Other Publications

By Mail

Books, maps, and other publications are available by mail from—

USGS Information Services
Box 25286, Federal Center
Denver, CO 80225

Publications include Professional Papers, Bulletins, Water-Supply Papers, Techniques of Water-Resources Investigations, Circulars, Fact Sheets, publications of general interest, single copies of permanent USGS catalogs, and topographic and thematic maps.

Over the Counter

Books, maps, and other publications of the U.S. Geological Survey are available over the counter at the following USGS Earth Science Information Centers (ESIC's), all of which are authorized agents of the Superintendent of Documents:

- Anchorage, Alaska–Rm. 101, 4230 University Dr.
- Denver, Colorado–Bldg. 810, Federal Center
- Menlo Park, California–Rm. 3128, Bldg. 3, 345 Middlefield Rd.
- Reston, Virginia–Rm. 1C402, USGS National Center, 12201 Sunrise Valley Dr.
- Salt Lake City, Utah–2222 West, 2300 South (books and maps available for inspection only)
- Spokane, Washington–Rm. 135, U.S. Post Office Building, 904 West Riverside Ave.
- Washington, D.C.–Rm. 2650, Main Interior Bldg., 18th and C Sts., NW.

Maps only may be purchased over the counter at the following USGS office:

- Rolla, Missouri–1400 Independence Rd.

Electronically

Some USGS publications, including the catalog "New Publications of the U.S. Geological Survey" are also available electronically on the USGS's World Wide Web home page at **http://www.usgs.gov**

Preliminary Determination of Epicenters

Subscriptions to the periodical "Preliminary Determination of Epicenters" can be obtained only from the Superintendent of Documents. Check or money order must be payable to the Superintendent of Documents. Order by mail from—

Superintendent of Documents
Government Printing Office
Washington, DC 20402

Information Periodicals

Many Information Periodicals products are available through the systems or formats listed below:

Printed Products

Printed copies of the Minerals Yearbook and the Mineral Commodity Summaries can be ordered from the Superintendent of Documents, Government Printing Office (address above). Printed copies of Metal Industry Indicators and Mineral Industry Surveys can be ordered from the Center for Disease Control and Prevention, National Institute for Occupational Safety and Health, Pittsburgh Research Center, P.O. Box 18070, Pittsburgh, PA 15236–0070.

Mines FaxBack: Return fax service

1. Use the touch-tone handset attached to your fax machine's telephone jack. (ISDN [digital] telephones cannot be used with fax machines.)
2. Dial (703) 648–4999.
3. Listen to the menu options and punch in the number of your selection, using the touch-tone telephone.
4. After completing your selection, press the start button on your fax machine.

CD-ROM

A disc containing chapters of the Minerals Yearbook (1993–95), the Mineral Commodity Summaries (1995–97), a statistical compendium (1970–90), and other publications is updated three times a year and sold by the Superintendent of Documents, Government Printing Office (address above).

World Wide Web

Minerals information is available electronically at **http://minerals.er.usgs.gov/minerals/**

Subscription to the catalog "New Publications of the U.S. Geological Survey"

Those wishing to be placed on a free subscription list for the catalog "New Publications of the U.S. Geological Survey" should write to—

U.S. Geological Survey
903 National Center
Reston, VA 20192

Geologic Studies in Alaska by the U.S. Geological Survey, 1996

John E. Gray *and* J.R. Riehle, *Editors*

U.S. GEOLOGICAL SURVEY PROFESSIONAL PAPER 1595

UNITED STATES GOVERNMENT PRINTING OFFICE, WASHINGTON : 1998

DEPARTMENT OF THE INTERIOR

BRUCE BABBITT, *Secretary*

U.S. GEOLOGICAL SURVEY

Thomas J. Casadevall, *Acting Director*

Manuscript approved for publication, November 25, 1997

Library of Congress catalog-card No. 92-32287

For sale by
U.S. Geological Survey, Map Distribution
Box 25286, MS 306, Federal Center
Denver, CO 80225

COVER PHOTO: Kaguyak Crater is the northernmost collapse caldera in the Aleutian volcanic arc and the only Holocene caldera on the Alaska Peninsula whose age has not been determined directly. Recent tephra studies (see article by Riehle and others) establish an age by correlation of about 3,600 yr B.P. The age is significant because it means that, in addition to major eruptions at other volcanoes, four of the six Holocene calderas on the Alaska Peninsula formed between 3,400 and 4,000 yr B.P.

CONTENTS

GEOLOGIC FRAMEWORK—*Continued*

BIBLIOGRAPHIES

CONTRIBUTORS TO THIS PROFESSIONAL PAPER

Anchorage

U.S. Geological Survey
4200 University Drive
Anchorage, Alaska 99508

Bradley, Dwight C.
Dumoulin, Julie A.
Keith, William J.
Miller, Marti L.
Riehle, James R.

U.S. Geological Survey
4230 University Drive
Anchorage, Alaska 99508

Dorava, Joseph M.

Denver

U.S. Geological Survey MS-
P.O. Box 25046, Denver Federal Center
Denver, Colorado 80225

Blome, Charles D., MS 913
Gent, Carol A., MS 973
Gray, John E., MS 973
Meier, Alan L., MS 973
Snee, Lawrence W., MS 913
Taylor, Cliff D., MS 973
Theodorakos, Peter M., MS 973

Fairbanks

U.S. Geological Survey
800 Yukon Drive
Fairbanks, Alaska 99775

Weber, Florence R.

Menlo Park

U.S. Geological Survey MS-
345 Middlefield Road
Menlo Park, California 94025

Brew, David A., MS 904
Calk, Lewis C., MS 910
Cole, Frances, MS 969
Ford, Arthur B., MS 904
Galloway, John P., MS 904
Gromme, Sherman, MS 937
Meyer, Charles E., MS 975
Toussaint, Susan, MS 955

Ocala

U.S. Geological Survey
4500 S.W. 40th Avenue
Ocala, Florida 34474

d'Angelo, William M.

Reston

U.S. Geological Survey
National Center MS-
12201 Sunrise Valley Drive
Reston, Virginia 20192

Harris, Anita G., MS 926A

Vancouver

U.S. Geological Survey
5400 MacArthur Blvd
Vancouver, Washington 98661

Scott, Kevin M.
Waitt, Richard B.

Others

Bundtzen, Thomas K.
Pacific Rim Geological Consulting

P.O. Box 81906
Fairbanks, Alaska 99708

Burleigh, Roger E.

4401 E. 145th Ave.
Anchorage, Alaska 99516

Layer, Paul W.

Geology and Geophysics and Geophysical Institute
University of Alaska
Fairbanks, Alaska 99775

Meier, Jonathan M.

Burns and McDonnell Waste Consultants, Inc.
P.O. Box 281647
San Francisco, California 94128

Mortensen, James K.

Department of Earth and Ocean Sciences
University of British Columbia
Vancouver, British Columbia, Canada

Newberry, Rainer J.
Solie, Diana N.

Department of Geology
University of Alaska
Fairbanks, Alaska 99775

Reed, Katherine M.

Washington Division of Geology and Earth Resources
Olympia, Washington 98504-7007

Toro, Jaime

Department of Geological and Environmental Sciences
Stanford University
Stanford, California 94305

Geologic Studies in Alaska by the U.S. Geological Survey, 1996

By John E. Gray *and* James R. Riehle

INTRODUCTION

This collection of 12 papers continues the annual series[1] of U.S. Geological Survey (USGS) reports on geologic investigations in Alaska. The annual volume presents results from new or ongoing studies in Alaska that are of interest to scientists in academia, industry, land and resource managers, and the general public. The Geological Studies in Alaska volume reports the results of studies that cover a broad spectrum of earth science topics from many parts of the state (fig. 1).

The papers in this volume are organized under the topics Environment and Climate, Resources, and Geologic Framework, in order to reflect the objectives and scope of USGS programs that are currently active in Alaska. Environmental studies are the focus of two articles in this volume: One study addresses the relation between glaciers and aquatic habitat on the Kenai River and another study evaluates the geochemistry of water draining chromite deposits in Alaska. Two papers address mineral resources in southwestern Alaska including a geochemical study of the Fortyseven Creek prospect and a geological and geochemical study of the Stuyahok area. Eight geologic framework studies apply a variety of techniques to a wide range of subjects throughout Alaska, including biostratigraphy, geochemistry, geochronology, paleomagnetism, sedimentology, and tectonics.

Two bibliographies at the end of the volume list reports about Alaska in USGS publications released in 1996 and reports about Alaska by USGS authors in non-USGS publications in 1996.

[1] From 1975 through 1988, the Geological Studies in Alaska series was published as USGS Circulars. During 1989–1994, the volumes were published as USGS Bulletins; since 1995, the volumes have been USGS Professional Papers. The most recent change is the result of reorganization of USGS publications. The volume was originally titled, "The United States Geological Survey in Alaska: accomplishments during 1975," but in 1986 the title was changed to "Geological studies in Alaska by the U.S. Geological Survey, 1985." This 1996 volume is the twelfth since the change in title.

Figure 1. Index map of Alaska showing 1:250,000-scale quadrangles and locations of study areas discussed in this book.

Role of Glaciers and Glacial Deposits in the Kenai River Watershed and the Implications for Aquatic Habitat

By Joseph M. Dorava *and* Kevin M. Scott

ABSTRACT

The Kenai River in south-central Alaska supports a multi-million-dollar, world-class salmon fishery. Recent studies indicate that numerous aquatic-habitat features along the river can be directly attributed to the effect of glaciers in its watershed. An extensive period of sustained high flows during salmon migration, two large glacially sculpted lakes, coarse streambed material, and a stable channel are examples of glacier-affected features. The extent of the watershed covered by glaciers significantly affects the seasonal and daily fluctuation in streamflow and the concentrations of suspended sediment. The historical extent of glaciers in a watershed has influenced channel morphology and stability. The glacial influences subsequently affect aquatic-habitat attributes such as protective cover, navigable water velocities, and appropriately sized substrate, which are most important to rearing juvenile salmon in the Kenai River.

INTRODUCTION

The Kenai River watershed drains an area of about 5,700 km^2 of the Kenai Peninsula in south-central Alaska (fig. 1). The Kenai River begins at the outlet of Kenai Lake, a narrow, 35-km-long, glacially sculpted, moraine-impounded lake; it flows about 27 km before it passes through Skilak Lake, another large moraine-impounded lake approximately 19 km long. From Skilak Lake, the river flows another 80 km before entering Cook Inlet near the city of Kenai.

The Kenai River has no man-made dams, and most of the residential and commercial development in the watershed is concentrated near the river's mouth and along a narrow corridor adjacent to the river downstream from Skilak Lake. Approximately 10 percent of the watershed is presently covered by glaciers (fig. 1).

The Kenai River is Alaska's most popular sport fishery, and more than 330,000 angler-days are representative of the annual sport-fishing effort (Liepitz, 1994). The commercial and sport fisheries contribute as much as $78 million annually to the economy of Alaska (Mills, 1994). During the past 10 years, the Kenai River has produced approximately 30 percent of the total commercial chinook salmon harvest in Cook Inlet. In addition, an estimated 20,452 chinook salmon were taken by sport fishing in the Kenai River during 1995, and the annual harvest has more than quadrupled since 1974 (table 1). The strength of these fisheries results in part because the aquatic habitat in the Kenai River is of high quality. The emigrating juvenile salmon are numerous, healthy, and adequately prepared for 4-5 years of life in the ocean before returning to the river as mature adults. The reasons for the highly productive chinook salmon runs on the Kenai River have been poorly understood. We have not known why so many chinook salmon return to this river and why they are among the largest in the world.

Several studies by the U.S. Geological Survey (Dorava, 1995; 1996; Dorava and Liepitz, 1996; Karlstrom, 1964; Post and Mayo, 1971; Scott, 1982) have identified specific geomorphic, hydrologic, and aquatic-habitat features of the Kenai River that have been derived primarily from glaciers, which are or were within the watershed. This report discusses the roles of glaciers in the watershed as they relate to chinook salmon habitat. For example, high-quality spawning and rearing habitat is provided by a stable river channel that has sustained high flows for extended periods, abundant protective cover, and appropriate substrate sizes. Past and present glaciers in the watershed have influenced the stability of the river channel, the river flow, and therefore the aquatic habitat.

ROLE OF GLACIERS IN THE KENAI RIVER WATERSHED

As recently as 12,000 years ago, the Kenai River watershed was nearly covered by glaciers (Karlstrom, 1964; Scott, 1982). Several specific features of the Kenai River can be attributed to the past or present glaciers. Kenai and Skilak Lakes (fig. 1) were formed by glaciers scouring a deep channel, retreating, and then leaving a lake impounded behind terminal moraines. These lakes now provide over-wintering habitat for juvenile salmon, trap sediment from the upstream tributaries, and moderate streamflow variations.

Glaciers significantly influence hydrologic and geomorphic characteristics of rivers that drain them. The expected variations in river flow influenced by glaciers in a river's

watershed are described by Fountain and Tangborn (1985). The influence of glaciers on the hydraulic characteristics near streamside structures along the Kenai River has been described by Dorava (1995). The potential links between salmon productivity and several unique glacier features of the Kenai River have been described by Dorava and Liepitz (1996). The influence of glaciers on river morphology and streambank erosion along the Kenai River is described by Scott (1982). Data describing the influence of glaciers on streamflow and sediment transport in the Kenai River can be found in annual reports by the U.S. Geological Survey (1957-96). The quality of the aquatic habitat in the Kenai River is described by Estes and Kuntz (1986) and Liepitz (1994).

AQUATIC-HABITAT FEATURES IN THE KENAI RIVER

The large number of chinook salmon harvested from the Kenai River by sport fishermen (table 1) reflects the high quality of the available aquatic habitat (Liepitz, 1994). The three most important habitat attributes for rearing juvenile chinook salmon are abundant streamside and instream cover, navigable water velocities, and appropriately sized substrate (Estes and Kuntz, 1986; Liepitz, 1994). Recent studies that pertain to salmon habitat in the Kenai River include those of Reger and others (1996; Quaternary deposits), Scott (1982; erosion and sedimentation), Dorava (1995; hydraulic characteristics near streamside structures), Dorava (1996; effects of flooding); and Dorava and Moore (1997; effects of boatwakes on streambank erosion). Results of these studies illustrate the relation between the quality of aquatic habitat and the past and present influence of glaciers in the Kenai River watershed.

Salmon generally require cool, clear, unpolluted water, with an adequate depth to support migrating and spawning adults, egg incubation, and rearing of juveniles. Although adult salmon may not eat while spawning in freshwater, juveniles spend as much as three years in freshwater and obtain their food primarily from benthic macroinvertebrates. Water velocities must not be greater than about 64 cm/s, the sustained swimming ability of juvenile salmon, or they will

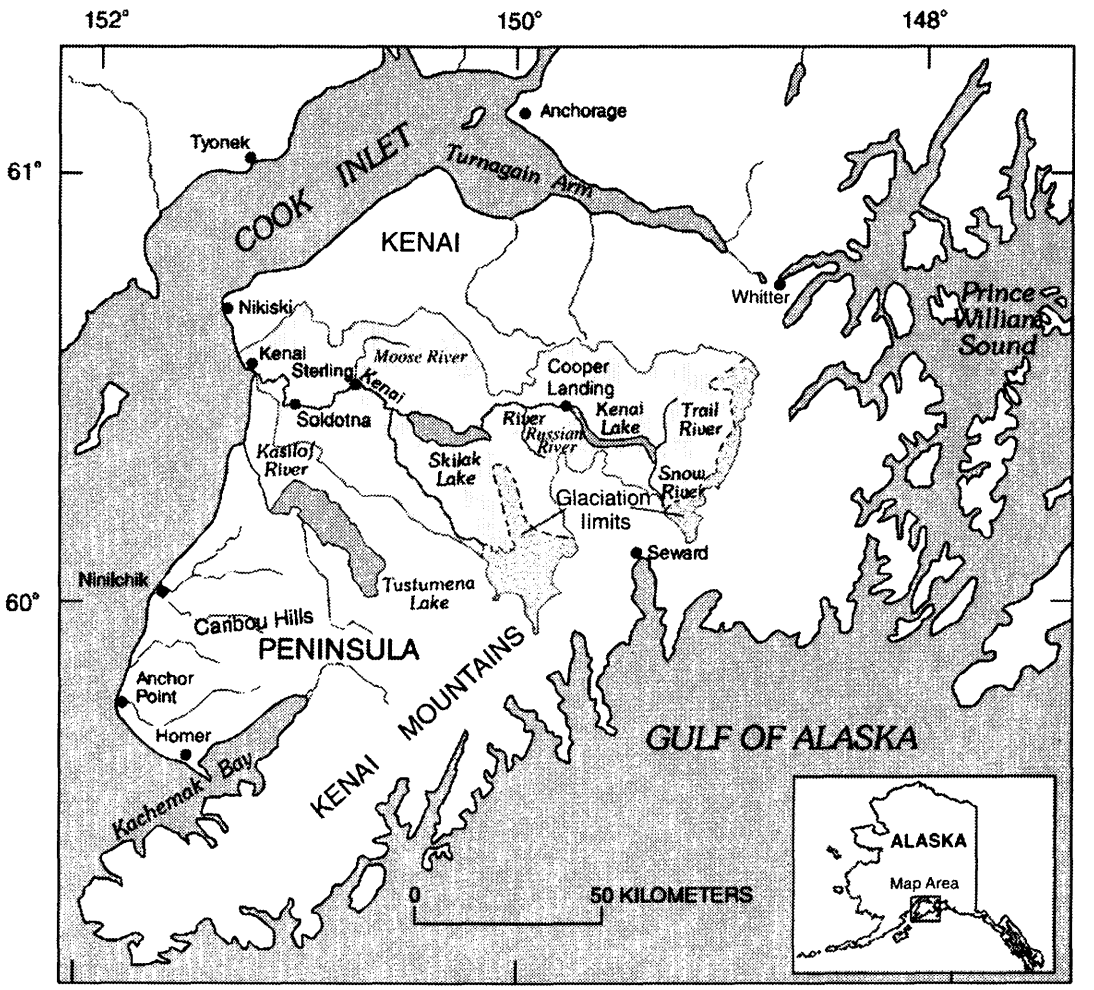

Figure 1. Kenai River watershed (shaded) on Kenai Peninsula, Alaska, and approximate limit of present glaciation (stippled).

Table 1. Number of chinook salmon taken by sport fishing in the Kenai River, 1974-95.

[Data from Alaska Department of Fish and Game. Annual catch is limited by State regulation]

Year	Total	Year	Total
1974	4,910	1985	16,026
1975	2,970	1986	16,565
1976	7,018	1987	25,608
1977	7,321	1988	30,259
1978	7,120	1989	16,383
1979	8,295	1990	7,982
1980	5,554	1991	7,740
1981	9,810	1992	8,045
1982	10,276	1993	23,006
1983	15,534	1994	20,022
1984	12,332	1995	20,452

not be able to navigate and find food (Liepitz, 1994). Juvenile chinook salmon in the Kenai River are most commonly found where water velocities are between about 3 and 18 cm/s (Burger and others, 1982). During winter low-flow periods, water velocity must remain above some minimum value that circulates adequate water and oxygen through spawning beds. The magnitude of these minimum velocities depends on the permeability of the substrate. There must also be adequate in-stream cover provided by vegetation, debris, or large substrate to protect juvenile fish from predators and to allow resting areas for migrating adults.

Historically, urban and residential development in the Kenai River watershed has been sparse, and thus sources of water pollution have been few. This lack of development also means that an abundance of undisturbed riparian areas is available to contribute streamside cover and food for salmon migrating or rearing in the river. Salmon also provide the Kenai River with a source of nutrients from spawned-out dead carcasses. Glacier-fed rivers can be nutrient-poor systems, and the salmon themselves are an important source of nutrients for streamside vegetation and benthic macroinvertebrates. Extensive periods of sustained flow during the months of June through September provide adequate water depths and navigable water velocities, giving the salmon ample opportunities to migrate into and spawn in the river and its tributaries. When flows are reduced in the winter, Kenai and Skilak Lakes provide over-wintering habitat for rearing salmon. The Kenai River is providing salmon with a healthy environment, and much of the river's environment is influenced by the effects of glaciers.

GLACIER EFFECTS ON AQUATIC HABITAT IN THE KENAI RIVER

The effect of glaciers on the aquatic habitat in the Kenai River's watershed has been documented in an investigation of erosion and sedimentation along the river (Scott, 1982). Glaciers formed terminal moraines along the river during various stages of advance (fig. 2). Steep-gradient segments or rapids are found where the river crosses these moraines. Immediately downstream from these rapids, material in the stream channel and banks is coarse and resistant to movement. The stability of these steep segments of the river is evident in constancy in their bank positions over time (Scott, 1982). The instability of segments of the river upstream and downstream from these steep segments is shown by greater changes in their bank positions over time (Scott, 1982). The streambank material in these segments of greater channel movement is easily eroded unconsolidated alluvium, deposited by past glaciation in the watershed.

Scott (1982) describes a period between 12,000 and 8,420 years ago, when the Kenai River was diverted upstream from Skilak Lake into Hidden Lake and flowed down the East Fork of the Moose River (fig. 2). The diversion probably existed until the final advance of Skilak Glacier. During the subsequent period when the Kenai River entered and exited Skilak Lake, glaciers were more extensive in the watershed than they are now, and meltwater runoff was much greater than it is at present (Karlstrom, 1964; Reger and others, 1996; Scott, 1982). These large flows carved a large river channel. However, the present Kenai River is smaller, and much of its channel is under-fit and stable under the present flow regime. This channel stability helps maintain spawning and rearing habitat, as long as there is no increased siltation caused by anthropogenic influences. The short-term effect of channel stability is to maintain aquatic habitat. However, during the long term, habitat created by the stable channel is degraded as fine-grained sediments accumulate when the streamflow is not adequate to move the streambed. Accumulation of fine-grained sediment significantly reduces the quality of important spawning and rearing habitat by suffocating or entrapping incubating eggs and by reducing the clarity of the water, making it difficult for juvenile salmon to find food. Any mitigation of human activities on the river will be more effective if it can be tailored to local differences in hydrologic and geologic characteristics.

The effects of glaciers on aquatic habitat in the Kenai River may be illustrated by a comparison of chinook salmon escapement numbers from another river without glaciers in its watershed. The Deshka River is a popular chinook salmon fishing river that drains about 950 km^2 on the west side of Cook Inlet. This river is about 58 km northwest of Anchorage, extends for nearly 100 km inland, and is not easily accessible from the road system. Thus, far fewer people use this river than use the Kenai River. The Deshka River watershed is generally in its natural state, and the chinook salmon

escapement numbers represent annual totals available for reproduction (table 2). The chinook salmon escapement from the Deshka River is as much as 55 percent and as little as 27 percent of that in the Kenai River (table 2). The mean escapement for the Kenai River is about 5.6 times that for the Deshka River. However, these escapement numbers can be normalized for differences in available habitat between the Kenai River (5,700 km^2) and the Deshka River (950 km^2) by dividing each escapement value by the square root of the drainage area. This results in an approximation of salmon escapement per unit length of each river and indicates a 2.28 times greater escapement in the Kenai River.

Hydrologic and geomorphic differences associated with the absence or presence of glaciers in the watersheds of the two river systems probably contribute to the difference in salmon escapement numbers. For example, the mean summer flow for the months of June, July, and August—when chinook salmon escapement takes place—is much lower in the Deshka River than in the Kenai River (U.S. Geological Survey, 1986 and 1996). The mean summer flow in the Deshka River as runoff per kilometer of watershed area is 0.03 (m^3/s)/km, and in the Kenai River it is 0.06 (m^3/s)/km. The unit runoff values indicate the significant hydrologic effect of glaciers providing melt water to sustain flows in the Kenai River during the escapement period. As a result, the primary period for spawning in the Deshka River will be shorter than that in the Kenai River. In the Deshka River, however, streamflow results primarily from rainfall and snowmelt runoff. Although detailed geomorphic information is not available to compare the Deshka River with the Kenai River, it might provide additional evidence of the role of glaciers to influence channel stability and provide aquatic habitat.

The nature of the streambed and streambank material along the Kenai River is also influenced by the past and present glaciers in the watershed. The riverbed is generally coarser and more armored than that of the Deshka River, as a result of glacial activity. Larger porous substrate provides

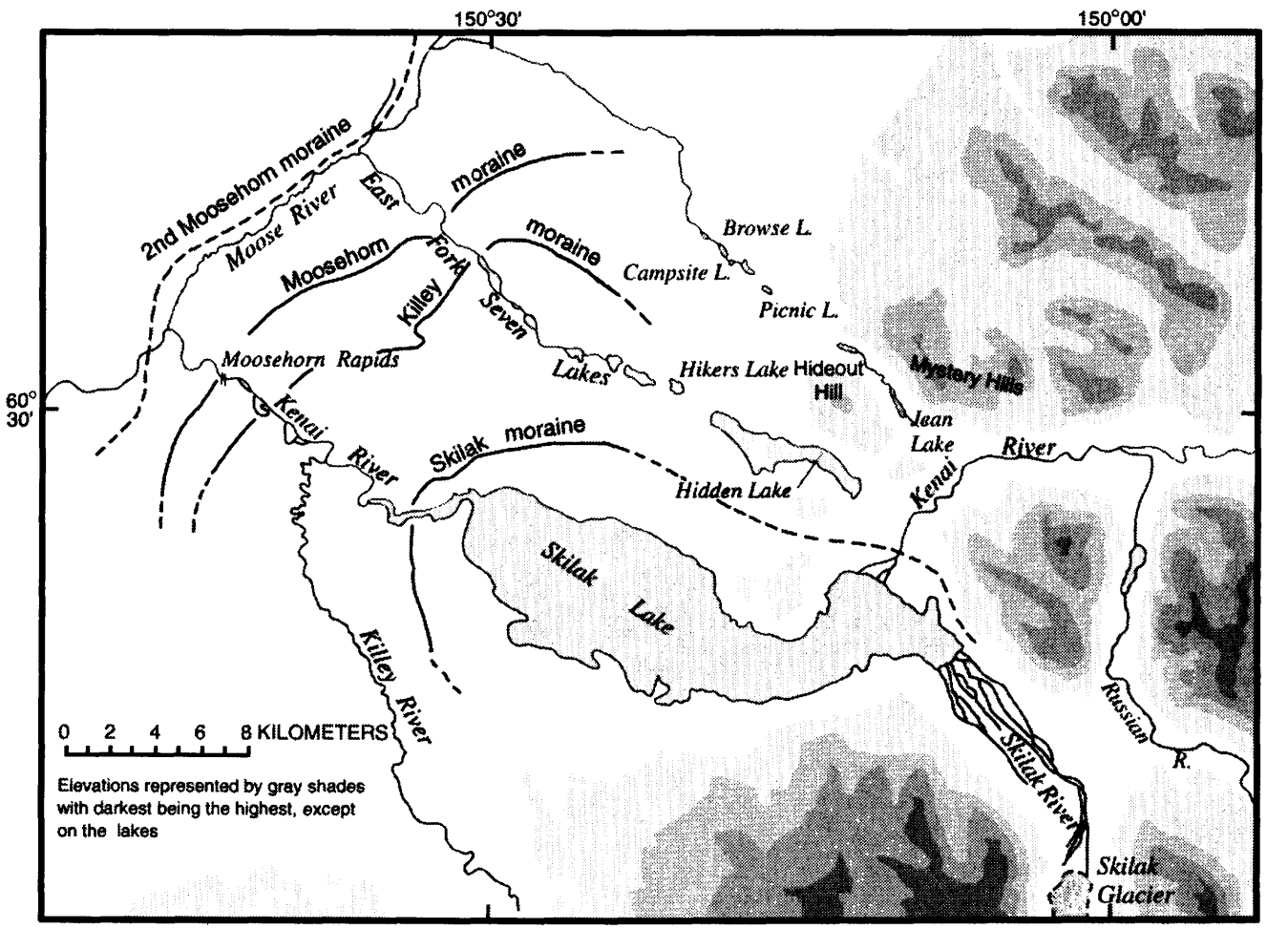

Figure 2. Kenai River watershed around Skilak Lake near front of Kenai Mountains. Limits of subsidiary moraines within Naptowne Glaciation are shown; lines dashed were approximate (modified from Karlstrom, 1964, pl. 4, and Reger and others, 1996, pl. 2).

Table 2. Escapement of chinook salmon in the Deshka River and Kenai River, 1987-96

[Data from Alaska Department of Fish and Game]

Year	Deshka River	Kenai River
1987	15,028	70,036
1988	19,200	72,888
1989	5,036	47,027
1990	18,166	33,036
1991	8,112	45,824
1992	7,736	40,401
1993	5,769	69,595
1994	2,665	71,877
1995	10,048	66,220
1996	14,354	77,439

a stable environment and allows adequate water and oxygen flow through the substrate in spawning sites. Streambanks composed of unconsolidated alluvium are more easily eroded than are armored streambeds or banks composed of coarse outwash or cohesive tills.

Coarse bed material that may be naturally resistant to erosion is, however, susceptible to siltation of the gravel interstices. Once deposited, fine-grained sediment within the coarse gravel is rarely washed away. On the Kenai River, this washing away of accumulated fine-grained sediment occurs only when streamflow is great enough to erode the armored bed material. During a large flood in September1995, which has an estimated recurrence interval of 100 years, the streambed was eroded as much as 1.5 m at the stream-gaging station in Soldotna (Dorava, 1996). In comparison, during the 10-year period between 1980-90, less than 0.5 m of total erosion occurred at this site. Additionally, large gravel dunes in the river channel downstream from Skilak Lake did not move significantly during the 100-year flood in 1995. Periodic releases of water stored by glaciers in headwater tributaries have also produced outburst floods on a 2- to 3-year cycle on the Kenai River (Post and Mayo, 1971). At present, it is uncertain whether these periodic outburst floods erode the streambed or at what discharge the armored streambed on the Kenai River will erode.

The change in aquatic habitat near a streamside structure is influenced primarily by the alterations the structure makes to available cover for fish, to water velocity, and to substrate size. Antecedent conditions in the river, which are influenced by glaciers in the watershed and inherited effects from ancient glaciers, generally control the quality of existing aquatic habitat. The hydraulic characteristics of the Kenai River near structures (such as jetties, docks, and boat launches) are influenced by the presence of upstream glaciers in the watershed (Dorava, 1995). During most of the year when temperatures are low, glacier melting and runoff are also low, and structures along the Kenai River are above the water line. During periods of increased flow in the summer, many of the structures along the Kenai River are in the water. These structures modify aquatic habitat in terms of cover they provide; they also alter the natural water velocity and flow direction. A jetty or groin extending into the river is more likely to cause erosion where the channel is narrow, where bank and bed materials are relatively small and unconsolidated, and where water velocities are high.

The potential effects of increased urbanization of the watershed and increased power-boat use on the river are also influenced by glaciers. When new structures are built or power-boat use is concentrated in areas having unconsolidated glacial deposits that are easy to erode, rapid destruction of aquatic habitat will result. The degradation of aquatic habitat will be slower in areas where large material was deposited as glacial outwash or where clay-rich glacial tills are more resistant to erosion. For example, large boulders deposited in the river near Soldotna reduce the speed of local boat traffic and also naturally mitigate the erosive boatwake energy. Other areas of unconsolidated alluvium near Sterling erode easily and are more susceptible to human activities.

SUMMARY

Recent U.S. Geological Survey investigations of aquatic habitat, erosion, and hydraulics on the Kenai River have identified the important role of glaciers in creating and maintaining aquatic habitat in the watershed. The Kenai River is different from rivers that do not have glaciers in their watersheds because the glaciers affect the river's aquatic habitat by controlling its hydrologic and geomorphic characteristics. Many of the unique glacial features of the Kenai River (such as the sustained high flows for extended periods, the two large lakes in the watershed, and the stable channel configuration) provide juvenile chinook salmon with their most important aquatic-habitat attributes: Navigable water velocities, abundant cover, and appropriate substrate sizes. Recognizing the role of glaciers in the watershed has implications for mitigating potential damage to the aquatic habitat resulting from human activities.

REFERENCES CITED

Burger, C.V., Wangaard, D.B., Wilmot, R.L., and Palmisano, A.N., 1982, Salmon investigations in the Kenai River, Alaska, 1979-1981: U.S. Fish and Wildlife Service National Fisheries Research Center, 139 p.

Dorava, J.M., 1995, Hydraulic characteristics near streamside structures along the Kenai River, Alaska: U.S. Geological Survey Water-Resources Investigations Report 95-4226, 41 p.

Dorava, J.M., 1996, Salmon habitat alterations resulting from recent flooding along the Kenai River, Alaska [abs.]: American Water Resources Association, Alaska Chapter Annual Meeting, April 1996.

Dorava, J.M., and Liepitz, G.S., 1996, Balancing the three R's (regulation, research, and restoration) on the Kenai River, Alaska: U.S. Geological Survey Fact Sheet FS-160-96, 2 p.

Dorava, J.M., and Moore, G.W., 1997, Effects of boatwakes on streambank erosion, Kenai River, Alaska: U.S. Geological Survey Water-Resources Investigations Report 97-4105, 84 p.

Estes, C.C., and Kuntz, K.J., 1986, Kenai River habitat study: Alaska Department of Fish and Game, Federal Aid in Fish Restoration F-10-1 and Anadromous Fish Studies, v. 27, variously paged.

Fountain, A.G., and Tangborn, W.V., 1985, The effect of glaciers on streamflow variation: Water Resources Research, v. 21, no. 4, p. 579-586.

Karlstrom, T.N.V., 1964, Quaternary geology of the Kenai Lowlands and glacial history of the Cook Inlet region Alaska: U.S. Geological Survey Professional Paper 443, 69 p.

Liepitz, G.S., 1994, An assessment of the cumulative impacts of development and human uses on fish habitat in the Kenai River: Alaska Department of Fish and Game Technical Report No. 94-6, 63 p.

Mills, M.J., 1994, Harvest, catch, and participation in Alaska sport fisheries during 1993: Alaska Department of Fish and Game, Division of Sport Fish, Fishery Data Series 94-42, variously paged.

Post, Austin, and Mayo, L.R., 1971, Glacier-dammed lakes and outburst floods in Alaska: U.S. Geological Survey Hydrologic Investigations Atlas HA-455, 3 sheets, scale 1:1,000,000.

Reger, R.D., Pinney, D.S., Burke, R.M., and Wiltse, M.A., 1996, Catalog and initial analyses of geologic data related to middle to late Quaternary deposits, Cook Inlet region, Alaska: Alaska Division of Geological and Geophysical Surveys Report of Investigations 95-6, 188 p.

Scott, K.M., 1982, Erosion and sedimentation in the Kenai River, Alaska: U.S. Geological Survey Professional Paper 1235, 35 p.

U.S. Geological Survey, 1957-96, Water resources data, Alaska—water years 1947-95: U.S. Geological Survey Water-Supply Papers from 1957 to 1976 and U.S. Geological Survey Water-Data Reports from 1977 to 1996 (Surface-water data for water years 1947-96).

Reviewers: Roy Glass and Dennis Trabant.

A Reconnaissance Study of the Chemistry of Natural Waters Draining Chromite-Bearing Ultramafic Complexes in Alaska

By Cliff D. Taylor, Alan L. Meier, *and* William M. d'Angelo

ABSTRACT

Twelve surface-water samples were collected from creeks and abandoned mines at Red Mountain on the Kenai Peninsula and from creeks and lakes at the Siniktanneyak Mountain ultramafic complex in the western Brooks Range, Alaska. The waters at both locations are neutral to alkaline (pH 6.7 to 9.3) magnesium-bicarbonate type, with total chromium concentrations of less than 2 ppb (0.5 to 1.0 ppb Cr in five samples from Red Mountain). Under normal climatic conditions and pH ranges of most natural waters, Cr-contamination from chromite-bearing ultramafic complexes does not appear to pose a significant environmental threat.

INTRODUCTION

The majority of the world's supply of chromium (Cr) is mined from ultramafic igneous complexes. The ultramafic complexes are generally vast flat-lying intrusions, covering many hundreds of square kilometers in stable continental areas, or much smaller alpine-type intrusions that are several tens of square kilometers in size in dismembered sections of obducted oceanic crust at continental margins. The complexes consist of homogenous to distinctly layered, dark-colored rock sequences composed of simple magnesium-, iron-, and calcium-rich mineralogy dominated by olivine, pyroxenes, and plagioclase feldspar. The chromium resides in chromite ($FeCr_2O_4$), a spinel-group oxide that is resistant to chemical and physical weathering and therefore has a low solubility in natural waters. Ultramafic complexes weather to a distinct orange-brown color and are generally devoid of vegetation (fig. 1).

When chromite ore is present in ultramafic complexes, it is found as monomineralic black layers or seams called "chromitite." Chromitite seams (fig. 2) vary from 0.5 mm to 2 m in width. In alpine-type chromite deposits, chromitite orebodies are podiform in shape and irregularly distributed. Chromium is used in the plating industry, steel alloys, catalysts used for industrial-scale polymerization processes, pigments and dyes, and in chromic acid products such as wood preservatives (Simon and others, 1994; Duke, 1988).

The maximum contaminant level (MCL) for drinking water recommended by the State of Alaska is 100 parts per billion (ppb or 1 ng/g) total chromium (Alaska Department of Environmental Conservation, 1994). Federal water-quality standards for chromium include criteria for maximum concentrations (CMC) of trivalent (Cr^{3+}) and hexavalent (Cr^{6+}) chromium; the limits are 1,700 and 16 ppb, respectively (Environmental Protection Agency, 1992). Chromium in cationic and anionic forms is soluble in aqueous systems over a wide pH range. Under reducing and acidic to near-neutral pH conditions, the dominant form of soluble chromium is as Cr^{3+} (largely as hydroxide complexes such as $CrOH^{2+}$ and $Cr(OH)_2^+$, fig. 3). Similarly, chromium in the mineral chromite is in the Cr^{3+} form. The resistance of chromite to physical and chemical weathering and the less than 1 ppb solubility of chromium in natural waters (Hem, 1977) indicates that in waters of near-neutral pH, effluent draining chromium mines is unlikely to be an environmental contaminant. However, under alkaline oxidizing conditions Cr^{6+} is stable (as CrO_4^{2-}, fig. 3), and chromium is therefore soluble in a potentially toxic state. Although Cr^{3+} is generally benign, Cr^{6+} is a mutagen and a possible carcinogen (Simon and others, 1994).

While there are numerous studies of Cr^{6+} entering freshwater and saltwater ecosystems from industrial sources (Perlmutter and others, 1963; Kharkar and others, 1968; Elderfield, 1970; Casagrande and Erchull, 1977; Kaczynski and Kleber, 1993), there are presently few studies of chromium-mine drainage and its effect on surrounding environments. To evaluate the environmental effect of chromium-mining in Alaska, we sampled surface waters at a mined and at an undisturbed ultramafic complex.

The mined site is located at Red Mountain, an alpine-type ultramafic complex 16 km from the town of Seldovia, on the Kenai Peninsula (fig. 4*A*). Red Mountain contains the only mined chromite deposits in Alaska.

More than 35,000 tonnes of ore have been mined from Red Mountain through 1976. A large, low-grade resource may remain, containing at least 27,000,000 tonnes grading 5.1 percent Cr_2O_3 (Bundtzen and others, 1996). The local ecosystem supports a rich and diverse wildlife population as well as an important saltwater fishery. We also collected water samples from Siniktanneyak Mountain, an undisturbed alpine-type ultramafic complex in the western Brooks Range about 240 km northeast of Kotzebue (fig. 4*B*).

METHODS

SAMPLE COLLECTION AND FIELD METHODS

Seven surface water samples were collected on July 22, 1994, from the Red Mountain ultramafic complex. Five of the samples represent stream runoff, and two are effluent issuing from abandoned chromite mines (figs. 4*A*, 5; table 1). During the site work, the weather was overcast and drizzly with an average air temperature of

Figure 1. Northern contact of the Red Mountain ultramafic complex showing distinct color and vegetation contrasts between bare orange-colored ultramafic rock on left and well vegetated soil on right.

Figure 2. Seam of dark black chromitite 0.7 m thick in ultramafic rocks at Red Mountain.

about 4.5°C (40°F). Snowpack was present on the north-facing slopes at the head of the Windy River drainage upstream of sample RM-02.

Five surface-water samples were collected from the Siniktanneyak complex on July 16, 1994. The weather was clear and sunny, and snowmelt was above average for this time of year. Three samples (SN-01, SN-02, and SN-03, fig. 4*B*, table 1) were from drainages having no known chromite occurrences. Two more samples (SN-04 and SN-05, fig 4*B*, table 1) were collected from a river and lake below chromite-bearing rocks.

At each site, the water temperature, pH, and specific conductivity were recorded using digital meters with temperature corrections. Hach colorimetric kits were used in the field for determination of alkalinity. Two samples were obtained at each site: (1) A filtered (0.45-µm membrane), nitric-acid-acidified water sample collected in a 60-ml polyethylene bottle for determination of dissolved cations, and (2) a filtered (0.45-µm membrane) unacidified water sample collected in a 125-ml polyethylene bottle for anion determinations. Samples for anion determinations were kept cool until analyzed.

ANALYTICAL METHODS

Major, minor, and trace element concentrations were determined in the filtered acidified water samples by inductively coupled plasma mass spectrometry (Meier and others, 1994). This semiquantitative method allows for

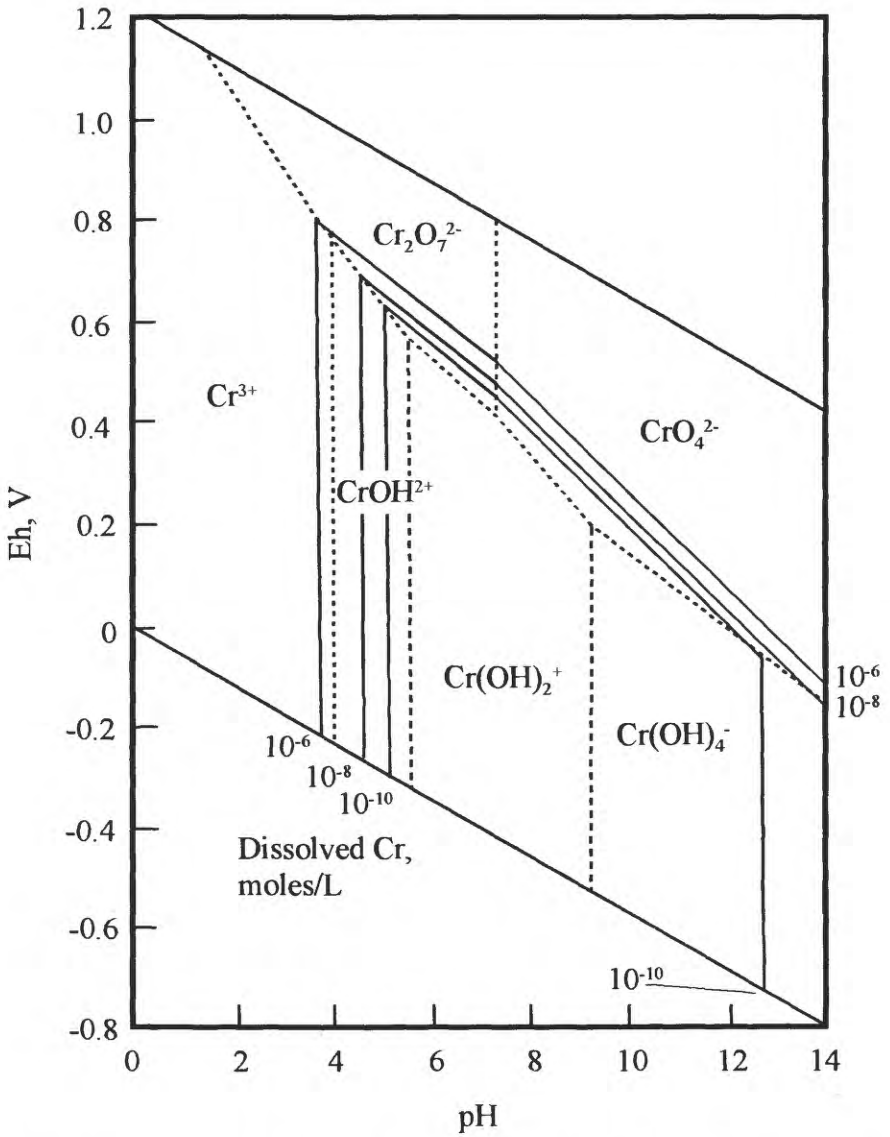

Figure 3. Equilibrium solubility characteristics of chromium as a function of Eh and pH in the system $Cr+H_2O+O_2$ with fixed total activities of sulfur=$10^{-4.00}$M and carbon=$10^{-3.00}$M at 25°C and 1 atm. Areas of dominance of solute species (dashed lines) and dissolved chromium activity (solid lines) in the presence of Cr_2O_3(c) (modified from Hem, 1977).

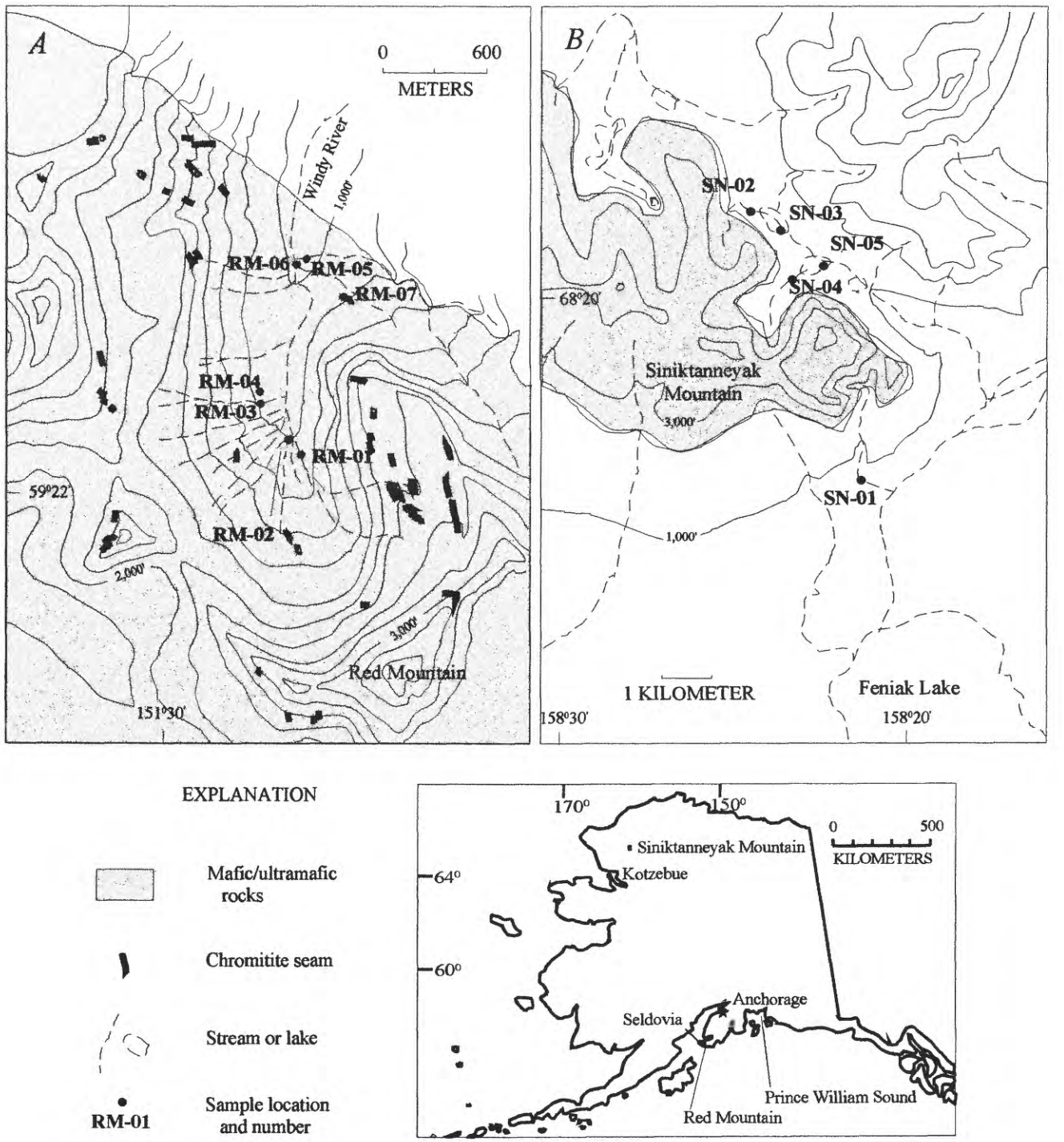

Figure 4. Simplified maps showing locations of Red Mountain (*A*) and Siniktanneyak Mountain (*B*) and collection sites of water samples discussed in text. Red Mountain geology modified from Guild (1942) and Siniktanneyak Mountain geology modified from Nelson and Nelson (1982).

sub-ppb determinations of more than 60 elements (including Cr) directly from a water sample. The relative standard deviation for Cr is 15 percent. The lower limit of detection for Cr was 0.5 ppb and 2 ppb for the Red Mountain and Siniktanneyak Mountain samples, respectively. Anion concentrations were determined in the filtered unacidified stream-water samples by ion chromatography (Fishman and Pyen, 1979). The relative standard deviation for this method was about 10 percent.

RESULTS

Waters draining the two complexes contain low concentrations of most trace metals determined. The waters at both locations are neutral to alkaline and vary from pH 6.7 to 9.3. Of the twelve samples collected, five of the seven samples from Red Mountain had detectable Cr (0.5 to 1.0 ppb). No Cr was detected at Siniktanneyak Mountain above the slightly higher detection limit of 2 ppb. In general, samples containing detectable chromium have pH values ranging from 7.5 to 9.3. The major cations in solution at both locations are magnesium (Mg), calcium (Ca), and sodium (Na); Mg concentrations are an order of magnitude greater than the concentrations of Ca or Na. Potassium (K), iron (Fe), and aluminum (Al) are present at low concentrations similar to those in surface waters in Prince William Sound, southern Alaska (Goldfarb and others, 1996; table 1). In general, concentrations of the major cations are slightly higher in water collected from Red Mountain than in those from Siniktanneyak Mountain.

Figure 5. Effluent issuing from mouth of abandoned chromium mine at Red Mountain.

At the pH values determined (pH 6.7 to 9.3), the measured alkalinity range of 10,000 to 55,000 pbb is probably present as the bicarbonate anion (HCO_3^-). Other possible contributors to alkalinity that we have not analyzed for are non-carbonate solute species such as hydroxide, silicate, borate, and organic ligands. In order of decreasing importance, chlorine, sulfate, and nitrate are also present in the waters of both complexes. As with the major cations, the total concentration of solute anions is slightly higher at Red Mountain.

In addition to Cr, other potentially toxic trace elements that were detected include nickel (Ni, 6 ppb), copper (Cu, 0.9-4.9 ppb), lead (Pb, 0.3-6.5 ppb), and zinc (Zn, 0.9-10 ppb). These concentrations are all similar to, or less than, the average concentrations found in studies of river water throughout the U.S.A. (Kharkar and others, 1968; Durum and others, 1971; Hem, 1992). For Cu, Pb, and Zn, the concentrations are below the Federal CMC limits (Environmental Protection Agency, 1992). The Ni concentrations are all below the State of Alaska MCL of 100 ppb (Alaska Department of Environmental Conservation, 1994). Concentrations of barium (Ba), manganese (Mn), scandium (Sc), and strontium (Sr) are all present at levels less than 25 ppb.

DISCUSSION

Previous studies of the chemistry of spring waters flowing from ultramafic complexes have identified two distinct types of water (Barnes and others, 1967; Barnes and O'Neil, 1969; Barnes and others, 1972; 1978; Lahermo and Blomqvist, 1988; Kresic and Papic, 1990; Papic and Kresic, 1990). The most common is a magnesium-bicarbonate water with a pH range of about 8.3 to 8.6, that results from the interaction of rainwater with the magnesium-rich minerals in the rocks. A second, less common type is a highly alkaline calcium-hydroxide water with a range in pH of 11.2 to 11.8 that is produced during low temperature serpentinization (or alteration) of ultramafic rocks. The waters sampled for this study are of the a magnesium-bicarbonate type.

The low concentrations of chromium are similar to the values predicted on the basis of the solubility charac-

Table 1. Analytical data on water samples collected at Red Mountain and Siniktanneyak Mountain ultramafic complexes.

[An acidified and an unacidified sample were collected at each site. Acidified samples were analyzed by inductively coupled plasma mass spectrometry; unacidified samples were analyzed by ion chromatography. TDS is obtained by totalling the unqualified values for cation and anion solute species. TDS values with a "less than" include the minimum reporting values for alkalinity and Ca in the total. Data on background water-sample chemistry from Goldfarb and others (1996)]

Field No.	Location	Temp. °C	pH	Cond. µS/cm	Alkalinity ppb	Na ppb	Mg ppb	Al ppb	K ppb	Ca ppb
Background surface waters, Prince William Sound		11-14	6.4-7.6	44-47	14,500-21,000	800-1,200	310-380	15-21	40-88	5,800-6,000
RM-01	East fork at head of valley	6	7.5	53	26,000	600	5,400	12	60	800
RM-02	South fork at head of valley	5	7.9	112	55,000	730	12,000	12	62	700
RM-03	Creek just south of mine	8	7.7	63	33,000	680	6,100	7	50	1,000
RM-04	Mine dump, crack in rock face	4	9.3	73	39,000	750	6,900	6	66	1,000
RM-05	Main east fork, 25 ft above junction	5	7.6	56	27,000	670	4,200	11	73	2,800
RM-06	Main river, 15 ft above junction	7	7.6	64	39,000	660	6,400	4	50	700
RM-06	Main river, 15 ft above junction, replicate analysis	7	7.6	64	39,000	730	6,800	5	50	700
RM-07	Kenai chrome mine, partially caved	8	7.8	72	40,000	760	7,600	5	67	600
SN-01	Creek on SE side of complex	8	7.5	55	32,000	<300	7,100	20	<400	<20,000
SN-02	ENE side, creek above uppermost lake	3	6.7	0	<10,000	<300	170	20	<400	<20,000
SN-03	ENE side, uppermost lake 50 m SW of outlet	8	6.9	7	<10,000	<300	220	57	<400	<20,000
SN-04	ENE side, creek above middle lake	4	7.1	19	10,800	<300	2,000	20	<400	<20,000
SN-05	ENE side, middle lake 100 m south of outlet	9	7.1	13	<10,000	<300	1,100	20	<400	<20,000

teristics of chromium in natural waters (fig. 3) that are a function of the extreme insolubility of chromite (Hem, 1977; 1992). As the stability fields in figure 3 show, not only is chromium highly insoluble at the pH range measured, it is also likely to be present as the less toxic Cr^{3+}. The potentially carcinogenic Cr^{6+} only becomes dominant under oxidizing conditions. The solubility controls of both Cr^{3+} and Cr^{6+} indicate that the geochemical availability of chromium in natural waters depends upon an interplay of three types of reactions: Dissolution/precipitation, oxidation/reduction, and adsorption/desorption (Electric Power Research Institute, 1988, 1989). In the pH and oxidation range of most natural waters, the solubility of Cr^{3+} is low due to the precipitation of chromium and iron-chromium hydroxides. Under strongly oxidizing conditions Cr^{6+} becomes highly soluble as Mg-, Ca-, Na-, and K-chromates. At pH greater than about 9.0, Cr^{6+} availability rises dramatically due to the oxidation of ferric to ferrous iron and the concomitant decrease in the absorption capacity of Cr^{6+} by iron hydroxides (Electric Power Research Institute, 1988, 1989). Under such conditions, the equilibrium concentration of chromate anions in solution could conceivably rise to levels greater than the CMC limits through the oxidation of chromite. An example of naturally contaminated Cr^{6+}-bearing waters was reported by Robertson (1975), who found concentrations of 100-200 ppb Cr^{6+} in oxygenated groundwater in an aquifer beneath Paradise Valley, Arizona. The highest Cr^{6+} concentrations were associated with the most alkaline waters (pH 8.5-9.0).

Under such alkaline-oxidizing conditions it is conceivable that Cr^{6+} liberated from chromite-bearing ultramafic complexes could be an environmental problem. Of the studies that document calcium-hydroxide-type waters, only those of Barnes and others (Barnes and others, 1967; Barnes and O'Neil, 1969) list analyses for total chromium (measured at a lower detection limit of 20 ppb). They found 20 ppb chromium in one of three waters collected from springs issuing from alpine-type ultramafic complexes in California and Oregon.

Waters collected from the two sites we studied are chemically similar. Both are magnesium-bicarbonate waters with neutral to slightly alkaline pH. However, water samples collected from Siniktanneyak Mountain have consistently lower TDS values (table 1). The difference in TDS may be attributed to the greater accumulation of soil cover and vegetation at Red Mountain. Siniktanneyak Mountain is generally devoid of soil or vegetation. Water samples from the two sites have similar major-element and anion chemistry.

RECOMMENDATIONS AND CONCLUSIONS

Our study has determined that waters from the two Alaskan ultramafic complexes (1) are magnesium-bicarbonate dominated, (2) are neutral to slightly alkaline, and (3) contain Cr at concentrations below the state and federal drinking-water standards. Therefore, due to the above and to the lack of calcium-hydroxide-type waters, toxic Cr^{6+} is unlikely to present a problem. To further address the question of whether Cr^{6+}-contaminated water is generated at chromite-mineralized ultramafic complexes, studies should be conducted to specifically analyze calcium-hydroxide-type groundwaters from chromite-bear-

Table 1. Analytical data on water samples collected at Red Mountain and Siniktanneyak Mountain ultramafic complexes—Continued.

Field No.	Sc ppb	Cr ppb	Mn ppb	Fe ppb	Ni ppb	Cu ppb	Zn ppb	Sr ppb	Ba ppb	Pb ppb	Cl- ppb	SO_4^{2-} ppb	NO^{1-} ppb	TDS ppb
Background		<0.5	<0.2-3.5	<20-20	<6	0.3-0.6	0.8-1.4			<0.5	900-2,200	3,200-4,000		
RM-01	0.7	0.8	1.6	72	<6	0.9	10	1.6	2.4	6.0	1,400	480	<200	34,848
RM-02	0.9	0.5	0.9	40	<6	2.6	4.7	2.2	0.9	2.0	2,200	820	<200	71,579
RM-03	0.8	1.0	0.8	50	<6	1.6	3.4	2.5	1.4	6.5	2,000	550	<200	43,455
RM-04	<0.6	1.0	0.5	40	<6	1.6	1.6	2.6	1.1	5.1	2,200	540	260	50,776
RM-05	<0.6	0.5	0.7	40	<6	1.0	10	25	21	1.0	1,200	2,700	<200	38,753
RM-06	<0.6	<0.5	0.2	<20	<6	<0.3	0.9	2.2	0.8	1.0	560	560	250	48,189
RM-06	0.6	<0.5	0.3	20	<6	4.9	3.2	2.2	0.8	1.0	NA	NA	NA	47,318
RM-07	1.0	<0.5	<0.2	20	<6	0.4	1.5	2.8	1.0	<0.5	520	520	<200	50,099
SN-01	<20	<2	3.8	<200	6	<0.9	<3	0.4	0.9	<0.3	150	280	<200	<59,571
SN-02	<20	<2	<0.9	<200	<4	<0.9	<3	3.1	<0.2	<0.3	<100	<200	<200	<30,193
SN-03	<20	<2	3.7	<200	<4	1.0	5	3.3	0.3	0.4	<100	<200	<200	<30,301
SN-04	<20	<2	<0.9	<200	<4	<0.9	<3	2.0	<0.2	<0.3	150	<200	<200	<32,982
SN-05	<20	<2	1.0	<200	<4	<0.9	<3	2.6	0.5	0.3	110	<200	<200	<31,240

ing ultramafic complexes. In addition, analyses of river, lake, or marine sediments located at the points of outflow should be analyzed for chromium content due to the likelihood that once chromium is released to the environment in an oxidizing fluid, it will reprecipitate as amorphous chromium hydroxide ($Cr[OH]_3$) linked to the reduction of ferrous iron in sediments or to the degradation of organic material (Hem, 1977; Simon and others, 1994). Under normal climatic conditions and pH ranges of most natural waters, Cr^{6+} contamination from chromite-bearing ultramafic complexes does not appear to pose a significant environmental threat.

Acknowledgments.—Dick J. Goldfarb and Karen D. Kelley (USGS) assisted with fieldwork. David Taylor (U.S. Geological Survey volunteer) ably performed the duties of camp manager and cook during field work in the Brooks Range.

REFERENCES CITED

Alaska Department of Environmental Conservation, 1994, Drinking water regulations: State of Alaska, Department of Environmental Conservation Report 18-ACC-80, 195 p.

Barnes, Ivan, LaMarche, V.C., Jr., and Himmelberg, Glen, 1967, Geochemical evidence of present-day serpentinization: Science, v. 156, p. 830-832.

Barnes, Ivan, and O'Neil, J.R., 1969, The relationship between fluids in some fresh alpine-type ultramafics and possible modern serpentinization, western United States: Geological Society of America Bulletin, v. 80, p. 1947-1960.

Barnes, Ivan, Rapp, J.B., O'Neil, J.R., Sheppard, R.A., and Gude, R.J., III, 1972, Metamorphic assemblages and the direction of flow of metamorphic fluids in four instances of serpentinization: Contributions to Mineralogy and Petrology, v. 35, p. 263-276.

Barnes, Ivan, O'Neil, J.R., and Trescases, J.J., 1978, Present day serpentinization in New Caledonia, Oman and Yugoslavia: Geochimica et Cosmochimica Acta, v. 42, p. 144-145.

Bundtzen, T.K., Swainbank, R.C., Henning, M.W., Clough, A.H., and Charlie, K.M., 1996, Alaska's mineral industry 1995: Alaska Division of Geological and Geophysical Surveys, Special Report 50, 71 p.

Casagrande, D.J., and Erchull, L.D., 1977, Metals in plants and waters in the Okefenokee swamp and their relationship to constituents found in coal: Geochimica et Cosmochimica Acta, v. 41, p. 1391-1394.

Duke, J.M., 1988, Magmatic segregation deposits of chromite, *in* Roberts, R.G., and Sheahan, P.A., eds., Ore deposit models: Geoscience Canada, Reprint series 3, p. 133-143.

Durum, W.H., Hem, J.D., and Heidel, S.G., 1971, Reconnaissance of selected minor elements in surface waters of the United States, October, 1970: U.S. Geological Survey Circular 643, 49 p.

Elderfield,-H., 1970, Chromium speciation in seawater: Earth and Planetary Science Letters, v. 9, p. 10-16.

Electric Power Research Institute, 1988, Chromium reactions in geologic materials, Interim report of research project 2485-3, April 1988: Electric Power Research Institute Document No. EA-5741, 301 p.

Electric Power Research Institute, 1989, Chromium reactions in geologic materials: Electric Power Research Institute Technical Brief, Document No. TB.ENV.46.6.89, 4 p.

Environmental Protection Agency, 1992, Water quality standards; establishment of numeric criteria for priority toxic pollutants; States' compliance; final rule: Federal Register, 40 CFR Part 131, v. 57, no. 246, p. 60847-60916.

Fishman, M.J., and Pyen, G., 1979, Determination of selected anions in water by ion chromatography: U.S. Geological Survey Water Resources Investigation Report 79-101, 30 p.

Goldfarb, R.J., Nelson, S.W., Taylor, C.D., d'Angelo, W.M., and Meier, A.L., 1996, Acid mine drainage associated with volcanogenic massive sulfide deposits, Prince William Sound, Alaska, *in* Moore, T.E., and Dumoulin, J.A., eds., Geologic studies in Alaska by the U.S. Geological Survey, 1994: U.S. Geological Survey Bulletin 2152, p. 3-16.

Guild, P.W., 1942, Chromite deposits of Kenai Peninsula, Alaska: U.S. Geological Survey Bulletin 931-G, p. 139-175.

Hem, J.D., 1977, Reactions of metal ions at surfaces of hydrous iron oxide: Geochimica et Cosmochimica Acta, v. 41, p.527-538.

Hem, J.D., 1992, Study and interpretation of the chemical characteristics of natural water: U.S. Geological Survey Water-Supply Paper 2254, 263 p.

Kaczynski, S.E., and Kleber, R.J., 1993, Aqueous trivalent chromium photoreproduction in natural waters: Environmental Science and Technology, v. 27, p. 1572-1576.

Kharkar, D.P., Turekian, K.K., and Bertine, K.K., 1968, Stream supply of dissolved silver, molybdenum, antimony, selenium, chromium, cobalt, rubidium and cesium to the oceans: Geochimica et Cosmochimica Acta, v. 32, p. 285-298.

Kresic, N., and Papic, P., 1990, Specific chemical composition of karst groundwater in the ophiolite belt of the Yugoslav Inner Dinarides: a case for covered karst: Environmental Geology and Water Science, v. 15, p. 131-135.

Lahermo, P.W., and Blomqvist, R., 1988, Influence of mineralized rock on chemistry of deep bedrock groundwater in Finland—with reference to chemistry of surficial waters, *in* Lin, C.L., ed., Proceedings of the International Groundwater Symposium on Hydrogeology of Cold and Temperate Climates and Hydrogeology of Mineralized Zones; p. 112-118.

Meier, A.L., Grimes, D.J., and Ficklin, W.H., 1994, Inductively coupled plasma mass spectrometry—a powerful analytical tool for mineral resource and environmental studies [abs.] *in* Carter, L.M.H., Toth, M.I., and Day, W.C., eds., U.S. Geological Survey research on mineral resources—1994, Part A—Program and Abstracts, 9th V.E. McKelvey Forum on Mineral and Energy Resources, Tucson, Ariz., February 22-25, 1993: U.S. Geological Survey Circular 1103-A, p. 67-68.

Nelson, S.W., and Nelson, W.H., 1982, Geology of the Siniktanneyak Mountain ophiolite, Howard Pass quadrangle, Alaska: U.S. Geological Survey Miscellaneous Field Studies Map MF-1441, 1 sheet, 1:63,360 scale.

Papic, P., and Kresic, N., 1990, Ultrabasic groundwaters of the Zlatibor ultramafic massif, *in* Simpson, E.S., and Sharp, J.M., Jr., eds., Selected papers on hydrogeology from the 28th International Geological Congress: International Association of Hydrogeologists, Hydrogeology, Selected Papers, v. 1, p. 163-168.

Perlmutter, N.M., Lieber, M., and Frauenthal, H.L., 1963, Movement of waterborne cadmium and hexavalent chromium wastes in South Farmingdale, Nassau County, Long Island, New York: U.S. Geological Survey Professional Paper 475-C, p. C179-C184.

Robertson, F.N., 1975, Hexavalent chromium in the ground water in Paradise Valley, Arizona: Ground Water, v. 13, p. 516-523.

Simon, N.S., Demas, C., and d'Angelo, W., 1994, Geochemistry and solid-phase association of chromium in sediment from the Calcasieu River and estuary, Louisiana, U.S.A.: Chemical Geology, v. 116, p. 123-135.

Reviewers: Larry Jackson and Steve Wilson

Age, Isotopic, and Geochemical Studies of the Fortyseven Creek Au-As-Sb-W Prospect and Vicinity, Southwestern Alaska

By John E. Gray, Carol A. Gent, Lawrence W. Snee, *and* Peter M. Theodorakos

ABSTRACT

The Fortyseven Creek Au-As-Sb-W prospect consists of quartz veins that contain minor amounts of arsenopyrite, scheelite, stibnite, gold, pyrite, wolframite, jamesonite, and argentite, with locally abundant sericite. Mineralized veins are found in graywacke and shale hornfels of the Cretaceous Kuskokwim Group; locally, the sedimentary rocks are cut by small, Late Cretaceous to early Tertiary granite porphyry dikes. Although the lode has not been mined, about 28 kg of gold and 1,900 kg of scheelite have been recovered from a placer mine downstream from the prospect on Fortyseven Creek. Because there is considerable exploration for such gold deposits in southwestern Alaska, we collected stream-sediment and heavy-mineral-concentrate samples for exploration geochemical studies, as well as various samples of ore and gangue minerals from mineralized veins to evaluate the geochemistry, age, and formation of the deposit.

Stream-sediment and heavy-mineral-concentrate samples collected along Fortyseven Creek downstream from the prospect contain elevated concentrations of As, Ag, Au, Sb, Bi, and W, which are consistent with the mineralogy of the lode. For example, stream-sediment samples collected from Fortyseven Creek contain as much as 330 parts per million (ppm) As, 1.0 ppm Au, 8.7 ppm Bi, 29 ppm Sb, and 800 ppm W; heavy-mineral-concentrate samples contain as much as 300 ppm Ag, 2,000 ppm Bi, more than 1,000 ppm Au, and more than 20,000 ppm W.

We obtained a $^{40}Ar/^{39}Ar$ plateau age of 67.1±0.1 Ma for hydrothermal sericite separated from a sample of mineralized quartz vein. This age represents the best estimate for the timing of mineralization at Fortyseven Creek and is similar to ages for Late Cretaceous to early Tertiary subduction-related intrusions found throughout southwestern Alaska. The Fortyseven Creek age is also within the range of ages of about 63 to 71 Ma obtained for granite porphyry bodies near other southwestern Alaska gold deposits such as Donlin Creek and Golden Horn, which have similar geological, mineralogical, and geochemical characteristics to those of Fortyseven Creek.

Preliminary isotopic studies of ore and gangue minerals suggest that ore fluids were probably derived from both magmatic fluids and surrounding sedimentary rocks. Oxygen and hydrogen isotopic compositions of hydrothermal quartz and sericite yield calculated ore-fluid compositions of about 10.4 per mil $\delta^{18}O$ and –47 per mil δD (at 330°C), which were probably of magmatic origin or highly exchanged meteoric water. Sulfur isotopic compositions for arsenopyrite (–7.8 ‰ $\delta^{34}S$) and pyrite (–6.7 ‰ $\delta^{34}S$) indicate derivation of sulfur predominantly from surrounding sedimentary rocks of the Kuskokwim Group. These preliminary data suggest that Fortyseven Creek mineralization probably developed in response to high heat flow related to local Late Cretaceous igneous activity that initiated thermal convection and induced contact metamorphism in the sedimentary rocks. Resultant hydrothermal activity expelled fluids that flowed through local fractures and faults and reacted with surrounding sedimentary wallrocks.

INTRODUCTION

The Fortyseven Creek Au-As-Sb-W prospect is located about 80 km southwest of Sleetmute, on the ridge crest at the headwaters of Fortyseven Creek, a tributary of the Holitna River (fig. 1). This lode and an associated gold placer mine on Fortyseven Creek about 3 km downstream from the prospect was discovered in 1947 by Russell Schaeffer. The lode was first described by Cady and others (1955) as a quartz-scheelite-gold-bearing shear zone cutting silicified graywacke and shale of the Kuskokwim Group. Additional exploration and geologic mapping of the Fortyseven Creek area was conducted by Hawley (1989), who described quartz veins cutting silicified sedimentary rock hornfels of the Kuskokwim Group; granite porphyry intrusions cut the sedimentary rocks in the Fortyseven Creek area. Hawley (1989) also found minor amounts of arsenopyrite, scheelite, stibnite, gold, pyrite, wolframite, jamesonite, and argentite in the veins, with locally abundant sericite (hydrothermal-vein muscovite); these veins were traceable laterally for greater than 1,000 m. Some

mineralized samples contain more than 34 ppm Au (1 oz/t) (Hawley, 1989). The vein has not been mined. However, from 1948 to 1954, about 28 kg of gold (891 oz) and about 1,900 kg (5,000 lbs) of scheelite, containing 67 to 77 percent WO_3, were recovered by Schaeffer from the placer mine on Fortyseven Creek downstream from the lode (Hawley, 1989).

Several companies conducted exploration of the Fortyseven Creek area in the 1970's and 1980's, including Homestake, Amax, American Copper and Nickel, and Anaconda (Hawley, 1989). More recently, from 1991 to 1994, Nevada Star Resources conducted exploration of the area that included minor prospect trenching, an extensive soil geochemical survey, and exploration drilling (Maynard, 1995). Nevada Star collected more than 200 soil samples along the ridges at the headwaters of Fortyseven Creek and found highly elevated concentrations of Au (as much as 1.3 ppm), As (as much as 8,230 ppm), Bi (as much as 100 ppm), Cu (as much as 322 ppm), Sb (as much as 106 ppm), and W (as much as 510 ppm) in these soils. Nevada Star used soil anomalies of Au, As, and Bi to delineate several target areas for three exploration drill holes. Drilling was difficult due to circulation-loss and hole-caving problems. Consequently, only one drill hole penetrated significant mineralized rock about 44 to 105 m (145 to 345 ft) below the surface that contained as much as 1.2 ppm Au (Maynard, 1995).

The Fortyseven Creek prospect has similar geologic and geochemical characteristics to other gold deposits in southwestern Alaska such as the Au-As-W Golden Horn mine near Flat, and the Au-As-Sb Donlin Creek deposit (fig. 1). There is presently considerable exploration for such gold deposits in southwestern Alaska, but these deposits have not been well studied. We visited the Fortyseven Creek area in 1991 as part of U.S. Geological Survey (USGS) mineral resource assessments in southwestern Alaska. Our objective was to obtain

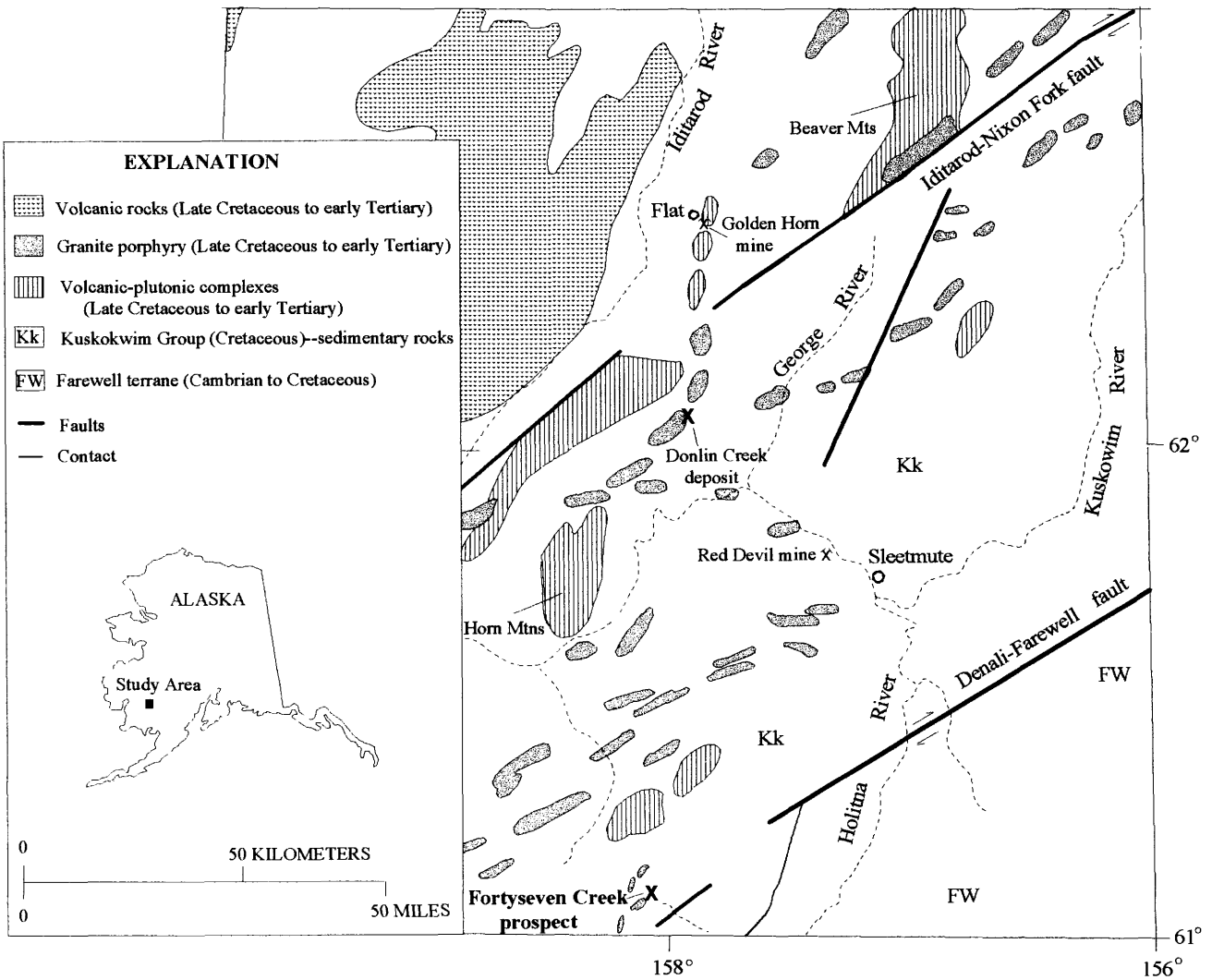

Figure 1. Geologic map of the Fortyseven Creek prospect and vicinity in southwestern Alaska, generalized from Cady and others (1955), Hoare and Coonrad (1959), Decker and others (1984), Decker and others (1994), Decker and others (1995), Miller and Bundtzen (1994), and Bundtzen and Miller (1997).

(1) exploration geochemical data for stream-sediment and heavy-mineral-concentrate samples collected from streams surrounding the prospect, (2) geochemical data for mineralized vein samples collected from the prospect, (3) a $^{40}Ar/^{39}Ar$ age for sericite from a hydrothermal quartz vein sample, and (4) oxygen and hydrogen isotopic compositions from vein gangue minerals and sulfur isotopic compositions from ore minerals for ore genesis studies.

GEOLOGIC SETTING

Rocks in the Fortyseven Creek area consist largely of interbedded graywacke and siltstone of the Cretaceous Kuskokwim Group that are cut by small granite porphyry intrusions of probable Late Cretaceous or early Tertiary age (Cady and others, 1955; Hawley, 1989). The Kuskokwim Group is a sequence of flysch representing turbidite fan, foreslope, shallow-marine, and shelf facies deposited into an elongate, northeast trending, fault-controlled Cretaceous basin (Decker and Hoare, 1982; Bundtzen and Gilbert, 1983). Fossil ages for the Kuskokwim Group range from Albian to Campanian (Cady and others, 1955; Hoare and Coonrad, 1959; Box and Murphy, 1987; Box and Elder, 1992; Miller and Bundtzen, 1994). Rocks of the Kuskokwim Group have undergone little or no regional metamorphism (Miller and others, 1989). The Kuskokwim Group is postaccretionary, overlying rocks of adjacent tectonostratigraphic terranes in the region (Miller and others, 1989).

Granite porphyry intrusions in the Fortyseven Creek area are similar to those found elsewhere in southwestern Alaska. These intrusions are generally peraluminous in composition, with Al_2O_3 exceeding Na_2O+K_2O+CaO, and locally contain igneous garnet (Bundtzen and Swanson, 1984; Moll-Stalcup, 1994). The granite porphyry near Fortyseven Creek has not been dated, but similar rocks in southwestern Alaska are Late Cretaceous and early Tertiary (about 72 to 61 Ma), based on K-Ar determinations (Reifenstuhl and others, 1984; Robinson and Decker, 1986; Decker and others, 1986; 1995; Miller and Bundtzen, 1994; Bundtzen and Miller, 1997). Late Cretaceous and early Tertiary magmatism is interpreted to be related to a broad subduction arc (Moll-Stalcup, 1994; Szumigala, 1993). Granite porphyry intrusions are important in southwestern Alaska because they show a close spatial and temporal association with Au-As-Sb-W vein and Hg-Sb vein deposits (Cady and others, 1955; Bundtzen and Miller, 1997; Gray and others, 1997).

SOUTHWESTERN ALASKA GOLD DEPOSITS SIMILAR TO FORTYSEVEN CREEK

The Fortyseven Creek prospect is similar geologically, geochemically, and mineralogically to other gold deposits in southwestern Alaska such as the Au-As-W Golden Horn mine and the Au-As-Sb Donlin Creek deposit (fig. 1). At the Golden Horn mine, quartz-carbonate veins contain scheelite, gold, arsenopyrite, pyrite, stibnite, chalcopyrite, galena, sphalerite, cinnabar, and lead-antimony sulfosalts; sericite and ankerite gangue are common (Bull, 1988; Bundtzen and others, 1992; Szumigala, 1993). Mineralized veins cut monzonitic rocks of the Black Creek Stock and surrounding sedimentary rocks of the Kuskokwim Group. Locally, granite porphyry dikes cut the stock (Bundtzen and others, 1992). Stocks in the Flat area yield K/Ar ages of 63.4 to 70.9 Ma and granite porphyries are 64.3 to 69.3 Ma in age (Bundtzen and others, 1992). Golden Horn was mined from 1925 to 1937 and produced 84,156 g of gold (2,706 oz), 81,482 g of silver (2,620 oz), and 4,243 kg of lead (9,336 lbs) (Bundtzen and others, 1992). In addition, numerous placer mines in the Flat area (the Iditarod district) have produced 48,560 kg of gold (1,561,524 oz) since 1909 (Bundtzen and others, 1996).

At Donlin Creek, quartz veins contain stibnite, pyrite, arsenopyrite, cinnabar, and antimony sulfosalts, as well as local carbonate, clay, limonite, and sericite gangue (Bundtzen and Miller, 1997). Mineralized veins are in peraluminous granite porphyry dikes and sills and in surrounding sedimentary rocks of the Kuskokwim Group. Granite porphyries in the Donlin Creek area yield K/Ar ages of 65.1 to 70.9 Ma (Miller and Bundtzen, 1994). Gold deposits at Donlin Creek are estimated to contain 44,000,000 t of ore grading 2.5 g/t (0.08 oz/t) of gold, or about 3,600,000 oz of gold (Millholland and Freeman, 1997). Placer mines in the Donlin Creek area have recovered about 733 kg (23,500 oz) of gold (Bundtzen and Miller, 1997).

Similarly, the Fortyseven Creek prospect consists primarily of hydrothermal quartz veins in sheared and faulted graywacke and siltstone of the Kuskokwim Group. Mineralized vein and adjacent altered wallrock samples that contain as much as 200 ppm As, 0.033 ppm Au, 6.7 ppm Sb, and 10 ppm W (table 1); these results are consistent with the ore mineralogy of the veins that contain arsenopyrite, scheelite, stibnite, gold, pyrite, wolframite, jamesonite, and argentite.

GEOCHEMICAL AND MINERALOGICAL METHODS

Stream-sediment and panned-concentrate samples were collected from 12 sites around the Fortyseven Creek prospect (fig. 2). The stream-sediment samples were air dried, sieved to minus-80 mesh, pulverized, and chemically analyzed. The panned-concentrate samples were separated using bromoform to remove lighter minerals, primarily quartz and feldspar, then separated magnetically into magnetic, paramagnetic, and nonmagnetic fractions. The nonmagnetic heavy-mineral fraction from each sample was ground and chemically analyzed.

The stream-sediment and rock samples were chemically analyzed by several techniques. Concentrations of Ag, As,

Sb, Bi, Cd, Cu, Mo, Pb, and Zn were determined by inductively coupled plasma (ICP) atomic-emission spectrometry using the procedure developed by Motooka (1996). Concentrations of Au were determined by an atomic-absorption spectrophotometry (AAS) technique adapted from Hubert and Chao (1985) or by graphite furnace atomic-absorption spectrophotometry (GFAAS) using the technique adapted from Meier (1980). Mercury was measured using a cold-vapor AAS technique (Kennedy and Crock, 1987). Tungsten was determined by a visual spectrophotometry technique described by Welsch (1983).

The nonmagnetic heavy-mineral-concentrate samples were analyzed by a semiquantitative arc-emission spectrographic (SQS) technique adapted from Grimes and Marranzino (1968) for 37 elements including Ag, As, Au, Bi, Sb, and W reported here. Using a binocular microscope, the abundance of gold, sulfide minerals (such as pyrite, cinnabar, stibnite, and arsenopyrite), and oxide minerals (such as scheelite) were identified in the nonmagnetic heavy-mineral concentrates samples.

STREAM-SEDIMENT AND HEAVY-MINERAL-CONCENTRATE RESULTS

Stream-sediment samples collected downstream from the Fortyseven Creek prospect are characterized by elevated concentrations of Au, As, Bi, Sb, and W (fig. 3), which is consistent with the vein mineralogy of the prospect. Generally, these elements show consistent geochemical dispersion patterns (fig. 3) and are diagnostic exploration guides for this type of mineral deposit. For example, stream-sediment sample FS08S, collected less than 1 km downstream from the Fortyseven Creek prospect trenches, contains 330 ppm As, 1.0 ppm Au, 8.7 ppm Bi, 29 ppm Sb, and 800 ppm W, which

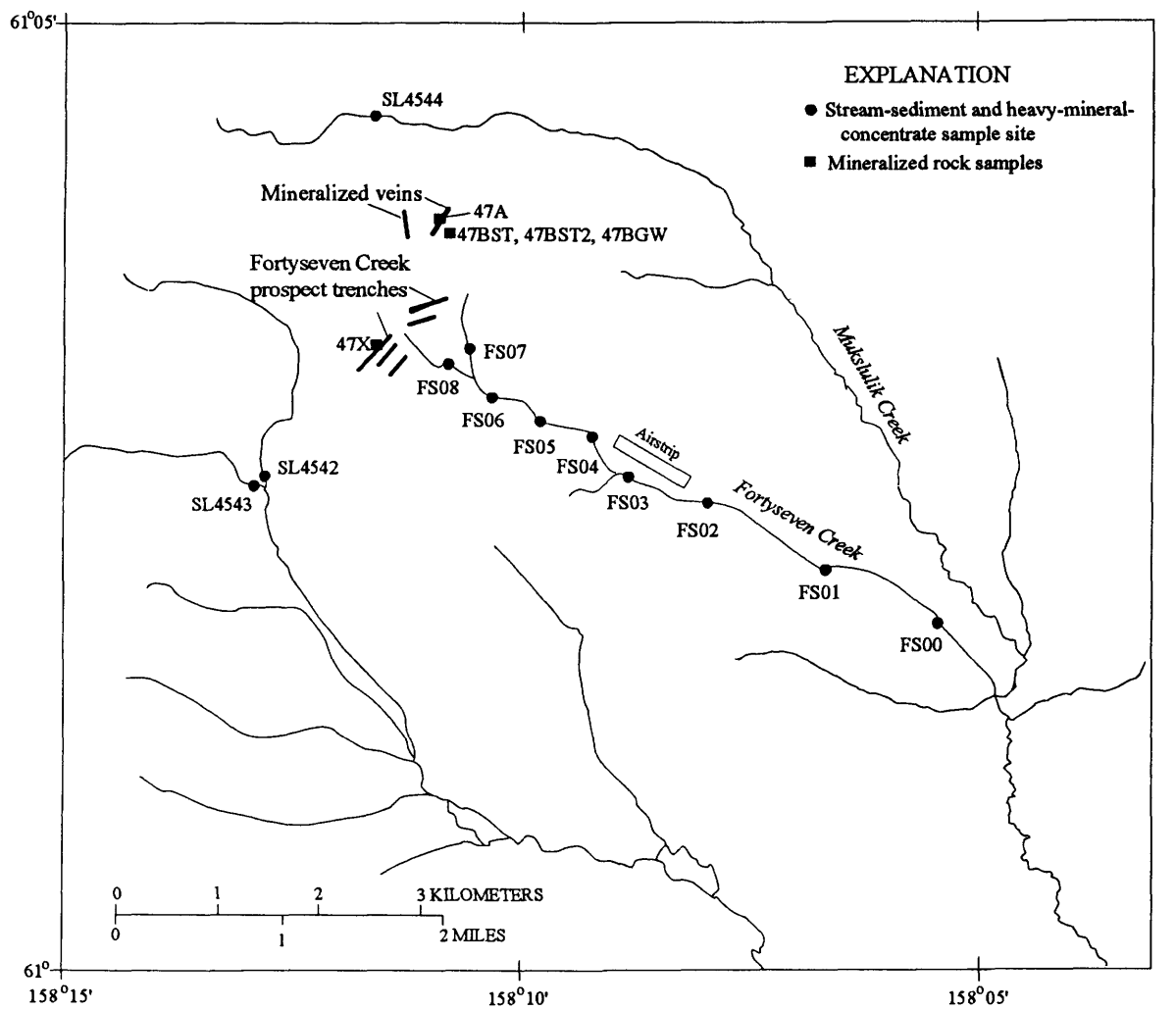

Figure 2. Location of mineralized rock, stream-sediment, and heavy-mineral-concentrate samples collected in this study.

are highly elevated relative to background concentrations for this region (table 1). In addition, stream-sediment sample FS01S, collected about 5 km downstream from the prospect, contains 110 ppm As, 0.008 ppm Au, 1.9 ppm Sb, and 11 ppm W, indicating the usefulness of such elements for tracing upstream mineral deposits of this type.

Similarly, anomalous concentrations of Au, Ag, Bi, Sb, and W are observed in the geochemical data of the heavy-mineral concentrates. For example, heavy-mineral-concentrate sample FS07C collected less than 1 km from the prospect, contains 300 ppm Ag, 2,000 ppm Bi, greater than 1,000 ppm Au, and 10,000 ppm W; three additional concentrate samples contain more than 20,000 ppm W (table 1). Concentrate sample FS00C, collected farthest from the prospect, contains 30 ppm Ag, 500 ppm Au, 1,000 ppm Sb, and 2,000 ppm W (table 1). Most of the heavy-mineral-concentrates collected along Fortyseven Creek downstream from the prospect contain visible gold, arsenopyrite, stibnite, pyrite, and significant quantities of scheelite. Concentrate sample FS07C contains 12 flakes of gold.

GEOCHRONOLOGY

Hydrothermal sericite in a vein sample containing quartz and minor scheelite and pyrite was collected from the Fortyseven Creek prospect (fig. 4). We separated the sericite by hand picking to obtain a sample with a purity of about 99 percent. The age of this sericite sample was determined using the $^{40}Ar/^{39}Ar$ technique (Dallmeyer, 1975; Dalrymple and others, 1981). A major advantage of the $^{40}Ar/^{39}Ar$ technique is that, for a single sample, a series of ages can be calculated for each of several progressively increasing temperature steps, usually 10 to 15 steps ranging from about 400 to 1,500°C. Although argon loss or gain is often observed in the initial heating steps, a plateau age is commonly produced by the later heating steps. A plateau age represents the average age of the undisturbed portion of the age spectrum and is defined by two or more successive heating steps with overlapping ages within analytical error. Generally, these gas fractions that yield similar ages make up more than 50 percent of the total gas released. Plateau ages are the best estimate of when the sample closed to diffusion of argon (Snee and others, 1988).

The Fortyseven Creek sericite sample yielded a plateau age of 67.1±0.1 Ma, based on five heating steps from 850 to 1,050°C (table 2, fig. 5). This hydrothermal-sericite age is within the range of ages of about 63 to 71 Ma obtained for granite porphyry near other southwestern Alaska gold deposits such as Donlin Creek and Golden Horn. If the granite porphyry at Fortyseven Creek has a similar age, there would be a temporal relationship between mineralization and magmatism. Two K-Ar ages previously reported for hydrothermal sericite from veins at the Fortyseven Creek prospect are 57 Ma (Nokleberg and others, 1987) and 60.9±1.8 Ma (Decker and others, 1995). The total gas age (65.8±0.1 Ma, table 2) for the sericite sample that we collected in this study does not overlap with these previously reported K-Ar ages at 1 sigma. It is possible that the range in ages indicates that the duration of mineralization at Fortyseven Creek was long-lived (57-67 Ma), although this seems unlikely. Our $^{40}Ar/^{39}Ar$ age spectrum shows significant argon loss in the lower temperature steps, and it is possible that the previously reported K-Ar hydrothermal sericite ages may have had similar argon loss. However, the advantage of the $^{40}Ar/^{39}Ar$ step-wise heating method is that it is possible to see through such argon loss, and therefore, we suggest that our $^{40}Ar/^{39}Ar$ plateau age (67.1 ±0.1 Ma) represents the most likely age of mineralization at Fortyseven Creek.

FLUID-INCLUSION STUDIES

Fluid-inclusion studies were conducted on quartz-vein samples from the Fortyseven Creek prospect primarily to provide ore-forming temperatures to be used in isotopic modeling calculations. Fluid-inclusion studies are presently ongoing and these results are preliminary. Fluid-inclusions studied were in hydrothermal milky-quartz crystals containing or intergrown with arsenopyrite or stibnite. The inclusions observed were small, generally about 10 microns in diameter, and were most commonly isolated inclusions along quartz-crystal growth planes. Fluid-inclusions studied were classified as primary using the criteria described by Roedder (1979). Secondary inclusions were also observed, but not studied. Microthermometry measurements have been hindered by the size of the inclusions, and thus only homogenization temperatures are reported in this study. Fluid-inclusion measurements were made on doubly polished thin sections of vein samples using a modified U.S. Geological Survey gas-flow heating and cooling stage. Inclusions were frozen and then slowly heated to determine homogenization temperatures. Homogenization temperatures for the fluid inclusions were determined when the vapor bubble disappeared and was thus homogenized into the liquid phase. Analytical reproducibility is about ±3°C for homogenization temperatures.

The fluid inclusions studied were a two-phase, liquid+vapor type. Fluid inclusion homogenization temperatures were measured for 40 inclusions, and these temperature ranged from 260 to 382°C (fig. 6). The average homogenization temperature is about 330°C. These are reasonable ore-forming temperatures for Fortyseven Creek and are similar to those reported for other gold deposits in southwestern Alaska. For instance, fluid-inclusion homogenization temperatures for the Golden Horn deposit average about 272°C, and equilibrium ore-fluid temperatures of 300 to 350°C were estimated using an arsenopyrite geothermometer (Bull, 1988; Bundtzen and others, 1992). Fluid-inclusion studies of samples from the Donlin Creek deposit indicate formation temperatures of about 250°C (Millholland and Freeman, 1997).

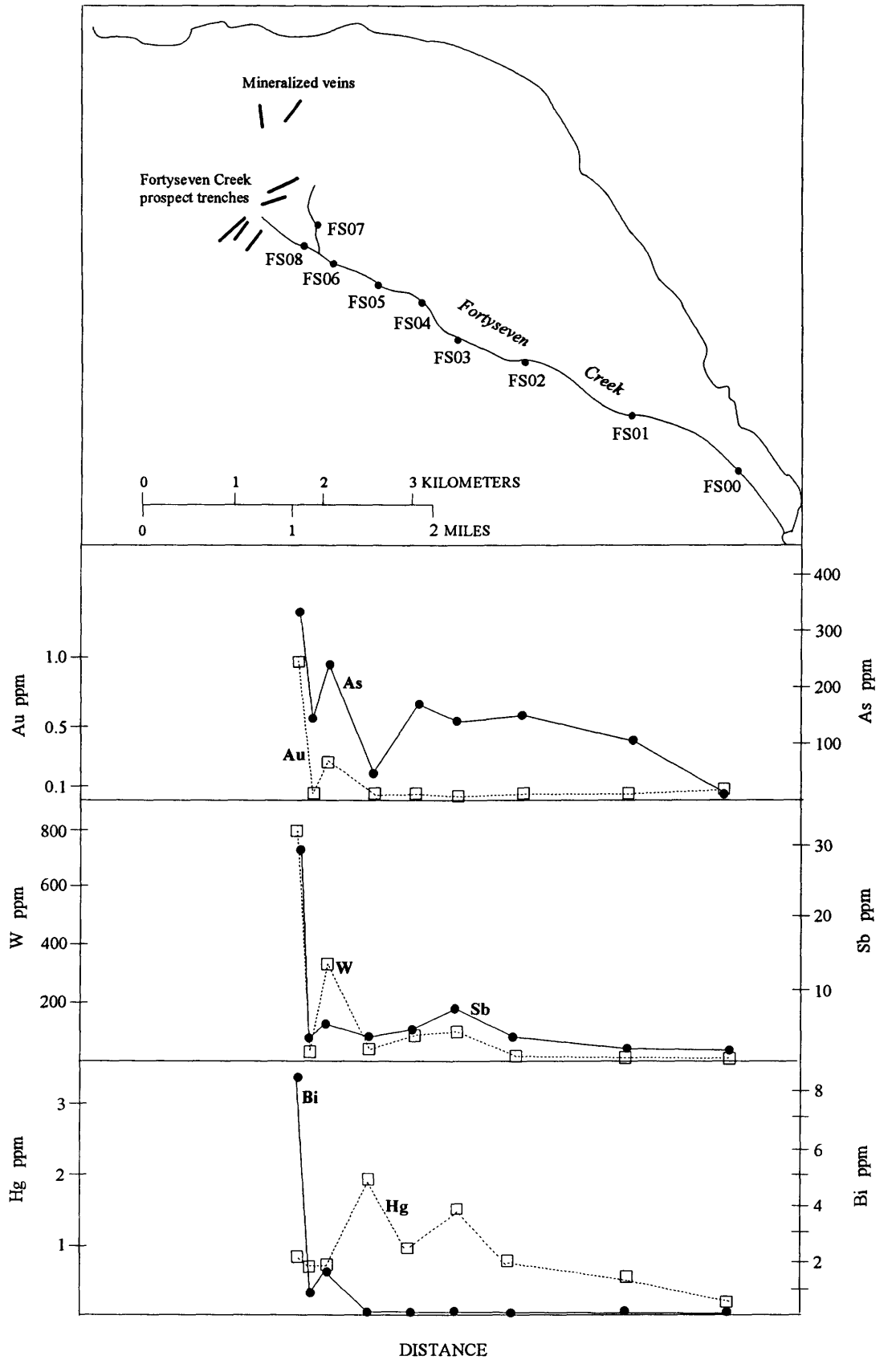

Figure 3. Plot showing the distribution of Au, As, W, Sb, Hg, and Bi concentrations in minus-80-mesh stream-sediment samples collected along Fortyseven Creek.

Table 1. Trace-element concentrations in mineralized rock, stream-sediment, and heavy-mineral-concentrate samples collected from the Fortyseven Creek prospect.

[For stream-sediment and rock samples, analysis of As, Ag, Bi, Cu, Sb, and Zn was by inductively coupled plasma spectrometry (ICP), Au and Hg by atomic absorption spectrophotometry (AA), and W by visual spectrophotometry (VS). All rock samples were collected from outcrop. All heavy-mineral-concentrate samples were analyzed by semiquantitative emission spectrography (SQS). Abbreviations are: ins, insufficient sample for analysis; aspy, arsenopyrite; py, pyrite, qtz, quartz; schl, scheelite; silcfd, silicified. Concentrations are listed in parts per million; background concentrations in brackets [ ] from regional geochemical studies in southwestern Alaska (Gray and Theodorakos, 1997)]

Rock samples

Sample	As (ICP) [20]	Ag (ICP) [0.1]	Au (AA) [0.002]	Bi (ICP) [0.5]	Hg (AA) [0.2]	Sb (ICP) [1.0]	W (VS) [1.0]	Description
47X	200	<0.067	0.002	<0.67	0.04	6.7	10	Qtz-schl-aspy veins in silcfd graywacke
47BST	72	<0.067	0.033	<0.67	0.03	5.0	3	Silcfd siltstone with minor py
47BST2	82	0.2	0.003	<0.67	0.05	4.7	2	Siltstone hornfels with py
47BGW	40	0.1	0.002	<0.67	0.03	4.9	3	Graywacke hornfels with qtz veins

Stream-sediment samples

Sample	As (ICP) [30]	Ag (ICP) [0.1]	Au (AA) [0.002]	Bi (ICP) [0.5]	Hg (AA) [0.3]	Sb (ICP) [1.0]	W (VS) [2.0]
FS08S	330	0.3	1.0	8.7	0.84	29	800
FS07S	140	0.2	0.004	0.8	0.78	2.7	25
FS06S	240	0.3	0.30	2.1	0.73	5.2	350
FS05S	50	0.2	0.008	<0.67	1.99	3.3	50
FS04S	170	0.2	0.004	<0.67	0.98	4.1	100
FS03S	140	0.2	<0.008	<0.67	1.55	7.8	108
FS02S	150	0.2	0.004	<0.67	0.81	3.4	26
FS01S	110	0.1	0.008	<0.67	0.56	1.9	11
FS00S	8.3	0.1	0.10	<0.67	0.26	0.9	12
SL4542S	110	0.1	0.002	<1.0	0.07	1.9	4
SL4543S	9.5	0.1	<0.002	<1.0	0.08	1.3	<1.0
SL4544S	10	0.1	<0.002	<1.0	0.10	1.7	<1.0

Heavy-mineral-concentrate samples

Sample	As (SQS)	Ag (SQS)	Au (SQS)	Bi (SQS)	Sb (SQS)	W (SQS)
FS08C	<500	7	<20	2,000	<200	>20,000
FS07C	<500	300	>1,000	2,000	<200	10,000
FS06C	<500	300	1,000	150	<200	>20,000
FS05C	<500	150	300	<20	1,000	>20,000
FS04C	<500	10	100	200	1,000	20,000
FS03C	<500	100	500	70	1,000	10,000
FS02C	ins.	ins.	ins.	ins.	ins.	ins.
FS01C	<500	70	300	<20	<200	2,000
FS00C	<500	30	500	<20	1000	2,000
SL4542C	<500	<1	<20	<20	<200	2,000
SL4543C	<500	<1	<20	<20	<200	<50
SL4544C	<500	<1	<20	<20	<200	<50

ISOTOPIC STUDIES

Oxygen, hydrogen, and sulfur isotopic compositions were determined for samples of ore and gangue minerals collected from the Fortyseven Creek prospect to identify possible fluid sources involved during the mineralizing event. Possible ore-fluid sources include meteoric water, local formation water in surrounding rocks, magmatic water, fluids derived during dehydration of minerals in surrounding wallrocks, or fluids derived from the deep crust.

OXYGEN AND HYDROGEN ISOTOPIC COMPOSITIONS

Oxygen isotopic ratios were measured in mineral separates of hydrothermal quartz and sericite (table 3). Hydrogen isotopic ratios were determined for sericite and for fluid-inclusion water extracted from a sample of hydrothermal quartz. Isotopic ratios were determined using standard extractions and mass-spectrometry techniques (Godfrey, 1962; Clayton and Mayeda, 1963). Isotope values are expressed relative to Vienna-Standard Mean Ocean Water (V-SMOW) in standard $\delta^{18}O$ notation for oxygen and δD for hydrogen. Hydrogen ratios were normalized to V-SMOW and Standard Light Antarctic Precipitation (SLAP). Analytical reproducibility is ± 0.2 per mil for oxygen and ± 3 per mil for hydrogen.

To estimate the oxygen and hydrogen isotopic composition of the Fortyseven Creek ore fluid, we used the measured isotopic compositions of gangue minerals (quartz and sericite) and the average ore-formation temperature (330°C) from the fluid-inclusion studies, and then calculated the isotopic ore-fluid compositions using equilibrium oxygen-isotope fractionation equations for quartz-water (Clayton and others, 1972) and muscovite-water (Friedman and O'Neil, 1977); the hydrogen isotopic ore-fluid composition was calculated using the equilibrium fractionation equation for muscovite-water (Suzuoki and Epstein, 1976).

The $\delta^{18}O$ value measured for hydrothermal quartz from the Fortyseven Creek prospect is 16.3 per mil, and 13.9 per mil for hydrothermal sericite; the δD for hydrothermal sericite is -89 per mil (table 3). The calculated $\delta^{18}O$ value is 10.4 per mil and 11.2 per mil for an ore fluid in equilibrium with quartz and sericite, respectively, at 330°C. The calculated δD value is -47 per mil for an ore fluid in equilibrium with sericite at 330°C. The isotopic composition of hydrogen measured for fluid-inclusion water in hydrothermal quartz from Fortyseven Creek is -117 per mil δD, a composition that is unreasonably isotopically light when compared to that calculated to be in equilibrium with hydrothermal sericite (-47 ‰ δD). The hydrogen composition for fluid-inclusion water in the sample of hydrothermal quartz analyzed here probably contains a significant amount of isotopically light secondary fluid inclusions, such as meteroric water, thus this δD value is not meaningful for the interpretation of ore-formation processes of the Fortyseven Creek deposit and is not considered further.

To evaluate the possible involvement of isotopically exchanged meteoric water in the formation of the Fortyseven Creek lode, modeling calculations were made using the iso-

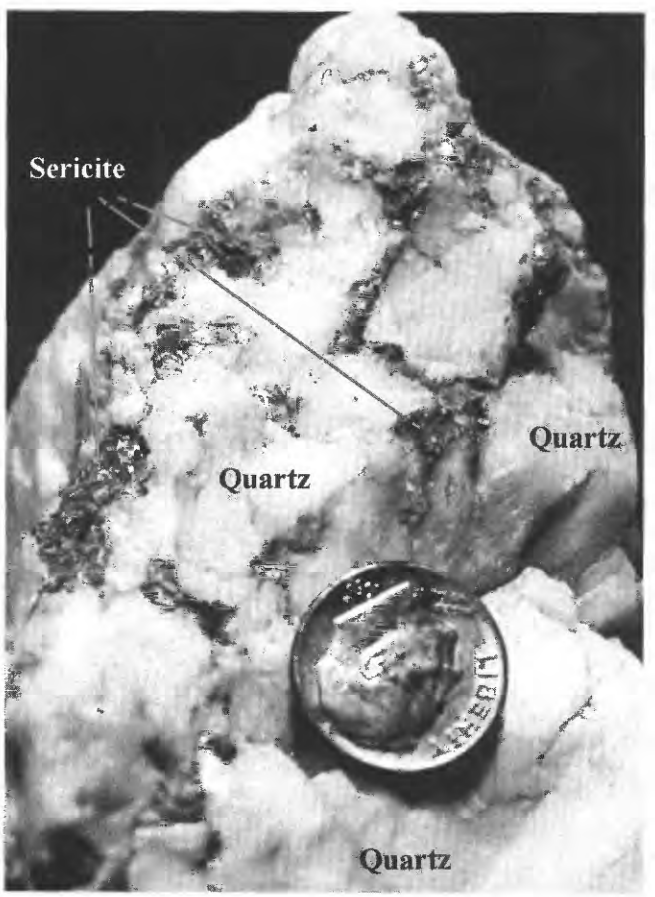

Figure 4. Sample of vein quartz with intergrown sericite from the Fortyseven Creek prospect.

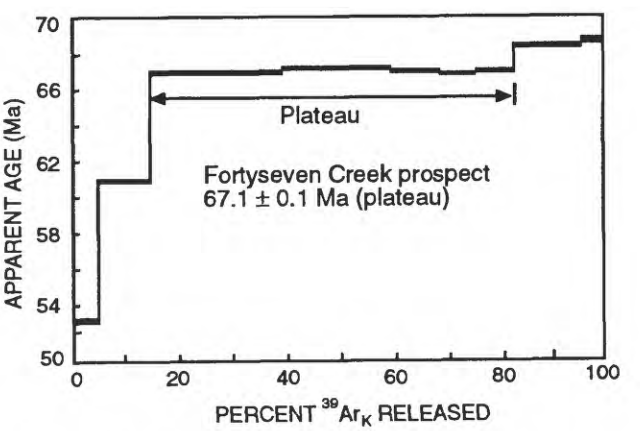

Figure 5. $^{40}Ar/^{39}Ar$ age spectrum for hydrothermal sericite sample collected from the Fortyseven Creek prospect. $^{39}Ar_K$, potassium-derived ^{39}Ar.

Table 2. $^{40}Ar/^{39}Ar$ data for hydrothermal-vein sericite sample collected from the Fortyseven Creek prospect.

Temp °C	$^{40}Ar_R$	$^{39}Ar_K$	F	$^{39}Ar_{rad}$ (% of total)	Radiogenic yield (%)	$^{39}Ar/^{37}Ar$	Apparent age ±1σ (Ma)
600	0.07317	0.02619	2.794	0.4	34.5	204	37.58 ± 2.53
700	1.00194	.26343	3.803	4.3	68.6	256	50.97 ± 0.08
800	2.96658	.65173	4.552	10.6	91.2	799	60.84 ± 0.09
850	8.45530	1.68466	5.019	27.5	98.1	6,134	66.97 ± 0.10
900	5.33447	1.05726	5.046	17.3	98.6	3,629	67.31 ± 0.10
950	2.96921	.59100	5.024	9.7	98.1	3,912	67.03 ± 0.10
1,000	1.97877	.39413	5.021	6.4	97.6	3,493	66.99 ± 0.18
1,050	2.24077	.44645	5.019	7.3	97.2	12,864	66.97 ± 0.10
1,150	3.89673	.76081	5.122	12.4	98.3	10,302	68.31 ± 0.10
1,300	1.27719	.24753	5.160	4.0	97.6	126,861	68.81 ± 0.16

Sample weight = 26.5 mg; J value = 0.007535.
F is the ratio of $^{40}Ar_R$ (radiogenic ^{40}Ar) to $^{39}Ar_K$ (potassium derived ^{39}Ar) of the sample.
$J = (e^{\lambda tm} - 1)/(^{40}Ar_R/^{39}Ar_K)_m$, where tm is the age of the primary flux monitor, $(^{40}Ar_R/^{39}Ar_K)_m$ is the measured ratio of the standard, $\lambda = 5.543 \times 10^{-10}$/yr.
Total gas age = 65.8 ± 0.1 Ma.
Plateau age = 67.1 ± 0.1 Ma.
Plateau on steps 850°C to 1,050°C and contains 68.2 percent of the gas.
Plateau minimum = 67.0 Ma. Plateau maximum = 67.3 Ma.

topic-exchange equation for water-rock systems of Field and Fifarek (1985). Variables in these calculations included (1) the initial isotopic composition of meteoric water in southwestern Alaska of $\delta^{18}O = -20$ per mil and $\delta D = -150$ per mil, (2) the average oxygen-isotopic composition of surrounding Kuskokwim Group wallrocks ($\delta^{18}O = +18‰$), (3) ore-formation temperatures ranging from about 260 to 380°C, and (4) water-to-rock ratios of 10, 1, 0.1, and 0.01. Using this approach, evolution paths of meteoric water were generated with varying water-to-rock ratios at 260 and 380°C (fig. 7). These calculations indicate that when meteoric water exchanges with surrounding sedimentary wallrocks at 380°C and low water-to-rock ratios (0.01), it is possible to shift the final fluid $\delta^{18}O$ to 12.9 per mil and δD to −62 per mil (fig. 7). These are the heaviest $\delta^{18}O$ and δD fluid compositions that can be obtained by isotopic exchange of meteoric water with surrounding Kuskokwim Group sedimentary wallrocks at 380°C.

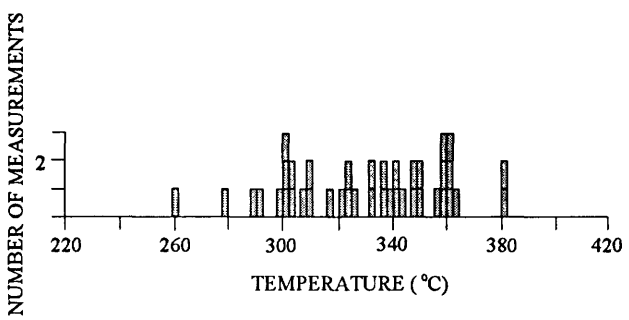

Figure 6. Homogenization temperatures for fluid inclusions in samples of vein quartz from the Fortyseven Creek prospect.

The oxygen and hydrogen isotopic data obtained for the Fortyseven Creek samples indicate that the fluids responsible for ore formation were probably of magmatic origin or highly exchanged meteoric water, or a mixture of both. For example, at 330°C (the average ore-forming temperature) the calculated $\delta^{18}O$ fluid compositions of 10.4 (quartz) and 11.2 (sericite), and a calculated δD value of −47 (sericite), plot near the magmatic water field (commonly $\delta^{18}O = +5$ to +10 per mil and $\delta D = -80$ to −40 per mil; Taylor, 1979). This ore-fluid composition is also similar to what would be obtained if meteoric water was isotopically exchanged with surrounding wallrocks at 330°C and a 0.01 water-rock ratio. The isotopic results for Fortyseven Creek suggest that the dominant ore-fluid source was probably of magmatic origin, which is consistent with the spatial association of a granite porphyry intrusion at the prospect; however, exchanged meteoric water also cannot be ruled out.

SULFUR ISOTOPIC COMPOSITIONS

Sulfur isotopic ratios were determined for separates of arsenopyrite and pyrite from mineralized vein samples to iden-

Table 3. Summary of isotope data for the Fortyseven Creek prospect.

[V-SMOW, Vienna Standard Mean Ocean Water; CDT, Canyon Diablo Troilite; all values are per mil; —, not applicable]

Mineral	$\delta^{18}O_{V\text{-}SMOW}$	$\delta D_{V\text{-}SMOW}$	$\delta^{34}S_{CDT}$
Hydrothermal quartz	16.3	-117	--
Hydrothermal sericite	13.9	-89	--
Pyrite	--	--	-6.7
Arsenopyrite	--	--	-7.8

tify possible sources of sulfur involved during the formation of the Fortyseven Creek deposit. Sulfur isotopic ratios were measured using mass spectrometry procedures similar to those described by Yanaglsawa and Sakal (1983). Sulfur isotope ratios are expressed relative to Canyon Diablo Troilite and have a precision of ±0.2 per mil.

The $\delta^{34}S$ values for arsenopyrite (−7.8‰) and pyrite (−6.7‰) from Fortyseven Creek (table 3, fig. 8) are within the range of $\delta^{34}S$ values (−26.5 to −5.2‰) determined for sedimentary rocks of the Kuskokwim Group (Gray and others, 1997); in fact, the pyrite and arsenopyrite values are most similar to the −8.3 per mil $\delta^{34}S$ value determined for a sample of graywacke from the Kuskokwim Group collected near to the Fortyseven Creek prospect (fig. 8). In addition, assuming sulfide precipitation at about 300°C and using the isotope fractionation equation for pyrite-H_2S (Ohmoto and Rye, 1979), the isotopic composition of ore-fluid H_2S calculated to be in equilibrium with this pyrite is −7.9 per mil $\delta^{34}S$, which is also similar to the composition of the nearby Kuskokwim Group shale. This result is also consistent with derivation of sulfur from surrounding sedimentary rocks during the formation of the Fortyseven Creek deposit. The negative $\delta^{34}S$ values for sulfide minerals from Fortyseven Creek indicate derivation from a light sulfur source, which may be sedimentary pyrite and organic sulfur leached from surrounding sedimentary rocks during ore formation.

Similar to the oxygen and hydrogen isotopic data, a small component of magmatic sulfur ($\delta^{34}S=0\pm3$‰; Ohmoto and Rye, 1979) cannot be ruled out because the average $\delta^{34}S$ composition (about −15%) of the Kuskokwim Group sedimentary rocks is slightly lighter than that of the Fortyseven Creek sulfide samples and indicates minor involvement of a heavier sulfur isotope source. A Late Cretaceous to early Tertiary granite porphyry intrusion near the Foryseven Creek prospect is a potential source of magmatic sulfur that may have been part of the ore-forming fluids. Such magmatic sulfur could be derived directly from magmatic fluids or from the dissolution of sulfide minerals in the igneous rocks during hydrothermal alteration.

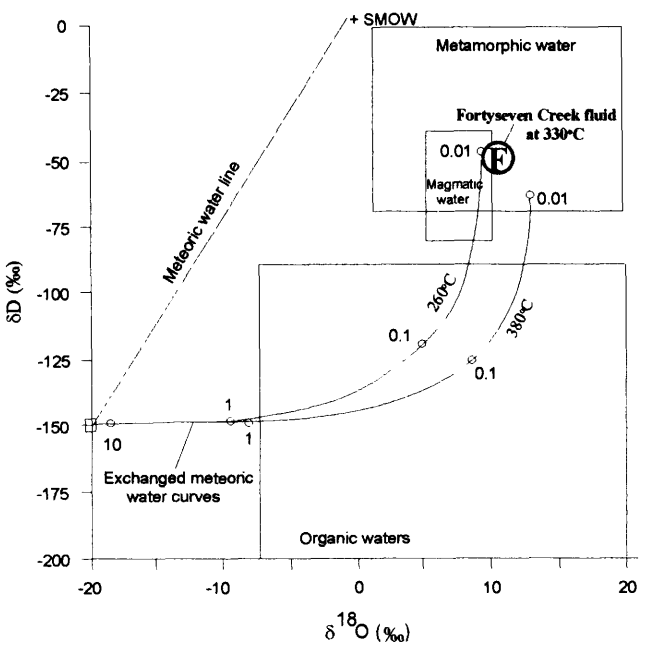

Figure 7. Isotopic compositions of oxygen and hydrogen for the Fortyseven Creek ore fluids, calculated at 330°C using the fractionation equation from Clayton and others (1972). Fields shown for reference are metamorphic and magmatic waters (Taylor, 1979), and organic waters (derived from organic matter during processes such as dehydration, dehydrogenation, or oxidation) (Sheppard, 1986). Water-rock curves were calculated at 260 and 380°C (the range in ore-forming temperatures) from equation of Field and Fifarek (1985), using water-rock ratios of 10, 1, 0.1, and 0.01 as shown. SMOW, standard mean ocean water.

SUMMARY

Geochemical dispersion patterns in stream-sediment and heavy-mineral-concentrate samples indicate that Au, As, Sb,

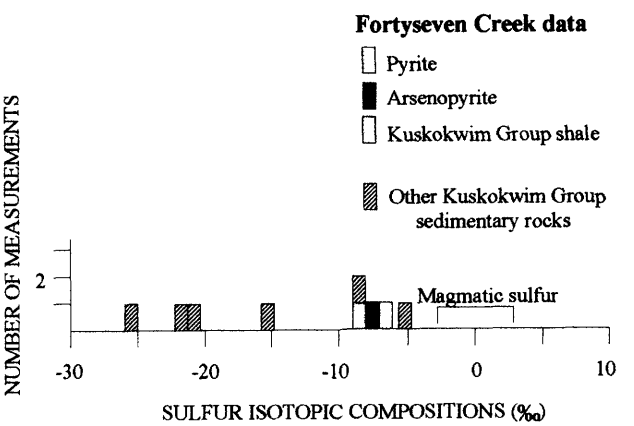

Figure 8. Sulfur isotopic compositions for pyrite and arsenopyrite separated from mineralized vein samples collected from the Fortyseven Creek prospect. Sulfur isotope compositions for sedimentary rocks of the Kuskokwim Group (Gray and others, 1997) shown for reference.

Bi, and W are diagnostic of the upstream Fortyseven Creek prospect. These results are consistent with the ore mineralogy of the prospect that contains scheelite, arsenopyrite, stibnite, and gold. Thus, anomalous concentrations of these elements can be used in exploration for deposits of similar type throughout southwestern Alaska.

We suggest that the age of mineralization at Fortyseven Creek is 67.1±0.1 Ma on the basis of a $^{40}Ar/^{39}Ar$ plateau age obtained for a sample of sericite intergrown with hydrothermal vein quartz that was collected from the prospect. This hydrothermal-sericite age is within the range of ages of about 63 to 71 Ma obtained for granite porphyry bodies near other southwestern Alaska gold deposits such as Donlin Creek and Golden Horn, which have geologic, mineralogical, and geochemical characteristics similar to those of Fortyseven Creek. Assuming that granite porphyry at Fortyseven Creek has a similar age, there may be a temporal relation between mineralization and Late Cretaceous and early Tertiary magmatism.

Oxygen, hydrogen, and sulfur isotopic data for the Fortyseven Creek prospect probably indicate that ore fluids were derived during the interaction of a nearby granite porphyry intrusion with surrounding sedimentary rocks of the Kuskokwim Group. Calculated oxygen and hydrogen isotopic compositions of the ore fluids suggest that they were of magmatic origin, but that the source of sulfur was probably the surrounding sedimentary wallrocks. High heat flow related to local igneous activity probably initiated thermal convection and induced contact metamorphism in the surrounding sedimentary rocks. Resultant hydrothermal activity expelled fluids that flowed through local fractures and faults and reacted with wallrocks.

Acknowledgments.—We thank Stanley B. Pleninger (Anchorage) for permission to visit the Fortyseven Creek prospect. We especially thank Monte Moore and Jim Sanders (Nevada Star Resources Corp., Seattle) for the opportunity to evaluate geochemical data collected by Nevada Star during exploration of the Fortyseven Creek prospect in 1991. We also thank Chuck Hawley (Hawley Resource Group, Inc., Anchorage) for providing a copy of his 1989 report on Fortyseven Creek. John Bullock, Phil Hageman, Rich O'Leary, and Jerry Motooka (USGS) provided chemical analyses of stream-sediment and heavy-mineral-concentrate samples.

REFERENCES CITED

Box, S.E., and Elder, W.P., 1992, Depositional and biostratigraphic framework of the Upper Cretaceous Kuskokwim Group, southwest Alaska, *in* Bradley, D.C., and Ford, A.B., eds., Geologic studies in Alaska by the U.S. Geological Survey, 1990: U.S. Geological Survey Bulletin 1999, p. 8-16.

Box, S.E., and Murphy, J.M., 1987, Late Mesozoic structural and stratigraphic framework, eastern Bethel quadrangle, southwest Alaska, *in* Hamilton, T.D., and Galloway, J.P., eds., Geologic studies in Alaska by the U.S. Geological Survey during 1986: U.S. Geological Survey Circular 998, p. 78-82.

Bull, K.F., 1988, Genesis of the Golden Horn and related mineralization in the Flat area, Alaska: Fairbanks, University of Alaska, M.S. thesis, 149 p.

Bundtzen, T.K., and Gilbert, W.G., 1983, Outline of geology and mineral resources of upper Kuskokwim region, Alaska: Journal of the Alaska Geological Society, v. 3, p. 101-119.

Bundtzen, T.K., and Miller, M.L., 1997, Precious metals associated with Late Cretaceous-early Tertiary igneous rocks of southwestern Alaska, *in* Goldfarb, R.J., and Miller, L.D., eds., Mineral deposits of Alaska: Economic Geology Monograph 9, p. 242-286.

Bundtzen, T.K., Miller, M.L., Laird, G.M., and Bull, K.F., 1992, Geology and mineral resources of the Iditarod mining district, Iditarod B-4 and eastern B-5 quadrangles, southwestern Alaska: Alaska Division of Geological and Geophysical Surveys Professional Report 97, 46 p.

Bundtzen, T.K., and Swanson, S.E., 1984, Geology and petrology of igneous rocks in the Innoko River area, western Alaska: Geological Society of America Abstracts with Programs, v. 16, no. 5, p. 273.

Bundtzen, T.K., Swainbank, R.C., Clough, A.H., Henning, M.W., and Charlie, K.M., 1996, Alaska's mineral industry, 1995: Alaska Division of Geological and Geophysical Surveys Special Report 50, 71 p.

Cady, W.M., Wallace, R.E., Hoare, J.M., and Webber, E.J., 1955, The central Kuskokwim region, Alaska: U.S. Geological Survey Professional Paper 268, 132 p.

Clayton, R.N., O'Neil, J.R., and Mayeda, T.K., 1972, Oxygen isotope exchange between quartz and water: Journal of Geophysical Research, v. 77, p. 3057-3067.

Clayton, R.N., and Mayeda, T.K., 1963, The use of bromine pentafluoride in the extraction of oxygen from oxides and silicates for isotopic analyses: Geochimica et Cosmochimica Acta, v. 27, p. 43-52.

Dallmeyer, R.D., 1975, Incremental $^{40}Ar/^{39}Ar$ ages of biotite and hornblende from retrograded basement gneisses of the southern Blue Ridge: Their bearing on the age of Paleozoic metamorphism: American Journal of Science, v. 275, p. 444-460.

Dalrymple, G.B., Alexander, E.C., Lanphere, M.A., and Kraker, G.P., 1981, Irradiation of samples for $^{40}Ar/^{39}Ar$ dating using the Geological Survey TRIGA reactor: U.S. Geological Survey Professional Paper 1176, 56 p.

Decker, John, Bergman, S.C., Blodgett, R.B., Box, S.E., Bundtzen, T.K., Clough, J.G., Coonrad, W.L., Gilbert, W.G., Miller, M.L., Murphy, J.M., Robinson, M.S., and Wallace, W.K., 1994, Geology of southwestern Alaska, *in* Plafker, George, and Berg, H.C., eds., The Geology of Alaska: Boulder, Colo., Geological Society of America, The Geology of North America, v. G-1, p. 285-310.

Decker, John, and Hoare, J.M., 1982, Sedimentology of the Cretaceous Kuskokwim Group, southwest Alaska, *in* Coonrad, W.L., ed., U.S. Geological Survey in Alaska: accomplishments during 1980: U.S. Geological Survey Circular 844, p. 81-83.

Decker, John, Reifenstuhl, R.R., Robinson, M.S., and Waythomas, C.F., 1986, Geologic map of the Sleetmute A-5, A-6, B-5, and B-6 quadrangles, Alaska: Alaska Division of Geological and

Geophysical Surveys Professional Report 93, 22 p., 1 sheet, scale 1:250,000.

Decker, John, Reifenstuhl, R.R., Robinson, M.S., Waythomas, C.F., and Clough, J.G., 1995, Geology of the Sleetmute A-5, A-6, B-5, and B-6 quadrangles, southwestern Alaska: Alaska Division of Geological and Geophysical Surveys Professional Report 99, 16 p.

Decker, John, Robinson,M.S.,Murphy,J.M.,Reifenstuhl, R.R., and Albanese, M.D., 1984, Geologic map of the Sleetmute A-6 quadrangle: Alaska Division of Geological and Geophysical Surveys Report of Investigations 84-8, scale 1:40,000.

Field, C.W., and Fifarek, R.H., 1985, Light stable-isotope systematics in the epithermal environment, *in* Berger, B.R., and Bethke, P.M., eds., Geology and geochemistry of epithermal systems: Society of Economic Geologists, Reviews in Economic Geology, v. 2, p. 99-128.

Friedman, I., and O'Neil, J.R., 1977, Compilation of stable isotope fractionation factors of geochemical interest, *in* Fleischer, M., ed., Data of geochemistry, 6th edition: U.S. Geological Survey Professional Paper 440-KK, p. KK1-KK12.

Godfrey, J.D., 1962, The deuterium content of hydrous minerals from the east-central Sierra Nevada and Yosemite National Park: Geochimica et Cosmochimica Acta, v. 26, p. 1215-1245.

Gray, J.E., Gent, C.A., Snee, L.W., and Wilson, F.H., 1997, Epithermal mercury-antimony and gold-bearing vein deposits of southwestern Alaska, *in* Goldfarb, R.J., and Miller, L.D., eds., Mineral deposits of Alaska: Economic Geology Monograph 9, p. 287-305.

Gray, J.E., and Theodorakos, P.M., 1997, Areas favorable for metallic mineral resources and newly discovered mineral occurrences in the Buckstock Mountains, southwestern Alaska, *in* Dumoulin, J.A., and Gray, J.E., eds., Geologic studies by the U.S. Geological Survey, 1995: U.S. Geological Survey Professional Paper 1574, p.111-123.

Grimes, D.J., and Marranzino, A.P., 1968, Direct-current arc and alternating-current spark emission spectrographic field methods for the semiquantitative analysis of geological materials: U.S. Geological Survey Circular 591, 6 p.

Hawley, C.C., 1989, The Forty Seven Creek prospect, southwest Alaska, summary of data and recommendations: Unpublished report prepared for Holitna Basin Mining and Exploration, Inc., Hawley Resources Group, 9200 Lake Otis Parkway, Anchorage, AK 99507, 7 p.

Hoare, J.M., and Coonrad, W.L., 1959, Geology of the Bethel quadrangle, Alaska: U.S. Geological Survey Miscellaneous Geologic Investigations Series Map I-285, scale 1:250,000.

Hubert, A.E., and Chao, T.T., 1985, Determination of gold, indium, tellurium and thallium in the same sample digestion of geological materials by atomic-absorption spectroscopy and two-step solvent extraction: Talanta, v. 32, p. 383-387.

Kennedy, K.R., and Crock, J.G., 1987, Determination of mercury in geological materials by continuous flow, cold-vapor, atomic-absorption spectrophotometry: Analytical Letters, v. 20, p. 899-908.

Maynard, G.B., 1995, 47 Creek property, southwestern Alaska, results of the Phase Three Exploration Program: Unpublished report prepared for Nevada Star Resource Corp., 10735 Stone Avenue North, Seattle, WA, 98133, 8 p.

Meier, A.L., 1980, Flameless atomic-absorption determination of gold in geological materials: Journal of Geochemical Exploration, v. 13, p. 77-85.

Miller, M.L., Belkin, H.E., Blodgett, R.B., Bundtzen, T.K., Cady, J.W., Goldfarb, R.J., Gray, J.E., McGimsey, R.G., and Simpson, S.L., 1989, Pre-field study and mineral resource assessment of the Sleetmute quadrangle, southwestern Alaska: U.S. Geological Survey Open-File Report 89-363, 115 p., 3 plates, scale 1:250,000.

Miller, M.L., and Bundtzen, T.K., 1994, Generalized geologic map of the Iditarod quadrangle, Alaska, showing potassium-argon, major-oxide, trace-element, fossil, paleocurrent, and archaelogical sample localities: U.S. Geological Survey Miscellaneous Field Studies Map MF-2219-A, scale 1:250,000.

Millholland, Madelyn, and Freeman, C.J., 1997, Exploration review, Alaska: Society of Economic Geologists Newsletter, no. 28, p. 32.

Moll-Stalcup, E.J., 1994, Latest Cretaceous and Cenozoic magmatism in mainland Alaska, *in* Plafker, George, and Berg, H.C., eds., The Geology of Alaska: Boulder, Colo., Geological Society of America, The Geology of North America, v. G-1, p. 589-619.

Motooka, J.M., 1996, Organometallic halide extraction for 10 elements by inductively coupled plasma-atomic emission spectrophotometry, *in* Arbogast, B.F., ed., Analytical methods manual for the Mineral Resources Surveys Program, U.S. Geological Survey: U.S. Geological Survey Open-File Report 96-525, p. 102-108.

Nokleberg, W.J., Bundtzen, T.K., Berg, H.C., Brew, D.A., Grybeck, Donald, Robinson, M.S., Smith, T.E., and Yeend, Warren, 1987, Significant metalliferous lode deposits and placer districts of Alaska: U.S. Geological Survey Bulletin 1786, 104 p., 2 sheets.

Ohmoto, H., and Rye, R.O., 1979, Isotopes of sulfur and carbon, *in* Barnes, H.L., ed., Geochemistry of hydrothermal ore deposits (2nd ed.): New York, John Wiley and Sons, p. 509-567.

Reifenstuhl, R.R., Robinson, M.S., Smith, T.E., Albanese, M.D., and Allegro, G.A., 1984, Geologic map of the Sleetmute B-6 quadrangle, Alaska: Alaska Division of Geological and Geophysical Surveys Report of Investigations 84-12, scale 1:40,000.

Robinson, M.S., and Decker, John, 1986, Preliminary age dates and analytical data for selected igneous rocks from the Sleetmute, Russian Mission, Taylor Mountains, and Bethel quadrangles, southwestern Alaska: Alaska Division of Geological and Geophysical Surveys Public-Data File 86-99, 9 p.

Roedder, E., 1979, Fluid inclusions as samples of ore fluids, *in* Barnes, H.L., ed., Geochemistry of hydrothermal ore deposits, (2nd ed.): John Wiley and Sons, New York, p. 684-737.

Sheppard, S.M.F., 1986, Characterization and isotopic variations in natural waters, *in* Valley, J.W., Taylor, H.P., Jr., and O'Neil, J.R., eds., Stable isotopes in high temperature geological processes: Mineralogical Society of America, Reviews in Mineralogy, v. 16, p. 165-183.

Snee, L.W., Sutter, J.F., and Kelley, W.C., 1988, Thermochronology of economic mineral deposits: dating the stages of mineralization at Panasqueira, Portugal, by high-precision $^{40}Ar/^{39}Ar$ age spectrum techniques on muscovite: Economic Geology, v. 83, p. 335-354.

Suzuoki, T., and Epstein, S., 1976, Hydrogen isotope fractionation between OH-bearing minerals and water: Geochimica et Cosmochimica Acta, v. 40, p. 1229-1240.

Szumigala, D.J., 1993, Gold mineralization related to Cretaceous-

Tertiary magmatism in the Kuskokwim Mountains of west-central and southwestern Alaska: Los Angeles, University of California, Ph.D. dissertation, 301 p.

Taylor, H.P., Jr., 1979, Oxygen and hydrogen isotope relationships in hydrothermal mineral deposits, *in* Barnes, H.L., ed., Geochemistry of hydrothermal ore deposits (2nd ed.): New York, John Wiley and Sons, p. 236-277.

Welsch, E.P., 1983, A rapid geochemical spectrophotometric determination of tungsten with dithiol: Talanta, v. 30, p. 876-878.

Yanaglsawa, F., and Sakal, H., 1983, Thermal decomposition of barium sulfate-vanadium pentoxide-silica glass mixtures for preparation of sulfur dioxide in sulfur isotope ratio measurements: Analytical Chemistry, v. 55, p. 985-987.

Reviewers: Karen D. Kelley and David B. Smith.

Geology and Gold Resources of the Stuyahok Area, Holy Cross Quadrangle, Southwestern Alaska

By Marti L. Miller, Thomas K. Bundtzen, *and* William J. Keith

ABSTRACT

In 1995, under a cooperative agreement with Calista Corporation, the U.S. Geological Survey performed geologic mapping and geochemical sampling in the Stuyahok area of south-central Holy Cross quadrangle. The area is underlain largely by Lower Cretaceous tuff, volcaniclastic rocks, and lava flows of the Koyukuk terrane. These Lower Cretaceous rocks are cut by younger mafic and felsic dikes, which are similar to Late Cretaceous and early Tertiary dikes that are found in many parts of west-central and southwestern Alaska. Placer mining in the Stuyahok area has yielded an estimated 933 kg (30,000 oz) of gold, most of which was mined prior to 1940. The area is still actively mined. Results of this study indicate that additional placer gold resources are likely to be present, and that feldspar-quartz porphyry dikes (similar to peraluminous granite porphyry dikes found elsewhere in southwestern Alaska) are the probable source of at least some of the placer gold. Lode gold resources are difficult to evaluate on the basis of available information, but, if present, they most likely lie near the current placer workings, where they may be related to the feldspar-quartz porphyry dikes or possibly to the south near Chase Mountain, where they may be related either to felsic dikes or to an unexposed pluton.

INTRODUCTION

The Stuyahok study area lies north of the Yukon River in the south-central part of the Holy Cross 1:250,000-scale quadrangle (fig. 1). The study area encompasses approximately 142 km^2 surrounding placer gold deposits on Flat Creek and other small tributaries to the Stuyahok River (fig. 2). We estimate mineral production for the Stuyahok area to be about 933 kg (30,000 oz) of placer gold. Prior to this field investigation, little information was available about the geology or mineral resources of the Stuyahok area, and all published reports were based on site investigations made before 1940. Our work provides detailed information on the geologic setting of this gold-bearing area and gives an overview of the geochemical expression of the gold resources.

The Stuyahok area is characterized by wide, sediment-filled, heavily vegetated valleys that separate accordant rounded ridges. The lowest valley elevation is about 122 m; the highest point in the study area is the top of Chase Mountain[1] at 576 m (fig. 3). Hillsides are covered by thick brush up to about 274 m elevation. Access to the region is primarily by air. When the ground is frozen, a 19-km-long trail provides surface access from the Yukon River. Much of the study area is either owned or selected by Calista Corporation (an Alaska Native regional corporation established under the 1971 Alaska Native Claims Settlement Act). The remaining land within the study area is under selection by the State of Alaska (fig. 2).

This investigation was conducted in cooperation with Calista Corporation under a U.S. Geological Survey (USGS) Cooperative Research and Development Agreement (CRADA). The purpose of our joint study was to conduct geologic mapping and to collect samples for geochemical studies in the Stuyahok area. Field work was performed from August 7 to 25, 1995, by four people from the USGS, one from the Alaska Division of Geological and Geophysical Surveys, and two from Calista. Miller and others (1996) summarized the geological and mineral resource results of the project. Geochemical data were reported by Keith and others (1996) and Bailey and others (1996). In addition to providing new and more detailed information—point count and microprobe data, more detail on the geologic setting, and a geologic cross section—this paper interprets geologic data to specifically assess the gold resources of the Stuyahok area.

[1] Chase Mountain is the unofficial local name for this peak in honor of W.C. Chase, who was an early developer of the placer gold deposits. We have submitted the name to the Alaska Historical Commission for official consideration.

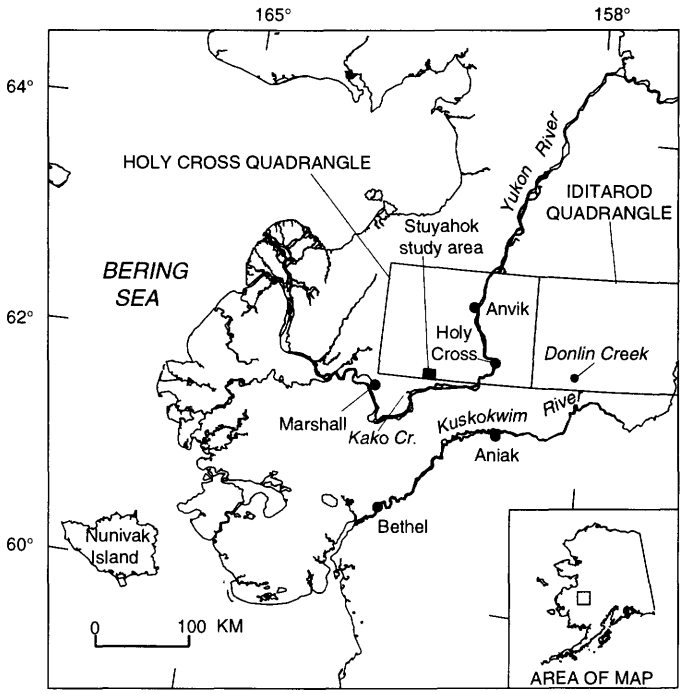

Figure 1. Map showing location of Stuyahok study area.

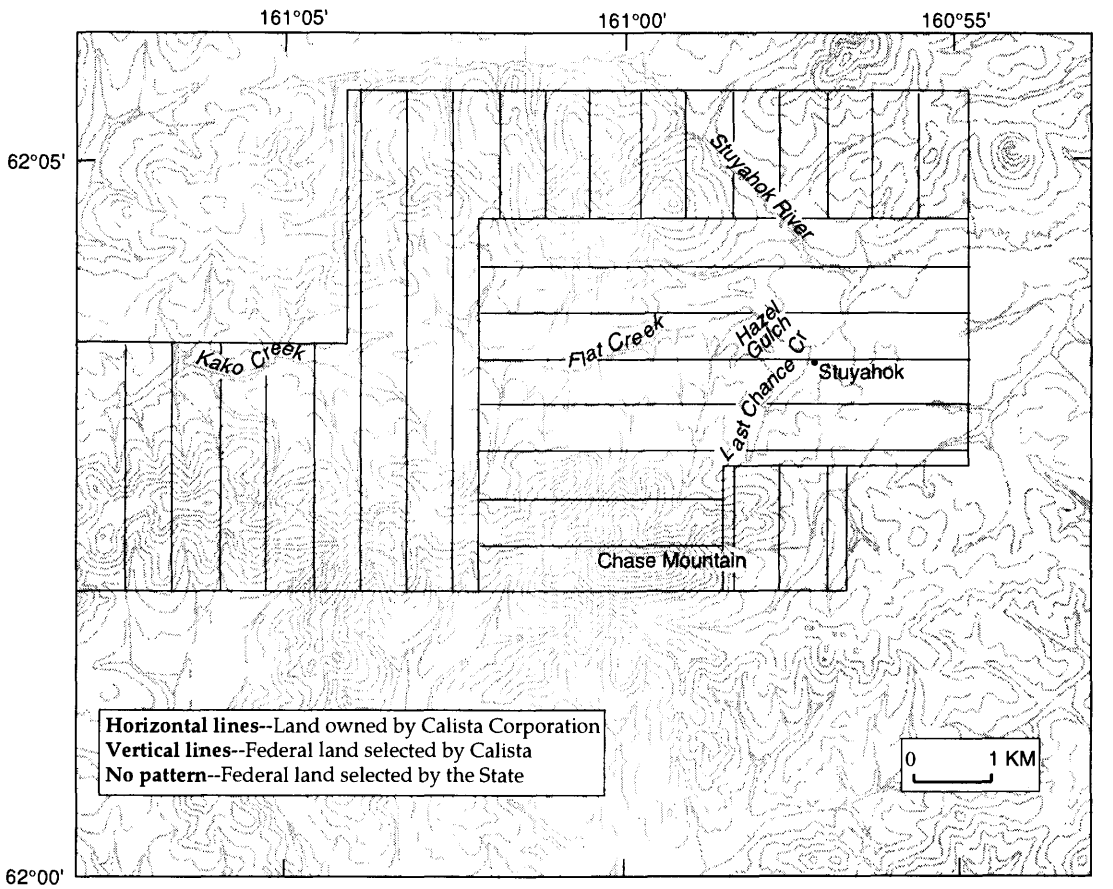

Figure 2. Map of Stuyahok study area showing land status and some topographic features referred to in the text. Contour interval 100 feet.

Figure 3. Chase Mountain from the north. Thermal alteration suggests mountain is underlain by an unexposed pluton.

GEOLOGY

REGIONAL GEOLOGY

The Stuyahok study area lies in the southern part of the Yukon-Koyukuk basin of western Alaska (Patton and Box, 1989) (fig. 4). The basin, which is offset along the Kaltag fault, occupies a wedge-shaped structural depression more than 560 km long that is filled with middle and Upper Cretaceous terrigenous sedimentary rocks. The flysch was deposited mainly on Lower Cretaceous island-arc-type volcanic rocks of the Koyukuk terrane (originally defined by Jones and others, 1987). Remnants of the Koyukuk terrane are now exposed as structural highs in the basin (Patton and others, 1994). The Koyukuk terrane, as described by Patton and others (1994), contains two distinct assemblages: (1) Jurassic tonalite-trondhjemite plutonic rocks and older(?) volcanic and plutonic rocks, which are unconformably overlain by (2) Upper Jurassic(?) and Lower Cretaceous, andesitic volcaniclastic rocks, tuffs, and flows. The Upper Jurassic(?) and Lower Cretaceous volcanic rocks, which form the bulk of the Koyukuk terrane, record an episode of andesitic magmatism marked by voluminous pyroclastic and epiclastic volcanic rocks and subordinate flows of basaltic to dacitic composition (Patton and others, 1994). Geochemical signatures indicate the magmatism was subduction-related (Patton and others, 1994; Patton and Moll-Stalcup, 1996), and structural data, isotopic evidence, and sandstone petrography suggest the Koyukuk terrane developed in an intraoceanic setting (Patton and others, 1994).

North of the Holy Cross quadrangle, the Koyukuk terrane is composed of two Lower Cretaceous volcanic units and two plutonic units of Jurassic age (Patton and Moll-Stalcup, 1996). The dominant volcanic unit is composed of andesitic crystal and lithic tuff, cherty tuff, tuff breccia, and volcanic sandstone and conglomerate. This andesitic volcaniclastic unit unconformably overlies Jurassic plutonic rocks and was assigned an Early Cretaceous age based on the presence of a Valanginian *Buchia* and radiolarians of possible Early Cretaceous (Valanginian) age (Patton and Moll-Stalcup, 1996).

GEOLOGY OF THE STUYAHOK AREA

The study area is underlain largely by tuff, volcaniclastic rocks, and flows that we believe correlate

with Lower Cretaceous rocks of the Koyukuk terrane found immediately north of the Holy Cross quadrangle. These Lower Cretaceous lithologies are cut by mafic to felsic dikes, which are petrographically similar to Late Cretaceous and early Tertiary dikes that are found in many parts of west-central and southwestern Alaska (for example, Miller and Bundtzen, 1994; Miller and others, 1989; Beikman, 1980). We assume the mafic to felsic dikes in the Stuyahok area are also Late Cretaceous and early Tertiary in age. Unconsolidated late Tertiary(?) and Quaternary deposits overlap the bedrock units (fig. 5) and are largely colluvial and alluvial deposits of variable thickness (to a maximum of 32 m in the older terraces). The Stuyahok area has not been glaciated.

KOYUKUK TERRANE

In the study area, rocks of the Koyukuk terrane are divided into three map units as distinguished by sandstone-dominant, volcanic-dominant, and heterogeneous compositions (fig. 5). The classification of magmatic rocks in the Stuyahok study area is based on major-element analyses, which are available in Miller and others (1996). The sandstone-dominant unit (Ks, fig. 5) is volumetrically minor and primarily consists of lithic sandstone, but also has felsic tuff and minor siltstone. The volcanic-dominant unit (Ka, fig. 5) is characterized by volcanic agglomerate (vent facies) and lapilli tuff, but it also has some volcanic flow rocks and minor felsic tuff and sedimentary rocks. The heterogeneous unit (Kt, fig. 5), which underlies most of the study area, is composed dominantly of andesitic crystal lithic and lapilli tuffs that are closely interbedded with volcaniclastic sandstones and tuffaceous siltstones and with minor felsic tuffs and andesitic to dacitic flow rocks. Bedding attitudes from a limited number of outcrops suggest that unit Kt structurally overlies unit Ka in the central part of the map area. However, the stratigraphic or structural relation between units Ka and Ks in the southeastern corner of the map area is unclear.

The sandstone-dominated map unit (Ks) is composed largely of light- to dark-gray, fine- to coarse-grained, moderately well- to poorly sorted lithic sandstone, interbedded with lesser water-laid felsic tuff, light-gray reworked felsic tuff-sandstone, and minor green fossiliferous siltstone. Graded bed sets of medium-grained sandstone, fine-grained sandstone, and siltstone are preserved locally and suggest sediment transport by turbidity currents. Clasts in the sandstones are subrounded to angu-

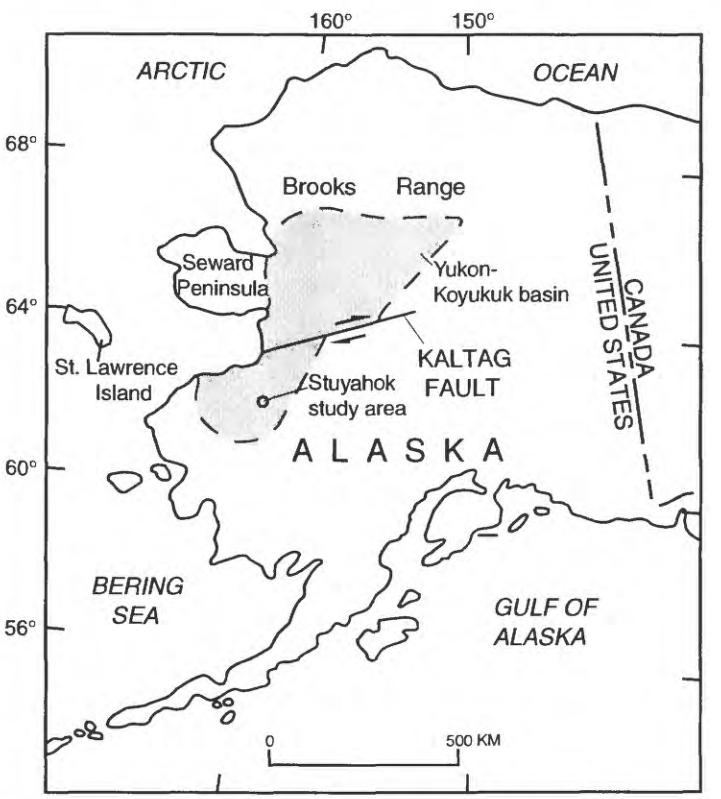

Figure 4. Map showing Yukon-Koyukuk basin (shaded) and location of Stuyahok study area. Arrows indicate relative direction of displacement on Kaltag fault (after Patton and Box, 1989, fig. 1).

lar and include a variety of rock fragments and some minerals. Framework point counts of five samples (table 1) range from 10 to 30 percent quartz grains, 9 to 28 percent feldspar, and 51 to 76 percent total lithic fragments. Trace amounts of detrital garnet, hornblende, epidote, and opaque grains are found locally. One moderately well-sorted, coarse- to very coarse grained sandstone sample (95AM080B, table 1) has crinoid debris that is probably Paleozoic in age (J.A. Dumoulin, oral commun., 1996), pieces of broken punctate brachiopod shells, and pumice clasts. The Paleozoic(?) debris suggests erosion of an older source terrane. Rubble of green siltstone is intermixed with graywacke at one site. The siltstone contains abundant sponge spicules and lesser radiolaria.

The volcanic-dominant map unit (Ka) is composed of about 70 percent basaltic to andesitic agglomerate and lapilli tuff, 25 percent volcanic flow rocks, and 5 percent felsic tuff and sedimentary rocks. The agglomerate consists of angular to subrounded volcanic blocks of a variety of sizes (as large as 25 cm in diameter) and textures (for example, porphyritic, pilotaxitic, vesicular, amygdaloidal, pumiceous), as well as crystals of clinopyroxene and plagioclase (locally broken). The lapilli tuff is essentially a finer grained version of the agglomerate—the clasts are poorly sorted, are 0.5 mm to 1 cm (and smaller), and include volcanic lithic grains, clinopyroxene, plagioclase, and locally hornblende and potassium feldspar crystals. One sample (95AM002B, table 1) yielded 84 percent volcanic lithic grains, 15 percent plagioclase, and trace amounts of potassium feldspar and quartz, but no clinopyroxene. The groundmass locally contains devitrified shard forms and is largely altered to chlorite. The volcanic agglomerate appears to be primarily a subaerial facies because it is unsorted and the clasts are largely angular. The lapilli tuff is also probably at least in part subaerial (consists of poorly sorted angular clasts in a matrix containing devitrified shards), but we cannot rule out that some of the juvenile material may have been reworked in a subaqueous environment. Lava flows of this volcanic-dominant unit are basaltic to andesitic in composition, range from less than 1 m to perhaps 5 m in thickness, and locally show pillow structures. The remainder of the volcanic-dominant unit is volumetrically minor, but includes some distinctive interbedded rocks. Fine-grained felsic tuff is exposed locally. Interbedded sedimentary rocks include fine-grained tuffaceous siltstone, soft-sediment-deformed silty mudstone, volcaniclastic sandstone, and reworked crystal lithic tuff, all of which indicate subaqueous deposition. Radiolarian tests in the tuffaceous siltstone and silty mudstone also indicate a marine environment. One sample of reworked tuff (95BF010, table 1) has 70 percent volcanic lithic grains, 28 percent plagioclase, 2 percent quartz, and no potassium feldspar.

The heterogeneous unit (Kt) is composed of about 75 percent tuffaceous rocks, 20 percent sedimentary rocks, and 5 percent volcanic flow rocks. The tuffaceous rocks are largely andesitic crystal lithic tuff and lapilli tuff, but minor amounts of felsic tuff and rhyolitic to dacitic ash flow tuff are also found. Petrographic point counts indicate that framework grains in crystal lithic tuff samples (n=4, table 1) consist of 60 to 81 percent volcanic lithic clasts (porphyritic andesite to basalt, and locally, porphyritic dacite, pumice, collapsed pumice, and scoria), 13 to 34 percent plagioclase, 2 to 5 percent clinopyroxene, and zero to 1 percent potassium feldspar. The matrix, which makes up 5 to 20 percent of the tuffs, is largely devitrified glass; relict shards are locally abundant. Sedimentary rocks of the heterogeneous unit include reworked crystal lithic tuff, volcaniclastic sandstone, and tuffaceous siltstone, which is locally rich in marine microfossils. These sedimentary rocks are locally finely layered or graded in 1- to 5-cm-thick beds. Some of the fine-grained varieties show soft-sediment deformation and bioturbation features. Point counts indicate that framework grains in reworked crystal lithic tuff samples of the heterogeneous unit (n=4, table 1) consist of 47 to 84 percent volcanic lithic clasts, 14 to 47 percent plagioclase, zero to 7 percent clinopyroxene, and zero to almost 1 percent potassium feldspar; a muddy matrix makes up 11 to 17 percent of these rocks. One volcaniclastic sandstone sample (95BF064, table 1) contains 73 percent volcanic lithic clasts, 22 percent plagioclase, 3 percent clinopyroxene, almost 1 percent potassium feldspar, and less than 1 percent quartz. Although compositionally similar to the crystal lithic tuffs, the clasts in the sedimentary rocks show evidence of reworking by water, because the grains are more rounded and better sorted. The tuffaceous siltstones commonly contain 100- to 200-micron-diameter round and locally triangular-shaped silica tests from pelagic radiolarians that we interpret to have been present in the marine water column at the time of deposition of the rock. Volcanic flows form a minor part of the heterogeneous unit. They consist primarily of 1- to 2-m-thick clinopyroxene andesite flows that we interpret to be interbedded with the tuffaceous rocks.

The three volcanic and sedimentary rock units (Ks, Ka, and Kt) of the Koyukuk terrane in the Stuyahok area have many features in common and probably represent different facies of the same depositional environment. Minor amounts of interbedded felsic tuff, reworked tuff, volcaniclastic sandstone, and radiolaria-bearing siltstone are common to all three units. Miller and others (1996) assigned an Early Cretaceous age to the heterogeneous unit (Kt) of the Stuyahok area on the basis of correlation with similar dated rocks to the north (Patton and Moll-Stalcup, 1996). On the basis of the presence of common lithologies among the sandstone-dominant, volcanic-dominant, and heterogeneous units (Ks, Ka, and Kt, fig. 5) of the

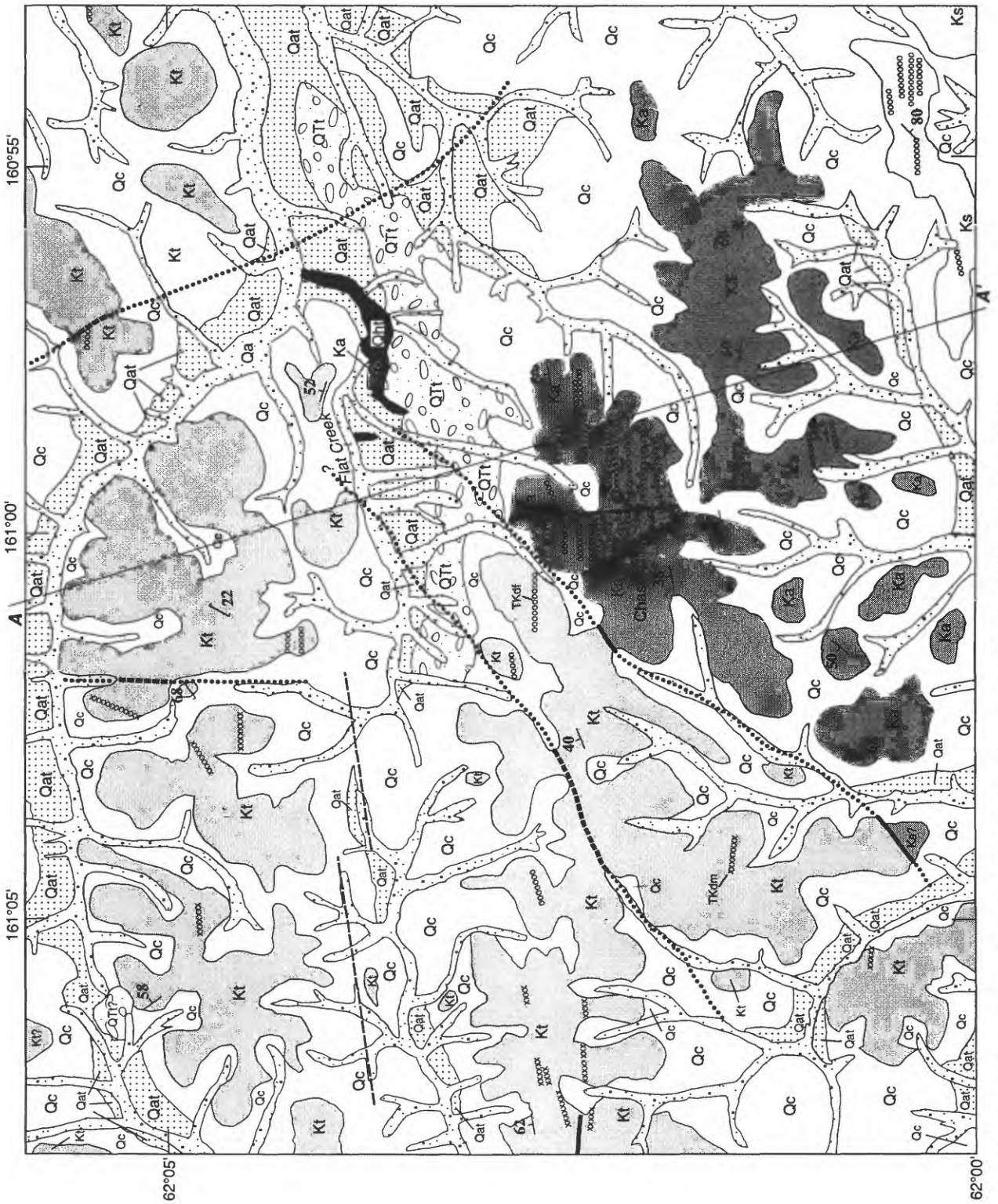

Figure 5. Geologic map and cross section of Stuyahok study area (modified from Miller and others, 1996).

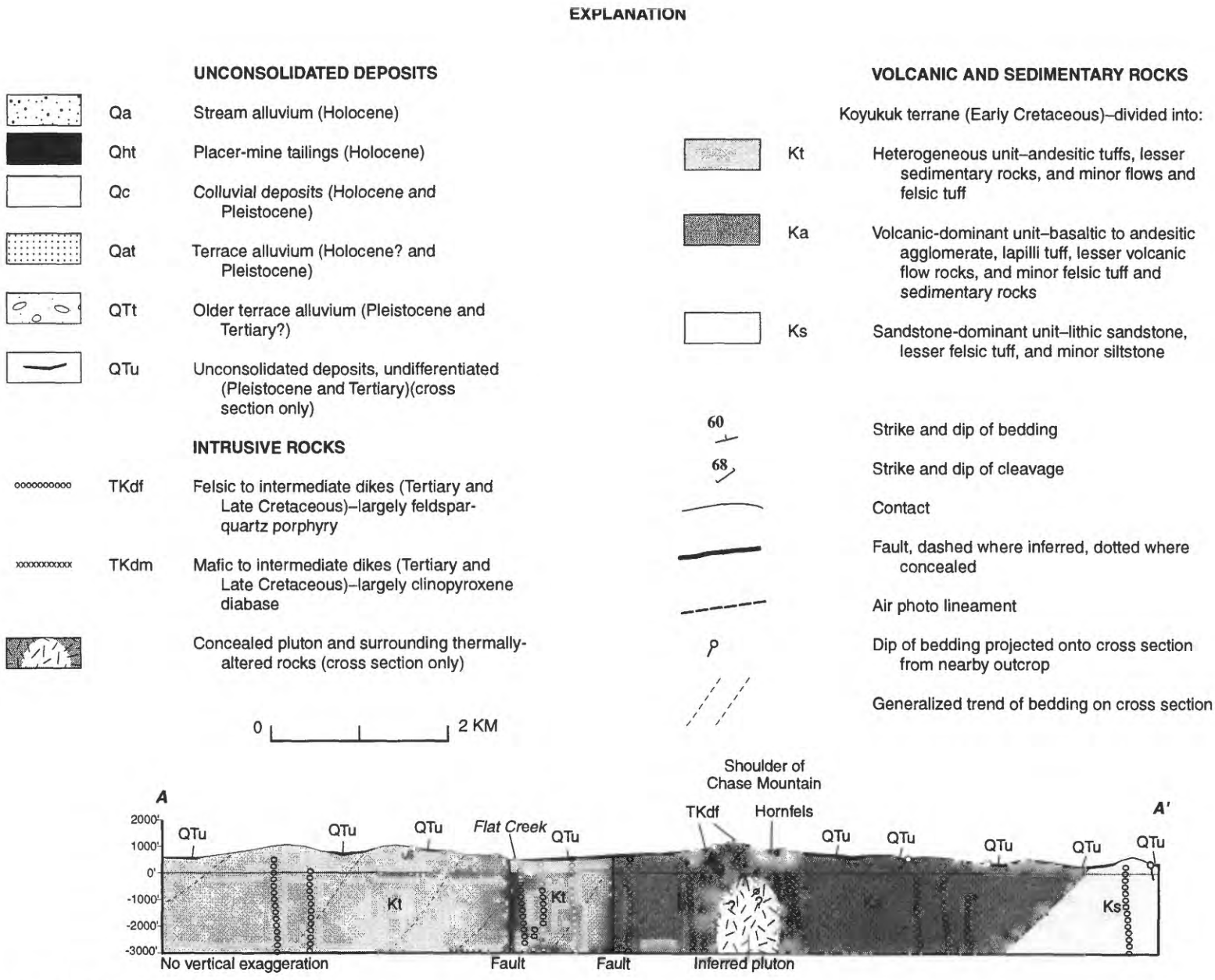

Figure 5. Continued.

Table 1. Petrographic point-count data for the Koyukuk terrane, Stuyahok study area.

[Map units: Ks, sedimentary dominant; Ka, volcanic dominant; Kt, heterogeneous (keyed to text and fig. 5). Rock types: ss, sandstone; lt, lapilli tuff; rt, reworked tuff; xt, crystal lithic tuff. Category abbreviations: Qm, monocrystalline quartz; Qp, polycrystalline quartz; udf, undifferentiated; fol, foliated; ct, chert; pl, plagioclase; ksp, potassium feldspar; Lv, volcanic lithic grains; pp, porphyritic (lathwork); dv, dark iron altered volcanic; mic, microlitic; vit, vitric; fel, felsic; Ls, sedimentary lithic grains; ss, sandstone; ms, metasandstone; ls, limestone; Lm, metamorphic lithic grains; fol, foliated metamorphic; nf, non-foliated metamorphic; cpx, clinopyroxene; hb, hornblende; gar, garnet; ep, epidote; op, opaque]

Map	Sample	Rock	Qm	Qp			Feldspar		Lv					Ls			Lm		cpx	hb	gar	ep	op	Matrix
unit	number	type		udf	fol	ct	pl	ksp	pp	dv	mic	vit	fel	ss	ms	ls	fol	nf						
Ks	95AM020A	ss	33	36	10	12	31	2	43	0	13	0	22	2	13	0	59	18	0	0	0	5	1	20
Ks	95AM023A	ss	26	14	3	2	40	3	120	0	0	0	29	0	5	0	57	0	0	1	0	0	0	29
Ks	95AM024A	ss	24	15	2	5	27	1	70	0	0	0	39	0	9	0	105	0	0	0	1	0	2	26
Ks	95AM025B	ss	9	11	2	9	41	5	83	0	0	0	38	0	12	0	65	24	0	0	0	0	1	36
Ks	95AM080B	ss	58	5	0	0	79	4	70	0	0	0	52	0	0	7	10	9	0	0	0	0	6	33
Ka	95AM002B	lt	1	0	0	0	47	1	249	0	0	1	1	0	0	0	0	0	0	0	0	0	0	33
Ka	95BF010	rt	5	0	0	0	84	0	203	0	0	0	7	0	0	0	0	0	0	0	0	0	1	42
Kt	95WK001A	xt	1	0	0	0	55	2	159	13	18	22	23	0	0	0	0	0	7	0	0	0	0	70
Kt	95WK010C	xt	0	0	0	0	103	1	175	1	3	1	1	0	0	0	0	0	14	0	0	0	1	54
Kt	95AM026A	xt	0	0	0	0	40	3	186	49	0	0	15	0	0	0	0	0	6	0	0	0	0	15
Kt	95BF039	xt	0	0	0	0	79	0	206	2	0	0	3	0	1	0	0	0	9	0	0	0	1	75
Kt	95AM050A	rt	1	0	0	0	88	1	197	1	0	0	0	0	0	0	0	0	12	0	0	0	0	54
Kt	95AM053A	rt	0	0	0	0	98	0	180	0	0	0	1	0	0	0	0	0	20	1	0	0	0	60
Kt	95AM039A	rt	2	0	0	0	142	0	97	39	4	0	0	0	0	0	0	0	11	0	0	0	5	51
Kt	95BF060	rt	0	1	0	0	41	2	204	34	0	7	8	0	0	0	0	0	0	0	0	0	3	36
Kt	95BF064	ss	1	0	0	0	67	2	195	24	1	0	0	0	0	0	0	0	8	0	0	0	2	27

Koyukuk terrane in the Stuyahok area, we assign all an Early Cretaceous age.

Information on the depositional environment for rocks of the Koyukuk terrane in the Stuyahok area may be gained from several sources. Chemical data from the volcanic rocks indicate a calc-alkaline differentiation trend (Miller and others, 1996). Some of the volcanic rocks show subaerial features (agglomerate and airfall tuffs); others are subaqueous (pillow lavas and water-laid tuffs); and the remainder could be either subaerial or subaqueous (crystal lithic tuffs and ash-flow tuffs). The Ks, Ka, and Kt units all have interbedded radiolarian-bearing siltstone or tuffaceous siltstone, which indicate deposition in a marine environment. This evidence suggests that deposition of the various Koyukuk terrane lithologies was near an emergent/submergent margin of a marine basin. A younger example of such an environment is well preserved on Adak Island (part of the Aleutian arc), where strata of the late Eocene Andrew Lake Formation include pyroclastic ejecta and radiolarian-bearing tuffaceous mudstones that accumulated in shallow sea water on the flanks of an active volcanic complex (Hein and McLean, 1980).

Five samples from sandstones from the sedimentary-dominant unit and one from the heterogeneous unit plot in or near the undissected magmatic-arc province of Dickinson (1985) on a Q-F-L diagram (fig. 6). However, the Paleozoic fossil debris in one sample from the Ks unit indicates that some older rocks were also being eroded. About 9 km to the west of the study area, Mesozoic and Paleozoic oceanic volcanic rocks contain pods of crinoid-bearing limestone. Similar limestone could have been the source of the crinoid clasts found in sandstones from the Stuyahok study area. The Mesozoic and Paleozoic volcanic unit appears to correlate with rocks of the Angayucham-Tozitna terrane, which was obducted onto the continental margin by mid-Cretaceous time (Patton and others, 1994).

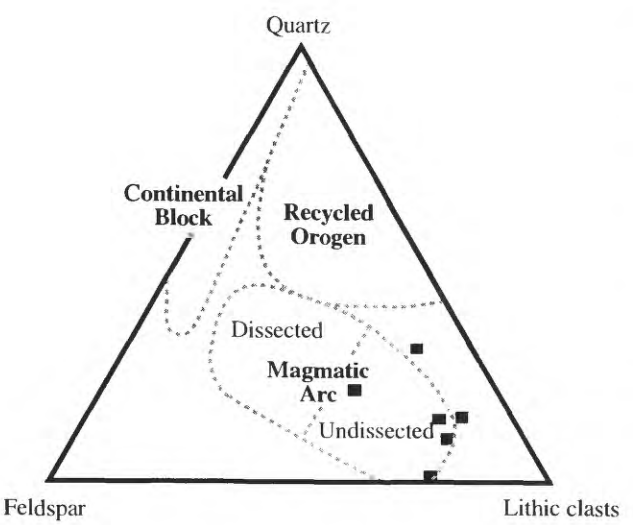

Figure 6. Framework modes of sandstones from Stuyahok study area. Provenance fields from Dickinson (1985).

INTRUSIVE ROCKS

Rocks of the Koyukuk terrane in the Stuyahok area are cut by two types of dikes—(1) felsic to intermediate (largely feldspar-quartz porphyry dikes) and (2) mafic to intermediate (largely clinopyroxene diabase dikes). The dikes are normally 1 to 3 m in width, but, on the basis of rubble exposure, some of the mafic dikes may be much wider. The dikes are poorly exposed and discontinuous; we cannot rule out that some may be sills.

Felsic dikes are found primarily in the central and eastern parts of the map area. They show a strong east-west orientation and form a dense swarm in the Chase Mountain area. The felsic dikes exhibit porphyro-aphanitic textures and contain 5 to 25 percent quartz, plagioclase, and biotite phenocrysts in a finer grained groundmass, hence we call them feldspar-quartz porphyry dikes. Clinopyroxene and hornblende grains are found locally. Granodiorite and granite are the most common compositions, but more intermediate varieties may be present locally. Alteration of the felsic dikes is extensive and includes assemblages of chlorite, white mica, calcite, and opaque minerals. On the basis of the presence of granite porphyry dike rubble in exploration trenches and soil auger holes, we believe that additional west-trending feldspar-quartz porphyry dikes lie concealed beneath the unconsolidated cover on the south side of Flat Creek, north and northwest of Chase Mountain (fig. 5). Although no isotopic age data are available, Miller and others (1996) assigned these dikes a Late Cretaceous and early Tertiary age because (1) they intrude Lower Cretaceous rocks, and (2) they are petrographically similar to Late Cretaceous and early Tertiary peraluminous granite porphyry mapped and dated 161 km to the east at Donlin Creek and elsewhere in the Iditarod quadrangle (Miller and Bundtzen, 1994), as well as at Willow Creek near Marshall (T.K. Bundtzen, unpub. data, 1991) (fig. 1). The felsic dikes in the Iditarod quadrangle and at Willow Creek are peraluminous, biotite-quartz-feldspar porphyritic granite and granodiorite, similar petrographically to the felsic dikes in the Stuyahok area. In all three areas, the dikes are generally 1 to 3 m thick and form subparallel swarms. In the Iditarod quadrangle, the felsic dikes generally trend northeast, but at Willow Creek and in the Stuyahok study area, they trend east-west.

Mafic to intermediate dikes are found primarily in the western half of the map area. They are diabasic to subophitic in texture and are primarily composed of clinopyroxene, plagioclase, and accessory magnetite; lo-

cally they contain minor quartz. The dikes commonly exhibit chloritic alteration. No isotopic age data are available, but these dikes were also assigned a Late Cretaceous and early Tertiary age by Miller and others (1996) because (1) they intrude Lower Cretaceous rocks of the Koyukuk terrane, and (2) they are petrographically similar to Late Cretaceous and early Tertiary mafic to intermediate dikes mapped and dated 130 km to the east (Miller and Bundtzen, 1994).

Tuffs and lava flows of the Koyukuk terrane in the study area have undergone low-grade regional metamorphism to laumontite and locally prehnite-pumpellyite facies. Thermally altered (maximum grade of hornblende-hornfels facies) volcaniclastic and flow rocks on Chase Mountain (fig. 3) suggest that the mountain is underlain by a buried pluton. Felsic dikes on Chase Mountain show no secondary minerals or textures indicative of thermal alteration, which suggests that the dikes postdate the pluton intrusion. However, their felsic composition would not necessarily yield diagnostic minerals under hornblende-hornfels facies conditions, so we cannot rule out that the dikes predate the pluton intrusion. Signs of hydrothermal alteration are present in both the felsic dikes and the enclosing volcaniclastic and flow rocks—the dikes are extensively sericite altered, and the enclosing country rock has disseminated pyrite.

UNCONSOLIDATED UNITS

Surficial deposits of late Tertiary(?) and Quaternary age cover about 70 percent of the study area. Placer mine tailings and stream alluvium of Holocene age are the youngest deposits. Ancestral stream drainages adjacent to modern streams are represented by locally extensive terrace gravels of two ages. The older terrace deposits may be as old as late Tertiary by analogy to similar older terrace gravels found throughout unglaciated interior Alaska (Karl and others, 1988). Extensive colluvial deposits cover the hillsides. The surficial deposits are commonly mantled by vegetation. Regional tilt to the west or northwest(?) in mid- to Late Quaternary time is suggested on the south side of Flat Creek by stream piracy of several small tributaries that may have been shifted to newer west-trending channels.

STRUCTURE

The study area has west-, northeast-, north-, and northwest-trending structural elements. Bedding strikes and dike trends are generally west; most faults trend northeast, but some trend north or northwest. The Lower Cretaceous rocks are tilted an average of 50 degrees, but structural control in the map area is too sparse for us to define folds. The rocks show no tectonic foliation in either outcrop or thin section. The study area is cut by several high-angle faults. Most significant of these are two northeast-trending faults, one of which forms the contact between the heterogeneous and volcanic-dominant units of the Koyukuk terrane (units Kt and Ka, fig. 5). These faults are not well exposed and their displacements are not known, but rocks that lie between the two faults have variable bedding strikes, suggesting structural disruption. North- and northwest-trending lineaments exposed on Chase Mountain are recognized on air photos but do not have demonstrable displacement. A northwest-trending fault in the northeast part of the study area was interpreted from air photos, but relative movement is not known. Dikes generally trend west and are interpreted to be near-vertical on the basis of their relatively straight trends across topography. Hence, they postdate the regional deformation, which must have occurred prior to Late Cretaceous-early Tertiary time.

The style of deformation in the Stuyahok study area closely resembles that displayed in rocks of the Koyukuk terrane that lie to the west and northwest (Patton and others, 1994; Patton and Moll-Stalcup, 1996). The Koyukuk terrane was accreted to continental North America in latest Jurassic to Early Cretaceous time (Patton and others, 1994). Subsequent east-west compression, probably related to convergence of the North American and Eurasian plates, led to the development of north- to northeast-oriented folds and faults in western Alaska in Late Cretaceous time (Patton and Box, 1989; Patton and Moll-Stalcup, 1996).

ECONOMIC GEOLOGY

Placer deposits of the Stuyahok area are part of the combined Marshall and Anvik mining districts (for example, Smith, 1933; Joesting, 1942; Malone, 1965; Cobb, 1973). Lower Flat Creek and limited sections of its gold-bearing tributaries were mined from 1921 to 1940, and again from 1986 to the present. On the basis of figures reported by Cobb (1973), we estimate that about 746 kg (24,000 oz) of placer gold was produced through 1940. No mining activity was reported from the area for the next 45 years. In 1971, under the Alaska Native Claims Settlement Act, Calista Corporation acquired entitlements to approximately 7 million acres in southwestern Alaska, including the Stuyahok placer mine area. Calista Corporation contracted Resource Associates of Alaska (RAA) to perform a geologic and geochemical reconnaissance investigation of the selected area in 1974 and 1975. From 1983 to 1992 Calista Corporation performed limited geologic mapping and geochemical sampling along Flat Creek and south to Chase Mountain. Placer mining began again in the Stuyahok-Flat Creek area in 1986 on

ground leased from Calista. Small-scale mining was performed from 1986 to 1989 by Chase Brothers Mining. Mining resumed again in 1991 under Stuyahok Mining Company (Retherford and McAtee, 1994) and continues to the present. Based on State of Alaska production records for the Marshall and Anvik districts, we estimate that a total of about 933 kg (30,000 oz) of gold has been produced in the Stuyahok area through 1996.

Lode sources for the placer gold in the Stuyahok study area are not known with certainty. In other parts of southwestern Alaska, placer gold is associated with four different bedrock sources (Bundtzen and Miller, 1997). The two main sources are (1) plutonic-hosted copper-gold-polymetallic deposits associated with volcanic-plutonic complexes and (2) peraluminous granite-porphyry-hosted gold-polymetallic deposits. In addition, some placer gold is derived from mid-Cretaceous granitic plutons; Jurassic zoned ultramafic complexes are a fourth, minor source. Possible lode sources in the Stuyahok area include peraluminous granite porphyry dikes and mineralized veins of uncertain origin (possibly related to the postulated buried pluton). To examine these possibilities, we will discuss the exploration geochemical data, the heavy-mineral placer deposits, and the potential bedrock sources.

EXPLORATION GEOCHEMICAL STUDIES

For this study, we collected 43 stream-sediment, 33 heavy-mineral-concentrate, 114 soil, and 270 rock samples that were geochemically analyzed. These new data were published by Bailey and others (1996) and Keith and others (1996), along with older geochemical data from samples collected by RAA in the 1970's and by Calista Corporation in the 1980's. Miller and others (1996) summarized the geochemical threshold values for elements of economic interest from various parts of the study area. Because the geochemical data base for the Stuyahok study area includes a variety of sample media analyzed by three different labs in different years, caution must be exercised in data comparison. For this paper, we did not use the original RAA data, but rather the data from splits of those samples that were reanalyzed in 1989 by Bondar-Clegg. Despite this precaution, some inconsistencies were noted between the older data (Bondar-Clegg's from 1989) and the newer data (Chemex Labs' from 1995), specifically that the Ag and As values are two to four times higher, and the Sb and Bi values are an order of magnitude higher in the older data set. With these limitations in mind, we note scattered Ag, As, Bi, Cd, Cu, Hg, Pb, Sb, and Zn anomalies in the study area, but the values are typically neither high enough, nor consistent enough, to define target areas for further exploration for these metallic resources. The rock sample data illustrate the relatively low values for these elements—anomalous values at the 90th percentile are 0.2 ppm Ag, 20 ppm As, 6 ppm Bi, 0.5 ppm Cd, 97 ppm Cu, 100 ppb Hg, 24 ppm Pb, 2 ppm Sb, and 108 ppm Zn.

Additional resources of gold in the study area are delineated by anomalous gold concentrations, which, for this reconnaissance study, are any gold values above the limit of determination. Combining the older and newer data sets, of the 293 rock samples, 5 carried gold $\geq$5 ppb; of the 96 stream-sediment samples, 16 carried gold $\geq$5 ppb; of the 33 heavy-mineral concentrate samples, 9 carried gold $\geq$10 ppb; and of the 116 soil samples, 5 carried gold >5 ppb. Collection sites of all the samples that contain gold above the detection limit are plotted in figure 7, and their gold concentrations are summarized in table 2, together with concentrations of other elements of interest, whether anomalously high or not. Anomalous concentrations of Hg, As, and Sb are sporadically present in the gold-bearing samples. Locally, the gold-bearing stream-sediment samples contain as much as 2 ppm Hg, 364 ppm As, and 28 ppm Sb; gold-bearing soil samples contain as much as 0.11 ppm Hg and 24 ppm As; and gold-bearing rock samples contain as much as 0.62 ppm Hg, 297 ppm As, and 90 ppm Sb. However, the values of these anomalies are relatively low, and the elemental suite is not consistently present, making it a poor pathfinder for gold resources. Likewise, anomalous concentrations of Zn, Pb, and Bi are inconsistent in the gold-bearing samples. The single best indicator of gold resources seems to be anomalous Au concentrations in stream sediments, heavy-mineral concentrates, soils, and rocks.

The gold data delineate areas that may contain additional gold resources. Last Chance Creek (fig. 7) has not been mined, but stream-sediment samples collected from the active channel contain 6 to 20 ppb gold (n = 9, table 2). Such consistent concentrations may indicate significant placer gold on this creek. A heavy-mineral-concentrate sample from a spring that drains into Last Chance Creek contains 33 ppm gold (map number 18, fig. 7 and table 2). Feldspar-quartz porphyry dike cobbles found at this spring suggest that felsic dikes are concealed beneath the unconsolidated cover. Two float samples, one of which is felsic dike, from Last Chance Creek contain 5 and 7 ppb gold (map numbers 20 and 26, fig. 7 and table 2), suggesting that gold is associated with some of the felsic dikes.

In addition to the 33 ppm Au in a concentrate sample, five other stream-sediment and heavy-mineral-concentrate samples yield gold values greater than 100 ppb. A heavy-mineral-concentrate sample from the active channel on Trail Creek (which drains Chase Mountain) contains 2.2 ppm gold (map number 29, fig. 7 and table 2); gold was not detected in the stream-sediment sample from

locality. While such gold is notable, it remains a one-sample anomaly. However, the four remaining stream-sediment and heavy-mineral-concentrate samples that have more than 100 ppb gold came from the Flat Creek area, where gold was detected in soil and rock samples as well.

One stream-sediment and three heavy-mineral-concentrate samples from two active channels and one spring that drain the terrace on the south side of Flat Creek, north and northwest of Chase Mountain (map numbers 7, 9, and 11, fig. 7 and table 2), contain 140 to 1,080 ppb gold. The current mine operator is working a north-limit bench of Flat Creek, which on air photos continues for as much as 3.2 km upstream from the present workings. Samples containing anomalous gold collected farther upstream suggest a potential for placer gold in extensions of the north-limit bench. Soil samples from one transect northwest of Hazel Gulch and from one transect just north of Flat Creek (map numbers 12 and 14, respectively, fig. 7 and table 2) contain up to 295 ppb gold. A secondary hematite-bearing, altered felsic tuff sample from the same general area (map number 13, fig. 7), contains 10 ppb gold. West-trending feldspar-quartz porphyry dikes are probably concealed beneath the unconsolidated cover in this same area. The collective data suggest a concealed bedrock gold resource in this area.

Rock samples from the Stuyahok study area yielded few anomalous gold concentrations. Besides the three rocks mentioned previously, only two other samples contain gold above the lower limit of determination. Both are from the north flank of Chase Mountain (map numbers 4 and 5, fig. 7 and table 2) and yielded 10 and 7 ppb

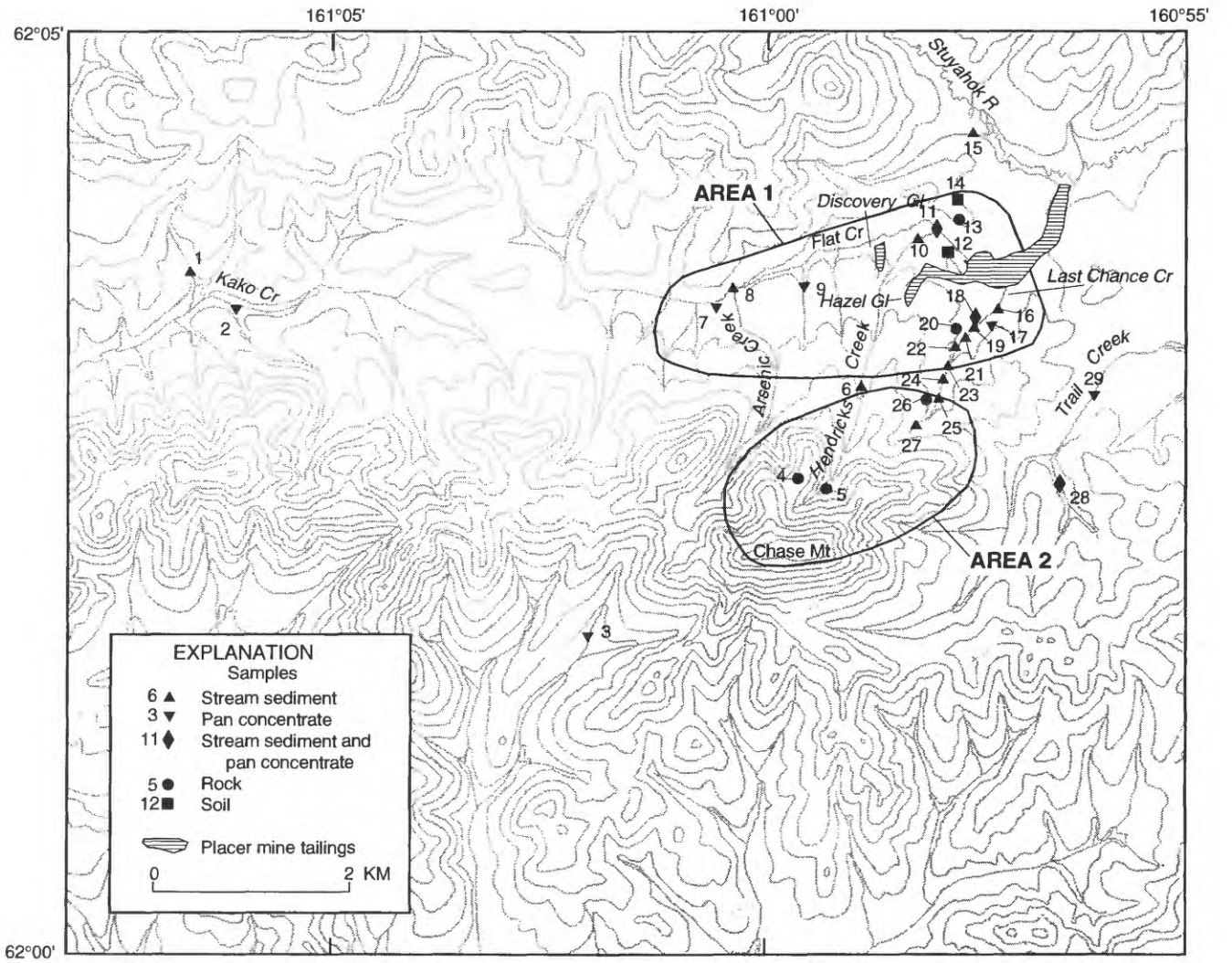

Figure 7. Map showing location of stream-sediment, heavy-mineral-concentrate, soil, and rock samples that have gold concentrations above lower limit of determination; map numbers are keyed to table 2. Placer mine tailings and possible bedrock resource Areas 1 and 2 are also shown. Gl, gulch.

Table 2. Concentrations of gold and other elements of interest in samples from the Stuyahok study area.

[Map number refers to fig. 7. Lower limit of gold determination is 10 ppb in the heavy-mineral-concentrate samples and 5 ppb in all other samples. Collector and lab: 1, collected by USGS and analyzed by Chemex Labs; 2, collected by Research Associates of Alaska in 1974-75 and reanalyzed in 1989 by Bondar-Clegg; 3, collected by Calista Corporation and analyzed by Bondar-Clegg in 1985]

Map number	Sample number	Gold[1, 2] (ppb)	Additional elements of interest[2] (ppm)	Geographic description and/or other information	Collector; lab
			Stream-sediment samples		
1	95AEb020	(-200) **35**	As(46), **Bi(2)**, **Hg(0.28)**, Zn(94)	Upper Kako Cr., active channel	1
11	95AEb043	(-80) **1080**	**Ag(0.2)**, As(54), **Bi(2)**, **Cd(1)**, **Pb(50)**, **Zn(178)**	Lower Hendricks Cr., active channel	1
18	95AEb041	(-200) **15**	**Ag(1.6)**, **As(96)**, **Cd(0.5)**, **Hg(0.37)**, **Sb(8)**, **Zn(154)**	Spring near Last Chance Cr.	1
28	95AEb032	(-200) **25**	**Bi(2)**, **Cd(0.5)**, **Hg(0.45)**, Zn(118)	Headwaters Trail Cr., active channel	1
6	RAA2233	**5**	**Ag(0.7)**, As(76), Bi(12), Hg(0.10), Sb(21)	North side of Chase Mt., active channel	2
8	RAA7816	**28**	Ag(0.4), **As(364)**, Bi(14), **Hg(2.05)**, **Pb(80)**, Sb(18), **Zn(131)**.	Arsenic Cr., active channel	2
10	RAA2241	**36**	Ag(0.2), As(106), **Bi(21)**, **Sb(28)**, Zn(109)	Lower Hendricks Cr., active channel	2
15	RAA8623	**10**	As(38), Bi(16), Sb(16)	Side creek draining into Stuyahok R.	2
16	RAA2396	**6**	As(73), Bi(11), Sb(17)	Last Chance Cr., active channel	2
19	RAA2394	**6**	As(71), Bi(13), Sb(18)	Last Chance Cr., active channel	2
21	RAA2393	**11**	As(66), Bi(12), Sb(12)	Last Chance Cr., active channel	2
22	RAA2392	**8**	As(86), Bi(15), Hg(0.10), Sb(20)	Last Chance Cr., active channel	2
23	RAA2391	**6**	As(73), Bi(11), Sb(20)	Last Chance Cr., active channel	2
24	RAA2390	**6**	As(82), Bi(14), Sb(18)	Last Chance Cr., active channel	2
25	RAA2388	**20**	As(57), Bi(12), Sb(15)	Last Chance Cr., active channel	2
27	RAA2385	**6**	As(65), Bi(16), Sb(21)	Last Chance Cr., active channel	2
			Heavy-mineral-concentrate samples[3]		
2	95AEb022	**20**	As(17), Sb(1)	Upper Kako Cr., active channel	1
3	95AEb010	**81**	As(56), Sb(5)	Southwest of Chase Mt., active channel	1
7	95AEb003A	**140**	As(11), Sb(8)	Spring near Arsenic Cr.	1
9	95AEb006*	**250**	**As(90)**, **Sb(14)**	Babe Cr., active channel	1
11	95AEb043*	**965**	As(37), **Sb(16)**	Lower Hendricks Cr., active channel	1
17	95AEb042*	**10**	As(40), Sb(9)	Last Chance Cr., active channel	1
18	95AEb041	**32,700**	**As(93)**, **Sb(30)**	Spring near Last Chance Cr.	1
28	95AEb032	**13**	As(15), Sb(2)	Headwaters of Trail Cr., active channel	1
29	95AEb009*	**2,160**	As(14), Sb(2)	Trail Cr., active channel	1
			Soil samples		
12	Line 7-1087	**120**	As(16), Hg(0.06)	Mineral soil and some felsic dike	1
12	Line 7-1088	**185**	As(16), Hg(0.10)	Mineral soil and decomposed bed rock	1
12	Line 7-1088B+	**95**	As(10), **Hg(0.11)**	Duplicate of 1088B	1
12	Line 7-1090	**230**	As(24), Hg(0.09)	Mineral soil and some felsic dike	1
14	Line 8-1100	**295**	As(6), Hg(0.04)	Medium-brown soil	1
			Rock samples		
4	95BF012	**10**	Bi(4), Cu(80), **Zn(120)**	Silicified tuff, secondary opaque minerals.	1
13	95AM001C	**10**	**Ag(0.4)**, **As(102)**, **Cu(97)**, **Hg(0.62)**, **Sb(8)**, **Zn(116)**.	Felsic tuff; secondary hematite	1
5	RAA2229	**7**	**As(297)**, Bi(42), Cu(77), Hg(0.45), **Sb(90)**	Unknown rock type	2
20	Calista S22	**5**	As(53), Hg(0.13)	Feldspar-quartz porphyry dike	3
26	RAA2389	**7**	As(150), Bi(23), Hg(0.29), Sb(33)	Unknown rock type	2

[1] Sieve mesh fraction given in parentheses.

[2] Boldface type indicates anomalous concentration (about the 90th percentile or greater). Note, percentiles were calculated separately for each sample media and laboratory combination (for example, stream-sediment samples analyzed by Chemex Labs, stream-sediment samples analyzed by Bondar-Clegg, heavy-mineral-concentrate samples analyzed by Chemex Labs, etc.).

[3] Samples marked by an asterix contained visible gold in the pan.

Au, respectively. The former sample is a silicified tuff containing secondary opaque minerals. We are not certain of the significance of these few gold values. Numerous felsic dikes trend west across Chase Mountain, which may be underlain by a concealed pluton.

HEAVY MINERAL PLACER DEPOSITS

The heavy-mineral placer deposits of the Stuyahok area are in stream gravels of Quaternary age, along about 3.2 km of Flat Creek and in two small tributaries or gulches of Flat Creek (fig. 7). We estimate total production through 1996 to be 933 kg (30,000 oz) gold and about 205 kg (6,600 oz) byproduct silver from approximately 573,500 m^3 gravel, or at an average recoverable-gold grade of 1.6 g/m^3. The auriferous gravels are shallow stream deposits averaging about 2.7 m in thickness that are covered by about 2.4 m of overburden. The gold occurs in the lowest 1.2 m of gravel, above the weathered bedrock surface and within weathered bedrock.

Mine-concentrate samples collected from Flat Creek contain abundant pyrite, magnetite, and ilmenite, and lesser amounts of cinnabar, arsenopyrite, garnet, stibnite(?), and monazite, in addition to gold. The gold grains are flat and locally exhibit pitted and vermicular textures. Only a small fraction of the gold exceeds 10-mesh size and no nuggets of size have been reported. We are uncertain if the vermicular texture observed in some of the grains is a primary texture or one developed during a silver-leaching (weathering) event. Some gold grains show intricate sunburst-like muscovite inclusions (fig. 8). This texture suggests the muscovite is a primary igneous mineral (Bart Cannon, Cannon Microprobe, oral commun., 1996).

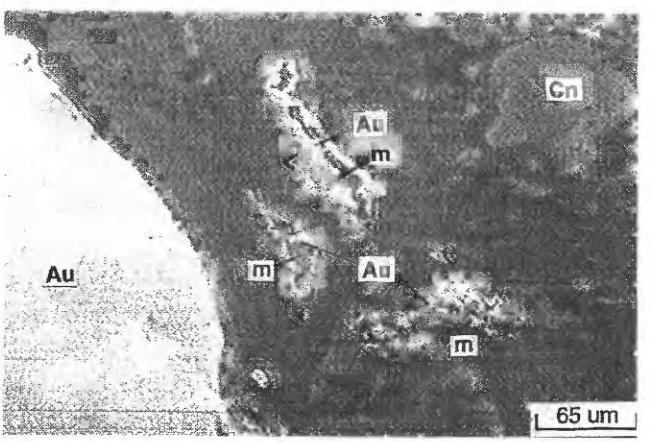

Figure 8. Photomicrograph of gold (Au) enclosing sunburst-shaped muscovite (m) and cinnabar (Cn) grains in iron oxide matrix. Photo by Cannon Microprobe, Inc.

Two records of gold fineness[2] from the Stuyahok area—presumably from Flat Creek—range from 772 to 802.5 and average 787 (Smith, 1941). An unpublished analysis of a gold sample collected in 1935 by J.B. Mertie, Jr., of the USGS, from a Stuyahok placer mine operation shows a gold fineness of 809.5. Microprobe analyses of 14 gold grains from a heavy-mineral-concentrate sample collected during this study (95BT246) show fineness values ranging from 644 to 891, and averaging 774 (table 3), similar to the 787 average fineness reported by Smith (1941) from the Stuyahok area. Most of the microprobed grains cluster between 731 and 835 in fineness (n=11); however, two grains have a lower fineness (about 650) and one has a high value of 891. Gold grains from the same lode source generally have similar fineness values, but chemical changes along the transport route can alter the fineness. Because our sample of 14 grains came from a single site in the active mine cut, the presence of these low and high values suggests that more than one lode zone contributed gold to the placer.

The microprobe data show that Ag is the most common impurity in the Flat Creek placer gold grains. In addition, Sb was detected in 5 of the 14 grains, Hg in 11, and Cu in only 1 grain. Problems with standards prevented reliable determination of Bi (Bart Cannon, Cannon Microprobe, written commun., 1996), so the totals have been recalculated to 100 percent without Bi, which did not exceed 2.8 percent. Other metals including PGEs, Pb, As, and Zn were not detected in the samples. The geochemistry of the gold grains suggests a Ag-Au-Sb-Hg-dominant metal suite in at least one of the lode sources. Such a suite is most characteristic of the epithermal Hg-Sb vein deposits that are widespread in southwestern Alaska (Sainsbury and MacKevett, 1965; Goldfarb and others, 1990). One grain of cinnabar from the Flat Creek concentrate (sample 95BT246) was microprobed, and contains 0.134 percent Au, which supports a genetic connection between Au and Hg.

POSSIBLE BEDROCK SOURCES

Gold was detected in only five rock samples (table 2), two of which were of unknown rock type (RAA2229 and RAA2389), so it is difficult to determine bedrock source(s) of the gold. Of the remaining three rocks that contain detectable gold, one is feldspar-quartz porphyry dike (Last Chance Creek drainage, map number 20, fig. 7), one is hematite-altered felsic tuff (north-limit cut bank of Flat Creek, map number 13, fig. 7), and the last is silicified tuff (north flank of Chase Mountain, map number 4, fig. 7).

[2] Fineness, calculated in parts per thousand, indicates the proportion of gold present in a gold grain. Thus a grain containing 77.2 percent Au has a fineness of 772.

Table 3. Microprobe analyses of fourteen 6- to 40-mesh placer-gold grains (sample 95BT246) from Flat Creek, Stuyahok River drainage, Marshall-Anvik district, Alaska.

[All values in percent. Gold grains were analyzed using ARL SEMQ electron microprobe (25 KV accelerating voltage, 0.05 μA beam current) by Cannon Microprobe Inc., which was equipped with six wavelength dispersive GE XRD-6 x-ray spectrometers (35 KV accelerating voltage, 10 mA beam current). Standards were pure metal for Au, Ag, Cu, and Sb; HgS for Hg. Backgrounds for other metals were obtained using mean atomic number]

Grain number	Au	Cu	Sb	Ag	Hg	Totals*
143	73.094	0.000	0.000	25.756	0.135	98.985
144	66.051	0.000	0.000	34.103	0.172	100.326
147	81.054	0.000	0.000	17.451	0.252	98.757
148	76.254	0.000	0.013	23.696	0.259	100.222
151	73.883	0.000	0.000	26.192	0.310	100.385
152	83.506	0.000	0.000	15.718	0.000	99.224
153	77.322	0.124	0.000	21.556	0.540	99.542
156	80.333	0.000	0.000	19.939	0.094	100.366
319	89.137	0.000	0.000	11.741	0.000	100.878
320	75.510	0.000	0.096	23.788	0.077	99.471
325	64.432	0.000	0.077	35.559	0.460	100.528
322	78.850	0.000	0.098	21.729	0.000	100.677
326	81.447	0.000	0.000	19.159	0.076	100.682
327	82.424	0.000	0.062	17.204	0.255	99.945
Average ---	77.378	0.009	0.025	22.399	0.188	99.999

* Totals recalculated less Bi, which ranged from 0 to 2.8%, but which was not reliable due to problems with standards.

On the basis of several lines of evidence, we suggest that the most promising lode targets in the study area are mineralized feldspar-quartz porphyry dikes and associated country rock, much like the gold-polymetallic-associated, peraluminous granite-porphyry dikes found in other parts of the Kuskokwim mineral belt (Bundtzen and Miller, 1997). The placer gold in Flat Creek is found downslope or downstream from west-trending feldspar-quartz porphyry dikes. Similarly, the gold anomalies in sediments from Last Chance Creek are also spatially associated with feldspar-quartz porphyry dikes. Mine concentrate samples from Flat Creek contain garnet, cinnabar, and arsenopyrite, characteristic of the heavy minerals associated with placer gold derived from granite-porphyry-hosted, gold-polymetallic deposits (Bundtzen and Miller, 1997). Soil samples from the Flat Creek area contain gold (from 95 to 295 ppb), and one feldspar-quartz porphyry dike from Last Chance Creek contains gold above the limit of determination. In peraluminous granite-porphyry-hosted, gold-polymetallic deposits, gold is found in both the dikes themselves and the enclosing country rock (Bundtzen and Miller, 1997). It is possible that the two gold-bearing tuff samples were spatially associated with unrecognized feldspar-quartz porphyry dikes.

Lode targets for further exploration are concentrated in two areas of mineralized feldspar-quartz porphyry dikes (fig. 7). The first area is defined by a west-trending, 2.4-km-long zone of feldspar-quartz porphyry and granodiorite dikes discontinuously exposed in Flat Creek, Hazel Gulch, and Discovery Gulch, and probably also in the lower reaches of Last Chance Creek (Area 1, fig. 7). The second area lies about 1.6 km south of the first and is defined by at least a dozen vertically-dipping felsic to intermediate dikes that intrude Chase Mountain (Area 2, fig. 7). Geochemical data for selected elements from all analyzed felsic dike samples from Area 1 (15 samples) and Area 2 (21 samples) are presented in table 4. Although the dikes are petrographically similar in these two areas, their geochemical signatures are slightly different.

In Area 1, feldspar-quartz porphyry dikes near the placer workings (fig. 7) locally contain sparsely disseminated arsenopyrite, pyrite, and stockwork quartz veins that extend into the volcanic country rocks in some places. Argillic, carbonate, and chalcedonic alteration are found locally in feldspar-quartz porphyry samples from both Hazel and Discovery Gulches. Four of six grab samples of dike rock from these gulches (table 4) contain elevated As (as much as 636 ppm), Hg (as much as 3,290 ppb), Sb (as much as 60 ppm), and locally Ag (as much as 0.36 ppm), but no detectable Au. Feldspar-quartz porphyry dike rocks from the lower part of Last Chance Creek in Area 1 are highly weathered and locally show extensive limonitic alteration. Three of five rock grab samples from here contain elevated concentrations of As (as much as 80 ppm), Hg (as much as 550 ppb), and locally Ag (as much as 0.4 ppm); one sample contains 5 ppb Au. Elevated values of As, Hg, Sb, and Ag are present locally in feldspar-quartz porphyry dike samples from the south side of Flat Creek. On the north side of Flat Creek (map

Table 4. Selected analytical results from all felsic dike (largely feldspar-quartz porphyry) samples collected in Area 1 and Area 2 (fig. 7).

[Sample locations and complete analytical results are given in Keith and others (1996). Samples collected for this study (sample numbers preceded by "95") were analyzed by Chemex Labs. All other samples were analyzed by Bondar-Clegg. Analytical methods used were as follows: fire assay for Au (detection by atomic absorption spectrometry), cold vapor atomic absorption for Hg, and inductively coupled plasma-atomic emission spectroscopy for other elements—except for samples collected by Calista. For these samples (sample numbers preceded by "Calista") Ag, Pb, and Zn were determined by atomic absorption spectrometry and As was determined by colorimetry. Detection limits for some elements varied by lab and (or) analytical method. Detection limits for each element are as follows (values in parentheses in the table had the limits that follow in parentheses here): Au, 5 ppb; Ag, 0.2 ppm (0.02 ppm); As, 2 ppm (5 ppm); Bi, 2 ppm; Cd, 0.5 ppm; Hg, 10 ppb (5 ppb); Pb, 2 ppm; Sb, 2 ppm (5 ppm); and Zn, 2 ppm (1 ppm). na, not analyzed]

Sample number	Secondary minerals or sulfides noted	Au (ppb)	Ag (ppm)	As (ppm)	Bi (ppm)	Cd (ppm)	Hg (ppb)	Pb (ppm)	Sb (ppm)	Zn (ppm)
				AREA 1						
95AEb003A	Not known if present	<5	<0.2	12	<2	2.0	20	6	<2	272
95AEb041	Not known if present	<5	0.2	80	<2	<0.5	550	22	<2	32
95AM085A	White mica, chlorite	<5	<0.2	10	<2	<0.5	20	4	<2	58
95AM085B	Hematite	<5	<0.2	20	<2	<0.5	360	6	2	14
95AM086A	Pyrite in quartz vein	<5	(0.36)	22	2	<0.5	10	20	<2	54
95BT243Z	Chalcedony	<5	(0.36)	34	2	<0.5	3,290	34	16	82
95BT244B	Hematite	<5	<0.2	16	<2	<0.5	340	16	2	62
95BT244Z	Chalcedony healed breccia	<5	<0.2	636	<2	3.0	2,270	28	60	328
95BT245	Hematite, white mica	<5	<0.2	14	4	<0.5	20	12	<2	58
RAA7814R	Opaques, silica, clay	<5	0.7	(148)	41	na	(3500)	60	(57)	(195)
RAA7815R	Disseminated pyrite	<5	0.3	(87)	20	na	(4400)	20	(27)	(184)
Calista S1	Not known if present	<5	0.4	37	na	na	(35)	17	na	(49)
Calista S7	Limonite, carbonate, quartz	<5	0.3	80	na	na	(1950)	7	na	(108)
Calista S10	Not known if present	<5	<0.2	38	na	na	(110)	7	na	(76)
Calista S22	Not known if present	5	<0.2	53	na	na	(130)	11	na	(40)
				AREA 2						
95AEb031	Not known if present	<5	<0.2	58	<2	<0.5	100	20	<2	46
95AM004C	Chlorite, calcite, opaques	<5	<0.2	4	<2	<0.5	20	<2	<2	48
95AM005D	White mica, chlorite, calcite	<5	<0.2	6	2	<0.5	30	82	2	76
95AM005E	Hematite, white mica	<5	<0.2	6	<2	<0.5	150	14	2	44
95AM005F	White mica, opaques	<5	<0.2	104	<2	<0.5	100	24	4	64
95AM006A	Pyrite, white mica, calcite	<5	<0.2	10	<2	<0.5	10	12	2	54
95AM007A	Opaques, white mica, chlorite	<5	<0.2	2	<2	<0.5	10	12	<2	58
95AM008C	Pyrite, white mica, chlorite	<5	(0.24)	12	2	<0.5	10	14	<2	82
95AM033A	Opaques, calcite, chlorite	<5	<0.2	6	<2	<0.5	<10	8	4	46
95AM035A	Opaques, calcite, chlorite	<5	<0.2	<2	<2	<0.5	<10	8	2	52
95AM083A	Limonite, white mica	<5	(0.40)	30	<2	5.0	170	224	2	460
95AM083B	Pyrite, calcite	<5	(0.32)	10	2	<0.5	<10	22	2	40
95BF003	Disseminated pyrite, chlorite	<5	<0.2	12	6	<0.5	<10	16	<2	44
95BF006	Chlorite, hematite	<5	0.8	4	8	1.5	10	150	<2	294
95BF011	Oxidized sulfides, white mica	<5	0.2	12	<2	0.5	<10	144	<2	206
95BF013	Chlorite, epidote, white mica	<5	0.4	12	<2	<0.5	10	88	2	118
95BF071B	Pyrite, white mica	<5	0.4	20	2	<0.5	10	36	<2	56
95BF072	Sulfides, chlorite	<5	0.8	6	6	<0.5	10	146	<2	130
Calista S4	Carbonate, limonite	<5	1.1	40	na	na	(15)	29	na	(40)
Calista S5	Pyrite, limonite	<5	0.2	150	na	na	(60)	11	na	(1177)
Calista S6	Disseminated pyrite	<5	1.4	12	na	na	(10)	20	na	(35)

location 13, fig. 7), a hematite-altered felsic tuff sample (95AM001C, table 2) contains 10 ppb Au, 102 ppm As, 620 ppb Hg, 8 ppm Sb, and 0.4 ppm Ag, similar to the geochemical signature expressed in some of the dike samples from Area 1. A few elevated concentrations of Bi, Cd, and Zn are found among the 15 feldspar-quartz porphyry dike samples analyzed from Area 1.

In Area 2, feldspar-quartz porphyry dikes are found within a pronounced hornfels aureole on Chase Mountain, about 3.2 km southwest of the placer tailings on Flat Creek (fig. 7). The hornfels aureole reached hornblende-hornfels facies conditions, which probably predated the felsic dike intrusion. Minor sericitic, argillic, and propyllitic alteration are found in many of the dikes.

Zones of disseminated pyrite are found in altered dike rocks, and in wall rock hornfels adjacent to the dikes. Unlike the mineralized feldspar-quartz porphyry dikes exposed in Flat Creek, which contain elevated concentrations of As, Hg, Sb, and Ag, the mineralized felsic dikes on Chase Mountain generally show elevated concentrations of Pb (as much as 224 ppm), Zn (as much as 1,177 ppm), and Ag (as much as 1.4 ppm). Altered country rocks near the dikes contain elevated concentrations of Bi (as much as 14 ppm) and locally Ag (as much as 0.6 ppm). Three rock samples from Area 2 (map numbers 4, 5, and 26, fig. 7) contain gold (7 to 10 ppb). A sample of lithic tuff (map number 4) that has secondary calcite, silica, and hematite, contains 10 ppb Au and 4 ppm Bi. Two samples of unknown rock type (RAA2229 and RAA2389, map numbers 5 and 26, respectively), contain 7 ppb Au and as much as 297 ppm As. The feldspar-quartz porphyry dikes and nearby volcanic country rocks are hydrothermally altered, locally contain sulfide minerals, and show slightly elevated concentrations of Pb, Zn, Ag, and Bi. The dikes are the most likely source for the anomalous concentrations of gold in rock samples collected from Area 2. However, the gold could be associated with the cupola of the postulated underlying pluton.

DISCUSSION

A likely lode source for placer gold deposits of Flat Creek, and perhaps also the placer gold anomalies of Last Chance Creek, are feldspar-quartz porphyry dikes and their country rock. These dikes, and their associated placer gold deposits, are similar to those found at Willow Creek (near Marshall) and Kako Creek, southwest of the Stuyahok study area (fig. 1). At both Willow Creek and Kako Creek, which together make up most of the Marshall mining district, west-trending swarms of feldspar-quartz porphyry dikes of granodiorite to granite composition cut volcanic-dominant rocks of the Koyukuk terrane (Bundtzen and Miller, 1997). These are the same type of felsic dike rocks and volcanic host rocks that we have mapped in the Stuyahok study area. K-Ar ages of 66 Ma (biotite) and 69 Ma (muscovite) have been obtained from mineralized intrusions at Willow Creek and Kako Creek, respectively (T.K. Bundtzen, unpub. data, 1996). The prominent dike swarm of the Willow Creek and Kako Creek areas projects toward the Stuyahok study area.

Geologic and mineralogical characteristics of the mineralized, feldspar-quartz porphyry dikes of the Flat Creek drainage (including alteration, trace-metal content, dike emplacement style, chemistry, and age), are similar to those of the dikes associated with peraluminous granite-porphyry-hosted, gold-polymetallic deposits in southwestern Alaska (Bundtzen and Miller, 1997). Such deposits commonly contain elevated concentrations of Hg, As, Sb, Ag, and Au. Late Cretaceous and early Tertiary peraluminous felsic dikes associated with this deposit type are interpreted to be the source of about 20 percent of the placer gold produced in the Kuskokwim mineral belt, and to host about 80 percent of the known lode gold (Bundtzen and Miller, 1997). An example of this deposit type is the Donlin Creek lode deposit near Aniak (fig. 1) that is currently being explored by Placer Dome U.S., Inc.; they have outlined a preliminary resource of 112,000 kg (3.6 million oz) of gold (Dodd, 1996).

The feldspar-quartz porphyry dikes exposed on Chase Mountain are similar to those of the Flat Creek drainage in chemical composition, alteration, and emplacement style, but their geochemical signature, which includes Pb, Zn, Ag, and Bi, is not typical of the peraluminous granite-porphyry-hosted gold deposit type. Elsewhere in southwestern Alaska, this geochemical signature is found in cupolas and overlying hornfels associated with plutonic-related, boron-enriched, silver-tin-polymetallic deposits (Bundtzen and Miller, 1997). Such polymetallic deposits generally have high Ag-to-Au ratios and significant amounts of Pb, Zn, Sn, As, and Bi. The geochemical signature recognized on Chase Mountain could be related to an unexposed pluton. We are uncertain whether the gold anomalies associated with Chase Mountain are related to the feldspar-quartz porphyry dikes or to the postulated pluton.

SUMMARY AND CONCLUSIONS

The bedrock geology of the Stuyahok area consists primarily of Lower Cretaceous tuff, volcaniclastic rocks, and flows of the Koyukuk terrane. These rocks show both subaerial and subaqueous features that indicate deposition near an emergent/submergent margin of a marine basin. Modal analysis of interbedded sandstones indicates erosion of an undissected magmatic arc, but local sources of Paleozoic limestone were also present. The rocks were tilted and regionally metamorphosed (locally reaching prehnite-pumpellyite facies) prior to intrusion by dominantly west-trending Late Cretaceous and early Tertiary felsic and mafic dikes. High-angle faults of unknown displacement trend northeast and northwest across the study area. Unconsolidated Quaternary deposits overlap the older rocks and cover about 70 percent of the area.

Approximately 933 kg (30,000 oz) of gold has been produced from placer deposits in the Stuyahok area, and gold remains the area's most significant mineral resource. Additional placer resources probably lie in Area 1 (fig. 7), particularly upstream from the present workings on Flat Creek, and also on Last Chance Creek. We are not certain about the source of the placer gold, but our results are consistent with the suggestion made by earlier

workers (Joesting, 1938; Retherford and McAtee, 1994) that feldspar-quartz porphyry dikes in the area of the placer workings (Area 1, fig. 7) may be a source of gold. This conclusion is based mainly on the similarity between the geology and geochemistry of the Stuyahok placer deposits and those at Willow Creek, Kako Creek, and Donlin Creek, where the gold is derived from peraluminous granite porphyry dikes and associated country rock (Bundtzen and Miller, 1997). Anomalous concentrations of Hg ± As ± Sb were found in samples collected in Area 1. Although this geochemical signature is consistent with peraluminous granite-porphyry-hosted gold, it is also consistent with the signature of other epithermal lodes found in southwestern Alaska (Sainsbury and MacKevett, 1965; Goldfarb and others, 1990), so we cannot rule out the possibility of an additional lode source of gold. The gold fineness data from Flat Creek suggest that more than one lode zone contributed gold to the placer. This could mean that more than one lode zone is present within the feldspar-quartz porphyry dikes or that two different lode types exist.

If lode gold resources are present, they will probably be found in an area that encompasses the present placer workings and much of the terrace on the south side of Flat Creek (Area 1, fig. 7) or perhaps on Chase Mountain and its north flank (Area 2, fig. 7). In Area 1, gold appears to be spatially associated with west-trending felsic dikes that are largely concealed under Quaternary deposits. The granite porphyry-hosted, gold-polymetallic mineral deposit type described for the Kuskokwim mineral belt in Bundtzen and Miller (1997) is consistent with the overall characteristics of the mineralized dikes in this area. The mineralized area probably extends for several kilometers up valley but may be low grade. Area 2 is also characterized by closely spaced, near-vertical feldspar-quartz porphyry dikes, but hornblende-hornfels facies contact metamorphism indicates Chase Mountain may be underlain by an unexposed pluton. The elemental signature exhibited on Chase Mountain (Pb, Zn, Ag, and Bi) is similar to that associated with some plutonic-related deposits found in other parts of southwestern Alaska that have high Ag-to-Au ratios (Bundtzen and Miller, 1997). We are uncertain if the minor gold anomalies found in rock samples from Chase Mountain are related to the hornfels or to the feldspar-quartz porphyry dikes. However, given the presence of feldspar-quartz porphyry dikes like those of Area 1 and the possibility of plutonic-related mineralized rock, we must include Chase Mountain as a possible gold resource area.

Acknowledgments.—We thank Elizabeth Bailey for her invaluable contribution to the geochemical studies that assisted this report. We thank June McAtee (Calista Corporation) and Damon Bickerstaff (now with Placer Dome U.S., Inc.) for their contributions to the fieldwork. We appreciate the logistical and analytical support provided by Calista Corporation. We also thank the miners at Stuyahok, who not only provided logistical assistance but also important technical information on the placer gold.

REFERENCES CITED

Bailey, E.A., Keith, W.J., Bickerstaff, Damon, Dempsey, David, and Miller, M.L., 1996, Analytical results and sample locality maps of stream-sediment, panned concentrate, streamwater, and soil samples from the Stuyahok study area, part of Holy Cross A-4 and A-5 quadrangles, Alaska: U.S. Geological Open-File Report 96-505-C, 44 p.

Beikman, Helen M., 1980, compiler, Geologic map of Alaska: U.S. Geological Survey, 2 sheets, scale 1:2,500,000.

Bundtzen, T.K., and Miller, M.L., 1997, Precious metals associated with Late Cretaceous-early Tertiary igneous rocks of southwestern Alaska, *in* Goldfarb, R.J., and Miller, L.D., eds., Mineral deposits of Alaska: Economic Geology Monograph 9, p. 242-286.

Cobb, E.H., 1973, Placer deposits of Alaska: U.S. Geological Survey Bulletin 1374, 213 p.

Dickinson, W.R., 1985, Interpreting provenance relations from detrital modes of sandstones, *in* Zuffa, G.G., ed., Provenance of arenites: Boston, D. Reidel, p. 333-362.

Dodd, Stan, 1996, Donlin Creek Project, southwest Alaska [abs.], *in* Alaska mining—No longer just a dream: Alaska Miners Association Annual Convention, Anchorage, Alaska, 1996, [Abstracts], p. 27-28.

Goldfarb, R.J., Gray, J.E., Pickthorn, W.J., Gent, C.A., and Cieutat, B.A., 1990, Stable isotope systematics of epithermal mercury-antimony mineralization, southwestern Alaska, *in* Goldfarb, R.J., Nash, J.T., and Stoeser, J.W., Geochemical studies in Alaska by the U.S. Geological Survey, 1989: U.S. Geological Survey Bulletin 1950, p. E1-E9.

Hein, J.R., and McLean, Hugh, 1980, Paleogene sedimentary and volcanogenic rocks from Adak Island, central Aleutian Islands, Alaska, *in* Shorter contributions to stratigraphy and structural geology, 1979: U.S. Geological Survey Professional Paper 1126-E, 16 p.

Joesting, H.R., 1938, The Kaiyuh Hills and the Stuyahok-Marshall district: Alaska Territorial Department of Mines Miscellaneous Report MR-195-20, 6 p.

Joesting, H.R., 1942, Strategic mineral occurrences in interior Alaska: Territory of Alaska, Department of Mines Pamphlet No. 1, 46 p.

Jones, D.L., Silberling, N.J., Coney, P.J., and Plafker, George, 1987, Lithotectonic terrane map of Alaska, west of the 141st meridian; folio of the lithotectonic terrane maps of the North American Cordillera: U.S. Geological Survey Miscellaneous Field Studies Map MF-1874-A, scale 1:2,500,000.

Karl, S.M., Ager, T.A., Hanneman, Karl, and Teller, S.D., 1988, Tertiary gold-bearing gravel at Livengood, Alaska, *in* Galloway, J.P., and Hamilton, T.D., eds., Geologic studies in Alaska by the U.S. Geological Survey during 1987: U.S. Geological Survey Circular 1016, p. 61-63.

Keith, W.J., Miller, M.L., Bailey, E.A., Bundtzen, T.K., and Bickerstaff, Damon, 1996, Analytical results and sample locality maps of rock samples from the Stuyahok area, part of

Holy Cross A-4 and A-5 quadrangles, Alaska: U.S. Geological Open-File Report 96-505-B, 47 p.

Malone, Kevin, 1965, Mercury in Alaska, *in* Mercury potential of the United States: U.S. Bureau of Mines Information Circular 8252, p. 31-59.

Miller, M. L., Belkin, H.E., Blodgett, R.B., Bundtzen, T.K., Cady, J.W., Goldfarb, R.J., Gray, J.E., McGimsey, R.G., and Simpson, S.L., 1989, Pre-field study and mineral resource assessment of the Sleetmute quadrangle, southwestern Alaska: U.S. Geological Survey Open-File Report 89-363, 115 p., 3 plates, scale 1:250,000.

Miller, M.L., and Bundtzen, T.K., 1994, Generalized geologic map of the Iditarod quadrangle, Alaska, showing potassium-argon, major-oxide, trace-element, fossil, paleocurrent, and archaeological sample localities: U.S. Geological Survey Miscellaneous Field Studies Map MF-2219-A, 48 p., scale 1:250,000.

Miller, M.L., Bundtzen, T.K., Keith, W.J., Bailey, E.A., and Bickerstaff, Damon, 1996, Geology and mineral resources of the Stuyahok area, part of Holy Cross A-4 and A-5 quadrangles, Alaska: U.S. Geological Open-file Report 96-505-A, 30 p., scale 1:63,360.

Patton, W.W., Jr., and Box, S.E., 1989, Tectonic setting of the Yukon-Koyukuk basin and its borderlands, western Alaska: Journal of Geophysical Research, v. 94, no. B11, p. 15,807-15,820.

Patton, W.W., Jr., Box, S.E., Moll-Stalcup, E.J., and Miller, T.P., 1994, Geology of west-central Alaska, Chapter 7 *in* Plafker, George, and Berg, H.C., eds., The geology of Alaska: Boulder, Colo., Geological Society of America, The Geology of North America, v. G-1, p. 241-269.

Patton, W.W., Jr., and Moll-Stalcup, E.J., 1996, Geologic map of the Unalakleet quadrangle, west-central Alaska: U.S. Geological Survey Miscellaneous Investigations Map I-2559, 39 p., scale 1:250,000.

Retherford, Rob, and McAtee, June, 1994, The Stuyahok Property, southwestern Alaska: Anchorage, Alaska, Calista Corporation, unpublished company report, 4 p.

Sainsbury, C.L. and MacKevett, E.M., Jr., 1965, Quicksilver deposits of southwestern Alaska: U.S. Geological Survey Bulletin 1187, 89 p.

Smith, P.S., 1933, Mineral industry of Alaska in 1931 and administrative report: U.S. Geological Survey Bulletin 844-A, 117 p.

———1941, Fineness of gold from Alaska placers: U.S. Geological Survey Bulletin 910-C, 272 p.

Reviewers: Dwight C. Bradley and Richard J. Goldfarb

Radiolarian and Conodont Biostratigraphy of the Type Section of the Akmalik Chert (Mississippian), Brooks Range, Alaska

By Charles D. Blome, Katherine M. Reed, *and* Anita G. Harris

ABSTRACT

Radiolarians recovered from 21 of 112 samples from the nearly 73-m-thick type section of the Akmalik Chert and its counterpart on the opposite side of Akmalik Creek (lat. 68°23.13'N., long. 154°19.2'W., Killik River quadrangle, Alaska) are Mississippian (middle Osagean to probably late Meramecian) in age. Sparse albaillellids include, from oldest to youngest, *Albaillella perforata,* *A.* sp. cf. *A. ramsbottomi*, *A.* sp. cf. *A. cartalla,* and *A. furcata.* Also present are *Pylentonema* sp. cf. *P. antiqua* and *Archocyrtium* sp., several spumellarians including scharfenbergiids, and an unidentified conical radiolarian. A dolomitic limestone at the base of the Akmalik Chert type section contains conodonts that indicate a Mississippian age (early half of the Osagean); they range from the *Gnathodus typicus* Zone into the *Scaliognathus anchoralis-Doliognathus latus* Zone. Conodonts restricted to the uppermost Upper *G. typicus* Subzone through most of the *S. anchoralis-D. latus* Zone (middle Osagean) are present in samples collected from 12.1 to 16.2 m above the base of the type section. A middle Osagean to Pennsylvanian conodont, most likely no younger than early Chesterian, was found at 39.7 m. One specimen of *G. texanus* (late Osagean to early Chesterian) was found 8 m below the top of the Akmalik Chert in a section about 0.2 km west of the type section. Conodont biofacies and taphonomy suggest that conodonts in the Akmalik Chert may have been deposited in a dominantly foreslope and basin (near toe-of-slope) depositional setting; some conodonts were subsequently hydraulically transported farther basinward.

INTRODUCTION

Microfossils have substantially aided correlation of Paleozoic units in the central Brooks Range in northern Alaska (for example, Murchey and others, 1988; Holdsworth and Murchey, 1988; Dumoulin and Harris, 1993; Dumoulin and others, 1993, 1994). One of the most widespread Paleozoic units in the central Brooks Range is the Carboniferous Lisburne Group (fig. 1*A*). In the subsurface of northern Alaska and in outcrop in the northeastern and east-central Brooks Range, the Lisburne Group is dominantly thick gray limestone. However, to the southwest and west (north of 68° and between about 159° and 165°W) in the western Endicott Mountains (northern front of the Brooks Range) and the De Long Mountains, it includes dark siliceous mudstone and chert units that are generally older than the limestone (Moore and others, 1994; Krumhardt and others, 1996). These black mudstones and cherts, originally referred to as "black Lisburne" by Tailleur and others (1966), represent facies deposited south (present coordinates) of the limestone facies adjacent to the northern basin margin. These siliceous sediments may have been deposited first in the area that is now the southwestern Brooks Range and adjacent parts of the National Petroleum Reserve in Alaska, to the north, in areas of deeper water that were possibly related to creation of extensional basins (Mayfield and others, 1988). These dark siliceous rocks and associated sedimentary units deposited in various parts of the Mississippian basin were thrust faulted in a series of telescoped allochthons (fig. 1*A*) during the Late Jurassic to Cretaceous development of the Brooks Range orogen (Moore and others, 1994).

The black siliceous rock units are radiolarian bearing and occur predominantly in the lithologic sequences of three allochthons that constitute most of the central and western Brooks Range. The units consist of (1) the Kuna Formation (Mull and others, 1982), which is part of the Endicott Mountains allochthon (fig. 1*A*), the structurally lowest of the major allochthons, (2) the Akmalik Chert (Mull and others, 1987), which is part of the Picnic Creek allochthon (fig. 1*A*), and (3) the Rim Butte unit (informal name, Dumoulin and others, 1994), included in the Picnic Creek and Ipnavik River allochthons (fig. 1*A*). However, according to C.G. Mull (Alaska Division of Geological and Geophysical Surveys, written commun., 1996), the Rim Butte unit occurs only in the Ipnavik River allochthon. The Kuna, Akmalik, and Rim Butte units include, in many places, distal turbidites and radiolarian-rich sediments deposited on a basin floor that

was less well oxygenated than that of the older Kayak Shale or the coeval and younger platform carbonates of the Lisburne Group (Dumoulin and Harris, 1993).

The dark-colored rock assemblages of the Lisburne Group that include siliceous mudstone and chert have similar conodont and stratigraphic ages that range from the early Osagean to about middle Meramecian (Dumoulin and others, 1994). However, a limestone sample collected in 1985 from near the base of the type section (section A, fig. 1*B*) of the Akmalik Chert yielded chiefly Osagean conodonts, as well as a few anomalous latest Mississippian and Pennsylvanian conodonts (Mull and others, 1987). We resampled the section in detail because of the mixed conodont fauna as well as to test the increasing reliability of Paleozoic radiolarian biostratigraphy. We collected and processed 112 samples for radiolarians from section A and its counterpart (section B, fig. 1*B*) on the opposite side of Akmalik Creek, considered unpublished data of A.K. Armstrong (U.S. Geological Survey, retired) from a nearby third section (section C, fig. 1*B*), and used co-occurring conodonts from 19 limestone and chert samples for independent biostratigraphic control.

GEOLOGIC SETTING

The Akmalik Chert (Mull and others, 1987) is exposed along both sides of Akmalik Creek, a tributary of the Killik River, about 3 km south-southwest of Kikiktat

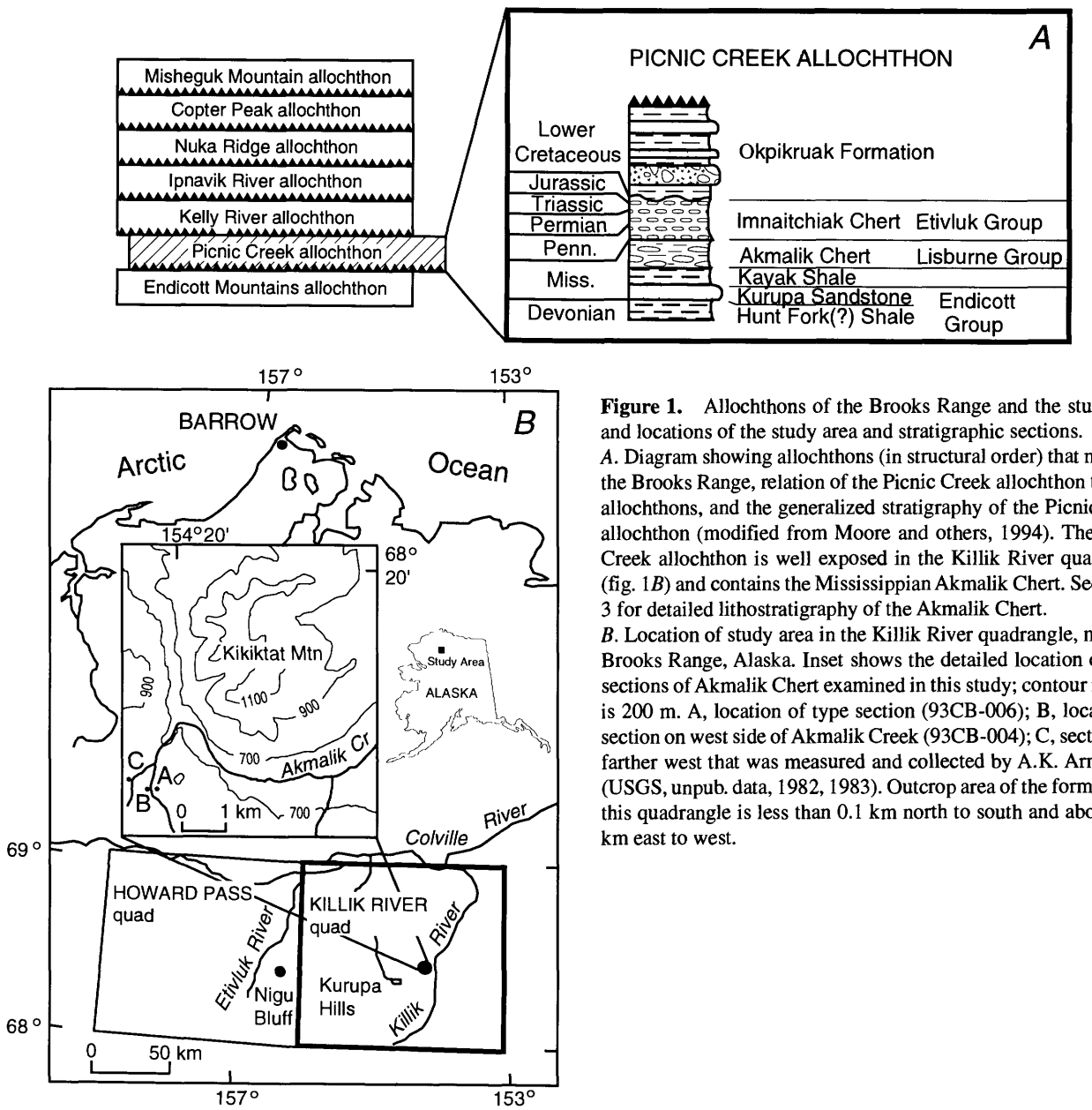

Figure 1. Allochthons of the Brooks Range and the study area and locations of the study area and stratigraphic sections.
A. Diagram showing allochthons (in structural order) that make up the Brooks Range, relation of the Picnic Creek allochthon to other allochthons, and the generalized stratigraphy of the Picnic Creek allochthon (modified from Moore and others, 1994). The Picnic Creek allochthon is well exposed in the Killik River quadrangle (fig. 1*B*) and contains the Mississippian Akmalik Chert. See figure 3 for detailed lithostratigraphy of the Akmalik Chert.
B. Location of study area in the Killik River quadrangle, northern Brooks Range, Alaska. Inset shows the detailed location of three sections of Akmalik Chert examined in this study; contour interval is 200 m. A, location of type section (93CB-006); B, location of section on west side of Akmalik Creek (93CB-004); C, section still farther west that was measured and collected by A.K. Armstrong (USGS, unpub. data, 1982, 1983). Outcrop area of the formation in this quadrangle is less than 0.1 km north to south and about 0.25 km east to west.

Mountain in the Killik River quadrangle (figs. 1-3). The type section, section A (figs. 1*B* and 2*A*, *B*), is on the east side of the creek, and the top of the Akmalik is well exposed on the west side of the creek at section B (fig. 3). The third partial section, section C (figs. 1*B*, 3), on a short westward tributary of Akmalik Creek about 200 m west of section B, was measured and collected in 1982 by A.K. Armstrong. The geology of the area was mapped at a scale of 1:20,000 by Alexander (1990) and at a regional scale of 1:125,000 by Mull and others (1994).

The outcrops of sections A and B (figs. 2, 3) are part of a gentle east-trending synform. The strata at section A (fig. 2) also dip west toward the creek. That dip fluctuates from an average of 14° near the base of the section, decreases to an average of 4° in the middle part, and increases to 7-13° near the top. The north side of section A is partly separated from the main outcrop by a high-angle fault. About 40 m of section was measured in section B (fig. 3), which also dips toward the creek. The rocks in both sections A and B are highly fractured, and low-angle (possibly bedding-plane) faults complicate precise measurement. Offset on most of these faults cannot be determined, but it appears to be small. Section B also displays steeper faults, slickensides, and common calcite stringers. Section C (fig. 3) consists of about 28 m of dark chert containing little argillite.

The Akmalik Chert overlies the Kayak Shale (Kinderhookian), but the contact is covered at all three sections (fig. 3). Mull and others (1987) reported that the contact was gradational in other exposures of the Akmalik Chert. The Akmalik Chert underlies the Imnaitchiak Chert (Mull and others, 1987), which was originally thought to be Pennsylvanian to Middle or Late Triassic in age but is now known to be as young as Middle Jurassic (Mull and others, 1997). The upper contact of the Akmalik Chert is preserved in three sections. In the Picnic Creek allochthon (fig. 1*A*), the basal contact of the Imnaitchiak Chert is a disconformity, and the lower beds are glauconitic, phosphatic sandstone and, in one place, an oncolitic conglomerate (Mull and others, 1987). Even though the Akmalik-

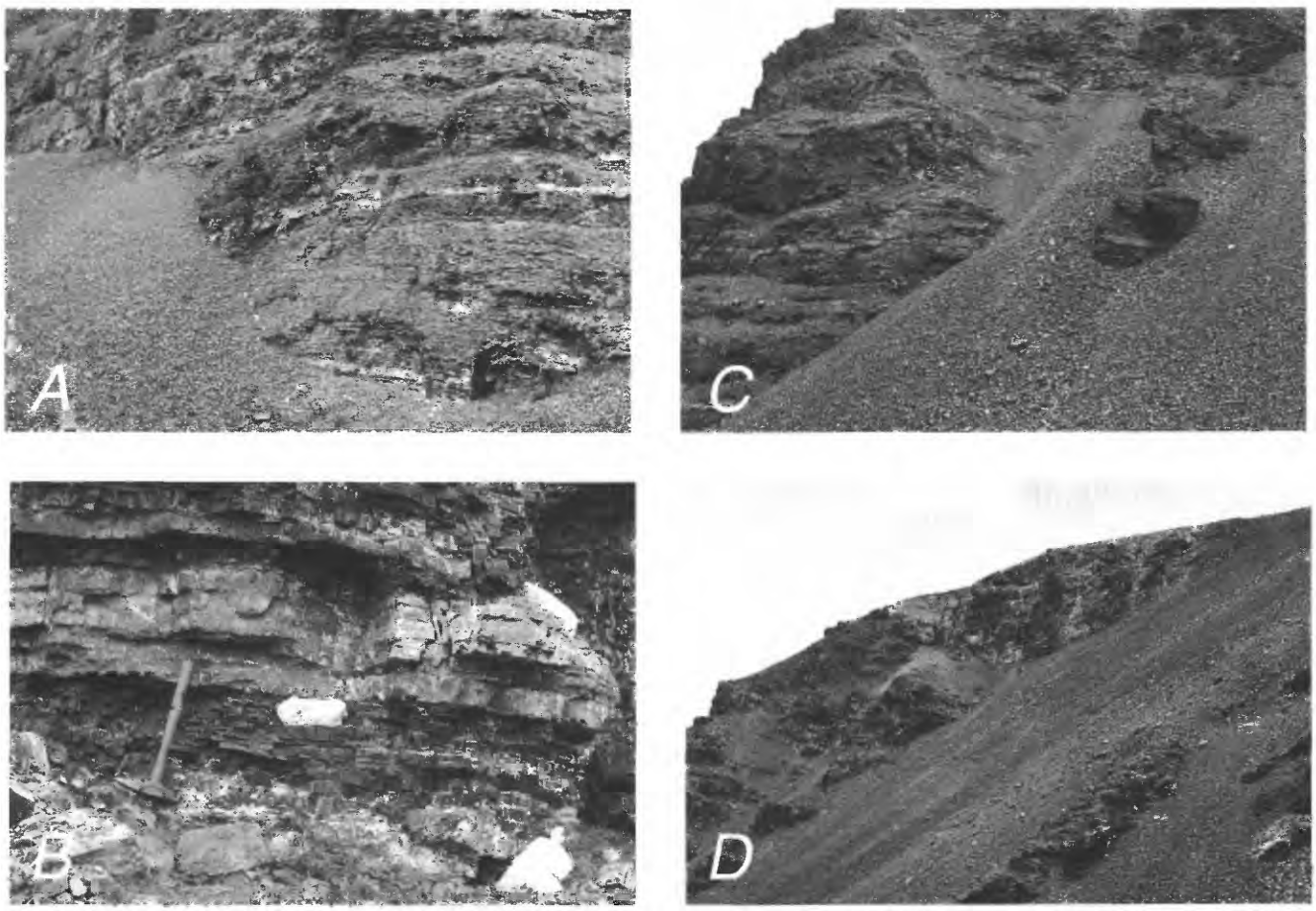

Figure 2. Type section of the Akmalik Chert, east side of Akmalik Creek. *A*, North side of outcrop showing sampling sites (white bags) from the base to about 22 m; note person in lower right corner. *B*, Silicified(?) dolomitic limestone at base of measured section. *C*, South side of type section showing sampling sites (white bags); light-colored bed in lower left corner of this photograph is bed about half-way up the exposure shown in *A*. *D*, Upper part of south side of section; uppermost sample was taken at top of outcrop.

Imnaitchiak contact was not studied in detail by us, we estimate that more than 15 million years of deposition is represented in the Akmalik on the basis of the age range of the conodont and radiolarian faunas.

Our measured sections A and B (fig. 3) indicate that the Akmalik Chert consists of as much as 72.8 m of black and dark-gray (rarely green) argillaceous chert, chert, and minor dark-colored argillite. Locally, the siliceous rock weathers red, yellow, orange, or brown. The chert beds are generally 2 to 6 cm thick; argillite beds are thinner (1-2 cm). Section B contains less argillite and argillaceous chert than section A. Most cherty beds display some pinch and swell features.

A few limestone horizons are also present in sections A and B (figs. 2*B*, *C*, 3) near the base of the formation. Two 15- to 20-cm-thick yellowish-brown-weathering beds of silicified(?) dolomitic limestone crop out at the base of section A and about 3 m above the base of section B. Dark limy beds were noted higher on the north side of section A, but they are separated from the measured part of that section by a high-angle fault. Dolomitic limestone beds are present near the base of the Akmalik Chert in the Kurupa Hills, 20 km west of section A (fig. 1*B*).

PALEONTOLOGY OF THE AKMALIK CHERT

Previous studies (for example, Mull and others, 1987) and the stratigraphic position of the Akmalik Chert indicated that it was Mississippian to Pennsylvanian in age, but more recent studies (Dumoulin and Harris, 1993) show it to be restricted to the Mississippian. Mull and others (1987) reported that chert from several intervals yielded Late Mississippian radiolarians belonging to the radiolarian assemblages A and B of Murchey and others (1979) and to the lower part of the Chesterian *Albaillella*-3 assemblage of Holdsworth and Jones (1980). Mull and others (1987) also noted that spongy latentifistulid radiolarians at the top of the Akmalik Chert near Kurupa Lake (just north of the Kurupa Hills, fig. 1*B*) suggested an Early Pennsylvanian (Morrowan) age, but that the age could be as old as Late Mississippian (Chesterian). In addition, Mull and others (1987) reported that one well-preserved plant fossil from Akmalik Chert float resembled a Chesterian form from the Soviet Union (R.A. Spicer, Oxford University, written commun., 1984); however, inasmuch as the fossil was from float, its stratigraphic position is unknown. To the west and north in the Howard Pass quadrangle (fig. 1*B*), the Akmalik Chert contains relatively rare conodonts of both shallow-water and pelagic biofacies that are "probably early Viséan" or middle Osagean to middle Meramecian according to Dumoulin and others (1994, p. 79, 81). A mix of mostly Early Mississippian (Osagean) and a few latest Mississippian and Early Pennsylvanian (Morrowan) conodonts was recovered in 1985 from limestone collected at the base of the type section (fig. 3) of the Akmalik Chert (Mull and others, 1987). The younger conodont fauna appeared to us to be anomalous because (1) nearly all of the conodonts were Early Mississippian (Osagean) and (2) section A is well exposed and contains no evidence of structural complications that would fault older Mississippian rocks over Pennsylvanian rocks.

CONODONTS

We sampled the dolomitic limestone layers at and near the base of sections A and B (figs. 2, 3) to resolve the latest Mississippian and Pennsylvanian ages for the conodonts previously reported at the base of the type section. Our study shows that the basal sample from section A (fig. 3 and table 1, sample 93CB-006A) contains only early to middle Osagean conodonts indicative of the Lower *Gnathodus typicus* Subzone into the *Scaliognathus anchoralis-Doliognathus latus* Zone; no conodonts of younger Mississippian or Pennsylvanian age were recovered from this large sample. The conodont species association and its taphonomy indicate postmortem transport from or within a depositional setting no shallower than the upper foreslope (table 1). We believe that the dolomitic limestone is the same interval that in 1985 yielded the mix of latest Mississippian and Early Pennsylvanian conodonts. We conclude that the few latest Mississippian and (or) Early Pennsylvanian conodonts in the 1985 sample (USGS colln. 29702-PC) resulted from laboratory contamination because (1) there are no structural features in the section to suggest the placement of latest Mississippian or Pennsylvanian units (such as Imnaitchiak Chert) at the base of the Akmalik Chert and (2) all other conodont collections from higher in the Akmalik Chert section yielded coevel Osagean or possibly younger Mississippian conodonts (table 1). Laboratory contamination is also the most likely conclusion because a large number of samples from various Mississippian and Pennsylvanian units in the same area were being processed in the U.S. Geological Survey conodont laboratory in 1985 and 1986. The color alteration indices (CAIs) of the conodonts in the 1985 collection are consistent within this collection and with past collections in the area.

The other well-dated conodont samples from section A (fig. 3 and table 1, samples 93CB-006C, P, S2, T) have the same age as, or a slightly narrower age range than, the collection at the base of the section;

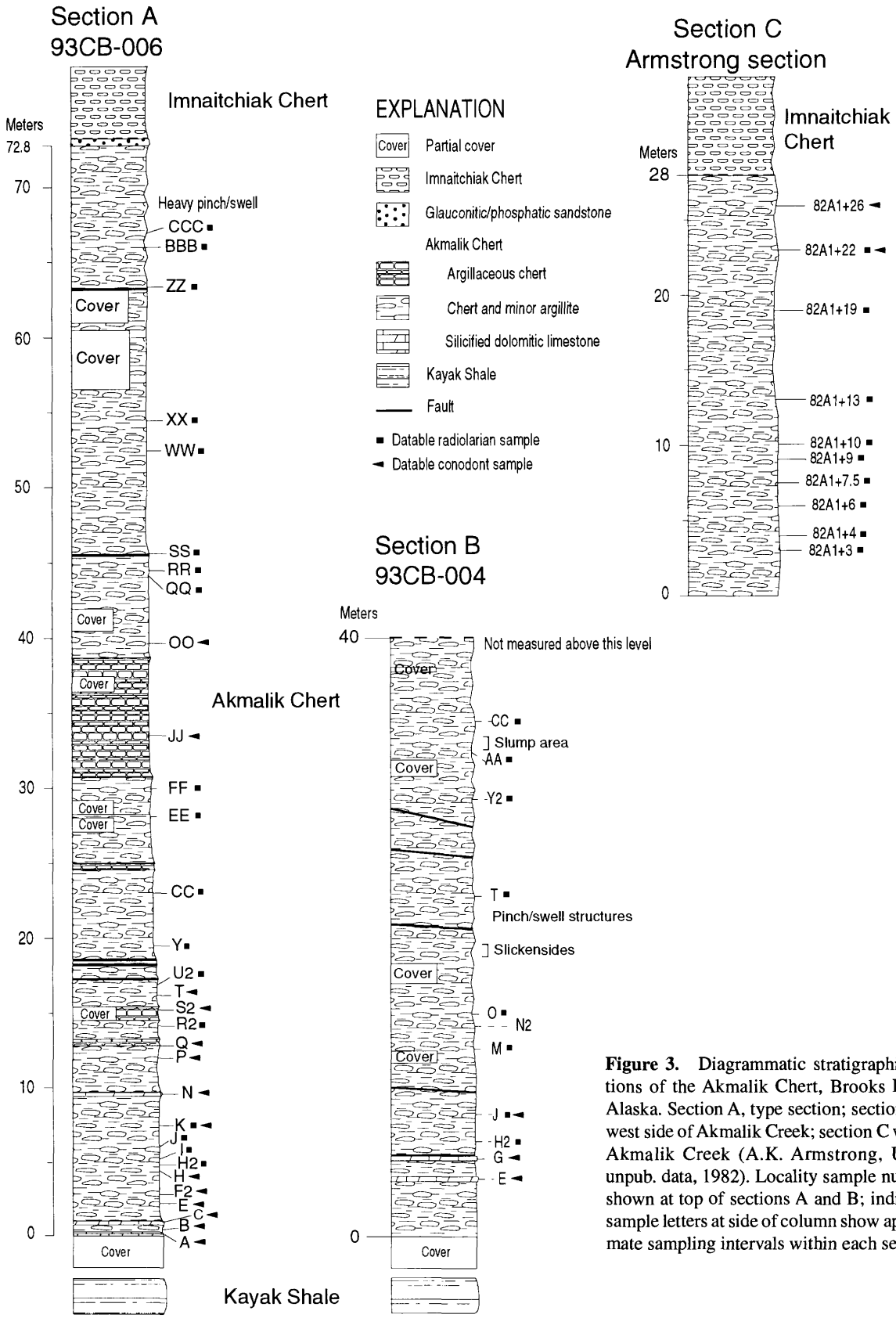

Figure 3. Diagrammatic stratigraphic sections of the Akmalik Chert, Brooks Range, Alaska. Section A, type section; section B on west side of Akmalik Creek; section C west of Akmalik Creek (A.K. Armstrong, USGS, unpub. data, 1982). Locality sample numbers shown at top of sections A and B; individual sample letters at side of column show approximate sampling intervals within each section.

they range from the uppermost Upper *G. typicus* Subzone through most of the *S. anchoralis-D. latus* Zone (fig. 4 and table 1). The highest conodont sample from section A (table 1, 93CB-006OO) yielded one juvenile Pa element of a hindeodid or synclydognathid (fig. 5J). Hindeodids range into the very earliest Triassic, but synclydognathids do not extend beyond the early Chesterian. The stratigraphic position of the sample, however, restricts the age range to middle Osagean through Pennsylvanian, and the sample most likely is no younger than early Chesterian because the diagnostic radiolarian species *Albaillella* sp. cf. *A. cartalla* (fig. 4) was found in the section above 93CB-006OO. Chert beds in section A generally yield only a few small conodont fragments or juveniles, indicating that the conodonts were deposited as distal winnows. The conodont genera and species also suggest derivation from chiefly foreslope and basin biofacies.

Section C (figs. 1*B*, 3) lies along an unnamed tributary to Akmalik Creek about 0.2 km west of section A. Two samples from this section collected by A.K. Armstrong in 1982 produced two forms: a juvenile *Gnathodus texanus* Roundy in a sample from 22 m above the base of the section (USGS colln. 29103-PC; figs. 5N, O) and an even smaller juvenile *Gnathodus* sp. indet. from 4 m higher (USGS colln. 29104-PC) (A.G. Harris, written commun., 1983). *Gnathodus texanus* ranges from the late Osagean (base of *Polygnathus mehli*-Lower *G. texanus* Zone) into the early Chesterian; representatives of that genus, however, extend into the very earliest Pennsylvanian. Thus, it seems unlikely that the top of the Akmalik Chert extends much, if at all, beyond the early Chesterian because the contact with the overlying Imnaitchiak Chert at section C is at 28 m above the base of the section (C.G. Mull, Alaska Division of Geological and Geophysical Surveys, written commun., 1996) and only 6 m above the level that produced *G. texanus*.

The CAI values of conodonts from the Akmalik Creek exposures are generally 3-3.5, and less commonly, 3 and 3.5-4. The two rather small conodonts from section C have an apparent CAI of 2-2.5, but it is more likely to be 3 or 3.5. These CAI values indicate the Akmalik Chert along Akmalik Creek reached about 130° to 180°C during metamorphism.

RADIOLARIANS

Preservation of the Akmalik Creek radiolarians (figs. 6, 7) is generally poor. Of the 63 samples collected from section A and 49 samples from section B, only about 20 percent yielded biostratigraphically useful taxa. Most samples collected from the upper part of section A contain poorly preserved radiolarians that could not be used for age determination. We were unable to safely measure and collect the upper part of section B. Nonetheless, the 21 samples containing identifiable radiolarians greatly enlarge the published database for Mississippian radiolarians from the northern Brooks Range. Excluding samples mentioned in theses, less than 25 samples (most of them not taken from measured sections) containing Mississippian radiolarians are mentioned in the published literature (Murchey and others, 1988, p. 703-709). Four samples of Mississippian age are from the Nigu Bluff section in the Howard Pass quadrangle (Holdsworth and Murchey, 1988) on the higher Ipnavik River allochthon (C.G. Mull, written commun., 1997).

Studies by Won (1983, 1990, 1991a, b) of faunas in Germany provide important identifications and age correlations for the Akmalik Chert specimens. Our sparse faunas are not particularly diverse, but they do contain some taxa (primarily albaillellids and scharfenbergiids) in common with the German faunas. Specimens assigned to *Pylentonema* sp. cf. *P. antiqua* Deflandre and *Archocyrtium* sp. cf. *A. coronasimilae* Won are the first of these taxa to be described from the North Slope. Also, the albaillellid, *Albaillella* sp. cf. *A. ramsbottomi* Schwartzapfel and Holdsworth (fig. 7:5) from 32.4 m in section B, appears to be a new morphotype for North Slope faunas.

Radiolarians from samples collected at section A indicate an age range from early/middle Osagean to at least late Meramecian (or even Chesterian). This age range is slightly longer than that indicated by the conodonts from the darker facies of the Lisburne Group (Dumoulin and others, 1994).

A comparison of the radiolarians and conodonts from section C with those from sections A and B shows that the lower part of section C contains younger Mississippian faunas than those in the lower parts of the sections along Akmalik Creek. Tests and h-frames of *Albaillella cartalla* (K.M. Reed, unpub. data, 1983) are well preserved at 6 m above the base of section C. *Scharfenbergia impella* also is present at the base of section C. At least one specimen similar to *Albaillella* sp. aff. *A. cylindra*, of middle(?) to late Meramecian age (Schwartzapfel and Holdsworth, 1996, pls. 29, 35) was found about midway through this section. As noted above, the conodont *Gnathodus texanus*, found at 22 m above the base of the section, ranges from the late Osagean into the early Chesterian.

RADIOLARIAN SYSTEMATICS

The following is an abbreviated systematic discussion of the Mississippian radiolarian taxa found in the cherty samples of the Akmalik Chert. Refer to Gourmelon

(1987), Holdsworth and Murchey (1988), Won (1983, 1990, 1991a, b), and Schwartzapfel and Holdsworth (1996) for expanded synonymies for most of the taxa discussed.

Class ACTINOPODA
Subclass RADIOLARIA
Order POLYCYSTIDA Ehrenberg 1838, emend. Riedel 1967
Suborder ALBAILLELLARIA Deflandre 1953; emend. Holdsworth 1969
Superfamily Albaillellacea Cheng 1986
Family Albaillellidae Deflandre 1952; emend. Holdsworth 1977
Genus *Albaillella* Deflandre, 1952; emend. Holdsworth 1966
Type species *Albaillella paradoxa* Deflandre 1952

The Akmalik Chert contains representatives of two broad groupings of albaillellids and several other related forms.

Albaillella indensis group
Figures 6:1-4; 7:1, 3, 4

Remarks–The older of the two groups is the *Albaillella indensis* group. The forms in this group de-

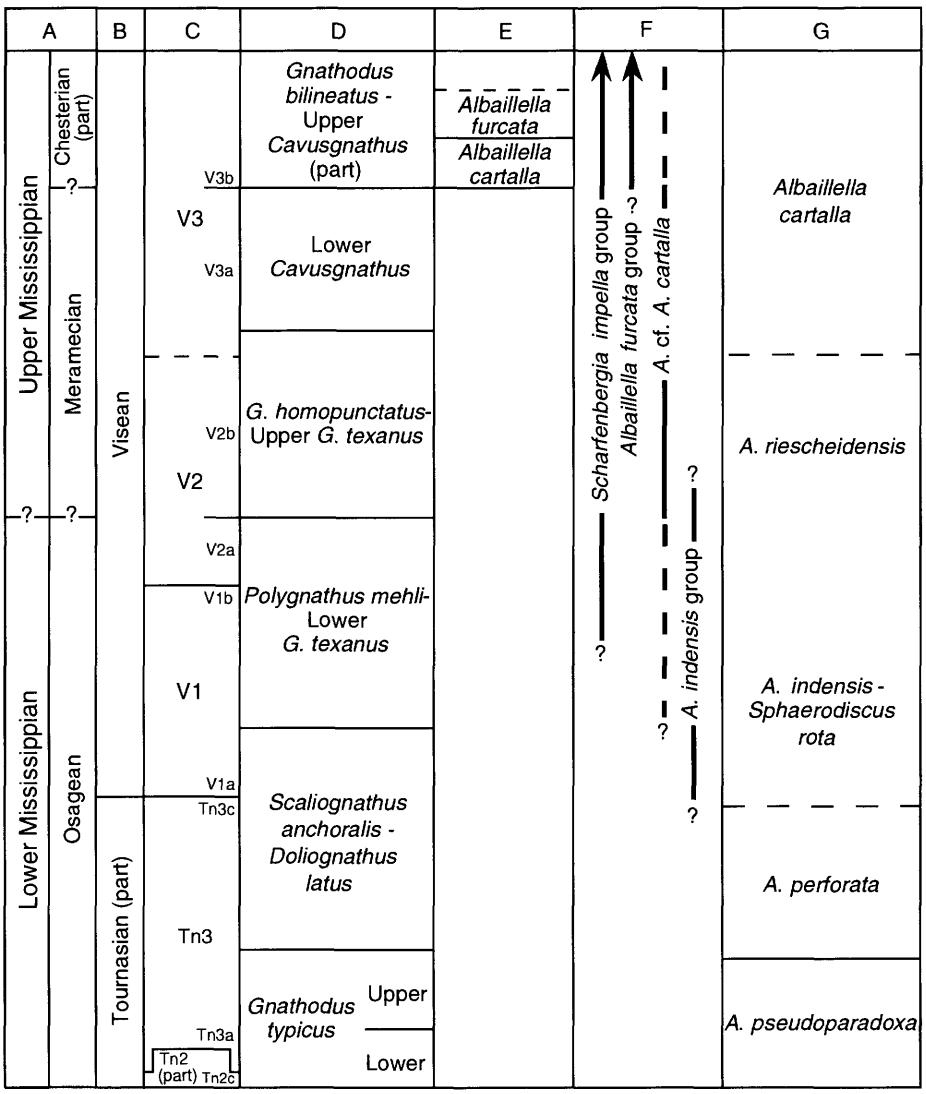

Figure 4. Conodont and radiolarian zonations for rocks of Osagean to early Chesterian (Mississippian) age. Columns A-C, chronostratigraphic units: A, North American series; B, Western European stages; C, Belgian zones. D, Western United States conodont zones (from Poole and Sandberg, 1991); E, radiolarian zones of Schwartzapfel and Holdsworth (1996). F, ranges of selected North Slope radiolarian taxa (Holdsworth and Murchey, 1988); the younger groups and taxon are as young as Pennsylvanian. G, preliminary radiolarian zonation of Won (1991a). Correlation of series, stages, and zones interpreted from Higgins and others (1991), Poole and Sandberg (1991), and Schwartzapfel and Holdsworth (1996, p. 46).

Table 1. Conodont data from the type section and nearby section of the Akmalik Chert, Killik River quadrangle, Brooks Range, Alaska.

[Samples prefixed 93CB-006 are from the type section (figs. 1, 2, and 3, section A) and 93CB-004 are from nearby section B (figs. 1 and 3). R, rare (<5 specimens); C, common (5-20 specimens); indets., bar, blade, and (or) platform fragments indeterminate to element morphotype; CAI, color alteration index; *, biostratigraphically important taxon]

SAMPLE NO. (USGS colln. no.)	STRATIGRAPHIC POSITION	CONODONT FAUNA	AGE	BIOFACIES	CAI	REMARKS
93CB-006A (33279-PC)	Dolomitic limestone at base of section.	*Dollymae hassi* Voges (R)* (fig. 5C) *Do. hassi* Voges? (R)* *Gnathodus cuneiformis* Mehl and Thomas? (R)* (fig. 5D) *G.* spp. indet. (C) *Kladognathus* sp. (Sb-Sc elements) (C) *Polygnathus communis carina* Hass (C) (fig. 5B) *Po. c. communis* Branson and Mehl (C) (fig. 5A) *Po.* sp. indet. (R) *Protognathodus*? sp. indet. (R) *Pseudopolygnathus* spp. indet. (C) +200 unassigned elements and indets.	Lower *G. typicus* Subzone into *S. anchoralis-D. latus* Zone (early to middle Osagean).	Postmortem transport within or from the polygnathid-gnathodid biofacies. Virtually all conodonts are incomplete. The presence of *Dollymae hassi* with gnathodids suggests an upper foreslope or deeper water depositional setting.	3-3.5	7.8 kg of dolomitic limestone was processed (2.56 kg +20 mesh and 900 g 20-200 mesh insoluble residue).
93CB-006B	Thin-bedded black chert with pinch-and-swell argillite partings; 0.6 m above base of section.	4 unassigned elements and indets.	Lower *G. typicus* Subzone into *S. anchoralis-D. latus* Zone (early to middle Osagean) on the basis of under- and overlying collections.	Indeterminate (too few conodonts); postmortem winnow.	3	No weights recorded.
93CB-006C (33280-PC)	Dolomitic limestone; 1 m above base of section.	*Bispathodus* sp. indet. (R) Juvenile protognathodid or gnathodid (R) *Polygnathus communis carina* Hass (R) *Po. communis* Branson and Mehl subsp. indet. (R) *Pseudopolygnathus multistriatus* Mehl and Thomas morphotype 1 (R)* (fig. 5E) *Ps.* sp. indet. (R) 34 indets.		Indeterminate (too few conodonts); postmortem transport from normal-marine environment.	3.5-4	3.7 kg of dolomitic limestone was processed (912 g of 20-200 mesh insoluble residue).
93CB-006E (33281-PC)	Thin-bedded black chert with pinch-and-swell argillite partings; 2.25 m above base of section.	*Pseudopolygnathus* sp. indet. (R) 12 unassigned elements or indets.	Early to middle Osagean on the basis of under- and overlying collections.	Indeterminate (too few conodonts).	3-3.5	No weights recorded.
93CB-006F2	Same lithology as above; 3.0 m above base of section.	2 indets.			Indet.	No weights recorded.
93CB-006H	Same lithology as above; 4.5 m above base of section.	1 indet.			3.5	No weights recorded.
93CB-006K	Same lithology as above; 7.55 m above base of section.	Juvenile *Bispathodus*? sp. indet. (R) 5 unassigned elements and indets.			3	No weights recorded.

Table 1. Continued.

SAMPLE NO. (USGS colln. no.)	STRATIGRAPHIC POSITION	CONODONT FAUNA	AGE	BIOFACIES	CAI	REMARKS
93CB-006N	Limestone (0.25 m thick), 10.4 m above base of section.	5 indets.	Early to middle Osagean on the basis of under- and overlying collections.	Indeterminate (too few conodonts).	3.5	4.1 kg of limestone was processed (1.23 kg of 20-200 mesh insoluble residue).
93CB-006P (33282-PC)	Thin-bedded black chert with pinch-and-swell argillite partings; 12.05 m above base of section.	Bar fragments of "*Hindeodella*" *segaformis* Bischoff s.f. (R)* (Fragments of "*H.*" *segaformis* are common to abundant in the Akmalik Chert in the Howard Pass quadrangle (Dumoulin and others, 1993; 1994).	Uppermost Upper *G. typicus* Subzone through most of *S. anchoralis-D. latus* Zone (middle Osagean).	Indeterminate (too few conodonts); postmortem winnow within or into basin environment.	3-3.5	No weights recorded.
93CB-006Q	Same lithology as above; 13.5 m above base of section.	2 indets.		Indeterminate (too few conodonts).	3.5	No weights recorded.
93CB-006S2 (33283-PC)	Same lithology as above; 15.3 m above base of section.	Bar fragments of "*Hindeodella*" *segaformis* Bischoff s.f. (C)* (figs. 5G-I)		Indeterminate (too few conodonts); postmortem winnow within or into basin facies.	3.5	No weights recorded.
93CB-006T (33284-PC)	Same lithology as above; 16.2 m above base of section.	Bar fragments of "*Hindeodella*" *segaformis* Bischoff s.f. (R)* (fig. 5F) 4 unassigned elements and indets.			3.5	No weights recorded.
93CB-006JJ	Same lithology as above; 33.5 m above base of section.	1 indet.	No older than middle Osagean.		~3.5	No weights recorded.
93CB-006OO (33286-PC)	Same lithology as above; 39.7 m above base of section.	Juvenile *Hindeodus* sp. indet. or *Synclydognathus* sp. indet. (fig. 5J) 1 indet.	Middle Osagean to Pennsylvanian, probably no younger than early Chesterian.	Indeterminate (too few conodonts); postmortem winnow.	~3	No weights recorded.
93CB-004E (33276-PC)	Dolomitic limestone unit 0.2 m thick; 3.8 m above base of section	Bar fragment of "*Hindeodella*" *segaformis* Bischoff s.f. (R)* 6 indets.	Uppermost Upper *G. typicus* Zone into *S. anchoralis-D. latus* Zone (middle Osagean).	Indeterminate (too few conodonts); postmortem winnow within or into basin environment.	3.5	1.8 kg of dolomitic limestone was processed (720 g of 20-200 mesh insoluble residue).
93CB-004G (33277-PC)	Massive limestone 0.2 m thick just below low-angle fault; 5.2 m above base of section.	Bar fragments of "*Hindeodella*" *segaformis* Bischoff s.f. (R)* (fig. 5M) *Protognathodus*? sp indet. (fig. 5K) 22 unassigned elements and indets.			3.5	Original sample weight not recorded (1120 g of 20-200 mesh insoluble residue).
93CB-004J (33278-PC)	Thin-bedded black chert with very little argillite; 8.3 m above base of section.	Bar fragment of "*Hindeodella*" *segaformis* Bischoff s.f. (R)* (fig. 5L) 17 unassigned elements and indets.	Uppermost Upper *G. typicus* Zone through most of *S. anchoralis-D. latus* Zone (middle Osagean).		3.5	Sample weights not recorded.

scribed by Won (1990, 1991a, b) in probable phylogenetic/stratigraphic order are, from oldest to youngest: *A. perforata* Won 1991b, *A. perforata uniramosa* Won 1991b, *A. indensis* Won 1983, and *A. riescheidensis* Won 1990. In order to distinguish these species, the external stapia must be present. *A. riescheidensis* has a large dorsal spine on the lowest part of the cavea. None of our specimens has vestiges of this spine preserved. We conclude that our *A. indensis* group specimens are older than *A. riescheidensis*. The first appearance of this group in section A (fig. 3) is at 4.9 m, and the uppermost specimen was recovered at 7.55 m. In section B (fig. 3), specimens were recovered at 8.3 m and 29.3 m.

Range and occurrence–(Middle to late Osagean; worldwide. The *A. indensis* group is as old as Early Mississippian (middle Osagean, according to Holdsworth and Murchey, 1988). Radiolarians belonging to Won's (1991a) *A. perforata* Zone are found with the conodont *"Hindeodella" segaformis* Bischoff s. f., whose range is uppermost Upper *G. typicus* Zone through most of the *S. anchoralis-D. latus* Zone. Won's (1991a) *A. indensis-S. rota* Zone is placed between the *A. perforata* Zone and the *P. mehli*-Lower *G. texanus* Zone.

Albaillella cartalla group
Figures 6:5, 7-17

*Remarks–*The second group of albaillellids is the *A. cartalla* group (*A. cartalla* Ormiston and Lane 1976), characterized by forms having a short, nearly pentagonal test and a u-shaped h-frame that has several spines on the external side. None of the *A. cartalla* group specimens from the Akmalik Creek sections preserves the h-frame. Specimens we interpret as cf. *A. cartalla* are present upsection from 16.85 m, which is less than a meter above the highest conodont sample (fig. 3, 93CB-006T, and table 1) firmly assignable to the *S. anchoralis-D. latus* Zone. In section C (fig. 3), complete specimens were recovered, and numerous detached h-frames are also preserved. It is not possible to assign our few poorly preserved specimens from sections A and B to one of the five *A. cartalla* morphotypes described by Schwartzapfel and Holdsworth (1996).

*Range and occurrence–*Osagean? to early Chesterian; North America and Germany (probably worldwide). On the basis of the Akmalik sections, we suggest that *A.* sp. cf. *A. cartalla* extends down into the Osagean. Ormiston and Lane (1976) described *A. cartalla*, but the age of the Sycamore Limestone in which it was found was in dispute for some

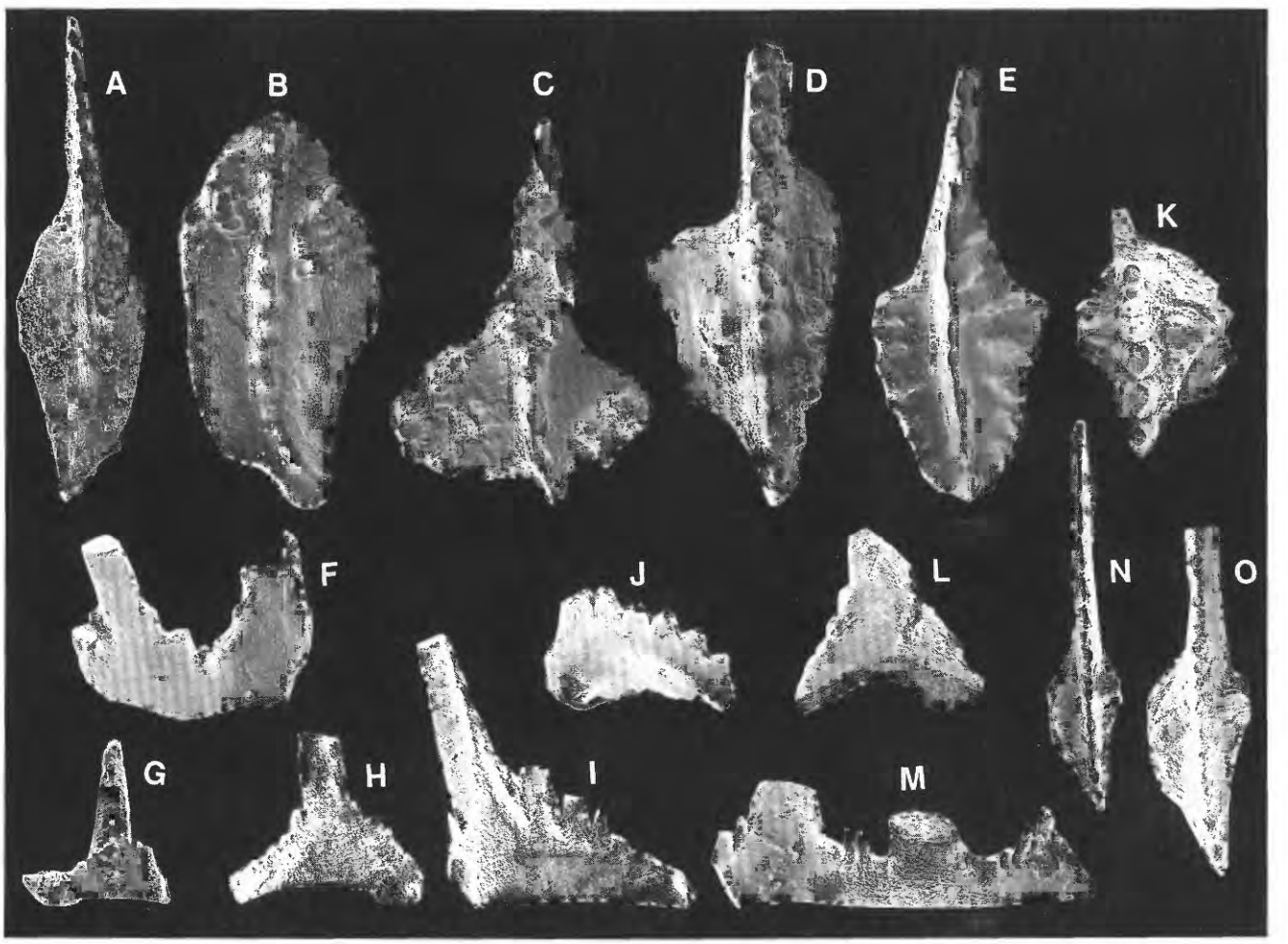

time because of reworked conodonts. However, three conodont collections now date the basal 0.5 m as early Meramecian, *G. homopunctatus*-Lower *G. texanus* Zone (C.A. Sandberg, USGS, written commun., 1997). An analysis by Schwartzapfel and Holdsworth (1996, p. 18) indicates that the vast majority of the Sycamore Limestone in their study area is younger than at least middle Meramecian and some of it is as young as early Chesterian. Bender and others (1991) place the upper *Albaillella cartalla* Zone in (at least) the Upper *G. texanus* Zone and, for the most part, in the *G. bilineatus* Zone. Holdsworth and Murchey (1988) indicated a range for the group as Meramecian to Chesterian. Won's (1991a) *A. cartalla* Zone is middle Meramecian or younger.

Albaillella furcata Won
Figure 6:18
Albaillella furcata Won, 1983, p. 126-127, pl. 12, figs. 3 -5, 7

Remarks–The apical portion of this specimen collected from the type section on Akmalik Creek is not strongly annulated but is fairly long and split at the tip. No trace of an h-frame was found. We question the identifications of Braun (1989b) and Aitchison and Flood (1990) of *A. furcata* in samples in which faunas are characterized by *A. paradoxa* Deflandre and *A. indensis* Won.

The specimen shown in figure 7:6 was found at 32.4 m in section B, higher than any conodont sample; whereas the apical portion appears to be forked, we cannot assign the specimen to this species with certainty.

Range and occurrence–(The species is found with *A. cartalla* in Germany and ranges into the Pennsylvanian (Morrowan); it is also found with *Declinognathodus noduliferus* group conodonts (Holdsworth and Murchey, 1988, p. 782). In section A, this species was recovered only at 66.9 m.

Albaillella sp. cf. *A. ramsbottomi* Schwartzapfel and Holdsworth
Figure 7:5
Albaillella ramsbottomi Schwartzapfel and Holdsworth, 1996, p. 74-76, pl. 43, figs. 6, 8-10, 14, 15, 17, 18

Remarks–In the sample from 32.4 m in section B, this crenulated, short-bodied albaillellid with one prominent and strong dorsal wing dominates the bilateral radiolarians. This form differs from the type in lacking the pointed apical portion. No trace of the h-frame was found. Schwartzapfel and

◄Figure 5. Mississippian conodonts from the Akmalik Chert at and near the type section, Killik River quadrangle, Brooks Range, Alaska. Scanning electron micrographs; upper views of Pa elements except as noted; illustrated specimens are reposited in the U.S. National Museum (USNM), Washington, D.C. See figure 3 for stratigraphic position of samples and table 1 for faunal assemblage, age assignment, and biofacies. A-J, from type section of Akmalik Chert (section A); A-D, from dolomitic limestone at base of section, sample 93CB-006A. K-M from section B. N-O from section C.

A. *Polygnathus communis communis* Branson and Mehl, ×70, USNM 491450.
B. *Polygnathus communis carina* Hass, incomplete gerontic specimen, ×50, USNM 491451.
C. *Dollymae hassi* Voges, ×70, USNM 491452. This species restricts the age range for the base of the Akmalik Chert to the *G. typicus* Zone into the succeeding *S. anchoralis-D. latus* Zone (lower half of the Osagean). It is a rare component of Osagean conodont faunas in the Brooks Range and has only been reported in two other collections (from Rim Butte unit in Howard Pass C-3 and Killik River B-5 quadrangles) where, as in this collection, it occurs with *Gnathodus cuneiformis*, *Kladognathus* sp., *Polygnathus communis*, pseudopolygnathids, and few other taxa (Dumoulin and others, 1993, table 1 and figs. 9*P*, *V*).
D. *Gnathodus cuneiformis* Mehl and Thomas?, ×100, USNM 491453. Specific assignment is uncertain because the specimen is a juvenile.
E. *Pseudopolygnathus multistriatus* Mehl and Thomas morphotype 1, ×35, USNM 491454; from dolomitic limestone 1 m above the base of section, sample 93CB-006C. Morphotype 1 of *Ps. multistriatus* indicates the collection is probably no younger than the lower half of the *S. anchoralis-D. latus* Zone.
F-I. "*Hindeodella*" *segaformis* Bischoff s.f., lateral views, ×100, USNM 491455-58; from black chert (F, sample 93CB-006T; and G-I, sample 93CB-006S2). These bar fragments are part of the posterior process of vicarious S elements of *Scaliognathus* spp. (middle Osagean). Their hindeodellid denticulation and pronounced sigmoidal character make them easily recognizable, even as very small fragments. These distinctive, delicate fragments can be hydraulically transported great distances so that "*H.*" *segaformis* is often the only or most biostratigraphically diagnostic form recovered from hemipelagic basinal deposits of middle Osagean age (table 1, our study; Dumoulin and others, 1993, table 1).
J. *Hindeodus* sp. indet. or *Synclydognathus* sp. indet., juvenile, lateral view, ×100, USNM 491459; from black chert, sample 93CB-006OO, 39.7 m above base of section.
K. *Protognathodus*? sp. indet., juvenile, ×100, USNM 491460; from limestone, sample 93CB-004G.
L. "*H.*" *segaformis* Bischoff s.f., lateral view, ×100, USNM 491461; from black chert, sample 93CB-004J; only taxonomically identifiable specimen in this sample.
M. "*H.*" *segaformis* Bischoff s.f., lateral view, ×100, USNM 491462; same sample as K.
N, O. *Gnathodus texanus* Roundy, juvenile, ×70 and ×100, USNM 491463, USGS colln. 29103-PC, 8 m below top of Akmalik Chert, section C.

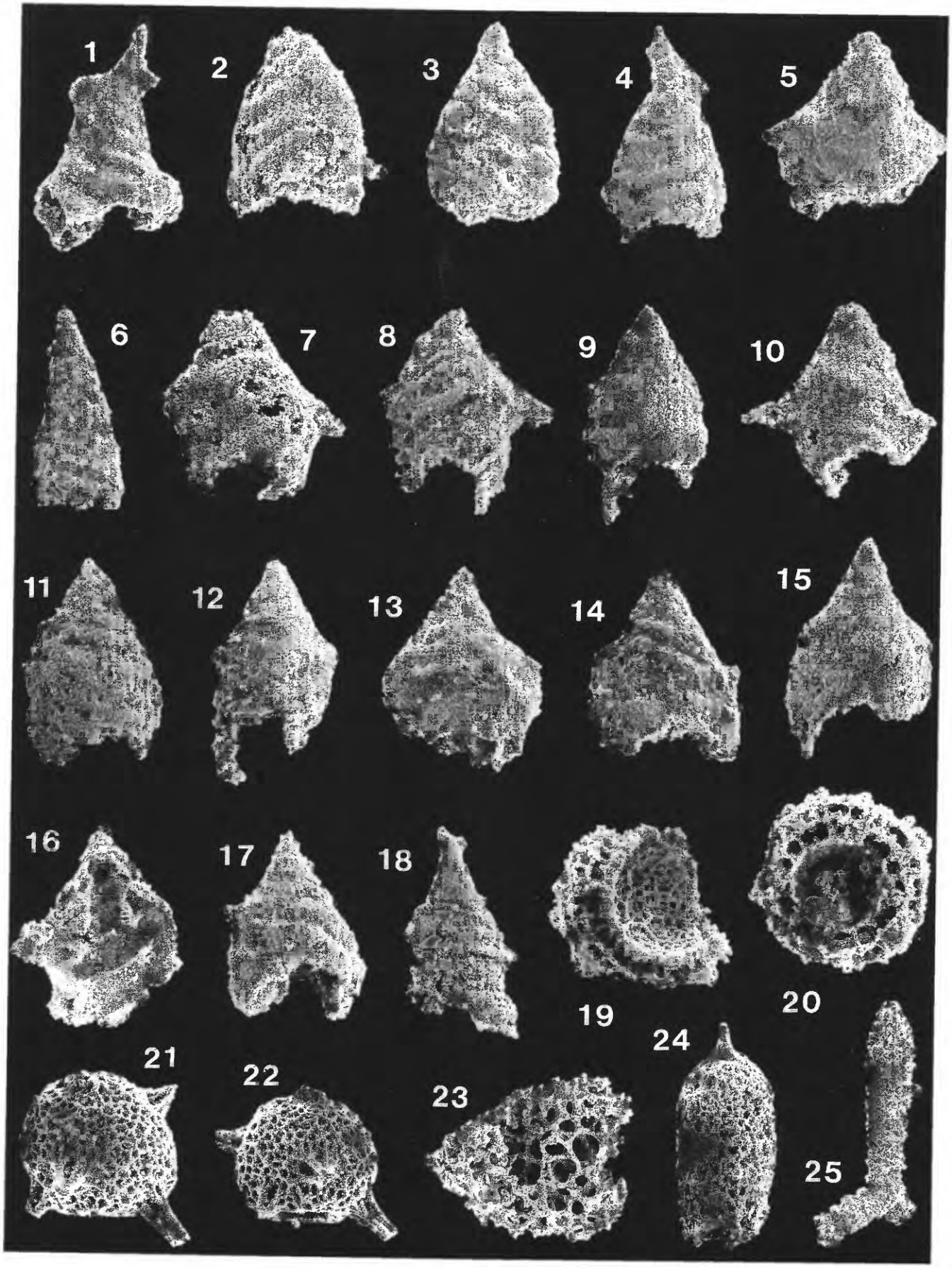
1
2
3
4
5
6
7
8
9
10
11
12
13
14
15
16
17
18
19
20
21
22
23
24
25

Holdsworth (1996) state that *A. ramsbottomi* may be conspecific or at least phylogenetically related to *A. unusalata* (Cheng, 1986) (which they also emend, Schwartzapfel and Holdsworth, 1996, p. 79-80); *A. unusalata* is typically less strongly crenulated but somewhat variable in form.

Range and occurrence–The named species is found in middle Chesterian strata in the Ouachita Mountains of Oklahoma. The Akmalik specimen is certainly older.

Albaillella sp.
Figures 6:6; 7:2

Remarks–This weakly segmented, tall, conical form from 19.5 m in section A and 14.9 m in section B resembles *Albaillella* sp. A described by Won (1991b) from faunas belonging to her *A. perforata* Zone, within strata that contain conodonts of the lower part of the *S. anchoralis-D. latus* Zone. Because these morphotypes are higher in the sections than identifiable conodonts from this zone, this form may extend the range of *A.* sp. A or represent a younger undescribed species.

Suborder SPUMELLARIINA Ehrenberg 1875
Superfamily Latentifistulidea Nazarov and Ormiston 1983; emend. Holdsworth and Murchey 1988
Genus *Scharfenbergia* Won 1983
Type species *Scharfenbergia concentrica* (Rüst 1892)

Scharfenbergia impella (Ormiston and Lane)
Figures 6:24, 25; 7:10, 13

Paronaella impella Ormiston and Lane, 1976, p. 176, pl. 3, figs. 1-5
Scharfenbergia impella (Ormiston and Lane 1976); Won, 1983, p. 160, pl. 9, fig. 9; pl. 10, figs. 1-4

Remarks–The specimens in which the rays are reasonably well preserved (for example, 6:25, 93CB-006RR at 44.5 m, section A) show the classic double tapering. Other specimens (for example, fig. 7:10, 13) have more cylindrical rays with more or less open meshwork, the variation being typical of this species. The oldest scharfenbergiids were found in samples 93CB-006CC at 23.0 m in section A and in sample 93CB-004N2 at 14.2 m in section B. Both of these samples are above the highest recovered middle Osagean conodonts, but they lack other age control. The lowest sample in which the taxon appears is unlikely to be the first occurrence in our section because of the spacing of our samples and poor preservation.

Range and occurrence–Mississippian and Pennsylvanian (late Osagean to possibly Morrowan); essentially worldwide. Holdsworth and Murchey (1988, p. 785) noted that stauraxon radiolarians (here *Scharfenbergia impella* (Ormiston and Lane)) range from the late Osagean to Morrowan(?). Murchey (1990, fig. 4) showed the *S. impella* group extending down to the middle Osagean. Harms and Murchey (1992, fig. 4) showed the range of *S. impella* extending to the earliest Osagean. In the absence of other information, we accept the Holdsworth and Murchey (1988) lower age limit for the taxon, partly because the underlying Kayak Shale, at least in the Ivotuk Hills about 50 km west of the study area, is early Osagean.

◄ **Figure 6.** Scanning electron photomicrographs of radiolarians from the type section of the Akmalik Chert, Killik River quadrangle, Alaska. All magnifications are approximate. Field numbers are followed by Denver radiolarian laboratory number. Stratigraphic position of field numbers is given in meters above base of section (figure 3). USNM number is repository number at U.S. National Museum, Washington, D.C.

1. *Albaillella perforata* Won 1991b, 93CB-006H2, DR 1691, 4.9 m; ×270, USNM 491463.
2. *Albaillella perforata* Won 1991b, 93CB-006J, DR 1694, 6.6 m; ×180, USNM 491464.
3. *Albaillella indensis* Won 1983, 93CB-006I, DR 1693, 7.55 m; ×180, USNM 491465.
4. *Albaillella perforata uniramosa* Won 1991b, 93CB-006K, DR 1696, 7.55 m; ×180, USNM 491466.
5. *Albaillella* sp. cf. *A. cartalla* Ormiston and Lane 1976, 93CB-006U2, DR 1827, 16.85 m; ×220, USNM 491467.
6. *Albaillella* sp., 93CB-006Y, DR 2073, 19.5 m; ×200, USNM 491468.
7. *Albaillella* sp. cf. *A. cartalla* Ormiston and Lane 1976, 93CB-006CC, DR 1717, 23.0 m; ×200, USNM 491469.
8-12. *Albaillella* sp. cf. *A. cartalla* Ormiston and Lane 1976, 93CB-006QQ, DR 1702, 44.1 m. 8, ×240, USNM 491470; 9, ×220, USNM 491471; 10, ×270, USNM 491472; 11, ×220, USNM 491473; 12, ×200, USNM 491474.
13-15. *Albaillella* sp. cf. *A. cartalla* Ormiston and Lane 1976, 93CB-006XX, DR 1830, 54.5 m. 13, ×220, USNM 491475; 14, ×240, USNM 491476; 15, ×180, USNM 491477.
16, 17. *Albaillella* sp. cf. *A. cartalla* Ormiston and Lane 1976, 93CB-006CCC, DR 1894, 66.9 m. 16, ×220, USNM 491478. View of interior of test showing columellae. 17, ×200, USNM 491479. Note faint vertical "costae."
18. *Albaillella furcata* Won 1983, 93CB-006CCC; DR 1894, 66.9 m; ×220, USNM 491480.
19, 20. Unidentified multi-shelled spumellarians. 19, 93CB-006SS, DR 1825, 45.7 m; ×200, USNM 491481, 20, 93CB-006BBB, DR 1893, 66 m; ×220, USNM 491482.
21, 22. *Pylentonema* sp. cf. *P. antiqua* Deflandre 1963, 93CB-006R2, DR 1704, 14.2 m. 21, ×180, USNM 491483; 22, 30(tilt, x160, USNM 491484.
23. *Scharfenbergia* sp. cf. *S. concentrica* (Rüst 1892), 93CB-006ZZ, DR 1833, 63.3 m; ×120, USNM 491485.
24, 25. *Scharfenbergia impella*, 93CB-006RR, DR 1733, 44.5 m. 24, ×110, USNM 491486; 25, ×80, USNM 491487.

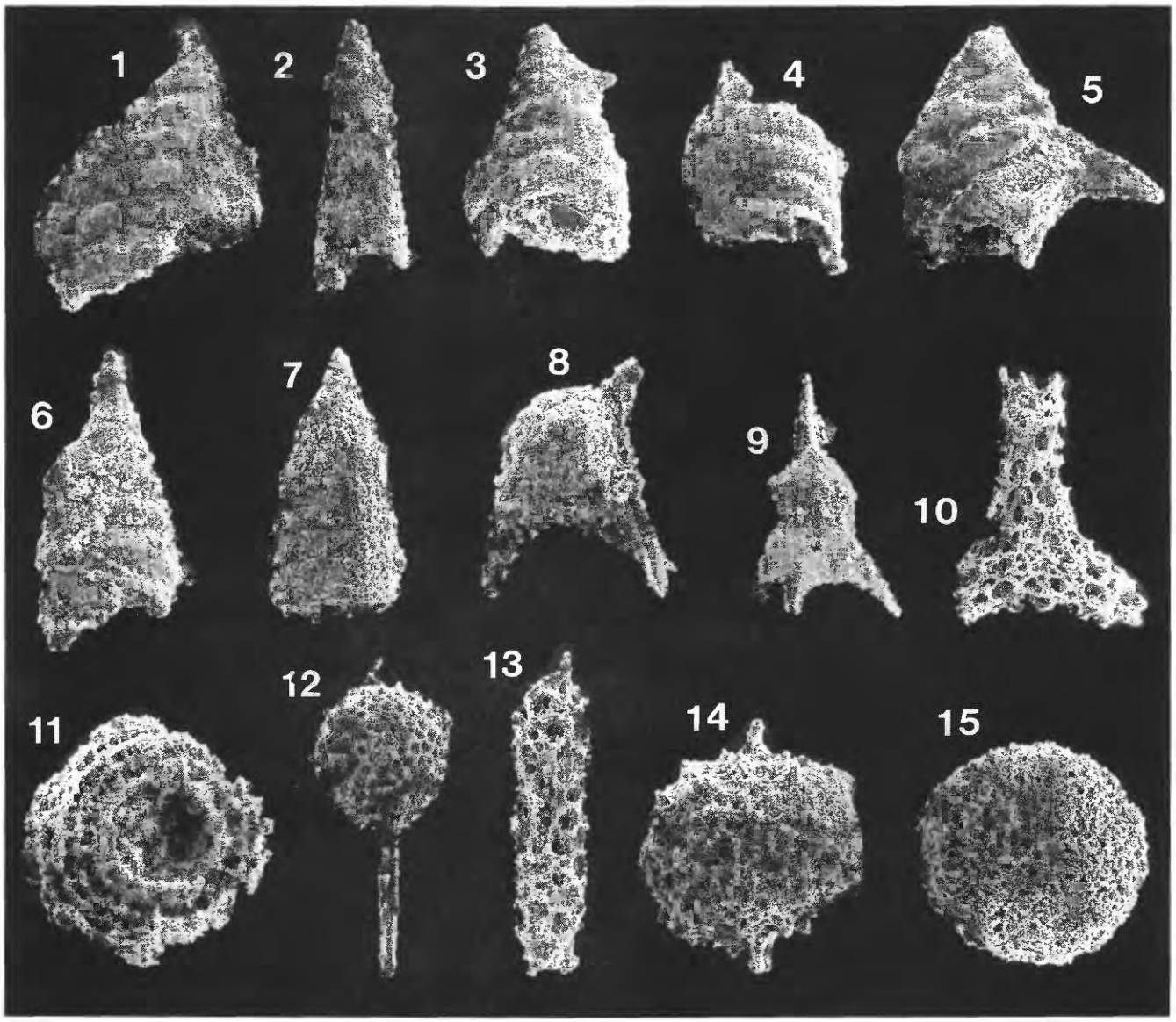

Figure 7. Scanning electron photomicrographs of radiolarians from section B, west side of Akmalik Creek, opposite type section (nos. 12 and 14 are from section A). All magnifications are approximate. Field numbers are followed by Denver radiolarian laboratory number. Stratigraphic position of field numbers is given in meters above base of section (figure 3). USNM number is repository number at U.S. National Museum, Washington, D.C.

1. *Albaillella indensis* Won 1983, 93CB-004J, DR 2001, 8.3 m; ×360, USNM 491488.
2. *Albaillella* sp., 93CB-004O, DR 2044, 14.9 m; ×360, USNM 491489.
3-4. *Albaillella perforata* Won 1991b, 93CB-004Y2, DR 2074, 29.3 m. 3, ×400, USNM 491490; 4, ×400, USNM 491491.
5. *Albaillella* sp. cf. *A. ramsbottomi* Schwartzapfel and Holdsworth 1996, 93CB-004AA, DR 2077, 32.4 m; ×540, USNM 491492.
6. *Albaillella* sp. cf. *A. furcata*, 93CB-004AA, DR 2077, 32.4 m; ×440, USNM 491493.
7. Unidentified cone-shaped radiolarian, 93CB-004H2, DR 1998, 6.8 m; ×360, USNM 491494.
8. ?*Pylentonema*, 93CB-004J, DR 2001, 8.3 m; ×360, USNM 491495.
9. *Archocyrtium* sp. cf. *A. coronasimilae* Won, 93CB-004J, DR 2001, 8.3 m; ×480, USNM 491496.
10, 13. *Scharfenbergia impella* s.l., 93CB-004CC, DR 2079, 34.4 m. 10, ×240, USNM 491497; 13, ×220, USNM 491498.
11. Multishelled spumellarian, 93CB-004M, DR 2041, 12.7 m; ×360, USNM 491499.
12. Unidentified spumellarian, 93CB-006QQ, DR 1702, 44.1 m; ×260, USNM 491500.
14. Unidentified spumellarian, 93CB-006H2, DR 1691, 36.8 m, ×320, USNM 491501.
15. Unidentified spumellarian, 93CB-004CC, DR 2079, 34.4 m, ×330, USNM 491603. This morphotype also occurs in 93CB-006 EE, FF, and 93CB-004T.

Scharfenbergia sp. cf. *S. concentrica* (Rüst)
Figure 6:23
Spongotripus concentricus Rüst, 1892, p. 173, pl. 25, fig. 4
Scharfenbergia concentrica (Rüst 1892); Won, 1983, p. 159, pl. 9, figs. 1-7, pl. 11, figs. 1, 2a, 3a

Remarks–This fragmentary specimen collected at 63.3 m in section A retains traces of two edges and the open spongy meshwork of this species (for example, Won, 1983, pl. 9, fig. 5). The meshwork fines toward the surface. Won's (1983) specimens are considered to be late Viséan (latest Meramecian or early Chesterian) in age.

Range and occurrence–Late Mississippian, North America and Germany.

Superfamily Entactinacea Riedel 1967
Subsuperfamily Pylentonemilae Cheng 1986; emend. Schwartzapfel and Holdsworth 1996
Family Pylentonemidae Deflandre 1963; emend. Holdsworth 1977; emend. Holdsworth, Jones, and Allison 1978; emend. Cheng 1986
Type genus *Pylentonema* Deflandre 1963; emend. Holdsworth, Jones and Allison 1978; emend. Cheng 1986; emend. Gourmelon 1987

Pylentonema sp. cf. *P. antiqua (P. antiqua,* s.l.)
Figures 6:21, 22
Pylentonema antiqua Deflandre, 1963, p. 3981-3984, figs. 1-5; emend. Gourmelon, 1987, p. 284, pl. 1, figs. 1-5

Remarks–No trace of the single inner shell is preserved in our specimen, and the pores are not as regularly spaced or uniformly rounded as in the older Ford Lake Shale specimens (Holdsworth and others, 1978). At least one of the apertural spines is not placed adjacent to the faint, simple pylome rim; these spines are broken but show no curvature toward the pylome. None of the spines appears to be twisted as in the approximately coeval *P. eucosmeta* Braun (1989a). There are seven spines, like the *S. anchoralis-D. latus* Zone specimen shown in Sandberg and Gutschick (1984, pl. 6, fig. P). At least one of the non-apertural grooved spines is shorter than the others, as in M3 of Gourmelon (1987, p. 286). The specimen illustrated in Braun (1990, pl. II, fig. 1), from the *S. anchoralis-D. latus* Zone of the Frankenwald, shares many features with the Akmalik specimen. The specimen in 93CB-006R2 (fig. 3, section A) represents the first reported occurrence of *Pylentonema* in North Slope sequences.

Range and occurrence–Late Devonian (pre-latest Famennian in the Ford Lake Shale, Alaska, possibly Early Carboniferous, Holdsworth and others, 1978) and Early Carboniferous (middle and late Tournaisian; Gourmelon, 1987) and Woodman Formation (Delle Phosphatic Member; Sandberg and Gutschick, 1984), Utah. Germany, North America, Turkey; essentially worldwide.

?*Pylentonema*
Figure 7:8

Remarks–This poorly preserved morphotype, recovered 8.3 m above the base of section B (93CB-004J, fig. 3) is questionably assigned to *Pylentonema* because it possesses a subspherical cortical shell and collar spines and one lateral spine, but it lacks other lateral spines and a centrally located apical spine. This form is present with middle Osagean conodonts assigned to the uppermost Upper *G. typicus* Subzone through most of the *S. anchoralis-D. latus* Zone.

Family Archocyrtiidae Kozur and Mostler 1981; emend. Cheng 1986
Type genus: *Archocyrtium* Deflandre 1972; emend. Won 1983; emend. Cheng 1986

Archocyrtium sp. cf. *A. coronasimilae* Won
Figure 7:9
Archocyrtium coronasimilae Won, 1983, p. 128-129, pl. 1, figs. 1-3

Remarks–It is not possible to determine the number of pores or the details of the pore frames, but the weak apical spine, the "waist" above the attachment of the feet, and the well-developed skirt resemble *A. coronasimilae* somewhat more than other described species. Braun and Schmidt-Effing (1988) illustrated an earliest Viséan ("*Pericyclus*-Delta Stufe") specimen of *A.* sp. aff. *A. babini* Gourmelon that has the less spherical cephalis profile of our specimen. Photographs in Cheng (1986) of *A. wonae* Cheng showed a more robust apical horn and a shallower skirt connecting the feet. Won (1990) illustrated four specimens of *Archocyrtium* from Riescheid, Germany ("not older than the lower *texanus* Zone", p. 111), all of which have deep skirts but more robust apical spines. The genus is quite variable according to M.-Z. Won (Pusan National University, oral commun., 1996).

Range and occurrence–The genus ranges from the Early Silurian (Cheng, 1986) to the early Meramecian *G. homopunctatus*-Upper *G. texanus* Zone (Sandberg and Gutschick, 1984); worldwide. Cheng (1986) gave the youngest end of the range simply as Early Carboniferous. Gourmelon (1986, p. 194) showed the range of the genus from late Famennian to Namurian.

Unidentified spumellarians
Figures 6:19, 20; 7:11, 12, 14, 15

Remarks–Spumellarians were recovered from nearly every sample. However, their internal spicules are not visible, and preservation is too poor to allow assignment even to family. The wide variety of sizes and shapes includes discoidal forms and those with cylindrical, grooved, and (or)

twisted spines, those with one spine far longer than the others, bipolar forms, and spherical forms with both polar and equatorial spines. Only a few examples are shown in the plates.

Radiolaria *incertae sedis*
Figure 7:7

Remarks–Holdsworth and others (1978, fig. 2 x, p. 779) illustrated a conical radiolarian from the Ford Lake Shale, which they concluded spans the Devonian-Mississippian boundary. They noted that the form is imperforate and that it consists of distinct chambers. The conical form from sample 93CB-004H2 at 6.8 m in section B (fig. 3) is clearly perforate, and chambers are less clearly separated. We found conodonts of middle Osagean age above and below this sample (table 1).

DISCUSSION

The type section (section A; figs. 2, 3) of the Akmalik Chert appears to record nearly continuous deposition from early Osagean to at least middle and probably late Meramecian time. The radiolarian samples contain forms representative of the *A. perforata* Zone of Won (1991a) and species that are characteristic of her *A. cartalla* Zone (particularly the *cartalla-concentrica* Subzone; Won, 1991a, p. 18). The age of the lower part of the section is well constrained by conodonts (mostly the middle Osagean *S. anchoralis-D. latus* Zone; fig. 4, table 1).

There are no apparent ancestors to the scharfenbergiid radiolarian group in any of the samples examined from the Akmalik Creek area or from any other locality in northern Alaska. Questions regarding their origin and the paleoecologic or paleogeographic conditions favorable to this group remain unresolved. The Akmalik faunas do not confirm the first appearance of scharfenbergiids any more precisely than do the nearby cherts at Nigu Bluff (Holdsworth and Murchey, 1988). We can only demonstrate that scharfenbergiids are present above Akmalik strata containing conodonts of the *S. anchoralis-D. latus* Zone (fig. 4).

In addition, we found no specimens belonging to the robust tetrahedral *Scharfenbergia tailleurense* Holdsworth and Murchey in the Akmalik Chert. This species is widespread in western North America and Europe and is generally recognizable even in poorly preserved faunas. Holdsworth and Murchey (1988) gave the range of this species as late Meramecian to Morrowan and possibly younger (fig. 4). They also showed that *S. tailleurense* is present in the Imnaitchiak Chert at Nigu Bluff, where the age range was given as the upper two-thirds of the Chesterian and the Morrowan. *Scharfenbergia tailleurense* is also found in samples above 28 m at section C (fig. 3).

The absence of identifiable radiolarians at the top of section A (72.8 m) prevents us from determining its upper age limit. The presence of *A. furcata* at 66.9 m suggests at least a late Meramecian age (fig. 4). The Won (1991a) *cartalla-concentrica* Subzone, which can contain *A. furcata,* ranges from the upper part of the *Pericyclus*-delta to the *Goniatites*-alpha Zones, which are at least middle Meramecian to early Chesterian in age. However, Braun (1993) shows the Osagean-Meramecian boundary between *Pericyclus*-Stufe gamma and delta Zones and the Meramecian-Chesterian boundary between the *Goniatites*-Stufe alpha and beta Zones. Schwartzapfel and Holdsworth (1996, p. 47) indicate that the *Albaillella cartalla-Albaillella furcata* Interval Zone begins no lower than the middle Meramecian; their next youngest interval zone, which also contains *A. furcata,* ranges from late Meramecian to early Chesterian. Holdsworth and Murchey (1988) gave the range of their *A. furcata* group simply as Meramecian to Morrowan; they did not record *A. furcata* specimens in their Nigu Bluff samples. The presence of the conodont *Gnathodus texanus* (late Osagean through early Chesterian) near the top of section C with *A. cartalla* strengthens our conclusion that this section is at least as young as middle and probably late Meramecian.

CONCLUSIONS

Our biostratigraphic study of the Akmalik Chert sections on and near Akmalik Creek adds important data to the North Slope Carboniferous conodont and radiolarian record. Our study is also one of the few that document a Mississippian lithostratigraphic section that has both sequential radiolarian faunas and independent conodont age control. In contrast, some of the work on correlative German Carboniferous sequences records few samples collected from sections that are reasonably well dated. Neither the radiolarian nor conodont data for the Akmalik Creek sections suggest a Pennsylvanian age for the base of the type section or suggest that the section is inverted. These results resolve the uncertainty about the 1985 conodont sample reported in Mull and others (1987) and restricts the age of the section to Mississippian.

Radiolarians recovered at the type section (section A) indicate that the Akmalik Chert ranges in age from Early to Late Mississippian (middle Osagean to probably late Meramecian). We cannot document a broader range because the contact with the underlying Kayak Shale is not exposed and no diagnostic radiolarians were found in the highest samples at any of the sections studied.

Because little is known about the paleoecology of Paleozoic radiolarians, their associated conodont faunas should be used as one of the primary indicators of depositional environments for the rocks in which both are found. There is an implication that the Akmalik radiolarians could have been

transported because the conodont faunas indicate postmortem transport of middle shelf to upper slope taxa within or basinward of the polygnathid-gnathodid biofacies (table 1). Unless there was further postmortem transport, the conodonts in the lower part of the section indicate that the chert samples collected at Akmalik Creek were deposited no shallower than an upper foreslope setting. Small delicate bar fragments of "*Hindeodella*" *segaformis* s.f., however, are the only taxonomically identifiable conodonts in many of these chert samples (table 1). We agree with Chauff (1981) that the sigmoidal bar fragments identified by most workers as "*H.*" *segaformis* s.f. are posterior bar fragments of vicarious S elements of some *Scaliognathus* species. Dumoulin and others (1994, fig. 3*C*) showed a nearly complete Sa element of *Scaliognathus* from the type section of the Kuna Formation. Chauff (1983, text-fig. 3) assigned scaliognathids to the most offshore (deeper water) habitats of the lower Osagean of the North American mid-continent. Subsequently, Sandberg and Gutschick (1984) further refined the habitat of scaliognathids on the basis of their extensive biostratigraphic and lithostratigraphic Osagean studies in the Rocky Mountains and Great Basin of the western United States. These authors regarded scaliognathids as "mesopelagic nektonic dwellers of the dysphotic and aphotic zones" (p. 150), and thus those remains would most likely be found in upper foreslope to basinal deposits adjacent to the lower foreslope. The presence of tiny fragments of the long, delicate bars of "*H.*" *segaformis* in many chert samples collected from the lower Akmalik Chert may indicate that these were carried basinward as distal winnows from a middle foreslope to toe-of-slope setting.

Acknowledgments.—We thank the Alaska Division of Geological and Geophysical Surveys for making it possible for Blome and Reed to spend a week at the outcrop and to bring back nearly 2,000 lb of rock to process and examine. We are grateful to James Vigil for preparing some of the chert samples. Comments from J.A. Dumoulin and C.A. Sandberg helped us improve this paper. However, the authors take full responsibility for the interpretations presented in the final version of the manuscript.

REFERENCES CITED

Aitchison, Jonathan, and Flood, Peter, 1990, Early Carboniferous radiolarian ages constrain the timing of sedimentation within Anaiwan terrane, New England orogen, eastern Australia: Neues Jahrbuch für Geologie und Paläontologie, v. 180, no. 1, p. 1-19.

Alexander, R.J., 1990, Structure and lithostratigraphy of the Kikiktat Mountain area, central Killik River quadrangle, north-central Brooks Range, Alaska: Fairbanks, University of Alaska, M.S. thesis, 248 p., 5 pl.

Bender, Peter, Braun, Andreas, and Königshof, Peter, 1991, Radiolarien und Conodonten aus unterkarbonischen Kieselkalken und Kieselschiefern des nördlichen Rheinischen Schiefergebirges: Geologica et Palaeontologica, v. 25, p. 87-97.

Braun, Andreas, 1989a, Neue unterkarbonische Radiolarien-Taxa aus Kieselschiefer-Geröllen des unteren Maintales bei Frankfurt a. M.: Geologica et Palaeontologica, v. 23, p. 83-99.

Braun, Andreas, 1989b, Unterkarbonische Radiolarien aus Kieselschiefergeröllen des Mains dei Frankfurt am Main: Jahresberichte und Mitteilungen des Oberrheinischen Geologischen Vereines, N. F. 71, p. 357-380.

Braun, Andreas, 1990, Evolutionary trends and biostratigraphic potential of selected radiolarian taxa from the early Carboniferous of Germany: Marine Micropaleontology, v. 15, p. 351-364.

Braun, Andreas, 1993, Die Anwendung der Radiolarien-Biochronologie auf Gesteine des Thüringischen Unterkarbons—Ergebniss und Möglichkeiten: Geologisches Jahrbuch Hessen, v. 121, p. 11-16.

Braun, Andreas, and Schmidt-Effing, Reinhard, 1988, Radiolarienfaunen aus dem tiefen Visé (Unter-Karbon) des Frankenwaldes (Bayern): Neues Jarhbuch für Geologie und Paläontologie, Mh., v. 11, p. 645-660.

Chauff, K.M., 1981, Multielement conodont species from the Osage (lower Carboniferous) in Midcontinent North America and Texas: Palaeontographica, Abteilung A, v. 175, no. 4-6, p. 140-169.

Chauff, K.M., 1983, Multielement conodont species and an ecological interpretation of the Lower Osagean (Lower Carboniferous) conodont zonation from midcontinent North America: Micropaleontology, v. 29, no. 4, p. 404-429.

Cheng Yen-Nien, 1986, Taxonomic studies on Upper Paleozoic Radiolaria: National Museum of Natural Science [Taiwan] Special Publication No. 1, 311 p.

Deflandre, Georges, 1952, *Albaillella*, nov. gen., Radiolaire fossile du Carbonifère inférieur, type d'une lingée aberrante éteinte: Comptes Rendus de l'Académie des Sciences, Paris, v. 223, série D, p. 872-874.

Deflandre, Georges, 1953, Radiolaires fossiles, *in* Grassé, P.P., Traité de Zoologie: Paris, Masson & Cie., v. 1, pt. 2, p. 389-436.

Deflandre, Georges, 1963, *Pylentonema*, nouveau genre de Radiolaire du Viséen; Sphaerellaire ou Nassellaire(?): Comptes Rendus de l'Académie des Sciences, Paris, v. 257, série D, p. 3981-3984.

Deflandre, Georges, 1972, Le système trabéculaire interne chez les Pylentonémidés et les Popofskyellidés, Radiolaires du Paléozoïque: Comptes Rendus de l'Académie des Sciences, Paris, v. 274, série D, p. 3535-3540.

Dumoulin, J.A., and Harris, A.G., 1993, Lithofacies and conodonts of the Carboniferous strata in the Ivotuk Hills, western Brooks Range, Alaska, *in* Dusel-Bacon, Cynthia, and Till, A.B., eds., Geologic studies in Alaska by the U.S. Geological Survey, 1992: U.S. Geological Survey Bulletin 2068, p. 31-47.

Dumoulin, J.A., Harris, A.G., and Schmidt, J.M., 1993, Deep-water lithofacies and conodont faunas of the Lisburne Group, west-central Brooks Range, *in* Dusel-Bacon, Cynthia, and Till, A.B., eds., Geologic studies in Alaska by the U.S. Geological Survey, 1992: U.S. Geological Survey Bulletin 2068, p. 12-30.

Dumoulin, J.A., Harris, A.G., and Schmidt, J.M., 1994, Deep-water facies of the Lisburne Group, west-central Brooks Range, Alaska, *in* Thurston, D.K., and Fujita, Kazuya, eds., 1992 Proceedings, International Conference on Arctic Margins, Anchorage, Alaska, September 1992: Anchorage, Minerals Manage-

ment Service, Outer Continental Shelf Study MMS 94-0040, p. 77-82.

Ehrenberg, C.G., 1838, Über die Bildung der Kreidefelsen und des Kreidemergels durch unsichtbare Organismen: Abhandlungen der Königlische Akademie der Wissenschaften, aus dem Jahre 1838, Berlin, p. 59-147.

Ehrenberg, C.G., 1875, Forsetzung der Mikrogeologischen Studien als gesammt Übersicht der mikroskopischen Palaontologie gleichartig analysierter Gebirgsarten der Erde, mit specieller Rucksicht aus den Polycystinen Mergel von Barbados: Abhandlungen der Königlische Akademie der Wissenschaften, aus dem Jahre 1875, Berlin, 226 p.

Gourmelon, Françoise, 1986, Étude des radiolaires d'un nodule phosphaté du Carbonifère inférieur de Bareilles, Hautes-Pyrénées, France: Geobios, v. 19, no. 2, p. 179-197.

Gourmelon, Françoise, 1987, Revision of the genus *Pylentonema* Deflandre 1963 and its lower Carboniferous species from Montagne Noire, France: Micropaleontology, v. 33, no. 3, p. 282-288.

Harms, T.A., and Murchey, B.L., 1992, Setting and occurrence of Late Paleozoic radiolarians in the Sylvester allochthon, part of a proto-Pacific ocean floor terrane in the Canadian Cordillera: Palaeogeography, Palaeoclimatology, Palaeoecology, v. 96, p. 127-139.

Higgins, A.C., Richards, B.C., and Henderson, C.J., 1991, Conodont biostratigraphy and paleoecology of the uppermost Devonian and Carboniferous of the western Canada sedimentary basin, *in* Orchard, M.J., and McCracken, A.D., eds., Ordovician to Triassic conodont paleontology of the Canadian Cordillera: Geological Survey of Canada Bulletin 417, p. 215-251.

Holdsworth, B.K., 1966, Radiolaria from the Namurian of Derbyshire: Palaeontology, v. 9, pt. 2, p. 319-329.

Holdsworth, B.K., 1969, The relationship between the genus *Albaillella* Deflandre and the ceratoikiscid Radiolaria: Micropaleontology, v. 15, no. 2, p. 230-236.

Holdsworth, B.K., 1977, Paleozoic Radiolaria; stratigraphic distribution in Atlantic borderlands, *in* Swain, F. M., ed., Stratigraphic micropaleontology of Atlantic Basin and borderlands: Elsevier Publishing Co., p. 167-184.

Holdsworth, B.K., and Jones, D.L., 1980, A provisional Radiolaria biostratigraphy, Late Devonian through Late Permian: U.S. Geological Survey Open-File Report 80-876, 32 p., 2 oversize sheets.

Holdsworth, B.K., Jones, D.L., and Allison, Carol, 1978, Upper Devonian Radiolarians separated from chert of the Ford Lake Shale, Alaska: U.S. Geological Survey Journal of Research, v. 6, no. 6, p. 775-788.

Holdsworth, B.K., and Murchey, B.L., 1988, Paleozoic radiolarian biostratigraphy of the northern Brooks Range, Alaska, *in* Gryc, George, ed., Geology and exploration of the National Petroleum Reserve in Alaska, 1974 to 1982: U.S. Geological Survey Professional Paper 1399, p. 777-797.

Kozur, Heinz, and Mostler, Helfried, 1981, Beiträge zur Erforschung der mesozoischen Radiolarien; Teil IV(Thalassosphaeracea Haeckel, 1862, Hexastylacea Haeckel, 1882 emend., Petrushevskaya, 1979, Sponguracea Haeckel, 1862 emend. und weitere triassische Lithocycliacea, Trematodiscacea, Actinommacea und Nassellaria: Geologische-Paläontologische Mitteilungen Innsbruch, Sonderband, 208 p.

Krumhardt, A.P., Harris, A.G., and Watts, K.F., 1996, Lithostratigraphy, microlithofacies, and conodont biostratigraphy and biofacies of the Wahoo Limestone (Carboniferous), eastern Sadlerochit Mountains, northeast Brooks Range, Alaska: U.S. Geological Survey Professional Paper 1568, 70 p.

Mayfield, C.F., Tailleur, I.L., and Ellerseick, Inyo, 1988, Stratigraphy, structure, and palinspastic synthesis of the western Brooks Range, northwestern Alaska, *in* Gryc, George, ed., Geology and exploration of the National Petroleum Reserve in Alaska, 1974 to 1982: U.S. Geological Survey Professional Paper 1399, p. 143-186.

Moore, T.E., Wallace, W.K., Bird, K.J., Karl, S.M., Mull, C.G., and Dillon, J.T., 1994, Geology of northern Alaska, *in* Plafker, George, and Berg, H.C., eds., The geology of Alaska: Boulder, Colo., Geological Society of America, The Geology of North America, v. G-1, p. 49-140.

Mull, C.G., Crowder, R.K., Adams, K.E., Siok, J.P., Bodnar, D.A., Harris, E.E., Alexander, R.A., and Solie, D.N., 1987, Stratigraphy and structural setting of the Picnic Creek allochthon, Killik River quadrangle, central Brooks Range, Alaska—A summary, *in* Tailleur, I.L., and Weimer, Paul, eds., Alaskan North Slope geology, Volume Two: Society of Economic Paleontologists and Mineralogists, Pacific Section [and the Alaska Geological Society], p. 649-661.

Mull, C.G., Harris, A.G., and Carter, J.L., 1997, Lower Mississippian (Kinderhookian) biostratigraphy and lithostratigraphy of the western Endicott Mountains, Brooks Range, Alaska, *in* Dumoulin, J.A., and Gray, J.E., eds., Geologic studies in Alaska by the U.S. Geological Survey, 1995: U.S. Geological Survey Professional Paper 1574., p. 221-242.

Mull, C.G., Moore, T.E., Harris, E.E., and Tailleur, I.L., 1994, Geologic map of the Killik River quadrangle, Brooks Range, Alaska: U.S. Geological Survey Open-File Report 94-697, 1 sheet, scale 1:125,000.

Mull, C.G., Tailleur, I.L., Mayfield, C.F., Ellersieck, I.F., Curtis, S., 1982, New upper Paleozoic and lower Mesozoic stratigraphic units, central and western Brooks Range, Alaska: American Association of Petroleum Geologists Bulletin, v. 66, no. 3, p. 348-362.

Murchey, B.L., 1990, Age and depositional setting of siliceous sediments in the upper Paleozoic Havallah sequence near Battle Mountain, Nevada; implications for the paleogeography and structural evolution of the western margin of North America, *in* Harwood, D.S., and Miller, M.M., eds., Paleozoic and early Mesozoic paleogeographic relations; Sierra Nevada, Klamath Mountains, and related terranes: Geological Society of America Special Paper 255, p. 137-155.

Murchey, B.L., Jones, D.L., Holdsworth, B.K., and Wardlaw, B.R., 1988, Distribution patterns of facies, radiolarians, and conodonts in the Mississippian to Jurassic siliceous rocks of the northern Brooks Range, Alaska, *in* Gryc, George, ed., Geology and exploration of the National Petroleum Reserve in Alaska, 1974 to 1982: U.S. Geological Survey Professional Paper 1399, p. 697-724.

Murchey, B.L., Swain, P.B., and Curtis, Steve, 1979, Late Mississippian to Pennsylvanian radiolarian assemblages in the Siksikpuk(?) Formation at Nigu Bluff, Howard Pass quadrangle, Alaska, *in* Albert, N.R.D., and Hudson, Travis, eds., The U.S. Geological Survey in Alaska—Accomplishments during 1979: U.S. Geological Survey Circular 823-B, p. B17-B19.

Nazarov, B.B., and Ormiston, A.R., 1983, A new superfamily of stauraxon polycystine Radiolaria from the Late Paleozoic of

the Soviet Union and North America: Senckenbergiana Lethaea, v. 64, no. 2/4, p. 363-379.

Ormiston, A.R., and Lane, H.R., 1976, A unique radiolarian fauna from the Sycamore Limestone (Mississippian) and its biostratigraphic significance: Palaeontographica, Abteilung A, v. 154, no. 4-6, p. 158-180.

Poole, F.G., and Sandberg, C.A., 1991, Mississippian paleogeography and conodont biostratigraphy of the Western United States, *in* Cooper, J. D., and Stevens, C. H., eds., Paleozoic paleogeography of the Western United States II: Pacific Section Society of Economic Paleontologists and Mineralogists Book 67, p. 107-136.

Riedel, W.R., 1967, Chapter 8, Protozoa, *in* Harland, W.B., and others, eds., The fossil record; a symposium with documentation: Geological Society of London, p. 291-298.

Rüst, David, 1892, Beiträge zur Kentniss der fossilen Radiolarien aus Gesteinen der Trias und der paleozoischen Schichten: Palaeontographica, v. 38, p. 107-200.

Sandberg, C.A., and Gutschick, R.C., 1984, Distribution, microfauna, and source-rock potential of Mississippian Delle Phosphatic Member of Woodman Formation and equivalents, Utah and adjacent states, *in* Woodward, Jane, Meissner, F.F., and Clayton, J.L., eds., Hydrocarbon source rocks of the greater Rocky Mountain region: Denver, Colorado, Rocky Mountain Association of Geologists, p. 135-176.

Schwartzapfel, J.A., and Holdsworth, B.K., 1996, Upper Devonian and Mississippian radiolarian zonation and biostratigraphy of the Woodford, Sycamore, Caney and Goddard Formations, Oklahoma: Cushman Foundation for Foraminiferal Research Special Publication 33, 275 p.

Tailleur, I.L., Kent, B.H., Jr., and Reiser, H.N., 1966, Outcrop/geologic map of the Nuka Etivluk region, northern Alaska: U.S. Geological Survey Open-File Report 66-128, 7 sheets, scale 1:63,360.

Won, Moon-Zoo, 1983, Radiolarien aus dem Unterkarbon des Rheinischen Schiefergebirges (Deutschland): Palaeontographica, Abteilung A, v. 182, no. 4-6, p. 116-175.

Won, Moon-Zoo, 1990, Lower Carboniferous radiolarian fauna from Riescheid (Germany): Paleontological Society of Korea Journal, v. 6, no. 1, p. 111-143.

Won, Moon-Zoo, 1991a, Phylogenetic study of some species of genus *Albaillella* Deflandre 1952 and a radiolarian zonation in the Rheinische Schiefergebirge, West Germany: Paleontological Society of Korea Journal, v. 7, no. 1, p. 13-25.

Won, Moon-Zoo, 1991b, Lower Carboniferous radiolarians from siliceous boulders in western Germany: Paleontological Society of Korea Journal, v. 7, no. 1, p. 77-106.

Reviewers: C.G. Mull, P.J. Noble, and D.J. Nichols

Sedimentology, Conodonts, Structure, and Regional Correlation of Silurian and Devonian Metasedimentary Rocks in Denali National Park, Alaska

By Julie A. Dumoulin, Dwight C. Bradley, *and* Anita G. Harris

ABSTRACT

A sequence of metasedimentary rocks in Denali National Park (Mt. McKinley and Healy quadrangles), previously mapped by Csejtey and others (1992) as unit DOs (Ordovician to Middle Devonian metasedimentary sequence) and correlated with rocks of the Nixon Fork terrane, contains both deep- and shallow-water facies that correlate best with rocks of the Dillinger and Mystic sequences (Farewell terrane), respectively, exposed to the southwest in the McGrath quadrangle and adjacent areas.

New conodont collections indicate that the deep-water facies are at least in part of Silurian age, and can be grouped into three broad subunits. Subunit A is chiefly very fine grained, thinly interbedded calcareous, siliceous, and siliciclastic strata formed mostly as hemipelagic deposits. Subunit B is characterized by abundant calcareous siliciclastic turbidites and may correlate with the Terra Cotta Mountains Sandstone in the McGrath quadrangle. Subunit C contains thin-bedded to massive calcareous turbidites and debris flows, locally intercalated with calcareous siliciclastic turbidites. Sedimentary features suggest that subunits B and C accumulated in a fan and (or) slope apron setting. All three subunits contain subordinate layers of altered tuff and tuffaceous sediment. Turbidites were derived chiefly from a quartz-rich continent or continental fragment and a carbonate platform or shelf, with subordinate input from volcanic and (possibly) subduction complex (accretionary prism) sources. Limited paleocurrent data from subunit B turbidites show generally southward transport. Stratigraphic relations between the three subunits are uncertain, although we believe that subunit A is probably the oldest. Shallow-water facies, at least in part of earliest Late Devonian (early Frasnian) age, are exposed locally and were deposited in intertidal to deeper subtidal settings.

Reconnaissance structural studies indicate that the most significant of two generations of folds have northerly vergence and presumably are the product of Mesozoic plate convergence.

Deep-water rocks of Silurian age have been recognized in six Alaskan terranes outside the Farewell terrane. Comparison of unit DOs with coeval strata in these terranes reveals closest sedimentologic and biostratigraphic similarities with rocks of east-central Alaska (Livengood terrane) and western Alaska (Seward terrane) and less striking similarities with rocks in southeastern Alaska (Alexander terrane) and northern Alaska (Hammond subterrane of Arctic Alaska terrane). Coeval sequences in easternmost Alaska (Porcupine and Tatonduk terranes) correlate least well with DOs because they lack both Silurian siliciclastic turbidites and Upper Devonian platform carbonate rocks. Our correlations permit the interpretation that all Alaskan terranes with Silurian deep-water strata originated along or adjacent to the North American continental margin, but imply a gradient in Silurian turbidite distribution along this margin. Volcanic material preserved in DOs and related rocks may have been derived from the island arc represented by the Alexander terrane.

INTRODUCTION

Lower and middle Paleozoic metasedimentary rocks (unit DOs, Ordovician to Middle Devonian metasedimentary sequence, of Csejtey and others, 1992) form an east-trending belt on the north side of the Denali fault in Denali National Park (Mt. McKinley and Healy quadrangles; figs. 1, 2). These rocks have been variously correlated (Jones and others, 1981, 1982, 1983; Mullen and Csejtey, 1986; Csejtey and others, 1992, 1996) with different parts of the Farewell terrane (Decker and others, 1994) but have received little detailed investigation. We report here the results of a reconnaissance study of the lithofacies, conodont age and biofacies, and structure of DOs in the Mt. McKinley B-1 and Healy B-6 quadrangles, and evaluate possible correlations between DOs and coeval sequences in the Farewell terrane and elsewhere in Alaska. Lower Paleozoic strata throughout Alaska are poorly understood and are considered by many authors to belong to numerous discrete tectonostratigraphic terranes (Jones and others, 1981; Silberling and others, 1994). Most of these terranes are interpreted as displaced pieces of the continental margin of North America, but some may repre-

sent fragments of other continental margins (for example, Siberia) or of island arcs (Nokleberg and others, 1994; Soja, in press). Detailed comparisons of Paleozoic rocks throughout Alaska are essential in understanding the ultimate origin of these terranes.

GEOLOGIC SETTING

The Farewell terrane of Decker and others (1994) incorporates three previously defined units: (1) the Nixon Fork terrane (Patton, 1978); (2) the Dillinger terrane (Jones and others, 1981) or sequence (Gilbert and Bundtzen, 1984); and the Mystic terrane (Jones and others, 1981) or sequence (Gilbert and Bundtzen, 1984). Different authors have proposed various definitions and boundaries for these three units and have disagreed on whether or not they are genetically related to each other and to the North American craton (compare Decker and others, 1994; Patton and others, 1994; Silberling and others, 1994). Most workers, however, favor a North American origin for these units (Decker and others, 1994; Nokleberg and others, 1994).

We follow here most of the conventions and interpretations outlined by Decker and others (1994). These authors (p. 288) interpreted the Farewell terrane as a coherent, but locally highly deformed, continental margin succession made up of the Middle Cambrian through Middle Devonian White Mountain sequence and the overlying Upper Devonian through Lower Cretaceous Mystic sequence. The contact between the two sequences is generally an angular unconformity, but it is locally conformable. The White Mountain sequence includes both platform and deeper water (slope and basinal) facies, called Nixon Fork and Dillinger terranes (or sequences), respectively, by previous authors. We agree with Decker and others (1994) that these two assemblages probably formed as part of a single continental margin succession, but we retain the term "Dillinger sequence" for convenience.

Rocks of the DOs unit, initially described as part of the Dillinger terrane by Jones and others (1981), are complexly folded and faulted and have been subjected to low-grade regional metamorphism; they contain conodonts with color alteration indices of 5 to 5.5, indicating that the host rocks reached temperatures of at least 300 to 350°C (Epstein and others, 1977). Parts of DOs in our study area retain little original fabric; some carbonate intervals are pervasively recrystallized, and some siliciclastic layers are slightly to strongly semischistose. Other parts of DOs, however, particularly sections which are thick-bedded and (or) dolomitic, have well-preserved primary sedimentary textures.

As mapped by Csejtey and others (1992) and Jones and others (1983), the outcrop belt of DOs is bounded on the south by the Denali strike-slip fault, beyond which are rocks unrelated to DOs: the Windy terrane (melange), and a belt of

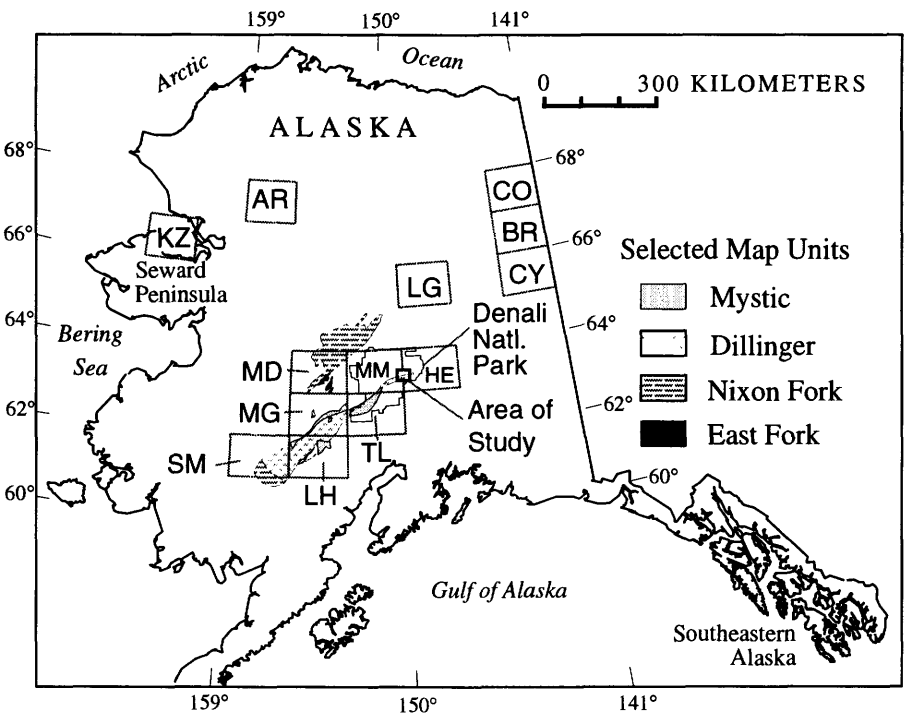

Figure 1. Location of quadrangles and selected tectonostratigraphic terranes mentioned in text; East Fork is East Fork subterrane of Minchumina terrane (Patton and others, 1994). Terranes from Silberling and others (1994), modified in the McGrath and Medfra quadrangles based on Decker and others (1994). Quadrangles: AR, Ambler River; BR, Black River; CO, Coleen; CY, Charley River; HE, Healy; LG, Livengood; LH, Lime Hills; KZ, Kotzebue; MD, Medfra; MG, McGrath; MM, Mt. McKinley; SM, Sleetmute; TL, Talkeetna.

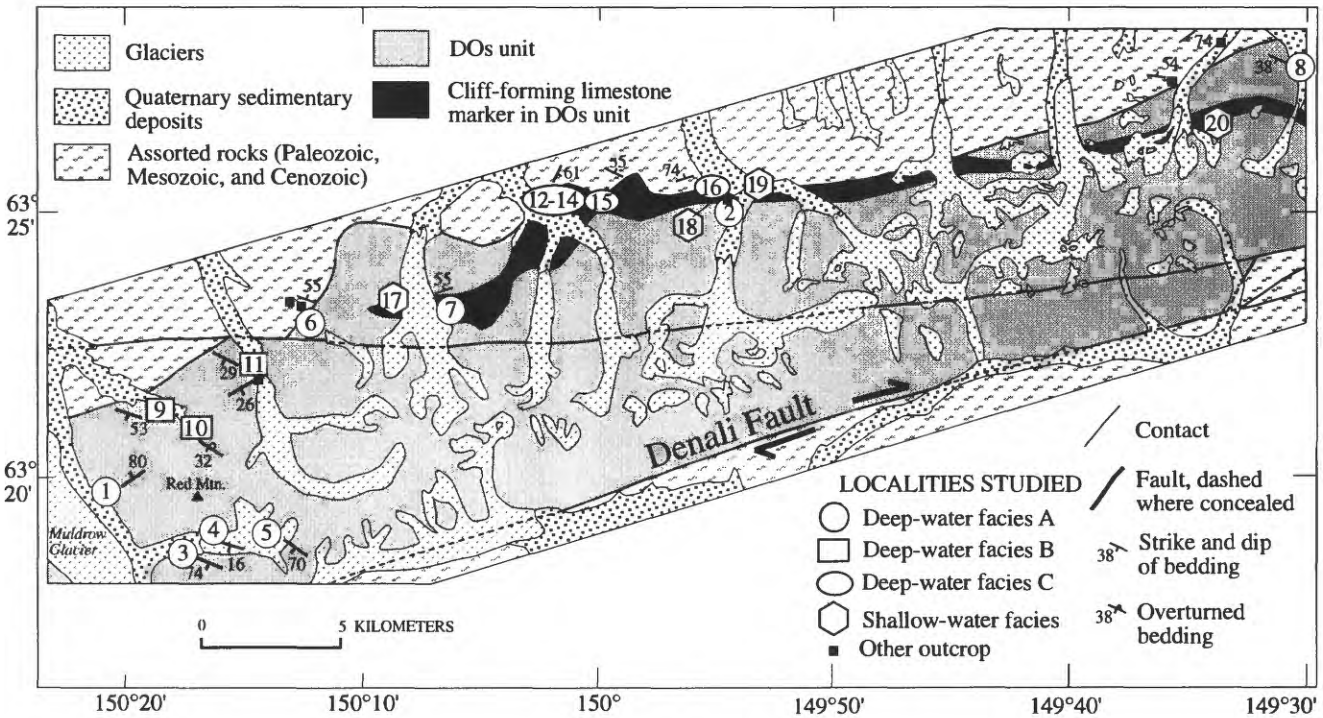

Figure 2. Location of lithologic and fossil collections and structural data from study area in Denali National Park (Healy and Mt. McKinley quadrangles). "Other outcrop" symbol within DOs map pattern indicates rocks assigned to DOs but not assigned to a facies or subunit; elsewhere, symbol indicates rocks other than DOs.

Jurassic-Cretaceous flysch (Kahiltna terrane). According to Csejtey and others (1992), DOs is bounded on the north by an unnamed fault (fig. 2), which they interpreted as a north-directed thrust fault. At various places along the footwall are Upper Triassic to Pennsylvanian flysch; Upper Triassic basalt, diabase, and sedimentary rocks; Lower Cretaceous and Upper Jurassic flysch; and the Upper Cretaceous (Ridgway and others, 1997) sedimentary member of the Cantwell Formation. Ridgway and others (1997) have shown that sediments that formed the Cantwell were shed northward from active thrusts in the ancestral Alaska Range. Fluvial conglomerates in the Cantwell include abundant limestone clasts that Csejtey and others (1992, 1996) traced to unit DOs.

PREVIOUS WORK AND METHODS

Lower and middle Paleozoic metasedimentary rocks in the study area were first described by Jones and others (1981, 1982, 1983; unit "Pzd") as "turbidites and basinal facies" (Jones and others, 1982, p. 3712). These publications included brief lithologic summaries and mentioned a single fossil collection, gastropods of Middle Ordovician to Devonian age, from the easternmost part of the unit in the Healy B-5 quadrangle. Mullen and Csejtey (1986) and Csejtey and others (1992) mapped these rocks as unit "DOs" in the Healy quadrangle, supplied additional descriptions of the deep-water facies, recognized and briefly described shallow-water facies in the unit, and reported a few additional fossil localities. Constraints on the age of DOs were provided chiefly by conodont collections (Csejtey and others, 1992) from carbonate pebbles in nearby exposures of the Upper Cretaceous sedimentary part of the Cantwell Formation; these pebbles were interpreted as derived from DOs. Refinements of faunal ages for these cobbles, as well as new megafossil and conodont data from a single locality of Frasnian (early Late Devonian) age in the shallow-water facies of DOs (fig. 2, loc. 19), were given by Csejtey and others (1996). Savage and others (1995) reported additional faunal and lithologic details for locality 19.

We examined the DOs unit at 20 localities in the study area (fig. 2) and measured sections at five good exposures. Sedimentologic and petrographic descriptions are based on field observations and examination of 125 thin sections. Shallow-water carbonate rocks in which primary texture can be recognized are classified after Dunham (1962). Conodont age and biofacies determinations utilize data from seven new collections (table 1) and some older collections (Csejtey and others, 1992, map nos. 9-11 in table 2; ages revised by A.G. Harris, unpub. data, 1994, and reported in Csejtey and others, 1996). Interpretations of depositional environments follow models in Wilson (1975), Mutti and Ricci Lucchi (1978), Cook and others (1983), and Scholle and others (1983). Terrane designations generally follow Silberling and others (1994), except as noted.

SEDIMENTOLOGY, AGE, AND DEPOSITIONAL SETTING

Rocks of the DOs unit within the study area consist chiefly of calcareous and siliciclastic strata of Silurian and probable Silurian age deposited in a deep-water, off-platform setting. Shallow-water shelf or platform rocks have been recognized at several localities; where dated, these strata are earliest Late Devonian and Silurian or Devonian in age.

DEEP-WATER STRATA

Deep-water rocks can be grouped into three broad subunits (subunits A, B, and C) on the basis of lithology and bedding style. Subunit A is found throughout the study area, but subunits B and C are less widespread (fig. 2). Subunit B has been recognized only in the area north of Red Mountain; subunit C crops out in the central part of the study area.

SUBUNIT A

LITHOFACIES

Subunit A consists mainly of thinly interbedded, fine-grained, calcareous metasedimentary rocks, cherty argillite, phyllite, and tuff in various proportions (fig. 3A). It was examined at 8 localities across the study area (fig. 2, locs. 1-8); depositional textures are best preserved at localities 1 and 6 to 8. Most sections are strongly folded; some folds may be slumps. Sections at localities 6 and 7 consist chiefly of fine-grained carbonate; beds are 0.5 to 15 cm (mostly 2-4 cm) thick with abundant parallel laminae and local convolute and low-angle cross laminae. Most carbonate beds are gray to black on fresh and weathered surfaces, but more dolomitic layers weather yellow to olive gray. Carbonate beds consist mostly of micritic to sand-sized anhedral calcite crystals, with 5 to 95 percent euhedral to subhedral dolomite in some layers. Less than 1 percent quartz silt and sand is concentrated in local discontinuous laminae. Some beds are clearly graded; others contain outsize clasts, some of which may be crinoid columnals. Calcite-filled spheres and ovoids that are probably radiolarian ghosts form 2 to 5 percent of fine-grained samples at locality 7.

Black, carbonaceous, noncalcareous argillite, in intervals a few centimeters to several meters thick, is a subordinate part of the sections at localities 6 and 7. It is the predominate lithology at locality 1, where it weathers reddish-brown and forms parallel laminated beds 1 to 4 cm thick with gray phyllitic partings and millimeter- to centimeter-scale, yellow-weathering silty layers. Some beds are quite siliceous, with conchoidal fracture and stylolitic partings. Silty layers are largely quartz; laminae reflect local concentrations of radiolarian ghosts (made up of polycrystalline quartz) and lesser siliceous sponge spicules (fig. 3B).

The section at locality 8 is at least 15 m thick and consists chiefly of 0.5- to 3-cm-thick couplets of steel-gray phyllite and yellow- to tan-weathering siltstone. Sedimentary features include graded and flaser beds and parallel and cross laminae. Coarser grained material in these beds ranges from silt to fine sand and is mostly calcite (30-50%), quartz (30%), and subordinate sedimentary and volcanic lithic grains.

Calcareous siliciclastic rocks also crop out at locality 7, but they are noticably coarser grained and thicker bedded than the rocks at locality 8. The siliciclastic section at locality 7 crops out about 100 m east of the calcareous section described above; the contact between the two lithologies is not exposed. The section consists of about 70 percent orange- to gray-weathering, fine- to medium-grained sandstone, in beds 50 to 120

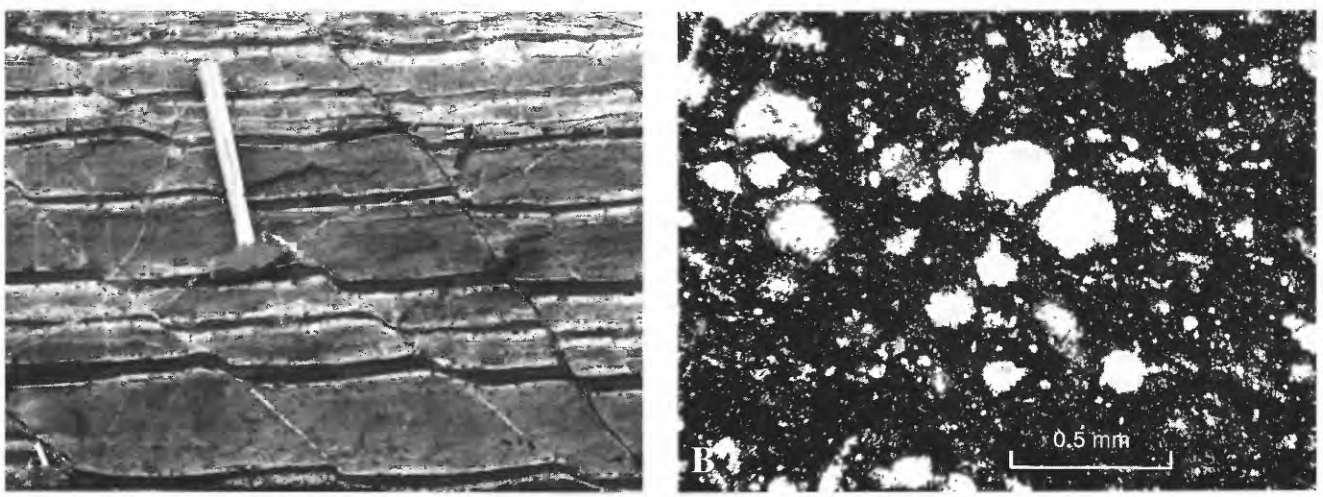

Figure 3. Sedimentary features of DOs subunit A. A, Thinly interlayered, chiefly phyllosilicate material (dark) and carbonate; dark layers contain metamorphic biotite (fig. 2, loc. 3). B, Photomicrograph of carbonaceous siliceous argillite containing abundant radiolarian ghosts made up of polycrystalline quartz (fig, 2, loc. 1).

cm thick, intercalated with gray- to black-weathering thinner beds of siltstone and phyllite. A sample of very fine to fine-grained sandstone consists of calcite (20-30%), quartz (30%), metamorphic lithic grains (10-20%) and phyllosilicate material (10-20%), with minor amounts of sedimentary and volcanic lithic grains, feldspar[1], and biotite.

Thin layers of altered tuff and tuffaceous sediment form a subordinate but notable part of the sections at localities 1, 6, and 8. Layers are a few millimeters to 3 cm thick and weather light to dark green, yellow, or brownish purple. They consist chiefly of euhedral crystals and crystal aggregates of feldspar and quartz in a fine-grained felty groundmass; one sample contains rounded, altered lapilli? (now mostly microcrystalline quartz) as much as 1 mm in diameter.

Pyrite, in 1- to 5-mm crystals and crystal aggregates, is a common minor component of dark, fine-grained calcareous and siliceous beds in subunit A. At locality 8, massive pyrite forms laterally continuous beds 0.5 to 3 cm thick that make up several percent of the outcrop. A grab sample of massive pyrite at this locality yielded 4.8 ppm Ag, 47 ppb Au, 110 ppm Co, 1,495 ppm Cu, 2.4 percent P, 75 ppm Pb, 102 ppm Sb, 39 ppm Se, and 155 ppm Zn.[2]

Rocks south of Red Mountain (fig. 2, locs. 3-5) are similar in general aspect and composition to those described above but have been contact metamorphosed by a small, previously unmapped plug at the snout of the glacier near locality 4. These rocks consist of pinkish-brown- to dark-gray-weathering siliciclastic layers and dark-gray, recessive calcareous layers, intercalated on a scale of 0.5 to 20 cm (fig. 3A). Strata are ductily folded, but locally preserve sedimentary structures such as parallel and cross laminae. Siliciclastic layers contain abundant phyllosilicate material, quartz, and metamorphic biotite. Calcareous layers consist of anhedral calcite with minor laminae of quartz silt.

AGE

Conodont samples were collected from graded, parallel and cross laminated, locally dolomitic metalimestone at localities 6 and 7, but no conodonts were found at either locality. Outcrop patterns (discussed further under "Stratigraphy" below) suggest that subunit A may be older than subunits B and C; this hypothesis implies an age of Silurian or older for subunit A. Lithologic correlations with rocks in the McGrath quadrangle to the southwest (see "Correlation" below) suggest that subunit A could be as old as Cambrian.

DEPOSITIONAL ENVIRONMENT

We interpret subunit A as chiefly hemipelagic sediment, with subordinate intercalated turbidites, deposited in a slope and (or) basinal setting adjacent to a continental landmass. Clay-sized "background" material in this facies originated as calcareous peri-platform ooze (Cook and others, 1983) (for example, locs. 6 and 7) or carbonaceous, siliceous, locally radiolarian-rich ooze (loc. 1). Both of these lithologies, but particularly the siliceous strata, have relatively high organic contents and are well-laminated with little or no bioturbation, suggesting that they were deposited in a dysaerobic (poorly oxygenated) to anoxic setting. Few calcareous planktonic organisms existed in the lower Paleozoic (Scholle and others, 1983, p. 622), so fine-grained calcareous material in these deposits must have been derived from a relatively nearby carbonate platform or shelf. Variations in calcareous versus siliceous background material in subunit A thus probably reflect chiefly temporal and (or) spatial differences in proximity to a carbonate source, although differences in depositional setting relative to position of the paleo-CCD (calcite compensation depth) may also be involved.

Millimeter- to centimeter-thick layers of silt and sand punctuate these clay-sized sediments and may have had various origins. Some may be the coarser half of basinal varves formed through cyclic (seasonal?) changes in productivity and (or) detrital influx; others are probably distal turbidites or lags left by bottom currents. Coarser and thicker layers such as those at localities 7 and 8 contain full or partial Bouma sequences and are clearly turbidites. The possible presence of slump folds suggests a slope setting for at least some of this facies.

The semischistose fabric and pervasive calcareous alteration of the turbidites in these facies preclude accurate point counts and thus precise use of point-count-based provenance analyses such as those of Dickinson and Suczek (1979). However, the general composition of subunit A turbidites compared to provenance interpretations by these and other authors (for example, Zuffa, 1980) indicates derivation chiefly from two sources: (1) carbonate platform or shelf (abundant calcareous grains) and (2) continent or continental fragment (abundant quartz). Notable metamorphic and sedimentary lithic grains could have been derived from a continental and (or) a subduction complex (accretionary prism) source. Volcanic lithic grains, as well as the discrete tuffaceous layers found throughout this facies, suggest some input from a volcanic arc.

SUBUNIT B

LITHOFACIES

Subunit B is characterized by abundant siliciclastic strata, includes thin layers of fine-grained carbonate and al-

[1] DOs thin sections examined in this study were not stained; feldspar grains were recognized petrographically. Most are plagioclase and contain polysynthetic twins.

[2] Au, Co, Se, and Zn determined by induced neutron activation analysis; all other values by inductively coupled plasma-atomic emission spectroscopy. All analyses were performed by ACTLABS.

tered ash, and was studied at localities 9 to 11 (fig. 2). A folded section 8 to 10 m thick at locality 9 consists chiefly of thin-bedded carbonate and subordinate thick-bedded siliciclastic rocks; sections 30 and 50 m thick at localities 10 and 11 comprise carbonate beds intercalated with 20 to 30 and 50 to 60 percent siliciclastic strata, respectively. Thus, thick-bedded siliciclastic strata are ubiquitous in subunit B and are consistently intercalated with carbonate rocks; similar siliciclastic rocks in subunit A are rare and, where found, are not interbedded with carbonate strata.

Siliciclastic rocks at all three localities in subunit B are medium-gray, gray- to brown- to reddish-brown-weathering siltstone to fine-grained sandstone. Beds are chiefly 30 cm to 1.5 m thick (fig. 4A); amalgamated beds as much as 3 m thick punctuated by thin mud drapes and mud chip layers (chips as much as 7 cm long) were noted at locality 11. Sedimentary structures in these rocks include common parallel and cross lamination, and local convolute laminae and flame structures. Some bed bottoms display abundant and well-preserved flutes (as large as 3 x 10 cm) and grooves (as large as 3 cm x 2 m) (fig. 4B). Coarser grained beds are clearly graded and have erosive, locally channeled, bases. Some beds contain 1- to 3-mm-thick horizontal trace fossils.

Eight siliciclastic samples from localities 9 to 11 were examined in thin section; their composition is quite uniform (fig. 4C, D) and is similar to that of the siliciclastic beds in subunit A (loc. 7). Sorting is poor to very poor; grains are chiefly subangular, but some are rounded. Quartz, mostly monocrystalline grains with straight extinction, is the major siliciclastic component and makes up 20 to 40 percent of all samples. Carbonate material (including monocrystalline and

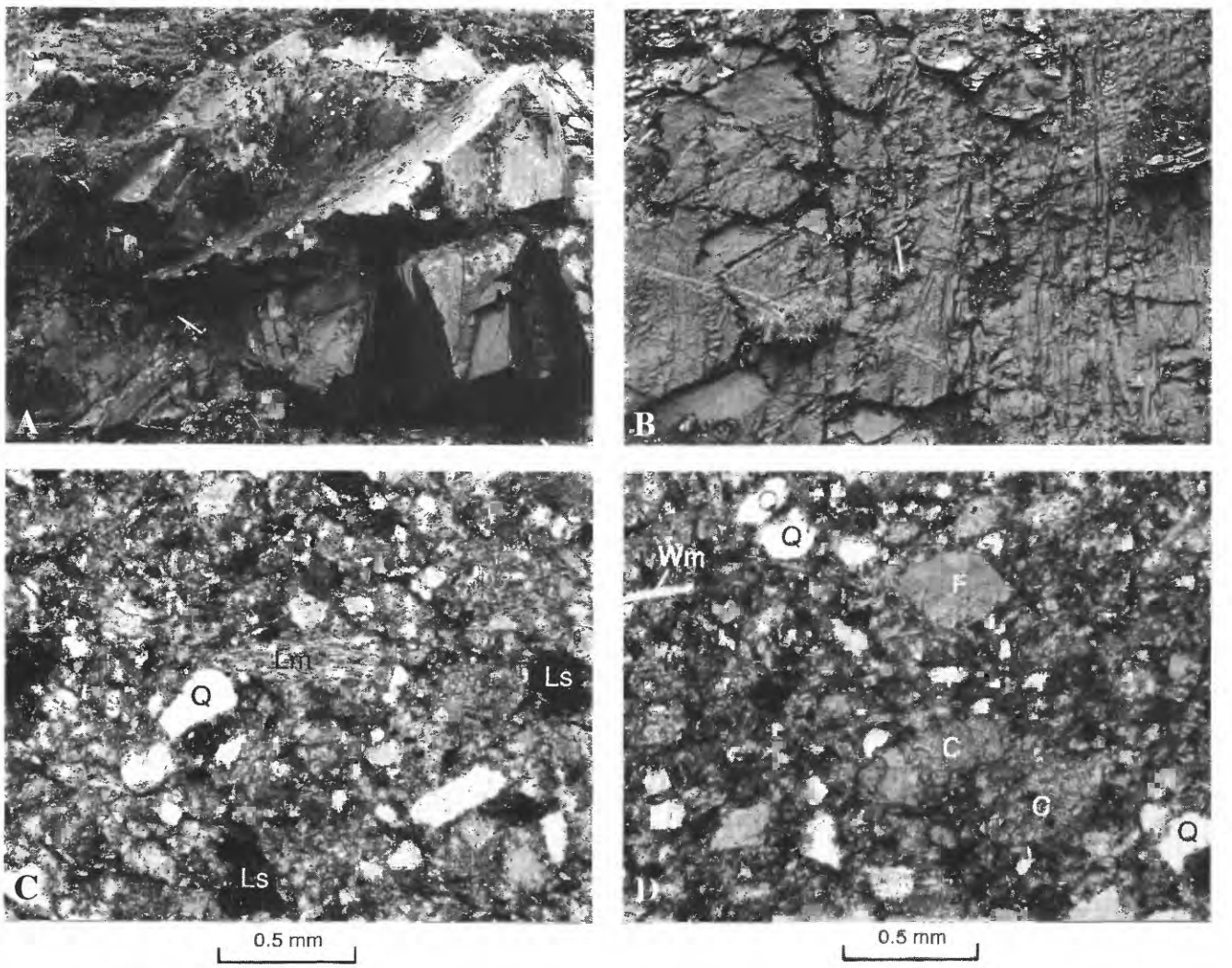

Figure 4. Sedimentary features of DOs subunit B. A, Thick-bedded fine-grained calcareous siliciclastic turbidites (fig. 2, loc. 11). B, Base of calcareous siliciclastic turbidite bed with abundant flutes and grooves (fig. 2, loc. 10). C and D, Photomicrographs of fine-grained calcareous siliciclastic turbidites (fig. 2, loc. 11); samples contain about 30 percent and 50 percent carbonate material, respectively. C, polycrystalline calcite fragment; F, feldspar; Lm, metamorphic rock fragment; Ls, sedimentary rock fragment; Q, quartz; Wm, white mica.

polycrystalline clasts, cement, and patchy replacement of feldspar and lithic grains) constitutes 15 to 50 percent. Other clasts include feldspar (trace to 5%), metamorphic lithic clasts such as phyllite and fine-grained schist (5-15%), and sedimentary lithic clasts such as mudstone and siltstone (5-15%). Volcanic lithic clasts and white mica are minor (<5%) but ubiquitous components of all samples; rare constituents include dolomite, chert, biotite, chlorite, and tourmaline. Fine-grained phyllosilicate matrix and pseudomatrix is pervasive, and makes up as much as 20 to 30 percent of the least calcareous samples. Original sedimentary fabric is better preserved in the siliciclastic strata of subunit B than in compositionally similar rocks in subunits A and C.

Very dark gray to black, light- to medium-gray-weathering calcareous layers are most abundant at locality 9, where they are 1 to 10 cm thick (fig. 5A) and contain obvious parallel and cross laminae (fig. 5B); cross-sets are low angle and less than 1 cm thick. All five samples of this lithology consist of calcitized radiolarite (fig. 5C), similar to, but richer in radiolarians than, the radiolarian-bearing beds in subunit A (locality 7). Radiolarians are chiefly ovoids and spheres, 150 to 300 μm in maximum diameter, that make up 5 to 40 percent of the samples. Most are filled with finely crystalline calcite or, less commonly, with calcite and chalcedony or chalcedony alone. Some contain concentrations of organic material that preserve details of the original test structure. Other bioclasts in these samples include calcareous sponge spicules (as much as 80 μm wide and 2.5 mm long), possible ostracodes, and a few unidentifiable fragments.

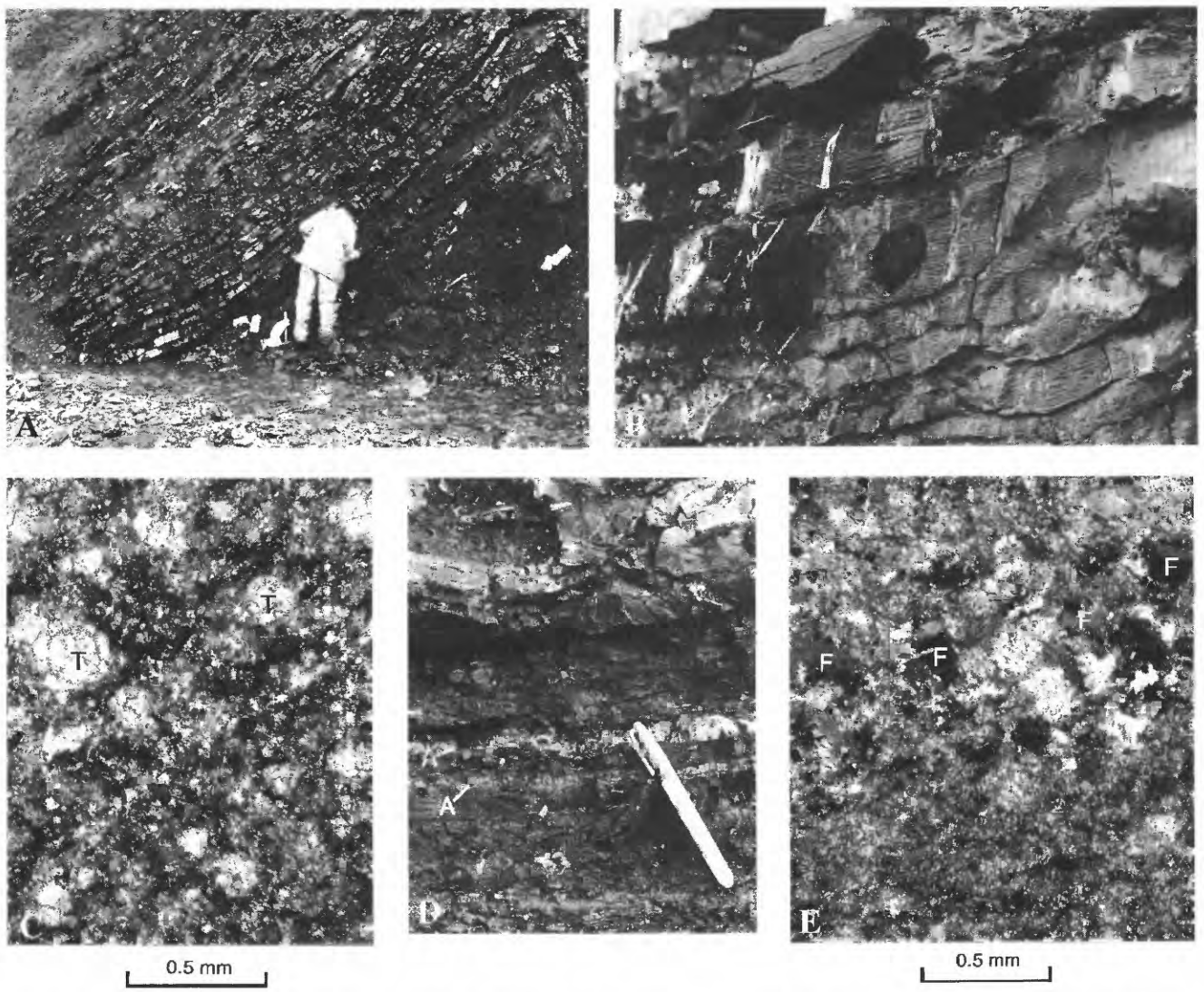

Figure 5. Sedimentary features of DOs subunit B (fig. 2, loc. 9). A-C, outcrop views and photomicrograph (C) of thin-bedded calcitized radiolarite that yielded conodonts of probable Silurian age. Note parallel and cross laminae in B, and locally preserved details of original test structure (T) in C. Outcrop view (D) and photomicrograph (E) (crossed nicols) of altered ash layers (A) intercalated with calcitized radiolarite. Note abundant feldspar crystals (F) in E.

The radiolarians and other bioclasts float in a matrix of very finely crystalline calcite, dolomite, and dark (organic?) material; crystals of calcite and dolomite are mostly 50 μm and less. The lamination in these samples reflects differing concentrations of radiolarians, dolomite, and (or) organic material.

Gray calcareous layers at localities 10 and 11 are 40 cm and less (mostly 8 cm and less) thick with parallel and cross laminae. Layers consist of recrystallized micrite; laminae concentrate various amounts of dolomite, organic material, quartz silt, and (or) phyllosilicate material.

Altered ash layers were noted at localities 9 and 10 in outcrop and thin sections. In outcrop, they are a few millimeters to 2 cm thick, have a friable, pasty, or indurated texture, and may be white, ivory, yellow, light gray, orange, red, or reddish brown. At least 12 discrete ash layers are intercalated with calcitized radiolarite through a 1.6-m-thick interval at locality 9 (fig. 5D), and a single 1-cm-thick pasty yellow ash layer was noted near the base of the section at locality 10. Abundant euhedral zircons were recovered from one ash at locality 9. Thin sections of calcitized radiolarite from locality 9 and of recrystallized micrite from locality 10 contain irregular lenses and laminae of ash, from 1 mm to a few hundred microns thick, rich in sand- and silt-sized euhedral to subhedral grains of feldspar (some zoned) and quartz (fig. 5E).

AGE

Conodonts from two collections of parallel- and cross-laminated calcitized radiolarite at locality 9 consist exclusively of elements of *Ozarkodina excavata*, which ranges from the late Early Silurian into the late Early Devonian (Wenlockian to early Emsian) (table 1, fig. 6A-F). We consider these collections to be of of probable Silurian age; if they were Devonian, they would most likely include other conodont taxa in addition to *O. excavata*. *O. excavata* is a eurytopic species that is the most abundant (and often the only) conodont in hemipelagic basinal deposits of post-Llandoverian Silurian age.

Figure 6.➤ Silurian and Devonian conodonts from metacarbonate rocks in Denali National Park (A-V and DD-II) and correlative rocks in the McGrath C-1 quadrangle (W-CC), Alaska (scanning electron micrographs; illustrated specimens are reposited in the U.S. National Museum, USNM, Washington, D.C.). See table 1 for faunal analysis, age assignment, and lithostratigraphic description of samples and figure 2 for geographic and geologic position of Denali localities.

A-F, Oz*arkodina excavata* (Branson and Mehl), two Pa, Pb, M, Sb, and Sc elements, lateral views, A-E x50 and F x80, USNM 491604-09; loc. 9, subunit B of deep-water facies, USGS colln. 12537-SD.

G, Distomodontid? M? element, lateral view, x100, USNM 491610; loc. 15, subunit C of deep-water facies, USGS colln. 12533-SD.

H-K, N, Loc. 16, subunit C of deep-water facies, USGS colln. 12532-SD.

H, *Ozarkodina* sp., Pa element, lateral view, x100, USNM 491611.

I, *Walliserodus* sp., outer lateral view, x100, USNM 491612.

J, *Panderodus unicostatus* (Branson and Mehl), inner lateral view, x75, USNM 491613.

K, Unassigned Sb compressed coniform element of Early Silurian morphotype, x100, USNM 491614.

N, *Belodella* sp., Sc element, outer lateral view, x100, USNM 491617.

L, *Panderodus unicostatus* (Branson and Mehl) inner lateral view, x75, USNM 491615; loc. 14, subunit C of deep-water facies, USGS colln. 12535-SD.

M, Distomodontid or icriodellid P element fragment, upper view, x100, USNM 491616; loc. 15, subunit C of deep-water facies, USGS colln. 12534-SD.

O-Q, Distomodontid and (or) pelekysgnathid coniform S elements; subunit C of deep-water facies.

O, Inner lateral view, x100, USNM 491618; loc. 15, USGS colln. 12534-SD.

P, Q, Anterior and oblique lower views, x60 and x75, USNM 491619-20; loc. 14, USGS colln. 12535-SD.

R-T, Unassigned compressed alate coniform elements of Early Silurian morphotype, Pb? element (outer lateral view), M element (posterior view), and Sb element (inner lateral view), x90, USNM 491621-23; loc. 14, subunit C of deep-water facies, USGS colln. 12535-SD.

U, V, *Panderodus* sp. element and Sb element *Belodella*? sp., outer lateral views, x100, USNM 491624-25; loc. 18, shallow-water facies, USGS colln. 12531-SD.

W, X, Distomodontid and (or) pelekysgnathid coniform S elements (like O-Q), lateral views, x100, USNM 491626-27; from 353-m-thick section of black to very dark gray micrite on north side of Dillinger River (SW1/4 sec. 6, T. 28 N., R. 20 W.), McGrath C-1 quadrangle, 86 m above base of section, USGS colln. 9736-SD.

Y-CC, Unassigned compressed alate coniform elements of Early Silurian morphotype (like R-T), x100; same locality as W.

Y, Z, CC, Pb?, M, and Sc elements, outer lateral and two inner lateral views, USNM 491628-30; same collection as W.

AA, BB, Sa and Sb elements, posterior and inner lateral views, USNM 491631-32; USGS colln. 9738-SD, 126 m above base of section.

DD-GG, *Playfordia primitiva* (Bischoff and Ziegler), P elements, lower, lateral, and upper views of one specimen, x60, and upper view of another, x75, USNM 491633-34; loc. 19, shallow-water facies, USGS colln. 12358-SD.

HH, *Mesotaxis asymmetrica* (Bischoff and Ziegler), Pa element, upper view, x60, USNM 491635; same collection as DD.

II, *Icriodus subterminus* Youngquist, narrow morphotype, P element, upper view, x75, USNM 491636; same collection as DD.

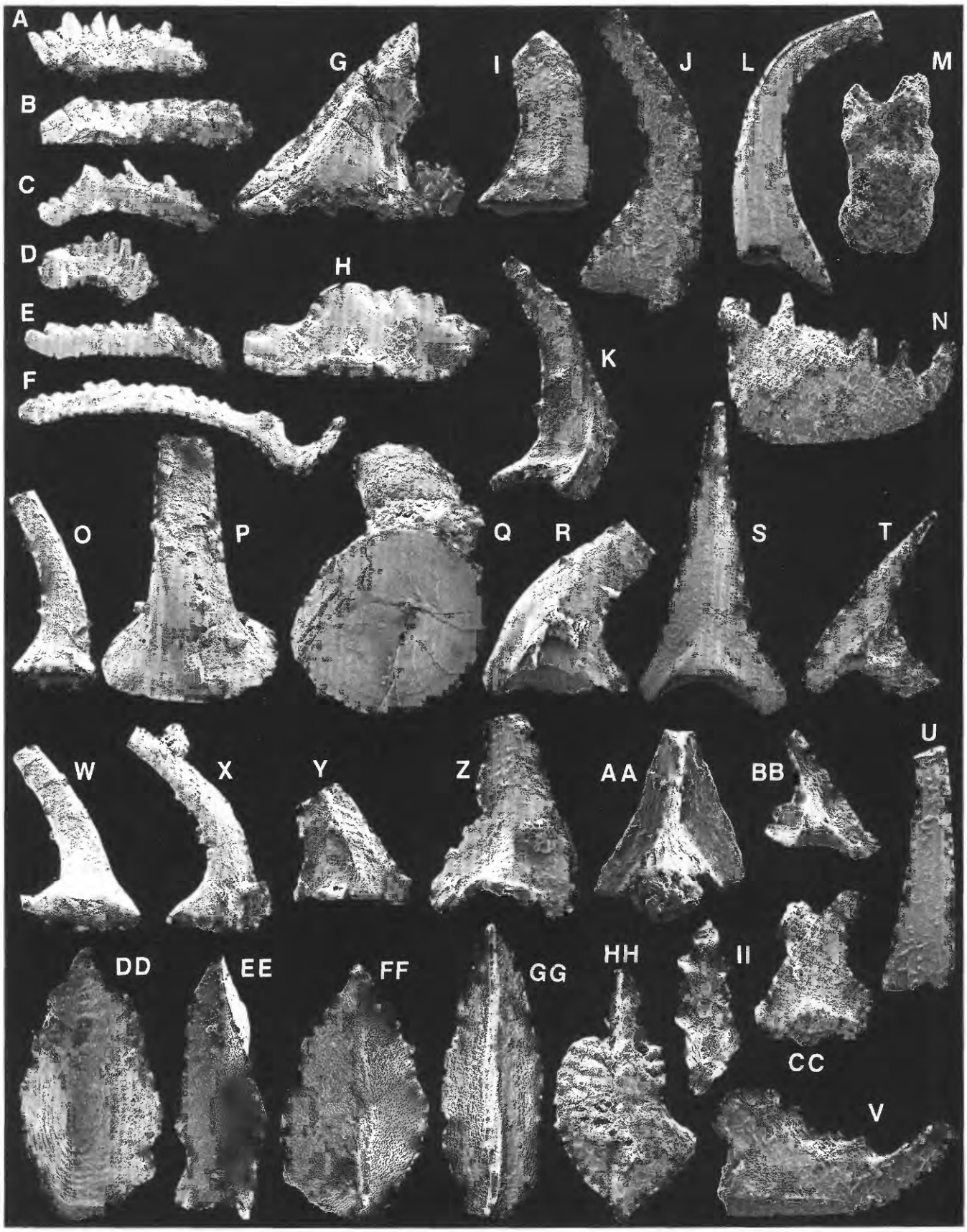
A
B
C
D
E
F
G
H
I
J
K
L
M
N
O
P
Q
R
S
T
U
V
W
X
Y
Z
AA
BB
CC
DD
EE
FF
GG
HH
II

Table 1. Conodont data for localities shown on figure 2.

[Letters in field number refer to collector: AD, J.A. Dumoulin; Cy, Béla Csejtey, Jr. Abbreviations: CAI, color alteration index; indets., indeterminate bar, blade, platform, and coniform fragments]

LOCALITY NO., (FACIES; SUBUNIT)	QUADRANGLE LATITUDE/ LONGITUDE	CONODONT FAUNA AND CAI (FIELD NO.; USGS COLLN. NO.)	AGE	BIOFACIES	REMARKS
9 (Deep-water facies; subunit B)	Mt. McKinley B-1 63°21'18"/ 150°18'38"	5 Pa elements *Ozarkodina excavata* (Branson and Mehl) 2 indets. CAI=5-5.5 (96AD8X; 12536-SD)	late Early Silurian into late Early Devonian (Wenlockian-early Emsian), probably Silurian—if collection was Devonian in age, other taxa would probably be represented.	Indeterminate (too few conodonts); probably deep-water open-marine setting.	Five-cm-thick bed of very dark-gray to black, light- to medium-dark-gray-weathering, parallel- to cross- laminated, calcitized radiolarite. From 10-m section of mostly thin-bedded, calcitized radiolarite with subordinate thick-bedded calcareous siliciclastic turbidites. Collected a few meters downstream from 96AD8Y. Sample weight 14.8 kg.
		Ozarkodina excavata (Branson and Mehl) (fig. 6A-F) 9 Pa, 4 Pb, 4 M, 4 Sb and 9 Sc juvenile to adult elements 33 fragments most probably of *O. excavata* CAI=5-5.5. (96AD8Y; 12537-SD)		*O. excavata* biofacies; this eurytopic, long-lived form is typically the most abundant or often the only conodont species recovered from deep-water, hemipelagic basin deposits of Wenlockian and younger Silurian age.	Same lithology as 96AD8X; 10-cm-thick bed within 1.6-m-thick measured section. Sample weight 13.4 kg.
14 (Deep-water facies; subunit C)	Mt. McKinley B-1 63°25'14"/ 150°01'25"	21 distomodontid and (or) pelekysgnathid coniform elements (fig. 6P, Q) 3 Pb, 1 M, and 1 Sb unassigned compressed alate coniform elements (fig. 6R-T) 8 *Panderodus unicostatus* (Branson and Mehl) elements (fig. 6L) 11 indets. CAI=5 (96AD7C; 12535-SD)	Early Silurian (late Llandoverian-Wenlockian). The compressed alate coniforms could belong to a new genus or to Silurian genera such as *Distomodus* or *Pterospathodus*. Coniform elements and more roundiform distomodontid and (or) pelekysgnathid coniforms like those in this collection were reported by Dumoulin and Harris (1988, figs. 4C-I) from the Ambler River quadrangle, Alaska, and considered Wenlockian or Ludlovian in age. Virtually the same fauna (fig. 6W-CC) is found in three collections from the McGrath C-1 quadrangle (Armstrong and others, 1977; USGS colln. 9736-38-SD) and are here considered late Llandoverian to Wenlockian in age. Similar coniform elements were also found in the late Llandoverian part of the Chicotte Formation on Anticosti Island, Québec (Uyeno and Barnes, 1983) but were not assigned to any taxon.	Postmortem transport from shallow-water depositional environment(s); all specimens are small and platform elements are notably absent.	Carbonate conglomerate containing micrite and dolomite clasts as much as 7 cm in size; some clasts contain radiolarian ghosts. Bed is 80 cm thick and has scoured base. Collected about 5 m above base of 21-m-thick measured section consisting of carbonate turbidites, debris flows, and hemipelagic "background" sediment. Sample weight 12.3 kg.

Table 1. Conodont data for localities shown on figure 2—Continued.

15 (Deep-water facies; subunit C)	Healy B-6/Mt. McKinley B-1 63°24'50"/ 150°00'00"	3 robust distomodontid element fragments of Llandoverian-Ludlovian morphotype (fig. 6G) 3 indets. CAI=5-5.5 (96AD4C; 12533-SD)	Early to early Late Silurian (Llandoverian-Ludlovian).	Indeterminate (too few conodonts); postmortem transport from shelf or platform depositional environment. Conodonts are tectonically deformed and fractured.	Sooty, black, laminated to cross-laminated dolomitic micrite in beds 2 mm to 4 cm thick. Sample weight 6.2 kg.
	Mt. McKinley B-1 63°24'48"/ 150°00'02"	1 P element fragment of a distomodontid or icriodellid (fig. 6M) 5 *Panderodus* sp. elements 2 distomodontid or pelekysgnathid coniform elements (fig. 6O) 1 unassigned M element of post-Ordovician morphotype 1 indet. CAI=5-5.5 (96AD4G; 12534-SD)	Silurian (Wenlockian, possibly early Wenlockian). The earliest pelekysgnathids and latest icriodellids overlap in the early Wenlockian. If the coniforms are distomodontids, an early Wenlockian age is still likely as these could belong in *Distomodus? dubius* (Rhodes).	Indeterminate (too few conodonts); coniform elements were probably derived from shallow-water depositional environments.	Black to light-gray, grayish-orange-weathering, massive carbonate conglomerate at least 20 m thick. Clasts up to 5 cm across are micrite and dolomite; matrix mostly dolomite. Some clasts contain relict fossils including possible algae. This sample may be from a channel cut into the deposits represented by 96AD4C. Sample weight 14.1 kg.
16 (Deep-water facies; subunit C)	Healy B-6 63°25'19"/ 149°55'05"	*Belodella* sp. 1 Sa and 3 Sc elements (fig. 6N) 1 ozarkodinid? Sb (plectospathodan) element of Silurian-Devonian morphotype 1 Pa *Ozarkodina* sp. (fig. 6H) 4 *Panderodus unicostatus* (Branson and Mehl) elements (fig. 6J) 1 pelekysgnathid? coniform element 2 *Walliserodus* sp. elements (fig. 6I) 1 Sb compressed coniform element of Early Silurian morphotype (fig. 6K) 10 indets. CAI=5 (96AD3D; 12532-SD)	Early Silurian (probably Wenlockian)	Indeterminate (too few conodonts); postmortem transport from shelf or platform depositional environment(s).	Dark-gray to black, medium-gray-weathering, fetid dolomitic limestone from 10 to 30-cm-thick graded bed containing chiefly micritic clasts (as much as 5 cm in diameter) and some dolomitic clasts and fossil fragments (colonial corals and crinoids?) in dolomitic matrix; partly cross laminated in upper part of bed. Collected 2 m above base of 42-m-thick measured section of thin- to thick-bedded carbonate turbidites intercalated with calcareous hemipelagic "background" sediments. Sample weight 10.1 kg.
18 (Shallow-water facies)	Healy B-6 63°25'18"/ 149°55'02"	1 Sb element *Belodella*? sp. (fig. 6V) 4 *Panderodus* sp. elements (fig. 6U) 4 indets. CAI=5-5.5 (96AD2G; 12531-SD)	Silurian or Devonian; no younger than earliest Late Devonian (earliest Frasnian).	Indeterminate (too few conodonts); relict peloidal texture and spar-filled fenestral fabric seen in thin-section indicates shallow-water depositional environment.	Medium- to light-gray and pinkish-gray, massive, mottled dolostone bed 1.6 m thick in base of 16-m-thick measured section; sample from basal 20 cm. Sample weight 8.4 kg.

Table 1. Conodont data for localities shown on figure 2—Continued.

LOCALITY NO., (FACIES; SUBUNIT)	QUADRANGLE LATITUDE/ LONGITUDE	CONODONT FAUNA AND CAI (FIELD NO.; USGS COLLN. NO.)	AGE	BIOFACIES	REMARKS
19 (Shallow-water facies)	Healy B-6 63°25'16"/ 149°54'43"	*Belodella devonica* (Stauffer)? 2 Sa and 2 Sb elements *Dvorakia*? cf. *D.* sp. of Klapper and Barrick, 1983 1 Sb, 2 Sc, and 1 Sd elements 20 P elements *Icriodus subterminus* Youngquist, narrow morphotype (fig. 6II) 4 Pa element fragments *Mehlina* sp. 1 Pa element *Mesotaxis asymmetrica* (Bischoff and Ziegler) (fig. 6HH) 62 P elements *Playfordia primitiva* (Bischoff and Ziegler) (fig. 6DD-GG) 81 Pa elements of *Polygnathus*, chiefly *Po. aequalis* Klapper and Lane 18 Pa element fragments *Polygnathus* spp. indet. 148 indets. CAI=5 (94ACY-6a; 12358-SD)	earliest Late Devonian (early Frasnian; upper part of Lower *Mesotaxis falsiovalis* Zone into the *Palmatolepis punctata* Zone). *Playfordia primitiva* is the most biostratigraphically restricted conodont in the fauna and is best known from the *Pa. transitans* and succeeding *Pa. punctata* Zones of Ziegler and Sandberg (1990). A list of conodont and brachiopod species from locality 19 is given in Savage and others (1995) and Csejtey and others (1996); these authors also considered the faunas early Frasnian in age.	Postmortem transport within the playfordid-polygnathid biofacies; normal-marine, probably middle shelf near shallow-shelf depositional setting because of relative abundance of small icriodid platform elements. *Playfordia primitiva* is generally a rare though cosmopolitan component of early Frasnian faunas. Its unusual abundance here suggests this locale lay within its preferred habitat.	Massive, medium-dark-gray to black, light- to medium-gray-weathering, fine-grained fossiliferous limestone that is sheared and partly recrystallized; fossils include solitary and colonial corals, brachiopods, gastropods, and pelmatozoan fragments. Sample weight 11.2 kg.

DEPOSITIONAL ENVIRONMENT

We interpret subunit B as turbidites, probably deposited in a submarine fan or fan complex, intercalated with subordinate hemipelagic deposits. Hemipelagic layers originated chiefly as calcareous peri-platform ooze; they contain locally common, largely calcitized radiolarians. The turbidites are similar in general aspect to those in subunit A but are more abundant. They represent facies B, C, and D of Mutti and Ricci Lucchi (1978), an association most typical of an outer fan setting. Their composition is also similar to the turbidites in subunit A, suggesting a similar mixed provenance of carbonate platform or shelf, continent, and volcanic arc.

PALEOCURRENT DATA

Paleocurrent data were obtained from subunit B at two locations (fig. 7). The more reliable and conclusive results are from locality 11, where 6 flutes, 5 grooves, and 9 cross laminae give a visual mean direction of about 195°. As products of the upper flow regime, the flutes and grooves are likely to be more meaningful than the more scattered cross laminae. Bedding at locality 11 is upright and dips 30 to 60°; beds and sedimentary structures were restored to horizontal by the standard single-tilt rotation (see, for example, Potter and Pettijohn, 1977, p. 372). There is little risk of significant paleocurrent error with moderate bedding dips such as these. Less reliable but broadly similar results were obtained from 2 grooves and 3 cross laminae at locality 10, which give a visual mean paleocurrent direction of about 135°. Bedding dips 45 to 55° and is overturned. For lack of any evidence for a more complex retrodeformation path, the standard single-tilt rotation was used here as well, but the chances of a substantial paleocurrent error are much greater than at locality 11 because the beds are overturned.

SUBUNIT C

LITHOFACIES

Subunit C consists mainly of thin-bedded to massive, fine-grained to conglomeratic calcareous metasedimentary rocks; it was studied at localities 12 to 16 (fig. 2). Thick-bedded to massive, coarse-grained to conglomeratic carbonate rocks, not observed in subunits A and B, are the distinguishing feature of subunit C and are found at all 5 localities. Calcareous siliciclastic rocks and altered tuffs and tuffaceous sediment are notable intercalated lithologies at locality 15.

Original sedimentary features are best preserved at localities 14 and 16, at which sections of 21 and 42 m, respectively, were measured. At locality 14, beds are chiefly 0.5 to 10 cm thick, with subordinate thick-bedded to massive intervals 0.8 to 5 m thick. At locality 16, beds range from less than 1 cm to 1.5 m thick, but about one-third of the section consists of 30- to 70-cm-thick beds. Grain-size at both localities ranges from micrite to clast- and matrix-supported conglomerate with clasts as much as 12 cm long (fig. 8A); conglomeratic beds range from less than 5 cm to at least 5 m thick. Many beds are graded (fig. 8B); some of these are at least 60 to 70 m in lateral extent. Some coarser beds have scoured bases with as much as 0.5 to 2 cm of relief; other coarse beds are amalgamated. Finer grained intervals contain abundant parallel and rare cross and convolute laminae.

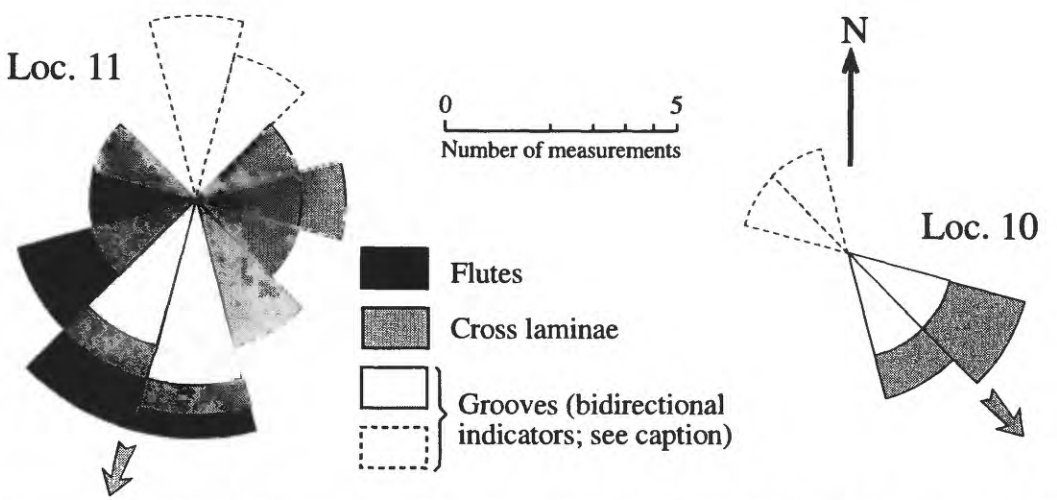

Figure 7. Paleocurrent rose diagrams for calcareous siliciclastic turbidites of DOs subunit B at two localities (fig. 2, locs. 10, 11) in Denali National Park. Arrows showing inferred paleoflow directions are visual estimates of vector mean. Grooves record line of paleoflow but not azimuth (for example, 40° or 220°). Rose petals representing grooves are dashed on side opposite from inferred paleoflow azimuth.

Clasts are typically rounded to elongate and locally imbricated; some contain parallel laminae. Most clasts have irregular outlines and appear to have been relatively unlithified when deposited; these clasts were probably partially cemented during early diagenesis. Most samples contain micritic and lesser dolomitic clasts in a chiefly dolomitic matrix (figs. 8C and D). Some clasts consist of rare, fine-grained bioclasts in a micritic matrix; bioclasts include probable dasycladacean algae, crinoidal debris, and calcitized radiolarians. Other clasts, commonly silicified, consist of single sand- to pebble-sized fragments of colonial coral and (or) stromatoporoids. Siliciclastic material is rare or absent in these sections.

At locality 15, however, thin-bedded to massive metacarbonate is intercalated at several scales with orange- and gray-weathering calcareous siliciclastic strata (fig. 9). Three sequences, each consisting of 20 to 50 m of relatively pure carbonate rocks overlain by an equivalent or slightly thicker interval of more siliciclastic strata, are clearly visible on cliff faces at this locality; the highest sequence is capped by massive carbonate. It is unclear whether these sequences are structural or stratigraphic repeats—only the lowermost of the three sequences is accessible and was examined and sampled for this study.

In this lowermost sequence, the lower, carbonate interval consists of two dissimilar lithologies that appear to be laterally equivalent. The first is a 20-m-thick section of thick-bedded to massive, clast- and matrix-supported carbonate conglomerate similar to that described above from localities 14 and 16. Clasts (as much as 5 cm long) are chiefly micritic and float in a dolomitic matrix; some clasts contain relict algal(?) bioclasts. The second lithology is yellowish-gray to

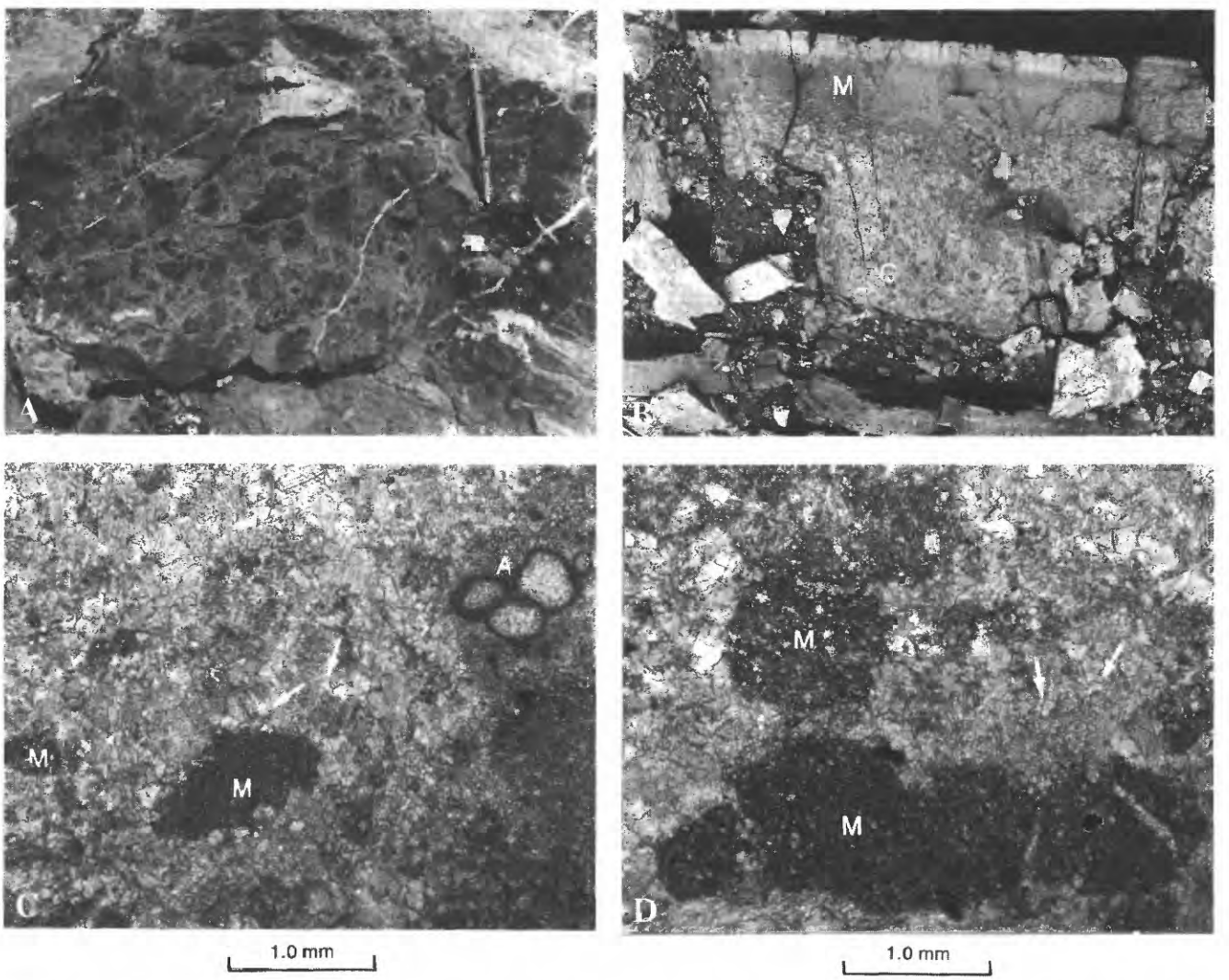

Figure 8. Sedimentary features of DOs subunit C. A, Debris flow consisting of carbonate clasts in carbonate matrix (fig. 2, loc. 14). B, Carbonate turbidite, grading upward from calcirudite (C) to micrite (M) (fig. 2, loc. 16). C and D, Photomicrographs of graded carbonate turbidite (fig. 2, loc. 16). Clasts mostly micrite (M); matrix chiefly dolomite (arrows indicate discrete dolomite crystals). Some clasts contain algal (A) and other fossil (F) fragments.

black, locally dolomitic and (or) carbonaceous micrite in thin beds (most 0.5-4 cm, rarely as much as 10 cm) with abundant parallel laminae and locally scoured bases.

The upper, more siliciclastic interval of the lowermost sequence is more than 100 m thick and consists chiefly of subequal amounts of gray- to black-weathering phyllite and siltstone and tan- to orange-weathering calcareous siltstone to fine-grained sandstone. Beds are generally ≤20 cm thick and graded, with parallel and cross lamination. Sandstones are similar to those described above in subunit B but are more calcareous (50-95%) and proportionately richer in feldspar and volcanic lithic clasts; grains with both felsitic and lathwork volcanic textures were noted. Subordinate lithologies in this interval (<5% each) include black carbonaceous argillite, black dolostone, and orange- to red-weathering tuffaceous sediment. Argillite and dolostone form 1 to 6 m intervals of thin (<3 cm) beds. Tuffaceous layers are a few centimeters to several decimeters thick and medium grained to pebbly; they grade upward into calcareous siltstone and phyllite and contain abundant highly altered feldspar laths.

AGE

Four samples from three localities in this facies yielded conodonts (table 1, fig. 6). Conodonts of Early Silurian (late Llandoverian-Wenlockian) age were obtained at locality 14 from a conglomerate bed 80 cm thick of (dolo)micritic clasts as much as 7 cm long in a dolomitic matrix. At locality 15, a few deformed distomodontid element fragments were recovered from 3-cm-thick beds of carbonaceous dolomitic micrite; massive carbonate conglomerate at least 20 m thick at this same locality produced conodonts of early(?) Wenlockian age. The collections from locality 14 and the conglomerate at locality 15 contain coniform elements derived from shallow-water biofacies (fig. 6O-T). At locality 16, a conglomerate bed 20 to 30 cm thick of coral fragments and (dolo)micritic clasts as much as 5 cm long in a calcareous matrix produced a mixture of Early Silurian (probably Wenlockian) coniform conodonts representing a range of shelf or platform depositional environments.

We believe that the conodonts recovered from subunit C accurately date the subunit and were not reworked from significantly older beds. Although conodonts in this subunit have been redeposited—most are shallow-water forms transported, chiefly by turbidity currents, into a deeper water setting—several lines of evidence suggest that the shallow-water source facies and the deeper water depositional facies were essentially coeval. As noted above, most carbonate clasts in subunit C were relatively unlithified when deposited, indicating that clast transport took place soon after initial sedimentation of the clast material. In addition, both coarse-grained redeposited beds (table 1, locs. 14, 15 [sample 12534-SD], and 16) and fine-grained hemipelagic "back-

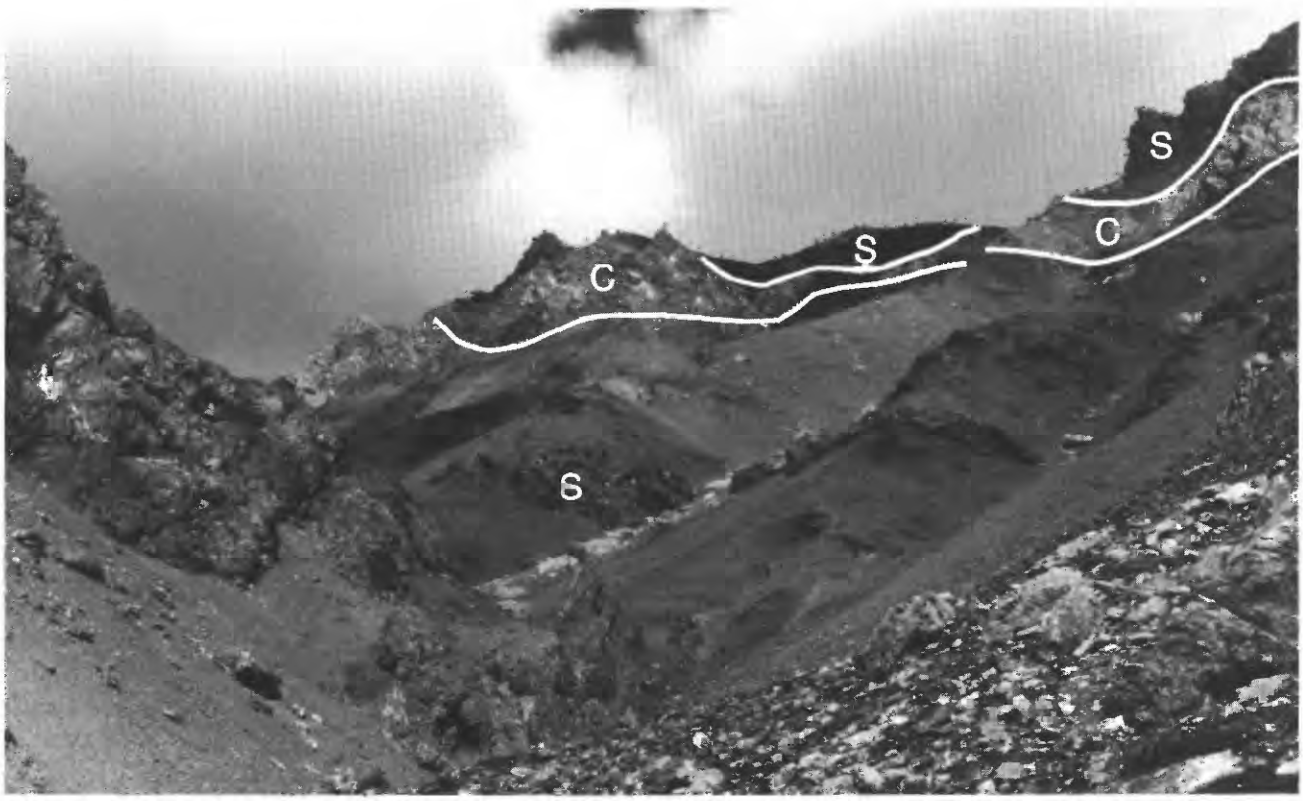

Figure 9. Alternations of massive carbonate (C) and thin-bedded, more siliciclastic rocks (S) (fig. 2, loc. 15). Cliff face is about 200 m high.

ground" material (table 1, loc. 15, sample 12533-SD) in this subunit yield relatively similar conodont faunas. Regional correlations, however, suggest that subunit C could be at least in part of Late Silurian or younger age; this possibility is discussed further below.

DEPOSITIONAL ENVIRONMENT

Turbidites and debris flows (clast- and matrix-supported carbonate conglomerate) derived almost exclusively from a carbonate platform and (or) shelf source form the bulk of this unit. Clasts of calcareous radiolarite in some beds indicate input from coeval slope and (or) basinal sediments. Locally (loc. 15), calcareous strata are overlain by siliciclastic turbidites (with a mixed provenance like that interpreted for turbidites in subunits A and B) intercalated with subordinate tuffaceous and calcareous hemipelagic layers. Submarine fans composed of carbonate detritus are rare (Cook and others, 1983; Scholle and others, 1983), and the carbonate turbidites and debris flows in subunit C probably accumulated in slope and (or) base-of-slope aprons. Aprons are laterally more continuous and internally less organized than fans; they characterize carbonate margins because such margins act as "line" rather than "point" sources (Scholle and others, 1983, pp. 567-569).

SHALLOW-WATER FACIES

Rocks that apparently formed in relatively shallow-water settings have been recognized at several localities within DOs (fig. 2, locs. 17-20). All of these fall within the "massive limestone interbed" mapped by Csejtey and others (1992, p. 27).

Massive, light- to medium-gray-weathering, medium-dark-gray to black dolomitic metalimestone at locality 19 contains brachiopods and conodonts of early Frasnian age (Savage and others, 1995; Csejtey and others, 1996; this report, table 1 and fig. 6DD-II), as well as solitary and colonial corals, gastropods, pelmatozoan and trilobite(?) fragments, red algae, and calcispheres (figs. 10A-C). Most samples are bioclastic-peloidal wackestones and packstones; some skeletal fragments have micritic rims (fig. 10C). These rocks form an interval about 20 to 30 m thick and overlie at least 50 m of black shale (fig. 10A). Dark gray, nodular, argillaceous carbonate beds near the top of this shale contain an early Frasnian conodont and brachiopod fauna similar to that in the massive metalimestone (Savage and others, 1995).

Fossils and sedimentary features at locality 19 suggest that these rocks were deposited below wave base in a shelf or platform setting. The massive metalimestone contains some fossils tolerant of relatively restricted circulation (calcispheres, gastropods) as well as forms typical of settings with normal salinity (corals). The conodont fauna indicates a normal-marine, middle-shelf or shallower depositional setting.

At least 16 m of light-gray to pink to orange, locally dark-gray to black, well-bedded dolostone crops out at locality 18. These rocks consist of cyclic alternations of gray-weathering, mottled beds 40 to 180 cm thick, and orange-weathering, parallel-laminated beds 5 to 40 cm thick. Some gray beds contain vague cross laminae in 20- to 40-cm sets; the mottled texture in this lithology may reflect partial bioturbation. The orange beds contain some crinkly laminae as well as rip-up clasts, commonly laminated, as much as 4 cm long. Both gray and orange beds consist of a mosaic of euhedral to subhedral dolomite crystals, 20 to 400 μm in diameter, in which a ghostly relict texture of brownish peloids is preserved (fig. 10D). Peloids are rounded to ovoid and 40 to 200 μm in size; they may have formed as fecal pellets and (or) micritized skeletal grains. A few possible pelmatozoan fragments occur locally. Fenestral fabric is well developed in both lithologies; fenestrae range from elongate to irregular in shape and from less than 1 mm to 3 cm in size (fig. 10D). Most fenestrae are filled with clear calcite spar; some contain layers of micritic sediment and spar or are partly rimmed with solid hydrocarbons.

Sedimentary structures, particularly fenestral fabric, crinkly (algal?) laminae, and the abundance of peloids, suggest a shallow subtidal to intertidal setting for these rocks. A bed of mottled dolostone yielded only a few specimens of *Panderodus* sp. and *Belodella*? sp. (fig. 6, U and V) that suggest a Silurian or Devonian age no younger than earliest Frasnian (table 1).

More recrystallized rocks that may also have formed in relatively shallow water settings are exposed at localities 17 and 20. These rocks are very light gray- to tan-weathering, dark-gray, fine- to medium-crystalline metalimestone that forms massive cliffy outcrops 35 to 50 m high. Samples in which sedimentary texture is best preserved are bioclastic wackestones and packstones; some samples contain probable pelmatozoan fragments. These rocks lack features such as graded bedding, parallel and cross laminae, and lithic clasts observed in the deep-water facies described above. We suggest they formed in shallow-water shelf or platform settings. Recrystallized bioclastic wackestone at locality 20 was sampled for conodonts but none were found.

STRATIGRAPHY

Because some of the subunits and facies described above are undated or only broadly dated, the stratigraphy of the DOs unit in the study area is poorly constrained. We offer here our best interpretation of the data in hand to facilitate comparison with possibly correlative sequences elsewhere in the state.

Subunits A, B, and C are at least 15 m, 50 m, and 40 m thick, respectively, based on sections at localities 8, 11, and 16. If the alternations of more calcareous and more siliciclastic intervals at locality 15 are stratigraphic and not structural repeats, that section could be 300 to 400 m thick. Conodont data presented above permit the interpretation that subunits A, B, and C are all the same age, that is, late Early Silurian (Wenlockian). The conodont data also permit the interpretation that subunit B is slightly younger than subunit C. Conodont faunas from carbonate cobbles in the Upper Cretaceous sedimentary part of the Cantwell Formation, interpreted in Csejtey and others (1996) as derived from limestone turbidites of DOs, are of Silurian, Late Silurian, and Early Devonian age and provide an upper age limit for the deep-water part of DOs. At least part of the shallow-water facies is younger than any of the deep-water facies; strata at locality 19 are early Frasnian (earliest Late Devonian) in age.

One interpretation of the stratigraphy, based on available fossil data and geographic distribution of subunits, is that the DOs unit is generally older to the south and younger to the north. In this interpretation, subunit A, which is the most laterally extensive of the three subunits and is exposed chiefly in the southern part of the study area, is the oldest subunit. Subunits B and C, exposed chiefly in the western and central parts of the study area, respectively, are both

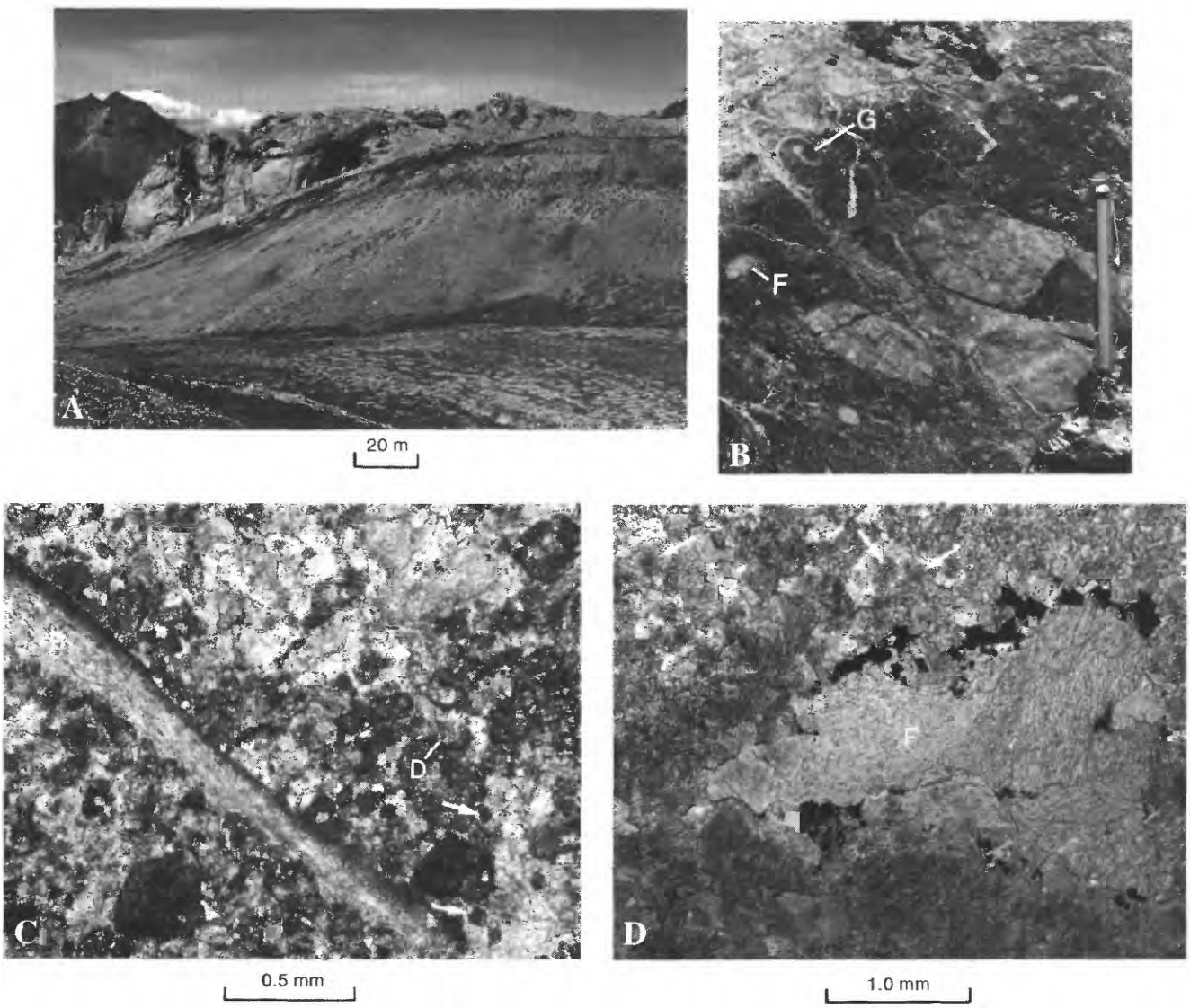

Figure 10. Sedimentary features of DOs shallow-water facies. A-C, Bioclastic-peloidal wackestone-packstone of early Frasnian age (fig. 2, loc. 19). Carbonate forms massive, light-colored layer above darker, recessive shale in A. Gastropods (G) and other fossil fragments (F) evident in outcrop in B. Photomicrograph (C) shows abundant peloids (indicated by arrows) and a brachiopod fragment (B) with dark micritic rim in partially dolomitized (D) matrix. D, Photomicrograph of mottled dolostone of Silurian or Devonian age with relict peloids (indicated by arrows); fenestrae (F) are partly rimmed with solid hydrocarbons and filled with clear calcite spar (fig. 2, loc. 18).

probably Silurian and could be younger than subunit A. Subunits B and C could be age equivalent but lithologically distinct facies with different provenances, which interfinger near the center of the study area (for instance, around locality 15). The nature of the contact between the deep-water strata which make up most of DOs and the youngest (Frasnian) strata exposed to the north is unclear—it could be an unconformity, perhaps structurally complicated, or a fault.

Mullen and Csejtey (1986) proposed the following stratigraphic succession for DOs: (1) 300 m of calcareous siliciclastic turbidites intercalated with limestone and shale; (2) 250 m of dark-gray to black, well-bedded lime mudstone to wackestone with rare argillite and chert interbeds; and (3) 20 m of massive to thick-bedded, partly dolomitic limestone of uniform age (Devonian), facies (shallow-water), and stratigraphic position (near the top of the unit) that can be traced along strike for at least 45 km. The thickness of the massive limestone was later given as 200 m (Csejtey and others, 1992) and then 40 to 70 m (Csejtey and others, 1996).

Our findings suggest at least three modifications to this stratigraphic succession. First, coarse-grained, thick-bedded to massive carbonate turbidites and debris flows like those described above in subunit C are an important part of DOs. Second, we could not confirm the presence of a thick interval of chiefly fine-grained carbonate overlying the calcareous siliciclastic turbidite interval. Third, massive limestone is an important part of the DOs unit, but it encompasses both deep-water facies of Silurian age (for example, locs. 14, 15) and shallow-water facies of Devonian age (loc. 19), as well as recrystallized, probably shallow-water metalimestone of uncertain age (locs. 17 and 20). Thus, although this massive limestone has been mapped as a single unit at 1:250,000 scale (for example, Csejtey and others, 1992), in detail it appears to consist of several cliff-forming limestone horizons whose relations with one another have not yet been determined.

STRUCTURE

Our reconnaissance studies of unit DOs reveal glimpses of a complex history of contractional deformation. Homoclinal sections were not recognized, and as noted above, piecing together a comprehensive stratigraphic section of the entire unit is not possible with our present knowledge. Nonetheless, certain broad tracts do appear to be dominated by a particular subunit. For example, sections containing abundant, relatively thick-bedded calcareous siliciclastic turbidites (subunit B) predominate in the area north of Red Mountain.

Within unit DOs, bedding typically strikes east and dips moderately to the south, although there is considerable variation in strike (fig. 11). The clustering of both upright and overturned bedding poles suggests the presence of north-vergent overturned folds. Such folds are well displayed in Lower Cretaceous and Upper Jurassic flysch in a mountainside a few kilometers north of locality 20. Evidence from outcrops and stereonets discloses two fold generations; only those folds that are demonstrably F2 are identified as such on the stereonets (fig. 11). Poles to fold axial surfaces delineate two clusters. One set dips moderately to the south; these folds would account for the main cluster of bedding poles. The other set of axial surfaces, which includes some known F2 folds, dips steeply to the northeast. Most fold hinges plunge fairly gently. F1 hinges trend west, whereas F2 hinges trend northwest. Cleavage (fig. 11) shows considerable scatter, but there is fair correspondence, at least, to the two main clusters of fold axial surfaces.

Rocks similar to DOs that are exposed in the McGrath and Lime Hills quadrangles (further discussed below) have broadly similar structural histories. In both areas, the early isoclinal folds verge northwest (Bundtzen and others, 1988, 1994). This deformation is presumably a consequence of Mesozoic convergence between the Wrangellia superterrane and interior Alaska.

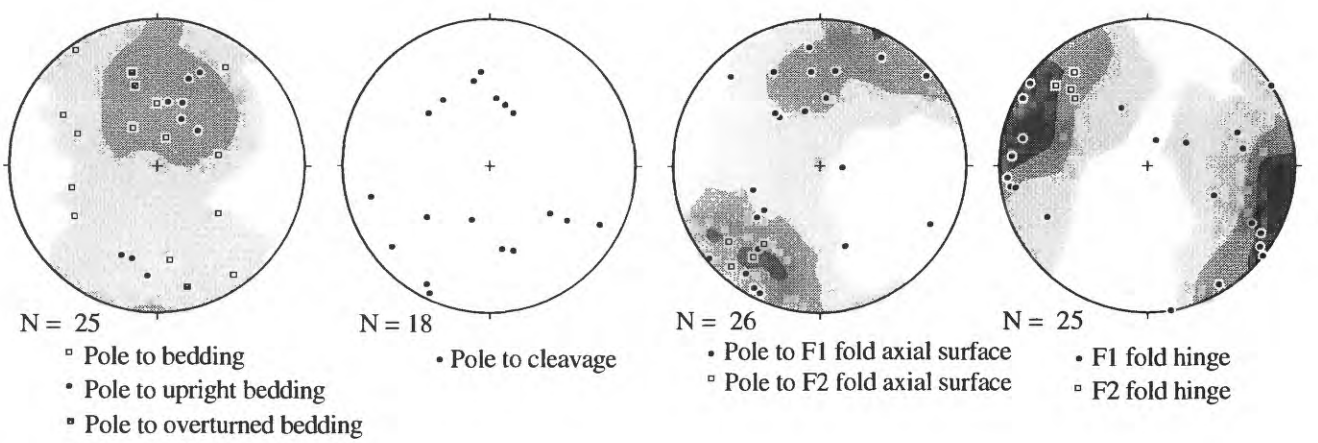

Figure 11. Lower hemisphere equal-area stereographic projections of structural data from unit DOs in Denali National Park. Contour interval is 2 sigma.

REGIONAL CORRELATION

Several aspects of the DOs unit in Denali National Park are distinctive and constrain correlations with coeval rocks (fig. 12). DOs consists chiefly of siliciclastic and calcereous turbidites, calcareous debris flows, and subordinate calcareous and siliceous hemipelagic deposits that accumulated in a slope and (or) basinal setting. The turbidites and debris flows are at least in part no older than Wenlockian (late Early Silurian) in age and have a mixed provenance including continental and subordinate volcanic sources. Deeper water strata are structurally (and stratigraphically?) overlain by shallower water carbonate facies at least in part of early Frasnian (earliest Late Devonian) age.

The DOs unit in the Denali area has been correlated with three sequences in central Alaska (fig. 1): (1) Rocks of the Dillinger terrane or sequence exposed to the southwest (for example, McGrath and Lime Hills quadrangles) (Jones and others, 1981, 1982, 1983); (2) rocks of the Mystic terrane or sequence exposed to the south (Talkeetna quadrangle) (Csejtey and others, 1996); and (3) rocks of the Nixon Fork terrane exposed to the west (for example, Medfra quadrangle) (Mullen and Csejtey, 1986; Csejtey and others, 1992). We consider these proposed correlations below.

In addition, we summarize below all other deep-water sequences of definite Silurian age known in Alaska, and compare their lithologies, faunas, specific depositional environments, and stratigraphic contexts to those of the DOs unit in the Denali area. Silurian deep-water sequences are known from east-central, eastern, southeastern, northern, and western Alaska; some of these sequences are overlain by Upper Devonian shallow-water carbonate rocks like those found in DOs.

CENTRAL ALASKA

MCGRATH QUADRANGLE

The Dillinger terrane or sequence, which consists chiefly of lower Paleozoic deep-water rocks, has been studied at several localities in the McGrath quadrangle (Armstrong and others, 1977; Churkin and others, 1977; Bundtzen and Gilbert, 1983; Bundtzen and others, 1988, 1997; Churkin and Carter, 1996). It is also exposed to the southwest (Lime Hills and Sleetmute quadrangles) and northeast (west-central edge of the Talkeetna quadrangle; unit Pzd of Reed and Nelson, 1980).

In the Terra Cotta Mountains, in the southeastern part of the McGrath quadrangle (fig. 12, column 2), the section begins with at least 300 m of rhythmically layered, thin-bedded, laminated to cross-bedded silty limestone and shale (Lyman Hills Formation of Bundtzen and others, 1994; lower siltstone member of Post River Formation of Churkin and Carter, 1996). This unit has yielded Late Cambrian conodonts (Bundtzen and others, 1997) and earliest Ordovician (Tremadocian) graptolites (Churkin and Carter, 1996). It is overlain by about 395 m of hemipelagic graptolitic shale, siltstone, and ribbon chert (upper four members of Post River Formation of Churkin and Carter, 1996) that contain a very complete succession of Early Ordovician through early Early Silurian graptolites. This unit is overlain by at least 685 m of fine- to coarse-grained, calcareous and micaceous, quartzofeldspathic to subarkosic turbidites intercalated with finely laminated dark limestone (Terra Cotta Mountains Sandstone of Churkin and Carter, 1996). About 30 km north of the Terra Cotta Mountains, a distinctive lens within this turbidite unit contains altered ash layers and discrete volcanic lithic clasts (T.K. Bundtzen, Alaska Division of Geological & Geophysical Surveys, written commun., 1997; Bundtzen and others, 1997). The Terra Cotta Mountains Sandstone produces late Early and Late Silurian graptolites (Churkin and Carter, 1996; Bundtzen and others, 1997) and grades upward into more than 380 m of calcareous (locally dolomitic) turbidites with interbeds of channelized limestone conglomerate and slumped carbonate breccia (Barren Ridge Limestone of Churkin and Carter, 1996.) No fossils were found in the Barren Ridge Limestone in the Terra Cotta Mountains, but Blodgett and Gilbert (1992) obtained conodonts of Lochkovian to Pragian (Early Devonian) age from correlative beds in the northern Lime Hills quadrangle. The Dillinger sequence in the Terra Cotta Mountains is interpreted as having formed in a shallowing-upward succession of basinal, fan turbidite, and foreslope depositional environments (Gilbert and Bundtzen, 1984).

Limited paleocurrent data reported by Churkin and others (1977) first suggested that the Terra Cotta Mountains Sandstone was deposited by currents that flowed toward the northwest and northeast, whereas the Post River Formation and Barren Ridge Limestone were deposited by southwest- and west-flowing currents, respectively. More recently, Bundtzen and others (1988) reported additional paleocurrent data from the Terra Cotta Mountains Sandstone. All of the available data now indicate that the predominant paleocurrent direction for this unit appears to have been toward the northeast, with minor components of flow toward the northwest and south.

A succession somewhat similar to that in the Terra Cotta Mountains is described from the Jones River area along the east-central edge of the McGrath quadrangle (Armstrong and others, 1977). This section (figure 12, column 3), in ascending order, consists of 300 m of lithic arenite turbidites; 250 m of well-bedded dolomitic, argillaceous lime mudstone with worm burrows and trails and fine cross and parallel laminae, and at least 360 m of subgraywacke turbidites. Graptolites from the limestone unit are of late Wenlockian and early Ludlovian (latest Early and earliest Late Silurian) ages. Conodonts from three collections 84 to 126 m above the base of a similar limestone sequence about 15 km to the northeast are here considered late Llandoverian to Wenlockian in age

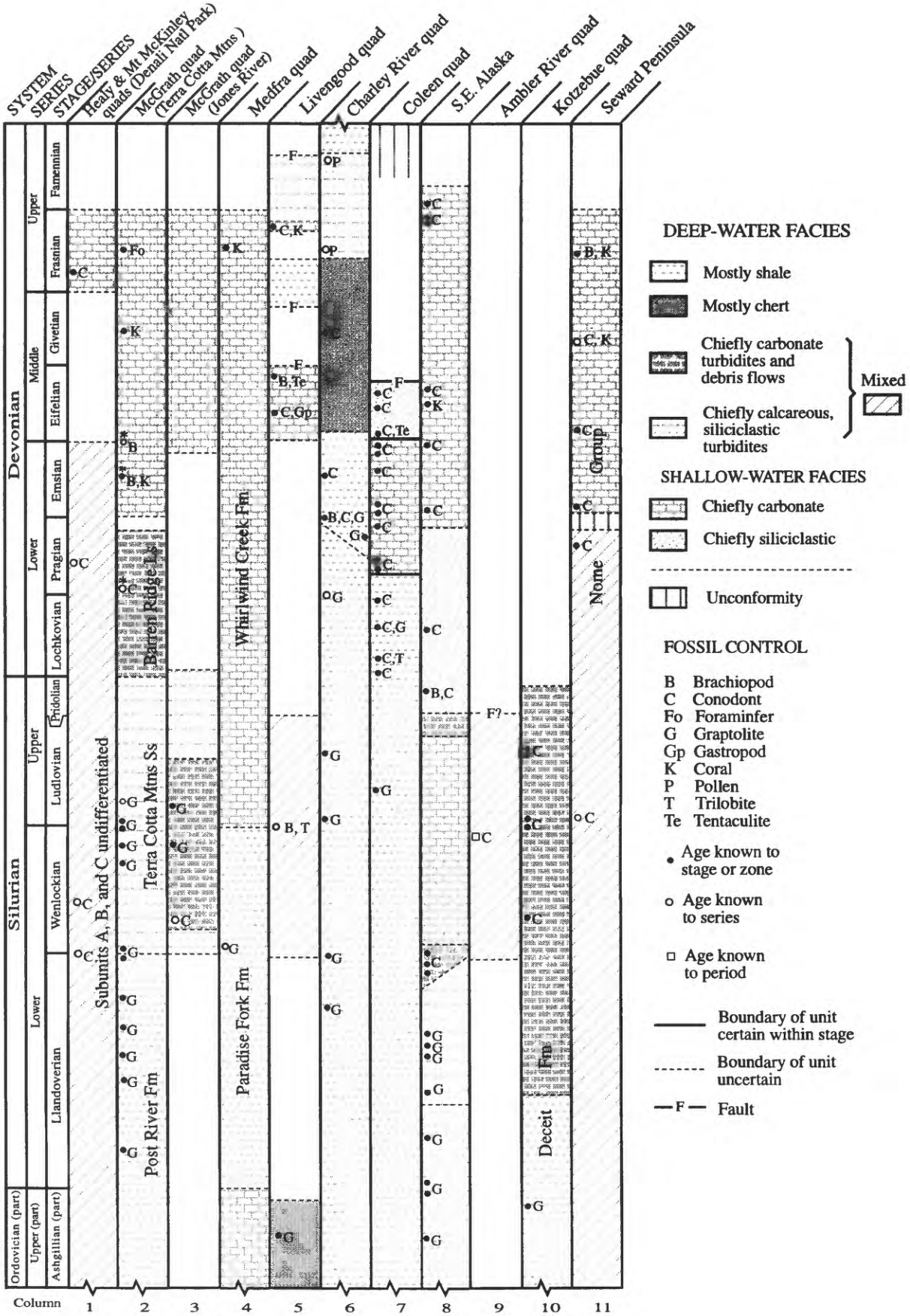
SYSTEM
SERIES
STAGE/SERIES
Healy & Mt McKinley quads (Denali Natl Park)
McGrath quad (Terra Cotta Mtns)
McGrath quad (Jones River)
Medfra quad
Livengood quad
Charley River quad
Coleen quad
S.E. Alaska
Ambler River quad
Kotzebue quad
Seward Peninsula
Devonian
Silurian
Ordovician (part)
Upper
Middle
Lower
Famennian
Frasnian
Givetian
Eifelian
Emsian
Pragian
Lochkovian
Pridolian
Ludlovian
Wenlockian
Llandoverian
Upper (part)
Ashgillian (part)
Subunits A, B, and C undifferentiated
Terra Cotta Mtns Ss
Post River Fm
Barren Ridge Ls
Paradise Fork Fm
Whirlwind Creek Fm
Deceit Fm
Nome Group
Column
1
2
3
4
5
6
7
8
9
10
11
DEEP-WATER FACIES
Mostly shale
Mostly chert
Chiefly carbonate turbidites and debris flows
Chiefly calcareous, siliciclastic turbidites
Mixed
SHALLOW-WATER FACIES
Chiefly carbonate
Chiefly siliciclastic
Unconformity
FOSSIL CONTROL
B Brachiopod
C Conodont
Fo Foraminfer
G Graptolite
Gp Gastropod
K Coral
P Pollen
T Trilobite
Te Tentaculite
Age known to stage or zone
Age known to series
Age known to period
Boundary of unit certain within stage
Boundary of unit uncertain
F Fault

(fig. 6W-CC) and are virtually identical to some conodonts from unit DOs (table 1, loc. 14).

Deep-water strata in the McGrath and northern Lime Hills quadrangles are conformably or unconformably overlain (Gilbert and Bundtzen, 1984) by Lower (Emsian) to Upper Devonian, chiefly shallow-water, carbonate and subordinate siliciclastic rocks of the Mystic sequence (Bundtzen and Gilbert, 1983; Blodgett and Gilbert, 1992; Bundtzen and others, 1994). These rocks include a carbonate platform sequence of Frasnian age that crops out both north and south of the Farewell fault and contains locally abundant foraminifers with Siberian biogeographic affinities (Mamet and Plafker, 1982; Blodgett and Gilbert, 1992).

TALKEETNA QUADRANGLE

The Mystic terrane or sequence consists largely of units Pzus and Dl of Reed and Nelson (1980) in the northwestern Talkeetna quadrangle (not shown in fig. 12). Pzus is a "depositionally and structurally complex terrane of chiefly marine flyschoid sedimentary rocks" (Reed and Nelson,1980, p. 7) that includes trench, slope, shelf, and terrestrial assemblages. The trench assemblage contains strata that are lithologically similar to deep-water parts of the DOs unit, but available fossil data suggest that they are mostly, perhaps completely, of Middle to Late Devonian and younger age. These lithologies include "terrigenous turbidites" (Reed and Nelson, 1980, p. 7), graywacke, and "wildflysch [that] locally contains house-sized blocks" of bedded limestone (Reed and Nelson, 1980, p. 8). No fossils of definitively Silurian or older age have been obtained from these deep-water rocks, but numerous collections of Devonian (including probable Middle and Late Devonian) age are reported by Reed and Nelson (1980) from limestones in Pzus. These limestones have chiefly shallow-water faunas; at least some appear to be blocks that were tectonically and (or) depositionally incorporated into coeval or younger deeper-water strata. Other parts of Pzus are definitely of post-Frasnian age; black shale and phosphatic chert contains Famennian (late Late Devonian) radiolarians, and some limestone layers are of Late Mississippian and Middle Pennsylvanian age (Reed and Nelson, 1980).

The Dl unit in the Talkeetna quadrangle provides a better match for the DOs unit, but only for the younger, shallow-water part of DOs. Dl consists of more than 95 m of intercalated thin-bedded micrite and massive, locally "reefoid" biostromal beds of colonial rugose corals, stromatoporoids, and bryozoans; it is interpreted as a series of small patch reefs and interreef beds (Reed and Nelson, 1980). Some parts of Dl may be of Early and (or) Middle Devonian age (Reed and Nelson, 1980), but much of the unit appears to be Late Devonian. Seven localities in Dl yielded megafossils of Frasnian or probable Frasnian age; brown to black shales with thin limestone interbeds near the top of the Dl unit contain conodonts of late Frasnian age (Reed and Nelson, 1980). Frasnian fossil assemblages in both DOs and Dl contain some of the same genera and species of atrypid and spiriferid brachiopods (Csejtey and others, 1996).

MEDFRA QUADRANGLE

The Nixon Fork terrane includes abundant lower Paleozic rocks; it is widely exposed and particularly well-studied in the Medfra quadrangle (Dutro and Patton, 1982) but also crops out to the northeast, south, and southwest (fig. 1). In the Medfra quadrangle, a thick Ordovician through Devonian, largely platform carbonate sequence is punctuated by an incursion of Silurian deeper water facies (fig. 12, column 4). This facies, named Paradise Fork Formation by Dutro and Patton (1982), consists of at least 1,000 m of dark-

◀Figure 12. Correlation, lithologies, fossil control, and depositional environments of uppermost Ordovician through Devonian rocks in selected areas of Alaska. See figure 1 for location of columns. Only fossils that most restrict age of collection or unit are listed; fossils listed alphabetically. Conodont collection of Early Devonian age in column 1 is from a cobble in Upper Cretaceous part of Cantwell Formation interpreted (Csejtey and others, 1996) as derived from DOs. Asterisk above some fossil symbols in column 2 indicates that these collections are from strata in northern part of Lime Hills quadrangle that are considered correlative (see for example, Bundtzen and others, 1994) with rocks in Terra Cotta Mountains. Silurian section in Black River quadrangle (not shown here but discussed in text) is identical to that from Coleen quadrangle shown in column 7; Devonian sections in the two areas are slightly different. Column 10 represents Deceit Formation, considered part of Nome Group by Till and Dumoulin (1994) and exposed only in the Kotzebue quadrangle; column 11 represents the Nome Group (part) exclusive of the Deceit Formation, exposed in the Kotzebue quadrangle and elsewhere on Seward Peninsula. Terranes represented as follows (Silberling and others, 1994): columns 1-3, Dillinger (Devonian and older deep-water facies) and Mystic (Devonian shallow-water facies); column 4, Nixon Fork; column 5, Livengood; column 6, ancestral North America; column 7, Porcupine; column 8, Alexander; column 9, Hammond subterrane of Arctic Alaska; columns 10 and 11, Seward. Data sources as follows: column 1, this paper, Csejtey and others (1996); column 2, Mamet and Plafker (1982), Bundtzen and Gilbert (1983), Blodgett and Gilbert (1992); Bundtzen and others (1994), Churkin and Carter (1996); column 3, Armstrong and others (1977), this paper; column 4, Dutro and Patton (1982); column 5, Blodgett and others (1988), Weber and others (1994); column 6, Churkin and Brabb (1965); column 7, Churkin and Brabb (1967); column 8, Churkin and Carter (1970), Savage (1977, 1985, 1992), Eberlein and others (1983), Soja (in press), A.G. Harris, unpub. data (1979, 1985); column 9, Dumoulin and Harris (1988); columns 10 and 11, Till and others (1986), Ryherd and Paris (1987), Till and Dumoulin (1994), A.G. Harris, unpub. data. A.G. Harris and Claire Carter revised the age of graptolite and conodont faunas in some of references listed above.

gray, thin-bedded, platy, silty limestone and black shale; limestone bodies and lenses as much as 5 m thick are found in the upper part of the unit. Graptolites from the lower part of the unit are latest Llandoverian to early Wenlockian; the uppermost beds are probably no younger than Wenlockian (Dutro and Patton, 1982). The unit is overlain by Upper Silurian through Devonian, predominantly shallow-water carbonate rocks of the Whirlwind Creek Formation; the upper part of this unit contains Frasnian (early Late Devonian) corals (Dutro and Patton, 1982).

Deeper water facies of Paleozoic age also crop out southeast of the Nixon Fork terrane in the Medfra quadrangle. These rocks, the East Fork Hills Formation of Dutro and Patton (1982), make up the East Fork subterrane (Patton and others, 1994) of the Minchumina terrane (Jones and others, 1981; Silberling and others, 1994) (fig. 1). (Decker and others, 1994, include the Minchumina terrane in the White Mountain sequence of the Farewell terrane.) The East Fork Hills Formation is poorly exposed and consists chiefly of thin-bedded limestone and dolostone and subordinate chert and siliceous siltstone. The formation has been assigned an Early Ordovician through Middle Devonian age on the basis of scattered, largely long-ranging conodont collections; definitively Silurian fossils have not been reported (Dutro and Patton, 1982; Patton and others, 1994).

SUMMARY

Jones and others (1981, 1982, 1983) included the DOs unit of Csejtey and others (1992) in their Dillinger terrane, correlating it with deep-water strata exposed in the northwestern Talkeetna and eastern McGrath quadrangles and adjacent areas to the southwest. Our data support this correlation and also suggest specific correlations between the subunits we recognize in DOs and the formations recognized by Churkin and Carter (1996) and Bundtzen and others (1994) in the McGrath and northern Lime Hills quadrangles.

Fine-grained, thin-bedded calcareous and siliceous strata of our subunit A are lithologically most like the Upper Cambrian to Lower Ordovician Lyman Hills Formation of Bundtzen and others (1994) (T.K. Bundtzen, written commun., 1997). Subunit A also has similarities with some members of the overlying Ordovician to lower Lower Silurian Post River Formation of Churkin and Carter (1996) but lacks the abundant graptolites characteristic of that unit. Graptolites could be present in parts of subunit A that were not examined during our reconnaissance investigations or could have been obscured by metamorphism and (or) structural complexities. Correlation with the Lyman Hills Formation and (or) the Post River Formation suggests an age of early Early Silurian or older for subunit A.

Upper Lower Silurian (Wenlockian or younger) siliciclastic turbidites of subunit B are similar in age and lithology to the Terra Cotta Mountains Sandstone of Churkin and Carter (1996) in the McGrath quadrangle. Both units contain carbonate interbeds, calcareous siliciclastic turbidites of mixed provenance, and subordinate volcanogenic components. The paleocurrent data we obtained from subunit B of DOs (flow to the south) differ from those reported by Churkin and others (1977) and Bundtzen and others (1988) from turbidites in the Terra Cotta Mountains (flow dominantly to the northeast), but the significance of this difference is unclear. It could be paleogeographically meaningful, but it could also reflect technical and (or) post-depositional complications such as small data sets, errors introduced during retrodeformation, and (or) large-scale structural rotations.

Thin-bedded to massive calcareous turbidites and debris flows of subunit C resemble the Barren Ridge Limestone of Churkin and Carter (1996), particularly as described by Bundtzen and others (1988, 1994) in the eastern McGrath and northern Lime Hills quadrangle. The Barren Ridge Limestone is considered Late Silurian (Ludlovian) or younger, however, whereas subunit C has produced late Early Silurian (Wenlockian) conodonts. As discussed above, lithologic and faunal evidence suggests that the conodonts recovered from subunit C reflect the depositional age of the subunit and were not reworked from significantly older beds. If so, subunit C may represent a coarser grained equivalent of the limy intervals recognized in the Terra Cotta Mountains Sandstone, rather than a correlative of the Barren Ridge Limestone.

The Frasnian part of the Mystic sequence platform carbonate rocks that overlie the Dillinger sequence in the McGrath quadrangle correlates well with the shallower water, Frasnian part of DOs.

Csejtey and others (1996) suggested that the DOs unit could be correlated with at least parts of units Pzus and Dl of Reed and Nelson (1980). However, there is no paleontological evidence that the Pzus unit contains any deep-water strata as old as Silurian; indeed, fossil collections reported by Reed and Nelson (1980) indicate that most, perhaps all of these rocks are Middle Devonian or younger. The Frasnian part of Dl is a good lithologic and paleontological match for the Frasnian part of DOs.

Mullen and Csejtey (1986) and Csejtey and others (1992) concluded that the DOs unit is a tectonically fragmented piece of the Nixon Fork continental margin that includes most or all of the deep-water segment, and part of the shallow-water segment, of the Nixon Fork terrane. However, although the deep-water segment of the Nixon Fork terrane (the Paradise Fork Formation of Dutro and Patton, 1982) is at least in part coeval with the deep-water part of the DOs unit, the Paradise Fork is more fine grained than DOs and lacks siliciclastic turbidites. The Frasnian part of the Whirlwind Creek Formation (part of the shallow-water segment of the Nixon Fork terrane) is correlative with the Frasnian part of DOs. Deep-water strata southeast of the Nixon Fork terrane in the Medfra quadrangle (the East Fork Hills Formation of Dutro and Patton, 1982) may correlate,

at least in part, with DOs, but they are finer grained and lack a significant siliciclastic component.

EAST-CENTRAL ALASKA

Deep-water Silurian strata crop out in the northwestern part of the Livengood quadrangle (fig. 1; fig. 12, column 5), in the Livengood stratigraphic belt (Dover, 1994) or Livengood terrane (Silberling and others, 1994). The Livengood belt has been interpreted as part of the North American continental margin (Selwyn Basin sequence) offset by strike-slip faulting along the Tintina fault (Dover, 1994). Other workers (for example, Grantz and others, 1991) have suggested that strata of the Livengood belt were deposited on Cambrian oceanic crust and may be of non-North American origin.

The Lost Creek unit (Blodgett and others, 1988) in the Livengood belt is a chiefly siliciclastic basinal succession about 50 m thick (R.B. Blodgett, oral commun., 1992) that includes a 15-m-thick carbonate limestone lens interpreted by Blodgett and others (1988) as a debris flow derived from a shallow-marine carbonate platform. The limestone includes brachiopods, crinoid columnals, ostracodes, trilobites, rugose corals, and possible calcareous algae; the brachiopods and trilobites indicate a Wenlockian to Ludlovian age (Blodgett and others, 1988). The Lost Creek unit overlies the Livengood Dome chert, a chiefly basinal succession that contains Late Ordovician (Ashgillian) graptolites, and is in turn overlain by a structurally complex and poorly exposed succession of Middle and Upper Devonian, chiefly shallow-marine siliciclastic and calcareous units (Weber and others, 1994). A discontinuous limestone, thought by Weber and others (1994) to represent a series of biogenic buildups at the base of their Quail unit, contains conodonts and corals that restrict its age to the late Frasnian.

The Lost Creek unit is similar in age and lithology to the deep-water part of DOs but is apparently thinner. Siliciclastic turbidites in the Lost Creek unit have not been described in sufficient detail to allow a precise correlation with those in DOs. The Frasnian limestone in the Quail unit is broadly correlative with the Frasnian part of DOs, although DOs may be slightly older.

EASTERN ALASKA AND ADJACENT PARTS OF CANADA

Basinal facies of Silurian age crop out discontinuously throughout eastern Alaska and adjacent Canada, particularly in the Charley River, Black River, and Coleen quadrangles (fig. 1; fig. 12, columns 6 and 7). In the Charley River quadrangle, these rocks are considered part of ancestral North America by Silberling and others (1994) but have been assigned to the Tatonduk terrane by some workers (for example, Howell and others, 1992). Correlative rocks in the Black River and Coleen quadrangles are generally called the Porcupine terrane (for example, Silberling and others, 1994). Most workers, even those who believe that rocks in eastern Alaska represent distinct terranes, infer that these terranes formed as part of the North American continental margin.

Throughout eastern Alaska and adjacent Canada, Silurian deep-water facies are assigned to the Road River Formation (Group in Canada) of Ordovician through Early Devonian age and consist chiefly of shale, with local thin beds of chert, dolostone, and limestone (Churkin and Brabb, 1965). The Silurian section is as much as 150 m thick in the Charley River quadrangle, but less than 10 m thick in the Black River and Coleen quadrangles (Churkin and Brabb, 1965, 1967). Upper Devonian rocks consist chiefly of siliciclastic turbidites of the Nation River Formation in the Charley River quadrangle (Churkin and Brabb, 1965) and have not been reported to the north (Black River and Coleen quadrangles).

Silurian deep-water facies in eastern Alaska thus are finer grained than those of DOs; siliciclastic sandstone turbidites are rare or absent. No rocks lithologically and biostratigraphically correlative with the Frasnian shallow-water carbonate part of DOs have been reported from this area.

Rocks of the Dillinger terrane or sequence in the McGrath and Lime Hills quadrangles have been correlated with Paleozoic rocks in the Selwyn Basin (Yukon and Northwest Territories, Canada) by previous workers. Bundtzen and Gilbert (1983) and Bundtzen and others (1988, 1994), for example, have correlated the Lyman Hills and Post River Formations with the Rabbitkettle Formation and Road River Group, respectively, of the Selwyn Basin. Like eastern Alaska, the Selwyn Basin lacks siliciclastic sandstone turbidites of Silurian age. However, the Sapper Formation (Gordey and Anderson, 1993), a sequence of several hundred meters of Silurian and Devonian limestone and silty limestone that is found in parts of the Selwyn Basin, could represent a distal equivalent of the proximal fan deposits of the Terra Cotta Mountains Sandstone (T.K. Bundtzen, written commun., 1997). Platform carbonate rocks of Frasnian age have not been reported from the Selwyn Basin or adjacent shelf successions; as in eastern Alaska, upper Devonian rocks in the Yukon are chiefly siliciclastic turbidites (Gordey and Anderson, 1993).

SOUTHEASTERN ALASKA

Silurian deep-water strata are an important part of the Alexander terrane (Silberling and others, 1994) in southeastern Alaska (fig. 1; fig. 12, column 8). The Alexander terrane is generally interpreted as a displaced fragment of an early through middle Paleozoic island arc, but the original position of this arc is controversial. Recent work suggests a position close to northern North America (Bazard and others,

1995).

The Silurian section in the Alexander terrane is summarized by Soja (in press). In the southern part of the terrane, the section begins with the deep-marine Descon Formation, about 3,000 m of Middle Ordovician through Lower Silurian volcanic rocks (including flows, breccias, tuffs, and agglomerates), graywackes, quartzofeldspathic arenites, mudstones, cherts, shales, and minor limestones. Upper Llandoverian carbonate turbidites and Ludlovian-Pridolian(?) turbidites and calcareous debris flows are found at the base and near the top of the overlying unit, the Heceta Formation, which is more than 3,000 m thick; shallow-water carbonate platform strata, however, make up most of the Heceta. The Heceta is overlain by the Karheen Formation, 1,800 m of Upper Silurian and (or) Lower Devonian terrigenous red beds and shallow-marine deposits. Deep-water strata may be somewhat younger in the northern part of the Alexander terrane; the Bay of Pillars Formation (middle Llandoverian-early Ludlovian) and Point Augusta Formation (Upper? Silurian), both interpreted as deep-marine deposits, contain abundant graywackes, subordinate limestones, and volcanic rocks. Volcanic lithic fragments are the most abundant clasts in samples point-counted from the Bay of Pillars and Point Augusta Formations (Karl and Giffen, 1992).

Devonian strata in the Alexander terrane consist primarily of shallow-marine carbonate rocks, siliciclastic strata, and (in the Middle and Upper Devonian) subordinate mafic-intermediate volcanic rocks (Gehrels and Berg, 1994). Megafossils and conodonts of Frasnian and Famennian age have been identified from the Wadleigh Limestone (Eberlein and others, 1983; Savage, 1992; A.G. Harris, unpub. data, 1985).

Deep-water Silurian strata in southeast Alaska have some similarities with the Silurian part of DOs. In particular, both sequences contain calcareous and siliciclastic turbidites as well as calcareous debris flows. However, Silurian turbidites in the Alexander terrane, particularly in the southern part of the terrane, are partly older (pre-Wenlockian) than those in DOs, which are at least in part Wenlockian and younger. Turbidites in the northern part of the Alexander terrane may correlate better with those in DOs, but age control in these northern units is poor (Karl and Giffen, 1992). Composition distinguishes all Silurian deep-water deposits in the Alexander terrane from Silurian strata in DOs, however. Throughout southeastern Alaska, volcanic rocks are a much larger part of the Silurian deep-water section, and volcanic lithic clasts are a correspondingly larger component of Silurian turbidites. The upper Frasnian and lowermost Famennian parts of the upper Wadleigh Limestone appear to be younger than the Frasnian part of DOs.

NORTHERN ALASKA

Deep-water Silurian metasedimentary rocks are exposed in the northeast Ambler River quadrangle in the western Brooks Range (fig. 1; fig. 12, column 9). These unnamed rocks are part of the Hammond subterrane of the Arctic Alaska terrane (Silberling and others, 1994). The Hammond subterrane has been interpreted as a composite of fragments displaced from the North American(?) and (or) Siberian(?) continental margins (Nokleberg and others, 1994).

Deep-water Silurian strata in the northeast Ambler River quadrangle consist of at least 200 m of intercalated fine- to coarse-grained siliciclastic and calcareous turbidites and contain late Early to Late Silurian (Wenlockian to Ludlovian) conodonts (Dumoulin and Harris, 1988) that are virtually identical to some conodonts in unit DOs (table 1, loc. 14). The turbidites overlie metacarbonate rocks of unknown age and underlie quartz metaconglomerate of Mississippian(?) age; the latter contact has been interpreted as an unconformity (Mayfield and Tailleur, 1978) but may be a fault. Siliciclastic turbidites in this unit consist chiefly of calcareous grains (as much as 30%), quartz (as much as 30%), and sedimentary lithic grains (5-10%), as well as lesser amounts of feldspar, volcanic lithic clasts, and chert (locally containing radiolarians). Dolomitic limestone turbidites form 10 to 20 percent of this unit and increase in abundance upward. Some beds contain clasts as large as 10 cm; many beds contain fossil fragments, including corals, gastropods, bryozoans, brachiopods, conularids, and orthocone cephalopods. This unit has been recognized in a small area near Kavachurak Creek, but lithologically similar strata that are at least in part stratigraphically correlative have been recognized throughout the Ambler River quadrangle (Dumoulin and Harris, 1988).

Deep-water Silurian strata in the Ambler River quadrangle are similar in age and lithology to the deep-water part of DOs. But Frasnian shallow-water carbonate rocks that could provide a match for the younger part of DOs have not been reported from this area.

WESTERN ALASKA

Lower Paleozoic rocks lithologically and stratigraphically correlative with DOs are found on the northern and southeastern Seward Peninsula (fig. 1); all are part of the Seward terrane (Silberling and others, 1994) and are included in the Nome Group by Till and Dumoulin (1994) (map units DObm, D€ks, and D€bm of Till and others, 1986)[3]. These rocks retain locally well-preserved sedimentary features but have been metamorphosed to blueschist, greenschist, and locally amphibolite facies. The Seward terrane has been interpreted as a metamorphosed and deformed fragment displaced from the North American continental margin (Nokleberg and others, 1994).

[3] DObm, Ordovician through Devonian black metalimestone and marble; D€ks, Cambrian through Devonian calcschist; D€bm, Cambrian through Devonian black marble.

In the north (southern part of the Kotzebue quadrangle; fig. 1; fig. 12, column 10), a fault-bounded interval about 300 m thick has been called the Deceit Formation and divided into three members by Ryherd and Paris (1987). These strata are less ductilely deformed than, but are thermally equivalent to, surrounding parts of unit DObm (J.A. Dumoulin and A.G. Harris, unpub. data, 1995) and are included in the Nome Group by Till and Dumoulin (1994). The lowest member is chiefly pelagic and hemipelagic deposits and contains graptolites of Middle and Late Ordovician age (Ryherd and others, 1995); the upper members consist of carbonate turbidites and debris flows deposited as a prograding base-of-slope apron (Ryherd and Paris, 1987). The middle member contains conodonts of Wenlockian and early to middle Ludlovian age (A.G. Harris, unpub. data, 1987); the upper member has not been dated but is considered of probable Late Silurian (and younger?) age (Ryherd and Paris, 1987). The coarsest beds in this formation are breccias at least 15 to 20 m thick that contain clasts as much as 5 m in diameter (Dumoulin and Till, 1985). Turbidites and debris flows in the Deceit Formation contain little siliciclastic material, but calcareous turbidites in adjacent and correlative strata of the DObm and DЄks units (Till and others, 1986) contain locally abundant quartz, albite, chlorite, white mica, and graphite.

The Nome Group on the southeastern Seward Peninsula (unit DЄbm of Till and others, 1986) includes metamophosed, pure and impure turbidites similar to those described above, although coarse-grained carbonate debris flows are rare or absent in these rocks (fig. 12, column 11). Conodonts of late Early to Late Silurian (Wenlockian to Ludlovian) and middle Early Devonian (Pragian) age were obtained from this unit.

Across Seward Peninsula, Devonian shallow-water metacarbonate rocks of the Nome Group (map unit Ddm of Till and others, 1986)[3] appear to have been unconformably deposited on older, deeper water Nome Group rocks (Till and Dumoulin, 1994). These shallow-water strata contain conodonts and (or) megafossils of late Early (Emsian), Middle, and early Late Devonian (Frasnian) age (Till and others, 1986).

DISCUSSION

As noted above, the DOs unit in the Denali area correlates well with parts of the Farewell terrane exposed in central Alaska. But sedimentologic and biostratigraphic similarities also exist between DOs and rocks elsewhere in Alaska that have been included by previous workers in six other tectonostratigraphic terranes. A full discussion of the paleogeographic and tectonic histories of Alaskan terranes is beyond the scope of this paper, but our comparisons of Silurian deep-water strata throughout the state provide several useful constraints for terrane analysis. Of particular interest are the distribution patterns of calcareous siliciclastic turbidites of Silurian (Wenlockian to Ludlovian) age and the presence of a volcanic component in (and intercalated with) these turbidites.

Lower Paleozoic rocks in the Farewell terrane have previously been correlated with coeval strata in the Selwyn Basin of western Canada (Bundtzen and Gilbert, 1983; Bundtzen and others, 1988, 1994), as have rocks of the Livengood, Porcupine, and Tatonduk terranes (Dover, 1994). These correlations imply that all of these sequences formed in relative proximity to each other along the North American continental margin. Our analyses suggest that if this interpretation is valid, these terranes record a gradient in Silurian turbidite deposition. Accumulations of calcareous siliciclastic sandstone are thickest (>500 m) in the Farewell terrane (Terra Cotta Mountains Sandstone), notably thinner (50 m) in the Livengood terrane (Lost Creek unit), and apparently absent in the Porcupine and Tatonduk terranes (Road River Formation).

Thick (200-300 m) turbidite successions of Silurian age are also found in terranes of possible North American affinity in northern and western Alaska. The similarity in age and composition of turbidite successions in the Hammond subterrane (unnamed rocks in the Ambler River quadrangle) and in the Seward terrane (parts of the Nome Group) to those of the Farewell terrane (Terra Cotta Mountains Sandstone) suggest that all three successions were derived from a common source and were deposited along the same continental margin. Thus, if a North American origin is accepted for the Farewell terrane, Silurian stratigraphic correlations support a North American origin for both the Seward terrane and the Hammond subterrane as well, and imply Silurian proximity between all three terranes.

A third implication of our stratigraphic comparisons is that volcanic material preserved in the DOs unit, the Terra Cotta Mountains Sandstone, and other Silurian turbidite sequences could have been derived from the island arc represented by the Alexander terrane. Volcanic rocks of Silurian age are recognized in the Alexander terrane (Churkin and Carter, 1970; Eberlein and others, 1983; Gehrels and Berg, 1994) but have not been reported from elsewhere in Alaska or adjacent parts of Canada. A position close to northern North America during Silurian and Early Devonian time has been proposed for the Alexander terrane based on paleomagnetic, detrital zircon, and paleontologic observations (Bazard and others, 1995). Faunal similarities suggest close paleogeographic ties between the Farewell and Alexander terranes during the Silurian (Bazard and others, 1995; Soja, in press). Careful analyses of the precise age and composition of volcanic components in these terranes could strengthen this interpretation.

[4] Ddm, Devonian dolostone, metalimestone, and marble.

CONCLUSIONS

The DOs unit in the Denali National Park area is a chiefly deep-water sequence, at least in part of Silurian age, of calcareous and siliciclastic turbidites, calcareous debris flows, and calcareous and siliceous hemipelagic deposits. The unit also contains shallow-water facies that are at least in part of Late Devonian (early Frasnian) age. DOs correlates best with rocks of the Dillinger sequence and the lower part of the Mystic sequence (Farewell terrane) exposed to the southwest in the eastern McGrath quadrangle. Intriguing sedimentologic and biostratigraphic similarities also exist with rocks of east-central Alaska (Livengood terrane) and western Alaska (Seward terrane). Less compelling correlations can be made between rocks in southeastern Alaska (Alexander terrane) and northern Alaska (Hammond subterrane of Arctic Alaska terrane). Rocks in easternmost Alaska (Porcupine and Tatonduk terranes) correlate least well because they lack the thick interval of calcareous siliciclastic turbidites that is characteristic of DOs.

Depositional patterns and composition of Silurian turbidites in terranes throughout Alaska provide constraints on the ultimate origin of these terranes. Previous studies have suggested that all Alaskan terranes which include Silurian deep-water strata could have originated along or adjacent to the North American continental margin. Our correlations yield some support for this interpretation but imply an uneven distribution of Silurian turbidites along this margin. The Alexander terrane contains the only volcanic rocks of Silurian age reported from Alaska or western Canada and could have provided a source for the volcanic material in DOs and related rocks.

REFERENCES CITED

Armstrong, A.K., Harris, A.G., Reed, Bruce, and Carter, Claire, 1977, Paleozoic sedimentary rocks in the northwest part of Talkeetna quadrangle, Alaska Range, Alaska, *in* Blean, K.M., ed., The United States Geological Survey in Alaska: Accomplishments during 1976: U.S. Geological Survey Circular 751-B, p. B61-B62.

Bazard, D.R., Butler, R.F., Gehrels, G.E., and Soja, C.M., 1995, Early Devonian paleomagnetic data from the Lower Devonian Karheen Formation suggest Laurentia-Baltica connection for the Alexander terrane: Geology, v. 23, p. 707-710.

Blodgett, R.B., and Gilbert, W.G., 1992, Upper Devonian shallow-marine siliciclastic strata and associated fauna and flora, Lime Hills D-4 quadrangle, southwest Alaska, *in* Bradley, D.C., and Dusel-Bacon, Cynthia, eds., Geologic studies in Alaska by the U.S. Geological Survey, 1991: U.S. Geological Survey Bulletin 2041, p. 106-115.

Blodgett, R.B., Zhang, N., Ormiston, A.R., and Weber, F.R., 1988, A Late Silurian age determination for the limestone of the Lost Creek unit, Livengood C-4 quadrangle, east-central Alaska, *in* Galloway, J.P., and Hamilton, T.D., eds., Geologic studies in Alaska by the U.S. Geological Survey during 1987: U.S. Geological Survey Circular 1016, p. 54-56.

Bundtzen, T.K., and Gilbert, W.G., 1983, Outline of geology and mineral resources of upper Kuskokwim region, Alaska, *in* Mull, Gil, and Reed, Katherine, eds., Proceedings of the 1982 Symposium on Western Alaska Geology and Resource Potential: Alaska Geological Society Journal, v. 3, p. 101-117.

Bundtzen, T.K., Harris, E.E., and Gilbert, W.G., 1997, Geology of the eastern half of the McGrath quadrangle, Alaska: Alaska Divison of Geological & Geophysical Surveys Report of Investigations 97-14a, 34 p., 1 pl., scale 1:125,000.

Bundtzen, T.K., Kline, J.T., Smith, T.E., and Albanese, M.D., 1988, Geology of the McGrath A-2 quadrangle, Alaska: Alaska Divison of Geological & Geophysical Surveys Professional Report 91, 20 p., 1 pl., scale 1:63,360.

Bundtzen, T.K., Laird, G.M., Blodgett, R.B., Clautice, K.H., and Harris, E.E., 1994, Geology of the Gagaryah River area, Lime Hills C-5 and C-6 quadrangles, southwest Alaska: Alaska Divison of Geological & Geophysical Surveys Public Data File 94-40, 17 p., 1 pl., scale 1:63,360.

Churkin, Michael, Jr., and Brabb, E.E., 1965, Ordovician, Silurian, and Devonian biostratigraphy of east-central Alaska: American Association of Petroleum Geologists Bulletin, v. 49, p. 172-185.

_____ 1967, Devonian rocks of the Yukon-Porcupine Rivers area and their tectonic relation to other Devonian sequences in Alaska, *in* Oswald, D.H., ed., International Symposium on the Devonian System: Alberta Society of Petroleum Geologists, Calgary, Alberta, Canada, p. 227-258.

Churkin, Michael, Jr., and Carter, Claire, 1970, Early Silurian graptolites from southeastern Alaska and their correlation with graptolitic sequences in North America and the Arctic: U.S. Geological Survey Professional Paper 653, 51 p.

_____ 1996, Stratigraphy, structure, and graptolites of an Ordovician and Silurian sequence in the Terra Cotta Mountains, Alaska Range, Alaska: U.S. Geological Survey Professional Paper 1555, 84 p.

Churkin, Michael, Jr., Reed, B.L., Carter, Claire, and Winkler, G.R., 1977, Lower Paleozoic graptolitic section in the Terra Cotta Mountains, southern Alaska Range, *in* Blean, K.M., ed., The United States Geological Survey in Alaska: Accomplishments during 1976: U.S. Geological Survey Circular 751-B, p. B37-B38.

Cook, H.E., Hine, A.C., and Mullins, H.T., 1983, Platform margin and deep water carbonates: Society of Economic Paleontologists and Mineralogists Short Course Notes No. 12, 573 p.

Csejtey, Béla, Jr., Mullen, M.W., Cox, D.P., and Stricker G.D., 1992, Geology and geochronology of the Healy quadrangle, south-central Alaska: U.S. Geological Survey Miscellaneous Investigations Series Map I-1961, 63 p., 2 pls., scales 1:250,000 and 1:360,000.

Csejtey, Béla, Jr., Wrucke, C.T., Ford, A.B., Mullen, M.W., Dutro, J.T., Jr., Harris, A.G., and Brease, P.F., 1996, Correlation of rock sequences across the Denali fault in south-central Alaska, *in* Moore, T.E., and Dumoulin, J.A., eds., Geologic studies in Alaska by the U.S. Geological Survey, 1994: U.S. Geological Survey Bulletin 2152, p. 149-156.

Decker, John, Bergman, S.C., Blodgett, R.B., Box, S.E., Bundtzen, T.K., Clough, J.G., Coonrad, W.L., Gilbert, W.G., Miller, M.L., Murphy, J.M., Robinson, M.S., and Wallace, W.K., 1994, Ge-

ology of southwestern Alaska, *in* Plafker, George, and Berg, H.C., eds., The geology of Alaska: Boulder, Colo., Geological Society of America, The Geology of North America, v. G-1, p. 285-310.

Dickinson, W.R., and Suczek, C.A., 1979, Plate tectonics and sandstone compositions: American Association of Petroleum Geologists Bulletin, v. 63, p. 2164-2182.

Dover, J.H., 1994, Geology of part of east-central Alaska, *in* Plafker, George, and Berg, H.C., eds., The geology of Alaska: Boulder, Colo., Geological Society of America, The Geology of North America, v. G-1, p. 153-204.

Dumoulin, J.A., and Harris, A.G., 1988, Off-platform Silurian sequences in the Ambler River quadrangle, western Brooks Range, Alaska, *in* Galloway, J.P., and Hamilton, T.D., eds., Geologic studies in Alaska by the U.S. Geological Survey during 1987: U.S. Geological Survey Circular 1016, p. 35-38.

Dumoulin, J.A., and Till, A.B., 1985, Sea cliff exposures of metamorphosed carbonate and schist, northern Seward Peninsula, *in* Bartsch-Winkler, Susan, and Reed, K.M., eds., The United States Geological Survey in Alaska: Accomplishments during 1983: U.S. Geological Survey Circular 945, p. 18-22.

Dunham, R.J., 1962, Classification of carbonate rocks according to depositional texture, *in* Ham, W.E., ed., Classification of carbonate rocks: American Association of Petroleum Geologists Memoir 1, p. 108-121.

Dutro, J.T., Jr., and Patton, W.W., Jr., 1982, New Paleozoic formations in the northern Kuskokwim Mountains, west-central Alaska, *in* Stratigraphic notes, 1980-1982: U.S. Geological Survey Bulletin 1529-H, p. H13-H22.

Eberlein, G.D., Churkin, Michael, Jr., Carter, Claire, Berg, H.C., and Ovenshine, A.T., 1983, Geology of the Craig quadrangle, Alaska: U.S. Geological Survey Open-File Report 83-91, 52 p., scale 1:250,000.

Epstein, A.G., Epstein, J.B., and Harris, L.D., 1977, Conodont color alteration—an index to organic metamorphism: U.S. Geological Survey Professional Paper 995, 27 p.

Gehrels, G.E., and Berg, H.C., 1994, Geology of southeastern Alaska, *in* Plafker, George, and Berg, H.C., eds., The geology of Alaska: Boulder, Colo., Geological Society of America, The Geology of North America, v. G-1, p. 451-468.

Gilbert, W.G., and Bundtzen, T.K., 1984, Stratigraphic relationship between Dillinger and Mystic terranes, western Alaska Range, Alaska [abs.]: Geological Society of America Abstracts with Programs, v. 16, no. 5, p. 286.

Gordey, S.P., and Anderson, R.G., 1993, Evolution of the northern Cordilleran miogeocline, Nahanni map area (1051), Yukon and Northwest Territories: Geological Survey of Canada Memoir 428, 214 p, 4 pls., scale 1:250,000.

Grantz, Arthur, Moore, T.E., and Roeske, S.M., 1991, Continent-ocean transect A-3: Gulf of Alaska to Arctic Ocean: Geological Society of America Centennial Continent/Ocean Transect No. 15, 72 p., 3 pls., scale 1:500,000.

Howell, D.G., Johnsson, M.J., Underwood, M.B., Huafu, Lu, and Hillhouse, J.W., 1992, Tectonic evolution of the Kandik region, east-central Alaska: preliminary interpretations, *in* Bradley, D.C., and Ford, A.B., eds., Geologic studies in Alaska by the U.S. Geological Survey, 1990: U.S. Geological Survey Bulletin 1999, p. 127-140.

Jones, D.L., Silberling, N.J., Berg, H.C., and Plafker, George, 1981, Map showing tectonostratigraphic terranes in Alaska, columnar sections, and summary description of terranes: U.S. Geological Survey Open-File Report 81-792, 20 p., 2 sheets, scale 1:2,500,000.

Jones, D.L., Silberling, N.J., and Coney, P.J., 1983, Tectonostratigraphic map and interpretive bedrock geologic map of the Mount McKinley region, Alaska: U.S. Geological Survey Open-File Report 83-11, 2 sheets, scale 1:250,000.

Jones, D.L., Silberling, N.J., Gilbert, Wyatt, and Coney, P.J., 1982, Character, distribution, and tectonic significance of accretionary terranes in the central Alaska Range: Journal of Geophysical Research, v. 87, no. B5, p. 3709-3717.

Karl, S.M., and Giffen, C.F., 1992, Sedimentology of the Bay of Pillars and Point Augusta Formations, Alexander Archipelago, Alaska *in* Bradley, D.C., and Dusel-Bacon, Cynthia, eds., Geologic studies in Alaska by the U.S. Geological Survey, 1991: U.S. Geological Survey Bulletin 2041, p. 171-185.

Klapper, Gilbert, and Barrick, J.E., 1983, Middle Devonian (Eifelian) conodonts from the Spillville Formation in northern Iowa and southern Minnesota: Journal of Paleontology, v. 57, p. 1212-1243.

Mamet, B.L., and Plafker, George, 1982, A Late Devonian (Frasnian) microbiota from the Farewell-Lyman Hills area, west-central Alaska: U.S. Geological Survey Professional Paper 1216-A, p. A1-A12.

Mayfield, C.F., and Tailleur, I.L., 1978, Bedrock geology map of the Ambler River quadrangle, Alaska: U.S. Geological Survey Open-File Report 78-120A, scale 1:250,000.

Mullen, M.W., and Csejtey, Béla, Jr., 1986, Recognition of a Nixon Fork terrane equivalent in the Healy quadrangle, *in* Bartsch-Winkler, Susan, and Reed, K.M., eds., Geologic studies in Alaska by the U.S. Geological Survey during 1985: U.S. Geological Survey Circular 978, p. 55-60.

Mutti, Emiliano, and Ricci Lucchi, Franco, 1978, Turbidites of the northern Apennines—introduction to facies analysis: International Geology Review, v. 20, p. 125-166.

Nokleberg, W.J., Moll-Stalcup, E.J., Miller, T.P., Brew, D.A., Grantz, Arthur, Reed, J.C., Jr., Plafker, George, Moore, T.E., Silva, S.R., and Patton, W.W., Jr., 1994, Tectonostratigraphic terrane and overlap assemblage map of Alaska: U.S. Geological Survey Open-File Report 94-194, 54 p., 1 sheet, scale 1:2,500,000.

Patton, W.W., Jr., 1978, Juxtaposed continental and ocean-island arc terranes in the Medfra quadrangle, west-central Alaska, *in* Johnson, K.M., ed., The United States Geological Survey in Alaska: Accomplishments during 1977: U.S. Geological Survey Circular 772-B, p. B38-B39.

Patton, W.W., Jr., Box, S.E., Moll-Stalcup, E.J., and Miller, T.P., 1994, Geology of west-central Alaska, *in* Plafker, George, and Berg, H.C., eds., The geology of Alaska: Boulder, Colo., Geological Society of America, The Geology of North America, v. G-1, p. 241-269.

Potter, P.E., and Pettijohn, F.J., 1977, Paleocurrents and basin analysis (2d ed.): New York, Springer-Verlag, 425 p.

Reed, B.L., and Nelson, S.W., 1980, Geologic map of the Talkeetna quadrangle, Alaska: U.S. Geological Survey Miscellaneous Investigations Series Map I-1174, 15 p., scale 1:250,000.

Ridgway, K.D., Trop, J.M., and Sweet, A.R., 1997, Thrust-top basin formation along a suture zone, Cantwell basin, Alaska Range: Implications for development of the Denali fault system: Geological Society of America Bulletin, v. 109, p. 505-523.

Ryherd, T.J., Carter, Claire, and Churkin, Michael, Jr., 1995, Middle through Upper Ordovician graptolite biostratigraphy of the Deceit Formation, northern Seward Peninsula, Alaska [abs.]: Geological Society of America Abstracts with Programs, v. 27, no. 5, p. 75.

Ryherd, T.J., and Paris, C.E., 1987, Ordovician through Silurian carbonate base-of-slope apron sequence, northern Seward Peninsula, Alaska, *in* Tailleur, I.L., and Weimer, Paul, eds., Alaskan North Slope geology: Bakersfield, Calif., Society of Economic Paleontologists and Mineralogists, Pacific Section, Book 50, p. 347-348.

Savage, N.M., 1977, Middle Devonian (Eifelian) conodonts of the genus *Polygnathus* from the Wadleigh Limestone, southeastern Alaska: Canadian Journal of Earth Sciences, v. 14, p. 1343-1355.

_____1985, Silurian (Llandovery-Wenlock) conodonts from the base of the Heceta Limestone, southeastern Alaska: Canadian Journal of Earth Sciences, v. 22, p. 711-727.

_____1992, Late Devonian (Frasnian and Famennian) conodonts from the Wadleigh Limestone, southeastern Alaska: Journal of Paleontology, v. 66, p. 277-292.

Savage, N.M., Blodgett, R.B., and Brease, P.F., 1995, Late Devonian (Early Frasnian) conodonts and brachiopods from Denali National Park, south-central Alaska [abs.]: Geological Society of America Abstracts with Programs, v. 27, no. 5, p. 76.

Scholle, P.A., Bebout, D.G., and Moore, C.H., 1983, Carbonate depositional environments: American Association of Petroleum Geologists Memoir 33, 708 p.

Silberling, N.J., Jones, D.L., Monger, J.W.H., Coney, P.J., Berg, H.C., and Plafker, George, 1994, Lithotectonic terrane map of Alaska and adjacent parts of Canada, *in* Plafker, George, and Berg, H.C., eds., The geology of Alaska: Boulder, Colo., Geological Society of America, The Geology of North America, v. G-1, plate 3, 1 sheet, scale 1:2,500,000.

Soja, C.M., in press, Silurian of Alaska, *in* Landing, E., and Johnson, M., eds., Silurian lands and shelf margins: New York State Museum Bulletin, James Hall Symposium, v. 2.

Till, A.B., and Dumoulin, J.A., 1994, Geology of Seward Peninsula and Saint Lawrence Island, *in* Plafker, George, and Berg, H.C., eds., The geology of Alaska: Boulder, Colo., Geological Society of America, The Geology of North America, v. G-1, p. 141-152.

Till, A.B., Dumoulin, J.A., Gamble, B.M., Kaufman, D.S., and Carroll, P.I., 1986, Preliminary geologic map and fossil data, Solomon, Bendeleben, and southern Kotzebue quadrangles, Seward Peninsula, Alaska: U.S. Geological Survey Open-File Report 86-276, 71 p., 3 sheets, scale 1:250,000.

Uyeno, T.T., and Barnes, C.R., 1983, Conodonts of the Jupiter and Chicotte Formations (Lower Silurian), Anticosti Island, Québec: Geological Survey of Canada Bulletin 355, 49 p.

Weber, F.R., Blodgett, R.B., Harris, A.G., and Dutro, J.T., Jr., 1994, Paleontology of the Livengood quadrangle, Alaska: U.S. Geological Survey Open-File Report 94-215, 24 p., 1 sheet, scale 1:250,000.

Wilson, J.L., 1975, Carbonate facies in geologic history: New York, Springer-Verlag, 471 p.

Ziegler, Willi, and Sandberg, C.A., 1990, The Late Devonian standard conodont zonation: Frankfurt am Main, Courier Forschungsinstitut Senckenberg, No. 121, 115 p.

Zuffa, G.G., 1980, Hybrid arenites: their composition and classification: Journal of Sedimentary Petrology, v. 50, p. 21-29.

Reviewers: T.K. Bundtzen and W.W. Patton, Jr.

Magnetic properties and paleomagnetism of the LaPerouse and Astrolabe Gabbro intrusions, Fairweather Range, Southeastern Alaska

By Sherman Gromme

ABSTRACT

The La Perouse and Astrolabe layered gabbro bodies were intruded in Oligocene time into late Mesozoic rocks of the Chugach allochthonous tectonostratigraphic terrane in southeastern Alaska. The Astrolabe gabbro has magnetic intensities comparable in magnitude to other gabbros, but the La Perouse gabbro is only one-tenth as magnetic and produces little or no aeromagnetic anomaly. Natural remanent magnetization in both gabbros is stable and is carried by low-titanium titanomagnetite. Orientation of magnetic fabric represented by anisotropy of magnetic susceptibility is generally controlled by primary mineral layering. Paleomagnetic directions measured in the two gabbro bodies are similar and uniform regardless of attitudes of mineral layering, which has structural dips as steep as 70°. Performing structural corrections based either on the mineral layering or on the magnetic fabric produced marked increases in angular dispersion of paleomagnetic directions. The average paleomagnetic direction is markedly discordant to what would be predicted by coeval data from the North American craton but is similar to that reported earlier for Paleocene sheeted dikes and pillow basalts of the Resurrection Peninsula in the Chugach terrane 700 km to the northwest. Both of these paleomagnetic results seem to imply similar counterclockwise rotations and northward translations of their respective parts of the Chugach terrane in Tertiary time. Although the Resurrection Peninsula data are derived from rocks that carry evidence of paleo-horizontal position, little or no such evidence exists for the Astrolabe and La Perouse gabbros. Correcting the paleomagnetic direction for a presumed 9° tilt of the gabbro bodies derived from the transverse regional metamorphic gradient of the enclosing rocks and associated with late Tertiary uplift of the Fairweather Range produces near coincidence with the results from the Resurrection Peninsula. Increasing the amount of the tilt correction to 37° brings the paleomagnetic direction for the gabbro bodies into close concordance with the North American craton reference, but such a correction is based only on the paleomagnetic data and has a large 95-percent confidence estimated as ±20°. This post-Oligocene displacement of part of the Chugach terrane is significantly younger than that previously interpreted from the Resurrection Peninsula paleomagnetic data but can be considered as a consequence of differential uplift subsequent to accretion.

INTRODUCTION

The Crillon-La Perouse and Astrolabe-De Langle gabbro intrusions are two of a chain of eight gabbro bodies distributed along the southern Fairweather Range and Yakobi and Chichagof Islands in southeastern Alaska (fig. 1). These igneous rocks were intruded into late Mesozoic metavolcanic, metasedimentary and sedimentary rocks assigned to the Chugach tectonostratigraphic terrane by Plafker and Campbell (1979). The Chugach terrane is one of a series of allochthonous terranes that border the Gulf of Alaska and is interpreted as former oceanic crust (Plafker and others, 1977). On mainland Alaska at the latitude of the gabbro bodies described here, the Chugach terrane is from 25 to 60 km wide and, as originally defined, extends from the Pacific coast northeastward to the Tarr Inlet suture zone (Brew and Morrell, 1978; Plafker and Campbell, 1979). The inboard tectonic boundary of the Chugach terrane in most areas is the Border Ranges fault. In the area of figure 1, the northeast boundary of the Tarr Inlet suture zone is now considered to coincide with the Border Ranges fault, so that the suture zone is part of the Chugach terrane (Decker and Plafker, 1982).

The Crillon-La Perouse and Astrolabe-De Langle gabbro intrusions were first mapped, named, and described by Rossman (1963). The larger of the two, the Crillon-La Perouse gabbro, was further investigated by Loney and Himmelberg (1983). Following the usage of Gromme and Hillhouse (1981) and Loney and Himmelberg (1983), the two intrusions will be referred to herein as the La Perouse and Astrolabe gabbros. Other gabbro bodies in this chain have been described by Plafker and MacKevett (1960) and Loney and others (1975).

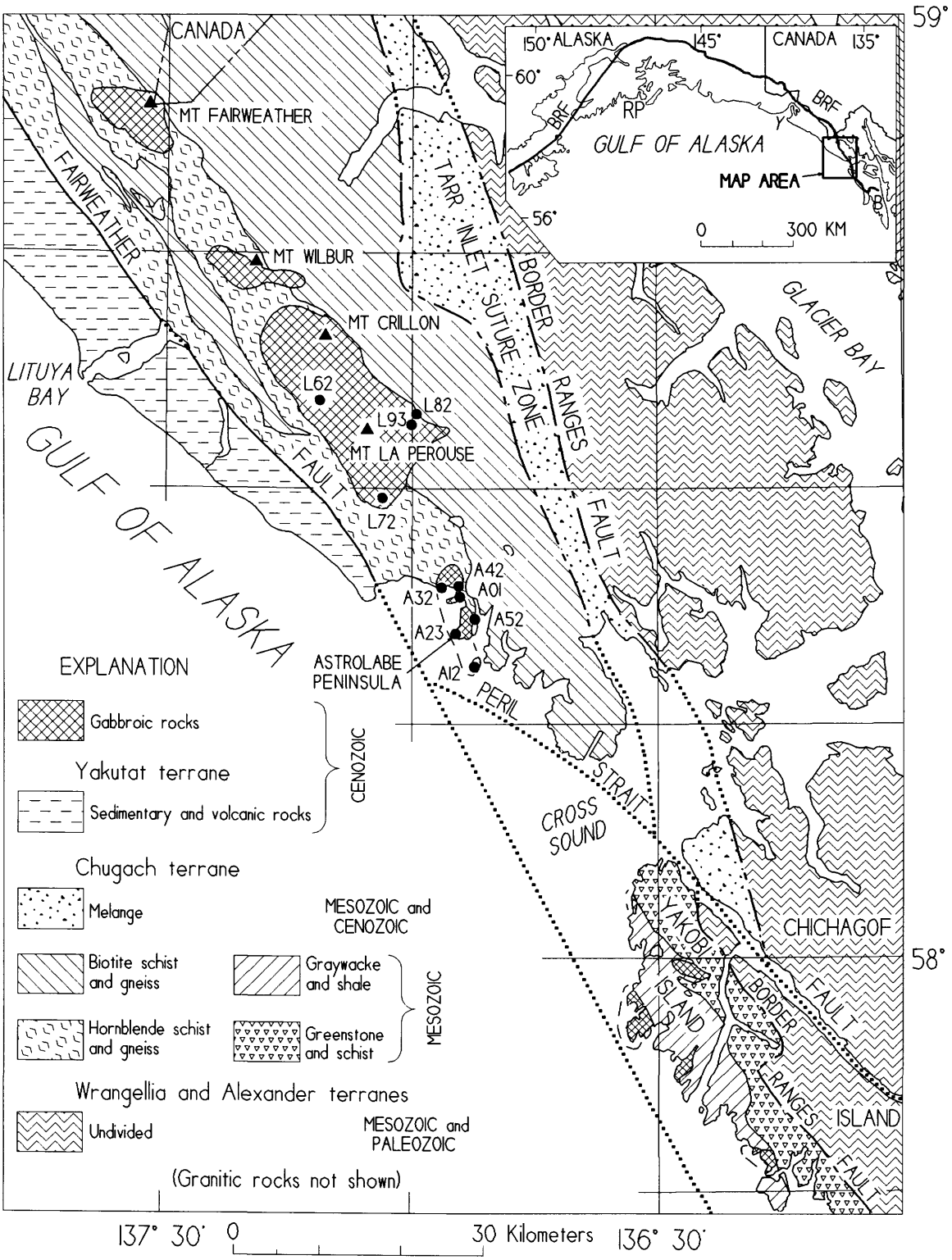

Figure 1. Index map of part of southeast Alaska, modified from Loney and Himmelberg (1983), showing geologic setting of gabbroic intrusions. Paleomagnetic sampling sites indicated by A01 to A52 (Astrolabe gabbro) and L62 to L93 (LaPerouse gabbro). Tectonostratigraphic terrane boundaries shown by heavy lines; solid where mapped, dashed where inferred, dotted where covered. Fairweather fault from Plafker and Campbell (1979). Peril Strait fault from Loney and others (1975). Tarr Inlet suture zone boundaries north of Cross Sound from Brew and others (1978b) and Brew and Morrell (1978, 1979). Tarr Inlet suture zone boundaries south of Cross Sound, Border Ranges fault, and combined extent of Wrangellia and Alexander terranes from Decker and Plafker (1982) and Karl and others (1982). Inset from Plafker and others (1977): BRF, Border Ranges fault; RP, Resurrection Peninsula. *Y*, Yakutat Bay. B, Baranof Island.

Some of the magnetic properties obtained during this study have been published by Brew and others (1978a). The most important aspect of the scalar magnetic properties is that the La Perouse gabbro is only weakly magnetic, about one-tenth as magnetic as the Astrolabe gabbro which is more typical of gabbroic rocks in this respect. A brief account of the paleomagnetic results (Gromme and Hillhouse 1981) showed that the paleomagnetic direction in the two gabbros was markedly discordant to the direction that would be predicted from coeval paleomagnetic data from the North American craton but was nearly coincident with the paleomagnetic directions obtained from the ophiolitic rocks of the Resurrection Peninsula in the Chugach terrane 700 km to the northwest. The purpose of this report is to provide a full description of the magnetic properties of the gabbro bodies, making use of recently developed methods for measuring and analyzing magnetic fabric, and to reevaluate the tectonic significance of the paleomagnetic directions.

The following description is taken from Rossman (1963) and Loney and Himmelberg (1983), supplemented by the author's observations in 1976. Both the Astrolabe and La Perouse gabbro bodies are layered. The layering is prominent in nearly all outcrops, and individual layers are commonly isomodal or modally graded, less commonly size graded. The modal layering (also termed phase layering) is defined by relative proportions of cumulus plagioclase and pyroxene, and the contacts between layers may be either abrupt or gradational over several millimeters. Thicknesses of individual layers range from less than 1 cm to 15 m but are generally 5 cm to 1.5 m. On outcrop scale the layering in both gabbro bodies is markedly planar and undisturbed. Moreover, there is no microscopic evidence of post-crystallization deformation in the gabbros. Rossman (1963) states that on the southern end of the La Perouse gabbro some individual layers can be traced for a distance of 1.5 km, but Loney and Himmelberg (1983) state that the lateral continuity of layers is no greater than that and commonly much less. In the Astrolabe gabbro the layering tends to be more lenticular, and dips range from 5° to 45° but are commonly between 10° and 20°. In the La Perouse gabbro, the layers dip steeply (as much as 70°) inward from the northeast and southwest margins, defining a synclinal structure approximately parallel to the long axis of the intrusion. This synclinal structure has a shallow plunge of about 10° to the southeast but is terminated at the southeast end by northwest-dipping (60° to 80°) layering in the gabbro (Loney and Himmelberg, 1983). The exposed stratigraphic thickness of the La Perouse gabbro is about 10 km, and in the Astrolabe gabbro the exposed thickness is about 600 m (Rossman, 1963). The strike of layering in the La Perouse gabbro is broadly concordant to the contact with country rock, but the contact relations are complicated by a subvertical fault surrounding the gabbro. In some places this fault lies a few hundred meters outside the igneous contact, but along the northeast margin of the gabbro the fault has evidently cut off at least 4,000 m of stratigraphic section of the gabbro. The remarkable transverse structural symmetry of the layering in the La Perouse gabbro is well illustrated in cross sections (Rossman, 1963; Loney and Himmelberg, 1983).

Radiometric age determinations of the La Perouse gabbro have been made difficult because of the presence of excess radiogenic argon (Himmelberg and Loney, 1981). K-Ar ages ranging from 19 to 44 Ma were determined for country rock and the metamorphic aureole at the southwest margin of the La Perouse gabbro (Hudson and Plafker, 1981). A subsequent determination by the $^{40}Ar/^{39}Ar$ incremental heating method of 28±8 Ma was reported by Loney and Himmelberg (1983); the dated mineral was plagioclase (R.A. Loney, U.S. Geological Survey, oral commun., 1997). The most recent age determination for the La Perouse gabbro is 29.54±0.13 Ma using the $^{40}Ar/^{39}Ar$ incremental heating method with biotite separated from a hornblende-biotite-muscovite pegmatite that intrudes the northeast flank of the gabbro. This plateau age was determined from eight contiguous heating steps representing 81.9 percent of the total argon gas released. The total gas age is 28.99±0.12 Ma (C.D. Taylor, R.J. Goldfarb, and L.W. Snee, U.S. Geological Survey, written commun., 1997). No age determinations have been made for the Astrolabe gabbro, but because the paleomagnetic directions in the two gabbros are concordant (Gromme and Hillhouse, 1981), for the purpose of this report the two bodies are assumed to be nearly coeval. Bradley and others (1993) have compiled radiometric ages of plutons that intrude the Chugach terrane for a distance along its trend of almost 2,200 km. Most of these plutons have ages ranging from 66 Ma in the west to 37 Ma in the southeast, and they are assigned to the Sanak-Baranof belt as originally defined by Hudson and others (1977). A group of younger granitic plutons in the southeastern Chugach terrane was also defined by Bradley and others (1993); these range in age from 18 to 33 Ma and extend from southeastern Chichagof Island approximately 500 km northwest to near the head of Yakutat Bay, but they are lacking along a 300-km gap between the latitude of Mt. Fairweather (fig. 1) southeast to Baranof Island. The gabbro bodies in the Fairweather Range may occupy the missing part of this younger plutonic trend, but only one of the four gabbros has been dated, and no genetic connection is implied here.

The gabbronorite bodies on Yakobi and western Chichagof islands (fig. 1) are enclosed by tonalite plutons; the emplacement age of the tonalite bodies is between about 40 and 43 Ma, and the gabbronorite is considered to be older (Himmelberg and others, 1987). Because of age differences and contrasting petrologic characteristics, Himmelberg and others (1987) emphasize that the Yakobi Island and Chichagof Island gabbronorites have no genetic connection to the tholeiitic gabbros in the Fairweather Range to the northwest.

At the latitude of the Astrolabe and La Perouse gabbros, two plutons intruding the eastern part of the Chugach terrane have been dated by the K-Ar method and are part of

Table 1. Locations of gabbro samples from the Fairweather Range

Site	Latitude	Longitude	1:63,360-scale sheet in Mt. Fairweather quadrangle
A01	58° 54.17′	136° 54.05′	B-3
A12	58° 18.90′	136° 52.15′	B-3
A23	58° 20.95′	136° 54.45′	B-3
A32	58° 23.92′	136° 55.93′	B-3
A42	58° 23.85′	136° 54.65′	B-3
A52	58° 21.58′	136° 52.35′	B-3
L62	58° 35.57′	137° 11.33′	C-4
L72	58° 29.57′	137° 03.05′	B-4
L82	58° 34.57′	136° 58.83′	C-3
L93	58° 33.78′	136° 59.68′	C-3

the Sanak-Baranof belt. Both are designated as unfoliated granitic rocks by MacKevett and others (1971). One is exposed as a large nunatak 7 km northeast of site L82 (fig. 1) and has an age of 39.4±1.2 Ma using muscovite; the other is 12 km east-northeast of site A12 (fig. 1) and has an age of 38.2±1.1 Ma using biotite (D.A. Brew, cited in Bradley and others, 1993). At this latitude there is no evidence for any igneous activity in the Chugach terrane that is younger than the 29-Ma age of the La Perouse gabbro.

FIELD AND LABORATORY METHODS

Field work was done by the author in the summer of 1976, assisted by Joseph C. Liddicoat. Because the La Perouse gabbro is mostly covered by glaciers and snowfields, and because bad weather restricted helicopter access, most paleomagnetic sampling was done along shoreline exposures of the Astrolabe gabbro. Sampling was done with a portable gasoline-powered diamond drill, and the cores were oriented with a magnetic compass. Compass readings were corrected for local magnetic anomalies by backsighting either to distant landmarks or to a second compass mounted on a tripod several meters away from the sampled outcrop. Corrections were usually zero and never exceeded 3°. Locations of the sampling sites are shown in figure 1 and are listed in table 1.

Remanent magnetizations were measured in the laboratory with spinner magnetometers or with a commercial superconducting magnetometer. Alternating-field (AF) demagnetization was done mostly with a four-axis tumbler in a 60-Hz field using the double demagnetization method of Hillhouse (1977) and also with a commercial 400-Hz uniaxial demagnetizer. Bulk susceptibilities were first measured with a commercial bridge in a field of approximately 0.05 mT at 1 kHz. The magnetic fabric represented by anisotropy of magnetic susceptibility (AMS) was measured with a commercial inductance meter in a 0.1-mT field at 800 Hz; this instrument also provides bulk susceptibilities. Thermal demagnetization was done in vacuum in a residual magnetic field less than 300 nT. Curie temperatures were determined in vacuum with a continuously recording thermomagnetic balance.

Pilot AF demagnetizations to 100-mT peak field strength were done for several specimens from each site. These results were used to determine the optimum demagnetization for the remaining specimens from a site in order to obtain the best estimate of the primary remanent magnetization direction. These experiments were supplemented by a limited number of thermal demagnetizations. Results of the two kinds of demagnetization were analyzed and averaged separately except in one instance where both methods isolated both normal and reversed polarities within the same site. The remanent magnetization directions were analyzed with Fisher (1953) statistics. The magnetic fabric measurements were analyzed for each site with the tensor-averaging method (Jelinek, 1978; Lienert, 1991). Representative polished thin sections from each sampling site in both gabbro bodies were examined in transmitted and reflected light at magnifications from 52 times to 1,050 times.

MAGNETIC PROPERTIES

The scalar magnetic properties of both gabbro bodies are summarized in table 2. As many single specimens as could be obtained from the oriented cores were used for the susceptibility measurements. As mentioned above, the susceptibilities of samples of La Perouse gabbro are consistently an order of magnitude less than for the Astrolabe gabbro. This difference is reflected in the amplitudes of aeromagnetic anomalies observed over the two gabbros (Brew and others, 1978a); there is no aeromagnetic expression of the southern half of the La Perouse gabbro and little expression of its northern half, whereas over the Astrolabe gabbro the amplitude of the anomaly remaining after subtraction of topographic enhancement is 200 nT. According to Rossman (1963), the La Perouse gabbro contains as much as 25 weight percent of ilmenite, with 0.2 percent being a representative overall value; Rossman reported no magnetite in these rocks. The Astrolabe gabbro contains roughly subequal amounts of ilmenite and magnetite (or titanomagnetite), and the total oxide content ranges from 3 to 22 percent by weight (Rossman, 1963).

Saturation isothermal remanent magnetizations were produced at room temperature in a selected group of speci-

mens, using a direct magnetic field of 0.8 T. These saturation IRM values are plotted with the corresponding susceptibility values on a bilogarithmic scale in figure 2. This figure emphasizes the wide range of magnetic properties in these two gabbros and shows that the retention of IRM is roughly proportional to the weak-field reversible susceptibility over most of the range. The departure from proportionality at low IRM values is probably due to the fact that the paramagnetic susceptibility of the pyroxene and of the antiferromagnetic ilmenite (and possibly hexagonal pyrrhotite as discussed below) in the rocks provides a minimum value when no ferrimagnetic oxide is present.

As a possible supplement to the measurements of attitude of layering in the gabbro bodies, the AMS, or magnetic fabric, was measured in the same specimens as the bulk susceptibilities. Even though the La Perouse gabbro is only weakly magnetic, both it and the Astrolabe gabbro possess easily measurable magnetic fabrics. The maximum fabric ratios range from 1.022 to 1.133 (table 2). These results will be discussed more fully below.

A magnetic hysteresis parameter that provides a partial estimate of the average magnetic domain configuration in the oxide grains contained in a rock specimen is the ratio of saturation IRM to the saturation magnetization determined from the slope of the high-field part of the hysteresis loop (Day and others, 1977). Values approaching 0.5 indicate predominance of single-domain (SD) configurations, while values lower than 0.05 indicate presence of multiple domains (MD) in each magnetic grain. The values of this ratio (SIRM/J_S) in table 2 indicate that the magnetic oxide grains in the Astrolabe gabbro are mostly pseudo-single domain (PSD), but in the much less magnetic La Perouse gabbro the magnetic oxide grains tend to be SD and therefore must be significantly smaller in diameter, concomitant with the much lower volume proportion. Petrographic examination of polished thin sections in reflected and transmitted light shows that in the Astrolabe gabbro the observable titanomagnetite grains are as large as 3,000 μm and as small as 5 μm. The larger titanomagnetite grains may be either optically homogeneous at magifications up to 1,050 times or may be subdivided by thin discontinuous lamellae along octahedral planes of the host. These lamellae are typically 0.5 to 1 μm wide by 20 to 40 μm long and, where they are thick enough to be identifiable, appear to be ilmenite.

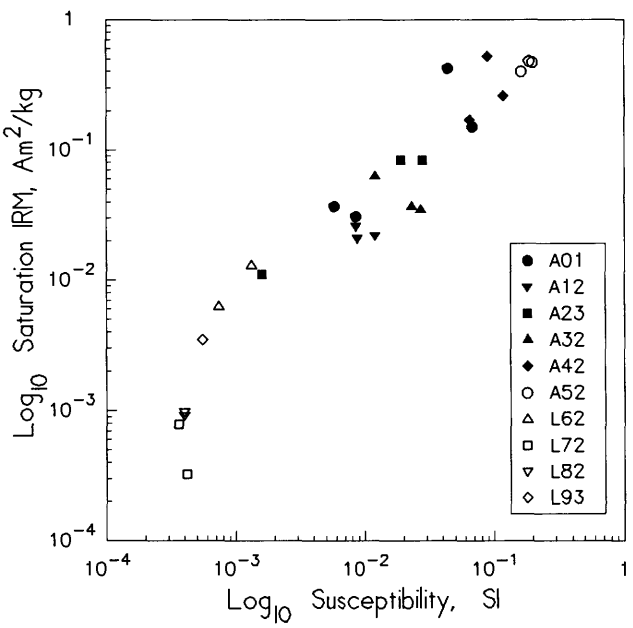

Figure 2. Scalar magnetic properties of gabbroic rocks. IRM, isothermal remanent magnetization produced by 800 mT field. Site designations as in figure 1.

A commonly used measure of stability of natural remanent magnetization (NRM) is the median destructive field (MDF), defined as the peak alternating field strength required to reduce the NRM to half its initial value. The ranges of MDF values for selected specimens from each site are listed in table 2. Both gabbro bodies are unusually stably magnetized; the maximum alternating field attainable is inadequate to reduce the NRM by one-half in some specimens from four of the sites in the Astrolabe gabbro. The La Perouse gabbro is somewhat less stably magnetized. With the exception of site L82, the MDF values were determined for specimens carrying little or no secondary magnetization. (The unique difficulty encountered with site L82 is discussed below.) The fact that the NRM in the Astrolabe gabbro is more stable against AF demagnetization than that in the La Perouse gabbro seems contradictory to the lower values of SIRM/J_S for the Astrolabe gabbro. A possible explanation is that in the Astrolabe gabbro the stable NRM (which is presumably natural thermoremanent magnetization) is carried by a subpopulation of oxide grains that are significantly smaller in effective grain size than the entire population of grains represented by the SIRM data and by the results of the other laboratory experiments that measure bulk magnetic properties.

Because secondary magnetization was found in many specimens at all the sites, the intensities of NRM before demagnetization have little intrinsic significance and are not given in table 2.

THERMOMAGNETIC RESULTS

Representative strong-field thermomagnetic curves are shown in figure 3. The presence of pyrrhotite is clearly evident in the curves for sites A01 and L82. On the heating curves, the increases in magnetization at 150°C and 210°C for sites A01 and L82 represent the transition from antiferromagnetic to ferrimagnetic hexagonal pyrrhotite with composition Fe_9S_{10} (Schwartz and Vaughn, 1972). The magnetization of the ferrimagnetic sulfide disappears at its Curie temperature, around 320 to 340°C for site A01 and 310°C for site L82; the latter value would be expected if no monoclinic pyrrhotite (Fe_7S_8) were also present (Schwartz,

Table 2. Room-temperature magnetic and thermomagnetic properties of specimens from the Astrolabe and La Perouse gabbros.

[N, number of specimens used for susceptibility measurements. K, bulk susceptibility. s.d., standard deviatin. K_{MAX}/K_{MIN}, tensor averageratio of maximum and inimum directional susceptibilities. $SIRM/J_s$, ratio of saturation remanent magnetization and saturation magnetization.MDF, median destructive alternating field for stable component of natural remanent magnetization. T_S, temperature of maximum negativeslope of thermal demagnetization of NRM. T_C, Curie temperature obtained from strong-field thermomagnetic curves. - -, not determined]

Site	N	K ± s.d. (SI)	K_{MAX}/K_{MIN}	$SIRM/J_s$	MDF (mT)	T_s (°C)	T_c (°C)
A01	28	0.022 ± 0.018	1.131	0.09 – 0.30 (4)	85 – 99 (2)	559 – 571 (3)	549 – 575 (4)
A12	27	0.014 ± 0.008	1.022	0.32 – 0.43 (4)	60 – >100 (3)	573 – 576 (3)	557 – 575 (4)
A23	19	0.013 ± 0.006	1.090	0.12 – 0.28 (3)	79 – >100 (3)	561 – 577 (3)	565 – 587 (3)
A32	19	0.014 ± 0.005	1.133	0.04 – 0.18 (3)	42 – >100 (3)	552 – 553 (3)	532 – 570 (3)
A42	25	0.085 ± 0.020	1.043	0.07 – 0.13 (3)	18 – >100 (4)	537 – 560 (3)	536 – 572 (3)
A52	24	0.121 ± 0.059	1.025	0.07 – 0.10 (3)	39 – 77 (2)	555 – 568 (3)	545 – 565 (3)
L62	22	0.0116± 0.0006	1.083*	0.5 (1)	37 (1)	563 – 569 (3)	569 – 570 (3)
L72	28	0.0048± 0.0006	1.036	0.3 (1)	29 – >100 (2)	- -	- -
L82	35	0.0047± 0.0012	1.050	0.4 (1)	4 – 7 (6)	- -	- -
L93	37	0.0071± 0.0015	1.040*	0.2 – 0.4 (3)	12 – 16 (3)	559 – 577 (3)	564 – 568 (3)

* Asterisks in K_{MAX}/K_{MIN} column denote inverse magnetic fabric

() Number of specimens used for $SIRM/J_s$, MDF, T_s, and T_c determinations are shown in parentheses; where more than one specimen was used, total range of values is shown

1975). Because hexagonal pyrrhotite is antiferromagnetic at room temperature, it does not contribute to the remanent magnetization, though it may contribute slightly to the measured susceptibility of the rock. The absence of the pyrrhotite peaks from the cooling curves is attributed to chemical breakdown. In the specimen from site L82, the breakdown is oxidation with formation of magnetite, as indicated by the large increase in magnetic moment. The release of reactive gas associated with this breakdown causes problems with the experimental apparatus, so that no thermal demagnetization experiments were done for sites L62, L72, and L82, all of which contain abundant pyrrhotite.

With the exception of the pyrrhotite peaks, the thermomagnetic curves in figure 3 are typical of ferrimagnetic spinel such as magnetite and titanomagnetite. The concave-upward parts of the curves for sites L62 and L82 represent the contribution of antiferromagnetic ilmenite and paramagnetic pyroxene; the concavity is enhanced by the large field strengths (400 mT) required for these weakly magnetic samples. The ranges of Curie temperatures obtained from the thermomagnetic curves are listed in table 2. The total range is from 532 to 587°C, which is typical of low-titanium titanomagnetite or pure magnetite. The lowest Curie temperature measured for any of the paleomagnetic sites, in a specimen from site A32 (fig. 3), is associated with the greatest degree of thermal irreversibility (excluding the irreversibility associated with pyrrhotite). The example of irreversibility in figure 3 is usually interpreted as partial rehomogenization of a magnetite-ilmenite intergrowth that originated from high-temperature oxidation of titanomagnetite.

A thermomagnetic curve for a magnetic separate from a sample of the Brady Glacier low-grade nickel-copper ore deposit at the largely unexposed southeast corner of the La Perouse gabbro (Czamanske and others, 1976) is also shown in figure 3. The ore deposit is in the basal cumulates of the gabbro, stratigraphically far below the main exposures (Himmelberg and Loney, 1981). The magnetic separate (furnished by G.K. Czamanske, U.S. Geological Survey, 1979) is a zoned chromium-iron spinel. The saturation magnetization is 10.1 Am^2/kg, and the Curie temperature is 518°C. This Curie temperature is significantly lower than any reported in table 2, and the chromium-iron spinel probably is not present in any of the paleomagnetic sampling sites.

Four examples of thermal demagnetization of NRM are shown in figure 4, illustrating the typically narrow range of unblocking temperatures. The unblocking temperatures can be represented by the temperatures of the midpoints of the steepest segments of these demagnetization diagrams. The ranges of observed values for eight sites are listed in table 2 as T_S. The typical unblocking temperatures are all close to (and below) the corresponding measured Curie temperatures. The narrowness of the unblocking temperature ranges and the closeness of these ranges to the maximum Curie temperatures are typical of thermoremanent magnetization in well-crystallized SD or PSD grains of magnetite or

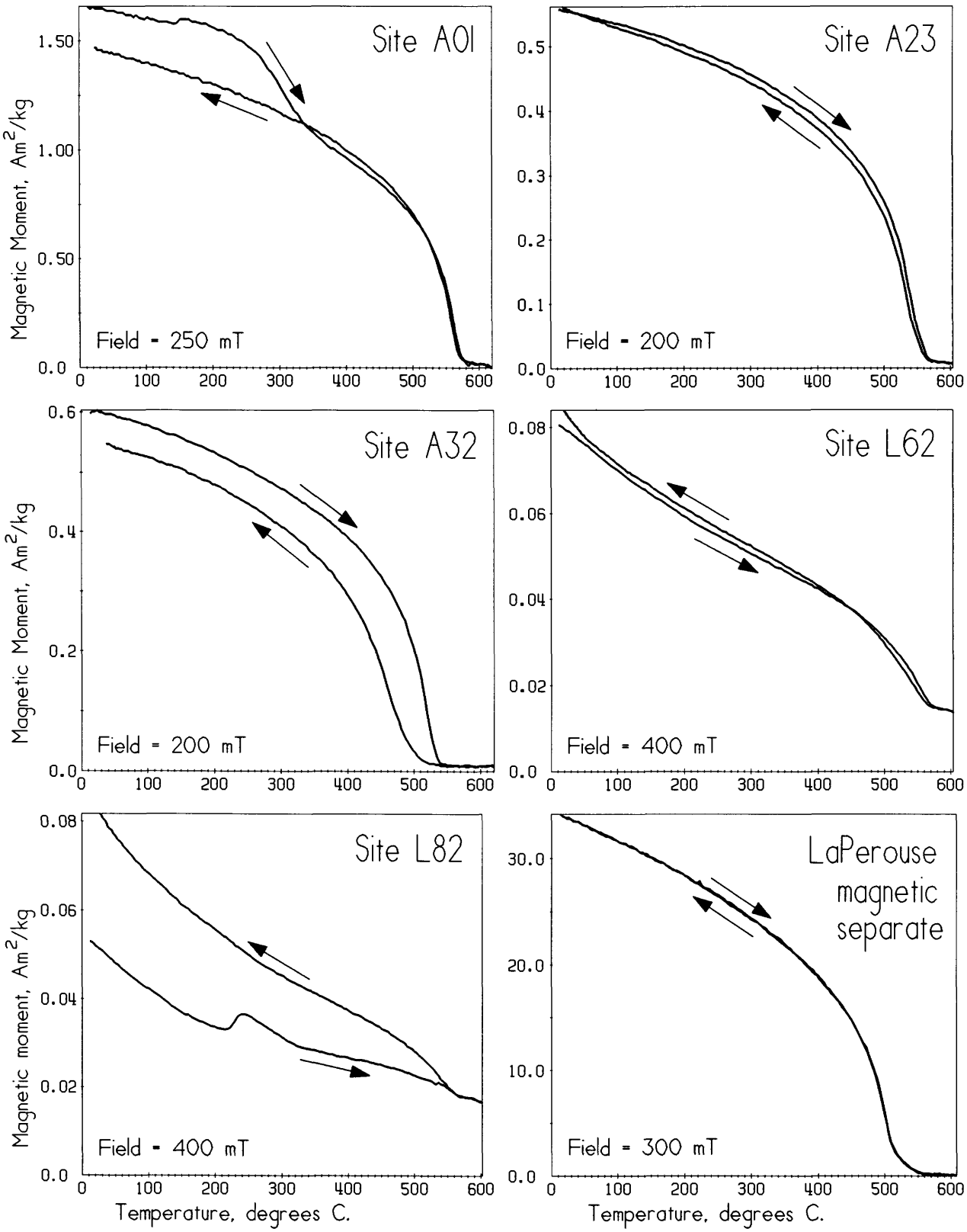

Figure 3. Continuous strong-field thermomagnetic curves illustrating variety of reversible and irreversible behavior. Heating and cooling (indicated by arrows) were done in vacuum. Pyrrhotite is evident in samples from sites A01 and L82. Magnetic separate is from a sample of drill core in nickel-copper ore deposit hosted by basal gabbro forming nunataks in Brady Glacier southeast of main exposures of LaPerouse gabbro (Czamanske and others, 1976). Other site designations as in figure 1.

low-titanium titanomagnetite. Together with the high MDF values, these thermal demagnetization results represent an unusually high degree of stability of NRM.

NATURAL REMANENT MAGNETIZATION

Site-mean paleomagnetic directions and associated statistics are given in table 3. Normal and reversed polarities were found, and two sites (A01 and A23) exhibited both polarities. At site A01, AF demagnetization isolated normal polarity in all samples, while thermal demagnetization of specimens from some of the same cores isolated reversed polarity. At site A23, both normal and reversed polarities were isolated by both AF and thermal demagnetization, but the polarity of a core depends on the location along the outcrop. The closest pair of cores with normal and reversed polarities are separated by only 2 m, but this interval also contains a pegmatite dike 0.5 m wide that is rich in green hornblende. Vector component diagrams illustrating AF demagnetization of a specimen from each of these adjacent cores are shown in figure 5. Except that secondary magnetization is more evident in the reversely magnetized specimen (core 30), there is no apparent difference in the response of the two specimens to demagnetization, and there is no other evidence supporting any difference in the magnetic minerals in the two specimens. Because no evidence for later reheating exists, all the normal and reversed polarities in these gabbro bodies must represent geomagnetic field reversals that occurred during initial cooling. The sense of reversal can only be surmised at site A01, where the high-temperature and hence presumably oldest magnetization is reversed, implying the sequence R→N. The total number of geomagnetic reversals represented by the data from the sampled sites is unknown but could be as few as one.

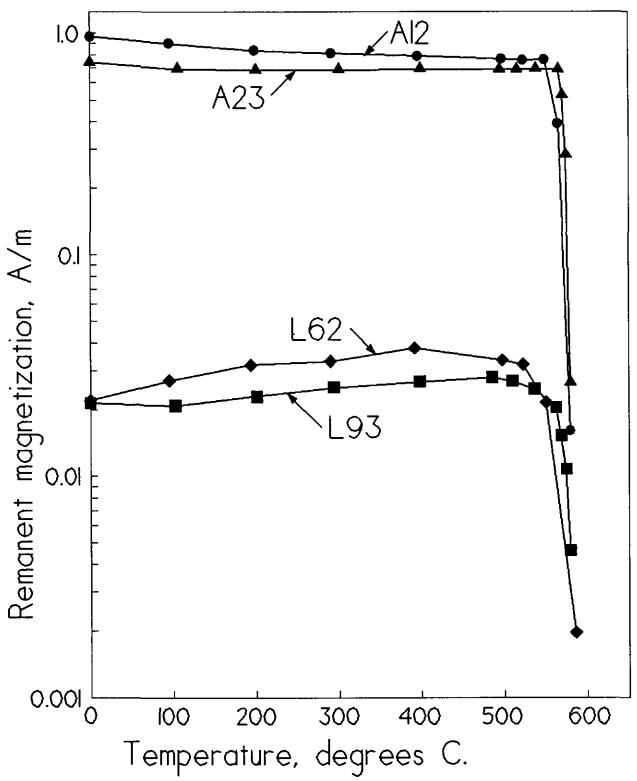

Figure 4. Thermal demagnetization of natural remanent magnetization (NRM). Data were chosen to illustrate typical narrowness of unblocking temperature distributions. Specimens were heated and cooled in vacuum. Site designations as in figure 1.

The data from site L82 were problematic and ultimately were discarded. The NRM directions were fairly well grouped, but their mean was excessively divergent from those for the rest of the sites. AF demagnetization only served to increase the within-site dispersion. Because of suspicion that the NRM's in these particular specimens were not responding well to 60-Hz tumbling demagnetization, triaxial sequential demagnetization in a 400-Hz static apparatus was also performed. The results were equally poor, so only the NRM data are reported in table 3. The MDF values for this site are atypically low (table 2) and all three principal susceptibility axes are oblique to the layering (see next section), but there is no further clue from either petrographic examination or the other magnetic parameters as to the origin of the divergent NRM. For eight of the nine remaining sites, it was necessary to reject one or more cores because AF demagnetization isolated no stable remanent direction (table 3).

The site-mean or treatment-mean remanent magnetization directions from table 3 are shown in figure 6*A*, except for site L82. Both normally and reversely polarized groups show sufficient clustering that the directions are considered to have paleomagnetic significance. The fifteen mean directions (table 3) were averaged using the two-tier method of Watson and Irving (1957) because this method gives each specimen unit weight and thus avoids giving excess weight to groups having only two or three specimens. For these calculations, the reversely magnetized directions (those on the upper hemisphere in figure 6*A*) were inverted through the vector origin, that is, their polarity was inverted to the normal sense. The overall two-level Fisher concentration parameter k for the directions without any structural correction was 227, corresponding to an angular standard deviation of 19°. When a structural correction was made for thirteen of the fifteen sites by rotating the mean direction around the strike of layering through the angle of dip (figure 6*B*), the overall two-level concentration parameter decreased to 71, corresponding to an increase of the angular standard deviation to 39°. This negative result of the classic paleomagnetic fold test is typical of layered gabbros, but a better result might have been expected in light of the positive fold test exhibited by the layered Cretaceous ultramafic intrusions at Duke Island in southeastern Alaska (Bogue and others, 1995). To try to get an improved paleohorizontal reference for the gabbro bodies, the AMS was measured in specimens from all sites.

Table 3. Paleomagnetic results from the Astrolabe and La Perouse gabbros.

[Strike, Dip: attitude of igneous lamination. N_C, number of oriented cores collected. N_R, number of cores rejected, as carrying no stable natural remanent magnetization. N, number of specimens used in averages after treatment indicated. Treatment; uniform maximum alternating-field strength, or range of temperatures reached by different specimens during thermal demagnetization. I, D, inclination (degrees, positive downward) and declination (degrees eastward), respectively, of mean remanent magnetization after treatment. R, vector sum of N unit vectors. k, Fisher (1953) concentration parameter. α_{95}, radius of 95-percent confidence cone (degrees) centered on mean direction (Fisher, 1953). Plo, Pla: east longitude and north latitude (degrees) of virtual geomagnetic pole corresponding to mean direction]

Site	Strike	Dip	N_C	N_R	N	Treatment	I	D	R	k	α_{95}	Plo	Pla
A01	116°	17°S	11	1	9	30 mT	48.7	243.2	8.8953	76.4	5.9	170.5	12.4
					3	565–580°C	-46.7	75.0	2.9717	70.6	14.8	160.4*	16.2*
A12	90°	30°S	11	1	10	30 mT	23.8	241.4	9.4125	15.3	12.8	164.0	-3.6
					3	548–566°C	50.2	256.0	2.9987	1543.	3.1	161.4	19.2
A23	Horizontal------		9	4	6	60 mT, 566°C	23.3	242.6	5.7728	22.0	14.6	162.6	-3.2
					3	60 mT, 495°C	-67.7	49.3	2.9677	61.8	15.8	190.7*	26.2*
A32	0°	15°E	10	0	10	30 mT	-53.2	95.0	9.9320	132.3	4.2	148.6*	30.8*
					3	496–539°C	-56.1	89.7	2.9246	26.5	24.4	154.6*	30.4*
A42	45°	9°SE	10	1	9	30 mT	-58.8	107.8	8.8187	44.1	7.9	143.4*	41.8*
					3	403–549°C	-68.4	87.7	2.5352	4.3	69.	168.0*	41.0*
A52	Unknown-------		10	2	8	15 mT	-69.9	152.7	7.5132	14.4	15.1	128.0*	74.2*
L62	347.5°	49.5°E	10	3	7	15 mT	-68.3	97.6	6.9423	104.0	6.0	161.4*	45.2*
L72	325°	44°E	10	8	2	10 mT	-59.4	130.5	1.9027	10.3	-	124.6*	54.1*
L82	180°	65°W	11	11	11	NRM	-1.6	351.5	8.9205	8.3	-	-	-
L93	167.5°	50.0°W	11	2	9	20 mT	-58.4	75.6	8.8679	60.6	6.7	166.3*	26.0*
					3	536–561°C	-55.3	71.9	2.9750	80.0	13.9	167.0*	21.6*

* Asterisks denote pole inverted through origin (reversed polarity).

ANISOTROPY OF MAGNETIC SUSCEPTIBILITY (AMS)

The number of specimens for each site that provided the AMS data (table 2) ranges from 19 to 37, sufficient to provide statistically robust mean results for all sites. The axial ratios of the mean susceptibiliy ellipsoids for each site are shown in figure 7. Most of the sites have distinctly oblate ellipsoids (representing a predominantly planar fabric), some have nearly equal axial ratios, and only one is prolate (a predominantly linear fabric). The mean susceptibility axes for each site are shown in figure 8 with the associated 95 percent confidence ellipses obtained from the bivariate tensor-averaging method. The attitudes of the layering measured at each site are also shown in figure 8. At site L93 the magnetic fabric is unambiguously inverse in relation to the layering; that is, the minimum and intermediate susceptibility axes are parallel to the layering. Site L93 is also the only one that exhibits prolate fabric. At site L62 the minimum susceptibility axis is parallel to the layering but the other two axes are oblique to it; the fabric at this site is also considered here to be inverse. At sites A01, A23, A32, A42, and L72 the fabric is clearly normal, in that the minimum susceptibility axis is approximately perpendicular to the layering. At sites A12 and L82 the fabric axes are oblique to the

layering, but both show a greater tendency toward normal fabric. At site A52 the layering was discernible in outcrop but not clearly enough to be measurable, so in accordance with attitudes of layering measured elsewhere on the Astrolabe Peninsula (Rossman, 1963, plate 1) the fabric is assumed to be normal at this site.

The normal magnetic fabric is caused by preferred orientation of longest axes of non-equant magnetite crystals; this is termed "shape" or "magnetostatic" anisotropy (Tarling and Hrouda, 1993). In the Astrolabe gabbro, where magnetite grains are large enough to be observed petrographically, they are interstitial to the cumulus crystals of pyroxene and plagioclase; that is, they are postcumulus. Inverse magnetic fabric is observed at only two sites, both in the La Perouse gabbro. Inverse fabric is most simply explained as the result of predominance of single-domain magnetic grains (Tarling and Hrouda, 1993). If the single-domain grains are preferentially oriented along their directions of spontaneous magnetization, then the axis of maximum susceptibility will be perpendicular to the axis of preferred orientation. If the single-domain grains are elongate parallel to their directions of spontaneous magnetization, the preferred orientation could have resulted from the same cause as that in multidomain grains. The SIRM/J_S ratios listed in table 2 show that, as would be expected from the fact that petrographically they are mostly submicroscopic and/or scarce, the titanomagnetite grains in the La Perouse gabbro tend to be more nearly single domain than those in the Astrolabe gabbro, so that the single-domain explanation for the inverse fabric is plausible. Site L93 has the most convincingly inverse fabric, and it is also the only site with strongly prolate fabric; this configuration helps to confirm the single-domain explanation.

The observation that at most sites the magnetic fabric is clearly related to the primary layering (fig. 8) indicates that the same factor or factors that produced the layering also governed the orientation of the fabric. Whether the layering originated by gravitational settling of cumulus minerals (Rossman, 1963) or by crystallization of cumulus silicates inward and upward from steeply or shallowly dipping margins (Loney and Himmelberg, 1983), in the complete absence of any evidence of penetrative deformation of the gabbro the magnetic fabric is evidently a reflection of pre-

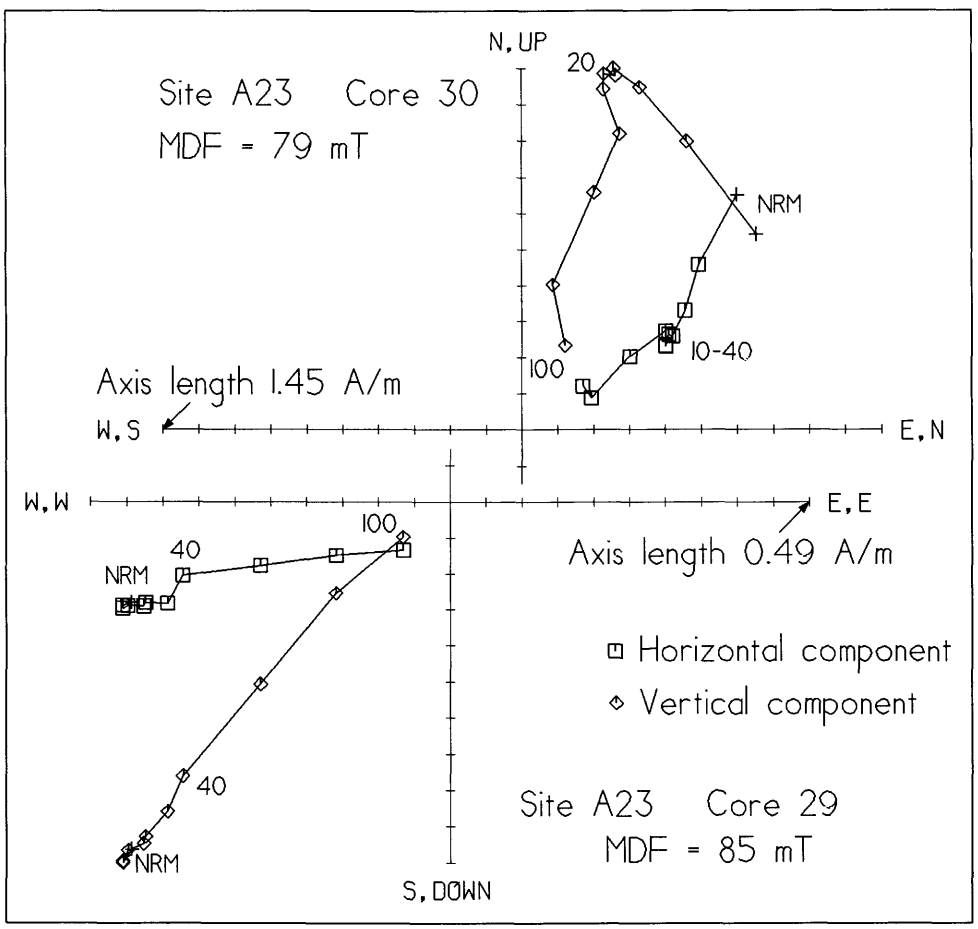

Figure 5. Vector component diagrams showing alternating-field demagnetization of natural remanent magnetization (NRM) in two oppositely polarized specimens from site A23. MDF, median destructive alternating field.

ferred orientation of margins of crystals of cumulus pyroxene and plagioclase. In other words the magnetic fabric, whether normal or inverse, is a primary characteristic of the rock. Rossman (1963, p. F19), referring to both gabbro bodies, stated that "Most of the rock within the layers has a discernible fabric in which the elongate or flat minerals lie with their long axes or flat sides parallel to the plane of the layering." Petrographic examination of the Astrolabe gabbro shows that the larger titanomagnetite grains are invariably surrounded by single post-cumulus pyroxene crystals of varying relative width and that the outlines of both are determined by the margins of the enclosing cumulus pyroxene and plagioclase crystals. Because magnetite grains are small and scarce in the La Perouse gabbro, a similar petrographic generalization cannot be made for it.

The mean AMS axes are used to calculate a revised paleomagnetic fold test in the following way. For all the sites having normal fabric, a pseudo-layering plane was chosen to pass through the maximum and intermediate axes. This construction was also done for site A52 where no layering could be measured on the outcrop. For sites L62 and L93, which have inverse fabric, the pseudo-layering plane was chosen to pass through the intermediate and minimum axes. Site L82 was omitted from the average, as discussed above. The result of this modified fold test is just as negative as that of the conventional test: The two-level Fisher concentration parameter k decreases from 227 to 82, and the equivalent angular standard deviation of the fifteen mean directions increases from 19° to 37°.

PALEOMAGNETIC INTERPRETATION

Loney and Himmelberg (1983) interpreted the present synclinal structure of the La Perouse gabbro as representing an initially laccolithic body that deformed with its country rock during intrusion and crystallization in a viscoelastic

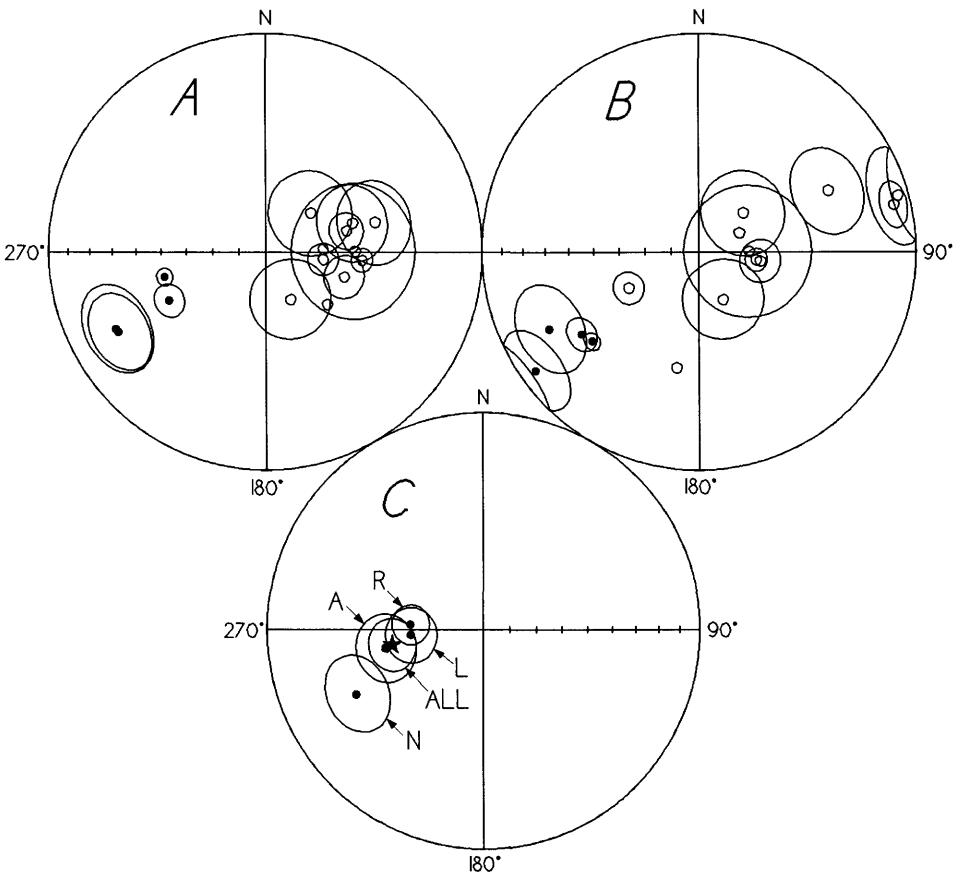

Figure 6. Equal-area projections of site-mean or treatment-mean (thermal or AF demagnetization) directions of magnetization, omitting site L82 (see text). *A*, *in-situ* directions. *B*, after unfolding using attitudes of mineral layering. *C*, comparisons of different combinations of *in-situ* data: N, all normally polarized and R, all reversely polarized. A, all Astrolabe gabbro and L, all LaPerouse gabbro. Overall mean indicated by star. Solid circles in lower hemisphere, open circles in upper hemisphere. In *C*, reversed directions (denoted by * in table 3) inverted through origin and shown on lower hemisphere. Mean directions and radii of 95-percent confidence circles obtained by method of Watson and Irving (1957).

manner in response to persistent subhorizontal regional compression. The negative results of both kinds of fold test as described above imply that the remanent magnetizations of the Astrolabe and La Perouse gabbro bodies were acquired after any deformation of the layering. The lack of any macroscopic evidence of penetrative deformation (Rossman, 1963; Loney and Himmelberg, 1983), the complete lack of any microscopic evidence of granulation, and the fact that the Curie temperatures are far below the solidification temperatures of these gabbros all combine to make this result predictable. Therefore, the paleomagnetic significance of these data must be evaluated from the *in situ* remanent magnetization directions. Various combinations of these directions, averaged by the two-level method of Watson and Irving (1957), are compared in figure 6*C*.

The normally and reversely polarized groups are not antiparallel. The most divergent mean directions in the normal group are from the AF-demagnetized specimens at site A12, and also from the AF- and thermally demagnetized specimens having normal polarity at site A23. The fact that both demagnetization methods gave the same result argues against incompletely removed secondary magnetization as the cause of the divergence. Moreover, any unremoved overprint such as might have been produced by the present geomagnetic field would tend to shallow the reversed directions, but the opposite relation is observed Thus, any such secondary magnetization would have to have been produced by a reversed geomagnetic field. It follows that the divergence

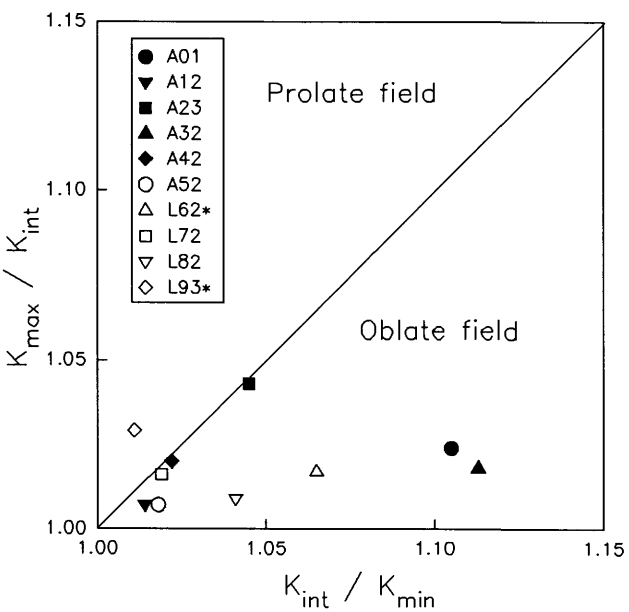

Figure 7. Flinn-type diagram (Tarling and Hrouda, 1993) showing that magnetic fabric of all but one site is marginally to dominantly oblate; that is, more nearly planar than linear. Site designations shown in figure 1. K_{max}, K_{int}, K_{min}, magnitudes of maximum, intermediate, and minimum orthogonal site-mean susceptibility axes, respectively. Asterisks in legend indicate sites with inverse fabric.

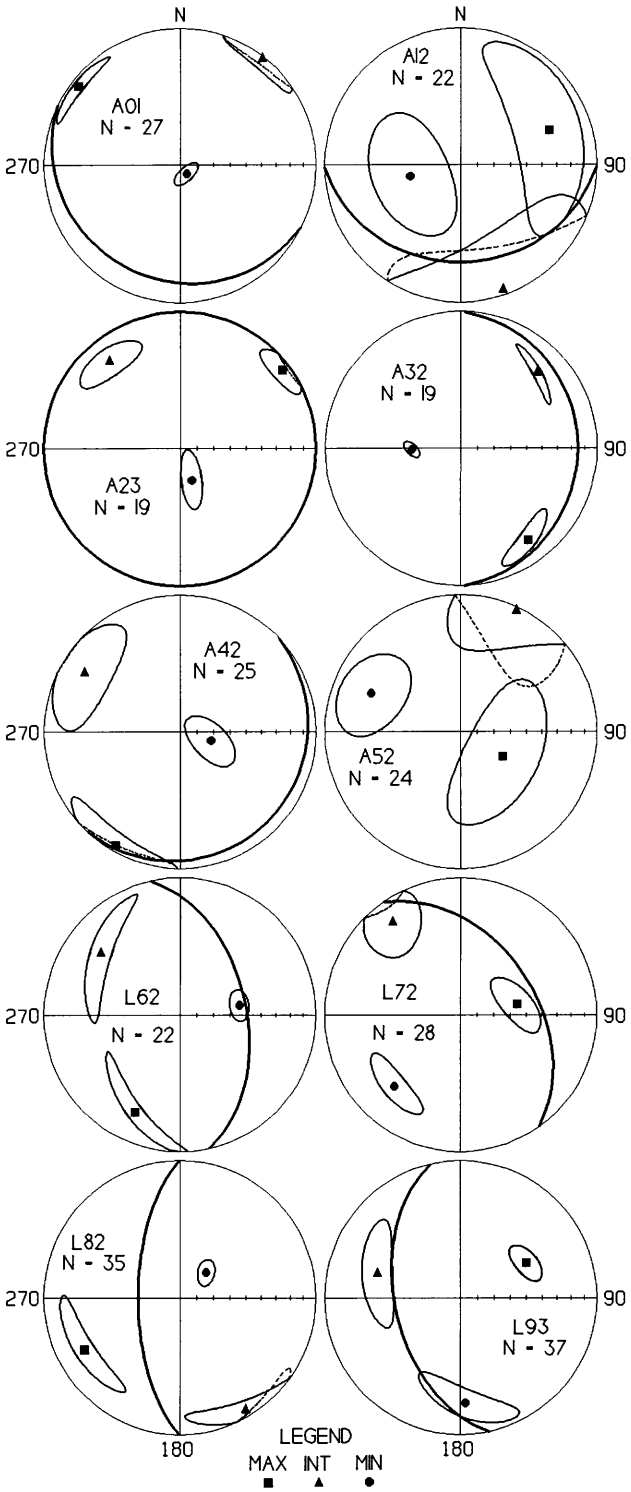

Figure 8. Magnetic fabric (AMS) diagrams for all sites. Orthogonal principal axes of site-mean susceptibility ellipsoids shown as equal-area projections on lower hemisphere. Means and 95-percent confidence ellipses obtained by tensor-averaging (Jelinek, 1978; Lienert, 1991). Measured igneous lamination attitudes indicated by heavy great circles (none visible in outcrop at site A52). Site designations as in figure 1; N is number of specimens analyzed from each site. Other symbols as in figure 7.

from antiparallelism is most reasonably attributed to geomagnetic secular variation.

The mean directions for the Astrolabe and La Perouse gabbros were averaged separately and are compared in figure 6*C*; they are not significantly different from each other. Therefore, the overall mean *in situ* paleomagnetic direction is used for comparison with coeval paleomagnetic data from the North American craton. Because the population of directions does not have a strictly Fisherian distribution, the consequent likelihood that these gabbro data do not average secular variation requires that the significance of the mean direction not be overemphasized. This direction has declination 260.7° and inclination 54.8° with a two-level 95-percent confidence radius 9.3° (fig. 6*C*). The equivalent paleomagnetic pole obtained by performing the two-level analysis of the fifteen virtual poles in table 3 has longitude 160.3°E., latitude 25.0°N., with an angular standard deviation 23° and 95-percent confidence radius 10.7°. This paleomagnetic pole is shown in figure 9 labeled AL.

The original reconnaissance paleomagnetic investigation of the sheeted dikes and pillow basalts of the Resurrection Peninsula, 700 km to the northwest in the Chugach terrane, was reported by Gromme and Hillhouse (1981). A more detailed study of these rocks has been published by Bol and others (1992), who cite a radiometric age of 57±1 Ma determined by the uranium-lead method from zircon separated from plagiogranite. The revised pole position is similar to that originally reported, at longitude 167°E., latitude 37°N, with a 95-percent confidence radius 11°; this pole is shown in figure 9 labeled RP. These two paleomagnetic poles (AL and RP) do not differ significantly from one another but are both highly discordant to the coeval poles for the North American craton, possibly implying that the two parts of the Chugach terrane that they represent shared a common displacement history in later Tertiary time.

This coincidence of paleomagnetic pole position must be qualified by the lack of a reference paleohorizontal for the Astrolabe and La Perouse gabbros. The paleomagnetic declination is fortuitously nearly perpendicular to the trend of the La Perouse synclinal structure, and, as a first approximation, the symmetry of this structure mentioned earlier might be evidence against tilt around its longitudinal axis. Moderate tilts around this axis would change the paleomagnetic inclination and hence the paleolatitude, but would hardly affect the declination. George Plafker (U.S. Geological Survey, written commun., 1996) has suggested that the metamorphic gradient across the segment of Chugach terrane between the Fairweather fault and the Tarr Inlet suture zone (Brew and others, 1978a) represents simple eastward tilt of a single structural block that resulted from the major uplift of the Fairweather Range that occurred during latest Tertiary time. This interpretation is complicated by the fault that cuts off much of the northeast part of the La Perouse gabbro (Loney and Himmelberg, 1983) and probably also by unknown structural complications in this area, which has not been mapped in detail. Nevertheless the simple tilt correction suggested by Plafker produces the following results.

The horizontal dimension is assumed to extend 30 km northeast from the head of Lituya Bay, a typical width for this structural block (fig. 1). At the southwest end the metamorphic grade is assumed to be about middle amphibolite facies, and at the northeast end the grade is assumed to be lowermost greenschist facies. Use of the pressure-temperature summary diagram of Winkler (1967, fig. 40), with assumed geothermal gradients of 30°C/km and 20°C/km, results in tilt angles toward the northeast of 9° and 17°, respectively. The axis of presumed tilt is taken as the azimuth of the two points where the contacts between hornblende schist and gneiss on the west and biotite schist and gneiss on the east intersect the La Perouse gabbro at its northwest and southeast ends (Loney and Himmelberg, 1983, fig. 2); this axis

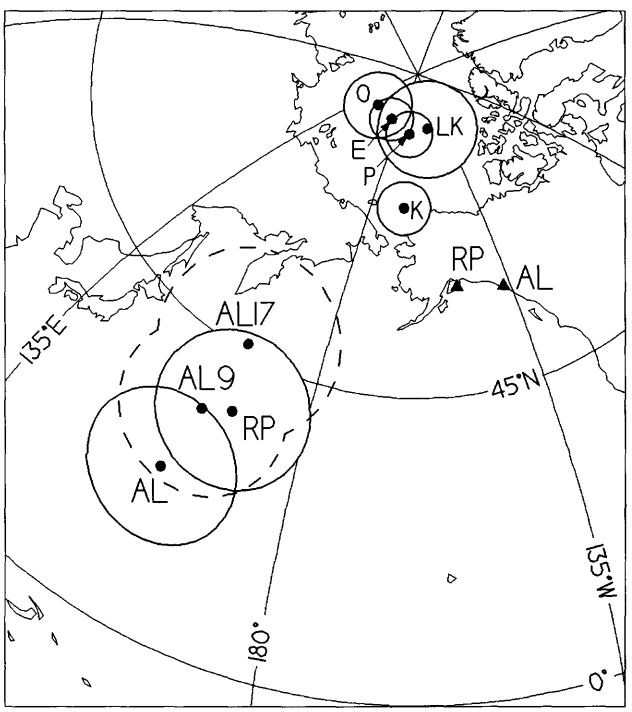

Figure 9. Equal-area map of part of northern hemisphere, showing paleomagnetic sampling areas (triangles) and paleomagnetic poles (solid circles). RP, pole for Resurrection Peninsula (Gromme and Hillhouse, 1981; Bol and others, 1992). AL, pole for Astrolabe and LaPerouse gabbros (this paper). AL9, AL17, modified pole positions for Astrolabe and La Perouse gabbros with hypothetical 9° and 17° tilts removed, respectively. Reference paleomagnetic poles for North American craton as follows: K, Cretaceous, 144-88 Ma (van Fossen and Kent, 1992). LK, Late Cretaceous, 76 Ma (Gunderson and Sheriff, 1991). P, Paleocene, 67-55 Ma; E, early to middle Eocene, 54-44 Ma; O, Oligocene to early Miocene, 38-22 Ma (Diehl and others, 1983). Large open circles are 95-percent confidence intervals from authors cited above or from table 2, and shown dashed for pole positions modified using hypothetical tilts.

trends at 329° and is representative of the major structural trend of the enclosing rocks of the Chugach terrane. These moderate tilt corrections do not greatly violate the symmetry of the La Perouse synclinal structure; that is, the corrections do not overturn any of the layering on the northeast flank of the gabbro. The sense of the corrections is to steepen the paleomagnetic inclination without significantly affecting the declination; thus the paleomagnetic pole is displaced toward the gabbro bodies, and this in turn decreases the amount of calculated northward transport. The corrected paleomagnetic poles are as follows: For the 9° tilt, the pole is at 162.3°E., 35.2°N., with 95-percent confidence radius 12.0°; for the 17° tilt, the pole is at 164.4°E., 46.2°N., with 95-percent confidence radius 13.1°. These two pole positions are shown dashed in figure 9; neither differs significantly from the Resurrection Peninsula pole of Bol and others (1992).

Another and more extreme tilt correction can be made by using only the trend of the longitudinal axis of the LaPerouse gabbro body as before, but also using just the paleomagnetic data themselves and ignoring the semiquantitative estimates from metamorphic facies differences. If a rotation of about 37° around a horizontal axis trending at 329° is used to remove the presumed eastward tilt of the gabbro bodies, their mean paleomagnetic direction moves into close coincidence with the direction that is calculated for the same location from the North American Oligocene reference pole of Diehl and others (1983). This tilt correction increases the 95-percent confidence interval around the corresponding paleomagnetic pole to nearly 17°, however, and therefore no numeric results are given except that the combined 95-percent confidence interval for the 37° rotation is roughly estimated at about ±20°, not including uncertainty in the azimuth and inclination of the assumed axis. A serious disadvantage to this method of estimation is that it analyzes the paleomagnetic data essentially in its own terms, including the sense of rotation, and for additional information makes use only of the azimuth of the major structure of the enclosing rocks of the Chugach terrane. Conversely, the assumption that the rocks of the Chugach terrane in this area were a rigid block without internal deformation during tilting is also unneeded.

Bol and others (1992), using a composite reference paleomagnetic pole for the North American craton, obtained for the Resurrection Peninsula rocks a northward displacement of 13°±9° and a counterclockwise rotation of 102°±16°. (These and the following 95-percent confidence intervals for displacements were calculated using the method of Demarest (1983) to convert from bivariate to univariate statistics.) For the Astrolabe and La Perouse gabbros, the appropriate reference pole is the Oligocene average for the interval 22 to 38 Ma of Diehl and others (1983) as shown in figure 9; note here that the choice of an older Tertiary reference pole would lessen the apparent northward displacement by a small amount but would scarcely affect the calculated rotation. The displacements calculated for the two gabbro bodies without tilt correction are 24°±9° northward transport and 86°±12° counterclockwise rotation. The 9° tilt correction yields 15°±10° of northward transport and 80°±15° of counterclockwise rotation, while the 17° tilt correction yields a northward transport of 6°±11° and a counterclockwise rotation of 70°±18°. Thus, the 9° tilt correction results in the best match of the Astrolabe and La Perouse gabbro results with those from the bedded ophiolitic rocks of the Resurrection Peninsula. The 17° tilt correction, however, results in a northward transport for the gabbro bodies that is not statistically significant at the 95-percent probability level. All three choices of correction result in significant counterclockwise rotation similar to that found by Bol and others (1992) for the Resurrection Peninsula.

SUMMARY AND CONCLUSIONS

The Astrolabe and La Perouse gabbro bodies were intruded in Oligocene time into late Mesozoic rocks of the Chugach terrane in southeastern Alaska (Loney and Himmelberg, 1983). The magnetic susceptibility and saturation magnetization of samples of the Astrolabe gabbro are typical of gabbro, whereas those of samples of the La Perouse are an order of magnitude lower. Thermomagnetic analysis and petrographic examination show that the magnetic mineral in both gabbro bodies is low-titanium titanomagnetite. The difference in magnetic properties reflects the far greater abundance of ilmenite relative to titanomagnetite in the La Perouse gabbro. The orientation of the magnetic fabric represented by anisotropy of magnetic susceptibility is mostly related to the macroscopic mineral layering; at least one and commonly two of the principal susceptibility axes are subparallel to the layering regardless of steepness of dip of the layering. Eight of the ten sample sites show normal magnetic fabric, but two of the sites, both in the La Perouse gabbro, show inverse fabric. The inverse fabric is interpreted to be the result of a high proportion of single-domain magnetic grains in the La Perouse gabbro.

Despite the large difference in magnetic properties, both gabbro intrusions share a common direction of natural remanent magnetization. Both normal and reversed magnetic polarities exist in the Astrolabe gabbro. Three of the four sampling sites in the the La Perouse gabbro are reversely magnetized, while the fourth has a divergent magnetization direction; the cause of the divergence is not known. The existence of both polarities is the result of one or more geomagnetic reversals that occurred during the initial cooling of the gabbro intrusions after they had become solid. All available evidence, both thermomagnetic and petrographic, indicates that the natural remanent magnetization is thermoremanent magnetization acquired while the gabbro intrusions cooled below their maximum Curie temperature of 580°C. Attempts to perform the paleomagnetic fold test using either

the attitudes of mineral layering observed in outcrop or the principal magnetic susceptibility axes cause marked increases in angular dispersion, hence yielding negative results. Little deformation other than faulting occurred within either gabbro body as they cooled below this temperature in Oligocene time.

The average direction of thermoremanent magnetization in the Astrolabe and La Perouse gabbros is compared with the Oligocene geomagnetic field direction predicted at their present location from the reference pole for the North American craton of Diehl and others (1983). In the gabbro bodies the inclination is 19°±8° shallower, and the declination is 86°±14° westward, or counterclockwise. This paleomagnetic discordance is similar to that found in Paleocene sheeted dikes and pillow basalts of the Resurrection Peninsula in the Chugach terrane 700 km to the northwest (Gromme and Hillhouse, 1981; Bol and others, 1992). If the Astrolabe and La Perouse gabbros were not tilted during postmagnetization uplift in latest Tertiary time, the paleomagnetic results imply post-Oligocene northward displacement of 2,700±1,000 km (confidence interval ±95%). The corresponding northward displacement for the Resurrection Peninsula rocks is 1,500±1,000 km (Bol and others, 1992), and the counterclockwise rotations are similar for both. On the basis of increasing regional metamorphic gradient from northeast to southwest across the block of Chugach terrane rock intruded by the gabbro bodies, arbitrary tilts around a northwest axis resulting from late Tertiary differential uplift can be estimated as between 9° and 17° southwestward by assuming geothermal gradients of 30°/km and 20°/km respectively. Application of the 9° tilt correction to the gabbro bodies reduces the apparent northward displacement to 1,700±1,100 km, in close agreement with the Resurrection Peninsula result of Bol and others (1992). Applying the 17° tilt correction further reduces the apparent northward displacement to 800±1,200 km, statistically not significant at 95-percent confidence. Another, more hypothetical tilt correction can be made using only the paleomagnetic data, the North American Oligocene reference pole (Diehl and others, 1983), and the major structural trend of the rocks of the Chugach terrane at the latitude of the gabbro bodies. That correction is approximately 37° southwestward, brings the paleomagnetic pole for the gabbro bodies into close coincidence with the reference pole, but has an associated 95 percent confidence roughly estimated at ±20°.

Applying the moderate and semiquantitative tilt corrections of 9° or 17° to the gabbro bodies does not change the apparent rotations significantly. The paleogeographic implications of this rotation have been discussed by Bol and others (1992) in the context of the extinct Kula-Farallon spreading ridge, of which the Resurrection Peninsula ophiolitic rocks are interpreted to be a part. Bol and others (1992) point out that the sense of rotation is the same as that implied by other paleomagnetic results farther north in Alaska and that the rotations might have resulted from oroclinal bending or from terrane translation along curved transcurrent fault systems. The sense of rotation is opposite, however, to that predicted for small passive structural blocks in a zone of oblique right-lateral tectonic convergence, as is observed along the western margin of North America at lower latitudes (Beck, 1980). Regardless of the similarity or dissimilarity between the paleomagnetic results from the Astrolabe and La Perouse gabbro bodies and the Resurrection Peninsula rocks, the differences in age and tectonic setting are significant. Bol and others (1992) concluded that if the Resurrection Peninsula ophiolitic rocks were part of the Kula-Farallon spreading ridge, their northward transport would have been completed by 45 Ma. Reviewing the previous paleomagnetic data from southern Alaska, Bol and others (1992) point out that all the data from rocks younger than about 55 Ma are concordant with the North American craton. The discordant result from the Oligocene gabbros constitutes an exception to that generalization and implies that counterclockwise rotation and also significant northward displacement of at least part of the Chugach terrane has occurred since Oligocene time. If the curved trace of the Border Ranges fault (fig. 1) is representative of the curved trasnscurrent fault systems referred to by Bol and others (1992), then explaining the rotations by northwestward displacements along them is unsatisfactory because, although the rotations for the Oligocene gabbros and the Paleocene ophiolitic rocks are similar, the strike of the Border Ranges fault is about 345° at the latitude of the Fairweather Range and approximately east-west north of the Resurrection Peninsula.

A further consequence of the apparently similar discordances of these two paleomagnetic poles from the North American craton reference is that if the La Perouse and Astrolabe magma chambers were deformed as they were intruded and began to crystallize (Loney and Himmelberg, 1983), the geometry of this deformation could not have been the result of regional subhorizontal compression associated with the final stages of accretion of the Chugach terrane, even though, as shown by Rossman (1963), by Brew and others (1978a), and by Loney and Himmelberg (1983), deformational structures within this part of the Chugach terrane are subparallel to its present major tectonic boundaries. This difficulty is removed, however, if the large estimated tilt correction of 37° is invoked. In this case the paleomagnetic discordance of the gabbro bodies implies only significant deformation of the inboard part of the Chugach terrane after 29 Ma, deformation which presumably was localized within the Tarr Inlet suture zone.

While the final outline and structure of the La Perouse gabbro are approximately parallel to the regional structural trend of its country rock, there is no necessity to invoke deformation of the magma chamber that it represents. As has been conclusively demonstrated for the Skaergaard intrusion of east Greenland (McBirney and Noyes, 1979), the orientation of mineral layering in the Astrolabe and La Perouse gab-

bros was evidently controlled mainly by thermal gradients normal to the contact with wall rock during crystallization and only subordinately by the direction of gravity.

REFERENCES CITED

Beck, M.E., Jr., 1980, Paleomagnetic record of plate-margin tectonic process along the western edge of North America: Journal of Geophysical Research, v. 85, p. 7115-7131.

Bogue, S.W., Gromme, Sherman, and Hillhouse, J.W., 1995, Paleomagnetism, magnetic anisotropy, and mid-Cretaceous paleolatitude of the Duke Island (Alaska) ultramafic complex: Tectonics, v. 14, no. 5, p. 1133-1152.

Bol, A.J., Coe, R.S., Gromme, C.S., and Hillhouse, J.W., 1992, Paleomagnetism of the Resurrection Peninsula, Alaska: implications for the tectonics of southern Alaska and the Kula-Farallon Ridge: Journal of Geophysical Research, v. 97, no. B12, p. 17,213-17,232.

Bradley, D.C., Haeussler, P.J., and Kusky, T.M., 1993, Timing of early Tertiary ridge subduction in southern Alaska, *in* Dusel-Bacon, C., and Till, A.B., ed., Geologic studies in Alaska by the U.S. Geological Survey, 1992: U.S. Geological Survey Bulletin 2068, p. 163-177.

Brew, D.A., Johnson, B.R., Grybeck, Donald, Griscom, Andrew, Barnes, D.F., Kimball, A.L., Still, J.C., and Rataj, J.L., 1978a, Mineral resources of the Glacier Bay National Monument Wilderness Study Area, Alaska: U.S. Geological Survey Open-File Report 78-494, chapter B, p. B1-B196.

Brew, D.A., Johnson, B.R., Ford, A.B., and Morrell, R.P., 1978b, Intrusive rocks in the Fairweather Range, Glacier Bay National Monument, Alaska, *in* Johnson, K.M., ed., The United States Geological Survey in Alaska: Accomplishments during 1977: U.S. Geological Survey Circular 772-B, p. B88-B90.

Brew, D.A. and Morell, R.P., 1978, Tarr Inlet suture zone, Glacier Bay National Monument, Alaska, *in* Johnson, K.M., ed., The United States Geological Survey in Alaska: Accomplishments during 1977: U.S. Geological Survey Circular 772-B, p. B90-B92.

———1979, The Wrangell terrane ("Wrangellia") in southeastern Alaska: the Tarr Inlet suture zone with its northern and southern extensions, *in* Johnson, K.M., and Williams, J.R.,ed., The United States Geological Survey in Alaska: Accomplishments during 1978: U.S. Geological Survey Circular 804-B, p. B121-B123

Czamanske, G.K., Himmelberg, G.R., and Goff, F.E., 1976, Zoned Cr, Fe-spinel from the La Perouse layered gabbro, Fairweather Range, Alaska: Earth and Planetary Science Letters, v. 33, p. 111-118.

Day, Ron, Fuller, M.D., and Schmidt, V.A., 1977, Hysteresis properties of titanomagnetites: Grain-size and compositional dependence: Physics of the Earth and Planetary Interiors, v. 13, p. 260-267.

Decker, J.E., and Plafker, George, 1982, Correlation of rocks in the Tarr Inlet suture zone with the Kelp Bay Group, *in* Coonrad, W.L., ed., The United States Geological Survey in Alaska: Accomplishments during 1980: U.S. Geological Survey Circular 844, p. 119-123.

Demarest, H.H., Jr., 1983, Error analysis for the determination of tectonic rotation from paleomagnetic data: Journal of Geophysical Research, v. 88, p. 4321-4328.

Diehl, J.F., Beck, M.E., Jr., Beske-Diehl, S., Jacobson, D., and Hearn, B.C., Jr., 1983, Paleomagnetism of the late Cretaceous–early Tertiary north-central Montana alkalic province: Journal of Geophysical Research, v. 88, p. 10,593-10,609.

Fisher, R.A., 1953, Dispersion on a sphere: Proceedings of the Royal Society of London, ser. A, v. 217, p. 295-305.

Gromme, Sherman, and Hillhouse, J.W., 1981, Paleomagnetic evidence for northward movement of the Chugach terrane, southern and southeastern Alaska, *in* Albert, N.R.D. and Hudson, Travis, eds., The United States Geological Survey in Alaska: Accomplishments during 1979: U.S. Geological Survey Circular 823-B, p. B70-B72.

Gunderson, J.A., and Sheriff, S.D., 1991, A new late Cretaceous paleomagnetic pole from the Adel Mountains, west central Montana: Journal of Geophysical Research, v. 96, no. B1, p. 317-326.

Hillhouse, J.W., 1977, A method for the removal of rotational remanent magnetization acquired during alternating field demagnetization: Geophysical Journal of the Royal Astronomical Society, v. 50, p. 29-34.

Himmelberg, G.R., and Loney, R.A., 1981, Petrology of the ultramafic and gabbroic rocks of the Brady Glacier nickel-copper deposit, Fairweather Range, southeastern Alaska: U.S. Geological Survey Professional Paper 1195, 26 p.

Himmelberg, G.R., Loney, R.A., and Nabelek, P.I., 1987, Petrogenesis of gabbronorite at Yakobi and northwest Chichagof Islands, Alaska: Geological Society of America Bulletin, v. 98, p. 265-279.

Hudson, Travis, Plafker, George, and Lanphere, M.A., 1977, Intrusive rocks of the Yakutat-St. Elias area, south-central Alaska: Journal of Research of the U.S. Geological Survey, v. 5, p. 155-172.

Hudson, Travis, and Plafker, George, 1981, Emplacement age of the Crillon-La Perouse pluton, Fairweather Range, *in* Albert, N.R.D. and Hudson, Travis, eds., The United States Geological Survey in Alaska: Accomplishments during 1979: U.S. Geological Survey Circular 823-B, p. B90-B94.

Jelinek, Vit, 1978, Statistical processing of anisotropy of magnetic susceptibility measured on groups of specimens: Studia Geophysica et Geodaetica, v. 22, p. 50-62.

Karl, S.M., Decker, J.E., and Johnson, B.R., 1982, Discrimination of Wrangellia and the Chugach terrane in the Kelp Bay Group on Chichagof and Baranof Islands, southeastern Alaska, *in* Coonrad, W.L., ed., The United States Geological Survey in Alaska: Accomplishments during 1980: U.S. Geological Survey Circular 844, p. 124-128.

Lienert, B.R., 1991, Monte Carlo simulation of errors in the anisotropy of magnetic susceptibility: a second-rank tensor: Journal of Geophysical Research, v. 96, no. B12, p. 19,539-19,544.

Loney, R.A., and Himmelberg, G.R., 1983, Structure and petrology of the La Perouse gabbro intrusion, Fairweather Range, southeastern Alaska: Journal of Petrology, v. 24, p. 377-423.

Loney, R.A., Brew, D.A., Muffler, L.J.P., and Pomeroy, J.S., 1975, Reconnaissance geology of Chichagof, Baranof, and Kruzof Islands, southeastern Alaska: U.S. Geological Survey Pro-

fessional Paper 792, 105 p., 4 plates, scale 1:250,000.

MacKevett, E.M., Jr., Brew, D.A., Hawley, C.C., Huff, L.C., and Smith, J.G., 1971, Mineral resources of Glacier Bay National Monument, Alaska: U.S. Geological Survey Professional Paper 632, 90 p., 12 maps.

McBirney, A.R., and Noyes, R.M., 1979, Crystallization and layering of the Skaergaard intrusion: Journal of Petrology, v. 20, p. 487-554.

Plafker, George, Jones, D.L., and Pessagno, E.A., Jr., 1977, A Cretaceous accretionary flysch and melange terrane along the Gulf of Alaska margin, *in* Blean, K.M., ed., The United States Geological Survey in Alaska: Accomplishments during 1976: U.S. Geological Survey Circular 751-B, p. B41-B43.

Plafker, George, and Campbell, R.B., 1979, The Border Ranges fault in the Saint Elias Mountains, *in* Johnson, K.M., and Williams, J.R., eds., The United States Geological Survey in Alaska: Accomplishments during 1978: U.S. Geological Survey Circular 804-B, p. B102-B104.

Plafker, George, and MacKevett, E.M., Jr., 1960, Mafic and ultramafic rocks from a layered pluton at Mount Fairweather, Alaska, *in* Short papers in the geological sciences, Geological Survey research 1960: U.S. Geological Survey Professional Paper 400B, p. B21-B26.

Rossman, D.L., 1963, Geology and petrology of two stocks of layered gabbro in the Fairweather Range, Alaska: U.S. Geological Survey Bulletin 1121-F, p. F1-F50.

Schwartz, E.J., 1975, Magnetic properties of pyrrhotite and their use in applied geology and geophysics: Geological Survey of Canada Paper 74-59, 24 p.

Schwartz, E.J., and Vaughn, D.J., 1972, Magnetic phase relations of pyrrhotite: Journal of Geomagnetism and Geoelectricity, v. 24, p. 441-458.

Tarling, D.H., and Hrouda, Frantisek, 1993, The Magnetic anisotropy of rocks: London, Chapman and Hall, 217 p.

van Fossen, M.C., and Kent, D.V., 1992, Paleomagnetism of 122 Ma plutons in New England and the mid-Cretaceous paleomagnetic field in North America: true polar wander or large-scale differential mantle motion?: Journal of Geophysical Research, v. 97, p. 19,651-19,661.

Watson, G.S., and Irving, Edward, 1957, Statistical methods in rock magnetism: Monthly Notices of the Royal Astronomical Society (London) Geophysical Supplement, v. 7, no. 6, p.289 300.

Winkler, H.G.F., 1967, Petrogenesis of metamorphic rocks: New York, Springer-Verlag, 237 p.

Reviewers: Peter J. Haeussler, Edward A. Mankinen, and Mark R. Hudson.

Petrology, Geochemistry, Age, and Significance of two Foliated Intrusions in the Fairbanks District, Alaska

By Rainer J. Newberry, Thomas K. Bundtzen, James K. Mortensen, *and* Florence R. Weber

ABSTRACT

Two foliated intrusions—the Pedro Creek ortho-gneiss and the O'Connor Creek alkali syenite—were examined in detail during recent remapping of the Fairbanks mining district. The older of the two bodies is a metaluminous granodiorite orthogneiss with a U-Pb age of 351±2 Ma. The presence of this body suggests that the amphibolite-facies metamorphic rocks that crop out in the Fairbanks mining district are equivalent to the Lake George subterrane, a subdivision of the Yukon-Tanana terrane. The younger body is a niobium-enriched, nepheline-bearing alkali syenite that displays magmatic foliation and gives a U-Pb age of 110±1 Ma. The age and composition of the younger intrusion supports the existence of an extensional event in the Yukon-Tanana region, which culminated at about 110 Ma, as previously hypothesized from structural fabrics and 110- to 120-Ma K-Ar and $^{40}Ar/^{39}Ar$ ages in high-grade metamorphic rocks. The 90-Ma metaluminous to slightly peraluminous calc-alkalic igneous rocks of the Fairbanks district are not related to the 110- to 120-Ma extensional event.

INTRODUCTION

With almost continuous mining since 1902, the Fairbanks district (fig. 1) has accounted for 8.3 million ounces (259 tonnes) of gold, or 26 percent of Alaska's historical gold output (Bundtzen and others, 1996). Because the district has thick loess and vegetation cover, little bedrock is exposed. The lack of rock exposures has hindered geologic studies in the past; significant lode gold resources have been found only in the past decade. Given the lack of geologic data, many conflicting proposals have been made concerning the ages and nature of the rock types present in the Fairbanks district (for example, Churkin and others, 1982; Forbes, 1982; Forbes and Weber, 1982; Aleinikoff and Nokleberg, 1989; Robinson and others, 1990; Pavlis et al, 1993). In the course of geologic mapping studies in the district in conjunction with detailed airborne geophysical surveys (Alaska Division of Geological and Geophysical Surveys, 1995), we identified several foliated intrusive bodies. To better understand the nature and significance of these bodies, we determined the mineralogy, U-Pb (zircon) ages, major- and trace-element compositions, and the compositions of biotites from the intrusions.

OCCURRENCE AND PETROLOGY OF TWO FOLIATED IGNEOUS INTRUSIONS

At least five major plutons and dozens of dikes and plugs of tonalitic to granitic composition have been recognized the Fairbanks area (fig. 1). Dating by Rb-Sr, K-Ar, U-Pb and $^{40}Ar/^{39}Ar$ techniques have consistently indicated primary ages of 88 to 92 Ma that postdate regional metamorphism of Yukon-Tanana terrane (YTT) host rocks (Forbes and Weber, 1982; Blum, 1983; Allegro, 1987; Newberry and others, 1995, 1996; Mortensen, unpub. data). Many plutons exhibit evidence of partial thermal resetting at 50 to 60 Ma (Newberry and others, 1996; Douglas, 1996). As a consequence, most workers have assumed that all plutonic rocks in the Fairbanks area are unfoliated and mid-Cretaceous in age. Given the extremely large degree of cover in the district, however, there is considerable room for discovery of atypical plutonic suites, such as the foliated granodiorite in lower Pedro Creek and the foliated syenite at O'Connor Creek (fig. 2).

PEDRO CREEK ORTHOGNEISS

The Pedro Creek orthogneiss (fig. 2) is part of a discontinuous belt of foliated granodioritic to granitic orthogneiss that crops out in a northeast-trending, 30-km-long zone, extending from Pedro Creek to Bear Creek (Newberry and others, 1996). The Pedro Creek body is the largest and best exposed orthogneiss in the belt. It possesses a distinctive aeromagnetic anomaly, which indicates an elliptical shape with a long axis of about 3 km and a short axis of about 1 km. The body exhibits a metamorphic foliation; structural measurements from rare outcrops indicate that the foliation is parallel to the body's elongation and to foliation

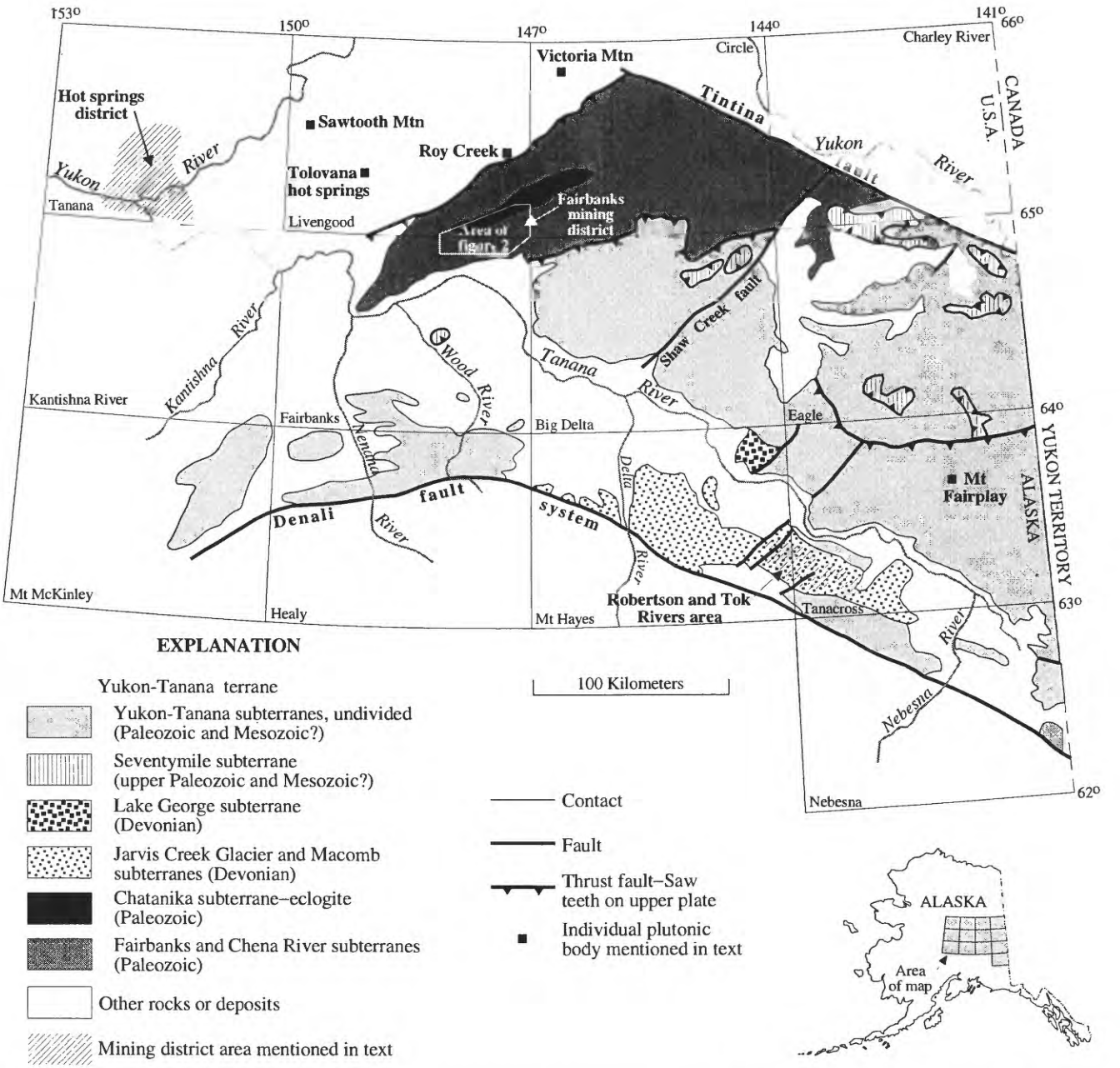

Figure 1. Map of eastern interior and east-central Alaska showing subterranes of Yukon-Tanana terrane, locations of selected Cretaceous plutons, and regional geographic features discussed in text; terrane nomenclature modified from Churkin and others (1982). Names given for U.S. Geological Survey 1:250,000 scale quadrangles.

Figure 2. Generalized geologic map of the Fairbanks district, eastern interior Alaska, showing foliated igneous intrusions described in text; simplified from Newberry and others (1996). ➤

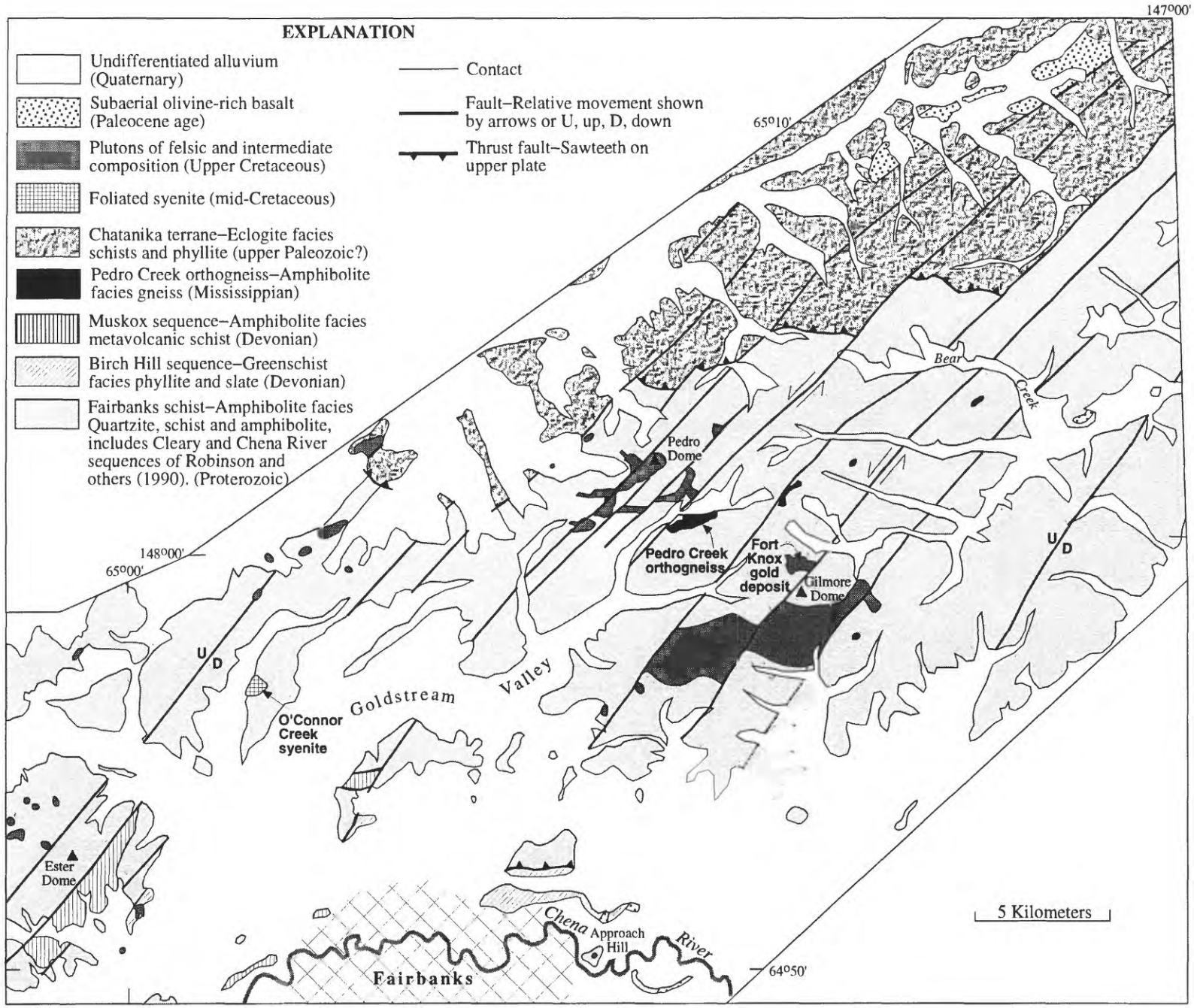
EXPLANATION
Undifferentiated alluvium (Quaternary)
Subaerial olivine-rich basalt (Paleocene age)
Plutons of felsic and intermediate composition (Upper Cretaceous)
Foliated syenite (mid-Cretaceous)
Chatanika terrane–Eclogite facies schists and phyllite (upper Paleozoic?)
Pedro Creek orthogneiss–Amphibolite facies gneiss (Mississippian)
Muskox sequence–Amphibolite facies metavolcanic schist (Devonian)
Birch Hill sequence–Greenschist facies phyllite and slate (Devonian)
Fairbanks schist–Amphibolite facies Quartzite, schist and amphibolite, includes Cleary and Chena River sequences of Robinson and others (1990). (Proterozoic)
Contact
Fault–Relative movement shown by arrows or U, up, D, down
Thrust fault–Sawteeth on upper plate
147°00'
65°10'
148°00'
65°00'
Bear Creek
Pedro Dome
Pedro Creek orthogneiss
Fort Knox gold deposit
Gilmore Dome
U
D
Goldstream Valley
O'Connor Creek syenite
Ester Dome
Chena Approach Hill
Chena River
Fairbanks
64°50'
5 Kilometers

in the surrounding amphibolite-facies metamorphic rocks. Thermobarometric and microprobe studies of metamorphic minerals (Joy and others, 1996) indicate that both the Fairbanks schist and the Pedro Creek orthogneiss sustained pressures of up to 4.8 kb and temperatures to 520°C. Although none of the contacts with the surrounding metamorphic rocks are exposed, the phaneritic texture, granitic mineralogy, and composition (table 1) support the inference that this body is an igneous intrusion. The original morphology of the body is unknown, but was probably more nearly circular in plan. Similar elongate, Mississippian granodioritic orthogneiss bodies intrude YTT units in the upper Chena River drainage 100 km northeast of the Fairbanks district (Smith and others, 1994).

The Pedro Creek intrusion consists of medium-grained quartz, plagioclase, K-feldspar, biotite, and minor hornblende and magnetite. Biotite is slightly chloritized, and plagioclase exhibits a dusting of sericite. No muscovite, garnet, or other diagnostic peraluminous-indicator minerals were noted in hand specimens or thin sections. Parallel alignment of K-feldspar megacrysts and biotite phenocrysts define a through-going planar fabric. Strained quartz crystals, broken feldspars, and bent biotite crystals seen in thin sections indicate that the foliation is a metamorphic feature superimposed on a plutonic fabric.

Chemical analysis of the metaplutonic rock (table 1) indicates that the rock is metaluminous to mildly peraluminous, assuming that postmagmatic alteration hasn't changed the alumina or alkali contents. Sericitic alteration is most developed in the sample having the highest normative corundum, however, suggesting some postmagmatic chemical changes. The normative and modal mineralogy indicates that the Pedro Creek orthogneiss was originally a granodiorite (Streckeisen and LeMaitre, 1979), which is consistent with hand-specimen observations that plagioclase feldspar is more abundant than potassium feldspar and megascopic quartz exceeds 15 percent. Trace-element analysis (table 1) indicates low concentrations of Nb, Y, Rb, Sn, Ta, and Ga, as is characteristic of I-type, volcanic arc-type granites (Pearce and others, 1984). Biotites (table 2) have compositions very similar to typical I-type granodioritic biotites (for example, those of the Sierra Nevada batholith); moderate concentrations of MgO, FeO, and TiO_2 reflect moderate degrees of fractionation of a typical metaluminous melt.

Although a small gold placer deposit occurs immediately downstream (west) of the Pedro Creek orthogneiss, there is no evidence for gold-related alteration or mineralization in the orthogneiss. Lode sources for the placer gold are probably the well-known mineralized zones in the upper Pedro Creek drainage (Chapman and Foster, 1969).

O'CONNOR CREEK ALKALI SYENITE

Chapman and Foster (1969) and Robinson and others (1990) mapped a small felsic intrusion just north of Goldstream Road about half-way between Ester Dome and Pedro Dome (fig. 2); however, both studies described the intrusion as a nonfoliated plutonic rock type, which is typical of the Fairbanks area. The significance of the O'Connor Creek intrusive body was first brought to our attention by Roger McPherson, a local prospector, who recognized both its lack of primary quartz and anomalous concentrations of Nb, Zr, U, and Th. The igneous intrusion body subcrops are seen as blocky rubble on the east side of O'Connor Creek valley; related (?) syenite dikes have been exposed on the ridge to the northeast by Roger McPherson's shallow trenching and drilling. An aeromagnetic high that correlates with exposures of the body suggests that it is sub-circular in plan with an approximately 1-km diameter. A weak foliation is commonly expressed by alignment of elongated K-feldspar and biotite grains, but the generally poor rock exposures made it impossible to determine the geometric relation between the weak foliation of the syenite and foliation in the surrounding metamorphic rocks.

Samples of the O'Connor Creek body are distinctly reddish-brown to black, fine- to medium-grained phaneritic syenite. Potassium-feldspar, albitic plagioclase, biotite, magnetite, and zircon are the dominant minerals. Electron microprobe analyses confirm the presence of zircon, nepheline, ilmenorutile [$(Ti,Nb,Fe,Ta)O_2$] and strontium-rich pyrochlore [$(Ca,Na)_2(Nb,Ta)_2O_6(O,OH,F)$]. The pyrochlore contains 1 to 5 percent K_2O and TiO_2 and 0.05 to 0.5 percent Sr, Cs, Nd, and Pb. The zircons are unusually rich in Nb. Except for rare apatite and monazite, no phosphate minerals were identified.

The outcrop and float of the O'Connor Creek body are generally homogeneous with respect to major mineralogy, although there are variations in grain size and degree of foliation. There are no indications of more mafic or of quartz-bearing igneous units either in the body or in the immediate vicinity. Lack of obvious metamorphic textures in thin section and the presence of variably foliated hand specimens suggest that the foliation is of igneous and not of metamorphic derivation.

Major-oxide analyses (table 1) indicate that the O'Connor Creek syenite can be classified as a nepheline-normative, alkali syenite that is enormously enriched in Nb, Y, Ga, Ta, Sn, REEs, Zr, and Na_2O but depleted in MgO, TiO_2, P_2O_5, and CaO. The depletion of compatible elements, combined with enrichment of incompatible elements and absence of modal or normative quartz, indicates high degree of fractional crystallization from a silica-poor, alkali-rich magmatic parent. Low K_2O/Na_2O, lack of normative corundum and quartz, and low Rb do not favor a crustal source for the melt (Collins and others, 1982). Concentrations of Nb and Y are sufficiently high for the rock to plot in the "within-plate granite" field of Pearce and others (1984). Given the unusual chemical composition, we believe that the O'Connor Creek body most likely represents a strongly fractionated, mantle-derived, alkalic melt.

Biotites from the O'Connor Creek body are enriched in FeO and especially MnO (table 2) and depleted in TiO_2 and MgO. In comparison to two biotites from the Sierra Nevada batholith, representative of typical I-type granodiorite (table 2) with atomic Fe:Mg of ~ 1.5:1, O'Connor Creek biotite has

Table 1. Chemical compositions of two foliated intrusions of the Fairbanks mining district, Alaska.

[Major oxides by Li metaborate fusion and ICP (Chemex Labs, Vancouver, B.C.), minor elements by wavelength dispersive X-ray fluorescence at the University of Alaska, Fairbanks, R.J. Newberry, analyst. Abbreviations: LOI, loss on ignition; QTZ, quartz; COR, corundum; OR, orthoclase; AB, albite; AN, anorthite; NE, nepheline; AC, acmite; DIOP, diopside; HYP, hypersthene; MT, magnetite; ILM, ilmenite; AP, apatite]

Site.....	Pedro Creek			O'Connor Creek	
Sample No.	RN118	RN179B	MC-1	BT300A	BT300B
			Major oxides (percentages)		
SiO_2.....	69.65	68.14	64.44	64.91	64.36
Al_2O_3.....	14.73	14.15	14.43	17.7	17.19
TiO_2.....	0.31	0.33	0.44	0.04	0.04
Fe_2O_3.....	2.88	3.32	5.19	2.43	2.81
MgO.....	0.94	0.97	1.33	0.06	0.04
CaO.....	2.39	2.16	5.55	0.05	0.17
Na_2O.....	3.19	3.00	2.45	8.18	9.15
K_2O.....	4.69	4.83	2.56	5.14	4.02
P_2O_5.....	0.13	0.14	0.08	0.02	0.02
MnO.....	0.05	0.03	0.09	0.15	0.15
LOI.....	1.05	1.44	1.16	0.52	0.75
Cr_2O_3.....	0.02	0.03	0.01	<0.01	0.01
TOTAL.....	100.00	98.5	97.7	99.2	98.7
			Minor elements (ppm)		
Y	32	36	20	30	33
Zr	149	164	110	850	1010
Ba	1050	1175	980	120	60
Nb	17	19	12	370	340
Rb	132	134	90	180	160
Sr	580	592	230	15	10
Ga	13	13	16	67	59
Sn	3	1	1	30	25
Ta	1	<1	<1	I8	22
La	45	48	43	92	105
Ce	65	70	61	195	225
Th	29	31	25	43	45
			CIPW norms (percentage)		
QTZ	27.3	26.4	25.3	0.0	0.0
COR	0.4	1.1	0.0	0.0	0.0
OR	28.0	29.3	15.4	30.8	24.2
AB	27.3	26.0	21.1	62.0	66.0
AN	11.1	10.1	21.2	0.0	0.0
NE	0.0	0.0	0.0	0.7	0.7
AC	0.0	0.0	0.0	4.1	5.3
DIOP	0.0	0.0	4.8	0.0	0.0
HYP	2.4	4.3	6.9	0.0	0.0
MT	2.6	2.0	4.4	0.0	0.0
ILM	0.6	0.6	0.9	0.0	0.0
AP	0.3	0.3	0.2	0.0	0.0

Table 2. Microprobe analyses of biotites from foliated intrusions, Fairbanks district and wet chemical analyses of biotites from the Sierra Nevada batholith, California.

[Alaska analyses performed using wavelength dispersive techniques, natural mineral standards, and a Chimeca SX-50 electron microprobe at the University of Alaska, Fairbanks, R.J. Newberry, analyst. Sierra Nevada analyses from Dodge and others (1969)]

Site.....	Pedro Creek				O'Connor Creek				Sierra Nevada batholith	
Rock type...	orthogneiss				syenite				granodiorite	
Sample No.	RN118	RN118	RN118	RN118	Occ-1	Occ-1	Occ-1	Occ-1	HL-4	FD-20
					Weight percent oxides					
Na_2O.....	0.20	0.06	0.07	0.11	0.10	0.06	0.15	0.13	0.04	0.44
MgO.....	8.02	9.09	8.82	9.06	1.49	1.61	0.82	0.98	10.9	6.78
Al_2O_3.....	14.95	14.81	15.01	14.45	15.09	13.87	19.94	17.79	15.4	18.59
SiO_2.....	36.31	36.77	36.94	35.36	37.47	36.83	39.38	37.81	36.9	34.72
K_2O.....	8.62	9.10	9.02	9.14	9.23	9.66	9.35	9.20	9.1	9.34
CaO.....	0.07	0.02	0.00	0.01	0.08	0.15	0.21	0.20	0.2	0.01
TiO_2.....	4.68	5.02	3.56	4.24	0.50	0.60	0.53	1.30	2.9	3.09
MnO.....	0.37	0.41	0.33	0.31	10.78	11.24	6.96	7.48	0.5	0.45
FeO.....	22.87	22.05	22.86	22.90	21.68	21.90	18.99	22.29	20.5	22.61
H_2O^*.....	3.68	3.67	3.62	3.66	3.46	3.40	3.82	3.84	3.1	3.38
F.....	0.33	0.51	0.46	0.27	0.30	0.36	0.29	0.00	0.18	0.36
Cl.....	0.22	0.18	0.24	0.20	0.00	0.00	0.00	0.02	0.56	NA
O=F,Cl.....	-0.19	-0.26	-0.25	-0.16	-0.13	-0.15	-0.12	-0.00	-0.28	-0.15
Total.....	100.12	101.42	100.70	99.56	100.06	99.53	100.31	101.0	100.00	99.62
					Cations per 22 oxygens					
Na.....	0.06	0.02	0.02	0.03	0.03	0.02	0.04	0.04	0.01	0.13
Mg.....	1.85	2.05	2.02	2.11	0.37	0.40	0.18	0.23	2.47	1.56
Al.....	2.72	2.64	2.72	2.66	2.87	2.35	3.74	3.27	2.76	3.39
Si.....	5.60	5.57	5.67	5.52	6.04	6.19	6.12	5.90	5.61	5.37
K.....	1.70	1.76	1.77	1.82	1.96	1.86	1.61	1.63	1.77	1.85
Ca.....	0.01	0.00	0.00	0.00	0.02	0.03	0.05	0.03	0.04	0.00
Ti.....	0.54	0.57	0.41	0.50	0.06	0.08	0.06	0.15	0.33	0.36
Mn.....	0.05	0.05	0.04	0.04	1.52	1.60	0.94	1.19	0.07	0.06
Fe.....	2.95	2.92	2.94	2.99	3.02	3.08	2.41	2.91	2.56	2.91

*H_2O calculated from stoichiometry

Fe:Mg of ~ 8:1. In addition, biotite from the Sierra Nevada batholith has Mn:Mg of ~ 1:25, compared to the O'Connor Creek biotite having Mn:Mg of ~ 4:1. The extremely high MnO contents are unusual in biotite and indicate extensive melt fractionation, almost certainly under conditions where ilmenite (a major Mn accumulator) did not crystallize.

Most surface samples of the alkali syenite are coated with Mn oxides, which are presumably derived from oxidation of the Mn-rich biotite (table 2). Uncommon quartz veins are probably of hydrothermal origin. Minor clay alteration is probably due to weathering of feldspar and nepheline. Trace analyses of weathered and altered syenite (table 3) indicate little change from unaltered syenite (table 2), even in mobile elements such as Rb, Ba, and Sr. Such compositional uniformity suggests that the rocks have experienced little hydrothermal alteration. Seven grab samples collected discontinuously across a 0.5-km-long transect of the alkali syenite intrusion average 350 ppm combined Nb and Ta, 1,000 ppm Zr, 52 ppm Th, and elevated U and Sn, which suggests that the O'Connor Creek intrusion might constitute a low-grade niobium-zirconium resource (table 3). However, the alkali syenite contains only slightly elevated values of As, Au, Mo, and Sb (table 3) relative to background values for these elements in plutonic rocks of the Fairbanks area (Newberry, 1996). We also analyzed a 0.5-m channel sample of quartz vein material in the O'Connor Creek alkali syenite; it shows low or undetectable As, Mo, Zn, Sb, and Au concentrations and no elevated Nb, Ta, Zr, U, or Th (table 3).

No gold placers are known downstream, but a small gold placer deposit is located about 1 km upstream of the O'Connor Creek body (Chapman and Foster, 1969), at the intersection of two major tributary streams. Given our limited assay data, we believe that the O'Connor Creek syenite did not contribute significantly to gold resources in the Fairbanks district.

Table 3. Trace element compositions (in ppm, except Au in ppb) from Alkali Syenite, O'Connor Creek intrusion, Fairbanks district, Alaska.

[All samples except BT60D (random chip sample) randomly collected at 100-m intervals in alkalic syenite rubble for a total transect of about 500 m. Ba, Nb, Rb, S, Sn, Sr, Y, and Zr by X-ray fluorescence (XRF); all others by Instrumental Neutron Activation Analysis (INAA). Uncertainty of elemental concentrations is approximately ±5 percent. Analyses performed by Nuclear Activation Services, Hamilton, Ontario, Canada]

Sample No.	BT405	BT404	BT60E	BT60A	BT60C	BT60D
Rock.....	Syenite	Syenite	Syenite	Syenite	Syenite	Qtz vein in syenite
Element			Parts per million			
As.....	200	150	49	35	16	9
Ba.....	280	260	180	200	290	60
Mo.....	2	<2	<2	27	2	<2
Nb.....	360	220	330	380	390	8
Rb.....	230	160	170	180	190	12
S.....	60	160	<10	140	60	<10
Sb.....	10	5	8	11	<1	8
Sn.....	22	12	18	20	13	4
Sr.....	74	92	66	76	64	12
Ta.....	18	4	14	23	22	3
Th.....	38	63	36	42	58	4
U.....	9	10	5	9	12	2
Y.....	49	33	50	55	62	<5
Zn.....	150	130	120	150	130	19
Zr.....	1,000	930	1,000	1,200	1,200	17
			Parts per billion			
Au.....	<5	25	15	<5	<5	<5

GEOCHRONOLOGY

Zircons and titanite were extracted from 5-kg samples of the Pedro Creek orthogneiss and the O'Connor Creek syenite by using heavy liquid (bromoform) and magnetic separations. The zircon and titanite were subsequently hand-picked, and all but one fraction were abraded. The separated minerals were dissolved; after adding a spike, U and Pb were extracted chemically, and isotopic compositions were determined in the Geochronology Laboratory at the University of British Columbia (table 4).

Four abraded and one unabraded zircon fractions and two abraded titanite fractions were analyzed from the Pedro Creek orthogneiss (table 4; fig. 3*A*). A regression through the four abraded zircon analyses gives calculated lower and upper intercept ages of 350.2+0.9/–1.5 Ma and 1.11±0.25 Ga. One of these fractions (B) is concordant with an age of 350.9+2.8/–1.2 Ma, based on both the $^{207}Pb/^{206}Pb$ and $^{206}Pb/^{238}U$ ages. We therefore assign a crystallization age of 351±2 Ma to the sample. The data array indicates the minor presence of an older inherited zircon component in most of the zircon fractions analyzed; this component has an average age of about 1.1 Ga. The unabraded zircon fraction (E) falls somewhat below the calculated regression line, reflecting both slight inheritance and post-crystallization Pb loss. The two fractions of titanite that were dated from the sample yield imprecise analyses with $^{206}Pb/^{238}U$ ages in the range of 347 to 360 Ma. These data indicate that the orthogneiss body was not exposed to metamorphic temperatures in excess of the blocking temperature of the U-Pb system in titanite (about 600°C) after emplacement.

Three fractions of abraded zircon were analyzed from the O'Connor Creek syenite (table 4, fig. 3*B*). The three analyses fall on or near concordia in the range of 108 to 111 Ma. Fraction A is concordant at 110.2±0.6 Ma. A weighted average of the $^{207}Pb/^{206}Pb$ ages of the three fractions is 110.3±1.1 Ma. There is no evidence for inheritance in any of the fractions; however, two fractions show evidence for very slight Pb loss, presumably caused by intrusion of nearby 90-Ma granitic dikes (Newberry and others, 1996). Lack of evidence for inheritance in the zircons confirms the geochemical evidence that this body is not contaminated by crustal materials and probably represents a highly fractionated mantle-derived melt.

SIGNIFICANCE TO YUKON-TANANA TERRANE GEOLOGY

Metamorphic rocks of the Fairbanks area have constituted an enigma with respect to the better studied rocks of the Yukon-Tanana terrane in east-central Alaska and the Yukon Territory, Canada. Churkin and others (1982) classified them as a separate subterrane, based on apparently lower metamorphic grades (for example, Forbes and Weber, 1982; Robinson and others, 1990) and lack of evidence for meta-

Table 4. U-Pb analytical data for zircons from two samples of foliated intrusions in the Fairbanks district, Alaska.

[N1, N2, non-magnetic at given degrees side slope on Frantz isodynamic magnetic separator; T, titanite; grain size given in microns; t, tabular grain; sp, stubby prism; ep, elongate prism; a, abraded. Pb (ppm) and percent radiogenic Pb corrected for blank, initial common Pb, and spike. $^{206}Pb/^{204}Pb$ (meas.) corrected for spike and fractionation. Pb/U ratios corrected for blank Pb and U and for common Pb; ratio errors (in parentheses) are 1 standard error of mean, in %; age errors are 2 standard errors, in Ma. Analyses performed at the University of British Columbia geochronology laboratory, J.K. Mortensen, analyst]

Sample: description	Wt (mg)	U (ppm)	Pb (ppm)	$^{206}Pb/^{204}Pb$ (meas.)	Total common Pb (pg)	Percent ^{208}Pb	$^{206}Pb/^{238}U$ (± % 1)	$^{207}Pb/^{235}U$ (± % 1)	$^{207}Pb/^{206}Pb$ (± % 1)	$^{206}Pb/^{238}U$ age, Ma (± 2 Ma)	$^{207}Pb/^{206}Pb$ age, Ma (± 2 Ma)
Pedro Creek orthogneiss, sample RN-95-118 (location: 65° 0.7′ N; 147° 27.5′ W)											
A: N2,+134,t,a.....	0.063	724	44.3	2,627	61	16.8	0.05602(0.07)	0.41412(0.11)	0.05361(0.08)	351.4(0.5)	354.7 (3.5)
B: N2,+134,t,a.....	0.041	680	41.6	4,891	20	17.9	0.05587(0.12)	0.41229(0.12)	0.05352(0.06)	350.5(0.8)	350.9 (2.8)
C: N2,+149,sp,a.....	0.135	681	41.8	3,210	101	16.9	0.05618(0.12)	0.41623(0.14)	0.05373(0.06)	342.4(0.8)	359.8 (2.7)
D: N2,+149,sp,a.....	0.113	655	40.6	5,294	49	17.2	0.05656(0.11)	0.42054(0.13)	0.05392(0.06)	354.7(0.7)	367.8 (2.6)
E: N2,74-105,ep.....	0.086	643	38.8	7,124	27	16.4	0.05556(0.08)	0.41249(0.09)	0.05385(0.03)	348.6(0.5)	364.6 (1.4)
AA: T,+149,a.....	0.655	137	11.3	126	2,950	37.2	0.05702(0.47)	0.42372(1.54)	0.05389(1.25)	357.5(3.3)	366.6(55.9)
BB: T,+149,a.....	0.565	130	9.6	131	2,280	31.2	0.05589(0.46)	0.41723(1.49)	0.05414(1.21)	350.6(3.1)	376.8(53.9)
O'Connor Creek syenite, sample 95-BT-300 (location: 64° 56.8′ N; 147° 52.7′ W)											
A: N1,+180,a.....	0.300	864	14.3	23,630	12	6.4	0.01724(0.28)	0.11461(0.28)	0.04823(0.07)	110.2(0.6)	110.4 (3.1)
B: N1,+180,a.....	0.338	811	13.1	63,35	46	5.3	0.01699(0.09)	0.11294(0.10)	0.04822(0.04)	108.6(0.2)	110.1 (1.8)
C: N1,+180,a.....	0.167	763	12.7	8,105	17	8.1	0.01692(0.08)	0.11245(0.09)	0.04823(0.04)	108.1(0.2)	110.4 (1.6)

igneous rocks. Pavlis and others (1993) subsequently divided the rocks of the Fairbanks area into an amphibolite-facies Chena River subterrane and a greenschist-facies Fairbanks subterrane. U-Pb dating of samples from the Fairbanks area by Aleinikoff and Nokleberg (1989) and Mortensen (1990) established a Late Devonian crystallization age for magmatic zircon from a metarhyolite assigned to the Muskox sequence by Newberry and others (1996) and Proterozoic ages for detrital zircons from several metaquartzite localities in the Fairbanks schist unit of Robinson and others (1990) previously (mis) identified as metarhyolite. These ages are compatible with U-Pb ages from

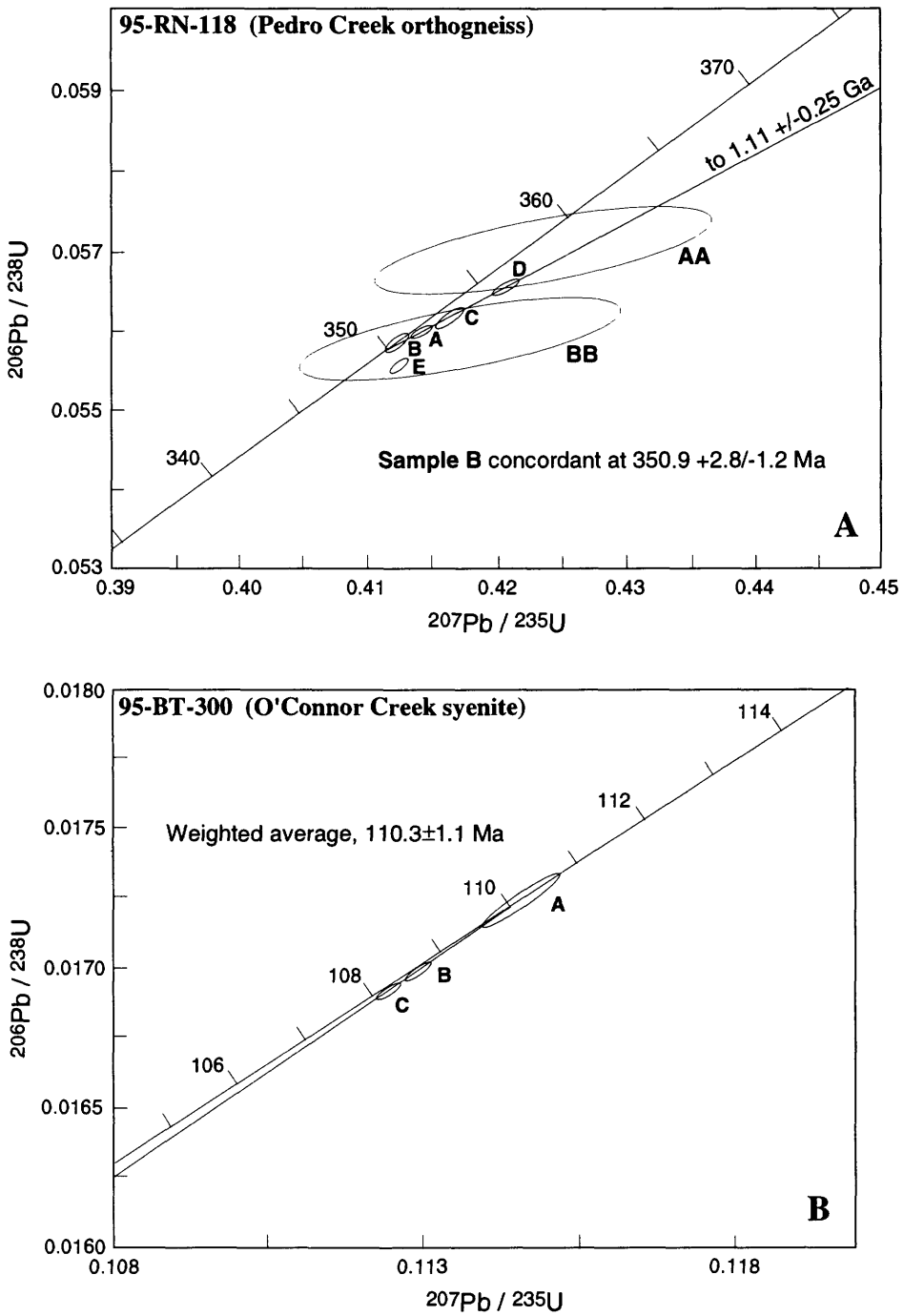

Figure 3. U-Pb concordia diagram for zircons and titanite from the Fairbanks district, Alaska. Bold letters designate samples (table 4). *A*, Pedro Creek orthogneiss, *B*, O'Connor Creek syenite.

metavolcanic and metasedimentary rocks of the Lake George subterrane of the Yukon-Tanana terrane (Aleinikoff and others, 1986; Dusel-Bacon and Aleinikoff, 1996).

Microprobe-based P-T determinations for garnet-bearing amphibolite and biotite schist found throughout the Fairbanks district (Joy and others, 1996; Newberry and others, 1996) indicate that both Chena River and Fairbanks subterranes of Pavlis and others (1993) experienced lower amphibolite-facies metamorphism with peak conditions of 480 to 550°C and 4 to 5 kb. Furthermore, amphibolites from the Chena River and Fairbanks subterranes have identical major- and minor-element compositions (Newberry and others, 1996) and exhibit similar ranges of plagioclase and hornblende compositions (Clautice and Newberry, 1996). On the basis of these considerations, the Fairbanks and Chena River subterranes closely resemble each other and the Lake George subterrane (Dusel-Bacon and others, 1993).

Documentation of orthogneiss (metagranodiorite) bodies in the Fairbanks area further establishes the correlation between most metamorphic rocks of the Fairbanks area and the Lake George subterrane, as Mississippian orthogneiss is diagnostic of the latter (Dusel-Bacon and Aleinikoff, 1985,1996). Identification of similar-appearing orthogneiss bodies in rocks previously mapped as both Fairbanks and Chena River subterranes in the Fairbanks area (Newberry and others, 1996) also ties these two subterranes together. Augen gneiss with a 340-Ma crystallization age was previously noted in southeastern Circle quadrangle (fig. 1) in contact with Chena River subterrane; however, Foster and others (1987) suggested that the augen gneiss was in thrust—and not intrusive—contact with the adjacent rocks. Field and map relations indicate that the Fairbanks orthogneiss bodies are intrusive into the surrounding rocks (Newberry and others, 1996). Consequently, the orthogneiss-bearing rocks northwest (Fairbanks and Circle quadrangles) and southeast (Tanacross, Mount Hayes, and Eagle quadrangles) of the sillimanite gneiss dome in the Big Delta quadrangle (Dusel-Bacon and others, 1993) are apparently correlative. Such a correlation suggests that a widespread, more-or-less continuous group of amphibolite-facies rocks, including the sillimanite gneiss dome group, existed prior to the mid-Cretaceous extension event that exposed the gneiss dome.

The O'Connor Creek syenite is an unusual igneous body. Only two ages of nepheline-normative plutons have been previously documented in the Yukon-Tanana area (fig. 1): (1) 90-Ma intrusions north and northwest of Fairbanks (for example, Roy Creek complex; Sawtooth pluton) and (2) 66- to 70-Ma intrusive bodies at Mount Fairplay east of Fairbanks, and at Tolovana hot springs and Victoria Mountain north of Fairbanks (Wilson and others, 1985; Burns and others, 1991; Weber and others, 1992). The O'Connor Creek body is unquestionably older than either of the above suites (fig. 3*B*) and is unquestionably alkalic (table 1). Furthermore, the O'Connor Creek body is compositionally distinct, with $Na_2O >> K_2O$ and Nb>Y, whereas rocks from the younger 90-Ma and 66- to 70-Ma suites have $K_2O > Na_2O$ and Y>Nb (Kerin, 1976; Burton, 1981; Foley, 1984; Light and Rinehart, 1988; Armbrustmacher, 1989; Burns and others, 1991; T.D. Light, written commun., 1996; Newberry, unpubl. data, 1996).

Because the Nb-rich O'Connor Creek alkali syenite represents a very strongly fractionated mantle-derived melt, somewhere in the Fairbanks district there must be an associated mafic alkalic plutonic rock. Either such rock is located in the subsurface or is buried under the extensive loess, alluvium, and vegetation of the area. Highly-fractionated, Nb-rich, Na>K alkalic rocks such as the O'Connor Creek alkali syenite are also commonly associated with carbonatites (Heinrich, 1966). If such were present in the Fairbanks district, the combined effects of extensive chemical weathering and surficial cover would make them difficult to identify. Nb-rich carbonatites have, however, recently been recognized in the Hot Springs mining district of eastern interior Alaska (Warner and others, 1986; fig. 1). Although undated, the carbonatite dikes postdate the tectonic emplacement of the Late Jurassic and Early Cretaceous Manley basin sedimentary rocks, indicating a post-Early Cretaceous age. The carbonatites and associated rocks of the Tofty district are also characterized by high Nb and Zr and low Y (Warner and others, 1986), a chemical signature similar to that of the O'Connor Creek alkali syenite (table 1).

The closest dated analogue to the O'Connor Creek syenite in the Yukon-Tanana terrane is represented by a series of lamprophyre and alkalic dikes in the upper Tok and Robertson Rivers area of the north-central Alaska Range (Foley, 1984), six of which were dated using K-Ar techniques. The alkalic intrusions in the eastern Alaska Range can be grouped into two different ages: (1) an older (92- to 108-Ma) suite of amphibole-rich lamprophyre, alkali gabbro, clinopyroxenite, and monzodiorite dikes; and (2) a younger (63- to 76-Ma) suite of biotite-rich lamprophyre dikes and related alkali gabbro to syenite and ultramafic stocks. On the basis of major-oxide data provided by (Foley, 1984), the older suite $Na_2O > K_2O$. Given the nearby presence of a 90-Ma granitic batholith (Burns and others, 1991), the K-Ar ages for the older dikes are compatible with magmatic ages of about 110 Ma, assuming some Ar losses in the latter suite.

There are few other documented examples of magmatic rocks with ages equivalent to the O'Connor Creek syenite in the YTT. A stock of peralkaline granite with a conventional K-Ar (biotite) age of 115±6 Ma was noted just south of the Chena River in the Fairbanks district by Forbes (1982). We were unable to relocate this rock during our recent field work but found instead a small body of tonalite yielding a $^{40}Ar/^{39}Ar$ (biotite) age of 92±1 Ma (Newberry and others, 1996). In the Big Delta quadrangle, about 150 km southeast of Fairbanks, an small unfoliated granite pluton having a U-Pb zircon age of 116±3 Ma intrudes sillimanite gneiss (Aleinikoff and others, 1984). Zircons from this pluton exhibit evidence for significant inheritance, while the granite

itself has Nb+Y content (University of Alaska-Fairbanks, unpub. major-oxide and trace-element XRF data, 1996) sufficiently high to be classified as "within-plate" (Pearce and others, 1984). If these examples are characteristic, then there may well be many more within-plate igneous bodies of this age in the YTT, (primarily?) expressed as small stocks and dikes.

The extensional geochemical character of these plutonic rocks with ages of approximately 110 to 115 Ma corresponds to most K-Ar and $^{40}Ar/^{39}Ar$ ages for metamorphic rocks of the YTT that have experienced the mid-Cretaceous extensional event (Hansen and others, 1991; Pavlis and others, 1993). Dusel-Bacon and Aleinikoff (1996) propose that extension began by 119 Ma (based on hornblende $^{40}Ar/^{39}Ar$ ages) and was essentially concluded by 109 Ma (based on mica $^{40}Ar/^{39}Ar$ ages). Given that, the logical explanation for the peculiar magmatic compositions of these 110- to 116-Ma rocks is that they represent magmatism associated with the extensional event. In contrast, the younger postextensional magmatism that characterizes much of the YTT has ages of 108 to 88 Ma (Wilson and others, 1985) and trace- and major-element compositions characteristic of a volcanic-arc setting (Bacon and others, 1990; Newberry and others, 1990; Burns and others, 1991; Newberry, 1996). In the Fairbanks district, the clear difference in magmatic compositions—as well as ages—between the O'Connor Creek syenite and the 90-Ma, metaluminous to weakly peraluminous granite-granodiorite-tonalite plutons (Newberry and others, 1996) indicates that the two have completely different origins. In the southern Eagle and northern Tanacross quadrangles (fig. 1), however, where plutons having volcanic-arc trace-element characteristics have K-Ar and $^{40}Ar/^{39}Ar$ biotite ages as old as 108 Ma (Wilson and others, 1985; C. Dusel-Bacon, written commun., 1996), subduction-related magmatism quickly followed or even overlapped extension.

CONCLUSIONS

The two foliated intrusions of the Fairbanks district have distinctive ages and compositions not previously documented for igneous rocks in the western Yukon-Tanana terrane. Although neither intrusion appears to be related to gold deposits of the area, the O'Connor Creek alkali syenite represents a potential Nb-REE target. The character and age of this intrusion also supports models of an extensional tectonic event in interior Alaska at about 110 Ma. The age and nature of the Pedro Creek intrusion provides supporting evidence for equivalence between Fairbanks area metamorphic rocks and those of the Lake George subterrane 200 km to the east. Given the poor exposures in this district (<3% of the bedrock is exposed) and in interior Alaska in general, it is likely that additional geologic surprises, such as carbonatites, wait to be discovered.

Acknowledgments.—We greatly appreciate the information and feedback we have received from U.S. Geological Survey geologists who have worked in the Yukon-Tanana region, including Tom Light, Cynthia Dusel-Bacon, Robert Hammond, Charles Bacon, Ted Armbrustmacher, and Helen Foster. We thank prospector Roger McPherson for sharing his knowledge and data base from plutons in the Fairbanks area; Ken Severin and Bart Cannon for assistance with the microprobe analyses; and Ellen Harris for drafting. Tom Light provided unpublished chemical analyses of plutonic rocks, and Cynthia Dusel-Bacon provided rock samples for analysis and unpublished major-oxide analyses and $^{40}Ar/^{39}Ar$ dates.

REFERENCES CITED

Alaska Division of Geological and Geophysical Surveys, 1995, Aeromagnetic map of the Fairbanks mining district: Alaska Division of Geological and Geophysical Surveys Report of Investigations, 95-5, 2 plates, 1:63,360.

Aleinikoff, J.N., Dusel-Bacon, Cynthia, and Foster, H.L., 1984, U-Pb ages of zircon from sillimanite gneiss and implications for Paleozoic metamorphism, Big Delta quadrangle, east-central Alaska, *in* Coonrad, W.L., and Elliot, R.L, eds., The United States Geological Survey in Alaska: accomplishments during 1981: U.S. Geological Survey Circular 868, p. 45-48.

Aleinikoff, J.N., Dusel-Bacon, C., and Foster, H.L., 1986, Geochronology of augen gneiss and related rocks, Yukon-Tanana terrane, east-central Alaska: Geological Society of America Bulletin, v. 97, p. 626-637.

Aleinikoff, J.N. and Nokleberg, W.J., 1989, Age of deposition and provenance of the Cleary sequence of the Fairbanks schist unit, Yukon-Tanana terrane, east-central Alaska, *in* Dover, J.H., and Galloway, J.P., eds., Geologic studies in Alaska by the U.S. Geological Survey, 1988: U.S. Geological Survey Bulletin 1903, p. 75-83.

Allegro, G.L., 1987, The Gilmore Dome tungsten mineralization, Fairbanks mining district, Alaska: Fairbanks, University of Alaska M.S. thesis, 114 p.

Armbrustmacher, T.J., 1989, Minor-element content, including radioactive elements and rare-earth elements in rocks from the syenite complex at Roy Creek, Mount Prindle area, Alaska: U.S. Geological Survey Open-File Report 89-146, 11 p.

Bacon, C.R., Foster, H.L., and Smith, J.G., 1990, Rhyolitic calderas of the Yukon-Tanana terrane, east central Alaska: volcanic remnants of a mid-Cretaceous magmatic arc: Journal of Geophysical Research, v. 95, No. B13, p. 21,451-21,461.

Blum, J.D., 1983, Petrology, geochemistry, and isotope geochronology of the Gilmore Dome and Pedro Dome plutons, Fairbanks mining district, Alaska: Alaska Division of Geological and Geophysical Surveys Report of Investigation 83-2, 62 p.

Bundtzen, T.K., Swainbank, R.C., Clough, A.H., Henning, M.W., and Charlie, K.M., 1996, Alaska's mineral industry—1995: Alaska Division of Geological and Geophysical Surveys Special Report 50, 72 p.

Burns, L.E., Newberry, R.J., and Solie, D.N., 1991, Quartz normative plutonic rocks of interior Alaska and their favorability for association with gold: Alaska Division of Geological and Geophysical Surveys Report of Investigation 91-3, 58 p.

Burton, P.J., 1981, Radioactive mineral occurrences, Mt. Prindle

area, Yukon-Tanana uplands, Alaska: Fairbanks, University of Alaska M.S. thesis, 72 p.

Churkin, Michael, Jr., Foster, H.L., Chapman, R.M., and Weber, F.R., 1982, Terranes and suture zones in east-central Alaska: Journal of Geophysical Research, v. 87, no. B5, p. 3718-3730.

Clautice, K.H., and Newberry, R.J., 1996, Microprobe Analyses of minerals from Fairbanks area metamorphic rocks, February-April, 1996: Alaska Division of Geological and Geophysical Surveys Public-Data File 96-24, 22 p.

Chapman, R.M. and Foster, R.L., 1969, Lode mines and prospects in the Fairbanks district, Alaska: U.S. Geological Survey Professional Paper 625-D, 25p.

Collins, W.J., Beams, S.D., White, A.J.R., and Chappell, B.W., 1982, Nature and origin of A-type granites with particular reference to southeastern Australia: Contributions to Mineralogy and Petrology, v. 80, p. 189-200.

Dodge, F.C.W., Smith, V.C., and Mays, R.E., 1969, Biotites from granitic rocks of the central Sierra Nevada batholith: Journal of Petrology, v. 10, p. 250-271.

Douglas, T.A., 1996, Metamorphic histories of the Chatanika eclogite and Fairbanks schist within the Yukon-Tanana terrane, Alaska, as revealed by electron microprobe thermobarometry and 40Ar/39Ar single grain dating: Fairbanks, University of Alaska M.S. thesis, 240 p.

Dusel-Bacon, Cynthia, and Aleinikoff, J.N., 1985, Petrology and tectonic significance of augen gneiss from a belt of Mississippian granitoids in the Yukon-Tanana terrane, east-central Alaska: Geological Society of America Bulletin, v. 96, p. 411-425.

Dusel-Bacon, Cynthia, and Aleinikoff, J.N., 1996, U-Pb zircon and titanite ages for augen gneiss from the Divide Mountain area, eastern Yukon-Tanana upland, Alaska, and evidence for the composite nature of the Fiftymile batholith, *in* Moore, T.E., and Dumoulin, J.A., eds., Geologic studies in Alaska by the U.S. Geological Survey, 1994: U.S. Geological Survey Bulletin 2152, pp. 131-142.

Dusel-Bacon, Cynthia, Csejtey, Béla, Jr., Foster, H.L., Doyle, E.O., Nokleberg, W.J., and Plafker, George, 1993, Distribution, facies, ages, and proposed tectonic associations of regionally metamorphosed rocks in east- and south-central Alaska: U.S. Geological Survey Professional Paper 1497-C, 73 p., 2 pls., scale 1:1,000,000.

Dusel-Bacon, Cynthia, and Hansen, V.L., 1992, High-pressure amphibolite-facies metamorphism and deformation within the Yukon-Tanana and Taylor Mountain terranes, eastern Alaska, *in* Bradley, D.C., and Dusel-Bacon, Cynthia, eds., Geologic studies in Alaska by the U.S. Geological Survey, 1991: U.S. Geological Survey Bulletin 2041, p. 140-159.

Foley, J.Y., 1984, Petrology, geochemistry, and geochronology of alkaline dikes and associated plutons in the eastern Mount Hayes and western Tanacross quadrangles, Alaska: Fairbanks, University of Alaska M.S. thesis, 95 p.

Forbes, R.B., 1982, Bedrock geology and petrology of the Fairbanks district, Alaska: Alaska Division of Geological and Geophysical Surveys Open-File Report AOF 169, 69 p.

Forbes, R.B., and Weber, F.R., 1982, Bedrock geologic map of the Fairbanks mining district, Alaska: Alaska Division of Geological and Geophysical Surveys Open-File Report AOF 170, 2 sheets, 1:63,360.

Foster, H.L., Keith, T.E.C., and Menzie, W.D., 1987, Geology of east-central Alaska: U.S. Geological Survey Open-File Report 87-188, 59p.

Foster, H.L., Menzie, W.D., Cady, J.W., Simpson, S.L., Aleinikoff, J.N., Wilson, F.H., and Tripp, R.B., 1987, The Alaska mineral resource assessment program: Background information to accompany folio of geologic and mineral resource maps of the Circle quadrangle, Alaska: U.S. Geological Survey Circular 986, 22 p.

Hansen, V.L., Heizler, M.T., and Harrison, T.M., 1991, Mesozoic thermal evolution of the Yukon-Tanana composite terrane: new evidence from $^{40}Ar/^{39}Ar$ data: Tectonics, v. 10, p. 51-76.

Heinrich, E.W., 1966, The geology of carbonatites: Chicago, Rand McNally, 555 p.

Joy, Brian, Keskinen, M.J., and Newberry, R.J., 1996, Preliminary Thermobarometry and microprobe mineral compositions, Fairbanks area schists and amphibolites: Alaska Division of Geological and Geophysical Surveys Public-Data File 96-12, 14 p.

Kerin, L.J., 1976, The reconnaissance petrology of the Mt. Fairplay igneous complex: Fairbanks, University of Alaska M.S. thesis, 95 p.

Light, T.D., and Rinehart, C.D., 1988, Molybdenite in the Huron Creek pluton, western Livengood quadrangle, Alaska, *in* Dover, J.H., and Galloway, J.P., eds., Geologic studies in Alaska by the U.S. Geological Survey, 1988: U.S. Geological Survey Bulletin 1903, p. 54-61.

Mortensen, J.K., 1990, Significance of U-Pb ages for inherited and detrital zircons from Yukon-Tanana terrane, Yukon and Alaska [abs.]: Geological Association of Canada Abstracts with Programs, v. 15, p. 274.

Newberry, R.J., 1996, Major and trace element analyses of Cretaceous plutonic rocks in the Fairbanks mining district, Alaska: Alaska Division of Geological and Geophysical Surveys Public-Data File 96-19, 16 p.

Newberry, R.J., Bundtzen, T.K., Clautice, K.H., Combellick, R.A., Douglas, T.A., Laird, G.M., Liss, S.A., Pinney, D.S., Reifenstuhl, R.R., and Solie, D.N., 1996, Preliminary geologic map of the Fairbanks mining district, Alaska: Alaska Division of Geological and Geophysical Surveys Public-Data File 96-16, 2 sheets, 32 p.

Newberry, R.J., Burns, L.E., Swanson, S.E., and Smith, T.E., 1990, Comparative petrologic evolution of the Sn and W granites of the Fairbanks-Circle area, interior Alaska, *in* Stein, H.J., and Hannah, J.L., eds., Ore-bearing granite systems; petrogenesis and mineralizing processes: Geological Society of America Special Paper 246, p. 121-142.

Newberry, R.J., McCoy, D.T., and Brew, D.A., 1995b, Plutonic-hosted gold ores in Alaska: igneous vs. metamorphic origins, *in* Ishihara, Shunso, and Czamanske, G.K., eds., Mineral resources of the NW Pacific Rim: Resource Geology Japan Special Issue, no. 18, p. 57-100.

Pavlis, T.L., Sisson, V.B., Foster, H.L., Nokleberg, W.J., and Plafker, George, 1993, Mid-Cretaceous extensional tectonics of the Yukon-Tanana terrane, Trans-Alaskan Crustal Transect (TACT), east-central Alaska: Tectonics, v. 12, p. 103-122.

Pearce, J.A., Harris, N.B.W., and Tindle, A.G., 1984, Trace element discrimination diagrams for the tectonic interpretation of granitic rocks: Journal of Petrology, v. 25, p. 956-983.

Robinson, M.S., Smith, T.E., and Metz, P.A., 1990, Bedrock geology of the Fairbanks mining district, Alaska: Alaska Division

of Geological and Geophysical Surveys Professional Report 106, 2 sheets, scale 1:63,360.

Smith, T.E., Robinson, M.S., Weber, F.W., Waythomas, C.W., and Reifenstuhl, R.R., 1994, Geologic map of the upper Chena River area, eastern interior Alaska: Alaska Division of Geological and Geophysical Surveys Professional Report 115, 19 p, scale 1:63,360.

Streckeisen, A.L., and LeMaitre, R.W., 1979, A chemical approximation to the modal QAPF classification of the igneous rocks: Neues Jahrbuch für Mineralogie Abhandlungen, v. 136, p. 169-206.

Warner, J.D., Mardock, C.L., and Dahlin, D.C., 1986, A columbium-bearing regolith on upper Idaho Gulch, near Tofty, AK: U.S. Bureau of Mines Information Circular 9105, 22 p.

Weber, F.R., Wheeler, K.L., Rinehart, C.D., Chapman, R.M., and Blodgett, R.B., 1992, Geologic map of the Livengood quadrangle, Alaska: U.S. Geological Survey Open-File Report 92-562, 7 p., scale 1:250,000.

Wilson, F.H., Smith, J.G, and Shew, Nora, 1985, Review of radiometric data from the Yukon crystalline terrane, Alaska, and Yukon Territory: Canadian Journal of Earth Sciences, v. 22, p. 525-537.

Reviewers: Cynthia Dusel-Bacon and Tom Light

New $^{40}Ar/^{39}Ar$ Dates for Intrusions and Mineral Prospects in the Eastern Yukon-Tanana Terrane, Alaska—Regional Patterns and Significance

By Rainer J. Newberry, Paul W. Layer, Roger E. Burleigh, *and* Diana N. Solie

ABSTRACT

Twenty $^{40}Ar/^{39}Ar$ mineral dates, representing samples from 16 locations in the eastern Yukon-Tanana terrane (YTT) of east-central Alaska indicate that within this area (1) Late Triassic to Early Jurassic granitic magmatism is more extensive than currently recognized and (2) mid-Cretaceous calc-alkalic igneous activity is significantly older (96-106 Ma) than it is in the western part of the YTT (89-92 Ma). Dating of Mo-Cu prospects indicates that the area includes mid-Cretaceous, Late Cretaceous, and early Tertiary porphyry systems. Gold-rich mineralization is documented in four different settings: Early Jurassic (about 185 Ma) Cu-A-Bi-Te-rich shear zones and stockworks in Late Triassic and Early Jurassic granitic intrusions; carbonate-altered mafic and ultramafic rocks mineralized by mid-Cretaceous magmatic-related fluids; mid-Cretaceous (94-106 Ma) felsic-pluton-hosted stockworks and veins; and early Tertiary (about 55 Ma) epithermal-style Ag-Au-Hg occurrences in Cretaceous-Tertiary continental sedimentary rocks. The variety of lode gold deposit types is consistent with the occurrence of gold placer deposits associated with a variety of rock types and in a variety of geologic subterranes. Our data suggest that the Mount Harper lineament is a major high-angle dip-slip fault that separates age-equivalent porphyry Mo-Cu-(Au) and epithermal-style Au-Ag prospects to the east (shallower exposures) from pluton-hosted mesothermal vein and stockwork Au and greisen Sn-W deposits to the west (deeper exposures).

INTRODUCTION

Fewer than a dozen of the thousands of igneous rock or base- and precious-metal mineralized rock occurrences of the Eagle quadrangle and vicinity (fig. 1), east-central Alaska, have been dated by radiometric methods (Wilson and others, 1985). Consequently, most plutonic rocks and mineral deposits of this region are assigned approximate ages based on broad, and not necessarily well-founded, correlations with units of known age. Despite the paucity of data, geologic maps of this region commonly show age designations indicating a much higher degree of certainty about the ages than can be supported by the data. Furthermore, subterranes of YTT, as first broken out by Churkin and others (1982), are distinguished in large part on the basis of igneous and metamorphic ages as well as metamorphic facies. In particular, subterrane Y_4 (fig. 1) is currently delineated by sparse Late Triassic to Early Jurassic radiometric ages (Foster and others, 1994; Dusel-Bacon and Aleinikoff, 1996).

Similarly, there is considerable controversy, but few reliable radiometric ages, concerning the ages and nature of base- and precious-metal mineralization in east-central Alaska. For example, Nokleberg and others (1987) suggest that Au vein deposits in this region are due to regional metamorphism, despite lack of temporal evidence for such an interpretation. Yeend (1996) suggests that placer gold of the region is derived from low-grade dispersed metamorphic source rocks unique to subterrane Y_4, and further suggests that gold is concentrated through several cycles of sedimentation. Porphyry Cu-Mo occurrences in the northern Tanacross quadrangle have been described as the continuation of the Carmacks belt of the central Yukon (fig. 2; Nokleberg and others, 1995), but K-Ar dates for the Alaskan deposits are significantly younger (55-58 Ma) than the Late Cretaceous (about 70 Ma) Carmacks deposits (Sinclair, 1986; Nokleberg and others, 1995).

PREVIOUS WORK

Available dates for igneous rocks of east-central Alaska fall dominantly into two groups: Late Triassic to Early Jurassic, and mid-Cretaceous to early Tertiary (DNAG time scale; Palmer, 1983; Wilson and others, 1985). Late Triassic to Early Jurassic magmatism consists of intermediate- to felsic-composition, holocrystalline, slightly foliated plutonic rocks restricted to the southeastern Eagle quadrangle (Foster, 1992); for example, those present near Taylor Mountain (fig. 1).

A wide range in K-Ar biotite dates (about 180-202 Ma), combined with a U-Pb zircon age of 214±2 Ma for rocks from the Taylor Mountain body suggests that these rocks were intruded during the Late Triassic and subsequently metamorphosed in the Middle Jurassic (Dusel-Bacon and Aleinikoff, 1996).

Mid-Cretaceous to early Tertiary igneous rocks in east-central Alaska exhibit nondeformed fabrics and both volcanic and plutonic varieties (Foster, 1992). On the basis of trace-element data, Bacon and others (1990) suggested that the mid-Cretaceous rocks probably formed in a magmatic-arc environment, whereas the early Tertiary rocks were probably formed in an extensional magmatic environment. Within the Eagle and Tanacross quadrangles, mid-Cretaceous magmatism is dominantly expressed by coarse-grained, calc-alkalic batholithic intrusions and voluminous tuff sheets; Late Cretaceous and early Tertiary magmatism is apparently dominated by volcanic and dike rocks (Bacon and others, 1990; Burns and others, 1991; Bacon and Lanphere, 1996). The apparent absence of Late Cretaceous and early Tertiary plutons in the Eagle and Tanacross quadrangles contrasts with their common occurrence in the Circle (fig. 12), Big Delta, and Mount Hayes quadrangles to the west (Wilson and others, 1985; Burns and others, 1991).

Most of the known base- and precious-metal occurrences in east-central Alaska are spatially associated with igneous rocks (Nokleberg and others, 1987). The most significant mineral occurrences include porphyry Cu-Mo prospects, vein and disseminated gold, Cu-Au skarns, disseminated platinum group metals (PGM), and polymetallic veins (U.S. Bureau of Mines, 1995). With the exception of two porphyry Cu-Mo prospects and one PGM occurrence, none have been dated, and their origins are speculative. Foster and others (1994) and Yeend (1996) suggest that certain pluton-associ-

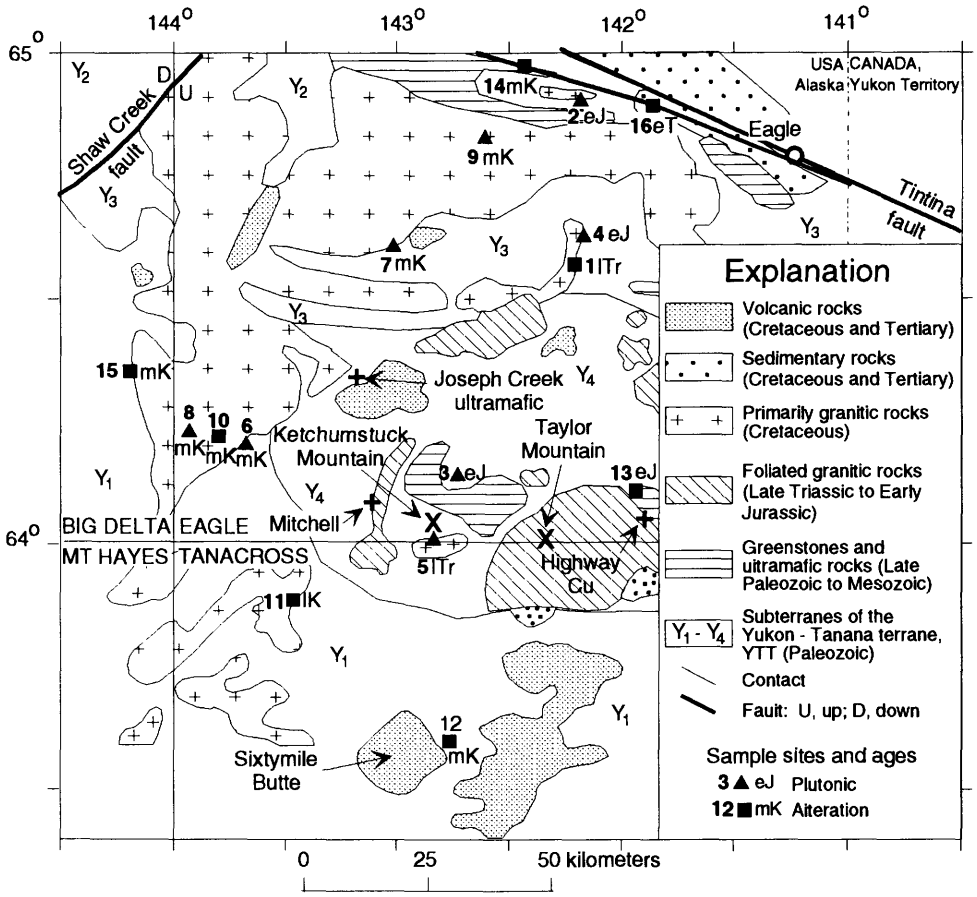

Figure 1. Generalized geologic map of Eagle quadrangle and vicinity, Alaska, showing locations of dated samples and some additional prospects. Numbers near symbols correspond to sample numbers in table 1; letters correspond to magmatic or alteration ages from table 1. Symbols: lTr, Late Triassic; eJ, Early Jurassic; JK, Jurassic or Cretaceous; mK, mid-Cretaceous, lK, Late Cretaceous; eT, early Tertiary; +, other prospect mentioned in text; YTT, Yukon-Tanana terrane. Relative fault movement: U, up; D, down. Geology modified from Foster and others (1994). Prospect locations from U.S. Bureau of Mines (1995). USGS 1:250,000 quadrangle names at 64° latitude.

ated deposit types and metals in this region are restricted to a particular subterrane, in part due to metal inheritance from the metamorphic wallrocks.

Tungsten occurrences in east-central Alaska include skarns, greisens, and porphyry prospects, all of unknown age. A notable tungsten-rich skarn is the Lucky 13 (fig. 1, No. 8), which has mineralogy, mineral compositions, and grades similar to the more abundant tungsten skarns in the Fairbanks area (Newberry and others, 1997). Greisen prospects are not common in the Eagle and Tanacross quadrangles; the most notable example is a small tungsten-bearing greisen vein in granite (fig. 1, No. 1). Several W (± Mo)-porphyry occurrences have been noted in the southwest Eagle quadrangle (U.S. Bureau of Mines, 1995), including the Section 21 prospect (fig. 1, No. 10), where rhyolite porphyry dikes contain a stockwork of quartz-wolframite veins with sericite alteration envelopes (U.S. Bureau of Mines, 1995).

Foster and Keith (1974) documented anomalous concentrations of PGM in several biotite-hornblendite and biotite-clinopyroxenite dikes in the Eagle quadrangle. One of these, in the Joseph Creek ultramafic body (fig. 1, west-central Eagle quadrangle) yielded a K-Ar (biotite) age of 185±3 Ma (Foster and others, 1976). Foley and others (1989) summarized an investigation of a biotite clinopyroxenite dike on Butte Creek (fig. 1, No. 4), where elevated concentrations of Au, Pt, and Pd are present. Assays indicate that Pt>Pd(Au>>Os, Ir, Ru, and Rh (Foley and others, 1989; U.S. Bureau of Mines, 1995).

Several porphyry Cu-Mo prospects in northern Tanacross quadrangle (fig. 2) form a belt that appears to con-

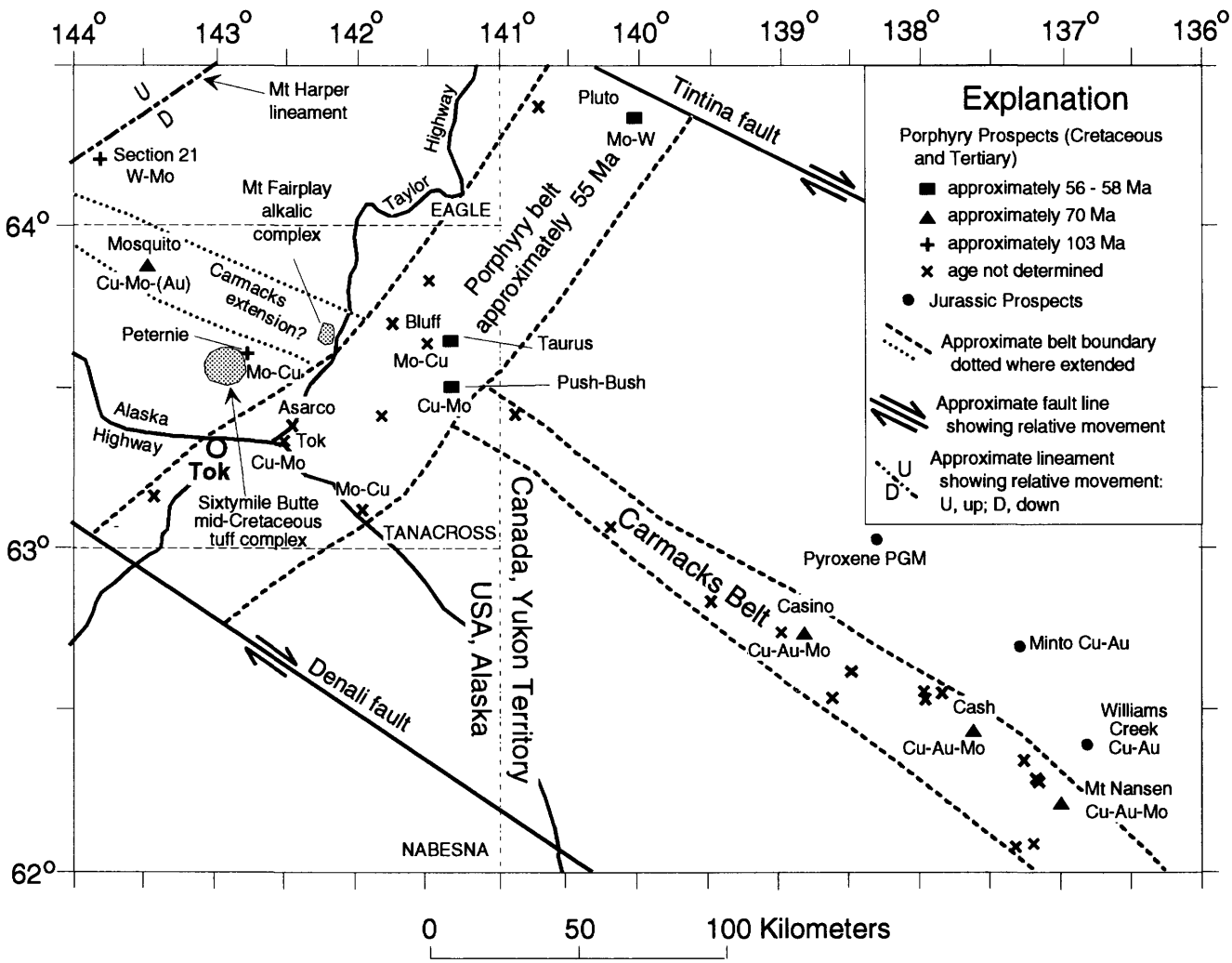

Figure 2. Map showing locations and ages of mid-Cretaceous to early Tertiary porphyry prospects and deposits of Yukon-Tanana terrane in east-central Alaska and western Yukon Territory and some Jurassic prospects in western Yukon Territory. All dates, except those from Peternie (No. 12), Section 21 (No. 10), and Mosquito (No. 11), are by conventional K-Ar techniques. Data from Hollister and others (1975), Singer and others (1976), Sinclair (1986), Indian and Northern Affairs Canada (1987, 1989), Foster (1992), and this study. Arrows on faults show relative fault movements. USGS 1:250,000 quadrangles shown.

tinue east into the central Yukon Territory, Canada (Nokleberg and others, 1995). K-Ar ages (secondary biotite) for the Taurus (Nokleberg and others, 1995) and Push-Bush prospects (Sinclair, 1986) of 57±2 and 56±2 Ma, respectively, generally similar Cu-Mo metallogeny, and association with granite-composition rocks may indicate that all the occurrences are of the same age and genesis (Hollister and others, 1975; Nokleberg and others, 1987; 1995). However, radiometric ages indicate serious complications in this interpretation. For example, a granite porphyry intrusion 3 km northeast of the Taurus prospect (fig. 2) has yielded K-Ar ages of 68±2 Ma (biotite) to 61±2 Ma (whole rock; Wilson and others, 1985), both significantly older than the Taurus deposit (Nokleberg and others, 1995). A felsic volcanic rock 3 km west of the nearby Bluff prospect (fig. 2; Wilson and others, 1985) yielded K-Ar ages of 97±3 Ma (biotite) and 70±2 Ma (whole rock) that indicate Late Cretaceous or early Tertiary reset of a mid-Cretaceous unit. In contrast, the porphyry deposits of the Carmacks belt in the central Yukon Territory (fig. 2) which may continue into Tanacross quadrangle, have consistent K-Ar ages of 71±2 Ma (Sinclair, 1986). The above dates indicate the presence of both mid-Cretaceous (about 90 to 100 Ma) and Late Cretaceous (about 70 Ma) porphyritic rocks and thermal resetting by Late Cretaceous and early Tertiary (about 56 Ma) magmatism. The Taurus porphyry Cu-Mo deposit is clearly of early Tertiary age, but, given the range in radiometric ages observed, the nearby (undated) Bluff prospect (fig. 2) could be mid-Cretaceous to early Tertiary. A rhyolite flow 2 km north of the Asarco prospect (fig. 2) exhibits within-plate (Pearce and others, 1984) major- and trace-element characteristics similar to those of prospects in other porphyry rhyolite bodies (Bacon and others, 1990; Burns and others, 1991; U.S. Bureau of Mines, 1995) and yielded a K-Ar age of 55±1.5 Ma. Because felsic igneous rocks in east-central Alaska that have within-plate trace-element characteristics are restricted to Late Cretaceous and early Tertiary ages (Newberry and others, 1995a) it is most likely that the Asarco and Tok porphyry Cu prospects (fig. 2) are in this age range. Other significant porphyry Cu-Mo occurrences of unknown age include the Peternie and Mosquito prospects (fig. 1, Nos. 11, 12).

Lode gold occurrences in east-central Alaska are of at least four different types, two of which exhibit a close spatial association with granitic rocks. The most abundant are gold-bearing quartz veins hosted by, or spatially associated with, granitic plutons of probable mid-Cretaceous age (Newberry and others, 1995b; McCoy and others, 1997) based on trace- and major-element similarities to dated interior Alaskan mid-Cretaceous plutonic rocks (Burns and others, 1991). A notable example is the Blue Lead mine in the southeastern Big Delta quadrangle (fig. 1, No. 15; Nokleberg and others, 1987). For this group of deposits, arsenopyrite, bismuthenite, and stibnite are commonly associated with ore, whereas copper concentrations are characteristically at or below crustal abundance, and molybdenum is only slightly anomalous (U.S. Bureau of Mines, 1995). Although referred to by some workers as porphyry Au deposits, few of these prospects are hosted by rocks with porphyry textures, and all show alteration and fluid-inclusion characteristics which differ dramatically from porphyry Cu-Mo deposits (McCoy and others, 1997). A second variety of lode gold deposits is present in, or adjacent to, foliated granitic rocks of presumably Late Triassic to Early Jurassic age, most notably the Purdy (fig. 1, No. 13) and Highway Copper prospects of Eagle quadrangle (Nokleberg and others, 1987; Burleigh and others, 1994). These deposits contain abundant chalcopyrite and anomalous Te and Bi concentrations (Burleigh and others, 1994; U.S. Bureau of Mines, 1995). The presence of local quartz+K-feldspar and quartz+secondary biotite veinlets, as well as high Cu concentrations, indicates similarities to porphyry Cu-Mo deposits. Some workers, however, have suggested a metamorphic origin for prospects of this group, perhaps due to reports of calcite in some of the veins (for example, Nokleberg and others, 1987).

Two other types of lode gold occurrences in the Eagle quadrangle exhibit little obvious relation to plutonic rocks. One type is represented by quartz veins in carbonate-altered, structurally emplaced mafic and ultramafic rocks, such as the Flume Creek prospect (fig. 1, No. 14) in the northern Eagle quadrangle (Clark and Foster, 1971). Gold prospects in this area are localized along a northwest-trending fault system south of and parallel to the Tintina fault. This group is similar to the listwaenite-hosted deposit type of Buisson and Leblanc (1986), thought to be related to late stages of ophiolite emplacement. A fourth type of gold deposit is represented by the Ptarmigan Hill occurrence, west of Eagle and just south of the Tintina fault (fig. 1, No. 16). Extensively silicified, Late Cretaceous, nonmarine, fluvial conglomeratic sedimentary rocks, which are locally cut by basalt and rhyolite dikes at Ptarmigan Hill, contain elevated concentrations of Au, Ag, and Hg (U.S. Bureau of Mines, 1995). The silicification, geochemistry, and dikes all suggest an epithermal mineralization style; that is, a near-surface, nonmarine, volcano-plutonic-related hydrothermal event.

PRESENT STUDY

As an outgrowth of our sampling and detailed prospect mapping in the Eagle and Tanacross quadrangles (U.S. Bureau of Mines, 1995) and to better understand the relations between plutonism and mineralization, we sampled several previously undated mineral occurrences for $^{40}Ar/^{39}Ar$ dating. We selected samples representing the major mineralization types, especially those in or near granitic rocks, and those for which we had sufficient geologic understanding to make $^{40}Ar/^{39}Ar$ dates meaningful. Our sampling focused on prospects containing alteration minerals datable by $^{40}Ar/^{39}Ar$ methods that were clearly related to significantly mineralized rocks (table 1, samples 1, 4, 8-16). Most of the deposits sampled

are in the Eagle quadrangle (fig. 1), but a few are in the adjacent Big Delta and Tanacross quadrangles. Samples were collected from the Y_1, Y_3, and Y_4 subterranes.

In the course of our detailed-scale mapping and sampling (U.S. Bureau of Mines, 1995), we observed slightly foliated granitic rocks in several places in the Eagle quadrangle in plutons previously mapped as Cretaceous(?) outside of the mapped limits of subterrane Y_4. The presence of foliation suggests a pre-Cretaceous age for the plutons (Foster, 1992), but the locations outside of Y_4 and previously assigned ages conflict with a pre-Cretaceous age. Because subterrane Y_4 was suggested as a source of placer gold in the southeastern Eagle quadrangle (Yeend, 1996), we wanted to determine if Late Triassic to Early Jurassic granitic bodies were present outside of subterrane Y_4, and the spatial distribution of any such older granitic bodies. Consequently, we also sampled several slightly foliated granitic bodies for $^{40}Ar/^{39}Ar$ dating (table 1, Nos. 1-5).

Finally, we noted leucocratic granites in a few locations, spatially associated with Tertiary volcanic rocks (fig. 1, No. 7) or with altered rhyolite dike swarms of possible Tertiary age (fig. 1, No. 6). Because early Tertiary leucocratic granites in interior Alaska are commonly associated with Sn-Ag greisens (Newberry and others, 1990), we selected several granites that were possibly Tertiary for dating.

Major- and minor-element compositional data for the plutonic rocks, rock descriptions, and trace-element data for the mineralized rocks are given in Alaska Division of Geological and Geophysical Surveys (1993), Burleigh and others (1994), and U.S. Bureau of Mines (1995). Geologic maps and descriptive material for the mineralized occurrences are given in U.S. Bureau of Mines (1995). Plutonic rock compositions are based on normative compositions, using the classification scheme of Streckeisen and LeMaitre (1979).

GEOCHRONOLOGIC TECHNIQUES

Twenty mineral separates for $^{40}Ar/^{39}Ar$ dating were concentrated to greater than 99% purity (visual inspection) using standard heavy liquid, magnetic separation, and paper friction techniques followed by hand-picking under a binocular microscope. Thin-section examination of the samples prior to crushing indicated that the chosen minerals were free from alteration and sufficiently coarse for mechanical separation. For all minerals, grains in the size range of 250 to 500 microns were used. For each sample, about 50 to 80 mg of biotite, potassium feldspar, or muscovite or 250 to 350 mg of hornblende was irradiated and subsequently analyzed. Six packages containing about 20 mg of the standard mineral MMhb-1 (Samson and Alexander, 1987) having an assumed age of 513.9 Ma (Lanphere and others, 1990) were also irradiated with our samples to determine the irradiation parameter (J) and the flux gradient in the reactor. Samples and standards were analyzed 45 to 90 days after irradiation.

The irradiated samples were step heated on-line in a Modifications Ltd. low-blank furnace. Temperature control is better than 1 degree, and a maximum temperature in excess of 1,600°C is achievable to ensure complete sample fusion. The extracted argon was purified in a two-stage process using a liquid-nitrogen cold finger and two SAES Zr-Al getters. The purified Ar gas was measured using a Nuclide 6-60-SGA 15-cm mass spectrometer. The sensitivity of the spectrometer is 6.5×10^{-15} mol/mV and system noise is generally around 0.02 mV. System blanks are generally better than 1×10^{-14} mol for ^{40}Ar. Argon isotopic measurements for both samples and standards were corrected for the system blanks, for decay of ^{37}Ar and ^{39}Ar, and for reactor-induced isotopic interferences. Ages were calculated using the equations and corrections from McDougall and Harrison (1988) and the constants from Steiger and Jaeger (1977). All errors on analyses are reported at the 1-sigma level. The age data for our 20 samples, including plateau and integrated ages and estimated Cl contents of the samples, are given in table 1. The Ar release data for each heating step are given in tables 2 and 3. Information concerning the interpretation of $^{40}Ar/^{39}Ar$ data is presented in the Appendix.

PLUTONIC ROCKS

LATE TRIASSIC TO EARLY JURASSIC MAGMATISM

A northeast-trending body of slightly foliated granite (fig. 1, No. 1), previously assigned a Cretaceous(?) age (Foster, 1992), is crosscut by a greisen vein containing muscovite with a late Triassic age of 214.4±0.6 Ma (tables1, 2; fig. 3). This age is similar to that of the granodioritic Taylor Mountain batholith, 50 km to the south (Dusel-Bacon and Aleinikoff, 1996) and probably represents an age close to that of magmatic crystallization. The Ar release spectra for this muscovite exhibits a slight reset at about 140 Ma (fig. 3), or late Jurassic time. This reset presumably indicates heating during a deformation event, although the presence of undeformed granitic dikes in the vicinity (U.S. Bureau of Mines, 1995) suggests this reset may be due in part to mid-Cretaceous magmatism.

Biotite and hornblende from a Cretaceous(?) quartz monzodiorite pluton (Foster, 1992) just south of the Tintina fault (fig. 1, No. 2), yield Early Jurassic plateau ages of 183.3±0.6 Ma and 183.6±0.6 Ma, respectively (tables 1, 2). The Ca/K ratios for the hornblende (fig. 4*B*), however, which indicate progressive changes in hornblende composition with heating, suggest that the lower temperature, lower Ca fractions represent fine-grained biotite inclusions in hornblende. Given this interpretation, the apparent age (table 2; fig. 4*A*) of the highest temperature fraction (about 198±10 Ma) is closer to the hornblende crystallization age, and the 183-Ma plateau represents the time at which the biotite closure temperature

Table 1. Data for $^{40}Ar/^{39}Ar$ dated samples from eastern interior Alaska

[Step-heat $^{40}Ar/^{39}Ar$ analyses were performed in the University of Alaska Geochronology Laboratory by P. Layer. See tables 2 and 3 for analytical details. Geologic units from Foster (1992): Pzp, Paleozoic peridotite; MzPzmu, Mesozoic and Paleozoic undifferentiated mafic rocks; JTrg, Jurassic and Triassic granite; TrKs, Triassic to Cretaceous sedimentary rocks; Kg, Cretaceous granite (?: unknown age); Kt?, Cretaceous(?) tuff. Deposit type: dssm= disseminated; additional details about prospects given in USBM (1996). All minerals are primary magmatic unless noted otherwise; musc, muscovite; Kspar, potassium feldspar; alt'n, alteration. Age period: lTr, Late Triassic; eJ, Early Jurassic; mK, middle Cretaceous; lK, Late Cretaceous. Reset ages are estimated from lowest temperature fractions of the $^{40}Ar/^{39}Ar$ spectra. Feldspars and most of the muscovites contained Ar isotope ratios indicating Cl/K < detection limit, hence no Cl is given. --, no data; ---do---, ditto]

No.	Name	Location		Geologic unit	Deposit type	Mineral dated	$^{40}Ar/^{39}Ar$ age (Ma)			Interpreted age of partial reset	Wt% Cl
		Latitude (N)	Longitude (W)				Plateau	Period	Integrated		
1	Happy granite---------	64° 31.1′	142° 15.2′	Kg?	W greisen----------	Vein musc----	214.4±0.6	lTr	211.0±0.6	Late Jurassic----------	--
2h	70-Mile pluton--------	64° 54.5′	142° 11.5′	Kg?	None----------	Hornblende---	183.3±0.6	eJ	183.6±0.6	Mid-Jurassic----------	0.09
2b	70-Mile pluton--------	---do---	---do---	Kg?	None----------	Biotite---------	183.6±0.6	eJ	180.2±0.6	Mid-Jurassic----------	0.05
3	Diamond Mtn.--------	64° 8.8′	142° 43.5′	Kg?	None----------	Hornblende---	197.3±0.7	eJ	196.4±0.7	Mid-Jurassic----------	0.1
4	Butte Creek hornblendite.	64° 38.4′	142° 11.0′	Pzp	Dssm PGM----------	Hornblende---	184.1±0.6	eJ	181.0±0.7	Early Cretaceous-----	0.25
5h	Ketchumstuck Mtn.--	64° 0.9′	142° 50.5′	MzPzmu	None----------	Hornblende---	205.6±1.0	lTr	203.9±0.8	Early Cretaceous-----	0.1
5b	Ketchumstuck Mtn.--	---do---	---do---	MzPzmu	None----------	Biotite---------	207.8±1.2	lTr	205.4±0.8	Mid-Cretaceous------	0.07
6	Ruby Creek granite---	64° 36.5′	143° 2.4′	Kg	None----------	Biotite---------	102.1±0.4	mK	100.8±0.4	Late K/early T-------	0.1
7	Mt. Harper granite----	64° 12.2′	143° 43.5′	Kg?	None----------	Biotite---------	105.8±0.4	mK	104.7±0.4	Early Tertiary--------	0.1
8	Lucky 13 prospect----	64° 14.0′	143° 54.1′	Kg?	W skarn----------	Biotite---------	94.2±0.3	mK	93.9±0.3	Late K/early T--------	0.1
9	Upper Granite Creek-	64° 50.1′	142° 37.6′	Kg	Plutonic Au----------	Biotite---------	93.3±0.5	mK	92.4±0.5	Tertiary----------	0.4
10	Section 21 prospect---	64° 12.5′	143° 47.9′	Kg?	Porphyry W-Mo-------	Vein musc----	102.7±0.4	mK	102.6±0.4	Late Cretaceous------	--
11	Mosquito prospect----	63° 53.1′	143° 27.9′	Kt?	Porphyry Cu-Mo-Au	Vein Kspar---	Saddle-----	lK	70.0±0.3	None----------	--
12	Peternie prospect------	63° 36.0′	142° 45.6′	Kg?	Porphyry Cu-Mo------	Vein Kspar---	102.8±0.5	mK	103.2±0.5	Late Cretaceous------	--
13	Purdy prospect--------	64° 7.0′	141° 56.8′	JTrg	Plutonic Au----------	Alt'n biotite--	185.9±0.8	eJ	183.7±0.8	Mid-Cretaceous------	0.03
14	Flume Creek prospect	64° 59.5′	142° 25.9′	Pzp	Mesothermal Au vein.	Alt'n musc---	100.3±3.3	mK	105.4±3.3	Mid-Cretaceous?-----	--
15	Blue Lead mine-------	64° 21.4′	144° 11.9′	Kg?	Plutonic Au----------	Alt'n musc---	105.6±0.5	mK	105.4±0.5	Late Cretaceous------	0.005
16a	Ptarmigan Hill--------	64° 54.1′	141° 51.1′	TrKs	Epithermal dssm Au-Ag.	Detrital musc	Saddle-----	lK	80.7±0.4	Early Tertiary--------	--
16b	Ptarmigan Hill--------	---do---	---do---	---do---	---do---	---do---	92.1±0.4	mK	91.9±0.4	Early Tertiary--------	--
16c	Ptarmigan Hill--------	---do---	---do---	---do---	---do---	---do---	90.3±0.4	mK	90.0±0.5	Early Tertiary--------	--

was reached. The lowest temperature fraction from this hornblende separate suggests a Middle Jurassic thermal event (fig. 4) and perhaps indicaties the time when this body became foliated.

Major progressive increases in the Ca/K ratios (fig. 4*E*) and slight increases in Cl/K ratios (fig. 4*F*) for the biotite separated from sample No. 2 suggest that it contains included hornblende. The most hornblende-rich, highest temperature, highest Ca/K fraction suggests a primary hornblende cooling age of nearly 190 Ma. This spectra also shows evidence for a 167 Ma (Middle Jurassic) thermal reset event (fig. 4*D*).

Hornblende from a Cretaceous(?) granodiorite in south-central Eagle quadrangle (table 1, fig. 1, No. 3) and a biotite- and PGM-bearing hornblendite dike in north-central Eagle quadrangle (table 1, fig. 1, No. 4) yield Early Jurassic plateau ages (197.3±0.7 and 184.1±0.6 Ma, respectively) and show evidence for a Middle Jurassic (about 170 Ma) to Early Cretaceous (about 130 Ma) reset event or multiple reset events (fig. 5*A, D*). As with the hornblende from sample No. 2, the low-temperature, low-Ca/K fractions (fig. 5*B, E*) most likely indicate inclusions of biotite in hornblende. Sample 3, however, appears to be almost entirely hornblende, whereas sample 4 contains significant biotite (fig. 5). The highest temperature fraction from sample 4 yields an age of 188±14 Ma (table 2; fig. 5*D*); as with sample 2, sample 4 may have a crystallization age closer to 190 Ma than to the integrated age of about 180 Ma.

Biotite and hornblende from the Mesozoic to Paleozoic granodiorite (Foster, 1992) at Ketchumstuck Mountain (tables 1, 2; fig. 1, No. 5) yield Late Triassic ages of 207.8±1.2 and 205.6±1.0 Ma, respectively, indistinguishable at analytical uncertainties. Their spectra also suggest inclusions of biotite in hornblende and hornblende in biotite, but the amounts of the included minerals are small (fig. 6*A-F*). Both minerals show evidence for a Cretaceous partial thermal reset: the lowest temperature biotite and hornblende fractions yield ages of 97±10.5 Ma and 117±31 Ma, respectively. These thermal resets are presumably caused by intrusion of a large mid-taceous(?) pluton 3 km northeast of the samples (fig. 1; Foster, 1992).

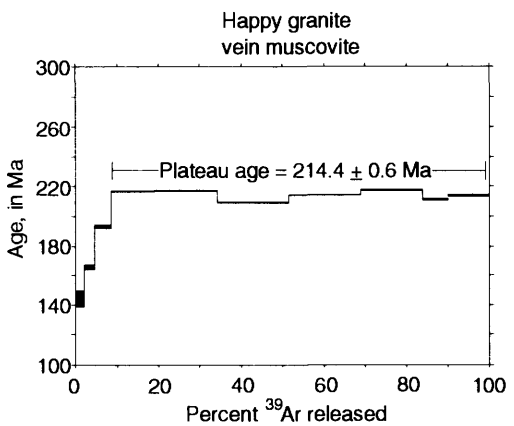

Figure 3. Ar release spectrum for greisen muscovite from Happy granite (sample 1). Error bars represent 1 sigma uncertainties.

In summary, the Ar release spectra (table 2; figs. 3-6) suggest that the five, slightly foliated igneous bodies represented by samples 1 through 5 crystallized at about 190 to 215 Ma, cooled to biotite-blocking temperatures at about 180 to 190 Ma, and experienced thermal events at about 150 to 170 Ma and about 100 Ma. The last heating event was caused by intrusion of mid-Cretaceous plutons; the earlier one presumably corresponds to a metamorphic (deformational) event, as plutons of that age are not known in east-central Alaska (Wilson and others, 1985; Newberry and others, 1995a). This structural event apparently predates the approximately 110- to 135- Ma extension event documented by K-Ar and sphene U-Pb ages for orthogneiss and gneiss domes in Tanacross and Big Delta quadrangles (Wilson and others, 1985; Pavlis and others, 1993; Dusel-Bacon and Aleinikoff, 1996).

The $^{40}Ar/^{39}Ar$ dates from these five igneous rocks clearly indicate that Late Triassic to Early Jurassic ages extend well beyond the current map limits of subterrane Y_4 (fig. 1), which suggests that either (1) Late Triassic to Early Jurassic pluton ages are not limited to subterrane Y_4, or (2) subterrane Y_4 is significantly more widespread than is currently mapped (fig. 1). In particular, the ages given by sample No. 2 imply that subterrane Y_4 extends as far north as the Tintina fault (fig. 1). Further work is clearly necessary to better define this subterrane, its boundaries, and the nature of its relationship to neighboring subterranes.

MID-CRETACEOUS MAGMATISM

All of the leucocratic, possibly Tertiary granites we dated in the study area have mid-Cretaceous $^{40}Ar/^{39}Ar$ ages (table 1, Nos. 6-9) of about 93 to 106 Ma. All the biotites give spectra with flat plateaus and minor Late Cretaceous to early Tertiary resets. Ca/K ratios indicate that traces of hornblende were present as inclusions in biotite, but these inclusions had no significant effect on the age spectra (fig. 7).

The ages of thermal resetting recorded in these plutonic biotites are difficult to quantify. The Ruby Creek sample exhibits an apparently Late Cretaceous reset, based on the lowest temperature step age of 77±2 Ma (fig. 7*A*, table 2). Comparison with the other spectra of fig. 7, however, suggests that the age of this relatively large first fraction is significantly older than the age of reset (McDougall and Harrison, 1988). The Mount Harper and Lucky 13 prospect samples (Nos. 7 and 8) are within a few kilometers of Tertiary(?) felsite dikes (Foster, 1976) and show resets which can be interpreted as early Tertiary. However, sample No. 14 also shows evidence for early Tertiary reset, despite the absence of any Tertiary igneous rocks within 10 kilometers (fig. 1; Foster, 1976). A similar phenomena is noted in the Fairbanks district, where virtually all metamorphic and igneous biotites show evidence

for an early Tertiary overprint (McCoy and others, 1997). Early Tertiary basalts crop out at the southeast and northeast edges of the Fairbanks district, but many of the samples with early Tertiary resets are located more than 30 kilometers from known Tertiary igneous rocks (Newberry and others, 1996). Apparently an early Tertiary thermal event in east-central Alaska is more widespread than the outcrop pattern of known Tertiary igneous rocks (Foster, 1992) would suggest.

MINERALIZED ROCKS

TUNGSTEN-RICH VEINS

Granite porphyry dikes contain quartz-wolframite-muscovite veins with and without molybdenite at the Section 21 prospect (tables 1, 2; fig. 1, No. 10). These veins are most likely related to either a porphyry Mo prospect (the upper

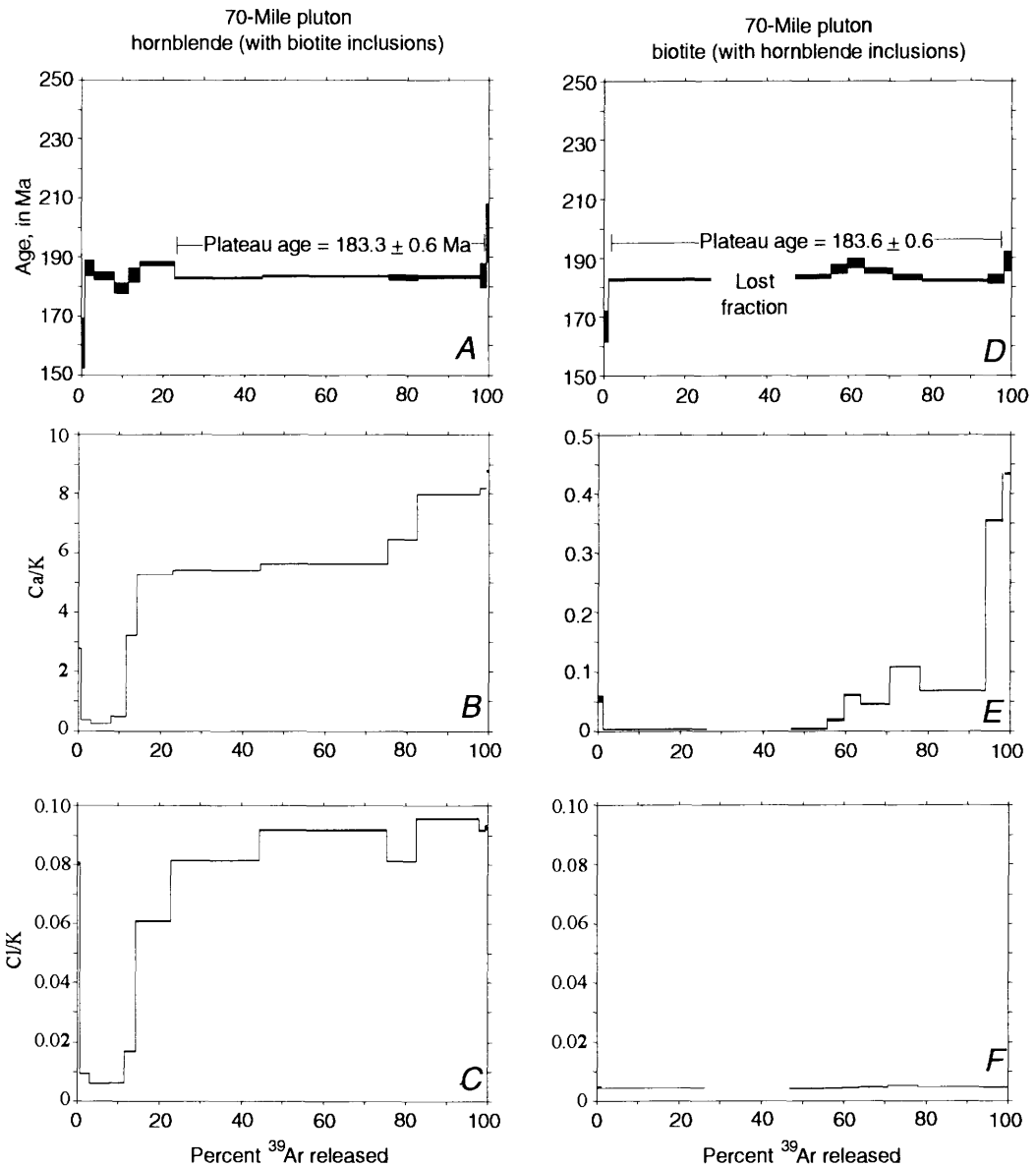

Figure 4. Ar release spectra for hornblende >> biotite (A-C) and biotite>> hornblende (D-F) from 70-mile quartz monzodiorite pluton (sample 2). Error bars represent 1 sigma uncertainties.

parts of which are commonly enriched in wolframite) or to a porphyry W-Mo prospect, such as the Logtung deposit, in northern British Columbia (Sinclair, 1986). Muscovite from a quartz-wolframite vein at the Section 21 prospect has both an integrated and a plateau age of 102.7±0.4 Ma (tables 1, 2; fig. 8). The Ar spectrum from this white mica shows a minor Late Cretaceous (86±15 Ma) reset. The Ca/K and Cl/K spectra, which are flat and nearly zero, indicate no contamination by other minerals.

PORPHYRY-TYPE PROSPECTS

Our dating of secondary potassium feldspar from the Mosquito and Peternie prospects (tables 1, 2; Nos. 11, 12) indicates ages of 70.0±0.3 and 102.8±0.5 Ma, respectively. Potassium feldspar from the Mosquito prospect shows no evidence for other thermal events (fig. 9*A, B*). Only the first and last Ar steps show significant deviation from about 70 Ma (excess Ar?), and both have slightly elevated Ca/K ratios

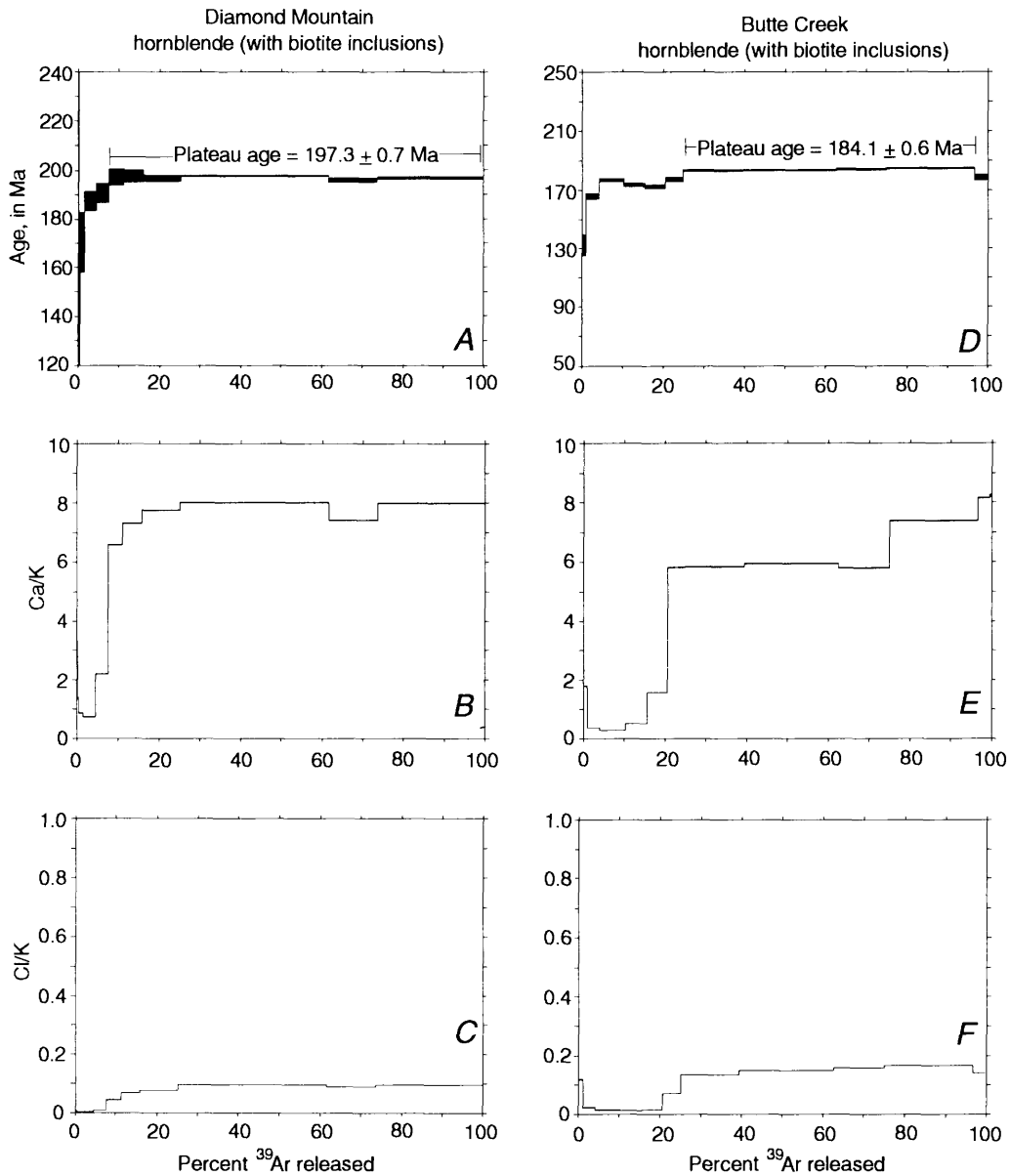

Figure 5. Ar release spectra for hornblende >> biotite from Diamond Mountain granodiorite (A-C; sample 3) and Butte Creek clinopyroxene biotite hornblendite (D-F; sample 4). Error bars represent 1 sigma uncertainties.

(fig. 9*B*)—most likely from minor plagioclase inclusions, as observed in thin section. Thus, the Mosquito prospect is the same age as the Au-rich Casino, Cash, and Mount Nansen porphyry deposits in the Carmacks belt of the central Yukon Territory (Sinclair, 1986) and is near the Alaskan extension of the Carmacks belt (fig. 2).

The $^{40}Ar/^{39}Ar$ spectrum of potassium feldspar from the Peternie prospect is slightly more complex than that from the Mosquito prospect. Peternie potassium feldspar also shows excess Ar in the high- and low-temperature fractions, which also correspond to high Ca/K ratios (fig. 9*C, D*) in the feldspar. However, the lowest temperature fraction seems to indicate a Late Cretaceous reset, which suggests the presence of unrecognized magmatism the age of that in the Carmacks belt (70 Ma).

GOLD-RICH PROSPECTS

We dated secondary biotite from the alteration envelope around an Au-Cu-Te-bearing quartz vein in granodiorite at the Purdy prospect (table 1, fig. 1, No. 13). This biotite yielded a complex spectrum having an integrated age of 186±1 Ma (fig. 10*A*). In thin section, the shreddy, secondary biotite

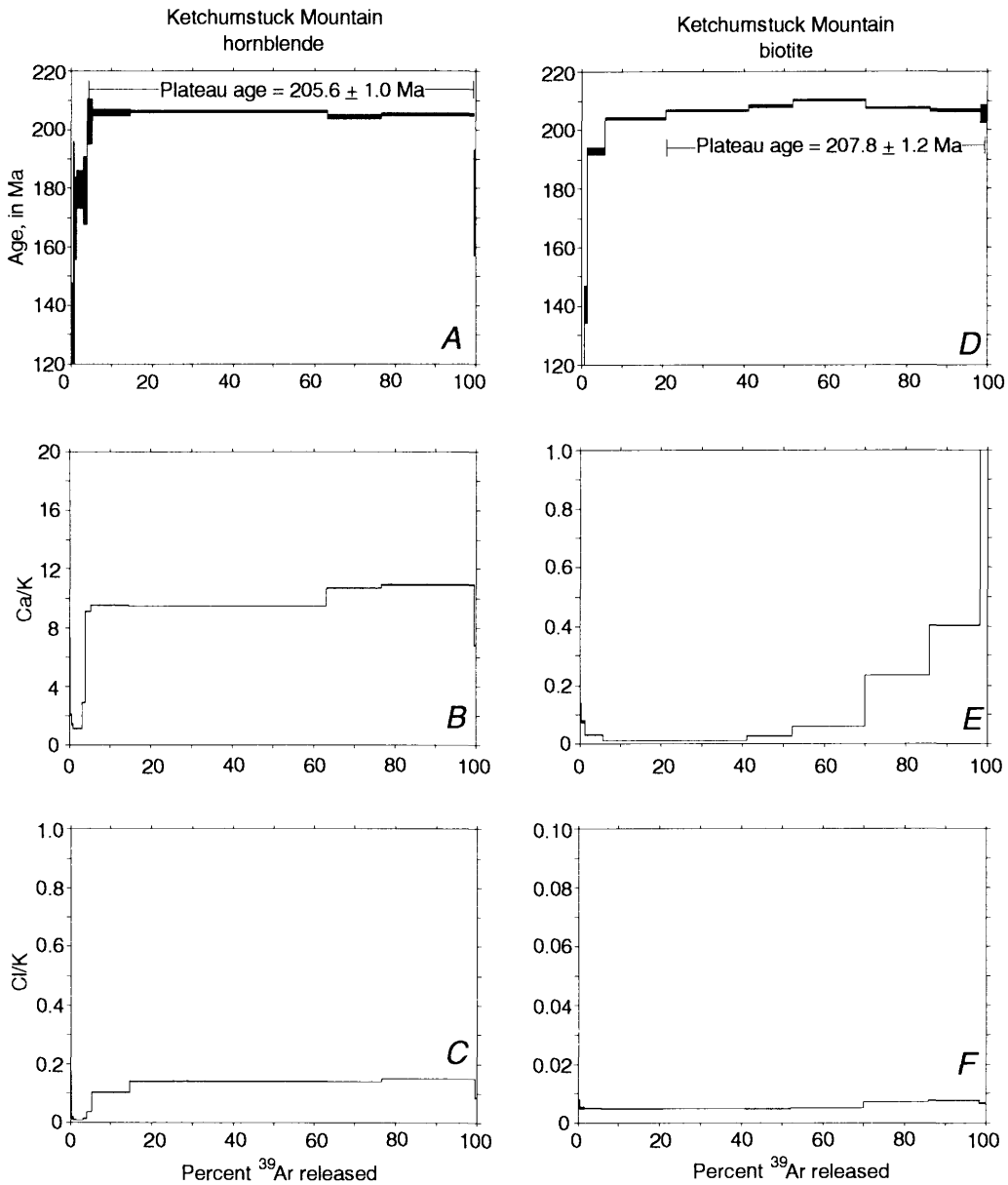

Figure 6. Ar release spectra for hornblende >> biotite (A-C) and biotite>> hornblende (D-F) from granodiorite of Ketchumstuck Mountain (sample 5). Error bars represent 1 sigma uncertainties.

in the vein envelope contains traces of magmatic(?) hornblende. The Ca/K spectrum (fig. 10*B*) indicates that this separate consists dominantly of biotite with minor hornblende. The biotite-rich part of the spectra indicates that ore-related alteration at Purdy is Early Jurassic, with an age similar to those of plutonic samples 2 and 4 (table 1). The lower temperature fractions indicate a slight mid-Cretaceous reset, possibly caused by Cretaceous or Tertiary granitic intrusions. The

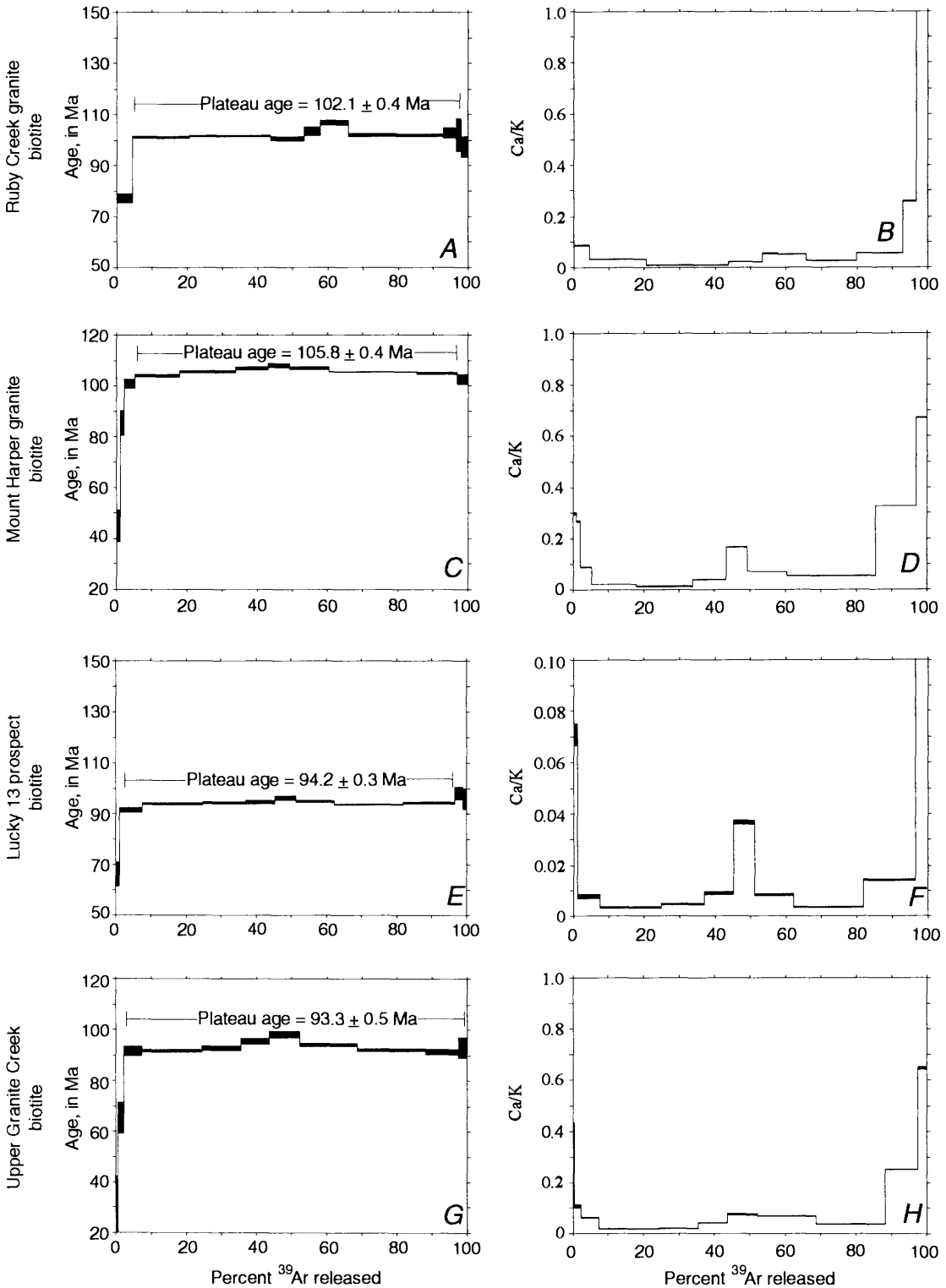

Figure 7. Ar release spectra from four mid-Cretaceous granitic biotites, Eagle quadrangle. A,B, Ruby Creek (sample 6). C,D, Mountt Harper (sample 7). E,F, Lucky 13 (sample 8). G,H, Upper Granite Creek (sample 9). Cl/K spectra for all four biotites are flat, having values of approximately 0.1. Error bars represent 1 sigma uncertainties.

age of the host granodiorite (fig. 1) is unclear from field relations. It may be a northern extension of the late Triassic Taylor Mountain batholith (fig. 1) as indicated by Foster (1992), in which case the Cu-Au mineralization would be related to a younger event. Alternatively, both the sheeted veins and the host granodiorite could be of Early Jurassic age. Because the highest temperature, most hornblende-rich fraction (fig. 10A) shows no evidence for a significantly older age, we favor the latter alternative and suggest that the alteration and mineralization is approximately contemporaneous with crystallization of the enclosing granodiorite.

The Flume Creek prospect, just south of the Tintina Fault (fig. 1, No. 14) is a gold prospect in silica-carbonate rock derived by hydrothermal alteration of gabbro and serpentinite (U.S. Bureau of Mines, 1995). Hydrothermal mica from silica-carbonate rock immediately adjacent to a quartz-arsenopyrite gold vein produced a complex spectrum (fig. 10*D*) with a plateau age of 100±3 Ma and an integrated age of 105±3 Ma (tables 1, 2). The Ca/K spectra (fig. 10*E*) suggest that minor included carbonate minerals released gas at low temperatures. Because carbonate minerals have a near-zero potassium content, Ar released from such contaminant minerals would affect only the uncertainties in the age spectrum and not the absolute age. The highest temperature fraction released Ar from both muscovite and an unknown mineral having elevated Ca/K and Cl/K ratios (figs. 10*E, F*). Comparison of these spectra with the $^{40}Ar/^{39}Ar$ spectra of hornblendes from the study area suggests that the contaminant mineral in this sample is most likely hornblende (of magmatic origin?), almost entirely replaced by secondary muscovite and carbonate minerals. Consequently, the age of the highest temperature fraction, 174±37 Ma, most likely represents a minimum age for included hornblende, which, in turn, represents a minimum age for crystallization or metamorphism of the parent mafic body. In contrast, the plateau age of about 100 Ma for the sample, taken from the alteration envelope around a gold-quartz vein, most likely indicates the time of alteration association with gold deposition.

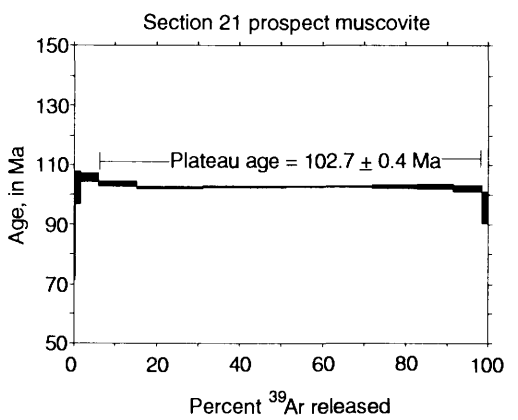

Figure 8. Ar release spectrum for secondary muscovite from Section 21 W-Mo porphyry prospect (sample 10). Error bars represent 1 sigma uncertainties.

Two mid-Cretaceous, pluton-hosted gold veins in the study area show age spectra that we interpret as pluton-related vein mineralization. At the Blue Lead mine (fig. 1, No. 15) the host granodiorite has a K-Ar date of 107±3 Ma (Wilson and others, 1985); the alteration muscovite has both integrated and plateau $^{40}Ar/^{39}Ar$ ages of 105.5±0.6 Ma (tables 1, 2, No. 15; fig. 11*A*). Lack of metamorphic textures in the host pluton and lack of evidence for metamorphism younger than 110 Ma in this region (Wilson and others, 1985) indicate that mineral deposit formation is unrelated to metamorphic-derived fluids. Because the gold vein and the host pluton are of analytically indistinguishable ages, it is most likely that the vein was formed by a pluton-related hydrothermal system. The Late Cretaceous reset (fig. 11*A*) presumably reflects the thermal effects of unmapped or subsurface Late Cretaceous or early Tertiary igneous rocks.

Biotite sample 9 from upper Granite Creek (table 1, fig. 1, fig. 7) was taken from granite adjacent to a gold-bearing, quartz-arsenopyrite vein, which showed the same elevated Te-Bi-Sb signature as the sample from the Blue Lead mine (U.S. Bureau of Mines, 1995) and presumably represents the same type of hydrothermal system. The mid-Cretaceous age of that biotite and the lack of evidence for significant reset (fig. 7*G*) suggests that this granite-hosted gold vein was also formed from a mid-Cretaceous granite-related hydrothermal system.

We dated three detrital muscovite grains from silicified, gold-bearing conglomeratic sandstone at the Ptarmigan Hill occurrence (fig. 1, No. 16); the resets indicate gold-related alteration is of early Tertiary age (tables 1, 2, No. 16; fig. 11*B*). The three detrital muscovites yielded plateau ages of about 81, 90, and 92 Ma, which record the ages of the original muscovite-bearing rocks that contibuted to the conglomerates (fig. 11*B*). Lack of a single plateau age indicates a multi-rock source for the immature conglomerate and a depositional age of less than 80 Ma (Late Cretaceous). All three muscovites show evidence for a low-temperature reset event (fig. 11*B*; table 3); the average age of the lowest temperature fractions for the three muscovites is 54 Ma.

REGIONAL PATTERNS OF MAGMATISM AND METAL DEPOSITION

TUNGSTEN-BEARING OCCURRENCES AND PROSPECTS

Tungsten vein occurrences in the study area were formed in both Late Triassic (table 1, No. 1) and mid-Cretaceous (table 1, No. 10) time. In addition, the Lucky 13 scheelite-bearing skarn (table 1, No. 8) is adjacent to the mid-Cretaceous granite (U.S. Bureau of Mines, 1995; Newberry and others, 1997) represented by sample 8. This garnet-pyroxene-scheelite skarn is not directly datable by $^{40}Ar/^{39}Ar$ techniques, but the localization of skarn to within 100 m of the

contact with a granite body suggests it formed at approximately the same time as the adjacent granite, about 94 Ma (tables 1, 2, No. 8). The likely age of about 90 Ma for this tungsten skarn is similar to the mid-Cretaceous ages determined for W skarns and adjacent intrusions in interior Alaska (Allegro, 1987; Newberry and others, 1990). Similarly, the mid-Cretaceous (103 Ma; table 1, 2) age for the wolframite-quartz veins at the Section 21 prospect (sample 10) is similar to mid-Cretaceous ages determined for porphyry Mo and W-Mo deposits in southern Yukon Territory and northern British Columbia (Sinclair, 1986). In contrast, the Late Triassic age (214 Ma; tables 1, 2) we determined for the tungsten-bearing greisen vein (sample 1) is a unique age for greisens in Alaska and northwestern Canada (Wilson and others, 1985; Sinclair, 1986). We are unaware of any greisen occurrences having ages between late Paleozoic and mid-Cretaceous in interior Alaska or the Yukon Territory, and we are uncertain of the significance of this age.

There are significant differences in the mineralogy, style (greisen versus porphyry versus skarn), ages (table 1), and the subterranes hosting the three dated tungsten occurrences (fig. 1). However, their common feature is an association with fractionated granitic bodies spatially and temporally associated with plutons of predominatly metaluminous granodiorite composition (Burns and others, 1991; U.S. Bureau of Mines, 1995; Newberry and others, 1997). These granitic rocks display the low Nb, Y, and Rb contents (U.S. Bureau of Mines, 1995; Newberry and others, 1997) characteristic of volcanic arc magmatism (Pearce and others, 1984).

On the basis of known occurrences in the Fairbanks and upper Chena areas (fig. 12), Foster and others (1994) suggested that tungsten skarns in east-central Alaska were restricted to subterrane Y_2, perhaps due to a tungsten source in the subterrane. The presence of the Lucky 13 tungsten skarn in the Y_1 subterrane (fig. 1, No. 8) indicates that tungsten skarns in interior Alaska are not restricted to a single subterrane. Given the large number of stream-sediment and heavy-mineral-concentrate tungsten geochemical anomalies in the Tanacross and Eagle quadrangles (Foster and Yount, 1972; Tripp and others, 1976) and the abundance of granitic rocks (fig. 1), it is likely that additional tungsten skarns are present in the area.

PLATINUM-RICH PROSPECTS

Foster and Keith (1974) concluded that the PGM-anomalous, biotite-hornblende clinopyroxenite bodies in the Eagle quadrangle were intrusions different in origin from the more numerous alpine-type ultramafic bodies in the same region.

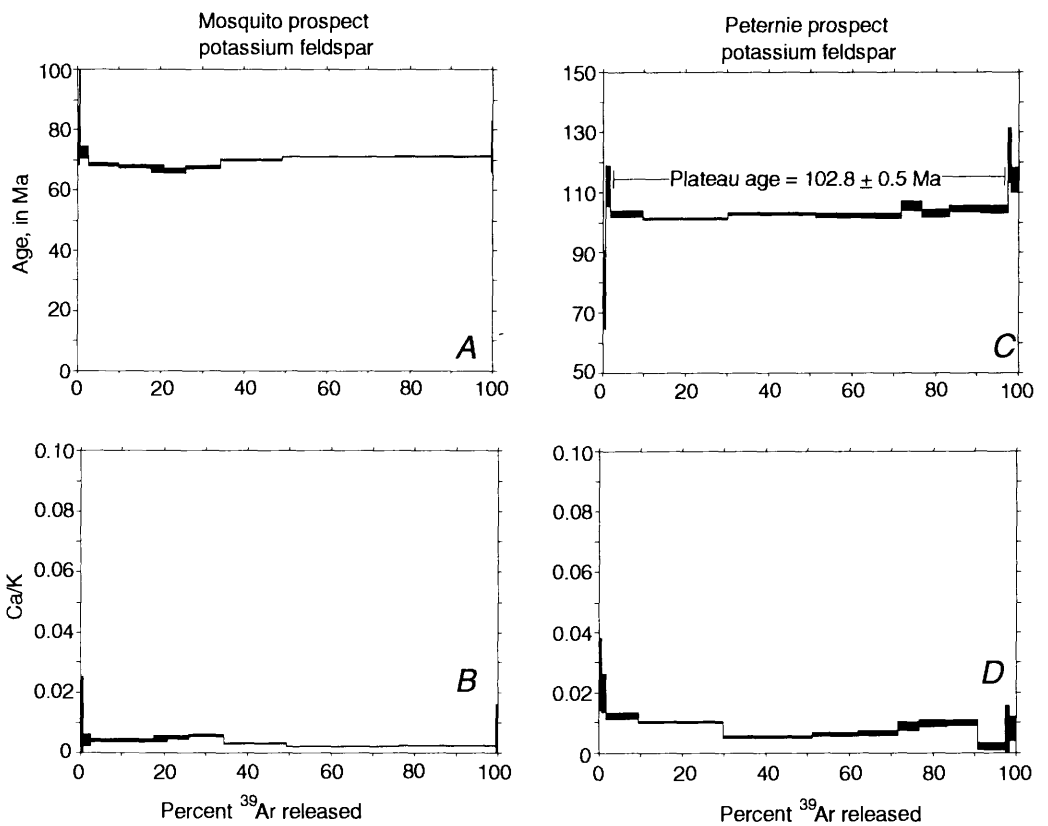

Figure 9. Ar release spectra for secondary K-feldspar from Mosquito (A,B; sample 11) and Peternie (C,D; sample 12) porphyry prospects. Error bars represent 1 sigma uncertainties.

Nokleberg and others (1987), however, interpreted the PGM-rich dikes as parts of an ophiolite complex, dated as Mississippian to Permian on the basis of ages of associated cherts (Foster, 1992). The Early Jurassic ages for the PGM-bearing Joseph Creek ultramafic rocks (K-Ar, hornblende; Foster and Keith, 1974) and Butte Creek hornblendite (fig. 1, No. 5; fig. 5; this study), however, are incompatible with the ophiolitic hypothesis. Furthermore, PGM mineralization associated with ophiolite complexes invariably contains Os, Ir > Pd > Pt >>Au (Page and others, 1986), a pattern not seen in the Joseph Creek or Butte Creek bodies (U.S. Bureau of Mines, 1995).

The alkalic nature of the Joseph Creek and Butte Creek dikes, together with their spatial association with Early Jurassic syenitic intrusions (U.S. Bureau of Mines, 1995) and their high PGM-Au abundances, suggests zoned (Alaska-type) ultramafic intrusions (Foley and others, 1989). If this is the case, these small alkalic bodies could be dikes above zoned intrusions. Several Late Triassic to Early Jurassic PGM-bearing zoned complexes associated with alkalic plutonic rocks are present in northern British Columbia; for example, Turnagain, Hickman, and Polaris (Clark, 1980). The Pyroxene prospect, in west-central Yukon (fig. 2), is another ex-

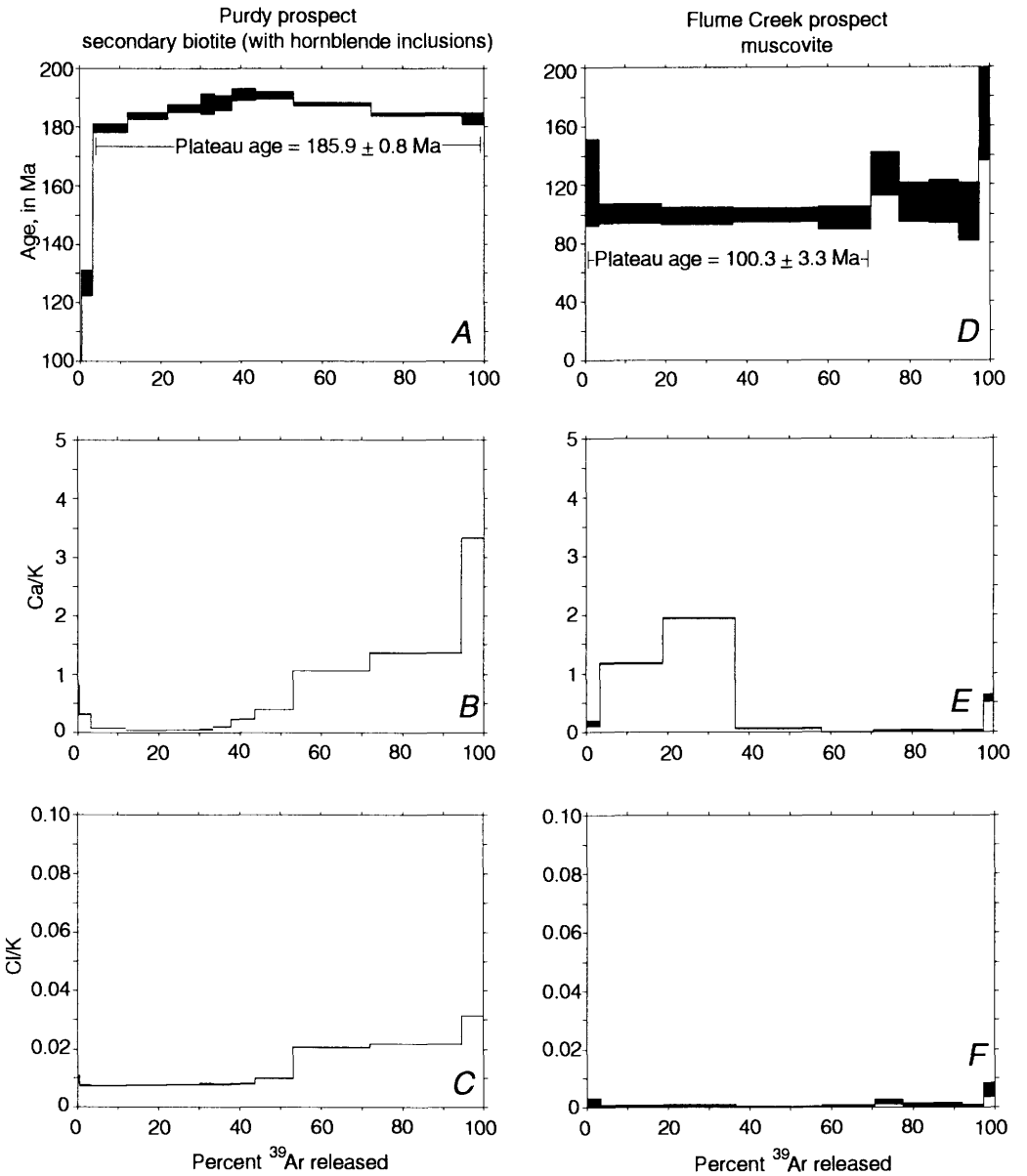

Figure 10. Ar release spectra for alteration minerals from Mesozoic Au-rich deposits, Eagle quadrangle. A,B,C, Spectra of secondary biotite >> primary(?) hornblende, Purdy prospect (sample 13). D,E,F, Spectra of muscovite with minor primary(?) hornblende from altered gabboric rock adjacent to gold vein, Flume Creek prospect (sample 14). Error bars represent 1 sigma uncertainties.

ample at which disseminated Pt-Au-Pd is hosted by an Early Jurassic alkalic gabbro (Indian and Northern Affairs Canada, 1987). However, the absence of significant PGM-bearing placers downstream from the biotite clinopyroxenite bodies in the Eagle quadrangle indicates either that the biotite clinopyroxenite bodies contain small amounts of PGMs or, alternatively, that only the tops of these systems are currently exposed.

PORPHYRY PROSPECTS AND OCCURRENCES

Our ages for the Mosquito and Peternie porphyry prospects are significantly older than those of the previously dated early Tertiary prospects of the northeastern Tanacross quadrangle (fig. 2) and indicate that the porphyry occurrences of east-central Alaska are not in a single belt. Indeed, there appear to be three ages of porphyry mineralization, about 100 Ma (Peternie, Section 21 prospects), about 70 Ma (Mosquito), and about 55 Ma (Taurus, Push-Bush, and Tok?). Each of these periods of porphyry deposit formation is characterized by a different metallogeny and by somewhat different igneous rock associations.

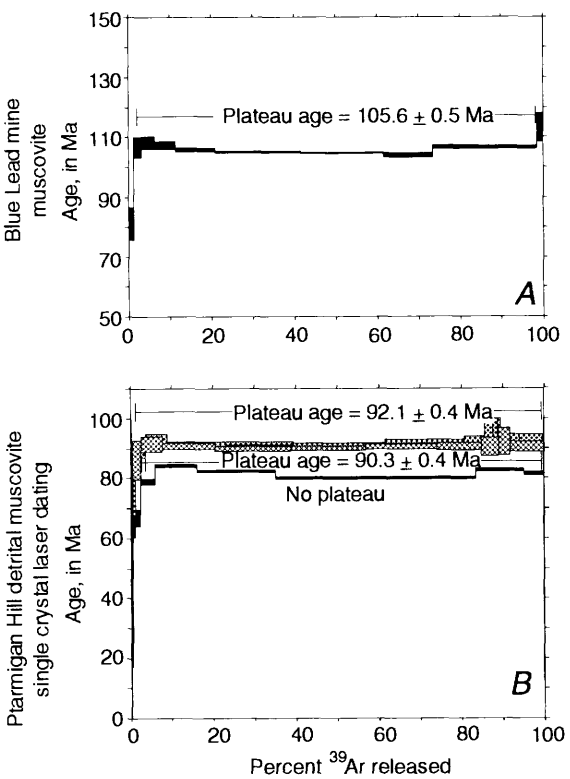

Figure 11. Ar spectra of white micas from Cretaceous and Tertiary deposits, east-central Alaska. A, Blue Lead mine, alteration muscovite (sample 15). B, Composite of three detrital muscovite grains, Ptarmigan Hill prospect (sample 16). Ca/K and Cl/K spectra are flat at near-zero values. Error bars represent 1 sigma uncertainties.

Mid-Cretaceous porphyry systems in the study area, as exemplified by the Section 21 and Peternie prospects (fig. 2), are Mo-, Ag-, and W-rich, but relatively Cu- and Au-poor (Alaska Division of Geological and Geophysical Surveys, 1993; Burleigh and others, 1994; U.S. Bureau of Mines, 1995). The host rocks are rhyolite porphyry dikes exhibiting volcanic-arc signatures (U.S. Bureau of Mines, 1995). Peternie is spatially associated with the mid-Cretaceous Sixtymile Butte tuff complex (fig. 2), characterized by volcanic rocks with andesitic to dacitic compositions and volcanic-arc-type minor-element abundances (Bacon and others, 1990). Porphyry occurrences of this age are rare both in east-central Alaska and in the adjacent Yukon Territory, perhaps because mid-Cretaceous igneous rocks are rarely exposed at subvolcanic levels in this region. The Peternie and Section 21 porphyry prospects are only slightly older than the mid-Cretaceous Red Mountain porphyry Mo prospect in the southcentral Yukon Territory (Sinclair, 1986). Given their significantly older age, it is unclear why the Section 21 and Peternie prospects are near an extension of the 70-Ma Carmacks porphyry belt into Alaska (fig. 2), although this age overlap suggests the existance of a northwest-trending structural zone which focused the intrusion of porphyry magmas over an extended period.

The Late Cretaceous Mosquito porphyry Cu-Mo-Au prospect appears to be within the extension into eastern Alaska of the approximately 70 Ma Au-rich Carmacks porphyry belt (fig. 2), based on similarity in age and anomalous Au, Bi, and Te concentrations (Alaska Division of Geological and Geophysical Surveys, 1993; Burleigh and others, 1994). At the Mosquito prospect the porphyritic rocks are strongly altered but appear to consist of a bimodal assemblage of quartz monzodiorite and alkali feldspar granite, both exhibiting within-plate trace-element characteristics (U.S. Bureau of Mines, 1995). The Mount Fairplay alkalic complex (fig. 2) is a composite syenite body, has a K-Ar (biotite) age of 67±2 Ma, and contains minor gold-bearing veins (Kerin, 1976; Wilson and others, 1985; McCoy and others, 1997). It represents a vein-type variation of Carmacks belt metallogeny commonly seen in the Mount Nansen-Cash area of the Yukon Territory (fig. 2; Indian and Northern Affairs Canada, 1989). On the basis of the approximately 70-Ma age of the Mosquito prospect (table 2) and the Mount Fairplay complex (Wilson and others, 1985), we predict that additional 70-Ma-type Au-rich plutonic systems are present between the Mosquito prospect and the Canadian border (fig. 2).

The early Tertiary ages for the Taurus and Push-Bush deposits (and for a rhyolite flow near the Asarco and Tok prospects) are similar to that of the Pluto porphyry Mo-W prospect (K-Ar biotite, 59±2 Ma; Sinclair, 1986) in the west-central Yukon Territory (fig. 2). Including the Pluto prospect, the early Tertiary east-central Alaskan porphyry prospects appear to be part of a northeast-trending belt of porphyry Mo-Cu systems that is different from the Carmacks belt (fig. 2). The 55- to 60-Ma ages characteristic of this belt are the same

as ages for the early Tertiary, granite-hosted, tourmaline-bearing, Sn-Ag-W greisens at Ketchem Dome (Circle district), in the upper Chena region, and at Lime Peak, Cache Mountain, and Manley Hot Springs (fig. 12) all in interior Alaska (Wilson and others, 1985; Smith and others, 1987, 1994; Newberry and others, 1990; Burns and others, 1991; Clautice and others, 1993). If the (shallow-level) 55- to 60-Ma porphyry systems in the eastern part of the area are the magmatic equivalents of the (deeper-level) 55- to 60-Ma granite-hosted greisen systems in the western part of the area (fig. 2) it is not coincidental that the porphyry mineralization at Taurus and Asarco is anomalous in W, Sn, Ag, B, and Bi, and that hydro-

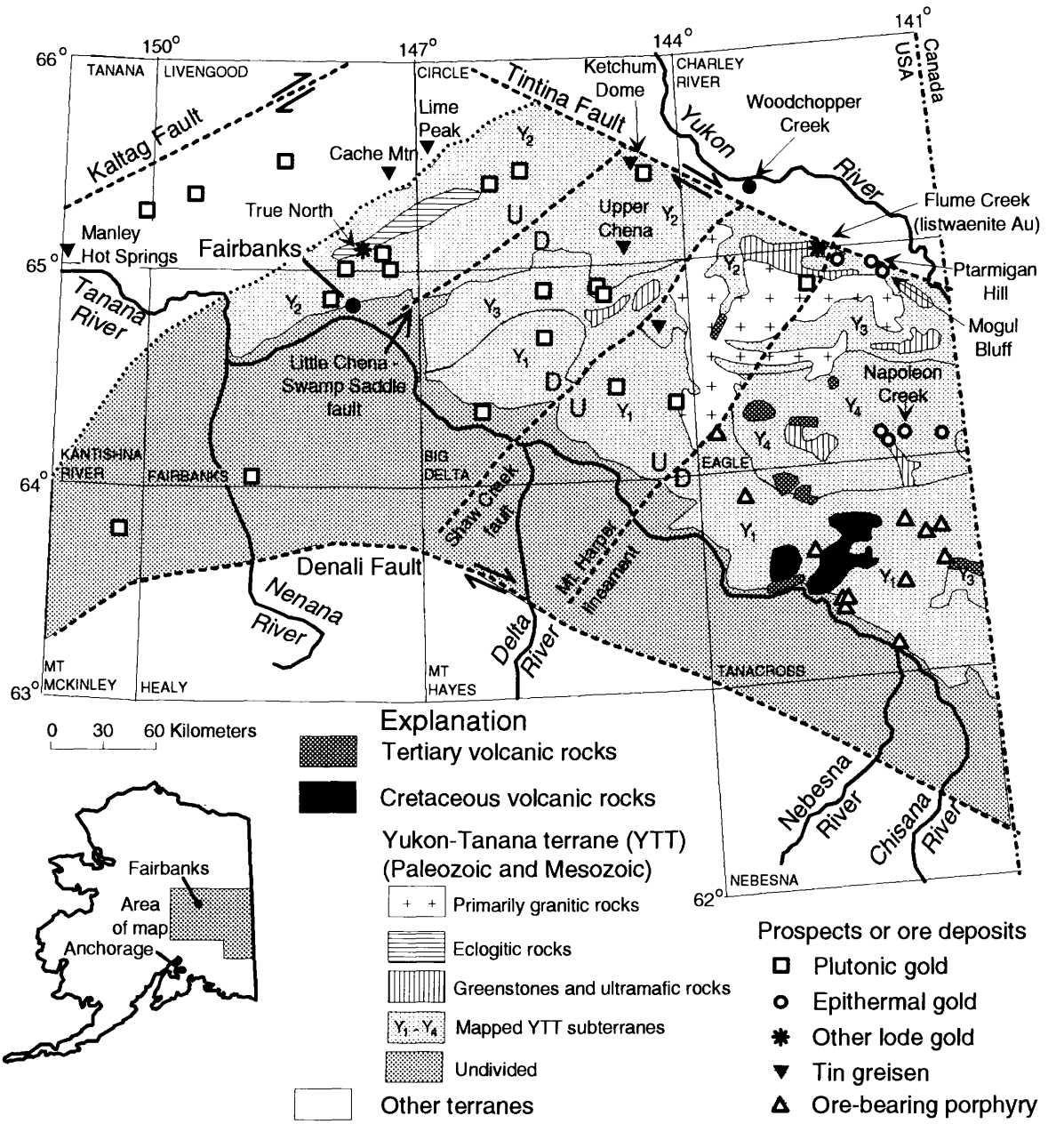

Figure 12. Locations of Cretaceous and Tertiary gold, greisen Sn, and porphyry prospects and deposits in eastern interior and east-central Alaska, related major geologic features, and 1:250,000 quadrangles. Dark dashed lines are major faults or lineaments; relative movement shown by arrows or U, up; D, down. Dotted line represents the approximate northwest limit of the Yukon-Tanana terrane. Thin continuous lines are geologic contacts. Geology modified from Wilson and others (1985), Foster (1992), Foster and others (1994), and Newberry and others (1996). Locations of deposits and prospects from Nokleberg and others (1987), Newberry and others (1990), Clautice and others (1993), Newberry and others (1995b), U.S. Bureau of Mines (1995), McCoy and others (1997), and this study. U.S.G.S. 1:250,000 quadrangle outlines and names are shown.

thermal tourmaline has been noted at Taurus (Singer and others, 1976; Alaska Division of Geological and Geophysical Surveys, 1993; U.S. Bureau of Mines, 1995). In addition, all of these early Tertiary porphyry prospects are gold-poor, as are the Sn greisen prospects to the west (Smith and others, 1987; Newberry and others, 1990; Alaska Division of Geological and Geophysical Surveys, 1993; U.S. Bureau of Mines, 1995). The porphyry prospects are associated with extensive hydrothermal alteration, but chemical analyses of least-altered rocks show that rhyolite porphyry is the predominant host rock type (Burns and others, 1991; Alaska Division of Geological and Geophysical Surveys, 1993; U.S. Bureau of Mines, 1995), similar in major- and trace-element contents to the similar-aged granites which host Sn greisens (Newberry and others, 1990; Burns and others, 1991).

The variation in ages among porphyry occurrences in east-central Alaska contradicts earlier descriptions of the occurrences as part of a single porphyry belt. However, similar variation in ages is seen in the better studied Yukon Territory (Sinclair, 1986). The systematic relation between mineralization age and metallogeny among porphyry and other magmatic-hydrothermal prospects in east-central Alaska suggests that magmatic sources, magmatic evolution trends, and levels of exposure are more important than host terrane or subterrane in determining metallogeny.

GOLD-BEARING PROSPECTS

$^{40}Ar/^{39}Ar$ dating of secondary biotite surrounding a Cu-Au-bearing quartz vein at the Purdy prospect (fig. 1, No. 13) indicates an Early Jurassic age for metal deposition (tables 1, 2). Shear zone and sheeted vein Cu-Au mineralization in early Jurassic granodiorite at the Minto and Williams Creek properties (fig. 2), west-central Yukon Territory, is also considered to be of Early Jurassic age (Indian and Northern Affairs Canada, 1995). Cu-Au-Bi-Te sheeted veins hosted by foliated granodiorite similar in composition and appearance to that hosting the Purdy prospect have been found at the Highway Cu prospect (fig. 1; Burleigh and others, 1994). A Cu-Au-Te-Bi-rich skarn is adjacent to foliated (pre-Cretaceous) granodiorite at the Mitchell prospect, 50 km west of Purdy (fig. 1; U.S. Bureau of Mines, 1995; Newberry and others, 1997). These examples appear to indicate a consistent Cu-Au-(Bi-Te) metal suite associated with Early Jurassic plutons, expressed at several different deposit types. Although only the Mitchell skarn is of clearly plutonic-hydrothermal origin, the systematic association with foliated, pre-Cretaceous, probably Early Jurassic and (or) Late Triassic intrusions, and the consistent metal suite suggests that all these occurrences and deposits are of similar affinity (Newberry and others, 1995b; McCoy and others, 1997). There are many drainage and bedrock geochemical anomalies of Cu and Bi in the Eagle quadrangle (Foster and Yount, 1972) and much of the placer gold in southeastern Eagle quadrangle contains anomalous concentrations of Bi±Te and Cu (Cathrall and others, 1989), data which suggest that there are additional undiscovered Early Jurassic Au-Cu occurrences in the Eagle quadrangle and vicinity.

Our $^{40}Ar/^{39}Ar$ spectrum for alteration muscovite from the Flume Creek listwaenite (altered ophiolite) gold prospect (fig. 1, No. 14; fig. 10*D*; table 2) shows a mid-Cretaceous plateau. This plateau age suggests that gold deposition was caused by mid-Cretaceous (hence, plutonic-related) fluids because it significantly post-dates the Jurassic emplacement of ophiolite fragments in this region (Templeman-Kluit, 1979; Dusel-Bacon and Hansen, 1992). A conventional model for gold associated with carbonate-altered mafic and ultramafic rocks (listwaenite) presumes that the carbonate alteration and gold deposition are caused by hydrothermal activity related to late stages of ophiolite emplacement (Buisson and Leblanc, 1986). However, as Buisson and Leblanc (1986, p. 129) point out, "it would be unwise to consider all such alteration and mineralization to be syn-emplacement." For the alteration muscovite from the Flume Creek prospect, the approximately 170-Ma minimum age of the highest-temperature fraction might be related to emplacement of the ophiolite fragment, whereas the approximately 100-Ma plateau age corresponds to that of mid-Cretaceous plutonism. A small, undated, but unfoliated (hence, post-Jurassic?) dioritic stock 200 meters from the prospect (Clark and Foster, 1971; U.S. Bureau of Mines, 1995) is a potential candidate for such fluids and (or) a heat source for convection-driven meteoric fluids.

Thrust slices(?) of variably altered ophiolitic fragments (greenstones and ultramafic rocks) are widespread in the Eagle quadrangle (fig. 1; Foster and Keith, 1974) and are present discontinously as far west as the Fairbanks area (fig. 12; Foster, 1992). These altered mafic and ultramafic rocks rarely contain lode gold mineralization and are rarely associated with gold placer deposits (Foster and Keith, 1974). The Flume Creek prospect data indicate that gold is not widespread in these ophiolitic rocks except where they are altered by mid-Cretaceous hydrothermal fluids.

The Flume Creek prospect bears similarities in rock compositions and Ar spectra to altered and gold-mineralized eclogitic rocks present at the recently discovered True North prospect, 30 km north of Fairbanks (fig. 12; McCoy and others, 1997). $^{40}Ar/^{39}Ar$ dating of relatively fresh eclogite from the region suggests it was metamorphosed in Early Jurassic time, structurally emplaced in Early Cretaceous time, but mineralized at about 90 Ma (Douglas, 1996). The True North prospect is spatially and temporally associated with Au-veins, skarns, and pluton-hosted Au stockworks of the Fairbanks region (fig. 12; McCoy and others, 1997). The recent discovery of significant gold resources at the True North prospect suggests that gold deposits in altered, magnesium- and carbonate-rich rocks of interior Alaska are more common than is currently recognized. Gold deposition in such deposits is apparently related to the unusual host rock

composition, high- and low-angle emplacement faults, and mid- Cretaceous, pluton-related, hydrothermal systems.

We propose that the average reset age (54 Ma) for detrital mica in silicified conglomeratic sandstone at the Ptarmigan Hill prospect (fig. 1, No. 16) represents the time of silicification and gold deposition. This age is the same as that of Tertiary basaltic volcanism in the Fairbanks area (Roe and Stone, 1993; Newberry and others, 1996) and that of bimodal volcanism in the Rampart district (fig. 12, 40 km NE of Manley Hot Springs; Reifenstuhl and others, 1997), Tanacross quadrangle (Wilson and others, 1985), and at Grew Creek in south-central Yukon (Christie and others, 1992). The Grew Creek prospect is an epithermal Au-Ag deposit in the Tintina fault zone, hosted by early Tertiary bimodal volcanic rocks and exhibiting strong Hg-Ag anomalies (Christie and others, 1992). The deposit indicates that 55-Ma bimodal volcanism is at least locally associated with epithermal gold deposition. Hitzman and others (1994) demonstrated that $^{40}Ar/^{39}Ar$ reset ages in detrital muscovites of hydrothermally altered Old Red Sandstone in southern Ireland were also consistent with geologic evidence for the age of hydrothermal alteration. On the basis of the Hg-Ag-Au metal signature (U.S. Bureau of Mines, 1995), our $^{40}Ar/^{39}Ar$ systematics, and the presence of silicification without other obvious hydrothermal alteration, we conclude that the Ptarmigan Hill occurrence is an early Tertiary epithermal deposit.

Mineralization similar to that at Ptarmigan Hill is present at Mogul Bluff, 5 kilometers to the east (fig. 12; U.S. Bureau of Mines, 1995). We also identified anomalous gold concentrations in silicified conglomerates underlying Tertiary basalt at Napoleon Creek (fig. 12; U.S. Bureau of Mines, 1995). Barker (1986) also noted mineralized altered Tertiary conglomerates in the Woodchopper Creek area, 30 kilometers north of Ptarmigan Hill, on the north side of the Tintina fault (fig. 12). Yeend (1996) noted that Tertiary conglomerates are apparently sources for Holocene gold placers at several locations in southeastern Eagle quadrangle, and he suggested that gold was concentrated in the early Tertiary conglomerates by stream concentration. However, on the basis of the Ptarmigan Hill, Mogul Bluff, and Napoleon Creek occurrences, we suspect that gold concentrations in Late Cretaceous-early Tertiary sedimentary rocks of east-central Alaska are primarly of epithermal origins.

Mid-Cretaceous pluton-hosted and pluton-related gold deposits are present throughout the YTT and vicinity in interior Alaska (Newberry and others, 1995b; McCoy and others, 1997) and are restricted neither to specific subterranes nor to specific ages within the 89- to 108-Ma subduction-related magmatic event (fig. 12; table 1). However, these deposits have not been found in interior Alaska east of the Mount Harper lineament (fig. 12). Similarly, early Tertiary granite-hosted Sn-W-Ag greisen deposits occur in several locations west of the Mount Harper lineament (Smith and others, 1987; Newberry and others, 1990) but are not known in interior Alaska west of the lineament (U.S. Bureau of Mines, 1995). Conversely, epithermal Au prospects (such as Ptarmigan Hill and Mogul Bluff) and Mo-Cu-W porphyry systems are only present east of the Mount Harper lineament (fig. 12). This northeast-trending linear further separates extensive exposures of Mesozoic plutonic rocks on the west side from large exposures of Cretaceous and early Tertiary volcanic rocks on the east side (fig. 12). The Mount Harper lineament is only one of several northeast-trending lineaments in interior Alaska (Wilson and others, 1985; Page and others, 1995), at least one of which (the Shaw Creek fault) is demonstrably a high-angle fault with significant (normal?) dip-slip movement. Northeast-trending zones of earthquake epicenters corresponding to mapped linear features suggest that these lineaments, including the Mount Harper lineament, are high-angle faults (Page and others, 1995).

We infer that the absence of porphyry and epithermal prospects west of the Mount Harper lineament does not reflect a difference in host subterrane or other local sources of metals, but rather that it reflects significant relative uplift west of the Mount Harper lineament and consequently different levels of erosion exposed across the lineament. In particular, we infer that levels of erosion appropriate to formation of porphyry and epithermal deposits are only present west of the lineament. Fluid-inclusion data combined with sphalerite and granite geobarometric data indicate that the pluton-hosted Au deposits in interior Alaska formed at pressures of 0.8 to 2 kb, whereas porphyry deposits form in subvolcanic environments characterized by pressures less than 0.5 kb (Newberry and others, 1995b; McCoy and others, 1997). Consequently, we infer 1 to 3 km of vertical movement along the Mount Harper lineament.

CRETACEOUS IGNEOUS ACTIVITY

Compilation of our $^{40}Ar/^{39}Ar$ ages with previous K-Ar and Pb-alpha ages of mid-Cretaceous, calc-alkalic, igneous rocks within the YTT and vicinity shows a systematic pattern (fig. 13)—magmatic ages apparently define northeast-trending belts across interior Alaska. Calc-alkalic magmatism apparently began at about 108 Ma (the oldest mid-Cretaceous plutonic K-Ar or $^{40}Ar/^{39}Ar$ age in this region) and continued to about 101 Ma in a 120-km-wide belt extending through southern Eagle and northern Tanacross quadrangles (fig. 12). Plutonic ages of 101 Ma or younger are found in belts northwest and southeast of the locus of earliest magmatism (fig. 13). Northwest of the belt of earliest mid-Cretaceous magmatism are two belts, the more southerly characterized by ages of 101 to 90 Ma and the more northerly by ages of 92 to 88 Ma (fig. 13). The initiation of magmatism, as defined by the oldest K-Ar or $^{40}Ar/^{39}Ar$ ages in a given region, sweeps from southeast to northwest across interior Alaska.

The above patterns cut across YTT subterranes (fig. 12) and the locus of postulated 135- to 110-Ma extension (outlined by subterrane Y_1, fig. 13) and is apparently truncated by both

the Denali and Tintina faults (fig. 13). North and northwest of this calc-alkalic plutonic belt is a narrow belt of mixed alkalic and quartz-normative plutons (Light and Rinehart, 1988; Burns and others, 1991) having K-Ar ages of 90 to 88 Ma (fig. 13). The net age pattern is one of east-northeast-trending bands of Cretaceous calc-alkalic magmatism (fig. 13). This pattern is similar to that observed in the central Sierra Nevada batholith of California, where magmatism sweept from west to east across the 200-km width of the batholith during the interval of 120 to 88 Ma (Bateman, 1992). In the Sierra Nevada, the resulting pattern is one of north-northwest bands of plutonic rocks with restricted age ranges, the bands oriented parallel to the paleosubduction zone (Bateman, 1992).

Analogy with the north-northwest bands of eastward-sweeping Cretaceous magmatism in the Sierra Nevada batholith, suggests that the age pattern for magmatic rocks of interior Alaska (fig. 13) was caused by north-northwest-directed (present coordinates) subduction. The

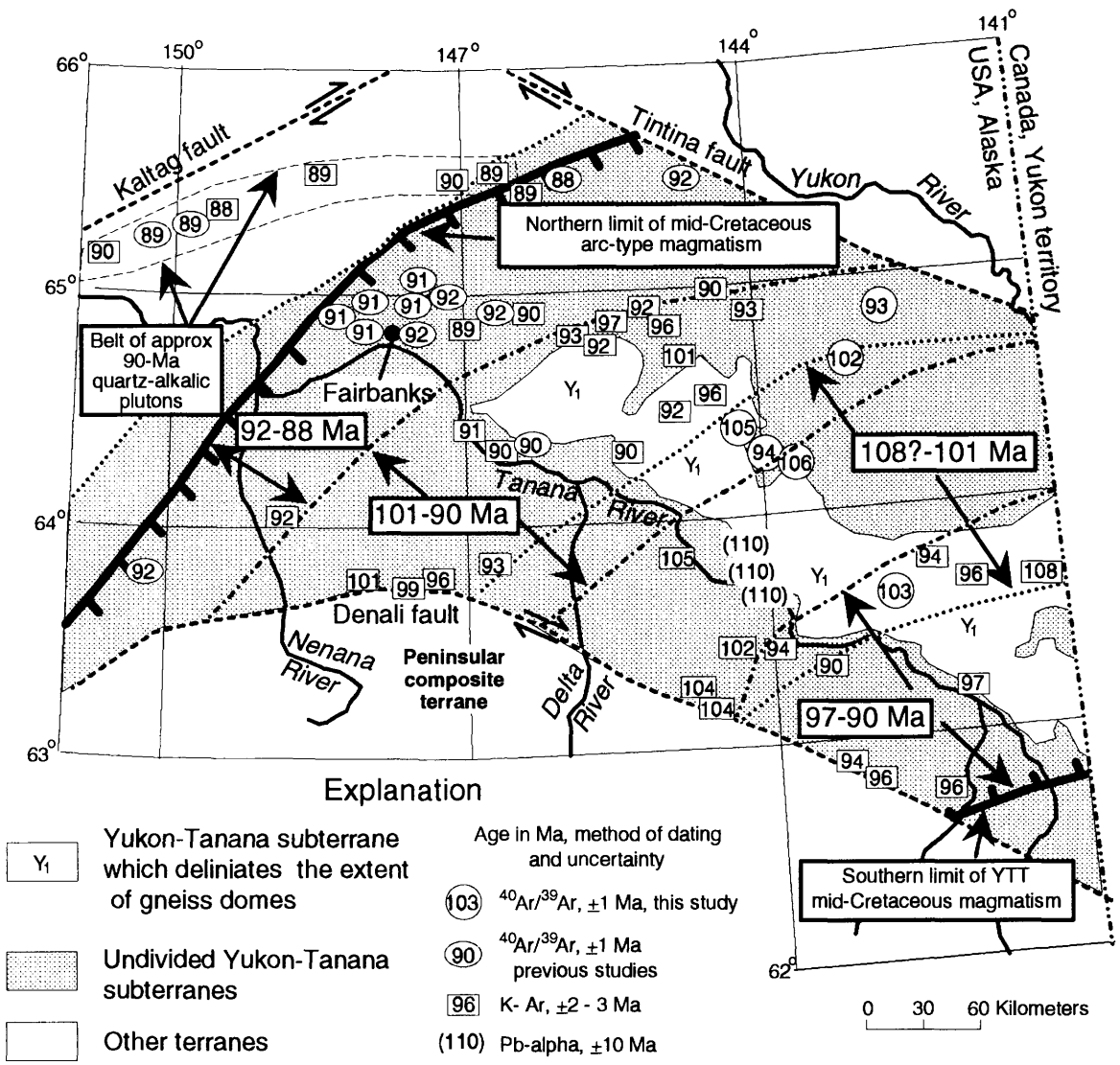

Figure 13. Map of same area of figure 12 showing ages of dated mid-Cretaceous calc-alkalic granitic and volcanic rocks in Yukon-Tanana terrane (YTT) and mixed alkalic/calc-alkalic plutonic rocks northwest of YTT. Larger boxes and arrows to related lines show ages and extent of Cretaceous magmatic and quartz-alkalic plutons across eastern interior and east-central Alaska. Boldest lines show extent of that magmatism. Spatial extent of sillimanite gneiss dome and major orthogneiss bodies is delineated by subterrane Y1, generalized from Foster (1992); gneissic rocks are variably intruded by younger calc-alkalic plutons. Dark dashed lines are major faults; relative movement shown by arrows. Unlabeled dotted line represents the approximate northwest limit of the Yukon-Tanana terrane. Thin continuous lines are geologic contacts. Data from Wilson and others (1985), Light and Rinehart (1988), Bacon and others (1990), Burns and others (1991), Weber and others (1992), Yesilyurt (1994), Newberry and others (1995a, b), McCoy and others (1997), and this study.

calc-alkalic plutonic rocks have volcanic-arc-trace-element signatures (Bacon and others, 1990; Burns and others, 1991; Newberry, 1996). The north-northwest migration of magmatism was approximately 2 cm/million years and could have been the result of shallowing of subduction beginning at about 101 Ma. Calc-alkalic magmatism in the vicinity of Fairbanks (fig. 13) is restricted to ages of 92 Ma or less and may represent the waning of the magmatic event. The narrow belt of alkalic and quartz normative magmatism northwest of (behind) the arc-related belt (fig. 13) is suggestive of back-arc magmatism, in both its location and its magmatic compositions, and further reinforces the possibility of a mid-Cretaceous arc. The cessation of mid-Cretaceous subduction-related magmatism may have been caused by the collision between the YTT and the Penninsular composite terrane (Csejtey and others, 1982), which is currently located south of the Denali fault (fig. 13). In this model, the approach of the Penninsular terrane toward the YTT along a northwest-dipping (present coordinates) subduction zone originally gave rise to the mid-Cretaceous magmatism (Csejtey and others, 1982).

Although mid-Cretaceous igneous rocks are present throughout the YTT region, mid-Cretaceous volcanic rocks are restricted to the far southeastern part (fig. 12; Bacon and others, 1990). Presumably this reflects the very shallow level of erosional exposure in that area. However, the volcanic rocks are restricted in time as well as space, with known ages of only 90 to 97 Ma compared to 89 to 108 Ma for plutonic rocks (Wilson and others, 1985; Bacon and others, 1990; this study, fig. 13). Ages for the plutonic rocks—given a ±2- to 3- Ma uncertainty for K-Ar ages—seem to define essentially continuous magmatism over this time interval. Mid-Cretaceous volcanic rocks older than 97 Ma have not been preserved, are covered by younger volcanic rocks, or did not exist in this region. If they did not exist, lack of surficial magmatism could be due to a compressional setting (making magma ascent through the crust difficult). A compressional setting is both consistent with the volcanic-arc signature of this mid-Cretaceous magmatism (Bacon and others, 1990; Newberry and others, 1996) and would indicate that the postulated mid-Cretaceous extension event of Pavlis and others (1993) had ended by about 108 Ma.

A narrow belt of quartz-alkalic plutonic rocks having U-Pb and K-Ar ages of about 90 Ma is present on the north side of the Tintina fault in the Tombstone Mountains, north of Dawson, Yukon Territory (Wheeler and McFeeley, 1991). Additionally, belts of apparently arc-related mid-Cretaceous plutons are present north of the Tintina fault and east of Dawson (Murphy and others, 1995). These belts are apparently the offset portions of the interior Alaskan belts described above (Mortensen and others, 1995); their positions are compatible with several hundred kilometers of post-mid-Cretaceous right-lateral offset and consistent with estimates of Tertiary and younger displacement along the Tintina fault.

CONCLUSIONS

Most of our $^{40}Ar/^{39}Ar$ spectra are quite complex (figs. 3-11). They indicate (1) the presence of several mineral phases in visually monomineralic samples, (2) exhibit evidence for Late Cretaceous and early Tertiary resets, and (3) contain high-temperature fractions that suggest primary ages significantly older than plateau or integrated ages. In particular, the evidence for widespread resets, especially in areas lacking mapped post-mid-Cretaceous igneous rocks, may indicate a widespread igneous-related(?) early Tertiary heating event, as seen in the Fairbanks district. In this region of multiple and complex igneous and metamorphic events, conventional K-Ar dating is severely limited relative to $^{40}Ar/^{39}Ar$ dating in unraveling the ages of geologic events.

Our ages provide a more realistic basis for understanding mineral prospects in east-central Alaska and for correlating them with the better studied deposits of the Yukon Territory. In particular, despite earlier suggestions to the contrary, we see no evidence for metal deposition associated with regional metamorphic events in the area; all the dated deposits can be clearly tied to known igneous events. The plutonic-hosted deposits studied also yielded age information indicating that alteration and metal deposition were essentially synchronous with crystallization of the host pluton. Despite earlier claims for correlation between specific host subterranes and specific metals, we see no such relations. Instead, we recognize a relation between depth of exposure in an igneous system and the style of alteration and metals deposited, and one between ages of magmatism (hence, magmatic source?) and metals deposited. In particular, only the Early Jurassic-associated deposits are characterized by high copper contents, and the early Tertiary deposits appear especially rich in tin.

Our dating of previously undated plutonic rocks and mineral deposits in the eastern YTT confirms that age estimates based on intuition and analogy are often incorrect. In this area—as in much of Alaska–published tectonic and metallogenic models have far overreached the available data. Because potentially significant mineral resources are near several of the major roads in this region (Singer and others, 1976), additional studies of the igneous rocks and their ages is feasible could be economically beneficial. The contrast between this apparently poorly endowed region and the adjacent deposit-rich but better studied Yukon Territory suggests that additional geologic data (including accurate dates) on igneous rocks and mineral occurrences is much needed. Rather than being of strictly academic importance, such data would be immediately useful.

Acknowledgments.—This study would not have been possible without the assistance of personnel from the USGS. Discussions with Helen Foster, Florence Weber, Charles Bacon, Cynthia Dusel-Bacon, Tom Light, Robert Hammond, and David Menzie helped to clarify our ideas concerning the nature of igneous rocks and mineral deposits in the study area. Florence Weber, Helen Foster, Cynthia Dusel-Bacon, and

Charles Bacon kindly donated samples for examination and compositional study. Cynthia Dusel-Bacon and Tom Light provided unpublished analytical data.

REFERENCES CITED

Alaska Division of Geological and Geophysical Surveys, 1993, Trace element and major oxide analyses of samples from the Eagle and Tanacross quadrangles, east-central Alaska: Alaska Division of Geological and Geophysical Surveys Public-Data File 93-4, 31 p.

Allegro, G.L., 1987, The Gilmore Dome tungsten mineralization, Fairbanks mining district, Alaska: Fairbanks, University of Alaska, M.S. thesis, 114 p.

Bacon, C.R., Foster, H.L., and Smith, J.G., 1990, Rhyolitic calderas of the Yukon-Tanana terrane, east-central Alaska: volcanic remnants of a mid-Cretaceous magmatic arc: Journal of Geophysical Research, v. 95, no. B13, p. 21,451-21,461.

Bacon, C.R., and Lanphere, M.A., 1996, Late Cretaceous age of the Middle Fork caldera, Eagle quadrangle, east-central Alaska, *in* Moore, T.E., and Dumoulin, J.A., eds., Geologic studies in Alaska by the U.S. Geological Survey, 1994: U.S. Geological Survey Bulletin 2152, p. 143-147.

Barker, J.C., 1986, Placer gold deposits of the Eagle trough, upper Yukon River region, Alaska: U.S. Bureau of Mines Information Circular 9123, 23 p.

Bateman, P.C., 1992, Plutonism in the central part of the Sierra Nevada batholith, California: U.S. Geological Survey Professional Paper 1483, 186 p.

Buisson, G. and Leblanc, M., 1986, Gold-bearing listwaenites (carbonatized ultramafic rocks) from ophiolite complexes, *in* Gallagher, M.J., Ixer, R.A., Neary, C.R. and Prichard, H.M., eds., Metallogeny of basic and ultrabasic rocks: London, Institute of Mining and Metallurgy, p. 121-131.

Burleigh, R.E., Fechner, S.A., and Lear, K.G., 1994, Preliminary results of the mineral resource evaluation of the Bureau of Land Management Black River and Fortymile River planning units: U.S. Bureau Mines Open-File Report 48-94, 117 p.

Burns, L.E., Newberry, R.J., and Solie, D.N., 1991, Quartz normative plutonic rocks of interior Alaska and their favorability for association with gold: Alaska Division of Geological and Geophysical Surveys Report of Investigation 91-3, 58 p.

Cathrall, J.B., Albanese, Mary, VanTrump, G., Mosier, E.L., and Lueck, Larry, 1989, Geochemical signatures, analytical results, mineralogical data, and sample locality map of placer and lode gold, and heavy-mineral concentrates from the Fortymile mining district, Eagle quadrangle, Alaska: U.S. Geological Survey Open-File Report 89-451, 52 p.

Christie, A.B., Duke, J.L., and Rushton, R., 1992, Grew Creek epithermal gold-silver deposit, Tintina trench, Yukon: Yukon Exploration and Geological Services Division, Indian and Northern Affairs Canada, Yukon Geology, v. 3, p. 223-259.

Churkin, Michael, Jr., Foster, H.L., Chapman, R.M., and Weber, F.R., 1982, Terranes and suture zones in east-central Alaska: Journal of Geophysical Research, v. 87, no. B5, p. 3718-3730.

Clark, S.B., and Foster, H.L., 1971, Geochemical and geological reconnaissance in the Seventymile River area, Alaska: U.S. Geological Survey Bulletin 1315, 21 p.

Clark, Thomas, 1980, Petrology of the Turnagain ultramafic complex, NW British Columbia: Canadian Journal of Earth Sciences, v. 17, p. 744-757.

Clautice, K.H., Burns, L.E., and Newberry, R.J., 1993, Land selection unit 5 (Big Delta, Mt Hayes, Fairbanks quadrangles): references, major oxides and geochemical data: Alaska Division of Geological and Geophysical Surveys Public-Data File 93-5, 18 p.

Csejtey, Bela, Jr., Cox, D.P., Evarts, R.C., Stricker, G.D., and Foster, H.L., 1982, The Cenozoic Denali fault system and the Cretaceous accretionary development of southern Alaska: Journal of Geophysical Research, v. 87, no. B5, p. 3741-3754.

Douglas, T.A., 1996, Metamorphic histories of the Chatanika eclogite and Fairbanks schist within the Yukon-Tanana terrane, Alaska, as revealed by electron microprobe thermobarometry and $^{40}Ar/^{39}Ar$ single grain dating: Fairbanks, University of Alaska, MS thesis, 240 p.

Dusel-Bacon, Cynthia, and Aleinikoff, J.N., 1996, U-Pb zircon and titanite ages for augen gneiss from the Divide Mountain area, eastern Yukon-Tanana upland, Alaska, and evidence for the composite nature of the Fiftymile batholith, *in* Moore, T.E., and Dumoulin, J.A., eds., Geologic studies in Alaska by the U.S. Geological Survey, 1994: U.S. Geological Survey Bulletin 2152, pp. 131-142.

Dusel-Bacon, Cynthia, and Hansen, V.L., 1992, High-pressure amphibolite-facies metamorphism and deformation within the Yukon-Tanana and Taylor Mountain terranes, eastern Alaska, *in* Bradley, D.C., and Dusel-Bacon, C., eds., Geologic studies in Alaska by the U.S. Geological Survey, 1991: U.S. Geological Survey Bulletin 2041, p. 140-159.

Foley, J.Y., Burns, L.E., Schneider, C.L., and Forbes, R.B., 1989, Preliminary report of platinum group element occurrences in Alaska: Alaska Division of Geological and Geophysical Surveys Public Data File 89-20, 33 p.

Foster, H.L., 1976, Geologic map of the Eagle quadrangle, Alaska: U.S. Geological Survey Miscellaneous Geologic Investigations Series Map I-922, scale 1:250,000.

Foster, H.L., 1992, Geologic map of the eastern Yukon-Tanana region, Alaska: U.S. Geological Survey Open-File Report 92-313, 26 p.

Foster, H.L., Albert, N.R.D., Barnes, D.F., Curtin, G.C., Griscom, A., Singer, D.A., and Smith, J.G., 1976, Background information to accompany folio of geologic and mineral resource maps of the Tanacross quadrangle, Alaska: U.S. Geological Survey Circular 734, 23 p.

Foster, H.L., and Clark, S.H.B., 1970, Geochemical and geologic reconnaissance of a part of the Fortymile area, Alaska: U.S. Geological Survey Bulletin 1312-M, 29 p.

Foster, H.L., and Keith, T.E.C., 1974, Ultramafic rocks of the Eagle quadrangle, east-central Alaska: U.S. Geological Survey Journal of Research, v. 2, p. 657-669.

Foster, H.L., Keith, T.E.C., and Menzie, W.D., 1994, Geology of the Yukon-Tanana area of east-central Alaska, *in* Plafker, George, and Berg, H.C., eds., The geology of Alaska: Boulder, Colo, Geological Society of America, The Geology of North America, v. G1, p. 205-240.

Foster, H.L., and Yount, M.E., 1972, Maps showing distribution of anomalous amounts of selected elements in stream-sediment and rock samples, Eagle quadrangle, Alaska: U.S. Geological Survey Miscellaneous Field Studies Map MF-356, 2 sheets, scale 1:250,000.

Hitzman, M.W., Layer, P.W., and Newberry, R.J., 1994, Argon-argon step heating studies of muscovite in the Upper Devonian Old

Red Sandstone: the first absolute dates for the age of Irish zinc-lead mineralization [abs.]: Geological Society of America Abstracts with Programs, v. 26, no. 7, p. 139.

Hollister, V.F., Anzalone, S.A., and Richter, D.H., 1975, Porphyry copper belts of southern Alaska and contiguous Yukon Territory: Canadian Institute of Mining and Metallurgy Bulletin, v. 68, p. 104-112.

Indian and Northern Affairs Canada, 1987, Yukon Exploration 1985-1986: Exploration and Geological Services Division, Yukon, Indian and Northern Affairs Canada, 451 p.

Indian and Northern Affairs Canada, 1989, Yukon Exploration 1988: Exploration and Geological Services Division, Yukon, Indian and Northern Affairs Canada, 304 p.

Indian and Northern Affairs Canada, 1995, Yukon Exploration and Geology 1994: Exploration and Geological Services Division, Yukon, Indian and Northern Affairs Canada, 112 p.

Kerin, L.J., 1976, The reconnaissance petrology of the Mt. Fairplay igneous complex: Fairbanks, University of Alaska, M.S. thesis, 95 p.

Lanphere, M.A., Dalrymple, G.B., Fleck, R.J. and Pringle, M.S., 1990, Intercalibration of mineral standards for K-Ar and $^{40}Ar/^{39}Ar$ age measurements [abs.]: EOS, Transactions, American Geophysical Union, v.71, p. 1658.

Light, T.D., and Rinehart, C.D., 1988, Molybdenite in the Huron Creek pluton, western Livengood quadrangle, Alaska, *in* Dover, J.H., and Galloway, J.P., eds., Geologic studies in Alaska by the U.S. Geological Survey, 1988: U.S. Geological Survey Bulletin 1903, p. 54-61.

McCoy, D., Newberry, R.J., Layer, P., DiMarchi, J.J., Bakke, A., Masterman, J.S. and Minehane, D.L., 1997, Plutonic related gold deposits of interior Alaska, *in* Goldfarb, R.J. and Miller, L.D., eds., Mineral deposits of Alaska: Economic Geology Monograph 9, p. 191-241.

McDougall, Ian, and Harrison, T.M., 1988, Geochronology and thermochronology by the $^{40}Ar/^{39}Ar$ method: New York, Oxford University Press, 212 p.

Mortensen, J.K., Murphy, D.C., Hart, C.J.R., and Anderson, R.G., 1995, Timing, tectonic setting, and metallogency of Early and mid-Cretaceous magmatism in Yukon Territory [abs.]: Geological Society of America Abstracts with programs, v. 27, no. 5, p. 65.

Murphy, D.C., Mortensen, J.K., and Bevier, M.L., 1995, U-Pb and K-Ar geochronology of Cretaceous and Tertiary intrusions, western Selwyn Basin, and implications for the structural and metallogenic evolution of central Yukon [abs.]: Geological Association of Canada Program and Abstracts, v. 20, p. A74.

Newberry, R.J., 1996, Major and trace element analyses of Cretaceous plutonic rocks in the Fairbanks mining district, Alaska: Alaska Division of Geological and Geophysical Surveys Public-Data File 96-19, 16 p.

Newberry, R.J., Allegro, G.L., Cutler, S.E., Hagen-Levelle, J.H., Adams, D.D., Nicholson, L.C., Weglarz, T.B.,Bakke, A.A.,Clautice, K.H.,Coulter, G.A., Ford, M.J., Myers, G.L., and Szumigala, D.J., 1997, Skarn deposits of Alaska, *in* Goldfarb, R.J., and Miller, L.D., eds., Mineral deposits of Alaska: Economic Geology Monograph 9, p. 355-395.

Newberry, R.J., Bundtzen, T.K., Clautice, K.H., Combellick, R.A., Douglas, T., Laird, G.M., Liss, S.A., Pinney, D.S., Reifenstuhl, R.R., and Solie, D.N., 1996, Preliminary geologic map of the Fairbanks mining district, Alaska: Alaska Division of Geological and Geophysical Surveys Public Data File 96-16, 2 sheets, 32 p.

Newberry, R.J., Burns, L.E., Swanson, S.E., and Smith, T.E., 1990, Comparative petrologic evolution of the Sn and W granites of the Fairbanks-Circle area, interior Alaska, *in* Stein, H.J., and Hannah, J.L., eds., Ore-bearing granite systems; petrogenesis and mineralizing processes: Geological Society of America Special Paper 246, p. 121-142.

Newberry, R.J., Layer, P.W., Solie, D.N., and Burleigh, R.E, 1995a, Mesozoic-Tertiary rocks of eastern interior Alaska: ages, compositions, and tectonic settings [abs.]: Geological Society of America Abstracts with Program, v. 27, no 5, p. 68.

Newberry, R.J., McCoy, D.T., and Brew, D.A., 1995b, Plutonic-hosted gold ores in Alaska: igneous vs. metamorphic origins, *in* Ishihara, Shunso, and Czamanske, G.K., eds., Mineral resources of the NW Pacific Rim: Resource Geology Japan Special Issue, no. 18, p. 57-100.

Nokleberg, W.J., Bundtzen, T.K., Berg, H.C., Brew, D.A., Grybeck, D., Robinson, M.S., Smith, T.E., and Yeend, W., 1987, Significant metalliferous lode deposits and placer districts of Alaska: U.S. Geological Survey Bulletin 1786, 104 p.

Nokleberg, W.J., Bundtzen, T.K., Brew, D.A., and Plafker, George, 1995, Metallogenesis and tectonics of porphyry copper and molybdenum (gold, silver) and granitoid-hosted gold deposits of Alaska, *in* Schroeter, Thomas, ed., Porphyry deposits of the northwestern cordillera: Canadian Institute of Mining, Metallurgy, and Petroleum, Special Vol. 46, p. 103-141.

Page, N.J, Singer, D.A., Moring, B.C., Carlson, C.A., McDade, J.M., and Wilson, S.A., 1986, Platinum-group element resources in podiform chromitites from California and Oregon: Economic Geology, v. 81, p. 1261-1271.

Page, R.A., Plafker, George, and Pulpan, Hans, 1995, Block rotation in east-central Alaska: a framework for evaluating earthquake potential?: Geology, v. 23, p. 629-632.

Palmer, A.R., 1983, The Decade of North American Geology 1983 geologic time scale: Geology, v. 11, p. 503-504.

Pavlis, T.L., Sisson, V.B., Foster, H.L., Nokleberg, W.J., and Plafker, George, 1993, Mid-Cretaceous extensional tectonics of the Yukon-Tanana terrane, Trans-Alaskan Crustal Transect (TACT), east-central Alaska: Tectonics, v. 12, p. 103-122.

Pearce, J.A., Harris, N.B.W., and Tindle, A.G., 1984, Trace element discrimination diagrams for the tectonic interpretation of granitic rocks: Journal of Petrology, v. 25, p. 956-983.

Reifenstuhl, R.R., Layer, P.W., and Newberry, R.J., 1997, $^{40}Ar/^{39}Ar$ Geochronology of 17 Rampart area rocks, Tanana and Livengood quadrangles, central Alaska: Alaska Division of Geological and Geophysical Surveys Public-Data File 97-29H, 22p.

Roe, J.T., and Stone, D.B., 1993, Paleomagnetism of the Fairbanks basalts, interior Alaska, *in* Solie, D.N., and Tannian, Fran, eds., Short notes on Alaskan geology: Alaska Division of Geological and Geophysical Surveys Professional Report 113, p. 61-70.

Samson, S.D., and Alexander, E.C., 1987, Calibration of the interlaboratory ^{40}Ar-^{39}Ar dating standard, MMhb-1; Chemical Geology, v. 66, p. 27-34.

Sinclair, W.D., 1986, Molybdenum, tungsten, and tin deposits and associated granitoid intrusions in the northern Canadian cordillera and adjacent parts of Alaska, *in* Morin, J.A., ed., Mineral deposits of the northern cordillera: Canadian Institute

of Mining and Metallurgy, Special Volume 37, p. 216-233.

Singer, D.A., Curtain, G.C., and Foster, H.L., 1976, Mineral resources map of the Tanacross quadrangle, Alaska: U.S. Geological Survey Miscellaneous Field Studies Map MF-767-E, scale 1:250,000.

Smith, T.E., Pessel, G.H., and Wiltse, M.A.,eds., 1987, Mineral assessment of the Lime Peak-Mt. Prindle area, Alaska: Fairbanks, Alaska Division of Geological and Geophysical Surveys, 663 p.

Smith, T.E., Robinson, M.S., Weber, F.W., Waythomas, C.W., and Reifenstuhl, R.R., 1994, Geologic map of the upper Chena River area, eastern interior Alaska: Alaska Division of Geological and Geophysical Surveys Professional Report 115, 19 p.

Steiger, R.H., and Jaeger, E., 1977, Subcommission on geo-chronology: convention on the use of decay constants in geo- and cosmochronology: Earth and Planet Science Letters, v. 36, p. 359-362.

Streckeisen, A.L., and LeMaitre, R.W., 1979, A chemical approximation to the modal QAPF classification of the igneous rocks: Neues Jahrbuch für Mineralogie Abhandlungen, v. 136, p. 169-206.

Templeman-Kluit, D.J., 1979, Transported cataclasite, ophiolite, and granodiorite in Yukon: evidence of arc-continent collision: Canada Geological Survey Paper 79-14, 27 p.

Tripp, R.B., Curtin, G.C., Day, G.W., Karlson, R.C., and Marsh, S.P., 1976, Maps showing mineralogical and geochemical data for heavy-mineral concentrates in the Tanacross quadrangle, Alaska: U.S. Geological Survey Miscellaneous Field Studies Map MF-7670, 2 sheets, scale 1: 500,000.

Turner, G., 1968, The distribution of potassium and argon in chondrites, *in* Ahrens, L.H., ed., Origin and distribution of the elements: London, Pergamon, p. 387-398.

U.S. Bureau of Mines, 1995, Final report of the mineral resource evaluation of the Bureau of Land Management Black River and Fortymile River subunits: U.S. Bureau of Mines Open-File Report 79-95, 197 p.

Weber, F.R., Wheeler, K.L., Rinehart, C.D., Chapman, R.M., and Blodgett, R.B., 1992, Geologic map of the Livengood quadrangle, Alaska: U.S. Geological Survey Open-File Report 92-562, 7 p.

Wheeler, J.O., and McFeeley, P., 1991, Tectonic assemblage map of the Canadian cordillera and adjacent parts of the United States of America: Geological Survey of Canada Map 1712A, scale 1:2,000,000.

Wilson, F.H., Smith, J.G, and Shew, Nora, 1985, Review of radiometric data from the Yukon crystalline terrane, Alaska and Yukon Territory: Canadian Journal of Earth Sciences, v. 22, p. 525-537.

Yeend, Warren, 1996, Gold placers of the historical Fortymile River region, Alaska: U.S. Geological Survey Bulletin 2125, 78 p.

Yesilyurt, Suleyman, 1994, Geology, geochemistry, and mineralization of the Liberty Bell gold mine, Alaska: Corvallis, Oregon State University, M.S. thesis, 189 p.

York, Derek, 1984, Cooling histories from $^{40}Ar/^{39}Ar$ age spectra: implications for Precambrian plate tectonics: Earth and Planetary Sciences Annual Review, v. 12, p. 383-409.

Reviewers: Jeanine Schmidt and Don Murphy

APPENDIX

Interpretation of $^{40}Ar/^{39}Ar$ data

For each mass spectrometer analysis, five Ar isotope abundances are measured. ^{36}Ar is used to determine the amount of atmospheric or initial Ar in the sample, ^{37}Ar provides an estimation of the Ca content in the mineral, ^{38}Ar provides an estimation of the Cl content, ^{39}Ar reflects the K content and ^{40}Ar is a mixture of initial and radiogenic Ar. The age of the sample is proportional to the the ratio of radiogenic ^{40}Ar to the amount of ^{39}Ar produced by neutron bombardment from ^{40}K. Using the previously determined potassium content of the standard, the absolute K, Ca and Cl contents can be calculated. These values are probably accurate to about 5 percent.

During a step heating experiment, a sample is heated to progressively higher temperatures, and for each step, or fraction, the argon isotopes are measured. Generally the first step is at 400 to 500°C and the last step is at 1,600°C, where the sample is completely melted and degassed of its argon. The sum of all gas released from all fractions is used to calculate what is called an "integrated" or "total gas" age. This age is equivalent to a conventional K-Ar age and is useful for comparing step heating results to K-Ar data. However, the $^{40}Ar/^{39}Ar$ method carries additional information in the age spectrum produced from the step heating process. Figures 3 to 11 show age spectra from our samples. The vertical axis is the apparent age of each fraction, shown by cross hatching. The height of each box reflects the ±1 sigma error bar. The width of each box shows the relative amount of argon (expressed as fraction of ^{39}Ar) released in each fraction. The lower temperature steps generally release argon from the margins of the minerals or from loosely bound sites and provide information about secondary, low-temperature events that could have caused slight argon loss or gain from the crystal. These reset ages are the first one or two fractions in the step heat process (Turner, 1968; York, 1984; McDougall and Harrison, 1988). Because of the small amount of gas released at low temperature, the calculated ages are generally not very precise. Detrital micas in hydrothermally altered sandstone yield $^{40}Ar/^{39}Ar$ reset ages that correlate well with the age of hydrothermal alteration based on geological evidence (Hitzman and others, 1994).

The higher temperature fractions reflect argon in the grain interiors or in tightly bound sites and most samples yield consistent ages for consecutive fractions. Three or more fractions whose ages are within 2 standard deviations of the mean and which have a total of more than 60 percent of the total gas released from the sample are considered to yield a plateau age. Plateau ages are conventionally interpreted as "true" formation ages, whereas integrated ages (and conventional K-Ar ages) are commonly subject to loss or gain of argon during later events. The plateau age of a sample reflects the time when the mineral cooled below its Ar closure temperature and argon was trapped in the crystal. The closure temperature is taken to be about 550°C for hornblende, about 300°C for muscovite, about 250 to 300°C for biotite, and about 200°C for K-feldspar (McDougall and Harrison, 1988). Consequently, one would expect the biotite plateau age to be younger than or equal to the hornblende plateau age from a given sample.

Ca/K and Cl/K ratios for fractions from samples present information about the distribution of Ca, K,and Cl in the materials heated, which can be useful in detecting contamination of mineral separates. Of the four minerals biotite, hornblende, K-feldspar, and muscovite, only hornblende contains appreciable Ca, and only biotite and hornblende contain appreciable Cl. Plagioclase and calcite (potential impurities) both have very high Ca/K and no Cl, and both release Ar at low temperatures. Because biotite has 5 to 10 times as much K as hornblende, but both contain similar levels of Cl when crystallized together, Cl/K is invariably much higher in hornblende

than in biotite. Consequently, whereas absolutely pure hornblende and biotite separates have Ca/K ratios of about 5 to 20 and less than 0.1, respectively, mixtures of these two minerals give rise to spectra having variable Ca/K ratios. Where the mineral separates have been hand picked, such mixtures invariably result from fine-grained inclusions of one mineral in another.

In our spectra, we note that such variable Ca/K ratios, implying inclusion behavior, is common in fractions where both hornblende and biotite occur in the same igenous rock. For such spectra, the lower temperature fractions with Ca/K<1 and Cl/K< 0.01 represent Ar released primarily from biotite, the highest temperature fraction (which typically shows maximum Ca/K and Cl/K ratios) represents Ar released predominantly from hornblende, and the mid-temperature fractions represent Ar released from combinations of the two (for example, fig. 5). Such spectra yield valuable information because the highest temperature fraction, even if a plateau is present, is more likely to indicate the primary crystallization age than is the plateau age. Conversely, potassium feldspar and muscovite spectra commonly exhibit a high Ca/K release at lower temperatures, which most likely reflects included plagioclase or calcite. Consequently, in addition to the age spectra, we present Ca/K and Cl/K spectra where they provide additional information about the age and thermal behavior of the main dated mineral (figs. 3-11).

Table 2. $^{40}Ar/^{39}Ar$ age data for samples from eastern interior Alaska

[Step-heat analyses performed at the University of Alaska Geochronology Laboratory by P. Layer using a Nuclide 6-60-SGA mass spectrometer system equipped with a Modifications Ltd. resistance-type furnace. Samples were heated for 45 minutes at the indicated temperatures. Irradiation parameter (J) calculated from standard MMhb-1 with an assumed age of 513.9 Ma. Fractions used in the calculation of plateau ages (table 1) are shown in bold. Measured $^{40}Ar/^{39}Ar$, $^{37}Ar/^{39}Ar$, and $^{36}Ar/^{39}Ar$ ratios are corrected for decay of ^{37}Ar and ^{39}Ar and for system blanks. Atmos., atmospheric; Kspar, potassium feldspar; $^{40}Ar^*$, radiogenic ^{40}Ar]

Temp. (°C)	Cumulative ^{39}Ar	$^{40}Ar/^{39}Ar$ measured	$^{37}Ar/^{39}Ar$ measured	$^{36}Ar/^{39}Ar$ measured	Volume ^{39}Ar x 10^{-12} mol/g	% Atmos. ^{40}Ar	$^{37}Ar_{Ca}/^{39}Ar_K$	$^{40}Ar^*/^{39}Ar_K$	Age (Ma)	±1σ (Ma)
1. Happy granite vein muscovite		Mass=0.0695 g		Weighted average of J from standards = 0.008140 ± 0.000025						
600	0.0201	14.689	0.060	0.015	4.040	30.147	0.060	10.241	144.5	5.6
700	0.0459	12.740	0.059	0.003	5.165	7.024	0.059	11.819	165.7	1.9
775	0.0857	14.899	0.004	0.003	7.987	6.675	0.004	13.878	193.1	1.2
850	**0.1912**	**16.093**	**0.000**	**0.001**	**21.163**	**2.527**	**0.000**	**15.658**	**216.4**	**0.5**
900	**0.3423**	**15.889**	**0.001**	**0.001**	**30.317**	**0.944**	**0.001**	**15.710**	**217.1**	**0.4**
950	**0.5152**	**15.271**	**0.000**	**0.000**	**34.677**	**0.743**	**0.000**	**15.129**	**209.5**	**0.3**
1,050	**0.6885**	**15.628**	**0.001**	**0.000**	**34.762**	**0.663**	**0.001**	**15.496**	**214.3**	**0.3**
1,100	**0.8381**	**15.853**	**0.001**	**0.000**	**30.012**	**0.425**	**0.001**	**15.757**	**217.7**	**0.4**
1,200	**0.9000**	**15.455**	**0.002**	**0.001**	**12.419**	**1.026**	**0.002**	**15.268**	**211.3**	**0.8**
1,600	**1.0000**	**16.133**	**0.002**	**0.002**	**20.060**	**3.910**	**0.002**	**15.475**	**214.0**	**0.5**
Integrated		15.606	0.004	0.001	200.602	2.165	0.004	15.240	211.0	0.6
2h. 70-Mile pluton hornblende		Mass=0.2790 g		Weighted average of J from standards = 0.008140 ± 0.000025						
600	0.0077	98.098	1.523	0.294	0.292	88.331	1.525	11.455	160.8	8.6
700	0.0319	17.087	0.201	0.013	0.911	21.637	0.201	13.369	186.4	2.7
775	0.0800	14.899	0.137	0.006	1.818	11.480	0.137	13.165	183.7	1.4
850	0.1164	14.059	0.269	0.004	1.376	8.408	0.269	12.853	179.5	1.8
925	0.1429	14.126	1.758	0.004	1.002	6.503	1.760	13.195	184.1	2.5
1,000	0.2284	14.049	2.866	0.003	3.228	3.989	2.871	13.487	187.9	0.8
1,050	**0.4440**	**13.409**	**2.949**	**0.002**	**8.140**	**2.214**	**2.955**	**13.109**	**182.9**	**0.4**
1,100	**0.7541**	**13.674**	**3.063**	**0.003**	**11.711**	**3.760**	**3.069**	**13.159**	**183.6**	**0.3**
1,150	**0.8251**	**13.434**	**3.511**	**0.002**	**2.680**	**2.224**	**3.519**	**13.137**	**183.3**	**0.9**
1,200	**0.9776**	**13.667**	**4.337**	**0.003**	**5.761**	**3.933**	**4.349**	**13.139**	**183.3**	**0.5**
1,300	**0.9930**	**13.571**	**4.451**	**0.002**	**0.582**	**2.971**	**4.464**	**13.178**	**183.8**	**4.2**
1,400	0.9996	17.389	4.784	0.012	0.247	18.056	4.799	14.270	198.3	9.8
1,600	1.0000	187.793	4.320	0.601	0.017	94.423	4.332	10.501	148.0	150.4
Integrated		14.550	2.923	0.005	37.763	9.546	2.929	13.160	183.6	0.6
2b. 70-Mile pluton biotite		Mass=0.0571 g		Weighted average of J from standards = 0.008140 ± 0.000025						
600	0.0124	72.693	0.030	0.206	2.306	83.626	0.030	11.898	166.8	5.3
700	**0.2641**	**14.372**	**0.002**	**0.004**	**46.975**	**8.696**	**0.002**	**13.096**	**182.7**	**0.3**
775	**0.4693**	**13.283**	**0.001**	**0.004**	**38.300**	**9.940**	**0.001**	**11.937**	**167.3**	**0.4**
825	**0.5570**	**13.327**	**0.002**	**0.000**	**16.355**	**1.003**	**0.002**	**13.165**	**183.7**	**0.8**
875	**0.5969**	**13.434**	**0.010**	**0.000**	**7.461**	**0.270**	**0.010**	**13.370**	**186.4**	**1.6**
925	**0.6377**	**13.602**	**0.033**	**0.000**	**7.608**	**0.524**	**0.033**	**13.503**	**188.1**	**1.6**
975	**0.7088**	**13.451**	**0.025**	**0.000**	**13.268**	**0.723**	**0.025**	**13.326**	**185.8**	**0.9**
1,025	**0.7807**	**13.232**	**0.059**	**0.000**	**13.422**	**0.418**	**0.059**	**13.149**	**183.4**	**0.9**
1,100	**0.9402**	**13.142**	**0.038**	**0.000**	**29.763**	**0.318**	**0.038**	**13.072**	**182.4**	**0.4**
1,200	**0.9806**	**13.352**	**0.193**	**0.001**	**7.534**	**1.688**	**0.193**	**13.100**	**182.8**	**1.6**
1,600	1.0000	17.974	0.235	0.015	3.621	24.479	0.235	13.555	188.8	3.3
Integrated		14.394	0.028	0.005	186.613	10.186	0.028	12.902	180.2	0.6
3. Diamond Mtn. hornblende		Mass=0.2298 g		Weighted average of J from standards = 0.008318 ± 0.000027						
600	0.0014	812.108	1.759	2.683	0.036	97.600	1.761	19.509	271.3	80.5
700	0.0048	41.754	0.749	0.111	0.085	78.365	0.750	9.032	130.7	36.8
800	0.0146	28.502	0.471	0.056	0.250	58.192	0.472	11.908	170.4	12.3
900	0.0453	19.420	0.402	0.021	0.783	32.161	0.402	13.158	187.4	3.9
1,000	0.0755	17.548	1.201	0.014	0.770	23.528	1.202	13.408	190.8	3.9
1,050	**0.1112**	**16.103**	**3.593**	**0.008**	**0.908**	**13.774**	**3.602**	**13.893**	**197.3**	**3.3**
1,075	**0.1590**	**15.233**	**3.979**	**0.005**	**1.218**	**8.711**	**3.989**	**13.916**	**197.6**	**2.5**
1,100	**0.2512**	**14.963**	**4.221**	**0.005**	**2.349**	**7.471**	**4.233**	**13.857**	**196.8**	**1.3**
1,150	**0.6163**	**14.535**	**4.356**	**0.003**	**9.304**	**4.190**	**4.368**	**13.938**	**197.9**	**0.4**
1,200	**0.7364**	**14.322**	**4.042**	**0.003**	**3.060**	**3.683**	**4.053**	**13.804**	**196.1**	**1.0**
1,600	**1.0000**	**15.592**	**4.346**	**0.007**	**6.715**	**11.039**	**4.358**	**13.885**	**197.2**	**0.5**
Integrated		16.520	3.988	0.010	25.479	16.358	3.998	13.830	196.4	0.7

Table 2. $^{40}Ar/^{39}Ar$ age data for samples from eastern interior Alaska - Continued

Temp. (°C)	Cumulative ^{39}Ar	$^{40}Ar/^{39}Ar$ measured	$^{37}Ar/^{39}Ar$ measured	$^{36}Ar/^{39}Ar$ measured	Volume ^{39}Ar x 10^{-12} mol/g	% Atmos. ^{40}Ar	$^{37}Ar_{Ca}/^{39}Ar_K$	$^{40}Ar^*/^{39}Ar_K$	Age (Ma)	±1σ (Ma)
4. Butte Creek hornblendite	**hornblende**	Mass=0.2681 g		Weighted average of J from standards = 0.008119 ± 0.000032						
600	0.0093	48.883	0.976	0.134	0.360	80.825	0.977	9.374	132.3	7.3
700	0.0421	15.892	0.195	0.014	1.266	25.343	0.195	11.845	165.6	2.0
775	0.1030	14.291	0.149	0.005	2.351	10.908	0.149	12.707	177.1	1.1
850	0.1546	13.467	0.284	0.003	1.992	7.354	0.284	12.452	173.7	1.3
925	0.2055	13.359	0.859	0.004	1.963	7.276	0.860	12.367	172.6	1.3
975	**0.2490**	**14.390**	**3.166**	**0.006**	**1.677**	**11.486**	**3.172**	**12.738**	**177.5**	**1.5**
1,025	**0.3945**	**13.871**	**3.184**	**0.003**	**5.617**	**5.008**	**3.191**	**13.176**	**183.4**	**0.5**
1,075	**0.6254**	**13.958**	**3.244**	**0.003**	**8.912**	**5.375**	**3.251**	**13.208**	**183.8**	**0.3**
1,125	**0.7497**	**13.977**	**3.159**	**0.003**	**4.798**	**5.297**	**3.166**	**13.237**	**184.1**	**0.6**
1,200	**0.9652**	**14.014**	**4.016**	**0.004**	**8.318**	**5.314**	**4.027**	**13.277**	**184.7**	**0.3**
1,300	0.9954	13.939	4.439	0 005	1.167	8.072	4.452	12.825	178.7	2.1
1,600	1.0000	52.237	4.473	0.132	0.176	74.230	4.486	13.493	187.5	13.9
Integrated		14.506	2.847	0.006	38.597	10.381	2.852	12.999	181.0	0.7
5h. Ketchumstuck Mtn.	**hornblende**	Mass=0.3372 g		Weighted average of J from standards = 0.008277 ± 0.000033						
600	0.0035	95.140	3.932	0.296	0.069	91.529	3.942	8.078	116.8	30.9
700	0.0051	19.104	1.142	0.054	0.031	83.244	1.143	3.199	47.1	72.4
775	0.0077	19.460	0.788	0.029	0.052	43.887	0.789	10.909	156.0	40.2
850	0.0152	18.098	0.617	0.021	0.148	34.076	0.617	11.917	169.7	14.1
925	0.0312	17.826	0.615	0.018	0.316	28.920	0.615	12.655	179.7	6.5
1,000	0.0402	14.828	1.586	0.008	0.178	14.844	1.587	12.616	179.2	11.6
1,050	**0.0535**	**15.747**	**4.952**	**0.006**	**0.263**	**8.832**	**4.968**	**14.377**	**202.8**	**7.8**
1,100	**0.1452**	**15.151**	**5.186**	**0.003**	**1.811**	**3.756**	**5.204**	**14.604**	**205.9**	**1.1**
1,150	**0.6314**	**14.837**	**5.156**	**0.002**	**9.608**	**1.560**	**5.173**	**14.627**	**206.2**	**0.3**
1,200	**0.7651**	**14.808**	**5.807**	**0.003**	**2.642**	**2.322**	**5.829**	**14.491**	**204.4**	**0.8**
1,300	**0.9942**	**14.914**	**5.928**	**0.003**	**4.526**	**2.532**	**5.951**	**14.565**	**205.3**	**0.5**
1,600	1.0000	41.497	3.709	0.100	0.115	70.367	3.718	12.318	175.2	18.0
Integrated		15.419	5.251	0.005	19.760	6.397	5.269	14.455	203.9	0.8
5b. Ketchumstuck Mtn.	**biotite**	Mass=0.0792 g		Weighted average of J from standards = 0.008277 ± 0.000033						
600	0.0055	34.137	0.073	0.093	0.879	80.408	0.073	6.683	97.1	10.5
700	0.0142	14.861	0.042	0.017	1.404	33.949	0.042	9.797	140.7	6.4
775	0.0579	15.525	0.017	0.006	7.037	12.050	0.017	13.629	192.8	1.3
850	0.2081	14.943	0.005	0.001	24.167	2.966	0.005	14.472	204.1	0.4
900	**0.4105**	**14.867**	**0.005**	**0.001**	**32.580**	**1.184**	**0.005**	**14.663**	**206.6**	**0.3**
950	**0.5208**	**15.060**	**0.015**	**0.001**	**17.751**	**1.755**	**0.015**	**14.768**	**208.0**	**0.5**
1,000	**0.6998**	**15.155**	**0.034**	**0.001**	**28.795**	**1.315**	**0.034**	**14.928**	**210.2**	**0.4**
1,050	**0.8583**	**14.836**	**0.128**	**0.000**	**25.515**	**0.561**	**0.128**	**14.726**	**207.5**	**0.4**
1,100	**0.9823**	**14.761**	**0.220**	**0.000**	**19.949**	**0.538**	**0.220**	**14.655**	**206.5**	**0.5**
1,600	**1.0000**	**15.937**	**0.669**	**0.005**	**2.856**	**8.394**	**0.670**	**14.579**	**205.5**	**3.0**
Integrated		15.086	0.071	0.002	160.934	3.246	0.071	14.569	205.4	0.8
6. Ruby Creek granite	**biotite**	Mass=0.0514 g		Weighted average of J from standards = 0.008140 ± 0.000025						
600	0.0463	7.894	0.047	0.008	8.106	31.850	0.047	5.360	77.0	1.7
700	**0.2055**	**7.430**	**0.020**	**0.001**	**27.878**	**4.375**	**0.020**	**7.078**	**101.1**	**0.5**
775	**0.4377**	**7.182**	**0.005**	**0.000**	**40.662**	**0.481**	**0.005**	**7.119**	**101.6**	**0.4**
850	**0.5328**	**7.123**	**0.013**	**0.000**	**16.652**	**0.726**	**0.013**	**7.043**	**100.6**	**0.8**
925	**0.5781**	**7.135**	**0.030**	**-0.001**	**7.925**	**-2.112**	**0.030**	**7.256**	**103.5**	**1.8**
975	**0.6579**	**7.429**	**0.029**	**0.000**	**13.979**	**-1.081**	**0.029**	**7.481**	**106.6**	**1.0**
1,025	**0.7986**	**7.207**	**0.016**	**0.000**	**24.642**	**0.562**	**0.016**	**7.138**	**101.9**	**0.6**
1,075	**0.9289**	**7.165**	**0.031**	**0.000**	**22.815**	**0.041**	**0.031**	**7.134**	**101.8**	**0.6**
1,125	**0.9668**	**7.106**	**0.141**	**0.000**	**6.628**	**-1.533**	**0.141**	**7.186**	**102.6**	**2.1**
1,200	**0.9792**	**6.970**	**0.747**	**0.000**	**2.172**	**-2.749**	**0.748**	**7.136**	**101.9**	**6.4**
1,600	1.0000	12.976	0.408	0.021	3.648	47.302	0.409	6.825	97.5	3.8
Integrated		7.383	0.041	0.001	175.108	4.003	0.041	7.060	100.8	0.4
7. Mt. Harper granite	**biotite**	Mass=0.0836 g		Weighted average of J from standards = 0.008277 ± 0.000033						
600	0.0094	44.808	0.164	0.141	1.440	93.188	0.164	3.051	45.0	6.3
700	0.0210	12.769	0.146	0.023	1.790	54.073	0.146	5.852	85.3	4.9
775	0.0518	9.821	0.049	0.010	4.736	29.056	0.049	6.947	100.9	1.8
850	**0.1790**	**7.788**	**0.012**	**0.002**	**19.582**	**7.564**	**0.012**	**7.173**	**104.0**	**0.5**
900	**0.3385**	**7.651**	**0.007**	**0.001**	**24.552**	**4.410**	**0.007**	**7.286**	**105.6**	**0.4**
950	**0.4314**	**7.799**	**0.021**	**0.001**	**14.305**	**5.079**	**0.021**	**7.376**	**106.9**	**0.6**
1,000	**0.4928**	**8.129**	**0.090**	**0.002**	**9.450**	**7.914**	**0.090**	**7.460**	**108.1**	**0.9**
1,050	**0.6050**	**7.594**	**0.038**	**0.001**	**17.257**	**2.398**	**0.038**	**7.384**	**107.0**	**0.5**
1,100	**0.8537**	**7.385**	**0.029**	**0.000**	**38.292**	**1.020**	**0.029**	**7.282**	**105.6**	**0.3**
1,200	**0.9691**	**7.403**	**0.178**	**0.000**	**17.763**	**1.821**	**0.178**	**7.240**	**105.0**	**0.5**
1,600	1.0000	7.864	0.366	0.003	4.749	9.746	0.366	7.073	102.6	1.8
Integrated		8.091	0.058	0.003	153.915	10.424	0.058	7.222	104.7	0.4

Table 2. $^{40}Ar/^{39}Ar$ age data for samples from eastern interior Alaska - Continued

Temp. (°C)	Cumulative ^{39}Ar	$^{40}Ar/^{39}Ar$ measured	$^{37}Ar/^{39}Ar$ measured	$^{36}Ar/^{39}Ar$ measured	Volume ^{39}Ar x 10^{-12} mol/g	% Atmos. ^{40}Ar	$^{37}Ar_{Ca}/^{39}Ar_K$	$^{40}Ar^*/^{39}Ar_K$	Age (Ma)	±1σ (Ma)
8. Lucky 13 Prospect	**biotite**	Mass=0.0656 g		Weighted average of J from standards = 0.008140 ± 0.000025						
600	0.0115	18.593	0.039	0.047	2.201	75.258	0.039	4.593	66.2	4.7
700	**0.0759**	**7.151**	**0.004**	**0.002**	**12.369**	**10.349**	**0.004**	**6.385**	**91.4**	**0.8**
775	**0.2480**	**6.567**	**0.002**	**0.000**	**33.069**	**-0.477**	**0.002**	**6.570**	**94.0**	**0.3**
825	**0.3703**	**6.527**	**0.002**	**0.000**	**23.476**	**-1.423**	**0.002**	**6.591**	**94.3**	**0.5**
875	**0.4518**	**6.496**	**0.005**	**-0.001**	**15.652**	**-2.438**	**0.005**	**6.625**	**94.8**	**0.7**
925	**0.5126**	**6.642**	**0.020**	**0.000**	**11.679**	**-1.786**	**0.020**	**6.731**	**96.2**	**0.9**
975	**0.6220**	**6.563**	**0.005**	**0.000**	**21.022**	**-1.602**	**0.005**	**6.639**	**95.0**	**0.5**
1,025	**0.8180**	**6.538**	**0.002**	**0.000**	**37.631**	**-0.651**	**0.002**	**6.551**	**93.7**	**0.3**
1,100	**0.9657**	**6.523**	**0.008**	**0.000**	**28.379**	**-1.577**	**0.008**	**6.597**	**94.4**	**0.4**
1,200	0.9891	6.199	0.079	-0.002	4.491	-11.246	0.079	6.865	98.1	2.4
1,600	1.0000	7.704	0.217	0.004	2.091	14.441	0.217	6.568	94.0	5.1
Integrated		6.728	0.009	0.000	192.061	1.968	0.009	6.567	93.9	0.3
9. Upper Granite Creek	**biotite**	Mass=0.0459 g		Weighted average of J from standards = 0.008268 ± 0.000034						
600	0.0057	44.716	0.225	0.146	0.914	96.344	0.225	1.634	24.2	18.1
700	0.0218	11.560	0.058	0.024	2.606	61.331	0.058	4.459	65.3	6.2
775	**0.0733**	**7.795**	**0.033**	**0.005**	**8.293**	**18.894**	**0.033**	**6.299**	**91.6**	**1.9**
850	**0.2442**	**6.585**	**0.009**	**0.001**	**27.547**	**3.602**	**0.009**	**6.320**	**91.9**	**0.6**
900	**0.3553**	**6.574**	**0.011**	**0.001**	**17.921**	**2.528**	**0.011**	**6.379**	**92.7**	**0.9**
950	**0.4370**	**6.777**	**0.022**	**0.001**	**13.161**	**2.526**	**0.022**	**6.578**	**95.5**	**1.2**
1,000	**0.5224**	**7.024**	**0.041**	**0.001**	**13.765**	**3.267**	**0.041**	**6.767**	**98.2**	**1.2**
1,050	**0.6870**	**6.569**	**0.037**	**0.000**	**26.547**	**0.911**	**0.037**	**6.481**	**94.2**	**0.6**
1,100	**0.8815**	**6.395**	**0.020**	**0.000**	**31.344**	**0.327**	**0.020**	**6.345**	**92.3**	**0.5**
1,200	**0.9746**	**6.402**	**0.137**	**0.000**	**15.006**	**1.316**	**0.137**	**6.290**	**91.5**	**1.1**
1,600	**1.0000**	**7.195**	**0.353**	**0.003**	**4.100**	**10.910**	**0.353**	**6.386**	**92.8**	**3.9**
Integrated		6.955	0.044	0.002	161.202	8.195	0.044	6.358	92.4	0.5
10. Sect. 21 Prospect	**vein muscovite**	Mass=0.0488 g		Weighted average of J from standards = 0.008140 ± 0.000025						
500	0.0046	35.218	-0.008	0.099	0.996	82.929	-0.008	6.007	86.1	14.9
600	0.0169	10.193	0.002	0.010	2.648	29.604	0.002	7.155	102.1	5.5
700	0.0608	8.175	0.000	0.002	9.502	8.953	0.000	7.417	105.8	1.5
775	**0.1516**	**7.639**	**-0.001**	**0.001**	**19.607**	**4.565**	**-0.001**	**7.263**	**103.6**	**0.8**
850	**0.3115**	**7.407**	**0.000**	**0.001**	**34.534**	**2.706**	**0.000**	**7.179**	**102.5**	**0.4**
900	**0.5106**	**7.330**	**0.000**	**0.000**	**43.028**	**1.528**	**0.000**	**7.190**	**102.6**	**0.4**
950	**0.7187**	**7.312**	**0.000**	**0.000**	**44.939**	**1.246**	**0.000**	**7.193**	**102.7**	**0.3**
1,000	**0.8284**	**7.320**	**0.000**	**0.000**	**23.712**	**1.251**	**0.000**	**7.200**	**102.8**	**0.6**
1,050	**0.9146**	**7.313**	**0.000**	**0.000**	**18.612**	**1.148**	**0.000**	**7.200**	**102.8**	**0.8**
1,100	**0.9835**	**7.317**	**0.000**	**0.000**	**14.892**	**1.846**	**0.000**	**7.154**	**102.1**	**1.0**
1,200	0.9961	8.928	0.002	0.007	2.724	24.791	0.002	6.693	95.7	5.4
1,600	1.0000	62.594	-0.001	0.193	0.839	91.201	-0.001	5.505	79.1	17.7
Integrated		7.799	0.000	0.002	216.033	7.515	0.000	7.186	102.6	0.4
11. Mosquito Prospect	**vein Kspar**	Mass=0.0785 g		Weighted average of J from standards = 0.008277 ± 0.000033						
500	0.0040	49.636	0.000	0.150	0.977	89.210	0.000	5.353	78.2	9.6
600	0.0062	23.826	0.005	0.059	0.542	73.353	0.005	6.341	92.3	17.2
700	0.0255	15.661	0.002	0.036	4.738	68.271	0.002	4.960	72.6	2.0
800	0.0974	10.796	0.002	0.021	17.633	56.583	0.002	4.675	68.5	0.6
900	0.1764	6.502	0.002	0.006	19.375	28.486	0.002	4.629	67.8	0.5
975	0.2080	5.803	0.003	0.004	7.752	20.710	0.003	4.578	67.1	1.2
1,050	0.2591	6.974	0.003	0.008	12.543	34.743	0.003	4.532	66.4	0.8
1,125	0.3434	7.384	0.003	0.009	20.665	37.279	0.003	4.613	67.6	0.5
1,200	0.4939	7.249	0.002	0.008	36.915	33.803	0.002	4.780	70.0	0.3
1,300	0.7639	7.386	0.001	0.008	66.237	34.019	0.001	4.854	71.1	0.2
1,600	0.9955	7.250	0.001	0.008	56.805	32.674	0.001	4.862	71.2	0.2
1,605	1.0000	9.105	0.004	0.013	1.098	43.898	0.004	5.092	74.5	8.6
Integrated		7.810	0.002	0.010	245.281	38.609	0.002	4.777	70.0	0.3

Table 2. $^{40}Ar/^{39}Ar$ age data for samples from eastern interior Alaska - Continued.

Temp. (°C)	Cumulative ^{39}Ar	$^{40}Ar/^{39}Ar$ measured	$^{37}Ar/^{39}Ar$ measured	$^{36}Ar/^{39}Ar$ measured	Volume ^{39}Ar x 10^{-12} mol/g	% Atmos. ^{40}Ar	$^{37}Ar_{Ca}/^{39}Ar_K$	$^{40}Ar^*/^{39}Ar_K$	Age (Ma)	±1σ (Ma)
12. Peternie prospect vein Kspar			Mass=0.0643 g		Weighted average of J from standards = 0.008277 ± 0.000033					
500	0.0061	47.899	0.014	0.144	0.886	88.889	0.014	5.319	77.7	12.9
600	0.0176	11.541	0.011	0.013	1.663	32.630	0.011	7.756	112.2	6.8
700	**0.0961**	**7.462**	**0.007**	**0.001**	**11.329**	**4.579**	**0.007**	**7.093**	**102.9**	**1.0**
800	**0.2994**	**7.068**	**0.006**	**0.000**	**29.359**	**0.826**	**0.006**	**6.981**	**101.3**	**0.4**
900	**0.5127**	**7.080**	**0.003**	**0.000**	**30.816**	**-0.498**	**0.003**	**7.086**	**102.8**	**0.4**
975	**0.6217**	**7.198**	**0.003**	**0.000**	**15.741**	**1.531**	**0.003**	**7.060**	**102.5**	**0.7**
1,050	**0.7170**	**7.340**	**0.004**	**0.001**	**13.764**	**3.613**	**0.004**	**7.047**	**102.3**	**0.8**
1,100	**0.7665**	**7.347**	**0.005**	**0.000**	**7.149**	**0.532**	**0.005**	**7.280**	**105.6**	**1.6**
1,150	**0.8328**	**7.432**	**0.005**	**0.001**	**9.575**	**3.925**	**0.005**	**7.113**	**103.2**	**1.2**
1,200	**0.9074**	**7.667**	**0.006**	**0.001**	**10.779**	**5.568**	**0.006**	**7.213**	**104.6**	**1.1**
1,275	**0.9734**	**7.807**	**0.001**	**0.002**	**9.532**	**7.495**	**0.001**	**7.196**	**104.4**	**1.2**
1,350	0.9819	8.257	0.004	-0.001	1.227	-2.877	0.004	8.465	122.2	9.1
1,600	1.0000	8.330	0.004	0.001	2.608	4.949	0.004	7.891	114.1	4.3
Integrated		7.608	0.004	0.002	144.428	6.191	0.004	7.110	103.2	0.5
13. Purdy prospect alteration biotite			Mass=0.0552 g		Weighted average of J from standards = 0.008268 ± 0.000034					
600	0.0057	21.844	0.427	0.055	0.610	73.892	0.427	5.697	83.0	21.8
700	0.0340	11.889	0.172	0.010	3.042	25.817	0.172	8.799	126.7	4.3
775	**0.1197**	**13.563**	**0.043**	**0.003**	**9.199**	**6.452**	**0.043**	**12.662**	**179.6**	**1.4**
825	**0.2206**	**13.174**	**0.027**	**0.001**	**10.824**	**1.295**	**0.027**	**12.975**	**183.9**	**1.2**
875	**0.3010**	**13.346**	**0.035**	**0.001**	**8.635**	**1.155**	**0.035**	**13.163**	**186.4**	**1.5**
875	**0.3336**	**13.312**	**0.037**	**0.000**	**3.502**	**0.038**	**0.037**	**13.279**	**187.9**	**3.6**
925	**0.3781**	**13.450**	**0.059**	**0.000**	**4.773**	**0.905**	**0.059**	**13.301**	**188.2**	**2.6**
975	**0.4368**	**13.831**	**0.130**	**0.001**	**6.304**	**2.106**	**0.130**	**13.513**	**191.1**	**2.0**
1,025	**0.5316**	**13.768**	**0.214**	**0.001**	**10.165**	**1.811**	**0.214**	**13.493**	**190.8**	**1.2**
1,100	**0.7202**	**13.362**	**0.575**	**0.000**	**20.251**	**0.563**	**0.575**	**13.263**	**187.7**	**0.6**
1,200	**0.9460**	**13.192**	**0.742**	**0.001**	**24.228**	**1.242**	**0.742**	**13.006**	**184.3**	**0.6**
1,600	**1.0000**	**13.765**	**1.812**	**0.003**	**5.800**	**6.300**	**1.814**	**12.886**	**182.7**	**2.2**
Integrated		13.417	0.422	0.002	107.332	3.188	0.422	12.965	183.7	0.8
14. Flume Creek Prospect alteration muscovite			Mass=0.0080g		Weighted average of J from standards = 0.007869 ± 0.000025					
600	**0.0346**	**12.691**	**0.077**	**0.013**	**3.605**	**29.883**	**0.077**	**8.879**	**121.8**	**29.7**
700	**0.1893**	**6.282**	**0.640**	**-0.003**	**16.105**	**-16.077**	**0.640**	**7.262**	**100.3**	**6.7**
775	**0.3663**	**6.255**	**1.057**	**-0.003**	**18.430**	**-15.021**	**1.057**	**7.167**	**99.0**	**5.9**
825	**0.5774**	**5.987**	**0.035**	**-0.004**	**21.978**	**-20.830**	**0.035**	**7.200**	**99.4**	**4.9**
875	**0.7056**	**5.414**	**-0.005**	**-0.006**	**13.349**	**-30.818**	**-0.005**	**7.045**	**97.3**	**8.1**
925	0.7743	4.370	0.006	-0.017	7.160	-114.487	0.006	9.311	127.6	14.9
975	0.8508	4.914	0.008	-0.010	7.963	-60.436	0.008	7.838	108.0	13.6
1,075	0.9214	4.739	0.005	-0.011	7.349	-67.286	0.005	7.879	108.5	14.7
1,200	0.9729	4.932	0.008	-0.008	5.367	-50.250	0.008	7.368	101.7	20.2
1,600	1.0000	15.572	0.323	0.009	2.818	17.441	0.323	12.835	173.6	37.0
Integrated		6.163	0.306	-0.005	104.126	-24.609	0.306	7.645	105.4	3.3
15. Blue Lead mine alteration muscovite			Mass=0.0587 g		Weighted average of J from standards = 0.008277 ± 0.000033					
600	0.0124	15.303	0.037	0.033	2.321	63.598	0.037	5.560	81.2	5.4
700	**0.0311**	**9.479**	**0.125**	**0.007**	**3.514**	**22.203**	**0.125**	**7.352**	**106.6**	**3.5**
775	**0.0628**	**8.694**	**0.061**	**0.004**	**5.945**	**13.943**	**0.061**	**7.457**	**108.1**	**2.1**
850	**0.1134**	**8.152**	**0.005**	**0.002**	**9.487**	**8.825**	**0.005**	**7.407**	**107.3**	**1.3**
900	**0.2087**	**7.819**	**0.001**	**0.002**	**17.892**	**6.335**	**0.001**	**7.296**	**105.8**	**0.7**
950	**0.4158**	**7.556**	**0.001**	**0.001**	**38.851**	**3.834**	**0.001**	**7.238**	**105.0**	**0.3**
1,000	**0.6161**	**7.548**	**0.002**	**0.001**	**37.571**	**3.995**	**0.002**	**7.219**	**104.7**	**0.3**
1,050	**0.7347**	**7.509**	**0.003**	**0.001**	**22.242**	**4.156**	**0.003**	**7.170**	**104.0**	**0.7**
1,100	**0.8454**	**7.564**	**0.003**	**0.001**	**20.772**	**2.265**	**0.003**	**7.364**	**106.7**	**0.6**
1,200	**0.9846**	**7.466**	**0.004**	**0.000**	**26.105**	**1.107**	**0.004**	**7.355**	**106.6**	**0.5**
1,600	1.0000	8.125	0.049	0.001	2.898	4.270	0.049	7.751	112.2	4.3
Integrated		7.769	0.008	0.002	187.597	6.118	0.008	7.267	105.4	0.5

Table 3. $^{40}Ar/^{39}Ar$ single crystal age data for Ptarmigan Hill samples, eastern interior Alaska

[Step-heat analyses performed at the University of Alaska Geochronology Laboratory by P. Layer using a VG3600 mass spectrometer system equipped with a 6 Watt argon-ion laser. Samples were heated for 30 seconds at the indicated laser power. Irradiation parameter (J) calculated from standard MMhb-1 with an assumed age of 513.9 Ma. Fractions used in the calculation of plateau ages (table 1) are shown in bold. Measured $^{40}Ar/^{39}Ar$, $^{37}Ar/^{39}Ar$, and $^{36}Ar/^{39}Ar$ ratios are corrected for decay of ^{37}Ar and ^{39}Ar and for system blanks. Atmos., atmospheric; $^{40}Ar^*$, radiogenic ^{40}Ar]

Laser power (mW)	Cumulative ^{39}Ar	$^{40}Ar/^{39}Ar$ measured	$^{37}Ar/^{39}Ar$ measured	$^{36}Ar/^{39}Ar$ measured	% Atmos. ^{40}Ar	$^{37}Ar_{Ca}/^{39}Ar_K$	$^{40}Ar^*/^{39}Ar_K$	Age (Ma)	±1σ (Ma)
16a. Ptarmigan Hill muscovite	Single crystal dating	Average of J from standards =0.006436 ± 0.000028							
50	0.0003	5.128	0.042	0.011	66.291	0.042	1.719	19.8	37.7
100	0.0034	9.274	0.003	0.015	48.368	0.003	4.774	54.6	4.1
150	0.0078	8.669	0.001	0.010	32.708	0.001	5.814	66.3	3.3
200	0.0131	6.567	0.006	0.002	11.182	0.006	5.807	66.2	1.8
300	0.0246	7.079	0.004	0.004	16.971	0.004	5.853	66.7	1.5
500	0.0592	7.225	0.000	0.001	3.668	0.000	6.932	78.7	0.6
700	0.1607	7.441	0.000	0.000	0.011	0.000	7.412	84.1	0.3
1,000	0.3515	7.282	0.000	0.000	0.034	0.000	7.251	82.3	0.2
1,500	0.8340	7.063	0.000	0.000	0.011	0.000	7.033	79.9	0.2
2,000	0.9497	7.280	0.000	0.000	-0.476	0.000	7.285	82.7	0.2
5,000	1.0000	7.098	-0.001	0.000	-0.462	-0.001	7.102	80.6	0.4
Integrated		7.186	0.000	0.000	0.691	0.000	7.108	80.7	0.4
16b. Ptarmigan Hill muscovite	Single crystal dating	Average of J from standards = 0.006436 ± 0.000028							
100	0.0019	15.976	0.004	0.037	68.052	0.004	5.095	58.2	19.5
300	0.0118	9.837	0.008	0.011	32.825	0.008	6.589	74.9	1.7
500	0.0363	10.246	0.004	0.008	22.558	0.004	7.913	89.6	1.3
650	**0.0885**	**8.549**	**0.000**	**0.001**	**3.325**	**0.000**	**8.237**	**93.2**	**0.7**
800	**0.2292**	**8.119**	**0.002**	**0.000**	**0.214**	**0.002**	**8.073**	**91.4**	**0.3**
900	**0.3937**	**8.162**	**0.010**	**0.000**	**0.564**	**0.010**	**8.088**	**91.5**	**0.2**
1,000	**0.6151**	**8.150**	**0.070**	**0.000**	**0.706**	**0.070**	**8.064**	**91.3**	**0.2**
1,100	**0.8079**	**8.195**	**-0.014**	**0.000**	**0.294**	**-0.014**	**8.142**	**92.1**	**0.3**
1,200	**0.8559**	**8.121**	**-0.086**	**0.000**	**-0.888**	**-0.086**	**8.164**	**92.4**	**0.8**
1,300	**0.8758**	**8.344**	**-0.221**	**0.000**	**-0.648**	**-0.221**	**8.368**	**94.6**	**1.7**
1,400	**0.8864**	**8.393**	**-0.441**	**-0.001**	**-3.471**	**-0.441**	**8.652**	**97.8**	**3.4**
1,500	**0.8939**	**8.531**	**-0.616**	**-0.002**	**-7.245**	**-0.616**	**9.115**	**102.8**	**6.7**
2,000	**0.9393**	**8.156**	**-0.102**	**0.000**	**-1.115**	**-0.102**	**8.217**	**93.0**	**0.9**
5,000	**0.9953**	**8.204**	**-0.082**	**0.000**	**-0.621**	**-0.082**	**8.226**	**93.1**	**0.7**
9,000	1.0000	9.050	-0.973	-0.002	-6.906	-0.972	9.638	108.6	5.9
Integrated		8.276	-0.017	0.000	1.568	-0.017	8.117	91.9	0.4
16c. Ptarmigan Hill muscovite	Single crystal dating	Average of J from standards = 0.006436 ± 0.000028							
100	0.0019	13.648	-0.040	0.026	56.833	-0.040	5.879	67.0	33.7
200	0.0060	12.583	-0.018	0.028	66.166	-0.018	4.247	48.7	16.4
450	0.0258	12.133	-0.002	0.015	37.292	-0.002	7.590	86.0	3.4
600	**0.0777**	**8.262**	**-0.001**	**0.001**	**1.930**	**-0.001**	**8.074**	**91.4**	**1.1**
750	**0.2047**	**8.022**	**-0.001**	**0.000**	**-0.262**	**-0.001**	**8.015**	**90.7**	**0.6**
900	**0.3883**	**7.982**	**0.000**	**0.000**	**0.264**	**0.000**	**7.932**	**89.8**	**0.4**
1,050	**0.5684**	**8.059**	**0.000**	**0.000**	**1.159**	**0.000**	**7.937**	**89.9**	**0.4**
1,200	**0.7403**	**8.045**	**0.000**	**0.000**	**0.460**	**0.000**	**7.980**	**90.4**	**0.5**
1,350	**0.8489**	**8.001**	**0.000**	**0.000**	**-0.263**	**0.000**	**7.993**	**90.5**	**0.6**
1,500	**0.8908**	**7.997**	**0.001**	**0.000**	**-0.101**	**0.001**	**7.976**	**90.3**	**1.8**
2,000	**0.9181**	**8.062**	**0.055**	**0.000**	**-1.335**	**0.055**	**8.141**	**92.1**	**2.0**
5,000	**0.9974**	**8.030**	**0.000**	**0.000**	**0.153**	**0.000**	**7.989**	**90.5**	**0.7**
9,000	1.0000	8.007	0.040	0.008	31.350	0.040	5.477	62.5	16.7
Integrated		8.147	0.001	0.001	2.129	0.001	7.945	90.0	0.5

Age of Formation of Kaguyak Caldera, eastern Aleutian arc, Alaska, Estimated by Tephrochronology

By James R. Riehle, Richard B. Waitt, Charles E. Meyer, and Lewis C. Calk

ABSTRACT

Kaguyak Crater is the only Holocene caldera on the Alaska Peninsula whose age of formation has not yet been determined. Datable materials in a dacitic block-and-ash-flow deposit around the caldera have been sought without success. However, tephra deposits at sites north and east of the caldera have been found that are mineralogically and chemically similar to the ash-flow deposits. These deposits can potentially provide an age by correlation, but a complication is that some Holocene pyroclasts of nearby Augustine Volcano are mineralogically and chemically similar to the Kaguyak deposits. Thus, source assignment of the distal Kaguyak-like tephra deposits has been uncertain.

We have found that the compositions of ilmenite grains in Kaguyak and Augustine lapilli are uniquely indicative of these sources and thereby provide a basis for inferring sources of the distal deposits. FeO and TiO_2 contents of ilmenite grains in most of the distal deposits plot in fields characteristic of either Kaguyak or Augustine. Deposits at two sites are a mixture of Kaguyak-like and Augustine-like grains; we interpret these deposits to be a mechanical mixture of ash from both volcanoes. Two such eruptions need not have been precisely synchronous because succeeding grainfalls even years apart can become mixed by freeze-thaw cycles and bioturbation.

Radiocarbon ages limit the mixed deposit to between 3,660±100 and 3,850±100 radiocarbon (RC) years at one site and 3,360±25 and 3,620±25 RC years at the second site. The proximal Kaguyak ash-flow deposit contains neither soils nor erosional unconformities to indicate that caldera formation comprised separate eruptive pulses, and the coincidence of two mixed deposits within centuries of one another seems unlikely. Consequently, we believe that the mixed deposits at the two sites are the same geologic age; the radiocarbon dates within limits of 1 sigma analytical uncertainty can be interpreted as a single age of about 3,600 years. An age of 3,600 years is significant because it adds to the list of major eruptions in the eastern Aleutian arc between 3,400 and 4,000 RC years ago. The cause of such an apparent pulse in eruptive activity is uncertain, but involvement of multiple vents across nearly 1,000 km of arc suggests a regional process such as glacial rebound or a plate-wide process such as a slight change in direction or rate of subduction.

INTRODUCTION

There are eight Quaternary collapse calderas in the eastern Aleutian volcanic arc (fig. 1). Two of these are historic (Katmai and Novarupta), two are Pleistocene in age (Emmons and Ugashik), and three others (Veniaminof, Black Peak, and Aniakchak) have been dated by the radiocarbon method (Miller and Smith, 1987). Kaguyak Crater, the northernmost caldera, is the only caldera on the Alaska Peninsula whose age has not yet been determined. Attempts by ourselves and by Swanson and others (1981) to find datable materials in pyroclastic-flow deposits that surround the caldera have not been successful. Thus, while sampling Holocene tephra deposits on the Alaska Peninsula, we specifically sought airfall equivalents of the Kaguyak pyroclasts. It became apparent that as many as three tephra deposits in the region resembled the near-vent Kaguyak deposits, which raised the possibility that there had been multiple Kaguyak eruptions. But then we discovered that Augustine Volcano, 100 km north of Kaguyak Crater, had produced tephra during late Holocene time that is chemically and mineralogically indistinguishable from the Kaguyak proximal deposits. We have found, however, that the composition of ilmenite grains in these Holocene deposits uniquely distinguishes an Augustine source from a Kaguyak source, and we infer that there was only one caldera-forming eruption of Kaguyak for which an age can be determined.

ROCKS AND DEPOSITS OF KAGUYAK CRATER

Kaguyak Crater comprises the remains of an andesitic stratocone that was truncated by collapse of a caldera 2.0 km in diameter (now lake-filled) and intruded by dacitic domes at least in part after caldera formation (Swanson, 1990; Riehle and others, 1993). A dacitic pyroclastic-flow deposit emplaced during caldera formation—the proximal deposit—surrounds the vent and is roughly 1 km^3 in volume (J. Riehle, unpub. data), which indicates a "moderate to large" eruption (volcano explosivity index, VEI, of 4; Newhall and Self, 1982). Subtle layering in the deposit is indicated by reversals in pumice and lithic concentrations, but there is no evidence for internal erosion or soil development (fig. 2). Fossil fumarole pipes are found only near the top of the deposit. Pumice lapilli throughout the deposit are uniformly high-silica dacite in bulk composition (67-70% SiO_2); no banded pumice has been found.

The total of the evidence indicates that the entire deposit was emplaced during a single eruptive event, not multiple events of geologically different ages. A VEI of 4 places the eruption roughly between those of Mount St. Helens and Pinatubo in size; there may have been precursory activity, but the main eruption probably occurred over 12 to 24 hours. Because the deposit is compositionally homogeneous, comparison of chemical compositions of distal ash samples with those of lapilli in the proximal deposit should be straightforward. The only reported date for the proximal deposit is a

radiocarbon age of 1,080 years[1] of soil closely atop the primary deposit (Swanson and others, 1981).

DISTAL AIRFALL (TEPHRA) DEPOSITS

Our tephra samples were collected during the course of regional sampling of Holocene tephra deposits on the Alaska Peninsula, and during a study of the eruptive history of Augustine Volcano. We can distinguish a subset of tephra samples from our larger set that are chemically and mineralogically similar to the Kaguyak proximal samples. Only these Kaguyak-like samples are discussed in this report.

Kaguyak-like tephra samples are from seven sites on the northern Alaska Peninsula, Afognak and Shuyak Islands, and southern Cook Inlet (numbered sites, fig. 3). Reference samples are samples from an unambiguous source to which fine-grained distal samples may be compared. Reference samples for Kaguyak Crater are two pumice lapilli from the ash-flow deposits and a composite sample of fine lapilli from proximal site 1 (25 km east of the vent). Reference samples for Augustine Volcano are three late Holocene lapilli from Augustine Island (R.B. Waitt, unpub. data) and composites of two deposits, one coarse ash and the other fine lapilli, at proximal site 7 (25 km northwest of the vent). Assignment of

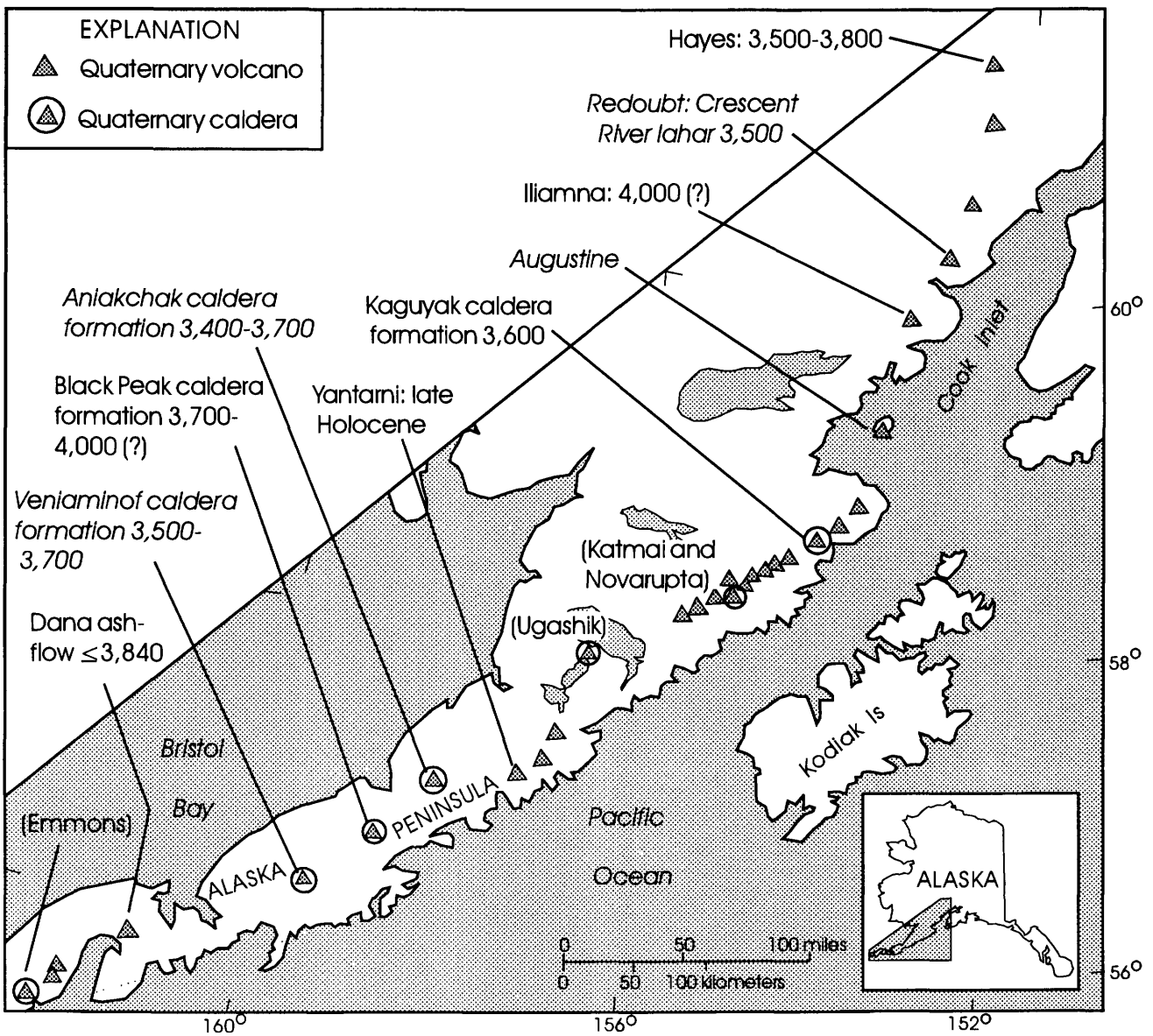

Figure 1. Quaternary volcanoes in the Alaska Peninsula segment of the Aleutian volcanic arc. Veniaminof, Black Peak, Aniakchak, and Kaguyak calderas formed during the period from 3.4 to 4.0 ka (uncorrected radiocarbon years), and Hayes, Redoubt, Iliamna, Augustine, Yantarni(?), and Dana had significant eruptions during the same period. Names of calderas that formed at times other than 3.4-4.0 ka are in parentheses. Radiocarbon ages (b.p.) of significant eruptions during the period 3.4-4.0 ka are shown; italics indicate volcanoes that also had other significant eruptions during Holocene time. Sources of ages: Hayes, Riehle (1985) and Riehle and others (1990); Redoubt, Riehle and others (1980); Iliamna, T.P. Miller, USGS, written commun., 1996; Augustine and Kaguyak, this paper; Yantarni, Riehle and others (1987); Aniakchak, Black Peak, and Veniaminof, Miller and Smith (1987) and Riehle, unpub. data; Dana, Yount (1990).

[1]All quantitative ages reported herein are in uncalibrated radiocarbon years.

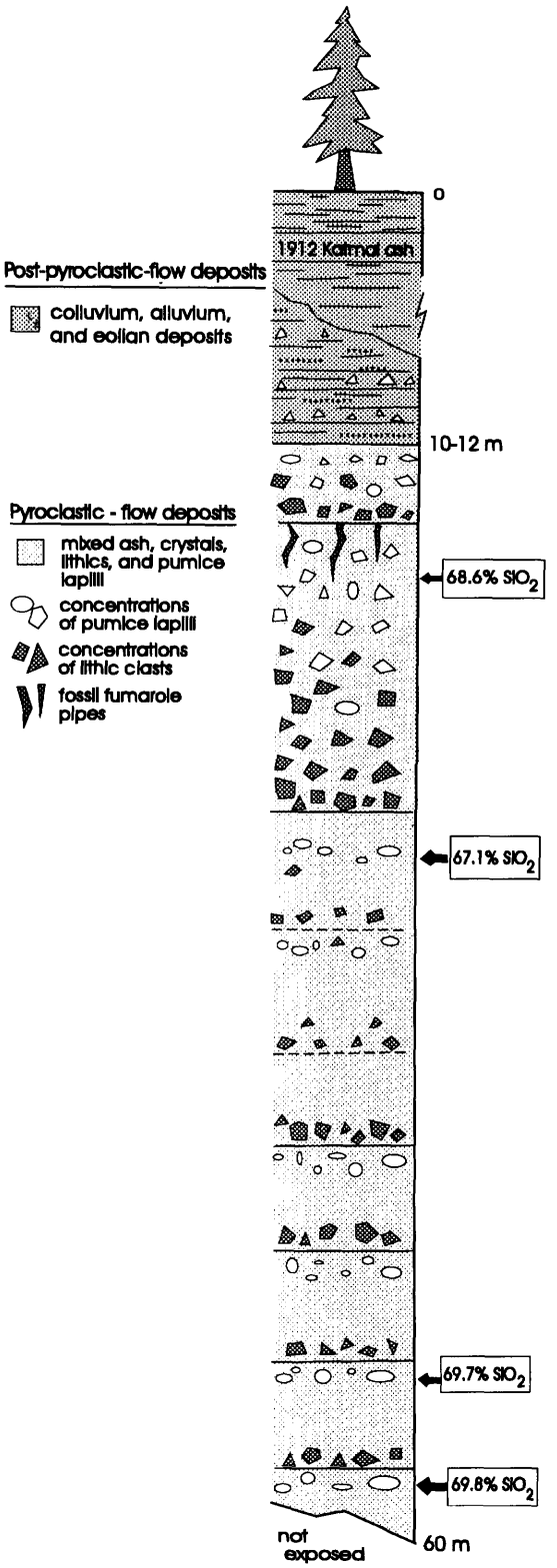

Figure 2. Composite section measured in pyroclastic-flow deposits formed during caldera collapse at Kaguyak Crater, Alaska. Bulk-rock silica contents of pumiceous lapilli, normalized to volatile-free basis, are shown in boxes (J.R. Riehle, unpub. data). Although the base is not exposed, nearby outcrops indicate that most of the deposit is exposed.

source for these reference samples is based on their coarse grain size close to the volcanoes. In contrast, Kaguyak-like samples of uncertain source at distal sites are mainly fine to medium ash.

All samples contain glass and minerals in subequal amounts. Mineral grains (fig. 4) are pyroxene, plagioclase, and opaque oxides; pleochroic brown-green hornblende is found in most samples as well. Analyses of glass separates from representative reference samples (table 1) indicate a high-silica rhyolitic composition for the glass.

CORRELATIONS AMONG THE SAMPLE SET

Because of the large differences among the densities of glass, mafic minerals, and plagioclase, the abundances of plagioclase and glass are not useful for comparison of tephra samples of different mean grainsize. The densities of amphibole and pyroxene are, however, more similar to one another, so unless one phase differs significantly from the others in mean grain size, the proportions among these phases

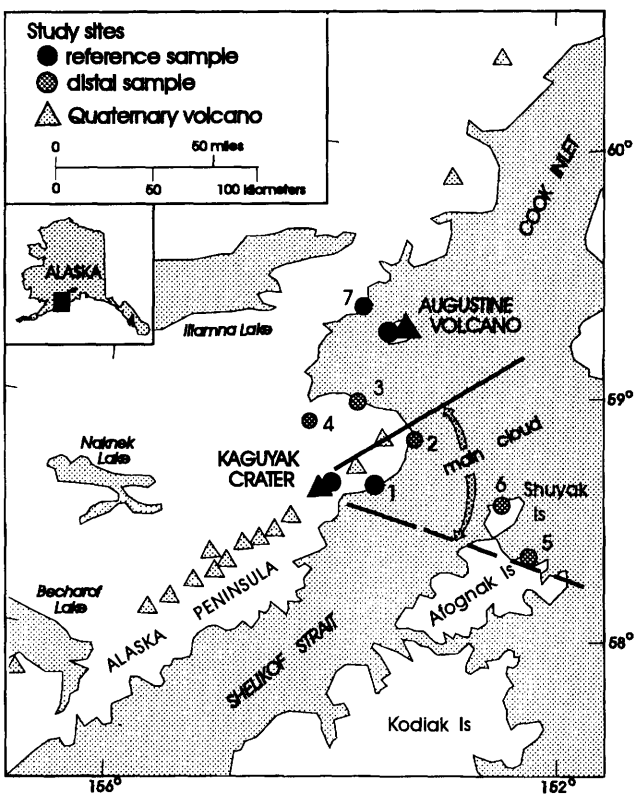

Figure 3. Sample sites in the region of Kaguyak Crater, northern Alaska Peninsula. Coarse-grained samples of unambiguous origin (reference samples) for Kaguyak Crater and Augustine Volcano are from proximal sites. Augustine samples are included because some are chemically and mineralogically indistinguishable from Kaguyak reference samples. Sites 2-6 are finer grained tephra deposits at distant sites that are chemically and mineralogically similar to Kaguyak reference samples. Because the coarsest and thickest airfall deposits that are attributed to Kaguyak Crater occur at sites 1 and 2, the main Kaguyak ash cloud is inferred to have dispersed to the east of the volcano (area shown by heavy lines, dashed where extrapolated).

Table 1. Major-element analyses of glass separates from representative reference samples of Kaguyak Crater (Site 1) and Augustine Volcano (33D).

[Oxides reported as weight percent; values in parentheses after each oxide are the standard deviation as a percent of the reported value. The number of shards that make up the average for each sample is in parentheses after the total. Totals are less than 100% largely because some elements are not included (chiefly magmatic volatiles and secondary water of hydration) and because of analytical uncertainty and the presence of microvesicles. Analyses by JEOL electron microprobe: 15 kev, 0.01 microamps sample current, defocussed beam and 15-second count times to minimize loss of alkalis. Basaltic and rhyolitic glass standards for all elements except Ti-hornblende and Mn_2O_3. A rhyolitic glass was used as an internal standard (RLS132). Analysts: J.R. Riehle and C.E. Meyer]

Sample No.—	Site 1	33D
Na_2O	4.04 (3.0)	3.80 (3.5)
MgO	0.32 (7.6)	0.34 (18)
Al_2O_3	11.9 (3.6)	12.2 (4.0)
SiO_2	76.0 (0.7)	73.2 (0.9)
K_2O	1.85 (1.7)	1.78 (2.0)
CaO	1.74 (3.0)	1.77 (3.3)
TiO_2	0.26	0.24
MnO	0.05	0.04
FeO_T	1.47 (3.8)	1.59 (4.1)
Total	97.6 (14)	95.0 (10)

can be a reliable basis for correlating proximal and distal deposits (fig. 4).

The major-element composition of glass has been widely used as a quantitative basis to correlate tephra samples (Smith and Okazaki, 1977; Sarna-Wojcicki and others, 1983), in part because the method affords a degree of precision that is difficult to attain by petrographic observations. In addition, microprobe analyses of glass separates are readily obtained, and (for homogeneous eruptions) the glass composition does not vary because of mechanical fractionation during transport in the ash cloud. The degree of similarity between two samples can be quantitatively expressed by the similarity coefficient (sc), which is the average of the ratios of the major oxides where the numerator is the lesser of the two values (for example, MgO_1/MgO_2; Borcherdt and others, 1972). A perfect match has an sc of 1.00, but due to analytical uncertainty and the inherent variability that typifies most glasses, perfect matches of even the same grainfall are rare. On the basis of a combination of empirical observation and replicate analyses of sample splits, an sc of 0.96 or greater is considered to be permissive, if not conclusive, evidence of correlation as the same grainfall (Riehle, 1985; Riehle and others, 1992).

The Kaguyak-like samples can be distinguished from other Alaska Peninsula tephra samples on the basis of their glass compositions. The high sc's of the Kaguyak reference samples with the Augustine reference samples (table 2) and, in some cases, the similarity in mafic-phenocryst contents as well (fig. 4), illustrate the difficulty in identifying the sources of these pyroclasts. Most Holocene tephras of Augustine Volcano have moderate to high ratios of amphibole to pyroxene (J. Riehle, unpub. data), but some of these Kaguyak-like Augustine tephras have low ratios. Thus, a moderate or high ratio of amphibole to pyroxene in a distal sample precludes a Kaguyak origin, but a low ratio does not unambiguously indicate a Kaguyak origin.

On the basis of amphibole-to-pyroxene ratios, two of three Kaguyak-like deposits at distal site 5 (fig. 5, deposits I, J, and G) could correlate with Kaguyak (5-G and 5-I). However, we know of only one low-amphibole deposit at site 6 (6-C), a site which is closer to Kaguyak Crater than site 5. This is a complication that we cannot resolve based only on glass composition and mineral contents.

ILMENITE COMPOSITIONS AS SOURCE INDICATORS OF THE TEPHRA SAMPLES

Magnetite and ilmenite compositions were used successfully by Downes (1985) to distinguish otherwise identical lobes of the White River ash deposit, Canada. We separated and analyzed a number of magnetite and ilmenite grains from our reference samples. Although the magnetite compositions are not separable by source, the ilmenite compositions unambiguously indicate the sources of these particular samples (fig. 6A). To investigate the reason for the success of this mineralogic source indicator, we converted the mineral compositions to temperature and oxygen fugacity. The late Holocene Augustine magmas had about 1 log unit higher oxygen fugacity (fig. 7) than the Kaguyak caldera-forming magma, a result that is consistent with the higher average amphibole content of the Augustine tephras.

Two Kaguyak-like deposits were sampled at distal site 6. Ilmenite in sample 6-C plots in the Augustine field of FeO-TiO_2, whereas that in sample 6-F plots in fields of both Kaguyak and Augustine (fig. 6B). We infer that 6-F is a mechanical mixture of ash from both sources. Mixing does not require that the two eruptions have occurred at precisely the same instant because two grainfalls even several years apart can become mixed over the succeeding millenia by freeze-

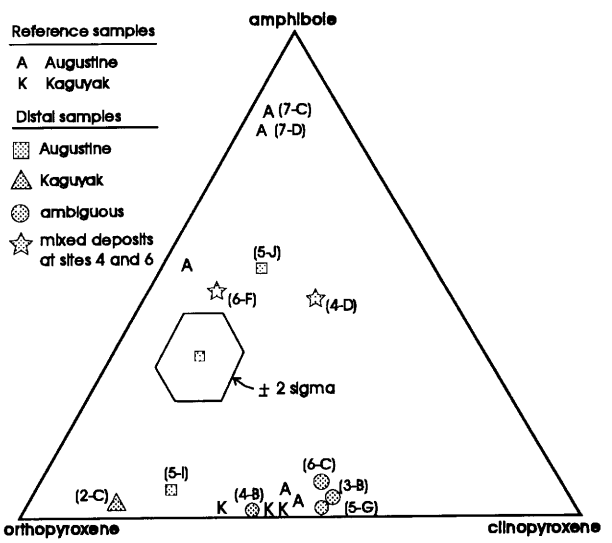

Figure 4. Mafic-phenocryst proportions of Kaguyak-like tephra deposits from the northern Alaska Peninsula and southern Cook Inlet region, Alaska. Reference samples are coarse, near-vent lapilli. Each distal sample has a glass composition that is highly similar to glass in Kaguyak reference samples. Assignment of distal samples to a source at Kaguyak or Augustine is based on the composition of ilmenite grains in the sample (discussed in the text). Phenocryst proportions determined by point counting of grain mounts, using a polarizing microscope; the typical uncertainty of measurement (± 2 sigma) is shown for one sample (150 points).

Table 2. Values of similarity coefficients sc for the glass composition of each Kaguyak-like sample compared with that of every other sample. [Perfectly identical compositions would have an sc of 1.00. Only values ≥ 0.95 are listed because smaller values do not support correlation as the same deposit. The high values here serve to (1) distinguish the samples in the data set from other Holocene samples in the region (J.R. Riehle, unpub. data), and (2) permit correlation of each sample in the data set with nearly every other sample. Mafic-phenocryst proportions (fig. 4) provide an additional basis for comparing these highly similar samples; underlined values are sample pairs that have similar phenocryst proportions. Note that Kaguyak reference samples are indistinguishable in both glass composition and phenocryst content from some Augustine reference samples. Ilmenite compositions have been used to distinguish between these sources.]

	Sample No.	1	37-D	37-H	5-G	5-I	5-J	7-C	7-D1	2-C2	3-B	4-B	4-D	75-A	33-B	33-D	6-C	6-F
Kaguyak reference tephras	1	--	0.97	0.96	0.97					0.96	0.96			0.95		0.97	0.96	
	37-D		--	0.97	0.96		0.96			0.98	0.96	0.97	0.96	0.95		0.97	0.96	
	37-H			--	0.96	0.95	0.97	0.96	0.96	0.96	0.99	0.97		0.98	0.96	0.98	0.98	0.96
	5-G				--			0.96	0.97	0.96	0.96		0.95	0.96		0.97	0.96	
	5-I					--	0.95	0.97	0.96		0.96			0.97	0.98	0.96	0.97	0.97
	5-J						--	0.96		0.95	0.97	0.97		0.98		0.95	0.96	
Augustine reference tephras	7-C							--	0.98		0.96		0.95	0.97	0.97	0.96	0.96	0.96
	7-D1								--	0.95	0.96			0.97	0.97	0.97	0.97	0.96
	2-C2									--	0.96	0.96	0.96	0.95		0.97	0.95	
	3-B										--	0.97	0.97	0.99	0.97	0.98	0.99	0.96
	4-B											--	0.97	0.96	0.95	0.97	0.97	
	4-D												--	0.97		0.96	0.96	
	75-A													--	0.97	0.97	0.98	0.95
	33-B														--	0.97	0.98	0.98
	33-D															--	0.99	0.97
	6-C																--	0.96
	6-F																	--

Underline, similar mafic-phenocryst contents

thaw cycles and bioturbation. Sample 4-D also contains grains that plot in FeO-TiO_2 fields of both sources (fig. 6C). Of the other samples from which ilmenite grains were analyzed, each plots chiefly in one field or the other (fig. 6C).

CORRELATIONS AMONG DISTAL SITES FOLLOWING PROVISIONAL SOURCE ASSIGNMENTS

Provisional source assignments based on ilmenite compositions can be tested for stratigraphic consistency (fig. 5). At distal sites 4, 5, and 6, there is only a single deposit that is either assigned to Kaguyak (5-G) or that is a postulated mixed deposit (4-D and 6-F). All other Kaguyak-like deposits at sites 4, 5, and 6 are assigned to Augustine. Ilmenite has not been analyzed from samples at sites 2 and 3. However, based on its coarse grain size and low amphibole-to-pyroxene ratio, 2-C is probably a Kaguyak deposit (although one which may include a fine-grained Augustine component). Deposit 3-B, which is presently classified as "uncertain," also has a low ratio of amphibole to pyroxene and so may consist chiefly of Kaguyak ash. Our mixed deposits have intermediate ratios of amphibole to pyroxene, which means that they cannot be exclusively Kaguyak ash (fig. 4). Examples of Augustine deposits that could be mixed with the Kaguyak ash include 7-C and 7-D, both of which have a high ratio of amphibole to pyroxene (fig. 4). Mixing of such a high-amphibole ash with Kaguyak ash would yield the observed intermediate ratios.

Grain-size differences among sites 1, 2, and 5 (fig. 5) indicate that the main Kaguyak ash cloud was dispersed approximately eastward (fig. 3). Mixed deposit 6-F is found near the center of this east-directed lobe; the pure Kaguyak deposit at site 5 must have been beyond the limit of significant Augustine fallout. Another mixed deposit (4-D) is located north of Kaguyak Crater, which because of the 90-degree difference in azimuth raises the possibility of two separate Kaguyak eruptions. It is not uncommon, however, for surface winds in lower Cook Inlet to flow northward while winds aloft flow eastward under influence of the jetstream (L. Kelly, National Weather Service, Anchorage, written commun., 1996). Thus, the occurrence of Kaguyak tephra both to the east and to the north of the vent does not require separate eruptions during different wind patterns.

AGE OF THE DISTAL KAGUYAK DEPOSIT

Peat deposits immediately above and below the ash deposits were dated by radiocarbon methods and limit the age of the mixed deposits at sites 4 and 6. The values that are midway between each pair of limiting peat ages are 3,750 years at site 4 and 3,500 years at site 6 (fig. 8). This 250-year difference suggests that the mixed deposit at site 4 may be older than that at site 6. However, the results can also be interpreted as a single age for both sites; 3.6 ka is within ±1 sigma analytical uncertainty of all four samples.

Closely succeeding eruptions of chemically similar pyroclasts from adjacent volcanoes may be unusual, but a second occurrence of such an event within 250 years of the first is even more improbable. Thus, we prefer the interpretation that the mixed deposits are the same geologic age and consist of a single Kaguyak ashfall, an interpretation that is consistent with the evidence for a single eruptive episode during emplacement of the Kaguyak ash flow. The August-

ine component of the mixed deposits could represent two different ashfalls; for example, one several years before and one several years after the Kaguyak eruption. Permissive evidence of this possibility is the presence of two closely succeeding Kaguyak-like deposits at site 7 (fig. 5, 7-C and 7-D).

Kaguyak tephra at site 5 (5-G) is found near the middle

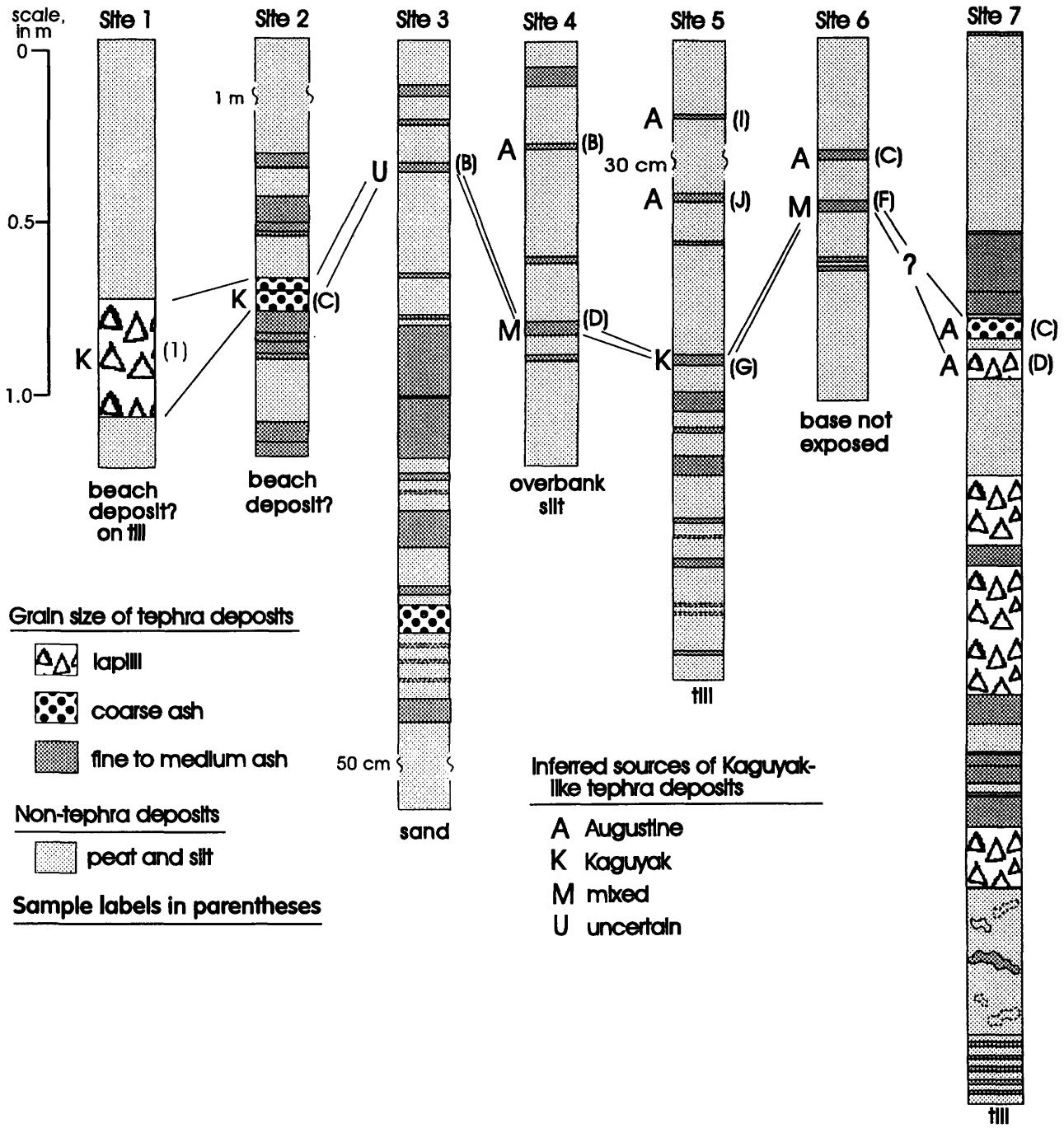

Figure 5. Geologic columns showing the stratigraphic setting of sampled Kaguyak-like tephra deposits from the northern Alaska Peninsula, Afognak and Shuyak Island, and southern Cook Inlet (fig. 3). Reference samples of Kaguyak Crater include the lapilli deposit at site 1 (25 km east of the vent). Reference samples of Augustine Volcano include coarse-grained deposits C and D at site 7 (25 km northwest of the vent). Distal deposits of Kaguyak-like tephra at sites 2 through 6 are labelled according to inferred sources on the basis of ilmenite compositions (discussed in the text). Only one deposit is inferred to be the airfall equivalent of the Kaguyak caldera-forming eruption; that deposit is indicated by lines that correlate from sites 1 through 6. Augustine reference deposits at site 7 (queried lines) represent ashfalls that are postulated to have mixed with Kaguyak deposits at sites 4 and 6.

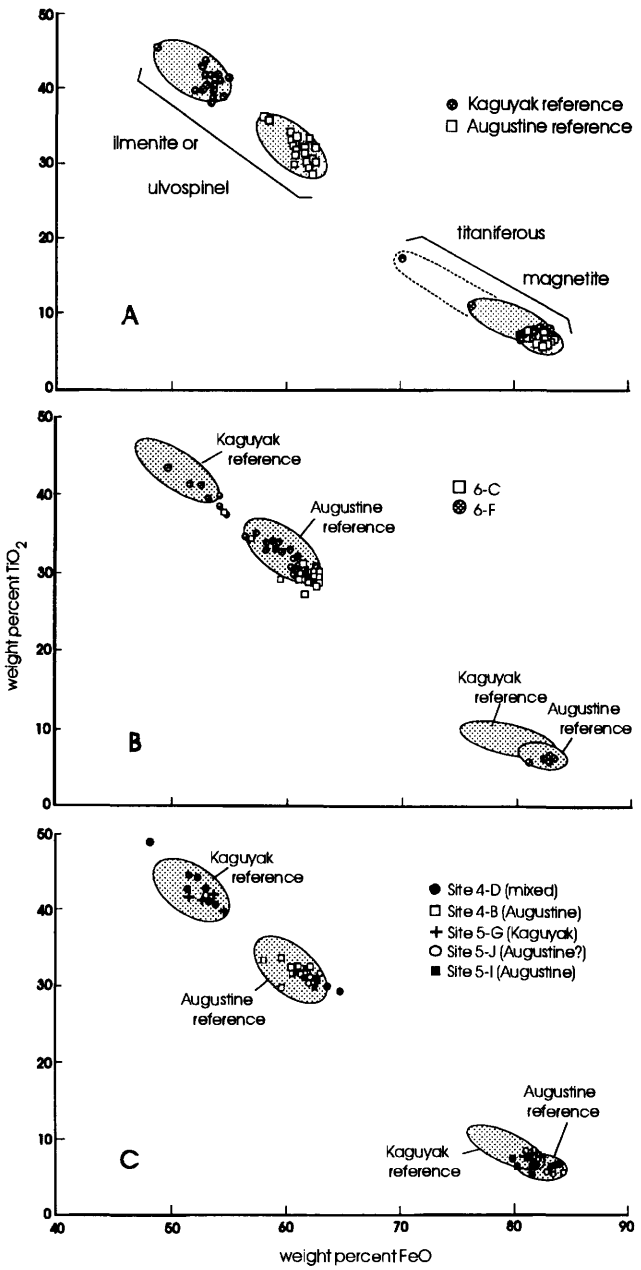

Figure 6. FeO and TiO^2 contents of magnetite and ilmenite grains in Kaguyak-like tephra deposits, northern Alaska Peninsula. See figures 3 and 5 for sample sources. Analyses by JEOL electron microprobe, 15 kev and 0.3 microamps sample current, focussed beam, 20-second count times. Standards: synthetic $MgAl_2O_4$ (Mg, Al), clinopyroxene (Si), Tiebaghi chromite (Cr), and synthetic oxides for Fe, Mn, Ti, Ni, and V. Analysts J.R. Riehle, C.E. Meyer, and L.C. Calk. (A) Magnetite and ilmenite grains in three reference samples of Kaguyak pyroclasts and four reference samples of Augustine pyroclasts. Ilmenite compositions uniquely indicate the sources of these late Holocene pyroclasts. Shaded areas outline the compositional fields for each volcano and are reproduced on parts B and C. (B) Distal deposit 6-C has chiefly Augustine-like ilmenite grains, but 6-F has both Kaguyak-like and Augustine-like ilmenite grains and is interpreted to be a mixture of Kaguyak and Augustine grainfalls. (C) Other distal deposits plot mainly in the field of either Kaguyak or Augustine ilmenite compositions, except that 4-D also appears to be a mixed deposit.

of a section that apparently represents the entire Holocene (fig. 8; section rests on glacial till). Assuming slightly greater compaction of the non-tephra deposits in the lower part of the section than in the upper part, the stratigraphic position of 5-G is broadly consistent with an age of 3.6 ka.

IMPLICATIONS OF THE NEWLY ESTIMATED AGE OF CALDERA FORMATION

An age of about 3.6 ka for formation of Kaguyak caldera is notable because it means that four of six Holocene calderas on the Alaska Peninsula formed within a few hundred years of one another, between about 3.4 and 4.0 ka (see ages in Miller and Smith, 1987). Moreover, a number of other volcanoes in the eastern Aleutian arc also had major eruptions during this period (fig. 1). These 3.4 to 4.0-ka eruptions were the only significant Holocene activity at some volcanoes, but other vents had many Holocene eruptions in addition to those during this period.

We have no evidence for the cause of such a remarkable pulse of eruptive activity in the eastern Aleutian arc at this time, nor do we know if the pulse involved the western part of the arc. But such widespread volcanic activity must somehow involve the tectonic plates, either by postglacial rebound of the upper plate or by a slight change in the direction, rate of convergence, or the dip of the downgoing plate. We suggest that vertical tectonism in the upper plate may have accompanied the eruptive pulse and that field evidence for such tectonism may still be preserved in uplifted marine terraces, river incisions, or tsunami deposits formed as a result of large earthquakes.

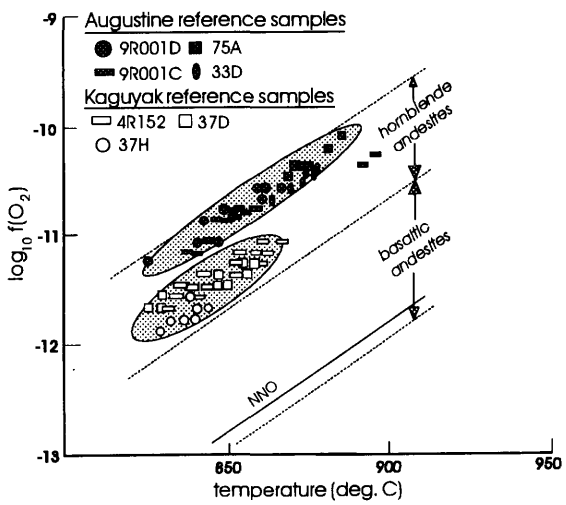

Figure 7. Temperature and oxygen fugacity calculated using the model of Andersen and Lindsley (1988) for magnetite and ilmenite pairs in Kaguyak and Augustine reference samples. Only pairs that satisfy the Mg/Mn equilibrium criteria of Bacon and Hirschmann (1988) are plotted. Fields for pyroxene (basaltic) andesites and hornblende andesites (Carmichael, 1991) show that the higher oxygen fugacity for the Augustine pyroclasts than that for the Kaguyak pyroclasts is consistent with the higher average amphibole content of the Augustine samples. Shaded areas emphasize the separation of the two sources.

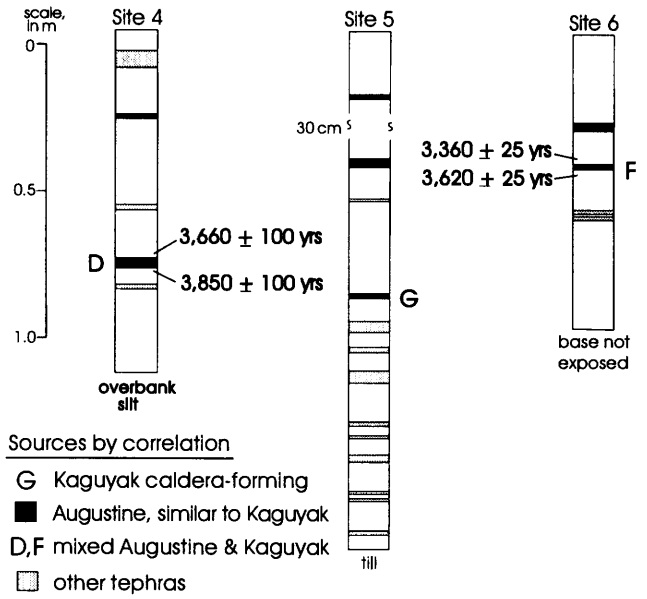

Figure 8. Peat samples dated by radiocarbon method limit the age of the mixed deposits at sites 4 and 6. The stratigraphic position of correlative deposit 5-G (approximately middle Holocene) is broadly consistent with the radiocarbon ages of deposits 4-D and 6-F. [Laboratory numbers: site 4, Isotopes I-16,120 (above) and I-16,121; site 6, University of Washington Quaternary Isotope Laboratory QL4813 (above) and QL4814.]

REFERENCES CITED

Andersen, D.J., and Lindsley, D.H., 1988, Internally consistent solution models for Fe-Mg-Mn-Ti oxides: Fe-Ti oxides: American Mineralogist, v. 73, p. 714-726.

Bacon, C.R., and Hirschmann, M.M., 1988, Mg/Mn partitioning as a test for equilibrium between coexisting Fe-Ti oxides: American Mineralogist, v. 73, p. 57-61.

Borcherdt, G.A., Aruscavage, P.J., and Millard, H.T., Jr., 1972, Correlation of the Bishop ash, a Pleistocene marker bed, using instrumental neutron activation analysis: Journal of Sedimentary Petrology, v. 42, p. 301-306.

Carmichael, I.S.E., 1991, The redox states of basic and silicic magmas: a reflection of their source regions?: Contributions to Mineralogy and Petrology, v. 106, p. 129-141.

Downes, Hillary, 1985, Evidence for magma heterogeneity in the White River ash (Yukon Territory): Canadian Journal of Earth Sciences, v. 22, p. 929-934.

Miller, T.P., and Smith, R.L., 1987, Late Quaternary caldera-forming eruptions in the eastern Aleutian arc, Alaska: Geology, v. 15, p. 434-438.

Newhall, C.G., and Self, Stephan, 1982, The volcanic explosivity index (VEI): an estimate of explosive magnitude for historical volcanism: Journal of Geophysical Research, v. 87, p. 1231-1238.

Riehle, J.R., 1985, A reconnaissance of the major Holocene tephra deposits in the upper Cook Inlet region, Alaska: Journal of Volcanology and Geothermal Research, v. 26, p. 37-74.

Riehle, J.R., Bowers, P.M., and Ager, T.A., 1990, The Hayes tephra deposits, an upper Holocene marker horizon in south-central Alaska: Quaternary Research, v. 33, p. 276-290.

Riehle, J.R., Detterman, R.L., Yount, M.E., and Miller, J.W., 1993, Geologic map of the Mount Katmai quadrangle and adjacent parts of the Naknek and Afognak quadrangles, Alaska: U.S. Geological Survey Miscellaneous Investigations Map I-2204, scale 1:250,000.

Riehle, J.R., Kienle, Jurgen, and Emmel, K.S., 1980, Lahars in the Crescent River valley, lower Cook Inlet, Alaska: Alaska Division of Geological and Geophysical Surveys, Geologic Report 53, 16 p.

Riehle, J.R., Mann, D.H., Peteet, D.M., Engstrom, D.R., Brew, D.A., and Meyer, C.E., 1992, The Mount Edgecumbe tephra deposits, a marker horizon in southeastern Alaska near the Pleistocene-Holocene boundary: Quaternary Research, v. 37, p. 183-202.

Riehle, J.R., Yount, M.E., and Miller, T.P., 1987, Petrography, chemistry, and geologic history of Yantarni Volcano, Aleutian volcanic arc, Alaska: U.S. Geological Survey Bulletin, v. 1761, 27 p., 23 fig., 1 pl.

Sarna-Wojcicki, A.M., Champion, D.E., and Davis, J.O., 1983, Holocene volcanism in the conterminous United States, and the role of silicic volcanic ash layers in correlation of latest Pleistocene and Holocene deposits, Chap. 5 in Porter, S.C., and Wright, H.E., Jr., eds., Late Quaternary environments of the United States: Minneapolis, University of Minnesota Press, p. 52-77.

Smith, H.W., and Okazaki, Rose, 1977, Electron microprobe data for tephra attributed to Glacier Peak, Washington: Quaternary Research, v. 7, p. 197-206.

Swanson, S.E., 1990, Kaguyak, in Wood, C.A., and Kienle, Jurgen, eds., Volcanoes of North America: New York, Cambridge University Press, p. 75-77.

Swanson, S.E., Kienle, Jurgen, and Fenn, P.M., 1981, Geology and petrology of Kaguyak Crater, Alaska [abs.]: EOS, Transactions of the American Geophysical Union, v. 62, p. 1062.

Yount, M.E., 1990, Dana, in Wood, C.A., and Kienle, Jurgen, eds., Volcanoes of North America: New York, Cambridge University Press, p. 54-55.

Reviewers: Elizabeth Bailey and Thomas Miller

$^{40}Ar/^{39}Ar$ Ages of Detrital Minerals in Lower Cretaceous Rocks of the Okpikruak Formation: Evidence for Upper Paleozoic Metamorphic rocks in the Koyukuk Arc

By Jaime Toro, Frances Cole, *and* Jonathan M. Meier

ABSTRACT

The Okpikruak Formation consists of Upper Jurassic and Lower Cretaceous turbidites interpreted as the first orogenic clastic rocks deposited during initiation of the Brooks Range orogeny. As such, detrital minerals and lithic fragments in rocks of the Okpikruak Formation contain information about the composition and age of the first uplifts exhumed in the Brooks Range. In this study, we present petrographic and detrital heavy-mineral analyses, including $^{40}Ar/^{39}Ar$ dating of detrital minerals, from samples of Lower Cretaceous rocks in the Okpikruak Formation collected in the western part of the Killik River quadrangle, near the Lisburne well. Detrital white mica yielded reliable Carboniferous $^{40}Ar/^{39}Ar$ ages, but detrital crossite yielded complex spectra that are difficult to interpret. On the basis of the heavy minerals and lithic fragments in our samples, the Carboniferous ages from the white mica, and previous provenance studies of the Okpikruak Formation, we interpret four distinct source terrains for the detritus in Okpikruak Formation: (1), Sedimentary rocks of the Arctic Alaska continental margin; (2), volcanic and plutonic rocks of the Koyukuk arc; (3), mafic and ultramafic rocks of the Angayucham terrane; and (4), metamorphic rocks of blueschist and greenschist grade from an unknown source terrain. It is unlikely that the Schist Belt of the Arctic Alaska terrane was a source for the metamorphic detritus in the Okpikruak Formation because the Schist Belt was deeply buried during the time that the Okpikruak Formation was deposited. It is more likely that the metamorphic detritus, including metamorphic or plutonic rocks containing Carboniferous white mica, were part of the upper plate that overrode the Arctic Alaska margin. These rocks may have been the roots of the Koyukuk arc or some other crustal fragment that was brought in with the arc during the initial Brookian collision.

INTRODUCTION

The Brooks Range orogen began with the collision of an intra-oceanic island arc against the continental margin of Arctic Alaska during Jurassic to Early Cretaceous time (Roeder and Mull, 1978; Box and others, 1985). Collision and the resultant obduction of this island arc are believed to be responsible for widespread blueschist metamorphism in the southern Brooks Range (Till, 1988). The blueschist-facies rocks have been difficult to study because they are largely overprinted by younger greenschist- to amphibolite- facies metamorphism (Dusel-Bacon and others, 1989). In addition, only small remnants of the colliding arc complex and its oceanic crust are presently exposed. Mafic and ultramafic rocks of Devonian to Jurassic age, representing the underpinnings of the island arc, are exposed in the uppermost thrust sheets in the northwestern Brooks Range and along a narrow belt that fringes the southern Brooks Range (fig. 1, Angayucham terrane). Additional arc rocks may have been removed from the Brooks Range by postcollisional processes that include erosion and perhaps extensional denudation (Miller and Hudson, 1991). Scattered outcrops of Jurassic and Lower Cretaceous igneous rocks, representing a younger, supracrustal part of the arc complex are found on structural highs in the Koyukuk basin (Patton and others, 1994) (fig. 1).

The Okpikruak Formation represents the first orogenic clastic sediments shed northward from the Brooks Range orogen. It consists of interbedded shale, greywacke, and minor conglomerate (Gryc and others, 1951) with fossils ranging from latest Jurassic (Tithonian) to Early Cretaceous (Valanginian). Fragments of sedimentary, igneous, and blueschist-facies metamorphic rocks that have been identified within the Okpikruak Formation along the northern flank of the Brooks Range (Wilbur and others, 1987; Siok, 1989; Meier, 1995; J.A. Dumoulin, U.S. Geological Survey, written commun., 1990; Till, 1992) indicate derivation from a diverse and complex orogenic source area (fig. 3).

In this paper, we present petrographic and detrital heavy-mineral analyses, including $^{40}Ar/^{39}Ar$ dating of detrital minerals from samples of Lower Cretaceous rocks in the Okpikruak Formation, collected in the western part of the Killik River quadrangle near the Lisburne well (figs. 1, 2). We use clast and lithic-grain compositions, as well as heavy minerals in the Okpikruak Formation, to infer the nature of

the orogenic source area that was exhumed in Early Cretaceous time. Our $^{40}Ar/^{39}Ar$ ages obtained from detrital white mica and blue amphibole are used to infer the age of metamorphic and possible plutonic source areas.

GEOLOGIC SETTING

Samples for this study were collected as part of a regional stratigraphic and structural investigation of the northern Brooks Range and Colville foreland basin (figs. 1, 2; Cole and others, 1997). In the study area, sedimentary rocks of the Colville foreland basin are involved in folding and thrusting at the leading edge of the Brooks Range orogen (Colville basin units, fig. 2). Deep-water shales and turbidite sandstones of the Torok and Fortress Mountain Formations and shallow-marine to nonmarine sandstones, shales, and conglomerates of the Nanushuk Group fill the Colville foreland basin (figs. 2, 3). This flysch and molasse sequence is Early to mid-Cretaceous in age and attains a thickness of 10 km north of the range front (fig. 2*B*); it represents the flexural response of the foreland to thrust loading in the orogen (Cole and others, 1997).

On a regional scale, the northern flank of the Brooks Range is made up of a series of northward-displaced allochthons, representing hundreds of kilometers of shortening (Tailleur and others, 1966; Mayfield and others, 1988). In our study area, these allochthons occupy the outcrop belt south of the foreland basin rocks, and they consist of distal facies of an upper Paleozoic-lower Mesozoic passive margin sequence (fig. 3); (Mull and others, 1985). The structurally lowest, largest, and most proximal is the Endicott Mountains allochthon, which includes imbricated Upper Devonian through Lower Cretaceous sedimentary rocks (Mull and others, 1994) (figs. 2, 3). The Endicott Mountains allochthon is structurally overlain by rocks of the the Picnic Creek and Ipnavik River allochthons, which represent the more distal parts of the Arctic Alaska passive margin (fig. 2). Turbidites of the Okpikruak Formation depositionally overlie the passive margin sequence, signalling a sudden change in the depo-

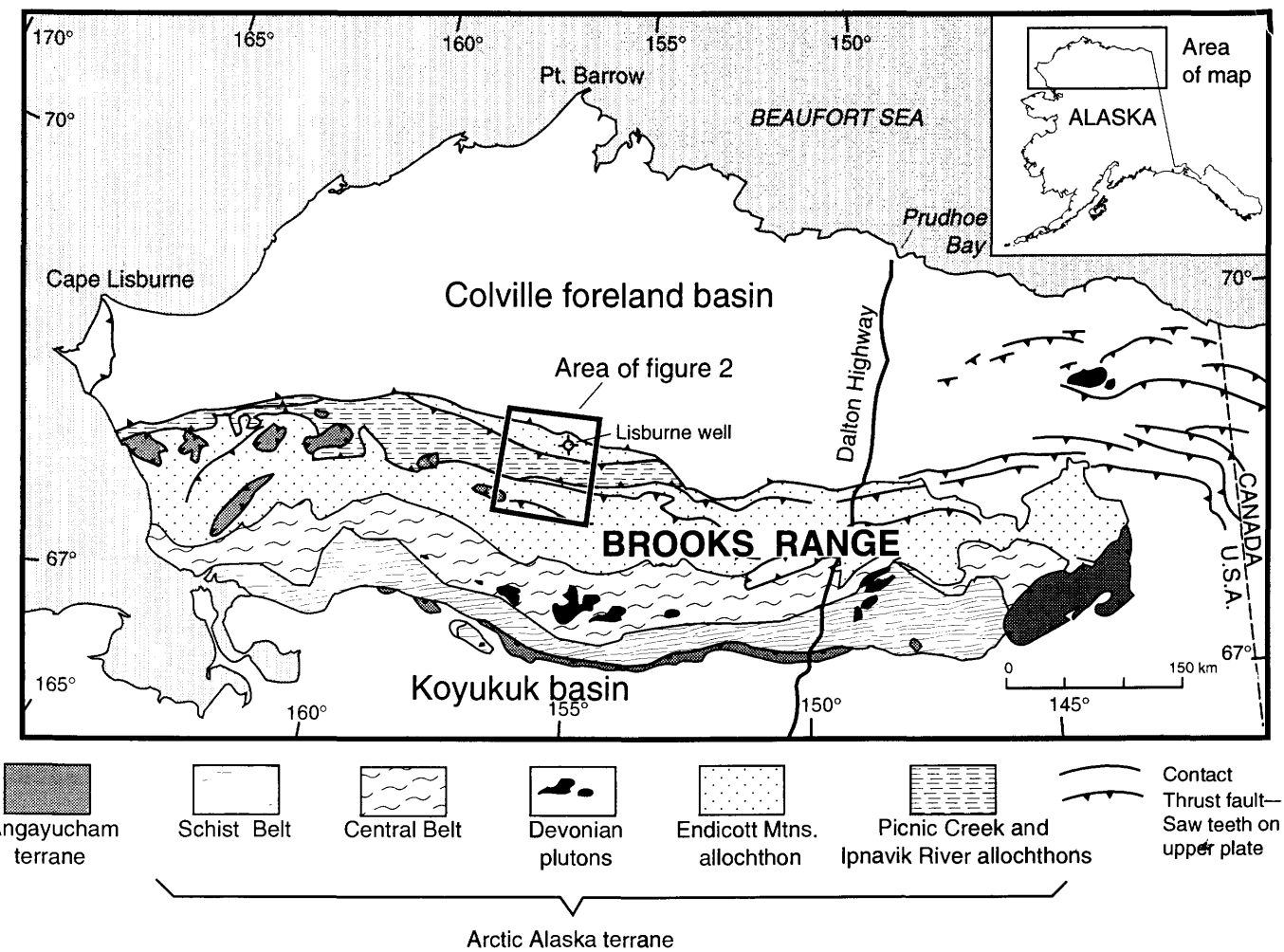

Figure 1. Generalized geologic map of northern Alaska showing structural units of the Brooks Range. Modified from Mull and others (1987) and Moore and others (1994).

sitional environment and tectonic setting of Arctic Alaska (Mayfield and others, 1988). The Okpikruak Formation analyzed in this study is part of the Ipnavik River allochthon (C.G. Mull, Alaska Division of Geological and Geophysical Surveys, written commun., 1997).

Small klippen of imbricated pillow basalt, diabase, chert, and limestone overlie the Picnic Creek and Ipnavik River allochthons. These oceanic rocks have been assigned to the Copter Peak allochthon of the Angayucham terrane (figs. 1, 2, 3) (Moore and others, 1994). Late Devonian to Early Jurassic fossils have been found in the cherts and limestones of the Copter Peak allochthon in several localities in the central and western Brooks Range (Moore and others, 1994). The basalts are tholeiitic in composition and may have formed in a midocean ridge or seamount setting (Harris, 1987; Moore, 1987). In the western Brooks Range, structurally above the Copter Peak allochthon is the Misheguk Mountain allochthon, also part of the Angayucham terrane (fig. 3). It is composed of mantle peridotite, ultramafic cumulates, gabbro, and locally sheeted dikes and basalts (Harris, 1995). The Misheguk Mountain rocks have geochemical characteristics of an ophiolite sequence transitional between midocean ridge and volcanic-arc type (Harris, 1995). The ophiolites crystallized during mid-Jurassic time according to U-Pb and $^{40}Ar/^{39}Ar$ ages (Moore and others, 1993; Wirth and others, 1993) and were emplaced onto the Copter Peak allochthon soon after their crystallization, signalling the beginning of Brookian overthrusting (Wirth and others, 1993).

The Koyukuk basin, which lies south of the Brooks Range (fig. 1), contains plutons and volcanic rocks interpreted as the supracrustal part of the ancient island arc known as the Koyukuk arc (Patton and Box, 1989; Patton and others, 1994). The oldest rocks exposed in the Koyukuk basin are Permian to Middle Jurassic pillow lavas and cherts. These rocks are intruded by Middle Jurassic tonalite-trondhjemite plutons thought to represent the oldest arc-related rocks of the basin. The most voluminous rocks in the Koyukuk basin are andesitic volcanic and volcaniclastic rocks of Jurassic(?) and mainly Early Cretaceous age, representing an extensive volcanic complex. The Middle Jurassic plutons and the Jurassic(?)-Early Cretaceous volcanic rocks all have geochemical characteristics associated with subduction-related magmatism in an intra-oceanic island-arc setting (Box and Patton, 1989; Patton and others, 1994). The Misheguk Mountain ophiolite described above is thought to represent an interarc basin or forearc limb to the Koyukuk arc (Harris, 1995; W.W. Patton, Jr., U.S. Geological Survey, oral commun., 1997).

The crest and south flank of the Brooks Range are made up of two extensive belts of metamorphic rocks, known as the Central Belt and Schist Belt (fig. 1). The Central Belt and Schist Belt include metasedimentary rocks of Proterozoic through Late Paleozoic age, thought to represent metamorphosed equivalents of the passive margin sequence and metamorphic substrate that underlie the Colville foreland basin (see for example, Moore and others, 1994). They also include metavolcanic rocks and Devonian metagranites. Along the southern margin of the Schist Belt is an imbricated panel of rocks known as the Phyllite Belt (not shown on fig. 1). These rocks are of lower metamorphic grade than the Schist Belt and are characterized by Devonian through Triassic quartzose metagreywacke and phyllite (Murphy and Patton, 1988). The Phyllite Belt represents the southernmost occurrence of continentally derived clastics associated with the Arctic Alaska plate.

The Central Belt and the Schist Belt underwent blueschist-facies metamorphism, probably by underthrusting beneath the Koyukuk arc (Till, 1988). The blueschist-facies event has been difficult to date with certainty because it is overprinted by a pervasive greenschist- to amphibolite-facies metamorphism. Most of the $^{40}Ar/^{39}Ar$ and K-Ar ages of the Schist Belt are between 130 to 90 Ma and are thought to represent the age of cooling after regional greenschist- to amphibolite-facies metamorphism, which for the most part obliterated evidence for earlier thermal events (Turner and others, 1979; Blythe and others, 1990; Little and others, 1994; Till and Snee, 1995). Christiansen and Snee (1994) reported an $^{40}Ar/^{39}Ar$ age of 171 Ma from white mica in a glaucophane-bearing metabasite that they interpreted as a minimum age for blueschist-facies metamorphism. Till and Snee (1995) suggested that high-pressure metamorphism persisted until 108 Ma (Albian) within rocks of the Central Belt, which exhibit a complex metamorphic history extending at least back to the late Proterozoic.

PREVIOUS STUDIES OF THE OKPIKRUAK FORMATION AND RELATED ROCKS

Heavy minerals were separated from well and outcrop samples of rocks in the Colville foreland basin and the northern thrust belt during early petroleum exploration, for use in stratigraphic correlation (Morris and Lathram, 1951). Patton and Tailleur (1964) analyzed heavy-mineral abundances in the Lower Cretaceous Okpikruak Formation and mid-Cretaceous(?) Fortress Mountain Formation. In these formations, they found the following heavy minerals, in decreasing order of abundance: garnet, tourmaline, apatite, augite, epidote, hornblende, mica, chromite, chloritoid, glaucophane, and rutile. The abundance of epidote, augite, and hornblende was used by Patton and Tailleur (1964) as evidence for a proximal volcanic source for the Okpikruak and Fortress Mountain Formations because those minerals are unstable in the sedimentary environment.

More recently, samples from mid-Cretaceous rocks of the Nanushuk Group and Torok Formation in the Colville basin were used to evaluate the unroofing history of the core of the Brooks Range by Till (1992), who showed that a suite of detrital metamorphic minerals, characterized by white mica, glaucophane, chloritoid, and garnet, was present in these rocks.

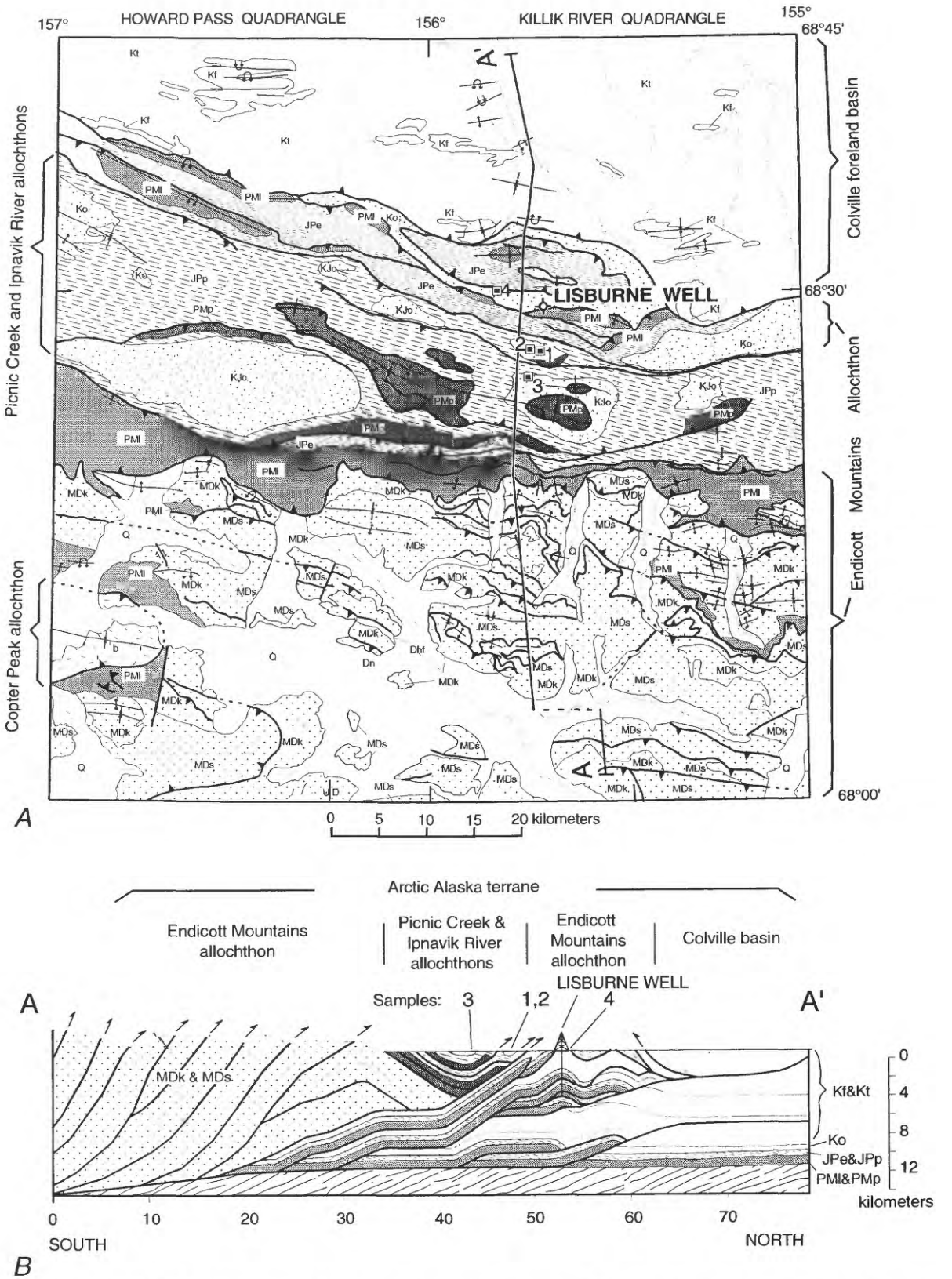

Figure 2. Generalized geologic map and cross section of southwestern Killik River quadrangle and southeastern Howard Pass quadrangle, northern Brooks Range, Alaska, and location of samples collected in this study. A., Geologic map. Modified from Mull and others (1994), Mull and Werdon (1994), and Cole and others (1995). Q, Quaternary Alluvium. B., Structural cross section through the study area. Modified from Cole and others (1997). Well and samples are projected to the section.

Till (1992) suggested that the Schist Belt had been exhumed and was contributing debris into the basin by middle Albian time and perhaps even earlier. Till (1992) does not report epidote, augite, and hornblende in the Torok Formation and Nanushuk Group samples, which suggests that the volcanic source for the Okpikruak and Fortress Mountain Formations had been decimated by erosion by mid-Albian time.

Mayfield and others (1978) collected igneous rock clasts from several outcrops of Lower Cretaceous conglomerate correlative with the Okpikruak Formation along the northern flank of the central and western Brooks Range. Clasts in the conglomerate were 55 percent quartz diorite or dacite, 29 percent diorite or andesite, and 16 percent quartz monzonite or granodiorite. Hornblende from two samples yielded K-Ar ages of 153±5 Ma and 186±9 Ma. Mayfield and others (1978) interpreted this data as evidence that a Jurassic igneous terrane was a source for the rocks of the Okpikruak Formation.

Petrographic studies of sandstones of the Okpikruak Formation collected in the central Brooks Range suggest that the sediment sources for the Okpikruak Formation were composed mostly of chert and quartz, plus minor volcanic, igneous, and metamorphic rocks (Siok, 1989; Wilbur and others, 1987). The sandstone composition varies significantly, but all of the petrographic data plotted on Q-F-L (quartz, feldspar, and lithic grains) ternary diagrams fall between the fields of recycled-orogenic and undissected magmatic arc, as defined by Dickinson and others (1983) (see for example fig. 4A). These data have been interpreted as evidence that the Okpikruak Formation received sediment from the distal parts of the Arctic Alaska continental margin and from the island arc that collided with the margin (Wilbur and others, 1987; Siok, 1989).

As part of a regional petrographic study of the western Killik River and eastern Howard Pass quadrangles, Meier (1995) conducted point counts on 24 samples collected from the Okpikruak Formation, including our sample 1 (fig. 2). Most of the sandstone samples of the Okpikruak Formation are litharenites and feldspathic litharenites. They are poorly sorted, with subangular to subrounded grains. The mean Q-F-L values for 21 fine-grain sandstones samples they are Q 48±10, F 14±5, and L 38±10; and for 3 coarse-grain sandstone samples are Q 26±8, F 15±5, and L 59±13 (fig. 4A). The coarse-grain samples show a greater igneous component, which suggests that the data from the fine-grained sandstones may be biased toward the recycled-orogenic field by removal of unstable arc-derived volcanic fragments during sedimentary transport.

Several diagnostic features can be seen in Meier's (1995) samples from the Okpikruak Formation: (1) Plagioclase is the dominant feldspar, although potassium-feldspar (5%) is present in some samples. (2) Lithic grains are mostly sedimentary rock fragments dominated by siliceous mudstone and shale. (3) Volcanic fragments are of intermediate composition and have an altered aphanitic matrix and plagioclase microphenocrysts. (4) Basaltic clasts are present but rare. (5) Metamorphic fragments are fine-grained quartz-muscovite phyllite and quartzite, including some highly strained quartz mylonites. (6) Some samples have as much as 11 percent heavy minerals. Although Meier (1995) did not list the heavy minerals present in his samples, we provide such a list below for the samples analyzed in this study.

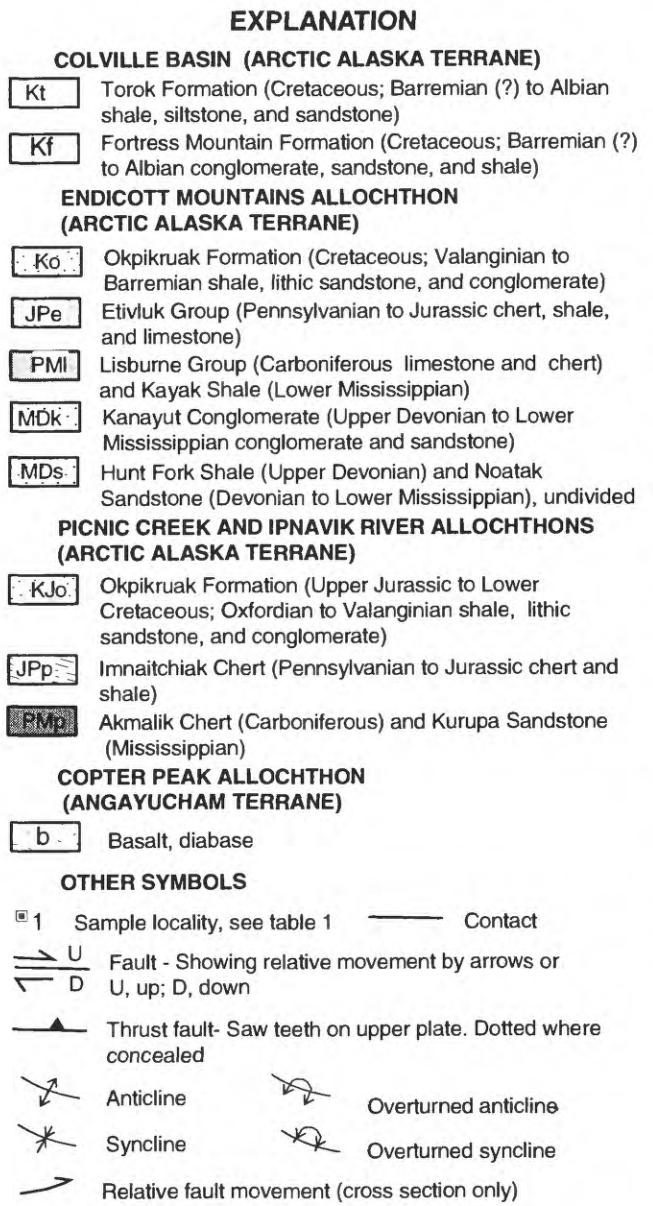

Figure 2. Continued.

THIS STUDY

In 1993, C.G. Mull guided us to an outcrop of the Okpikruak Formation where sandstones containing lithic fragments with abundant blue amphibole had been described (J.A.

Dumoulin, U.S. Geological Survey, written commun., 1990). In sandstones from the same locality, Dumoulin also observed limestone clasts with crinoid columnals, chert fragments, mafic volcanic clasts, and quartz-feldspar aggregates probably derived from intrusive rocks. We collected samples of sandstone of the Okpikruak Formation from the same locality for petrographic and heavy-mineral analysis (sample 1, fig. 2, table 1). The sampled outcrop consists of several meters of crudely stratified, channelized, and matrix-supported conglomerate and lithic sandstone that dips northwest. The conglomerate contains pebble- to boulder-size clasts of limestone, chert, mafic igneous rocks, and shale; it probably represents a debris flow that filled a submarine channel. Samples of interlayered siltstone and pebbly greywacke were also collected from the base and top of the channel fill.

The Okpikruak Formation at this locality is probably Valanginian age based on the presence of the bivalve *Buchia sublaevis* in correlative rocks 2 km to the west and 8 km to the northwest (samples 2, 4, fig. 2, table 1). In addition, *Buchia* sp., found in greywackes several kilometers to the south, are Oxfordian to Valanginian age (W. P. Elder, U.S. Geological Survey., written commun., 1993) (sample 3, fig. 2, table 1).

Detrital micas and heavy minerals were separated from sample 1 using standard heavy liquid, magnetic, and mechanical separation techniques. We found the following suite of heavy minerals in sample 1: epidote, actinolite, sulfides, garnet, hornblende, pyroxene, sphene, blue amphibole, chromite, chlorite, biotite, and white mica. This is a rich mineral suite, consistent with previous results from the Okpikruak Formation (for example, Patton and Tailleur, 1964). Several distinct source terrains are required by the heavy-mineral assemblage—a volcanic and plutonic source terrain to provide the coarse hornblende and pyroxene; blueschist-facies metamorphic rocks for the blue amphibole and possibly the garnet and white mica; a greenschist-grade metavolcanic terrain for the actinolite, epidote, and chlorite; and an ultramafic terrain to provide detrital chromite and possibly pyroxene.

Our sandstone petrography results for sample 1 also require a mixed provenance (fig. 4). Sample 1 yielded 35.2 percent quartz, 20.6 percent felspar, and 44.2 percent lithic grains; on a ternary plot it falls between the arc and the recycled-orogen fields of Dickinson and others (1983) (fig. 4A), indicating a mixed igneous, metamorphic, and sedimentary source. This is borne out by our determination of lithic compositions in sample 1 sandstone: 59.2 percent sedimentary, 2.9 percent metamorphic, and 37.9 percent volcanic (fig. 4B). This sample plots in the mixed magmatic arc and rifted continental margin field defined by Ingersoll and Suczek (1979).

$^{40}Ar/^{39}Ar$ DATING DETRITAL WHITE MICA

From the heavy-mineral fractions, we hand picked 1 to 2.5 mg of blue amphibole and white mica for $^{40}Ar/^{39}Ar$ dat-

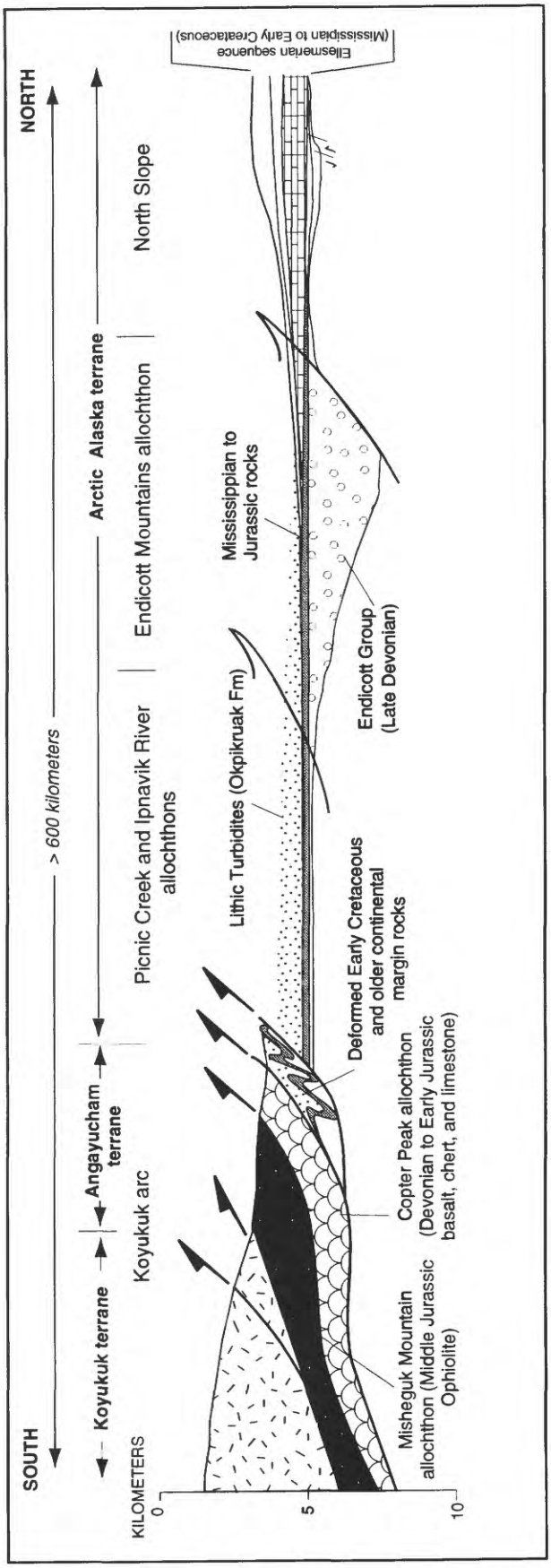

Figure 3. Cartoon showing possible depositional setting of Okpikruak Formation in Late Jurassic to Early Cretaceous time and its source areas as determined from its tectonic setting, sandstone petrography, heavy-mineral studies, and $^{40}Ar/^{39}Ar$ dating of detrital minerals (modified from Cole and others, 1997).

ing. The samples were irradiated at the TRIGA reactor at the University of Oregon, and the analyses were performed at Phil Gans' laboratory at Univ. of California, Santa Barbara. The complete analytical data and a summary of the laboratory methods are presented in table 3.

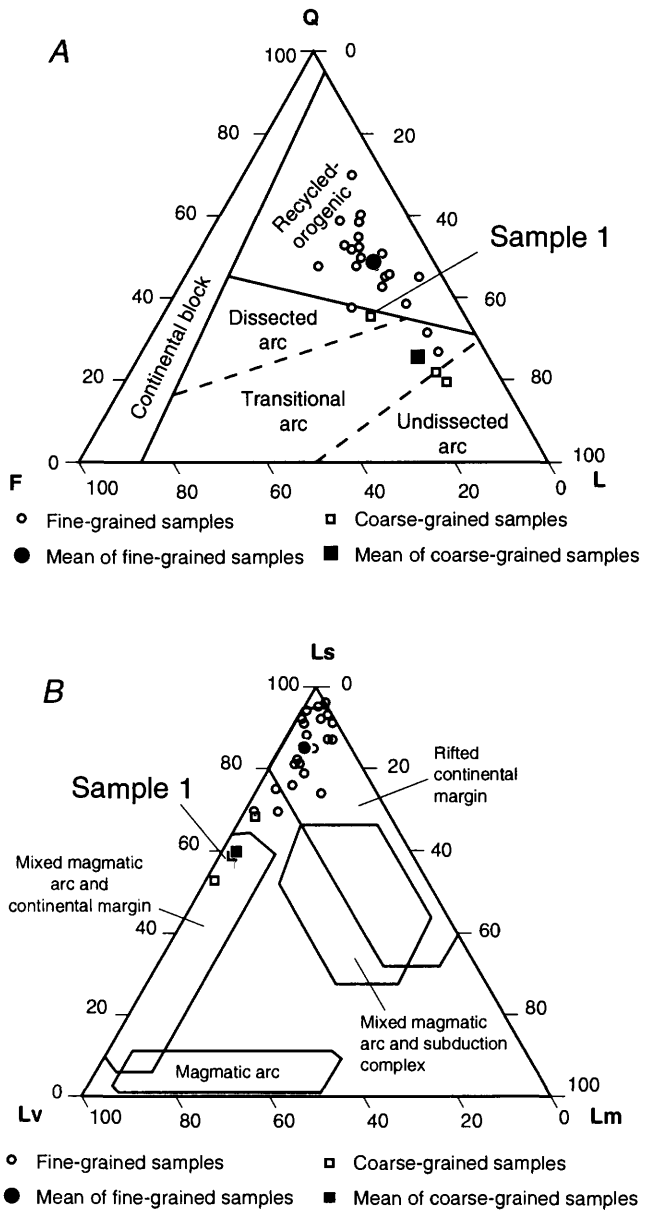

Figure 4. Sandstone petrographic data for Okpikruak Formation. Sample 1 from this study; other samples from Meier (1995). A, Ternary plot of Q-F-L data showing percentages of quartz, feldspar, and lithics. Provenance fields are from Dickinson and others (1983). B, Ternary plot of Ls-Lv-Lm data showing percentages of sedimentary lithic grains, volcanic lithic grains, and metamorphic lithic grains. Provenance fields from Ingersoll and Suczek (1979).

Two fractions of white mica separated from sample 1 were analyzed independently using the $^{40}Ar/^{39}Ar$ method (table 2 and 3). In the first experiment, a single flake of white mica was step heated in the resistance furnace. The single-grain age derived from the main step of the analysis was 332±2 Ma (Late Mississippian) representing 89 percent of the ^{39}Ar released (fig. 5A).

The second fraction was about 1 mg of detrital white micas of sizes ranging between 180 and 250 microns. Step heating yielded a spectrum with a total fusion age of 291±1 Ma (Late Pennsylvanian) (fig. 5A). In the spectrum, an age of 263±1 Ma (step 6) separates pseudo-plateaus of 291±1 Ma (steps 2-5) and 313±1 Ma (steps 7-9). Steps 2 to 5 define a well-correlated isochron age of 291±1 Ma with a $^{40}Ar/^{36}Ar$ ratio of 282±11 (fig. 5B). This $^{40}Ar/^{36}Ar$ ratio is close to the ideal atmospheric ratio (295.5), which indicates that excess Ar is not a problem in this sample. Steps 7-9 form a distinct, slightly older cluster of points near the radiogenic ($^{39}Ar/^{40}Ar$) axis. Step 6 also falls on the radiogenic axis. The apparent K/Ca ratio of the white mica sample is low, suggesting that the micas are not end-member muscovite. However we did not analyze their composition directly.

It is possible that the Carboniferous ages of this white-mica fraction are the result of a mixture of individual grains of widely different ages. We cannot discount this possibility entirely with our limited data set. However the fact that the single-grain age was also late Paleozoic, together with the systematic behavior of the data in the spectrum and isochron plots, suggests that all of the grains we analyzed were similar in age.

DETRITAL BLUE AMPHIBOLE

It is difficult to date blue amphibole (such as glaucophane or crossite) because it contains little potassium. In some studies, blue amphibole has yielded anomalously young ages attributed to the presence of small white-mica inclusions that contain most of the radiogenic argon (McDougall and Harrison, 1988; Sisson and Onstott, 1986). To determine if white mica was present in the blue amphibole separated from the Okpikruak Formation, we carried out microprobe analysis of a split of the amphibole. We found that our blue amphiboles were crossite (not end-member glaucophane) and that the grains have small inclusions of quartz, sphene, ilmenite, zircon, and zoisite but apparently no white mica. Similarly, Till (1992) found, by microprobe analysis of thin sections of the Okpikruak Formation from the same locality, that the blue amphiboles in her samples are also crossite containing inclusions of sulfides, iron oxides, and stilpnomelane, a potassium-bearing mineral likely to have a significant effect on $^{40}Ar/^{39}Ar$ dating.

Three splits of crossite separated from the Okpikruak Formation, ranging in mass from 1 to 2.5 mg, were analyzed using the $^{40}Ar/^{39}Ar$ step-heating method. The three

Table 1. Summary of four samples from the Okpikruak Formation, Brooks Range Alaska.
[Sample locations are shown on figure 2]

Sample locality	Field number	Location Latitude	Location Longitude	Sample type	Age	Fossils	Reported in
1	93FC19	68° 26.4'	156° 41.2'	Heavy minerals	Probably Valanginian--------	----------	This paper.
2	82AKy51	68° 26.3'	155° 43.5'	Fossils ----------	Valanginian ----------	*Buchia sublaevis*	Elder and others, 1989[1]
3	93FC58	68° 24.8'	155° 43.8'	Fossils ----------	Oxfordian to Valanginian ---	*Buchia sp.*	W.P.Elder, U.S.G.S., written commun., 1993.
4	90-Mu86-2	68° 30.0'	155° 49.0'	Fossils ----------	Early Valanginian ----------	*Buchia sublaevis*	W.P. Elder, U.S.G.S., written commun., 1991.

[1]Locations and ages in this report were modified in some cases according to W.P. Elder, written comm., 1995.

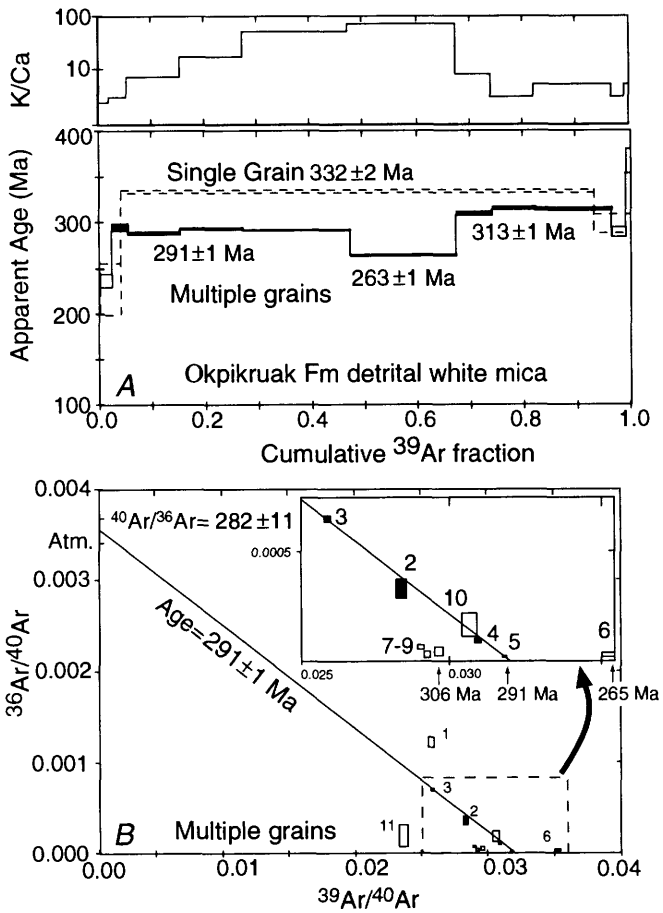

Figure 5. $^{40}Ar/^{39}Ar$ age spectra and inverse isochron plot for detrital white micas separated from Okpikruak Formation. A, $^{40}Ar/^{39}Ar$ spectra. Dashed spectrum corresponds to analysis of a single white-mica flake that yielded a Late Mississippian plateau age (332±2 Ma). Solid spectrum is for analysis of multiple white-mica grains; the corresponding K/Ca spectrum is shown above. This spectrum reflects a mixture of white-micas ages dominated by Late Mississippian to Early Permian grains. Vertical thickness of each step represents the error in age or K/Ca ratio of that step. B., Inverse isochron plot for analysis of multiple white-mica grains. Inset shows enlargement of area near intercept with the $^{39}Ar/^{40}A$ axis. Only data points represented as black rectangles were used to calculate isochron shown; numbers beside them are heating steps. Atm, $^{40}Ar/^{36}Ar$ atmospheric ratio (295.5).

spectra are highly disturbed, and the radiogenic ^{40}Ar yield for all the steps was low (fig. 6). Overall, these data are complex and difficult to interpret.

The largest sample (split A, table 2) yielded the best spectrum, with a pseudo plateau of 215±1 Ma using steps 2-7 (fig. 6A). Higher temperature steps from split A yielded older ages with highly disturbed patterns. The 215±1 Ma pseudo plateau corresponds to steps with K/Ca ratios of 0.1 to 0.3, whereas the higher temperature steps correlate with much lower K/Ca ratios (fig. 6A). The systematic variation of the K/Ca ratios, also observed in the other two crossite analyses, suggests that two different minerals were being degassed during the experiments. The inverse isochron plot of split A (fig. 6B) produced an $^{40}Ar/^{36}Ar$ intercept of 1,249±186, which is much higher than the 295.5 atmospheric ratio. This indicates that the sample contained large amounts of excess radiogenic argon, and therefore the age displayed in the spectrum can only be regarded as a maximum age. The isochron age calculated by using all but the first and last temperature steps is 147±15 Ma, which overlaps with the stratigraphic age of the Okpikruak Formation. However, the scatter of the data is higher than expected for a reliable linear regression. The mean square weighted deviation (MSWD, table 2), which is a measure of the goodness of fit (Wendt and Carl, 1991), is also too high. Therefore, the 147±15Ma isochron age is not reliable.

Split B produced an ^{39}Ar spectrum similar to that of split A, but it had an older pseudo plateau of 228±1 Ma calculated by using steps 2 and 3 (table 2, fig. 6A). The inverse isochron plot of split B yielded an $^{40}Ar/^{36}Ar$ ratio indicative of excess argon and an age of 154±16 Ma (table 2). Split C yielded a highly disturbed spectrum showing ages ranging between about 230 and 460 Ma.

The Ar isotopic variation between our three splits of detrital crossite separated from the same sample indicates that they contain a mix of amphibole grains having somewhat different ages that included different amounts of excess argon. In addition, the variable K/Ca ratios measured suggest that the $^{40}Ar/^{39}Ar$ ages are the product of more than one mineral. Stilpnomelane inclusions are a likely source for the Ar released in the low-temperature steps. A possible conclusion from these data is that the source area for the Okpikruak Formation contained blueschist-facies metamorphic rocks with

Table 2. Summary of $^{40}Ar/^{39}Ar$ data for sample 1 (fig. 2) from sandstone of the Okpikruak Formation, Alaska

[See table 3 for complete analytical data and laboratory methods. * Isochron age calculated for a single point assuming $^{40}Ar/^{36}$ Ar= 295.5. Steps used refers to the heating steps used to calculate the isochron and plateau ages respectively. MSWD is the mean square weighted deviation, a measure of the goodness of fit of the isochron (Wendt and Carl, 1991). Plateau age is the weighted mean plateau age of the release spectrum. None of the reported plateaus fulfills the strict definition of a plateau age (Dalrymple and Lanphere, 1974). $\%^{39}Ar$ used refers to the plateau age where shown, otherwise to the isochron. Do, ditto]

Sample type	Mineral	Total fusion age, Ma	Isochron age, Ma	Steps used	MSWD	$^{40}Ar/^{36}Ar$	Plateau age, Ma	Steps used	$\%^{39}Ar$ used
Single grain	White mica	327±2	----------	----------	---------	----------	332±2	2 of 3	89
Multiple grains	White mica	291±1	291± 1	2-5 of 11	1.8	282 ± 11	291±1	2-5 of 11	45
------Do----------	-----do--------	291±1	306± 10	7-9 of 11	2.8	696 ± 940	313±1	7-9 of 11	29
------Do----------	-----do--------	291±1	~263*	6 of 11	---------	----------	263±1	6 of 11	20
Split A ----------	Crossite ------	255±1	147 ± 15	2-14 of 15	32	1,249 ± 186	215±1	2-7 of 15	58
Split B ----------	Crossite ------	256±1	154 ± 16	2-8 of 9	27	1,283 ± 196	228±1	2-3 of 9	56
Split C ----------	Crossite ------	344±1	145 ± 17	2-14 of 14	9	1,543 ± 141	----------	----------	95

cooling ages younger than about 215 Ma (Late Triassic) and, therefore, distinct from the source of the late Paleozoic white mica. However, even this conclusion should be treated with caution.

DISCUSSION

Our petrographic, heavy-mineral, and age data, and the results of previous work on the Okpikruak Formation, indicate that several distinct source terrains contributed detritus into the Okpikruak sedimentary basin (fig. 3): (1) Distal continental margin rocks consisting of mudstone, chert, and carbonate debris would account for the sedimentary rock fragments in conglomerates and sandstones of the Okpikruak Formation (Wilbur and others, 1987; Siok, 1989; Meier, 1995; J. A. Dumoulin, U.S. Geological Survey, written commun., 1990; this study). (2) Felsic to intermediate plutonic and volcanic rocks, some of Middle to Late Jurassic age, would provide igneous rock clasts and igneous minerals including coarse hornblende (Patton and Tailleur, 1964; Mayfield and others, 1978; Meier, 1995; Dumoulin, U.S. Geological Survey, written commun., 1990; this study). (3) Ultramafic rocks would contribute pyroxene and chromite (Patton and Tailleur, 1964; this study). (4) One or more blueschist- to greenschist-grade metamorphic terranes containing blue amphibole, could account for the white mica, garnet, chlorite, actinolite, and epidote, as well as quartz mylonite and phyllite (J.A. Dumoulin, unpub. data, 1990; Meier, 1995; this study).

Some of these source terrains are readily identifiable in the Brooks Range. Upper Paleozoic and Lower Mesozoic rocks of the Endicott Mountains, Picnic Creek, and Ipnavik River allochthons include limestone, chert, and siltstone lithologies like those found as clasts and lithic fragments in the Okpikruak Formation. In many places, strata of the Okpikruak Formation overlie these passive margin rocks suggesting that some of the sedimentary detritus was locally derived. Likewise, the Misheguk Mountain and Copter Peak allochthons, which are found in klippen in the northern Brooks Range, probably provided nearby sources of ultramafic and mafic rock detritus in the Okpikruak Formation.

For the source of the metamorphic and plutonic minerals and rock fragments in the Okpikruak Formation, we need to look to the southern Brooks Range and the Koyukuk basin. The Middle Jurassic plutons in the Koyukuk basin are probably correlative with the dated igneous clasts in the Okpikruak Formation (Mayfield and others, 1978; Box and Patton, 1989). Although these plutons are limited in extent to the Koyukuk basin today, it seems likely that related rocks extended across the southern Brooks Range in Late Jurassic to Early Cretaceous time, when the Koyukuk arc was obducted over the Arctic Alaska margin. Presumably, this part of the arc was later removed by uplift and deep exhumation in the core of the Brooks Range, perhaps related to regional extension (Miller and Hudson, 1991).

The origin of the metamorphic minerals in rocks of the Okpikruak Formation is more difficult to determine. The Schist Belt is a possible source. Rocks in the Schist Belt contain the required white mica, glaucophane, garnet, and chlorite. However, the available $^{40}Ar/^{39}Ar$ cooling ages indicate that rocks of the Schist Belt were at depths of 10 to 15 km until 130 Ma (for example, Turner and others, 1979; Blythe and others, 1990; Christiansen and Snee, 1994), and fission-track ages suggest that these rocks were not exhumed until after 100 Ma (Blythe and Patrick, 1994). Therefore, it is unlikely that the presently exposed Schist Belt rocks could have contributed debris to the Valanginian (older than 131 Ma) rocks of the Okpikruak Formation that we studied.

Our $^{40}Ar/^{39}Ar$ data indicate that the white mica in the Okpikruak Formation was derived from metamorphic or plutonic rocks having Carboniferous cooling ages. Carbonifer-

ous metamorphic or plutonic rocks that could account for these white mica ages are not known in the Schist Belt, or elsewhere in northern Alaska. Generally, the Carboniferous was a time of tectonic quiescence and passive margin sedimentation on the Arctic Alaska continental margin (Moore and others, 1994). The stratigraphy beneath the Colville basin, and within the Endicott Mountains, Picnic Creek, and Ipnavik River allochthons attests to continuous passive margin subsidence in Late Paleozoic and Early Mesozoic time. The Central Belt, Schist Belt, and Phyllite Belt, which are thought to represent metamorphosed equivalents of the passive margin, also include Upper Paleozoic metasedimentary rocks, suggesting that these areas were also subsiding in Late Paleozoic time. In this framework, it is difficult to envision a scenario for uplift and cooling of these rocks to produce the Carboniferous white mica ages.

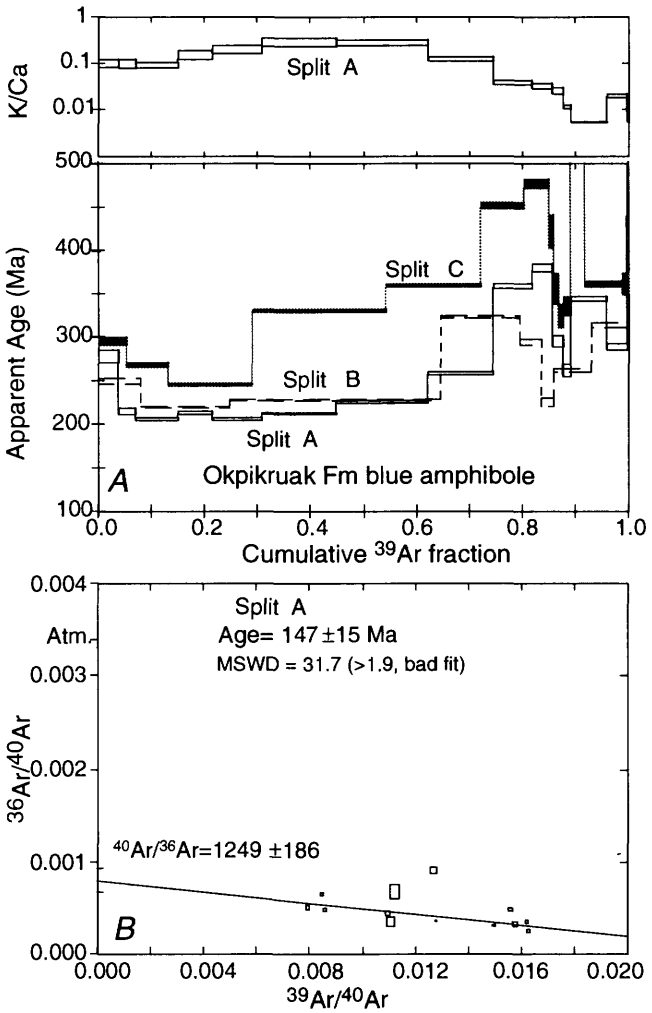

Figure 6. $^{40}Ar/^{39}Ar$ age spectra and inverse isochron plot of detrital blue amphibole sample from the Okpikruak Formation. A, $^{40}Ar/^{39}Ar$ age and K/Ca spectra. Splits A and B produced pseudo plateaus of low-temperature steps having ages of about 215 and 228 Ma, respectively. Higher temperature steps of split C are highly disturbed and correlate to low K/Ca ratios (above). They probably result from incorporation of excess argon and contribution of more than one mineral phase to the release spectrum. The vertical thickness of each step represents the error in age or K/Ca ratio of that step. B., Isochron plot for split A using all temperature steps except first and last. Data are highly scattered, and $^{40}Ar/^{36}Ar$ ratio is indicative of excess argon. Isochron age of 147±15 Ma is probably not geologically meaningful. This plot is typical of all three splits. Atm, $^{40}Ar/^{36}Ar$ atmospheric ratio (295.5); MSWD, mean square weighted deviation.

It is possible that a white-mica-bearing granite, belonging to the belt of Late Devonian plutons in the Central Belt of the Brooks Range (Dillon and others, 1987), cooled through the white mica-closure temperature in the Carboniferous and was exhumed during deposition of the Okpikruak Formation. However, it is difficult to envision how the required uplift and denudation could have occurred during regional passive-margin subsidence.

On the basis of stratigraphic and thermochronologic arguments described above, we suggest that the Arctic Alaska terrane is an unlikely source for the the metamorphic detritus in rocks of the Okpikruak Formation, including the white mica and crossite analyzed in this study. We propose that the metamorphic rock detritus was derived from a source terrain in the upper plate that was obducted onto the Arctic Alaska continental margin, perhaps part of the arc itself. The Angayucham terrane (including the Misheguk Mountain and Copter Peak allochthons), which represents an interarc basin or fore-arc limb of an island arc, is mostly prehnite-pumpellyite to greenschist facies, but garnet-bearing amphibolites are present locally in the Angayucham Mountains (Pallister and others, 1989). In addition, blue amphibole-bearing metabasalts have been found within Angayucham-equivalent rocks at the southern edge of the Koyukuk basin (Patton and Box, 1989). So it is possible that the detrital garnet and blue amphibole in samples of the Okpikruak Formation were derived from the Angayucham terrane.

The presence of white mica, quartz mylonite, and phyllite in rocks of the Okpikruak Formation suggests that the source area also included metamorphic and possibly plutonic elements of continental affinity not presently recognized in the Brooks Range. Such continental rocks may have been present in the Koyukuk arc or, alternatively, unknown crustal blocks may have been caught in the collision between the arc and the continent.

CONCLUSIONS

Our petrographic, heavy-mineral, and $^{40}Ar/^{39}Ar$ data from Lower Cretaceous rocks of the Okpikruak Formation indicate that the sources of the Okpikruak Formation included (1) the Arctic Alaska continental margin (sedimentary rocks of the Endicott Mountains, Picnic Creek, and Ipnavik River allochthons), (2) the island arc that collided with the continental margin (the Koyukuk arc), (3) the obducted ophiolites and oceanic basin rocks (the Misheguk Mountain and

Copter Peak allochthons of the Angayucham terrane), and (4) metamorphic rocks, of blueschist- to greenschist-metamorphicgrade, of unknown origin. The Carboniferous $^{40}Ar/^{39}Ar$ ages of detrital white micas separated from the Okpikruak Formation make it unlikely that the detrital metamorphic minerals were derived from the Schist Belt or any part of the Arctic Alaska continental margin. A more likely source for such detritus is the basement of the arc that overrode the Arctic Alaska margin and (or) an unknown continental block that was caught in the arc-continent collision. This would require that the Koyukuk arc had a more complicated history than has previously been recognized.

ACKNOWLEDGMENTS

Elizabeth Miller encouraged us to date the blueschist event in the Brooks Range. Julie Dumoulin's discovery of detrital blue amphibole in the Okpikruak Formation, Gil

Table 3. Argon analytical data for a sandstone sample from the Okpikruak Formation, Brooks Range, Alaska. [^{40}Ar(mol) = moles corrected for blank and reactor-produced ^{40}Ar. Ratios are corrected for blanks, decay, and interference. $\Sigma^{39}Ar$ is cumulative, ^{40}Ar radiog. = radiogenic fraction.

LABORATORY METHODS: From the heavy mineral fractions, 1 to 2.5 mg of blue amphibole and white mica were hand picked for $^{40}Ar/^{39}Ar$ dating. The samples were irradiated at the TRIGA reactor at the University of Oregon, and the analyses were performed at Phil Gans' laboratory at Univ. of California, Santa Barbara by J. Toro and A. Calvert. The laboratory is equipped with a Mass Analyzer Products model 216 mass spectrometer with a Baur-Signer source and a Johnston MM-1 multiplier, an all-metal extraction line/gas purification manifold, and a Staudacher-type double-vacuum resistance furnace manufactured by Modifications Limited. Samples are routinely analyzed on the multiplier at a gain of ~3,500, providing a sensitivity of ~$2.5x10^{-14}$ mol/volt. The dynamic background in the mass spectrometer ranges between 2 and $5x10^{-18}$ mol for all Ar isotopes. A typical system blank for a 15-minute heating step at 1,200°C is $2.5x10^{-16}$ mol ^{40}Ar and $5x10^{-18}$ mol ^{36}Ar (including mass-spectrometer backgrounds). The mass-spectrometer data were corrected for neutron flux gradient using Charcoal Ovens Sanidine, 35.88 Ma, an internal standard calibrated with Taylor Creek Sanidine (Dalrymple and Duffield, 1988). The analyses were corrected for decay since irradiation, mass discrimination, and interference of Ar isotopes produced by Cl, Ca, and K. Uncertainties reported are one sigma determined by using the uncertainties in monitor age, decay rates of ^{37}Ar, ^{39}Ar, and ^{40}Ar, rates of reactor-produced Ar-isotopes, duration of irradiation, time since irradiation, peak heights, blank values, and irradiation parameter J]

T (°C)	^{40}Ar (mol)	$^{40}Ar/^{39}Ar$	$^{37}Ar/^{39}Ar$	$^{36}Ar/^{39}Ar$	K/Ca	$\Sigma\ ^{39}Ar$	^{40}Ar radiog.	Age (Ma)
			White mica - single grain					J=0.0054570
550	1.7e-15	24.5264	0.4742	0.0653	1.0	0.038	0.560	226.6 ± 27.8
1100	3.5e-14	37.1390	0.0118	0.0047	41.0	0.930	0.964	332.9 ± 1.6
1350	2.5e-15	33.0764	0.1221	0.0081	4.0	1.000	0.933	299.3 ± 12.8
Total fusion age= 326.65±2.00 Ma								
Inverse isochron age =337.27±7.88 Ma. (MSWD =19.08; $^{40}Ar/^{36}Ar$=157.7±163.0). All steps.								
			White mica - multiple grains					J=0.005457
500	6.6e-15	25.5893	0.1822	0.0490	2.7	0.022	0.639	235.8 ± 6.8
575	8.2e-15	32.4519	0.1482	0.0131	3.3	0.053	0.893	294.1 ± 4.4
675	2.9e-14	31.6381	0.0653	0.0279	7.5	0.151	0.794	287.3 ± 1.9
725	2.9e-14	32.2214	0.0284	0.0034	17.0	0.270	0.970	292.2 ± 1.3
775	4.8e-14	32.0030	0.0100	0.0009	49.0	0.472	0.992	290.4 ± 0.9
850	4.3e-14	28.7837	0.0070	0.0011	70.0	0.672	0.989	263.2 ± 1.0
925	1.7e-14	34.1858	0.0565	0.0019	8.7	0.739	0.984	308.6 ± 2.4
1000	2.1e-14	34.8947	0.1500	0.0012	3.3	0.821	0.991	314.4 ± 1.8
1100	3.8e-14	34.7631	0.0904	0.0025	5.4	0.965	0.980	313.4 ± 1.3
1250	6.5e-15	31.7162	0.1583	0.0062	3.1	0.991	0.946	288.0 ± 5.1
1350	2.7e-15	41.1943	0.0848	0.0084	5.8	1.000	0.943	365.8 ± 13.5
Total fusion age= 290.93±0.71 Ma								

Table 3. Argon analytical data for a sandstone sample from the Okpikruak Formation, Brooks Range, Alaska—Continued.

Power (W)	^{40}Ar (mol)	$^{40}Ar/^{39}Ar$	$^{37}Ar/^{39}Ar$	$^{36}Ar/^{39}Ar$	K/Ca	$\Sigma\,^{39}Ar$	^{40}Ar radiog.	Age (Ma)
			Crossite, Split A					J=0.0021338
14	2.6e-14	178.1945	4.8025	0.3379	0.100	0.038	0.440	278.5 ± 7.8
16	1.1e-14	81.2534	4.9152	0.0742	0.100	0.070	0.730	215.0 ± 4.0
18	2.0e-14	66.0952	5.3288	0.0321	0.092	0.148	0.857	205.7 ± 1.9
19	1.7e-14	65.2753	3.1872	0.0217	0.150	0.215	0.902	213.4 ± 1.9
20	2.3e-14	63.5598	2.3985	0.0226	0.200	0.308	0.895	206.6 ± 1.6
21	3.5e-14	63.3963	1.7157	0.0160	0.290	0.448	0.926	212.7 ± 1.2
22	4.7e-14	68.8537	1.7440	0.0211	0.280	0.622	0.909	226.2 ± 1.1
23	3.9e-14	80.6785	4.0114	0.0288	0.120	0.746	0.894	258.1 ± 1.5
24	3.4e-14	120.3602	12.7873	0.0587	0.038	0.819	0.856	357.9 ± 2.7
26	1.9e-14	129.6945	15.2283	0.0660	0.032	0.857	0.850	380.4 ± 4.1
29	6.8e-15	92.9728	19.2011	0.0318	0.026	0.876	0.899	295.6 ± 6.0
32	5.2e-15	91.7980	43.1899	0.0627	0.011	0.891	0.798	261.7 ± 7.5
35	3.1e-14	122.0688	90.5824	0.0799	0.005	0.959	0.807	343.7 ± 3.0
38	1.4e-14	93.9196	24.4892	0.0417	0.020	0.998	0.869	289.4 ± 3.7
45	9.9e-16	139.5253	54.5398	0.0000	0.009	1.000	1.000	486.7 ± 48.0

Total fusion age= 254.67 ± 0.73 Ma
Inverse isochron age =147.14 ±15.01 Ma. (MSWD =31.64; $^{40}Ar/^{36}Ar$=1248.7±185.8)
Steps used in the isochron: 2 to 14 or 96% $\Sigma\,^{39}Ar$.

			Crossite, Split B					J=0.0021338
15	3.2e-14	112.4410	2.6563	0.1437	0.18	0.080	0.622	250.9 ± 3.4
19	4.1e-14	68.7872	3.6715	0.0261	0.13	0.247	0.888	220.9 ± 1.2
22	9.8e-14	69.5461	1.6886	0.0201	0.29	0.644	0.915	229.5 ± 0.8
24	5.8e-14	107.5354	6.2327	0.0515	0.079	0.795	0.858	324.1 ± 1.7
26	1.4e-14	94.3576	7.4410	0.0375	0.066	0.837	0.882	294.7 ± 3.3
28	5.4e-15	67.5731	5.4296	0.0163	0.090	0.859	0.929	226.7 ± 4.6
33	2.1e-14	87.0475	23.4381	0.0455	0.021	0.929	0.846	263.0 ± 2.4
39	2.4e-14	101.1352	16.4742	0.0397	0.030	0.997	0.884	314.9 ± 2.5
45	1.0e-15	115.1087	13.2804	0.0000	0.037	1.000	1.000	458.6 ± 38.8

Total fusion age= 255.99±0.68 Ma
Inverse isochron age =153.85±16.26 Ma. (MSWD =27.02; $^{40}Ar/^{36}Ar$=1283.0±196.2)
Steps used in the isochron: 2 to 8 or 92% $\Sigma\,^{39}Ar$.

			Crossite, Split C					J=0.0021338
14	2.2e-14	147.3413	2.3190	0.2159	0.21	0.052	0.567	295.6 ± 5.3
17	2.0e-14	87.5142	4.5309	0.0414	0.11	0.132	0.860	268.7 ± 2.6
19	3.4e-14	75.8738	1.9180	0.0248	0.26	0.291	0.903	246.2 ± 1.5
21	7.6e-14	105.9966	1.4309	0.0396	0.34	0.544	0.890	330.7 ± 1.3
22	6.0e-14	117.8113	2.2940	0.0488	0.21	0.723	0.878	359.5 ± 1.9
23	3.6e-14	156.8226	9.0546	0.0795	0.054	0.803	0.850	451.3 ± 3.7
24	2.2e-14	166.7369	18.7743	0.0843	0.026	0.850	0.851	476.1 ± 5.6
25	3.9e-15	147.8478	20.1838	0.0821	0.024	0.860	0.836	421.9 ± 18.7
26	2.5e-15	116.1003	14.5493	0.0472	0.034	0.867	0.880	355.4 ± 17.6
28	2.9e-15	106.5373	13.0004	0.0473	0.038	0.877	0.869	324.8 ± 13.7
31	4.7e-15	110.2675	18.2651	0.0484	0.027	0.892	0.870	335.9 ± 10.6
34	1.6e-14	222.3519	68.9369	0.1434	0.007	0.919	0.809	586.1 ± 9.7
38	2.3e-14	119.8815	23.2309	0.0534	0.021	0.988	0.868	361.8 ± 3.3
45	3.8e-15	117.2472	27.6619	0.0456	0.018	1.000	0.885	360.8 ± 12.7

Total fusion age= 344.14 ±0.99 Ma
Inverse isochron age =145.43±17.54 Ma. (MSWD =9.38; $^{40}Ar/^{36}Ar$=1543.3±141.6)
Steps used in the isochron: 2–14 or 95% $\Sigma\,^{39}Ar$

Mull's navigational skills, and David Howell's helicopter support led us to the right rocks. Phil Gans and Andy Calvert, from the University of California at Santa Barbara, helped us carry out the $^{40}Ar/^{39}Ar$ dating.

REFERENCES CITED

Blythe, A.E., Wirth, K.R., and Bird, J.M., 1990, Fission-track and $^{40}Ar/^{39}Ar$ ages of metamorphism and uplift, Brooks Range, northern Alaska [abs.]: Geologic Association of Canada Program and Abstracts, v. 15, p. A12.

Blythe, A.E., and Patrick, B.E., 1994, Tertiary cooling and deformation in the south-central Brooks Range, Alaska, deduced from apatite fission track analyses [abs.]: Geological Society of America Abstracts with Programs, v. 26, no. 2, p. 39.

Box, S.E., Patton, W.E., Jr., and Carlson, C., 1985, Early Cretaceous orogenic belt in northwestern Alaska: internal organization, lateral extent, and tectonic interpretation, in Howell, D.G., ed., Tectonostratigraphic terranes of the circum-Pacific region: Houston, Texas, Circum-Pacific Council for Energy and Mineral Resources, p. 137-146.

Box, S.E., and Patton, W.W., Jr., 1989, Igneous history of the Koyukuk terrane, western Alaska: constraints on the origin, evolution, and ultimate collision of an accreted island-arc terrane: Journal of Geophysical Research, v. 94, no. B11, p. 15,843–15,867.

Christiansen, P.P., and Snee, L.W., 1994, Structure, metamorphism, and geochronology of the Cosmos Hills and Ruby Ridge, Brooks Range schist belt, Alaska: Tectonics, v. 13, no. 1, p. 193-213.

Cole, F., Bird, K., Toro, J., Roure, F., O'Sullivan, P.B., Pawlewicz, M., and Howell, D.G., in 1997, A kinematic model for the north-central Brooks Range fold and thrust belt, Alaska: Journal of Geophysical Research, v. 102, p. 20685-20708.

Cole, F., Bird, K.J., Toro, J., Roure, F., and Howell, D.G., 1995, Kinematic and subsidence modeling of the north-central Brooks Range and North Slope of Alaska: U.S. Geological Survey Open-File Report 95-823, 3 sheets.

Dalrymple, G.B., and Lanphere, M.A., 1974, $^{40}Ar/^{39}$ Ar age spectra of undisturbed terrestrial samples: Geochimica et Cosmochimica Acta, v. 38, no. 5, p. 715-738.

Dalrymple, G.B., and Duffield, W.A., 1988, High-precision ^{40} Ar/^{39} Ar dating of Oligocene rhyolites from the Mogollon-Datil volcanic field using a continuous laser system: Geophysical Research Letters, v. 15, no. 5, p. 463-466.

Dickinson, W.R., Beard, L.S., Brakenridge, G.R., Erjavec, J.L., Ferguson, R.C., Inman, K.F., Knepp, R.A., Lindberg, F.A., and Ryberg, P.T., 1983, Provenance of North American Phanerozoic sandstones in relation to tectonic setting: Geological Society of America Bulletin, v. 94, no. 2, p. 222-235.

Dillon, J.T., Tilton, G.R., Decker, J., and Kelley, M.J., 1987, Resource implications of magmatic and metamorphic ages for Devonian igneous rocks in the Brooks Range, in Tailleur, I.L., and Weimer, P., eds., Alaskan north-slope geology: Bakersfield, Calif., Society of Economic Paleontologists and Mineralogists, Pacific Section, and Alaska Geological Society, Book 50, p. 713-723.

Dusel-Bacon, C., Brosgé, W.P., Till, A.B., Doyle, E.O., Mayfield, C.F., Reiser, H.N., and Miller, T.P., 1989, Distribution, facies, ages, and proposed tectonic associations of regionally metamorphosed rocks in northern Alaska: U.S. Geological Survey Professional Paper 1497-A, 44 p.

Elder, W.P., Miller, J.W., and Adam, D.P., 1989, Maps showing fossil localities and checklists of Jurassic and Cretaceous macrofaunaof the North Slope of Alaska, U.S. Geological Survey Open-File Report 89-0556; 7 p., 12 sheets.

Ellersieck, I., Mayfield, C.F., Tailleur, I.L., and Curtis, S.M., 1979, Thrust sequences in the Misheguk Mountain quadrangle, Brooks Range, Alaska, in Johnson, K.M., and Williams, J.R., eds., The United States Geological Survey in Alaska: accomplishments during 1978: U.S. Geological Survey Circular 804-B, p. B8-B9.

Gryc, G., Patton, W.W., Jr., and Payne, T.G., 1951, Present Cretaceous stratigraphic nomenclature of northern Alaska: Washington Academy of Sciences Journal, v. 41, no. 5, p. 159-167.

Harris, R.A., 1987, Structure and composition of sub-ophiolite metamorphic rocks, western Brooks Range ophiolite belt, Alaska [abs.]: Geological Society of America Abstracts with Programs, v. 19, no. 6, p. 387.

Harris, R.A., 1995, Geochemistry and tectonomagmatic affinity of the Misheguk massif, Brooks Range ophiolite, Alaska: Lithos, v. 35, no. 1, p. 1-25.

Ingersoll, R.V., and Suczek, C.A., 1979, Petrology and provenance of Neogene sand from Nicobar and Bengal fans, DSDP sites 211 and 218: Journal of Sedimentary Petrology, v. 49, no. 4, p. 1217-1228.

Little, T.A., Miller, E.L., Lee, J., and Law, R.D., 1994, Extensional origin of ductile fabrics in the Schist Belt, central Brooks Range, Alaska–I. Geologic and structural studies: Journal of Structural Geology, v. 16, no. 7, p. 899-918.

Mayfield, C.F., Tailleur, I.L., Mull, C.G., and Silberman, M.L., 1978, Granitic clasts from Upper Cretaceous conglomerate in the northwestern Brooks Range, in Johnson, K.M., ed., The United States Geological Survey in Alaska: accomplishments during 1977: U.S. Geological Survey Circular 772-B, p. B11–B13.

Mayfield, C.F., Tailleur, I.L., and Ellersieck, I., 1988, Stratigraphy, structure, and palinspastic synthesis of the western Brooks Range, northwestern Alaska, in Gryc, George, ed., Geology and exploration of the National Petroleum Reserve in Alaska, 1974 to 1982, U.S. Geological Survey Professional Paper 1399, p. 143–186.

McDougall, I., and Harrison, T.M., 1988, Geochronology and thermochronology by the $^{40}Ar/^{39}Ar$ method: New York, Oxford University Press, 212 p.

Meier, J.M., 1995, Petrographic evaluation of foreland basin sandstones, Brooks Range, north-central Alaska: Columbia, University of Missouri-Columbia M.S. thesis, 253 p.

Miller, E.L., and Hudson, T.L., 1991, Mid-Cretaceous extensional fragmentation of a Jurassic-Early Cretaceous compressional orogen, Alaska: Tectonics, v. 10, no. 4, p. 781–796.

Moore, T.E., 1987, Geochemical and tectonic affinity of basalts of the Copter Peak and Ipnavik River allochthons, Brooks Range, Alaska [abs.]: Geological Society of America Abstracts with Programs, v. 19, no. 6, p. 437.

Moore, T.E., Aleinikoff, J.N., and Walter, M., 1993, Middle Jurassic U-Pb crystallization age for Siniktanneyak Mountain ophiolite, Brooks Range, Alaska [abs.]: Geological Society of America Abstracts with Programs, v. 25, no. 5, p. 124.

Moore, T.E., Wallace, W.K., Bird, K.J., Karl, S.M., Mull, C.G., and Dillon, J.T., 1994, Geology of northern Alaska, in Plafker, George, and Berg, H.C., eds., The geology of Alaska: Boulder, Colo., Geological Society of America, The Geology of North

America, v. G1, p. 49-140.

Morris, R.H. and Lathram E.H., 1951, Heavy mineral studies, in Payne, T.G., and others, eds., Geology of the Arctic Slope ofAlaska: U.S. Geological Survey Oil and Gas Investigation Map OM-126, sheet 3.

Mull, C.G., Adams, K.E., Bodnar, D.A., and Siok, J.P., 1985, Stratigraphy of Endicott Mountains and Picnic Creek allochthons, Killik River and Chandler Lake quadrangles, north-central Brooks Range, Alaska: American Association of Petroleum Geologists, v. 69, no. 4, p. 671.

Mull, C.G., Moore, T.E., Harris, E.E., and Tailleur, I.L., 1994, Geologic map of the Killik River quadrangle, Brooks Range, Alaska: U.S. Geological Survey Open-File Report 94-0679; 1 sheet, scale 1:125,000.

Mull, C.G., Roeder, D.H., Tailleur, I.L., Pessel, G.H., Grantz, A., and May, S.D., 1987, Geologic sections and maps across Brooks Range and Arctic slope to Beaufort Sea, Alaska: U.S. Geological Survey Map and Chart Series MC-28S, 1 sheet.

Mull, C.G. and Werdon, M.B., 1994, Generalized geologic map of the western Endicott Mountains, central Brooks Range, Alaska: Alaska Division of Geological and Geophysical Surveys Public-Data File 94-55; 1 sheet, scale 1:250,000.

Murphy, J.M. and Patton, W.W., Jr., 1988, Geologic setting and petrography of the phyllite and metagreywacke thrust panel, north-central Alaska, in Galloway, J.P., and Hamilton,T.D., eds., Geologic studies in Alaska by the U.S. Geological Survey during 1987, U.S. Geological Survey Circular 1016, pp. 104-109.

Pallister, J.S., Budahn, J.R., and Murchey, B.L, 1989, Pillow basalts of the Angayucham terrane: oceanic plateau and island crust accreted to the Brooks Range: Journal of Geophysical Research, v. 94, no. B11, p. 15,901–15,923.

Patton, W.W., Jr., and Tailleur, I.L., 1964, Geology of the Killik-Itkillik region, Alaska: U.S. Geological Survey Professional Paper, v. 303-G, p. 409-500.

Patton, W.W., Jr., and Box, S.E., 1989, Tectonic setting of the Yukon-Koyukuk basin and its borderlands, western Alaska: Journal of Geophysical Research, v. 94, no. B11, p. 15,807–15,820.

Patton, W.W., Jr., Box, S.E., Moll-Stalcup, E.J., and Miller, T.P., 1994, Geology of west-central Alaska, in Plafker, George, and Berg, H.C., eds., The geology of Alaska: Boulder, Colo., Geological Society of America, The Geology of North America, v. G1, p. 241-269.

Roeder, D., and Mull, C.G., 1978, Tectonics of the Brooks Range ophiolites, Alaska: American Association of Petroleum Geologists Bulletin, v. 62, no. 9, p. 1696-1713.

Siok, J.P., 1989, Stratigraphy and petrology of the OkpikruakFormation at Cobblestone Creek, north-central Brooks Range, in Mull, C.G., and Adams, K.E., eds., Dalton Highway, Yukon River to Prudhoe Bay, Alaska, Bedrock geology of the eastern Koyukuk basin, central Brooks Range, and east central Arctic Slope: Alaska Division of Geological and Geophysical Surveys Guidebook 7, p. 285–292.

Sisson, V.B., and Onstott, T.C., 1986, Dating blueschist metamorphism; a combined $^{40}Ar/^{39}Ar$ and electron microprobe approach: Geochimica et Cosmochimica Acta, v. 50, no. 9, p. 2111-2117.

Tailleur, I.L., Kent, B.H., Jr., and Reiser, H.N., 1966, Outcrop geologic map of the Nuka-Etivluk region, northern Alaska: U.S. Geological Survey Open-File Report 66-128, 7 sheets, scale 1:63,360.

Till, A.B., 1988, Evidence for two Mesozoic blueschist belts in the hinterland of the western Brooks Range fold and thrust belt [abs.]: Geological Society of America Abstracts with Programs, v. 21, no. 7, p. A112.

Till, A.B., 1992, Detrital blue-schist facies metamorphic mineral assemblages in early Cretaceous sedimentary assemblages of the foreland basin of the Brooks Range, Alaska, and implications for orogenic evolution: Tectonics, v. 11, no. 6, p. 1207-1223.

Till, A.B., and Snee, L.W., 1995, $^{40}Ar/^{39}Ar$ evidence that formation of blueschists in continental crust was synchronous with foreland fold and thrust belt formation, western Brooks Range, Alaska: Journal of Metamorphic Geology, v. 13, no. 1, p. 41-60.

Turner, D.L., Forbes, R.B., and Dillon, J.T., 1979, K-Ar geochronology of the southwestern Brooks Range, Alaska: Canadian Journal of Earth Sciences, v. 16, p. 1789-1804.

Wendt, I., and Carl, C., 1991, The statistical distribution of the mean squared weighted deviation: Chemical Geology, v. 86, p. 275-285.

Wilbur, S.C., Siok, J.P., and Mull, C.G., 1987, A comparison of two petrographic suites of the Okpikruak Formation: a point count analysis, in Tailleur, I., and Weimer, P., eds., Alaskan North Slope Geology: Bakersfield, Calif., and Anchorage, Alaska, Society of Economic Paleontologists and Mineralogists, Pacific Section, and the Alaska Geological Society, p. 441–447.

Wirth, K.R., Bird, J.M., Blythe, A.E., and Harding, D.J., 1993, Age and evolution of western Brooks Range ophiolites, Alaska: result from $^{40}Ar/^{39}Ar$ thermochronometry: Tectonics, v. 12, no. 2, p. 410-432.

Reviewers: Kenneth J. Bird, Thomas E. Moore, and Sarah Roeske.

The Coast Mountains Structural Zones in Southeastern Alaska—Descriptions, Relations, and Lithotectonic Terrane Significance

By David A. Brew *and* Arthur B. Ford

ABSTRACT

The term "Coast shear zone" has been used informally in various ways for different large-scale structural, mostly fault-related features of different ages along the western side of the Coast Mountains Complex in southeastern Alaska. This report describes, from oldest to youngest, the five closely spaced structural zones that extend the length of southeastern Alaska.

(1) Gravina belt structural zone of mid- to Late Cretaceous age that shortened and thickened Lower to Upper Cretaceous sedimentary, volcanic, and conglomeratic rocks of the Gravina overlap assemblage.

(2) Behm Canal structural zone of latest Cretaceous age that juxtaposed rocks of the Gravina overlap assemblage with rocks of the Alexander and Wrangellia terranes of the Insular superterrane and with rocks of the Nisling (Yukon-Tanana terrane equivalent) terrane rocks of the Intermontane superterrane. (1) and (2) together form what has been called the "mid-Cretaceous thrust system."

(3) Great Tonalite Sill (GTS) shear zone of latest Cretaceous and Paleocene age that localized the emplacement of the GTS plutons within the Behm Canal structural zone, mostly between about 85 and 56 Ma.

(4) Great Tonalite Sill mylonite zone of Paleocene and Eocene age that localized near-vertical movements in a narrow space along the footwall of the GTS during and after its emplacement.

(5) Coast Range megalineament zone of inferred Eocene to Holocene age, which was the major western boundary of Coast Mountains uplift.

All of these features are within what we have called the "southeastern Alaska coincident zone" (Brew and Ford, 1985). All of these features, as well as other older ones not discussed here, are related to the long-lived tectonism that formed the back-arc rift basin that was the depocenter for rocks of the Gravina overlap assemblage. We, as well as others, interpret that tectonism to be related to the Insular-Intermontane superterrane boundary and interpret that boundary to have been a long-lived zone of compressive to transpressive and (or) transcurrent movement.

Each of the five structural zones is important in the sequence of tectonic events in the region, but their existence as separate and distinct features has not been discussed previously. Recognizing the zones and establishing their relations is critical to understanding the overall tectonic process. Difficulties arise in applying a specific name where one or more structural zones coincide. However, the different zones should be separated insofar as possible, and their geographic and structural relations should be described.

INTRODUCTION

Five structural zones of different ages and different types have been identified in the western part of the Coast Mountains Complex (Brew and others, 1995). Each structural zone has had an important role in the evolution of the Coast Mountains Complex, including effects on its constituent plutonic and metamorphic rocks. We describe here, together for the first time, each of the Coast Mountains structural zones and their ages, features, and relations to each other (fig.1). There has been some some confusion about the use of different terms for the structural zones; a few examples follow. (1) Umhofer and Schiarizza (1996) identify the "Coast Shear Zone" (CSZ on their figure 1) as a "major strike-slip fault" related spatially, but not genetically, to Tertiary transcurrent fault movements in southwestern British Columbia. (2) Karl and others (1996) use the term "Coast shear zone" to denote the structure that bounds the uplift of the Coast Mountains Complex on its west side; this same structure was described previously as the "Coast Range megalineament" by Brew and Ford (1978). (3) Smithson and others (1996a, b) used "Coast shear zone" in explaining the geophysical characteristics of some deep crustal features. (4) Hollister and Rohr (1996) and their colleagues in a recent symposium used the term loosely to

apply to any structural zone at the western margin of the Coast Mountains Complex. Unfortunately, these reports do not present any descriptions of the shear feature or any data to justify the use of the term "shear."

Our field studies indicate that, rather than a single "Coast shear zone" along the west side of the Coast Mountains Complex, there are actually five closely associated structural zones (fig. 2). Those five zones are discussed here from oldest to youngest. (1) The Gravina belt structural zone (GBSZ) of mid- to Late Cretaceous age that shortened and thickened Lower to Upper Cretaceous sedimentary, volcanic, and conglomeratic rocks of the Gravina overlap assemblage (2) The Behm Canal structural zone (BCSZ) of latest Cretaceous age that juxtaposed rocks of the Gravina overlap assemblage with rocks of the Alexander and Wrangellia terranes of the Insular superterrane and with rocks of the Nisling (Yukon-Tanana equivalent) terrane of the Intermontane superterrane. (3) The Great Tonalite Sill (GTS) shear zone (GTSSZ) of latest Cretaceous and Paleocene age, which is spatially within, but younger than, the Behm Canal structural zone and along which the GTS was emplaced, mostly between about 69 and 56 Ma. (4) The Great Tonalite Sill mylonite zone (GTSMZ) of Paleocene and Eocene age that localized near-vertical movements along the footwall of the GTS during and after its emplacement. (5) The Coast Range megalineament zone (CRMZ) of inferred Eocene to Holocene age that was the main western limit of uplift of the Coast Mountains. As discussed below, these zones are found in rocks of the Nisling, Stikine, Wrangellia, and Alexander terranes and in rocks of the Gravina overlap assemblage (fig. 2).

In this paper, we call attention for the first time to the close association of these five Coast Mountains structural zones and describe them, their relations, and their associated tectonic events. We hope to encourage distinction between the different zones and additional studies that will further define their characteristics and relations, and to promote use of appropriate descriptive nomenclature.

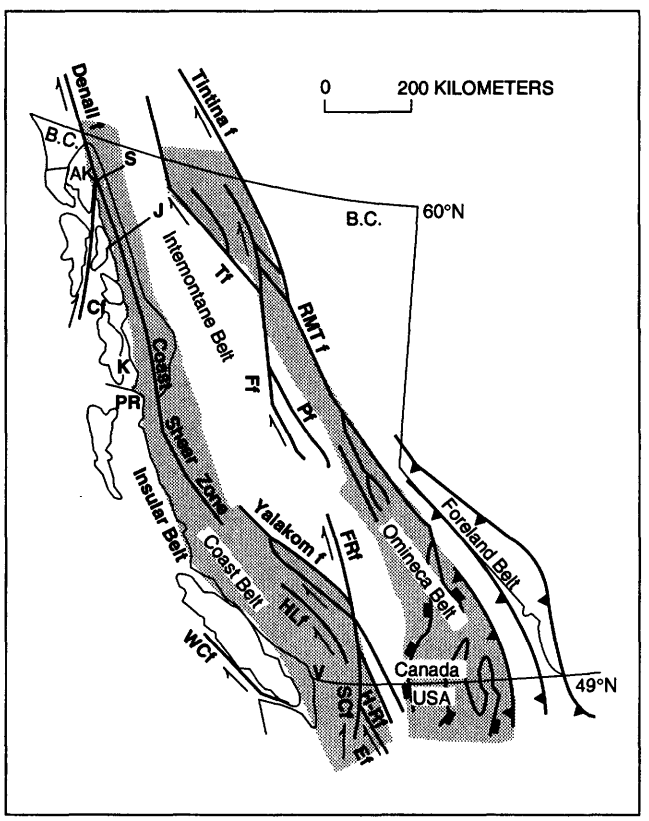

Figure 1. Index map of southeastern Alaska (AK), western British Columbia (BC), and northern Washington (USA), showing major strike-slip faults (f) of Late Cretaceous and early Tertiary age. From Umhoefer and Schiarizza (1996, p. 768). Other fault abbreviations are: Cf, Chatham Strait; Ef, Entiat; Ff, Finlay; FRf, Fraser River; HLf, Harrison Lake; HRf, Hozameen–Ross Lake; Pf, Pinchi; RMTf, Rocky Mountain Trench; SCf, Straight Creek; Tf, Teslin; WCf, West Coast. Community abbreviations are: J, Juneau, Alaska; K, Ketchikan, Alaska; PR, Prince Rupert, British Columbia; S, Skagway, Alaska; V, Vancouver, British Columbia. The Coast Mountains Complex is essentially the same as the Coast Belt shown on this map.

GRAVINA BELT STRUCTURAL ZONE (GBSZ) OF MID- TO LATE CRETACEOUS AGE

The Gravina belt structural zone (GBSZ) (figs. 3A, 4) is the westernmost structural zone in the Coast Mountains Complex. The GBSZ consists of graywackes and volcanic rocks of the Gravina overlap assemblage of Late Jurassic and Early Cretaceous age that have been shortened and thickened by dominantly west-vergent folds and faults and by some east-vergent antithetic faults(?). There are no estimates of the amount of shortening. The GBSZ may be rooted to the northeast and be largely confined to the Cretaceous rocks, although some older rocks of the Alexander terrane that were overlapped by the Gravina assemblage may also be included. The GBSZ is widest and best developed at the latitude of Ketchikan (Rubin and others, 1990; Rubin and Saleeby, 1991). The zone can be traced to the northwest as far as Haines, Alaska, but probably continues beyond into the Dezadeash Formation of British Columbia and Yukon Territory (Eisbacher, 1976; J.E. Mezger, Univ. of Alberta, oral commun., 1996). Evidence for the GBSZ is absent immediately south of southeastern Alaska, in the general vicinity of Prince Rupert, British Columbia (fig. 1) because of the few outcrops of Cretaceous rocks . The GBSZ reappears near Vancouver, British Columbia, as the "Coast Belt Thrust System" of Journeay and Friedman (1993). This zone and the Behm Canal structural zone (described below) together form the "mid-Cretaceous thrust system" of Rubin and others (1990).

The rocks deformed in the GBSZ in southeastern Alaska are Late Jurassic to Early and (or) mid-Cretaceous fossiliferous pelitic, psammitic, and intermediate to mafic volcanic rocks of the Gravina belt. Near Juneau, in northern southeastern Alaska, deformation generally preceded emplacement

of the Late Cretaceous plutons of the 90- to 95-Ma Admiralty-Revillagigedo plutonic belt and the associated contact metamorphism (Brew and others, 1989). To the south near Ketchikan, studies of the gabbros of the older (about 100- to 120-Ma) Alaskan-type mafic-ultramafic body and the adjacent aureole at Union Bay indicate that some deformation

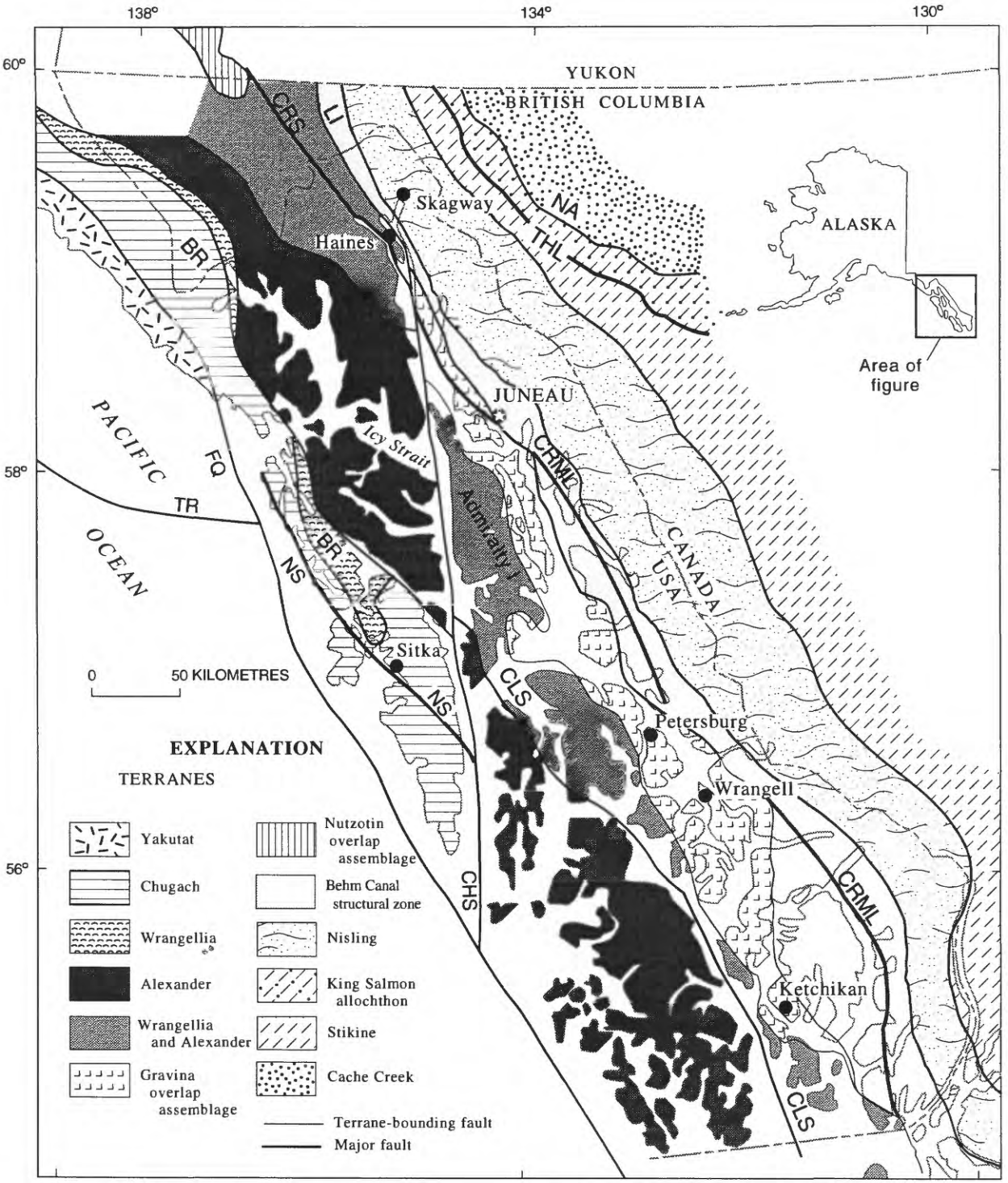

Figure 2. Lithotectonic terrane and major fault map of southeastern Alaska and adjacent parts of Canada. Major faults are indicated by heavy lines and are labeled as follows: BR, Border Ranges; CHS, Chatham Strait; CLS, Clarence Strait; CRML, Coast Range megalineament; CRS, Chilkat River; FQ, Fairweather–Queen Charlotte; LI, Lutak Inlet–Chilkoot River; NA, Nahlin; NS, Neva Strait–Sitka; THL, Tally Ho–Llwellyn; and TR, Transitional. Adapted from Brew and others (1992), Brew, D.A., in Nokleberg and others (1994), and Childe (1996). Area of King Salmon allochthon based on Childe and Thompson (1995) and on Childe (1996).

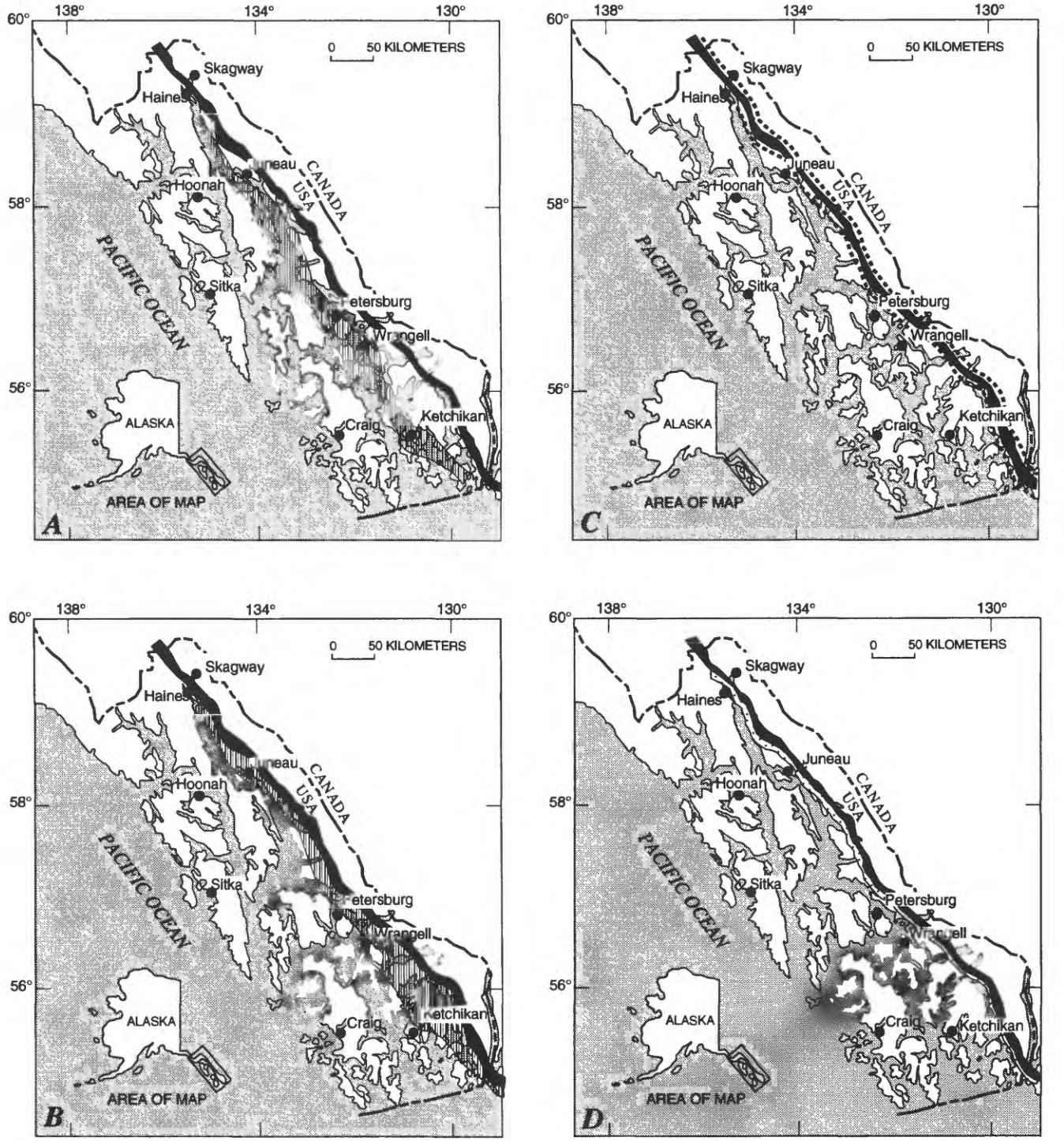

Figure 3. Maps of southeastern Alaska showing: ***A,*** Location of the Gravina belt structural zone (GBSZ; vertical hatching) of Late Cretaceous age (Rubin and others, 1990) and composite Great Tonalite Sill (solid black, about 69-56 Ma. ***B,*** Location of Behm Canal structural zone (BCSZ; vertical hatching) of latest Cretaceous age (Rubin and Saleeby, 1991) and composite Great Tonalite Sill (solid black about 69-56 Ma). ***C,*** Boundaries of Great Tonalite Sill shear zone (GTSSZ; heavy dotted lines) of latest Cretaceous to Paleocene and Eocene age (Ingram and Hutton, 1994), which localized the composite Great Tonalite Sill (solid black about 69-56 Ma.). ***D,*** Location of Great Tonalite Sill mylonite zone (GTSMZ; stipple pattern) of Paleocene and Eocene age at or near footwall of Great Tonalite Sill (Brew and Ford, unpub. data, 1985). The composite Great Tonalite Sill (solid black about 69-56 Ma). ***E,*** Location of Coast Range megalineament zone (CRMZ, heavy dashed line) of inferred Eocene to Holocene age (Brew and Ford, 1978) and composite Great Tonalite Sill (solid black about 69-56 Ma).

occurred during the intrusion of that mid-Cretaceous body (Himmelberg and Loney, 1995); however, Rubin and Saleeby (1992) interpreted the deformation to have been entirely synchronous with the emplacement of the 90– to 95-Ma plutons.

Almost all original thrust contacts in rocks of the Gravina belt structural zone are obscure because the main movements (1) pre-date or are inferred to have been synchronous with the Early to mid-Cretaceous regional M1 metamorphic event of Brew and others (1989), (2) preceded the 95- to 90-Ma intermediate plutons and the associated M4 metamorphic event, and (3) preceded the Late Cretaceous major M5 inverted Barrovian metamorphic sequence event.

In summary, the GBSZ, which is part of the major regional-scale "mid-Cretaceous thrust system" of Rubin and others (1990), is located where rocks of the Gravina belt over lap assemblage back-arc basin rocks were shortened and thickened in a west-vergent thrust system as the Insular superterrane completed its approach to the Intermontane superterrane to the east.

BEHM CANAL STRUCTURAL ZONE (BCSZ) OF LATEST CRETACEOUS AGE

The Behm Canal structural zone (BCSZ) is immediately east of the GBSZ (figs. 2, 3B, 4). The BCSZ juxtaposes graywackes and volcanic rocks of the Gravina overlap assemblage with rocks of the Alexander, Wrangellia, Nisling, and Stikine terranes. The BCSZ is widest and best developed at the latitude of Ketchikan, where it is part of the "mid-Cretaceous thrust system" of Rubin and others (1990) and Rubin and Saleeby (1991). In the rest of southeastern Alaska evidence for the BCSZ is obscure, although it is inferred to continue to the northwest to the latitude of Skagway (fig. 1) where it is poorly expressed, in part because the Coast Mountains Complex is narrowed down adjacent to the Denali fault. South of the Ketchikan area (fig. 1) it may correlate with a west-directed thrust zone inferred for the Prince Rupert area (Crawford and others, 1987). A structural zone somewhat like the BCSZ is found near Vancouver, British Columbia (fig. 1), where it is interpreted by Journeay and Friedman (1993) as the hinterland part of their Coast Belt Thrust System.

The oldest rocks in the BCSZ are Late Proterozoic(?)- and Paleozoic-age quartzofeldspathic gneiss, metacarbonate, pelitic schist, and minor metavolcanic rocks of the Nisling terrane (Wheeler and McFeely, 1991) about 50 km east-northeast of Ketchikan; they have been described as the "East Behm Canal Gneiss Complex" (Rubin and Saleeby, 1991). The youngest rocks in the BCSZ are early Mesozoic metapelitic, metacarbonate, and metavolcanic rocks of the Alava sequence near Ketchikan (Rubin and Saleeby, 1991) and early Late Cretaceous metapelitic, metapsammitic, and metavolcanic rocks near Juneau. Rubin and Saleeby (1991) assert that Gravina overlap assemblage rocks post-date the thrust package of older rocks, but we interpret their map and descriptions to indicate that the rocks of the Gravina overlap assemblage are instead part of the BCSZ.

Deformation in the BCSZ is west vergent and, as noted above, is interpreted by Rubin and Saleeby (1991) to post-date the Middle Triassic Alava sequence and to pre-date rocks of the Gravina overlap assemblage. In contrast, we consider the deformation to post-date the deposition of the rocks of the lower Upper Cretaceous Gravina overlap assemblage, to have been synchronous with, or post-dated, the Early to mid-Cretaceous regional M1 metamorphic event (Brew and others, 1989, 1992), and to have preceded the latest Cretaceous major M5 inverted Barrovian metamorphic sequence of events described by Brew and others (1989, 1992). The deformation also post-dates the emplacement of the 120- to 100-Ma ultramafic and mafic and the 95- to 90-Ma intermediate plutons mentioned above. Most of the faults in the BCSZ are near vertical, and their original character has been obscured by younger metamorphic events. There is no conclusive evidence for the amount of contractional displacement or for any lateral movement.

This major regional-scale structural zone is, like the GBSZ, near the preexisting boundary between the Insular superterrane to the west and the Intermontane superterrane to the east. It may, like the hinterland zone described by Journeay and Friedman (1993), actually be the root zone for the GBSZ thrusts, but this has not been confirmed.

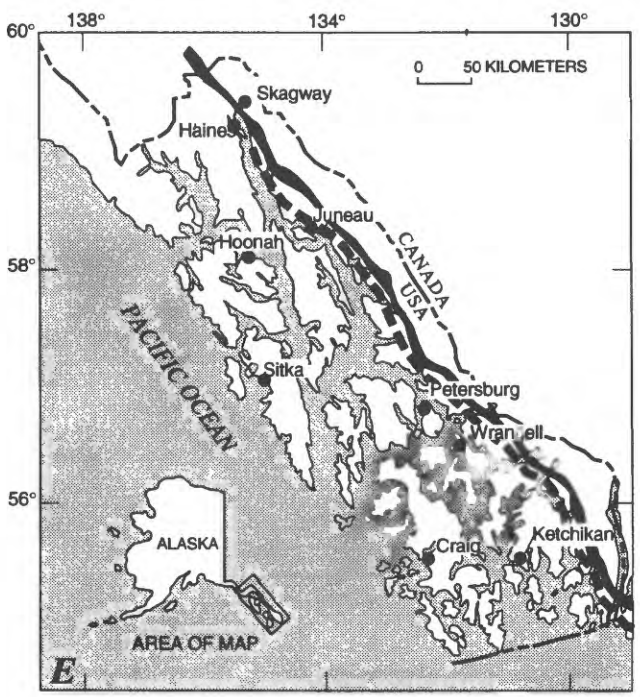

Figure 3. Continued.

GREAT TONALITE SILL SHEAR ZONE (GTSSZ) OF LATEST CRETACEOUS AND PALEOCENE AGE

The Great Tonalite Sill shear zone (GTSSZ) is a major crustal-scale shear zone more than 1,000 km long (fig. 3C, 4)

that localized the emplacement of the various bodies that make up the composite Great Tonalite Sill (Brew, 1994). The GTSSZ includes both the sill bodies and the adjacent hanging and footwall rocks. Himmelberg and others (1991) and Ingram and Hutton (1994) discussed the emplacement of the Great Tonalite Sill into this zone.

The oldest rocks involved in the shear zone are Triassic and Permian metavolcanic and fossiliferous metacarbonate rocks of the Wrangellia terrane to the west and late Proterozoic(?) and Paleozoic rocks of the Nisling terrane to the east. Rocks of the Nisling terrane may also be present west of the GTSSZ (Gehrels and others, 1990; Samson and others, 1991). The youngest rocks deformed by the GTSSZ are the Paleocene and early Eocene plutons of the composite Great Tonalite Sill (about 69 to 55 Ma; Gehrels and others, 1991; Brew, 1994). Highly metamorphosed Upper Jurassic to lower Upper Cretaceous metasedimentary and metavolcanic rocks belonging of the Gravina overlap assemblage are also interpreted to be in the GTSSZ near Juneau.

We believe that the GTSSZ was active during latest Cretaceous, Paleocene, and early Eocene time. Movement in the GTSSZ was synchronous with the major M5 inverted Barrovian metamorphic sequence event (Brew and others, 1989, 1992; Himmelberg and others, 1991, 1994) before, as well as during, the emplacement of the GTS bodies. Abundant mineral-lineation and shear-sense indicators show that the deformation was east over west and contractional. There is no conclusive evidence for the amount of shortening or for any translational deformation. This latter point is surprising, given the length and narrowness of the shear zone and its spatial association with the Insular-Intermontane superterrane boundary, for which some studies have inferred a significant lateral component (Umhoefer and Schiarizza, 1996).

GREAT TONALITE SILL MYLONITE ZONE (GTSMZ) OF PALEOCENE AND EOCENE AGE

The Great Tonalite Sill mylonite zone (GTSMZ) is in and adjacent to the footwalls of the GTS plutons (figs. 3D, 4). The GTSMZ also extends between individual plutons where they are separated. At some localities, such as in the Lemon Creek Glacier pluton near Juneau, the mylonite zone bifurcates, and a strand may extend a few meters into the interior of the pluton.

We interpret the GTSMZ to be the locus of minor movements along the west (footwall) side of GTS following emplacement of the different sill plutons. Inasmuch as plutons of the GTS vary in age (Gehrels and others, 1991; Brew, 1994), it is possible that the GTSMZ may also vary in age. Rocks affected by the mylonitization are mostly the tonalite, granodiorite, and quartz diorite of the footwall parts of the Paleocene and Early Eocene GTS. M5' metamorphic mineral assemblages (Brew and others, 1989, 1992; Himmelberg and others, 1991, 1994) of the pelitic schists in the footwall are interpreted to overprint the higher pressure M5 mineral assemblages. This overprint suggests that the latest phase of emplacement of the sill bodies was probably late adjustment of the already-emplaced bodies under lower pressure and higher temperature conditions. These late adjustments probably took place as uplift of the mountains started and magmatic heat was no longer transferred into the surrounding country rocks. A west-side-up sense in the GTSSZ north of Prince Rupert, British Columbia, has been reported (M.L. Crawford, Bryn Mawr College, oral commun., 1996), but other studies have not confirmed such movement. No estimates of the amount of displacement have been reported.

COAST RANGE MEGALINEAMENT ZONE (CRMZ) OF EOCENE TO HOLOCENE AGE

The Coast Range megalineament zone (CRMZ) is generally within a few kilometers of the western margin of the GTS (figs. 3E, 4). The CRMZ ranges from less than a kilometer to several kilometers wide and is defined locally by discontinuous and overlapping, en echelon topographic lineaments (Brew and Ford, 1978). Locally, such as near Juneau, the zone is a young fault; usually the zone is expressed only by topographic features developed by glacial erosion. The CRMZ marks both the western limit of the Paleocene and younger granitic and related rocks that form the Coast Mountains and the eastern limit of the Admiralty-Revillagigedo belt of 95-Ma magmatic-epidote-bearing plutons. The CRMZ is also the western limit of the post-middle Eocene uplift of the Coast Mountains Complex in southeastern Alaska (Brew and Ford, 1978; Donelick, 1988; Wood and others, 1991; Karl and others, 1996). Thus, we interpret the CRMZ to have been the primary shear zone along which the Coast Mountains to the east were uplifted relative to the rocks to the west. This deformation started some time after the emplacement of the GTS, continued during the emplacement of the great volume of 50-Ma granitic rocks of the Coast Mountains, and persisted through the Neogene until Holocene time. The close spatial and temporal association of the 50-Ma plutons with the overlying coeval subaerial Sloko Volcanics (Souther, 1971), about 75 km east-northeast of Juneau (fig. 1), indicates that much of the uplift was complete at the time of the 50-Ma pluton emplacement. We hypothesize that the Paleogene uplift and pluton emplacement occurred in an as-yet-undefined extensional fault system that was obliterated by the plutons. Brew and Ford (1978) suggested that the uplift was due to isostatic adjustment that occurred in response to the emplacement of the large volume of low-density granitic rocks. Currie and Rohr (1996) suggested that similar Neogene uplift in British Columbia (Parrish, 1983) south of southeastern Alaska was caused by a low-angle normal fault that thinned the lower lithosphere and allowed asthenosphere to rise, causing uplift and local volcanism.

The oldest rocks in the CRMZ are Triassic and Permian metavolcanic and fossiliferous metacarbonate rocks of the Wrangellia terrane to the west and Late Proterozoic(?) and Paleozoic rocks of the Nisling terrane to the east (and possibly to the west). The youngest materials affected by movements in the zone may be the young glacial deposits near Juneau; R.D. Miller (U.S. Geological Survey, oral commun., 1968) speculated that deltaic sediments of the Gastineau Channel Formation (Miller, 1973) might be offset vertically a few meters on the Gastineau Channel fault, which is the local expression of the CRMZ. Metamorphic-mineral assemblages, pressure-temperature data, and fission-track information all indicate that the rocks on the east side of the CRMZ have been elevated relative to those on the west, and suggest that the amount of uplift is probably several kilometers (Donelick, 1988; Wood and others, 1991; Himmelberg and others, 1991, 1994, 1995). Donelick (1988) documented cooling and uplift of the Coast Mountains Complex from 70 to 25 Ma; the fastest rates of cooling and uplift occurred between 50 and 30 Ma. Wood and others (1991) documented decreasing rates of uplift from 60 to 50 Ma for the GTS.

DISCUSSION OF RELATIONS AND EVOLUTION OF THE STRUCTURAL ZONES

All the Coast Mountains structural zones are in or close to the Gravina belt, which is defined as the rocks of the Gravina overlap assemblage. The depocenter for that assemblage is generally accepted (Monger and others, 1982; Brew and Ford, 1983) as marking the general location of the original boundary between the Insular and Intermontane superterranes. The only basement rocks known for the Gravina overlap assemblage are those of the Alexander terrane to the west. Berg and others (1972, 1978) interpreted the sedimentary and volcanic rocks of the Gravina belt to have been deposited in a back-arc basin. A volcanic arc is interpreted to have been to the west, constructed on the Alexander minicontinent. The original relations of the Gravina overlap assembage to lithotectonic terranes to the east is unresolved.

The Coast Mountains structural zones (figs. 3, 4) are close to each other and are in the "southeastern Alaska coincident zone," the part of southeastern Alaska where an unusual number of linear geologic and geophysical features, including the Gravina belt, either overlap or are in close proximity (Brew and Ford, 1985), although the features are of different ages and different origins. In particular, the Behm Canal structural zone (BCSZ) and the Great Tonalite Sill shear zone (GTSSZ) closely coincide and are located immediately to the east of the Gravina belt structural zone (GBSZ). The Great Tonalite Sill mylonite zone (GTSMZ) is essentially specific to the footwall of the Great Tonalite Sill (GTS) and both the GTS and GTSMZ are entirely within the Great Tonalite Sill shear zone (GTSSZ). The Coast Range megalineament zone (CRMZ) is related to the distribution of abundant 50-Ma granitic rocks at the surface and at depth but is located most closely to the Great Tonalite Sill shear zone (GTSSZ) at the surface. Overall, the five different structural zones, although of different ages and character, are all indirectly related to the original boundary between the Insular superterrane and the Intermontane superterrane.

The unresolved character of the contact of the Gravina overlap assemblage with the Intermontane superterrane is an important part of the superterrane boundary question because most of the Coast Mountains structural zones are east of rocks of the Gravina overlap assemblage. Those structural zones probably were localized indirectly or directly by the boundary between the Gravina belt and the Intermontane superterrane.

The nature of that boundary is probably the most significant unanswered tectonic question for southeastern Alaska. The factors involved in determining the boundary's location have been discussed by Brew and Ford (1994) and by Brew and others (1994). Focusing only on the lithotectonic terranes in the vicinity of the boundary (figs. 2, 4), we consider three points in attempting to explain the Insular-Intermontane superterrane relations. (1) Is the Nisling terrane in the Coast Mountains, with its continental-margin lithologic assemblages (Gehrels and others, 1990), really a separate terrane or is it instead the lowest part of the Stikine terrane that lies to its east? (2) If the Nisling is a separate terrane, then is the Insular-Intermontane superterrane boundary on the west or east side of the Nisling? (3) What was the original nature of the two superterrane margins, and how did they evolve during initial terrane accretion and subsequent tectonic events?

Questions (1) and (2) remain to be answered. If the rocks of the Nisling terrane underlie those of the Stikine terrane, then the Insular-Intermontane superterrane boundary is between the Alexander terrane to the west and Nisling/Stikine terrane to the east, and the original boundary thus lies between rocks of the Alexander terrane and the westernmost rocks of the Nisling terrane. For most of southeastern Alaska (figs. 2, 4), this means rocks of the Wrangellia terrane to the west and the Insular-Intermontane superterrane boundary would be generally close to the Great Tonalite Sill shear zone (GTSSZ), which they are (figs. 3C, 4). An exception to this is seen just north of Petersburg, where rocks of the Nisling terrane that lie several kilometers west of the Great Tonalite Sill shear zone (GTSSZ) suggest at least some local divergence or later fault complications.

Regarding point (2), if the Nisling terrane is a separate tectonic terrane, then its assignment to either the Insular or Intermontane superterrane is inappropriate, given the accepted definitions of those terranes (Monger and

Figure 4. Diagrams showing relations of Coast Mountains structural zones to plutonic belts, lithotectonic terranes, and to each other at a latitude between Ketchikan and Wrangell, southeastern Alaska. **A** Diagrammatic cross section. Limits of bracketed units are uncertain; arrows show relative movement on faults; question marks indicate uncertainty; queried line below "Plutonic Rocks" indicates base of granitic part of complex. **B** Age and distribution of structural zones. **C** Age and distribution of plutonic belts. **D** Age and distribution of lithotectonic terranes.

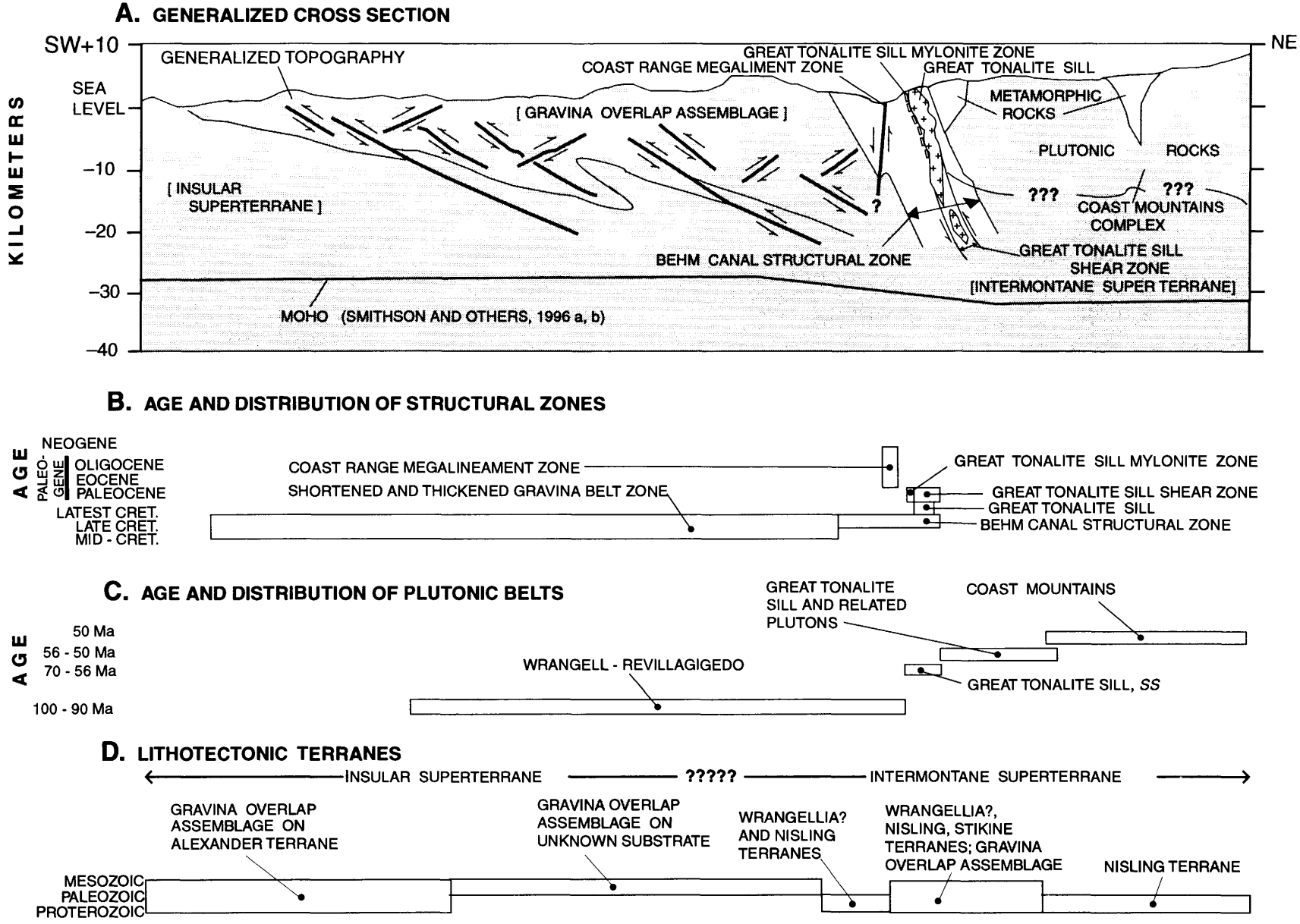

features along the east side of the Nisling terrane and their presence on the west side, such as in the Gravina belt structural zone (GBSZ), suggests that the original superterrane boundary does indeed lie in the area now occupied by the five Coast Mountains structural zones.

Considering point (3), it seems reasonable to assume that the original Insular-Intermontane superterrane margins were irregular before terrane accretion, rather than linear as is apparent from the present distribution of terrane boundaries, and that the present general configuration is the product of both the protracted middle to late Mesozoic accretion and subduction processes and of probable later transform movements. The linear distribution of the Gravina belt structural zone (fig. 3A) suggests that the depocenters for the Gravina overlap assemblage were also elongate and aligned; this suggests, in turn, that the margins of the orthogonally converging terranes that caused the depocenters to form were more or less linear and parallel in middle and Late Cretaceous time.

CONCLUSIONS

The five structural zones described together in this article are close to, or overlap, each other (fig. 4), but their relations to each other have not been examined previously. The five structural zones are in the western part of the Coast Mountains Complex in southeastern Alaska and represent the latest episodes in a long sequence of tectonism that began with the collision of the Insular superterrane against the Intermontane superterrane to the east and culminated in the subsequent uplift of what are now the Coast Mountains. The structural zones show a progressive change in style with time, starting with a broad zone of mid- to Late Cretaceous deformation of rocks of the Late Jurassic and Early Cretaceous back-arc basin that occupied elongate depocenters between the superterranes, progressing through three narrower shear zones of latest Cretaceous to Eocene age that were closely related to the emplacement of the Great Tonalite Sill, and ending with a very narrow zone that was the locus of uplift along the western margin of the dominantly granitic Coast Mountains. Detailed future studies of the structural zones and their relations should greatly advance our understanding of the Insular-Intermontane superterrane juxtaposition process.

REFERENCES CITED

Berg, H.C., Jones, D.L., and Coney, P.J., 1978, Map showing pre-Cenozoic tectonostratigraphic terranes of southeastern Alaska and adjacent areas: U.S. Geological Survey Open-File Report 78-1085, 2 sheets, scale 1:1,000,000.

Berg, H.C., Jones, D.L., and Richter, D.H., 1972, Gravina-Nutzotin belt—tectonic significance of an upper Mesozoic sedimentary and volcanic sequence in southern and southeastern Alaska, in Geological Survey Research 1972: U.S. Geological Survey Professional Paper 800-D, p. D1-D24.

Brew, D.A., 1994, Latest Mesozoic and Cenozoic magmatism in southeastern Alaska, *in* Plafker, G., and Berg, H.C., eds., The geology of Alaska: Boulder, Colo., Geological Society of America, The Geology of North America, v. G-1, p. 621-656.

Brew, D.A., and Ford, A.B., 1978, Megalineament in southeastern Alaska marks southwest edge of Coast Range batholithic complex: Canadian Journal Earth Science, v. 15, no. 11, p. 1763-1772.

———1983, Comment on Monger, J.W.H., Price, R.A., and Tempelman-Kluit, D.J., 1982, Tectonic accretion and the origin of the two major metamorphic and plutonic welts in the Canadian Cordillera: Geology, v. 11, p. 427-429.

———1985, The southeastern Alaska "coincident zone," in Bartsch-Winkler, S., ed., The United States Geological Survey in Alaska: Accomplishments during 1984: U.S. Geological Survey Circular 967, p. 82-86.

——— 1994, The Coast Mountains plutonic-metamorphic complex between Skagway, Alaska, and Fraser, British Columbia—Geologic sketch and road log: U.S. Geological Survey Open-File Report 94-268, 25 p.

Brew, D.A., Ford, A.B., and Himmelberg, G.R., 1989, Evolution of the western part of the Coast plutonic-metamorphic complex, southeastern Alaska, U.S.A.—a summary, *in* Daly, S.R., Cliff, R.A., and Yardley, B.W.D., eds., Evolution of metamorphic belts: Geological Society of London Special Publication 43, p. 447-452.

———1994, Jurassic accretion of Nisling terrane along the western margin of Stikinia, Coast Mountains, northwestern British Columbia: Comment: Geology, v. 22, no. 1, p. 89-90.

Brew, D.A., Ford, A.B., Himmelberg, G.R., and Drinkwater, J.L., 1995, The Coast Mountains Complex of southeastern Alaska and adjacent regions, in Koozmin, E.D., ed., Stratigraphic notes—1994: U.S. Geological Survey Bulletin 2135, p. 21-28.

Brew, D.A., Himmelberg, G.R., Loney, R.A., and Ford, A.B., 1992, Distribution and characteristics of metamorphic belts in the south-eastern Alaska part of the North American Cordillera: Journal of Metamorphic Geology, v. 10, p. 465-482.

Childe, F.C., 1996, Primitive Permo-Triassic volcanism in the Canadian Cordillera: Terrane implications [abs.]: Geological Society of America, Abstracts with Programs, v. 28, no. 7, p. A-312.

Childe, F.C., and Thompson, J., 1995, U-Pb age constraints and Pb isotopic signature of the Klutcho VMS deposit: Geological Association of Canada, The Gangue, no. 49, p. 6-8.

Crawford, M.L., Hollister, L.S., and Woodsworth, G.J., 1987, Crustal deformation and regional metamorphism across a terrane boundary, Coast plutonic complex, British Columbia: Tectonics, v. 6, no. 3, p. 343-361.

Currie, L., and Rohr, K.M., 1996, The Queen Charlotte basin and Coast Mountains: A paired belt of subsidence and uplift caused by a low-angle normal fault [abs.]: Geological Society of America Abstracts with Programs, v. 28, no. 7, p. A-195.

Donelick, R.A., 1988, Etchable fission track length reduction in apatite: Experimental observations, theory and geological applications: Troy, N.Y., Rensselaer Polytechnic Institute, Ph.D. thesis, 371 p.

Eisbacher, G.H., 1976, Sedimentology of the Dezadeash flysch and

its implications for strike-slip faulting along the Denali fault, Yukon Territory and Alaska: Canadian Journal of Earth Sciences, v. 13, p. 1495-1513.

Gehrels, G.E., McClelland, W.C., Samson, S.D., Patchett, P.J., and Brew, D.A., 1991, U-Pb geochronology and tectonic significance of Late Cretaceous-early Tertiary plutons in the northern Coast Mountains batholith: Canadian Journal of Earth Sciences, v. 28, no. 6, p. 899-911.

Gehrels, G.E., McClelland, W.C., Samson, S.C., Patchett, P.J., and Jackson, J.L., 1990, Ancient continental margin assemblage in the northern Coast Mountains, southeast Alaska and northwest Canada: Geology, v. 18, p. 208-211.

Himmelberg, G.R., Brew, D.A., and Ford, A.B., 1991, Inverted metamorphic isograds and P-T conditions, western metamorphic belt, Coast plutonic-metamorphic complex, Juneau, Alaska: Journal of Metamorphic Geology, v. 9, p. 165-180.

———1994, Petrologic characterization of pelitic schists in the western metamorphic belt, Coast plutonic-metamorphic complex, near Juneau, Alaska: U.S. Geological Survey Bulletin 2074, 18 p.

———1995, Low-grade, M1 metamorphism of the Douglas Island Volcanics, western metamorphic belt near Juneau, Alaska, in Schiffman, P., and Day, H.W., eds., Low-grade metamorphism of mafic rocks: Geological Society of America Special Paper 296, p. 51-66.

Himmelberg, G.R., and Loney, R.A., 1995, Characteristics and petrogenesis of Alaskan-type ultramafic-mafic intrusions, southeastern Alaska: U.S. Geological Survey Professional Paper 1564, 47 p.

Hollister, L.S., and Rohr, K.M., organizers, 1996, ACCRETE: An integrated study of continental growth at a convergent to transpressive margin [12 abs.]: American Geophysical Union, 1996 Fall Meeting, Supplement to EOS, Transactions, v. 77, no. 46, p. F651-652.

Ingram, G.M., and Hutton, D.H.W., 1994, The Great Tonalite Sill: Emplacement into a contractional shear zone and implications for Late Cretaceous to early Eocene tectonics in southeastern Alaska and British Columbia: Geological Society of America Bulletin, v. 106, p. 715-728.

Journeay, J.M., and Friedman, R.M., 1993, The Coast Belt Thrust System: Evidence of Late Cretaceous shortening in southwestern British Columbia: Tectonics, v. 12, no. 3, p. 756-775. [Correction in Tectonics, v. 12, no. 5, p. 1301-1302.]

Karl, S.M., Hammarstrom, J.M., Kunk, M., Himmelberg, G.R., Brew, D.A., Kimbrough, D.L., and Bradshaw, J.Y., 1996, Tracy Arm transect: Further constraints on the uplift history of the Coast plutonic complex in southeastern Alaska [abs.]: Geological Society of America Abstracts with Programs, v. 28, no. 7, p. A-312.

Miller, R.D., 1973, Gastineau Channel Formation, a composite glaciomarine deposit near Juneau, Alaska: U.S. Geological Survey Bulletin 1394-C, 20 p.

Monger, J.W.H., Price, R.A., and Tempelman-Kluit, D.J., 1982, Tectonic accretion and the origin of the two major metamorphic and plutonic welts in the Canadian cordillera: Geology, v. 10, p. 70-75.

Nokleberg, W.J., Moll-Stalcup, E.J., Miller, T.P., Brew, D.A., Grantz, A., Reed, J.C., Plafker, G., Moore, T.E., Silva, S.R., and Patton, W.W., Jr., 1994, Tectonostratigraphic terrane and overlap assemblage map of Alaska: U.S. Geological Survey Open-File Report 94-194, 53 p., scale 1:2,500,000.

Parrish, R.R., 1983, Cenozoic thermal evolution and tectonics of the Coast Mountains of British Columbia 1. Fission track dating, apparent uplift rates, and patterns of uplift: Tectonics, v. 2, no. 6, p. 601-631.

Rubin, C.M., and Saleeby, J.B., 1991, Tectonic framework of the upper Paleozoic and lower Mesozoic Alava sequence: a revised view of the polygenetic Taku terrane in southern southeast Alaska: Canadian Journal of Earth Sciences, v. 28, p. 881-893.

———1992, Tectonic history of the eastern edge of the Alexander terrane, southeast Alaska: Tectonics, v. 11, no. 3, p. 586-602.

Rubin, C.M., Saleeby, J.B., Cowan, D.S., Brandon, M.T., and McGroder, M.F., 1990, Regionally extensive mid-Cretaceous west-vergent thrust system in the northwestern cordillera: Implications for continental margin tectonism: Geology, v. 18, p. 276-280.

Samson, S.D., Patchett, P.J., McClelland, W.C., and Gehrels, G.E., 1991, Nd and Sr constraints on the petrogenesis of the west side of the northern Coast Mountains batholith, Alaskan and Canadian cordillera: Canadian Journal of Earth Sciences, v. 28, p. 939-946.

Smithson, S.B., Morozov, I., and Hollister, L.S., 1996a, Shear wave image of the crust along Portland Canal [abs.], *in* Hollister, L.S., and Rohr, K.M., organizers, 1996, ACCRETE: An integrated study of continental growth at a convergent to transpressive margin [12 abs.]: American Geophysical Union, 1996 Fall Meeting, Supplement to EOS, Transactions, v. 77, no. 46, p. F651.

Smithson, S.B., Morozov, I., and Vejmelek, L., 1996b, Seismic wide-angle reflection studies of accreted refraction terrain in southeastern Alaska [abs.]: Geological Society of America Abstracts with Programs, v. 28, no. 7, p. A-217.

Souther, J.G., 1971, Geology and ore deposits of the Tulsequah map-area, British Columbia: Geological Survey of Canada Memoir 362, 84 p.

Umhoefer, P.J., and Schiarizza, P., 1996, Latest Cretaceous to early Tertiary dextral strike-slip faulting on the southeastern Yalakom fault system, southeastern Coast Belt, British Columbia: Geological Society of America Bulletin, v. 108, no. 7, p. 768-785.

Wheeler, J.O., and McFeely, P., 1991, Tectonic assemblage map of the Canadian Cordillera and adjacent parts of the United States of America: Geological Survey of Canada Map 1712A, scale 1:2,000,000.

Wood, D.J., Stowell, H.S., Onstott, T.C., and Hollister, L.S., 1991, $^{40}Ar/^{39}Ar$ constraints on the emplacement, uplift, and cooling of the Coast plutonic complex sill, southeastern Alaska: Geological Society of America Bulletin, v. 103, p. 849-860.

Reviewers: R.A. Loney and T.E. Moore.

U.S. Geological Survey Reports on Alaska Released in 1996

Compiled by John P. Galloway *and* Susan Toussaint

[Reports dated 1994 or 1995 did not become available for indexing until 1996; they are included in this listing.]

Alpha, T.R., and Reimnitz, E., 1995, Arctic delta processes: a computer animation and paper models: U.S. Geological Survey Open-File Report 95-843A, 27 p., also 95-843B [diskette for Macintosh].

Bacon, C.R., and Lanphere, M.A., 1996, Late Cretaceous age of the Middle Fork caldera, Eagle quadrangle, east-central Alaska: *in* Moore, T.E., and Dumoulin, J.A., eds., 1996, Geologic studies in Alaska by the U.S. Geological Survey, 1994: U.S. Geological Survey Bulletin 2152, p. 143-147.

Bailey, E.A., Keith, W.J., Bickerstaff, Damon, Dempsey, David, and Miller, M.L., 1996, Analytical results and sample locality maps of stream-sediment, panned concentrate, stream-water, and soil samples from the Stuyahok area, part of Holy Cross A-4 and A-5 quadrangles, Alaska: U.S. Geological Survey Open-File Report 96-505-C, 44 p.1 diskette, scale 1:63,360.

Benoit, J.P., and McNutt, S.R., 1996, Global volcanic earthquake swarm database 1979-1989: U.S. Geological Survey Open-File Report 96-69, 333 p.

Brabets, T.P., 1996, Evaluation of the streamflow-gaging network of Alaska in providing regional streamflow information: U.S. Geological Survey Water-Resources Investigations Report 96-4001, 73 p.

Brabets, T.P., 1996, Geomorphology of the lower Copper River, Alaska: U.S. Geological Survey Open-File Report 96-500, 146 p.

Brew, D.A., compiler, 1996, Geologic map of the Craig, Dixon Entrance, and parts of the Ketchikan and Prince Rupert quadrangles, southeastern Alaska: U.S. Geological Survey Miscellaneous Field Studies Map MF-2319, 53 p. 1 sheet, scale 1:250,000.

Brew, D.A., Grybeck, D.J., Taylor, C.D., Jachens, R.C., Cox, D.P., Barnes, D.F., Koch, R.D., Morin, R.I., and Drinkwater, J.L., 1996, Undiscovered mineral resources of southeastern Alaska—Revised mineral-resource-assessment-tract descriptions: U.S. Geological Survey Open-File Report 96-716, 131 p. 1 sheet, scale 1:1,000,000.

Burns, L.E., 1996, Geology of part of the Nelchina River gabbronorite and associated rocks, south-central Alaska: U.S. Geological Survey Bulletin 2058, 32 p.

Carr, M.R., 1996, Description of wells drilled at the U.S. Coast Guard Support Center, Kodiak, Alaska, 1988-89: U.S. Geological Survey Open-File Report 96-134, 233 p.

Church, S.E., Kelley, J.S., and Bohn, D., 1996, Mineral resource assessment of the Chandler Lake quadrangle, Alaska: U.S. Geological Survey Miscellaneous Field Studies Map MF-2144-E, 37 p., 1 sheet, scale 1:250,000.

Churkin, Michael, Jr., and Carter, Claire, 1996, Stratigraphy, structure, and graptolites of an Ordovician and Silurian sequence in the Terra Cotta Mountains, Alaska Range, Alaska: U.S. Geological Survey Professional Paper 1555, 84 p., 4 plates.

Cole, F., Bird, K.J., Toro, J., Roure, F., and Howell, D.G., 1995, Kinematic and subsidence modeling of the north-central Brooks Range and North Slope of Alaska: U.S. Geological Survey Open-File Report 95-823, 4 p., 3 plates.

Cowan, J.R., 1995, Environmental overview and hydrogeologic conditions at Umiat, Alaska: U.S. Geological Survey Open-File Report 95-350, 13 p.

Csejtey, Béla, Jr., Wrucke, C.T., Ford, A.B., Mullen, M.W., Dutro, J.T., Jr., Harris, A.G., and Brease, P.F., 1996, Correlation of rock sequences across the Denali fault in south-central Alaska: *in* Moore, T.E., and Dumoulin, J.A., eds., 1996, Geologic studies in Alaska by the U.S. Geological Survey, 1994: U.S. Geological Survey Bulletin 2152, p.149-156.

Dawson, P.B., Chouet, B.A., Lahr, J.C., Page, R.A., Van Schaack, J.R., and Criley, E.E., 1996, Data report for a seismic study of the *P*- and *S*- wave velocity structure of Redoubt Volcano, Alaska: U.S. Geological Survey Open-File Report 96-703, 43 p.

Deming, D., Sass, J.H., and Lachenbruch, A.H., 1996, Heat flow and subsurface temperature, North Slope of Alaska: *in* Johnsson, M.J., and Howell, D.G., eds., 1996, Thermal evolution of sedimentary basins in Alaska: U.S. Geological Survey Bulletin 2142, p. 21-44.

Detterman, R.L., Case, J.E., Miller, J.W., Wilson, F.H., and Yount, M.E., 1996, Stratigraphic framework of the Alaska Peninsula, chapter A *of* Geologic studies on the Alaska Peninsula: U.S. Geological Survey Bulletin 1969-A, 74 p.

Dorava, J.M., 1995, Hydraulic characteristics near streamside structures along the Kenai River, Alaska: U.S. Geological Survey, Water-Resources Investigations Report 95-4226, 41 p.

Dorava, J.M., and Brekken, J.M., 1995, Overview of environmental and hydrogeologic conditions at Kotzebue, Alaska: U.S. Geological Survey Open-File Report 95-349, 11 p.

Dorava, J.M., and Liepitz, G.S., 1996, Balancing the three R's (regulation, research, and restoration) on the Kenai River, Alaska: U.S. Geological Survey Fact Sheet FS-160-96, 2 p.

Dusel-Bacon, Cynthia, and Aleinikoff, J.N., 1996, U-Pb zircon and titanite ages for augen gneiss from the Divide Mountain area, eastern Yukon-Tanana upland, Alaska, and evidence for the composite nature of the Fiftymile batholith: *in* Moore, T.E., and Dumoulin, J.A., eds., 1996, Geologic studies in Alaska by the U.S. Geological Survey, 1994: U.S. Geological Survey Bulletin 2152, p. 131-141.

Dusel-Bacon, C., Brew, D.A., and Douglass, S.L., 1996, Metamorphic facies map of southeastern Alaska—Distribution, facies, and ages of regionally metamorphosed rocks: U.S. Geological Survey Professional paper 1497-D, 42 p., 2 sheets, scale 1:1,000,000.

Dusel-Bacon, C., Doyle, E.O., and Box, S.E., 1996, Distribution, facies, ages, and proposed tectonic associations of regionally metamorphosed rocks in southwestern Alaska and the Alaska Peninsula: U.S. Geological Survey Professional Paper 1497-B, 30 p., 2 sheets, scale 1:1,000,000.

Evans, K.R., 1996, Marine geology of the Bering Sea: selected bibliography of U.S. Geological Survey studies (1970-present): U.S. Geological Survey Open-File Report 96-655, 11 p.

Fogleman, K.A., Rowe, C.A., and Hammond, W.R., 1996, Alaska earthquakes—1994: *in* Moore, T.E., and Dumoulin, J.A., eds., 1996, Geologic studies in Alaska by the U.S. Geological Survey, 1994: U.S. Geological Survey Bulletin 2152, p. 59-79.

Ford, A.B., Palmer, C.A., and Brew, D.A., 1996, Geochemistry of the andesitic Admiralty Island Volcanics, an Oligocene rift-related basalt to rhyolite volcanic suite of southeastern Alaska: *in* Moore, T.E., and Dumoulin, J.A., eds., 1996, Geologic studies in Alaska by the U.S. Geological Survey, 1994: U.S. Geological Survey Bulletin 2152, p. 177-204.

Frederiksen, N.O., Sheehan, T.P., Ager, T.A., Collett, T.S., Fouch, T.D., Franczyk, K.J., and Johnsson, M., 1996, Palynomorph biostratigraphy of Upper Cretaceous to Eocene samples from the Sagavanirktok Formation in its type region, North Slope of Alaska: U.S. Geological Survey Open-File Report 96-84, 44 p.

Gallant, A.L., Binnian, E.F., Omernik, J.M., and Shasby, M.B., 1995, Ecoregions of Alaska: U.S. Geological Survey Professional Paper 1567, 73 p.

Glass, R.L., 1996, Glaciers along proposed routes extending the Copper River Highway, Alaska: U.S. Geological Survey Water-Resources Investigations Report 96-4074, 39 p.

Glass, R.L., 1996, Ground-water conditions and quality in the western part of Kenai Peninsula, southcentral Alaska: U.S. Geological Survey Open-File Report 96-466, 94 p.

Glass, R.L., 1996, Hydrologic and water-quality data for U.S. Coast Guard Support Center Kodiak, Alaska, 1987-89: U.S. Geological Survey Open-File Report 96-498, 84 p., also 2 diskettes.

Goldfarb, R.J., Nelson, S.W., Taylor, C.D., d'Angelo, W.M., and Meier, A.L., 1996, Acid mine drainage associated with volcanogenic massive sulfide deposits, Prince William Sound, Alaska: *in* Moore, T.E., and Dumoulin, J.A., eds., 1996, Geologic studies in Alaska by the U.S. Geological Survey, 1994: U.S. Geological Survey Bulletin 2152, p. 3-16.

Grauch, V.J.S., and Castellanos, Esther, 1995, Revised digital aeromagnetic data for areas in and adjacent to the National Petroleum Reserve Area (NPRA), North Slope, Alaska: U.S. Geological Survey Open-File Report 95-835, 11 p.

Gray, J.E., Meier, A.L., O'Leary, R.M., Outwater, Carol, and Theodorakos, P.M., 1996, Environmental geochemistry of mercury deposits in southwestern Alaska: mercury contents in fish, stream-sediment, and stream-water samples: *in* Moore, T.E., and Dumoulin, J.A., eds., 1996, Geologic studies in Alaska by the U.S. Geological Survey, 1994: U.S. Geological Survey Bulletin 2125, p. 17-29.

Gray, J.E., and Sanzolone, R.F., eds., 1996, Environmental studies of mineral deposits in Alaska: U.S. Geological Survey Bulletin 2156, 40 p.

Grybeck, D.J., Nelson, S.W., Cathrall, J.B., Cady, J.W. and Le Compte, J.R., 1996, Mineral resource potential map of the Survey Pass Quadrangle, Brooks Range, Alaska: U.S. Geological Survey Miscellaneous Field Studies Map MF-1176-I, 16 p., 1 sheet, scale 1:250,000.

Hall, J.D., 1995, Overview of environmental and hydrogeologic conditions near Homer, Alaska: U.S. Geological Survey Open-File Report 95-405, 14 p.

Hogan, E.V., 1995, Overview of environmental and hydrogeologic conditions near Big Lake, Alaska: U.S. Geological Survey Open-File Report 95-403, 10 p.

Hogan, E.V., and Dorava, J.M., 1995, Overview of environmental and hydrogeologic conditions at seven Federal Aviation Administration facilities in interior Alaska: U.S. Geological Survey Open-File Report 95-341, 53 p.

Jackson, M.L., and Lilly, M.R., 1996, Ground-water and surface-water elevations in the University of Alaska Fairbanks area, 1992-95: U.S. Geological Survey Open-File Report 96-416, 219 p.

Jacobson, S.R., Blodgett, R.B., and Babcock, L.E., 1996, Organic matter and thermal maturation of lower Paleozoic rocks from the Nixon Fork subterrane of the Farewell terrane, west-central and southwestern Alaska: *in* Moore, T.E., and Dumoulin, J.A., eds., 1996, Geologic studies in Alaska by the U.S. Geological Survey, 1994: U.S. Geological Survey Bulletin 2152, p. 81-87.

Johnsson, M.J., and Howell, D.G., compilers, 1996, Generalized thermal maturity map of Alaska: U.S. Geological Survey Miscellaneous Field Investigations Map MF 2494, 1 sheet, scale 1:2,500,000; also *in pocket of* Johnsson, M.J., and Howell, D.G., eds., 1996, Thermal evolution of sedimentary basins in Alaska: U.S. Geological Survey Bulletin 2142.

Johnsson, M.J., and Howell, D.G., eds., 1996, Thermal evolution of sedimentary basins in Alaska: U.S. Geological Survey Bulletin 2142, 131 p.

Johnsson, M.J., and Howell, D.G., 1996, Thermal maturity of sedimentary basins in Alaska—an overview: *in* Johnsson, M.J., and Howell, D.G., eds., 1996, Thermal evolution of sedimentary basins in Alaska: U.S. Geological Survey Bulletin 2142, p. 1-9.

Jolly, A.D., Power, J.A., Stihler, S.D., Rao, L.N., Davidson, G., Paskievitch, J., Estes, S., and Lahr, J.C., 1996, Catalog of earthquake hypocenters for Augustine, Redoubt, Iliamna, and Mount Spurr Volcanoes, Alaska: January 1, 1991–December 31, 1993: U.S. Geological Survey Open-File Report 96-70-A, 90 p.; also 96-70-B, 1 diskette.

Keith, W.J., and Miller, M.L., 1996, Alaska Resource Data File: Iditarod quadrangle: U.S. Geological Survey Open-File Report 96-540, 35 p.

Keith, W.J., Miller, M.L., Bailey, E.A., Bundtzen, T.K., and Bickerstaff, Damon, 1996, Analytical results and sample locality maps of rock samples from the Stuyahok area, part of Holy Cross A-4 and A-5 quadrangles, Alaska: U.S. Geological Survey Open-File Report 96-505-B, 47 p., 1 sheet, scale 1:63,360.

Kelley, K.D., and Taylor, C.D., 1996, Natural environmental effects associated with the Drenchwater zinc-lead-silver massive sulfide deposit with comparisons to the Red Dog and Lik deposits, west-central Brooks Range, Alaska: *in* Moore, T.E., and Dumoulin, J.A., eds., 1996, Geologic studies in Alaska by the U.S. Geological Survey, 1994: U.S. Geological Survey Bulletin 2152, p. 31-45.

Kelley, K.D., Bailey, E.A., Briggs, P.H., Motooka, J.M., and Meier, A.L., 1996, Digital release of stream-sediment, heavy-mineral-concentrate, soil; water, and rock geochemical data collected in the Howard Pass quadrangle, Alaska: U.S. Geological Survey Open-File Report 96-711.

Kennedy, B.W., 1995, Air temperature and precipitation data, Wolverine Glacier basin, Alaska, 1967-94: U.S. Geological Survey Open-File Report 95-444, variously paged.

Krimmel, R.M., 1996, Columbia Glacier, Alaska: research on tidewater glaciers: U.S. Geological Survey Fact Sheet 96-91, 2 p.

Krumhardt, A.P., Harris, A.G., and Watts, K.F., 1996, Lithostratigraphy, microlithofacies, and conodont biostratigraphy and biofacies of the Wahoo Limestone (Carboniferous), eastern Sadlerochit Mountains, northeast Brooks Range, Alaska: U.S. Geological Survey Professional Paper 1568, 70 p., 6 plates.

Lilly, M.R., DePalma, K.L., and Benson, S.L., 1995, Selected environmental and geohydrologic reports for the Fort Wainwright and Fairbanks areas, Alaska, as of July 1995: U.S. Geological Survey Open-File Report 95-420, 65 p., 1 plate.

Lilly, M.R., McCarthy, K.A., Kriegler, A.T., Vohden, J., and Burno, G.E., 1996, Compilation and preliminary interpretations of hydrologic and water-quality data from the Railroad Industrial Area, Fairbanks, Alaska, 1992-94: U.S. Geological Survey Water-Resources Investigations Report 96-4049, 45 p.

March, R.S., and Trabant, D.C., 1996, Mass balance, meteorological, ice motion, surface altitude, and runoff data at Gulkana Glacier, Alaska, 1992 balance year: U.S. Geological Survey Water-Resources Investigations Report 95-4277, 32 p.

McCarthy, K.A., and Solin, G.L., 1995, Assessment of the subsurface hydrology of the UIC-NARL Main Camp, near Barrow, Alaska, 1993-94: U.S. Geological Survey Open-File Report 95-737, 23 p.

McGimsey, R.G., and Neal, C.A., 1996, 1995 volcanic activity in Alaska and Kamchatka: summary of events and response of the Alaska Volcano Observatory: U.S. Geological Survey Open-File Report 96-738, 22 p.

Meyer, D.F., 1995, Flooding in the Middle Koyukuk River Basin, Alaska, August 1994: U.S. Geological Survey Water-Resources Investigations Report 95-4118, 8 p., 2 sheets.

Meyer, J.F., Jr., and Saltus, R.W., 1995, Merged aeromagnetic map of interior Alaska: U.S. Geological Survey Geophysical Investigations Map 1014, 2 sheets, scale 1:500,000.

Meyer, J.F., Jr., Saltus, R.W., Barnes, D.F., and Morin, R.L., 1996, Bouguer gravity map of interior Alaska: U.S. Geological Survey Geophysical Investigations Map GP-1016, 2 sheets, scale 1:500,000.

Miller, M.L., Bundtzen, T.K., Keith, W.J., Bailey, E.A., and Bickerstaff, D., 1996, Geology and mineral resources of the Stuyahok area, part of Holy Cross A-4 and A-5 quadrangles, Alaska: U.S. Geological Survey Open-File Report 96-505-A, 30 p., 1 sheet, scale 1:63,360.

Molenaar, C.M., 1996, Thermal maturity patterns and geothermal gradients on the Alaska Peninsula: *in* Johnsson, M.J., and Howell, D.G., eds., 1996, Thermal evolution of sedimentary basins in Alaska: U.S. Geological Survey Bulletin 2142, p. 11-19.

Moll-Stalcup, E., Wooden, J.L., Bradshaw, J., and Aleinikoff, J.N., 1996, Elemental and isotopic evidence for 2.1-Ga arc magmatism in the Kilbuck terrane, southwestern Alaska: *in* Moore, T.E., and Dumoulin, J.A., eds., 1996, Geologic studies in Alaska by the U.S. Geological Survey, 1994: U.S. Geological Survey Bulletin 2152, p. 111-130.

Moore, T.E., and Dumoulin, J.A., eds., 1996, Geologic studies in Alaska by the U.S. Geological Survey, 1994: U.S. Geological Survey Bulletin 2152, 217 p.

Moore, T.E., and Dumoulin, J.A., eds., 1996, Introduction: *in* Moore, T.E., and Dumoulin, J.A., eds., 1996, Geologic studies in Alaska by the U.S. Geological Survey, 1994: U.S. Geological Survey Bulletin 2152, p. 1.

Morin, R.L., 1996, Complete bouguer and isostatic gravity maps of the Bethel and southern part of the Russian Mission quadrangles, southwestern Alaska: U.S. Geological Survey Miscellaneous Field Studies Map MF-2226-B, 1 map on two sheets, scale 1:250,000.

Morin, R.L., and Moore, T.E., 1996, Gravity models of the Siniktanneyak mafic-ultramafic complex, western Brooks Range, Alaska: evidence for thrust emplacement of Brooks Range ophiolites: *in* Moore, T.E., and Dumoulin, J.A., eds., 1996, Geologic studies in Alaska by the U.S. Geological Survey, 1994: U.S. Geological Survey Bulletin 2152, p. 101-110.

Mull, C.G., Moore, T.E., Harris, E.E., and Tailleur, I.L., 1994, Geologic map of the Killik River quadrangle, Brooks Range, Alaska: U.S. Geological Survey Open-File Report 94-679, 1 sheet, scale 1:125,000.

Neal, C.A., McGimsey, R.G., and Doukas, M.P., 1996, 1993 volcanic activity in Alaska: summary of events and response of the Alaska Volcano Observatory: U.S. Geological Survey Open-File Report 96-24, 21 p.

Neal, Christina, and McGimsey, Robert, 1996, Volcanoes of the Alaska Peninsula and Aleutian Islands, Alaska—selected photographs: U.S. Geological Survey Digital Data Series DDS 96-034, 1 CD-ROM.

Neal, Christina, and McGimsey, Robert, 1996, Volcanoes of the Wrangell Mountains and Cook Inlet Region, Alaska—selected photographs: U.S. Geological Survey Digital Data Series DDS 96-039, 1 CD-ROM.

Nokleberg, W.J., Bundtzen, T.K., Dawson, K.M., Eremin, R.A., Goryachev, N.A., Koch, R.D., Ratkin, V.V., Rozenblum, I.S., Shpikerman, V.I., Frolov, Y.F., Gorodinsky, M.E., Melnikov, V.D., Ognyanov, N.V., Petrachenko, E.D., Petrachenko, R.I., Pozdeev, A.I., Ross, K.V., Wood, D.H., Grybeck, Donald, Khanchuk, A.I., Kovbas, L.I., Nekrasov, I.Ya., and Disorov, A.A., 1996, Significant metalliferous lode deposits and placer districts for the Russian Far East, Alaska, and the Canadian Cordillera: U.S. Geological Survey Open-File Report 96-513-A, 385 p. [paper format].

O'Sullivan, P.B., 1996, Late Mesozoic and Cenozoic thermotectonic evolution of the Colville basin, North Slope, Alaska: *in* Johnsson, M.J., and Howell, D.G., eds., 1996, Thermal evolution of sedimentary basins in Alaska: U.S. Geological Survey Bulletin 2142, p. 45-79.

Patton, W.W., Jr., and Moll-Stalcup, E.J., 1996, Geologic map of the Unalakleet quadrangle, west-central Alaska: U.S. Geological

Survey Miscellaneous Investigations Map I-2559, 39 p., 1 sheet, scale 1:250,000.

Phillips, P.J., 1996, Sandstone composition and provenance of the Orca Group, Chugach National Forest study area, south-central Alaska: *in* Moore, T.E., and Dumoulin, J.A., eds., 1996, Geologic studies in Alaska by the U.S. Geological Survey, 1994: U.S. Geological Survey Bulletin 2152, p. 157-167.

Philpotts, J.A., Taylor, C.D., and Baedecker, P.A., 1996, Rare-earth enrichment at Bokan Mountain, southeast Alaska: *in* Moore, T.E., and Dumoulin, J.A., eds., 1996, Geologic studies in Alaska by the U.S. Geological Survey, 1994: U.S. Geological Survey Bulletin 2152, p. 89-100.

Plumb, E.W., and Lilly, M.R., 1996, Snow-depth and water-equivalent data for the Fairbanks area, Alaska, Spring 1995: U.S. Geological Survey Open-File Report 96-414, 24 p.

Reiser, E.R., compiler, 1996, Reports about Alaska in non-USGS publications released in 1994 that include USGS authors: *in* Moore, T.E., and Dumoulin, J.A., eds., 1996, Geologic studies in Alaska by the U.S. Geological Survey, 1994: U.S. Geological Survey Bulletin 2152, p. 205-211.

Reiser, E.R., compiler, 1996, U.S. Geological Survey reports on Alaska released in 1994: *in* Moore, T.E., and Dumoulin, J.A., eds., 1996, Geologic studies in Alaska by the U.S. Geological Survey, 1994: U.S. Geological Survey Bulletin 2152, p. 213-217.

Rickman, R.L., 1996, Effect of ice formation and streamflow on salmon incubation habitat in the Lower Bradley River, Alaska: U.S. Geological Survey Water-Resources Investigations Report 96-4202, 63 p.

Roach, A.L., Neal, C.A., and McGimsey, R.G., 1996, Photographs of the 1989-90 eruptions of Redoubt Volcano, Alaska: U.S. Geological Survey Open-File Report 96-689, 10 p., 20 slides.

Schmoll, H.R., Yehle, L.A., and Dobrovolny, E., 1996, Surficial geologic map of the Anchorage A-8 NE quadrangle, Alaska: U.S. Geological Survey Open-File Report 96-003, 49 p., 2 sheets, scale 1:25,000.

Schneider, J.L., ed., 1995, 1995 Annual report on Alaska's mineral resources: U.S. Geological Survey Circular 1127, 67 p.

Shelton, K.L., Underwood, M.B., Burstein, I.B., Haeussler, G.T., and Howell, D.G., 1996, Stable-isotope and fluid-inclusion studies of hydrothermal quartz and calcite veins from the Kandik thrust belt of East-Central Alaska—Implications for thermotectonic history and terrane analysis: *in* Johnsson, M.J., and Howell, D.G., eds., 1996, Thermal evolution of sedimentary basins in Alaska: U.S. Geological Survey Bulletin 2142, p. 111-131.

Snyder, E.F., 1996, Bibliography of glacier studies by the U.S. Geological Survey: U.S. Geological Survey Open-File Report 95-723, 35 p.

Snyder, E.F., 1996, Location maps and list of U.S. Geological Survey reports on water resources in Alaska 1950 to 1995: U.S. Geological Survey Open-File Report 96-335, 48 p.

Solin, G.L., 1996, Overview of surface-water resources at the U.S. Coast Guard Support Center Kodiak, Alaska, 1987-89: U.S. Geological Survey Open-File Report 96-463, 18 p., 2 sheets, scale 1:12,000 and 1:6,000.

Strobe, R., Rice, W., and Neal, T., 1995, Topographic maps of Novarupta Dome and parts of the Valley of Ten Thousand Smokes, Katami National Park and Preserve, Alaska: U.S. Geological Survey Open-File Report 95-619, 4 sheets, scale 1:200.

Trainor, T.P., Fleisher, S., Wildeman, T.R., Goldfarb, R.J., and Huber, C.S., 1996, Environmental geochemistry of the McKinley Lake gold mining district, Chugach National Forest, Alaska: *in* Moore, T.E., and Dumoulin, J.A., eds., 1996, Geologic studies in Alaska by the U.S. Geological Survey, 1994: U.S. Geological Survey Bulletin 2152, p. 47-57.

Underwood, M.B., Howell, D.G., Johnsson, M.J., and Pawlewicz, M.J., 1996, Thermotectonic evolution of suspect terranes in the Kandik region of east-central Alaska: *in* Johnsson, M.J., and Howell, D.G., eds., 1996, Thermal evolution of sedimentary basins in Alaska: U.S. Geological Survey Bulletin 2142, p. 81-110.

U.S. Geological Survey, 1995, Alaska: Reston, Va., The U.S. Geological Survey, 1 sheet, scale 1:2,500,000.

U.S. Geological Survey, 1996, Alaska Resource Data File: explanation of fields used in the Alaska Resource Data File of mines, prospects, and mineral occurrences in Alaska: U.S. Geological Survey Open-File Report 96-79, 4 p.

Waitt, R.B., and Begét, J.E., *with contributions from Juergen Kienle*, 1996, Provisional geologic map of Augustine Volcano, Alaska: U.S. Geological Survey Open-File Report 96-516, 44 p., 1 sheet, scale 1:25,000.

Walker, D.A., and Markon, C.J., eds., 1996, Circumpolar Arctic vegetation mapping workshop: U.S. Geological Survey Open-File Report 96-251, contract 1434-92-c-4004, variously paged.

Weems, R.E., and Blodgett, R.B., 1996, The pliosaurid *Megalneusaurus*: a newly recognized occurrence in the Upper Jurassic Naknek Formation of the Alaska Peninsula: *in* Moore, T.E., and Dumoulin, J.A., eds., 1996, Geologic studies in Alaska by the U.S. Geological Survey, 1994: U.S. Geological Survey Bulletin 2152, p. 169-176.

Wilson, F.H., 1996, Alaska Resource Data File: Unalaska quadrangle: U.S. Geological Survey Open-File Report 96-270, 48 p.

Wilson, F.H., and Light, T.D., 1996, Alaska Resource Data File: Adak quadrangle: U.S. Geological Survey Open-File Report 96-269, 12 p.

Wilson, F.H., White, W.H., Detterman, R.L., and Case, J.E., 1996, Maps showing the resource assessment of the Port Moller, Stepovak Bay, and Simeonof Island quadrangles, Alaska Peninsula, *with a section on* Geology of the Pyramid porphyry copper deposit, Alaska Peninsula, Alaska, by W.H. White, J.S. Christie, M.R. Wolfhard, and F.H.Wilson, *and a section on* Description of the Shumagin epithermal gold vein deposit, by W.H. White and L.D. Queen: U.S. Geological Survey Miscellaneous Field Studies Map MF-2155-F, 46 p., 2 sheets, scale 1:500,000 and 1:250,000.

Yamashita, K.M., Iwatsubo, E.Y., and Dvorak, J.J., 1996, Descriptions, photographs, and coordinates for Global Positioning System stations at Aniakchak Crater, Alaska: U.S. Geological Survey Open-File Report 96-46, 20 p.

Yeend, W.E., 1996, Gold placers of the historical Fortymile River region, Alaska: U.S. Geological Survey Bulletin 2125, 75 p., 1 sheet map, scale 1:63,360.

Reports about Alaska in Non-USGS Publications Released in 1996 that Include USGS Authors

Compiled by John P. Galloway *and* Susan Toussaint

*[Some reports dated 1993 and 1994 did not become available for indexing until 1996; they are included in this listing. USGS authors are marked with asterisks (*).]

*Alpha, T.R., 1996, Hypercard animations of sea-floor spreading and Arctic delta processes [abs.]: Geological Society of America Abstracts with Programs, v. 28, no. 5, p. 42.

Barley, M.E., and *Goldfarb, R.J., 1996, Exploration guides—Global tectonic settings of mesothermal gold deposits [abs.]: Mesothermal gold deposits—a global overview, extended abstracts: University of Western Australia Publication No. 27, p. 112-113.

Bence, A.E., *Kvenvolden, K.A., and Kennicutt, M.C., II, 1996, Organic geochemistry applied to environmental assessments of Prince William Sound, Alaska, after the Exxon Valdez oil spill —a review: Organic Geochemistry, v. 24, p. 7-42.

Bice, K.L., Arthur, M.A., and *Marincovich, L., Jr., 1996, Late Paleocene Arctic Ocean shallow-marine temperatures from mollusc stable isotopes: Paleoceanography, v. 11, no. 3, p. 241-249.

*Bond, K.R., 1993, Gravity studies of Annette Island: *in* Godwin, L.H., and Smith, B.D., eds., Special Symposium 1993 on Economic Mineral Resources of the Annette Islands Reserve, Alaska: Spokane, Wash., Northwest Mining Association, p. 73-76.

*Bogue, S.W., *Grommé, Sherman, and *Hillhouse, J.W., 1995, Paleomagnetism, magnetic anisotropy, and mid-Cretaceous paleolatitude of the Duke Island (Alaska) ultramafic complex: Tectonics, v. 14, p. 1133-1152.

*Brew, D.A., 1993, Regional geologic setting of mineral resources in southeastern Alaska: a synopsis: *in* Godwin, L.H., and Smith, B.D., eds., Special Symposium 1993 on Economic Mineral Resources of the Annette Islands Reserve, Alaska: Spokane, Wash., Northwest Mining Association, p. 13-20.

*Brew, D.A., *Drinkwater, J.L., *Ford, A.B., and *Himmelberg, G.R., 1996, The Taku transect, Coast Mountains Complex, Southeastern Alaska—emplacement styles and conditions, geochronology, and composition [abs.]: Geological Society of America Abstracts with Programs, v. 28, no. 5, p. 51.

*Brew, D.A., and * Ford, A.B., 1996, The coast shear zones in southeastern Alaska—how many and what are they? [abs.]: Geological Society of America Abstracts with Programs, v.28, no. 7, p. 444.

*Bufe, C.G., *Varnes, D.J., and Nishenko, S.P., 1996, Time-to-failure in the Alaska-Aleutian region: an update [abs.]: Eos (American Geophysical Union Transactions), v. 77, no. 46, suppl., p. 456.

Cai, Jinkui, Powell, R.D., Cowan, E.A., and *Kayen, R.E., 1996, Lithofacies, physical properties and seismic-reflection characteristcs of temperate glacimarine deposits in Glacier Bay, Alaska [abs.]: Eos (American Geophysical Union Transactions), v. 77, no. 46, suppl., p. 332.

Cai, Jinkui, Powell, R.D., Cowan, E.A., and *Kayen, R.E., 1996, Lithofacies, geotechnical properties and seismic-reflection characteristics of temperate glacial marine deposits in Alaskan fjords [abs.]: International Geological Congress, 30th, Beijing, 1996, Abstracts, v. 2, p. 192.

*Carlson, P.R., Cai, J., Powell, R.D., and Cowan, E.A., 1996, Acoustic profiles and PB ^{210} rates illuminate post Little Ice Age history in west arm, Glacier Bay, Alaska [abs.]: Geological Society of America Abstracts with Programs, v.28, no. 7, p. 507.

Cartee, S.L., Cowan, E.A., Johnson, N.E., *Kayen, R.E., Powell, R.D., and Cavin, O., 1996, Comparison of mineralogy, magnetic susceptibility and source area of glaciomarine sediment, Yakutat Bay, southern Alaska [abs.]: Geological Society of America Abstracts with Programs, v.28, no. 7, p. 58.

*Chouet, B.A., Long-period volcano seismicitiy: its source and use in eruption forecasting: Nature, v. 380, no. 6572, p. 309-316.

Cole, F., Toro, J., *Bird, K.J., and Roure, F., 1996, A forward model for thrusting and sedimentation in the north-central Brooks Range, Alaska [abs.]: Eos (American Geophysical Union Transactions), v. 77, no. 46, suppl., p. 642.

*Collett, T.S., 1996, Sources of surficial methane flux associated with natural gas hydrate accumulations in northern Alaska [abs.]: Eos (American Geophysical Union Transactions), v. 77, no. 46, suppl., p. 184.

Combellick, R.A., and *Lahr, J.C., 1996, Earthquake potential and hazards in south-central Alaska [abs.]: Geological Society of America Abstracts with Programs, v. 28, no. 5, p. 56-57.

Cowan, E.A., *Carlson, P.R., and Powell, R.D., 1996, The marine record of the Russell Fiord outburst flood, Alaska, U.S.A.: Annals of Glaciology, v. 22, p. 194-199.

Dawson, K.M., Monger, J.W.H., Gordey, S., and *Brew, D.A., 1996, 1:5,000,000 terrane metallogenic map of the Canadian

Cordillera and southeast Alaska, preliminary edition [abs.]: Geological Survey of Canada Mineral Colloquium 1995, Ottawa, Ontario, Canada, unpaged.

Drinkwater, J.L., Brew, D.A., and * Ford, A.B., 1996, Unique features of the magnetite-free plutons of the late Cretaceous Admiralty-Revillagigedo plutonic belt of southeastern Alaska [abs.]: Geological Society of America Abstracts with Programs, v. 28, no. 5, p. 63.

Eichelberger, J.C., *Keith, T.C., and Nye, C.J., 1996, New monitoring and geological investigations in the central Aleutian Arc, Alaska [abs.]: Eos (American Geophysical Union Transactions), v. 77, no. 46, suppl., p. 771.

Elias, S.A., Short, S.K.,* Nelson, C.H., and Birks, H.H., 1996, Life and times of the Bering land bridge: Nature, no. 382, no. 6586, p. 60-63.

Elias, S.A., Short, S.K., and *Waythomas, C.F., 1996, Late Quaternary environments, Denali National Park and Preserve, Alaska: Arctic, v. 49, p. 292-305.

*Evans, K.R., *Stevenson, A.J., *Barnes, P.W., *Carlson, P.R., *Hampton, M.A., and *Marlow, M.S., 1996, Sea-floor sediments in the Gulf of Alaska: new map compilation for studies of benthic biohabitats [abs.]: Eos (American Geophysical Union Transactions), v. 77, no. 46, suppl., p. 409.

*Ford, A.B., and *Brew, D.A., 1996, The Admiralty Island volcanics—Oligocene rift-related basalt to rhyolite volcanism in southeastern Alaska [abs.]: Geological Society of America Abstracts with Programs, v.28, no. 7, p. 504.

Ford, R.C., and *Snee, L.W., 1996, $^{40}Ar/^{39}Ar$ thermochronology of white mica from the Nome District, Alaska: the first ages of lode sources to placer gold deposits in the Seward Peninsula: Economic Geology, v. 91, p. 213-220.

*Fountain, A.G., 1996, Effect of snow and firn hydrology on the physical and chemical characteristics of glacial runoff: Hydrological Processes, v. 10, p. 509-521.

*Goldfarb, R.J., 1996, Metallogenic evolution of Alaska [abs.]: International Geological Congress, 30th, Beijing, 1996, Abstracts, v. 1, p. 395.

*Goldfarb, R.J., 1996, The early Tertiary of southern Alaska—a final episode of terrane accretion and gold vein genesis in the North American Cordillera [abs.]: University of Ballarat, Victoria Australia, Conference on Sedimentary-Hosted Gold Deposits—A Global Overview, Extended Abstracts, p. 33-38.

*Goldfarb, R.J., 1996, Ore fluids associated with mesothermal gold deposits in the North American Cordillera: Mesothermal gold deposits—a global overview, extended abstracts: University of Western Australia Publication No. 27, p. 88-92.

*Goldfarb, R.J., Landefeld, L.A., and Hart, C.J.R., 1996, Overview of the goldfields in metamorphosed rocks of the North American Cordillera [abs.]: Mesothermal gold deposits—a global overview, extended abstracts: University of Western Australia Publication No. 27, p. 58-64.

*Goldfarb, R.J., *Nokleberg, W.J., and Phillips, G.N., 1996, Tectonic setting of synorogenic gold deposits of the Pacific Rim [abs.]: Mesothermal gold deposits—a global overview, extended abstracts: University of Western Australia Publication No. 27, p. 22-28.

*Goldfarb, R.J., Skinner, D., Christie, A.B., *Haeussler, P.J., and *Bradley, D.C., 1995, Mesothermal gold deposits of Westland, New Zealand, and southern Alaska: products of similar tectonic processes?: Mauk, J.L., ed., and others, *in* Proceedings of the 1995 PACRIM Congress: Australian Institute of Mining and Metallurgy Publication Series, p. 239-244.

*Grantz, A., *Phillips, R.L., *Mullen, M.W., *Starratt, S.W., Jones, G.A., Naidu, A.S., and Finney, B.P., 1996, Character, paleoenvironment, rate of accumulation, and evidence for seismic triggering of Holocene turbidites, Canada abyssal plain, Arctic Ocean: Marine Geology, v. 133, no. 1-2, p. 51-73.

Greninger, M.L., Klemperer, S.L., and *Nokleberg, W.J., 1996, Geographic information system (GIS) database of the geology, geophysics, deep-crustal structure, and tectonics of the Russian Far East, Alaska, Canadian Cordillera, and adjacent offshore regions [abs.]: Eos (American Geophysical Union Transactions), v. 77, no. 46, suppl., p. 669.

*Griscom, A. and *Sauer, P.E., 1993, Aeromagnetic maps of Annette Island, Alaska: *in* Godwin, L.H., and Smith, B.D., eds., Special Symposium 1993 on Economic Mineral Resources of the Annette Islands Reserve, Alaska: Spokane, Wash., Northwest Mining Association , p. 33-41.

*Haeussler, P.J., and *Bradley, D.C., 1996, Structural characteristics of ridge-subduction related gold deposits in southern Alaska [abs.]: Geological Society of America Abstracts with Programs, v. 28, no. 5, p. 71-72.

*Haeussler, P.J., and Bruhn, R.L., 1996, Evidence for Holocene or late Pleistocene folding in Cook Inlet, Alaska [abs.]: Eos (American Geophysical Union Transactions), v. 77, no. 46, suppl., p. 686.

*Haeussler, P.J., *Karl. S.M., and *Bradley, D.C., 1996, Oblique accretion of part of the Mesozoic Kelp Bay Group in southeastern Alaska [abs.]: Geological Society of America Abstracts with Programs, v.28, no. 7, p. 437.

*Hammond, W.R., *Paskievitch, J.F., *Power, J.A., *Lockhart, A.B., Estes, S.A., Tytgat, G., and Benevento, J., 1996, The AVO central Aleutian expansion: seismic monitoring and instrumentation [abs.]: Eos (American Geophysical Union Transactions), v. 77, no. 46, suppl., p. 451-452.

*Hampton, M.A., *Lee, H.J., and Locat, Jacques, 1996, Submarine landslides: Reviews of Geophysics, v. 34, p. 33-59.

*Healy, J.H., *Dewey, J.W., Kossobokov, V.G., and Romashkova, L.L., 1996, Intermediate-term changes of seismicity in advance of the 10 June 1996 Delarof Islands earthquake [abs.]: Eos (American Geophysical Union Transactions), v. 77, no. 46, suppl., p. 502.

*Heinrichs, T.A., *Mayo, L.R., Echelmeyer, K.A., and Harrison, W.D., 1996, Quiescent-phase evolution of a surge-type glacier: Black Rapids Glacier, Alaska, U.S.A.: Journal of Glaciology, v. 42, no. 140, p. 110-122.

*Horton, R.J., 1993, Airborne electromagnetic surveys of the Annette Islands Reserve: *in* Godwin, L.H., and Smith, B.D., eds., Special Symposium 1993 on Economic Mineral Resources of the Annette Islands Reserve, Alaska: Spokane, Wash., Northwest Mining Association, p. 43-49.

*Horton, R.J., 1993, Airborne geophysical surveys of the Annette Islands Reserve: *in* Godwin, L.H., and Smith, B.D., eds., Special Symposium 1993 on Economic Mineral Resources of the Annette Islands Reserve, Alaska: Spokane, Wash., Northwest Mining Association, p. 27-31.

*Horton, R.J., *Karl, S.M., *Taylor, C.D., *Griscom, A., *Bond, K.R., and *Senterfit, R.M., 1993, Mineral resource assessment of the Annette Islands Reserve, Southeast Alaska: *in* Godwin, L.H., and Smith, B.D., eds., Special Symposium 1993 on Economic Mineral Resources of the Annette Islands Reserve,

Alaska: Spokane, Wash., Northwest Mining Association, p. 83-131.

*Horton, R.J., and *Senterfit, R.M., 1993, Site-specific geophysical surveys on the Annette Islands Reserve: *in* Godwin, L.H., and Smith, B.D., eds., Special Symposium 1993 on Economic Mineral Resources of the Annette Islands Reserve, Alaska: Spokane, Wash., Northwest Mining Association, p. 57-71.

Jolly, A.D., McNutt, S.R., Wiener, S., and *Lahr, J.C., 1996, An evaluation of b-value spatial mapping techniques based on an analysis of seismicity at Mt. Spurr, Alaska, and synthetic data [abs.]: Eos (American Geophysical Union Transactions), v. 77, no. 46, suppl., p. 514.

*Karl, S.M., 1993, The geology of Annette Island: in Godwin, L.H., and Smith, B.D., eds., Special Symposium 1993 on Economic Mineral Resources of the Annette Islands Reserve, Alaska: Spokane, Wash., Northwest Mining Association , p. 21-25.

*Karl, S.M., *Hammarstrom, J.M., *Kunk, M., Himmelberg, G.R., *Brew, D.A., Kimbrough, D., and Bradshaw, J.Y., 1996, Tracy Arm transect: further constraints on the uplift history of the Coast plutonic complex in southeastern Alaska [abs.]: Geological Society of America Abstracts with Programs, v.28, no. 7, p. 312.

*Keith, T.E.C., Nye, C.J., Eichelberger, J.C., *Miller, T.P., and *Power, J.A., 1996, March 1996 seismic crisis at Akutan Volcano, central Aleutian Arc, Alaska [abs.]: Eos (American Geophysical Union Transactions), v. 77, no. 46, suppl., p. 815.

*Kelley, K.D., *Goldfarb, R.J., *Gray, J.E., *Taylor, C.D., and *Plumlee, G.S., 1996, Geoenvironmental mineral deposit models of Alaska [abs.]: International Geological Congress, 30th, Beijing, 1996, Abstracts, v. 3, p. 53.

*Kenz, H.M., *Chouet, B.A., *Dawson, P.B.,* Lahr, J.C., *Page, R.A., and Hole, J.A., 1996, Three-dimensional *P*- and *S*- wave velocity structure of Redoubt Volcano, Alaska: Journal of Geophysical Research, v. 101, no. 4, p. 8111-8128.

*Kvenvolden, K.A., 1996, Gas hydrates—geological perspective and global change, *in* Piri, R.G., ed., Oceanography: contemporary readings in ocean sciences (3rd ed.): New York, Oxford University Press, p. 336-357.

*Lorenson, T.D., and *Kvenvolden, K.A., 1996, Nonmethane hydrocarbon gases in permafrost [abs.]: Eos (American Geophysical Union Transactions), v. 77, no. 46, suppl., p. 184.

*Lorenson, T.D., *Kvenvolden, K.A., Rust, T.M., Popp, B.N., Sanson, F.J., and Macdonald, R., 1996, Isotopic composition and concentration of methane in the Arctic Ocean [abs.]: Geological Society of America Abstracts with Programs, v.28, no. 7, p. 32.

McLaughlin, E.A., Lilley, M.D., Olson, E.J., *Kvenvolden, K.A., and *Lorenson, T.D., 1996, Methane oxidation in the Beaufort Sea [abs.]: Eos (American Geophysical Union Transactions), v. 77, no. 46, suppl., p. 187-188.

*McNutt, S.R., 1994, Volcanic tremor amplitude correlated with the volcanic explosivity index and its potential use in determining ash hazards to aviation: Acta Vulcanologica, v. 5, p. 193-196.

*McNutt, S.R., 1994, Volcanic tremor from around the world: 1992 update: Acta Vulcanologica, v. 5, p. 197-200.

*Miller, T.P., Begét, J.E., *Stephens, C.D., and *Moore, R.B., 1996, Geology and hazards of Iliamna Volcano, Alaska [abs.]: Eos (American Geophysical Union Transactions), v. 77, no. 46, suppl., p. 815.

Miller, L.D., and *Goldfarb, R.J., 1996, Metallogeny of the Juneau gold belt—Alaska's largest gold system [abs.]: International Geological Congress, 30th, Beijing, 1996, Abstracts, v. 2, p. 780.

*Miller, T.P., Begét, J.E., *Stephens, C.D., and *Moore, R.B., 1996, Geology and hazards of Iliamna Volcano, Alaska [abs.]: Eos (American Geophysical Union Transactions), v. 77, no. 46, suppl., p. 815.

*Molnia, B.F., 1996, Kettle formation in 1994 flood deposits—Bering Glacier, Alaska [abs.]: Eos (American Geophysical Union Transactions), v. 77, no. 46, suppl., p. 194.

*Molnia, B.F., *McGeehin, J.P., and *Post, A., 1996, Late Holocene history of Bering Glacier, Alaska [abs.]: Geological Society of America Abstracts with Programs, v.28, no. 7, p. 433.

*Molnia, B.F., *Post, A., and *Carlson, P.R., 1996, Glacial-marine acoustic stratigraphy in Gulf of Alaska fiords [abs.]: Geological Society of America Abstracts with Programs, v.28, no. 7, p. 507.

*Molnia, B.F., *Post, A., and *Carlson, P.R., 1996, 20th-century glacial-marine sedimentation in Vitus Lake, Bering Glacier, Alaska, U.S.A.: Annals of Glaciology, v. 22, p. 205-210.

Monger, J.W.H., *Nokleberg, W.J., Dawson, K.M., Parfenov, L.M., Bundtzen, T.K., and Shpikerman, V.I., 1996, Tectonic settings of Paleozoic through Cretaceous mineral deposits of the Canadian Cordillera and Alaska, with extensions into the Russian Northeast [abs.]: Canadian Cordilleran Roundup, Vancouver, Canada, January 30 to February 2, 1997, British Columbia and Yukon Chamber of Mines, Program with Abstracts, p. 27-28.

Mortera-Gutierrez, C.A., and *Geist, E., 1996, The subducted high relief of Rat Fracture Zone beneath the Aleutian accretionary prism [abs.]: Eos (American Geophysical Union Transactions), v. 77, no. 46, suppl., p. 659.

Nishenko, S.P., *Bufe, C., *Dewey, J., *Varnes, D., *Healy, J., Jacob, K., and Kossobokov, V., 1996, 1996 Delarof Islands earthquake—a successful earthquake forecast/prediction? [abs.]: Eos (American Geophysical Union Transactions), v. 77, no. 46, suppl., p. 456.

*Nokleberg, W.J., Parfenov, L.M., Shpikerman, V.I., Khanchuk, A.I., and Ratkin, V.V., 1996, Collaborative projects of the U.S. Geological Survey and participating agencies on metallogenesis and tectonics of Eastern Siberia, Mongolia, Northeast China, Russian Far East, Alaska, and the Canadian Cordillera [abs]: Northwest Mining Association Annual Meeting Spokane, Wash., December 2-6, Program with Abstracts, p. 41.

*Nokleberg, W.J., Dawson, K.M., Monger, J.W.H., Parfenov, L.M., Bundtzen, T.K., and Shpikerman, V.I., 1996, Circum-North Pacific metallogenesis [poster]: Canadian Cordilleran Roundup, January 30 to February 2, 1997, Program with Abstracts, Vancouver, Canada, British Columbia and Yukon Chamber of Mines, p. 33.

Nolan, M., Motkya, R.J., Echelmeyer, K., and *Trabant, D.C., 1995, Ice-thickness measurements of Taku Glacier, Alaska, U.S.A., and their relevance to its recent behavior: Journal of Glaciology, v. 41, no. 139, p. 541-553.

*Power, J.A., *Paskievitch, J.F., *Richter, D.H., *McGimsey, R.G., Stelling, P., Jolly, A.D., and Fletcher, H.J., 1996, 1996 seismicity and ground deformation at Akutan Volcano, Alaska [abs.]: Eos (American Geophysical Union Transactions), v. 77, no. 46, suppl., p. 514.

Reiners, P.W., Nelson, B.K., and *Nelson, S.W., 1996, Evidence for multiple mechanisms of crustal contamination of magma from

compositionally zoned plutons and associated ultramafic intrusions of the Alaska Range: Journal of Petrology, v.37, no. 2, p. 261-292.

*Riehle, J.R., *Waitt, R.B., *Meyer, C.E., and *Calk, L.C., 1996, Age of Kaguyak caldera, eastern Aleutian arc, Alaska, estimated by tephrochronology [abs.]: Eos (American Geophysical Union Transactions), v. 77, no. 46, suppl., p. 772.

*Sentefit, R.M., 1993, Audio-magnetotelluric (AMT) studies of the Annette Islands Reserve: *in* Godwin, L.H., and Smith, B.D., eds., Special Symposium 1993 on Economic Mineral Resources of the Annette Islands Reserve, Alaska: Spokane, Wash., Northwest Mining Association, p. 51-55.

Smart, K.J., Pavlis, T.L., Sisson, V.B., Roeske, S.M., and *Snee, L.W., 1996, The Border Ranges fault system in Glacier Bay National Park, Alaska: evidence for major early Cenozoic dextral strike-slip motion: Canadian Journal of Earth Sciences, v. 33, p. 1268-1282.

*Starratt, S.W., 1995, Latest Quaternary foraminifers and sediment transport in Pervenets Canyon, Bering Sea: Marine Micropaleontology, v. 26, p. 233-243.

Strasser, J.C., Lawson, D.E., Larson, G.J., *Denner, J., Evenson, E.B., and Alley, R.B., 1996, Glaciohydrological response to an intense rain event, Matanuska Glacier, Alaska [abs.]: Geological Society of America Abstracts with Programs, v.28, no. 7, p. 56.

Symonds, R.B., Ritchie, B.E., *McGimsey, R.G., and Ort, M.H., 1996, Preliminary report on 1995 gas seep and spring sampling in the vicinity of Gas Rocks, south shore of Becharof Lake; Alaska: Anchorage, Alaska, U.S. Department of Fish and Wildlife Services, Administrative Report 13 p.

*Taylor, C.D., 1996, Summary of geochemical data; Annette Islands Reserve, southeast Alaska: *in* Godwin, L.H., and Smith, B.D., eds., Special Symposium 1993 on Economic Mineral Resources of the Annette Islands Reserve, Alaska: Spokane, Wash., Northwest Mining Association, p. 77-82.

Truffer, M., Harrison, W.D., Echelmeyer, K.A., Gorda-DeMallie, J, and *Heinrichs, T.A., 1996, Velocity variations of surge type Black Rapids Glacier [abs.]: Eos (American Geophysical Union Transactions), v. 77, no. 46, suppl., p. 213.

*Walder, J.S., and *Costa, J.E., 1996, Outburst floods from glacier-dammed lakes: the effect of mode of lake drainage on flood magnitude: Earth Surface Processes and Landforms, v. 21, p. 701-723.

*Waythomas, C.F., 1996, Volcanigenic tsunamis from Augustine Volcano, Alaska: fact or fiction? [abs.]: Geological Society of America Abstracts with Programs, v.28, no. 7, p. 410.

*Waythomas, C.F., 1996, Late-Quaternary stratigraphy and environments of the Holitna lowland, southwest Alaska, *in* West, F.H., and Hoffecker, J.F., eds. American beginnings: University of Chicago Press, p. 35-52.

*Waythomas, C.F., *Walder, J.S., *McGimsey, R.G., and *Neal, C.A., 1996, A catastrophic flood caused by drainage of a caldera lake at Aniakchak Volcano, Alaska, and implications for volcanic hazards assessment: Geological Society of America Bulletin, v. 108, no. 7, p. 861-871.

☆ U.S. GOVERNMENT PRINTING OFFICE: 1998—673-048 / 20112 Region No. 8

Selected Series of U.S. Geological Survey Publications

Books and Other Publications

Professional Papers report scientific data and interpretations of lasting scientific interest that cover all facets of USGS investigations and research.

Bulletins contain significant data and interpretations that are of lasting scientific interest but are generally more limited in scope or geographic coverage than Professional Papers.

Water-Supply Papers are comprehensive reports that present significant interpretive results of hydrologic investigations of wide interest to professional geologists, hydrologists, and engineers. The series covers investigations in all phases of hydrology, including hydrogeology, availability of water, quality of water, and use of water.

Circulars are reports of programmatic or scientific information of an ephemeral nature; many present important scientific information of wide popular interest. Circulars are distributed at no cost to the public.

Fact Sheets communicate a wide variety of timely information on USGS programs, projects, and research. They commonly address issues of public interest. Fact Sheets generally are two or four pages long and are distributed at no cost to the public.

Reports in the **Digital Data Series (DDS)** distribute large amounts of data through digital media, including compact disc-read-only memory (CD-ROM). They are high-quality, interpretive publications designed as self-contained packages for viewing and interpreting data and typically contain data sets, software to view the data, and explanatory text.

Water-Resources Investigations Reports are papers of an interpretive nature made available to the public outside the formal USGS publications series. Copies are produced on request (unlike formal USGS publications) and are also available for public inspection at depositories indicated in USGS catalogs.

Open-File Reports can consist of basic data, preliminary reports, and a wide range of scientific documents on USGS investigations. Open-File Reports are designed for fast release and are available for public consultation at depositories.

Maps

Geologic Quadrangle Maps (GQ's) are multicolor geologic maps on topographic bases in 7.5- or 15-minute quadrangle formats (scales mainly 1:24,000 or 1:62,500) showing bedrock, surficial, or engineering geology. Maps generally include brief texts; some maps include structure and columnar sections only.

Geophysical Investigations Maps (GP's) are on topographic or planimetric bases at various scales. They show results of geophysical investigations using gravity, magnetic, seismic, or radioactivity surveys, which provide data on subsurface structures that are of economic or geologic significance.

Miscellaneous Investigations Series Maps or **Geologic Investigations Series (I's)** are on planimetric or topographic bases at various scales; they present a wide variety of format and subject matter. The series also incudes 7.5-minute quadrangle photogeologic maps on planimetric bases and planetary maps.

Information Periodicals

Metal Industry Indicators (MII's) is a free monthly newsletter that analyzes and forecasts the economic health of five metal industries with composite leading and coincident indexes: primary metals, steel, copper, primary and secondary aluminum, and aluminum mill products.

Mineral Industry Surveys (MIS's) are free periodic statistical and economic reports designed to provide timely statistical data on production, distribution, stocks, and consumption of significant mineral commodities. The surveys are issued monthly, quarterly, annually, or at other regular intervals, depending on the need for current data. The MIS's are published by commodity as well as by State. A series of international MIS's is also available.

Published on an annual basis, **Mineral Commodity Summaries** is the earliest Government publication to furnish estimates covering nonfuel mineral industry data. Data sheets contain information on the domestic industry structure, Government programs, tariffs, and 5-year salient statistics for more than 90 individual minerals and materials.

The Minerals Yearbook discusses the performance of the worldwide minerals and materials industry during a calendar year, and it provides background information to assist in interpreting that performance. The Minerals Yearbook consists of three volumes. Volume I, Metals and Minerals, contains chapters about virtually all metallic and industrial mineral commodities important to the U.S. economy. Volume II, Area Reports: Domestic, contains a chapter on the minerals industry of each of the 50 States and Puerto Rico and the Administered Islands. Volume III, Area Reports: International, is published as four separate reports. These reports collectively contain the latest available mineral data on more than 190 foreign countries and discuss the importance of minerals to the economies of these nations and the United States.

Permanent Catalogs

"Publications of the U.S. Geological Survey, 1879–1961" and **"Publications of the U.S. Geological Survey, 1962–1970"** are available in paperback book form and as a set of microfiche.

"Publications of the U.S. Geological Survey, 1971–1981" is available in paperback book form (two volumes, publications listing and index) and as a set of microfiche.

Annual supplements for 1982, 1983, 1984, 1985, 1986, and subsequent years are available in paperback book form.

ISBN 060790040-7
9 780607 900408